

Ingvar Lindgren

# Relativistic Many-Body Theory

A New Field-Theoretical Approach

*Second Edition*

# **Springer Series on Atomic, Optical, and Plasma Physics**

Volume 63

## **Editor-in-chief**

Gordon W.F. Drake, Windsor, Canada

## **Series editors**

James Babb, Cambridge, USA

Andre D. Bandrauk, Sherbrooke, Canada

Klaus Bartschat, Des Moines, USA

Philip George Burke, Belfast, UK

Robert N. Compton, Knoxville, USA

Tom Gallagher, Charlottesville, USA

Charles J. Joachain, Bruxelles, Belgium

Peter Lambropoulos, Iraklion, Greece

Gerd Leuchs, Erlangen, Germany

Pierre Meystre, Tucson, USA

The Springer Series on Atomic, Optical, and Plasma Physics covers in a comprehensive manner theory and experiment in the entire field of atoms and molecules and their interaction with electromagnetic radiation. Books in the series provide a rich source of new ideas and techniques with wide applications in fields such as chemistry, materials science, astrophysics, surface science, plasma technology, advanced optics, aeronomy, and engineering. Laser physics is a particular connecting theme that has provided much of the continuing impetus for new developments in the field, such as quantum computation and Bose-Einstein condensation. The purpose of the series is to cover the gap between standard undergraduate textbooks and the research literature with emphasis on the fundamental ideas, methods, techniques, and results in the field.

More information about this series at <http://www.springer.com/series/411>

Ingvar Lindgren

# Relativistic Many-Body Theory

A New Field-Theoretical Approach

Second Edition

 Springer

Ingvar Lindgren  
University of Gothenburg  
Gothenburg  
Sweden

ISSN 1615-5653                      ISSN 2197-6791 (electronic)  
Springer Series on Atomic, Optical, and Plasma Physics  
ISBN 978-3-319-15385-8              ISBN 978-3-319-15386-5 (eBook)  
DOI 10.1007/978-3-319-15386-5

Library of Congress Control Number: 2016932339

© Springer International Publishing Switzerland 2011, 2016

This work is subject to copyright. All rights are reserved by the Publisher, whether the whole or part of the material is concerned, specifically the rights of translation, reprinting, reuse of illustrations, recitation, broadcasting, reproduction on microfilms or in any other physical way, and transmission or information storage and retrieval, electronic adaptation, computer software, or by similar or dissimilar methodology now known or hereafter developed.

The use of general descriptive names, registered names, trademarks, service marks, etc. in this publication does not imply, even in the absence of a specific statement, that such names are exempt from the relevant protective laws and regulations and therefore free for general use.

The publisher, the authors and the editors are safe to assume that the advice and information in this book are believed to be true and accurate at the date of publication. Neither the publisher nor the authors or the editors give a warranty, express or implied, with respect to the material contained herein or for any errors or omissions that may have been made.

Printed on acid-free paper

This Springer imprint is published by Springer Nature  
The registered company is Springer International Publishing AG Switzerland

*To the memory of Eva*

## Preface to the Second Edition

In this second revised edition several parts of the first edition have been rewritten and extended. This is particularly the case for Chaps. 4, 6 and 8, which represent the central parts of the book. The presentation of numerical results concerning quantum-electrodynamical (QED) effects in combination with electron correlation is extended and now includes radiative QED effects (electron self-energy, vertex correction and vacuum polarization), involving the use of Feynman and Coulomb gauges.

A new section (Part IV) has been added, dealing with QED effects in *dynamical processes*. It turned out that the Green's operator, introduced primarily for structure problems, is particularly suitable also for dealing with dynamical processes, when bound states are involved. Here, certain singularities may appear of the same kind as in dealing with static processes, leading to so-called *model-space contributions*. These cannot be handled with the standard S-matrix formulation, which is the normal procedure for dynamical processes involving only free-particle states. This has led to a modification of the optical theorem applicable also to bound states, where the S-matrix is replaced by the Green's operator.

In addition, a number of misprints and other errors have been corrected for, and I am grateful to all readers who have pointed out some of them to me.

I wish to express my gratitude to Prof. Walter Greiner, Frankfurt, and to the Alexander von Humboldt Foundation for moral and economic support during the entire work with this book.

I am very grateful to my coworkers, Sten Salomonson, Daniel Hedendahl and Johan Holmberg, for valuable cooperation and for allowing me to include results that are unpublished or in the process of being published.

On behalf of our research group of theoretical Atomic Physics at the University of Gothenburg, I wish to express our deep gratitude to Horst Stöcker and Thomas Stöhlker at GSI, Darmstadt, as well as to the Helmholtz Association for moral and financial support during the final phase of this project, which has been of vital importance for the conclusion of the project.

Gothenburg

Ingvar Lindgren



## Preface to the First Edition

It is now almost 30 years since the first edition of my book together with John Morrison, *Atomic Many-Body Theory* [124], appeared, and the second edition appeared some years later. It has been out of print for quite some time, but fortunately it has recently been made available again by a reprint by Springer Verlag.

During the time that has followed, there has been a tremendous development in the treatment of many-body systems, conceptually as well as computationally. Particularly the relativistic treatment has expanded considerably, a treatment that has been extensively reviewed recently by Ian Grant in the book *Relativistic Quantum Theory of Atoms and Molecules* [79].

Also, the treatment of quantum-electrodynamical (QED) effects in atomic systems has developed considerably in the past few decades, and several review articles have appeared in the field [130, 159, 226] as well as in the book by Labzowsky *et al.*, *Relativistic Effects in Spectra of Atomic Systems* [114].

An impressive development has taken place in the field of many-electron systems by means of various coupled-cluster approaches, with applications particularly on molecular systems. The development during the past 50 years has been summarized in the book *Recent Progress in Coupled Cluster Methods*, edited by Čársky, Paldus and Pittner [246].

The present book is aimed at combining the atomic many-body theory with quantum electrodynamics, which is a long-sought goal in quantum physics. The main problem in this effort has been that the methods for QED calculations, such as the S-matrix formulation, and the methods for many-body perturbation theory (MBPT) have completely different structures. With the development of the new method for QED calculations, the *covariant evolution operator formalism* by the Gothenburg Atomic-Theory group [5], the situation has changed, and quite new possibilities has appeared to formulate a unified theory.

The new formalism is based on field theory, and in its full extent the unification process represents a formidable problem, and we can in the present book describe only how some steps towards this goal can be taken. The present book will be largely based upon the previous book *Atomic Many-Body Theory* [124], and it is

assumed that the reader has absorbed most of that book, particularly Part II. In addition, the reader is expected to have basic knowledge in quantum field theory, as found in books like *Quantum Theory of Many-Particle Systems* by Fetter and Walecka [67] (mainly parts I and II), *An Introduction to Quantum Field Theory* by Peskin and Schroeder [194], and *Quantum Field Theory* by Mandl and Shaw [143].

The material of the present book is largely based upon lecture notes and recent publications by the Gothenburg Atomic-Theory group [86, 89, 130–132], and I want to express my sincere gratitude particularly to my previous co-author John Morrison and to my present coworkers, Sten Salomonson and Daniel Hedendahl, as well as to the previous collaborators Ann-Marie Pendrill, Jean-Louis Heully, Eva Lindroth, Björn Åsén, Hans Persson, Per Sunnergren, Martin Gustavsson and Håkan Warston for valuable collaboration.

In addition, I want to thank the late pioneers of the field, Per-Olov Löwdin, who taught me the foundations of perturbation theory some 40 years ago, and Hugh Kelly, who introduced the diagrammatic representation into atomic physics—two corner stones of the later developments. Furthermore, I have benefitted greatly from communications with many other national and international colleagues and friends (in alphabetic order), Rod Bartlett, Erkki Brändas, Gordon Drake, Ephraim Eliav, Stephen Fritzsche, Gerald Gabrielse, Walter Greiner, Paul Indelicato, Karol Jankowski, Jüürgen Kluge, Leonti Labzowsky, Peter Mohr, Debashis Mukherjee, Marcel Nooijen, Joe Paldus, Vladimir Shabaev, Thomas Stöohlker, Gerhard Soff<sup>†</sup>, Joe Sucher, Peter Surjan and many others.

The outline of the book is the following. The main text is divided into three parts. Part I gives some basic formalism and the basic many-body theory that will serve as a foundation for the following text. In Part II three numerical procedures for calculation of QED effects on bound electronic states are described, the S-matrix formulation, the Green's function and the Green's operator methods. A procedure towards combining QED with MBPT is developed in Part III. Part IV contains a number of appendices, where basic concepts are summarized. Certain sections of the text that can be omitted at first reading are marked with an asterisk (\*).

Gothenburg  
November 2010

Ingvar Lindgren

# Contents

<b>1</b>	<b>Introduction</b> . . . . .	1
1.1	Standard Many-Body Perturbation Theory . . . . .	1
1.2	Quantum Electrodynamics . . . . .	2
1.3	Bethe–Salpeter Equation . . . . .	3
1.4	Helium Atom. Analytical Approach . . . . .	5
1.5	Field-Theoretical Approach to Many-Body Perturbation Theory . . . . .	5
1.6	Dynamical Processes . . . . .	7
 <b>Part I Basics. Standard Many-Body Perturbation Theory</b>		
<b>2</b>	<b>Time-Independent Formalism</b> . . . . .	11
2.1	First Quantization. . . . .	11
2.1.1	De Broglie’s Relations . . . . .	11
2.1.2	The Schrödinger Equation . . . . .	12
2.2	Second Quantization. . . . .	14
2.2.1	Schrödinger Equation in Second Quantization* . . . . .	14
2.2.2	Particle-Hole Formalism. Normal Order and Contraction . . . . .	16
2.2.3	Wick’s Theorem. . . . .	17
2.3	Time-Independent Many-Body Perturbation Theory . . . . .	18
2.3.1	Bloch Equation . . . . .	18
2.3.2	Partitioning of the Hamiltonian . . . . .	19
2.4	Graphical Representation. . . . .	23
2.4.1	Goldstone Diagrams . . . . .	23
2.4.2	Linked-Diagram Expansion . . . . .	27
2.5	All-Order Methods. Coupled-Cluster Approach . . . . .	29
2.5.1	Pair Correlation . . . . .	29
2.5.2	Exponential Ansatz: Coupled-Cluster Approach . . . . .	31
2.5.3	Various Models for Coupled-Cluster Calculations. Intruder-State Problem . . . . .	33

2.6 Relativistic MBPT. No-Virtual-Pair Approximation . . . . . 36

    2.6.1 QED Effects . . . . . 37

2.7 Some Numerical Results of Standard MBPT and CC Calculations, Applied to Atoms . . . . . 38

**3 Time-Dependent Formalism . . . . . 43**

    3.1 Transition Rate . . . . . 43

    3.2 Evolution Operator . . . . . 44

    3.3 Adiabatic Damping. Gell-Mann–Low Theorem . . . . . 48

        3.3.1 Gell-Mann–Low Theorem . . . . . 49

    3.4 Extended Model Space. The Generalized Gell-Mann–Low Relation . . . . . 50

**Part II Bound-State Quantumelectrodynamics: One- and Two-Photon Exchange**

**4 S-Matrix . . . . . 57**

    4.1 Definition of the S-Matrix. Feynman Diagrams . . . . . 58

        4.1.1 General . . . . . 58

        4.1.2 Bound States . . . . . 59

    4.2 Electron Propagator . . . . . 60

    4.3 Photon Propagator . . . . . 63

        4.3.1 Feynman Gauge . . . . . 64

        4.3.2 Coulomb Gauge . . . . . 66

    4.4 Single-Photon Exchange . . . . . 67

        4.4.1 Covariant Gauge . . . . . 68

        4.4.2 Non-covariant Coulomb Gauge . . . . . 71

        4.4.3 Single-Particle Potential . . . . . 73

    4.5 Two-Photon Exchange . . . . . 74

        4.5.1 Two-Photon Ladder . . . . . 74

        4.5.2 Two-Photon Cross\* . . . . . 76

    4.6 QED Corrections . . . . . 78

        4.6.1 Bound-Electron Self-energy . . . . . 78

        4.6.2 Vertex Correction . . . . . 81

        4.6.3 Vacuum Polarization . . . . . 83

        4.6.4 Photon Self-energy . . . . . 86

    4.7 Feynman Diagrams for the S-Matrix. Feynman Amplitude . . . . . 87

        4.7.1 Feynman Diagrams . . . . . 87

        4.7.2 Feynman Amplitude. Energy Diagram . . . . . 87

**5 Green’s Functions . . . . . 89**

    5.1 Classical Green’s Function . . . . . 89

    5.2 Field-Theoretical Green’s Function—Closed-Shell Case . . . . . 90

        5.2.1 Definition of the Field-Theoretical Green’s Function . . . . . 90

5.2.2	Single-Photon Exchange . . . . .	94
5.2.3	Fourier Transform of the Green's Function . . . . .	95
5.3	Graphical Representation of the Green's Function* . . . . .	99
5.3.1	Single-Particle Green's Function . . . . .	99
5.3.2	Many-Particle Green's Function . . . . .	104
5.3.3	Self-Energy. Dyson Equation . . . . .	107
5.3.4	Numerical Illustration . . . . .	108
5.4	Field-Theoretical Green's Function—Open-Shell Case* . . . . .	109
5.4.1	Definition of the Open-Shell Green's Function . . . . .	109
5.4.2	Two-Time Green's Function of Shabaev . . . . .	110
5.4.3	Single-Photon Exchange . . . . .	112
<b>6</b>	<b>The Covariant Evolution Operator and the Green's-Operator</b>	
	<b>Method . . . . .</b>	<b>117</b>
6.1	Definition of the Covariant Evolution Operator . . . . .	117
6.2	Lowest-Order Single-Particle Covariant Evolution Operator . . . . .	120
6.3	Single-Photon Exchange in the Covariant-Evolution-Operator Formalism . . . . .	122
6.4	Ladder Diagrams . . . . .	125
6.5	Multi-Photon Exchange . . . . .	127
6.5.1	General . . . . .	127
6.5.2	Irreducible Two-Photon Exchange* . . . . .	129
6.5.3	Potential with Radiative Parts . . . . .	131
6.6	Relativistic Form of the Gell-Mann–Low Theorem . . . . .	131
6.7	Field-Theoretical Many-Body Hamiltonian in the Photonic Fock Space . . . . .	132
6.8	Green's Operator . . . . .	135
6.8.1	Definition . . . . .	135
6.8.2	Relation Between the Green's Operator and Many-Body Perturbation Procedures . . . . .	136
6.9	Model-Space Contribution . . . . .	140
6.9.1	Lowest Orders . . . . .	141
6.9.2	All Orders* . . . . .	146
6.10	Bloch Equation for Green's Operator* . . . . .	152
6.11	Time Dependence of the Green's Operator. Connection to the Bethe–Salpeter Equation* . . . . .	156
6.11.1	Single-Reference Model Space . . . . .	156
6.11.2	Multi-reference Model Space . . . . .	159
<b>7</b>	<b>Examples of Numerical Calculations of One- and Two-Photon QED Effects . . . . .</b>	<b>161</b>
7.1	S-Matrix . . . . .	161
7.1.1	Electron Self-energy of Hydrogenlike Ions . . . . .	161
7.1.2	Lamb Shift of Hydrogenlike Uranium . . . . .	162
7.1.3	Lamb Shift of Lithiumlike Uranium . . . . .	164

7.1.4	Two-Photon Non-radiative Exchange in Heliumlike Ions . . . . .	164
7.1.5	Electron Correlation and QED Calculations on Ground States of Heliumlike Ions . . . . .	165
7.1.6	g-Factor of Hydrogenlike Ions. Mass of the Free Electron . . . . .	168
7.2	Two-Time Green's-Function and the Covariant Evolution Operator Method, Applied to He-Like Ions . . . . .	170

### **Part III Unification of Many-Body Perturbation Theory and Quantum Electrodynamics**

<b>8</b>	<b>Beyond Two-Photon Exchange: Combination of Quantum Electrodynamics and Electron Correlation . . . . .</b>	<b>177</b>
8.1	Non-radiative QED Effects, Combined with Electron Correlation . . . . .	178
8.1.1	Single-Photon Exchange with Virtual Pairs . . . . .	178
8.1.2	Fock-Space Treatment. . . . .	186
8.1.3	Continued Iteration. Combination of Non-radiative QED with Electron Correlation . . . . .	193
8.2	Radiative QED Effects, Combined with Electron Correlation . . . . .	196
8.2.1	Two-Electron Screened Self-Energy and Vertex Correction in Lowest Order . . . . .	197
8.2.2	All Orders . . . . .	200
8.2.3	Continued Coulomb Iterations . . . . .	202
8.3	Higher-Order QED. Connection to the Bethe–Salpeter Equation. Coupled-Cluster-QED. . . . .	202
8.3.1	General QED (Single-Transverse-Photon) Potential. . .	203
8.3.2	Iterating the QED Potential. Connection to the Bethe–Salpeter Equation . . . . .	204
8.3.3	Coupled-Cluster-QED Expansion . . . . .	205
<b>9</b>	<b>Numerical Results of Combined MBPT-QED Calculations Beyond Second Order . . . . .</b>	<b>209</b>
9.1	Non-radiative QED Effects in Combination with Electron Correlation . . . . .	209
9.1.1	Two-Photon Exchange . . . . .	209
9.1.2	Non-radiative Effects. Beyond Two-Photon Exchange . . . . .	210
9.2	Radiative QED Effects in Combination with Electron Correlation. Coulomb Gauge. . . . .	213
9.2.1	Radiative Effects. Two-Photon Effects. . . . .	213
9.2.2	Radiative Effects. Beyond Two-Photon Exchange. . . .	216

9.3	Comparison with Experiments . . . . .	217
9.4	Outlook . . . . .	218
<b>10</b>	<b>The Bethe–Salpeter Equation . . . . .</b>	<b>219</b>
10.1	The Original Derivations of the Bethe–Salpeter Equation . . . . .	219
10.1.1	Derivation by Salpeter and Bethe . . . . .	219
10.1.2	Derivation by Gell-Mann and Low . . . . .	222
10.1.3	Analysis of the Derivations of the Bethe–Salpeter Equation . . . . .	223
10.2	Quasi- and Effective-Potential Approximations. Single-Reference Case . . . . .	225
10.3	Bethe–Salpeter–Bloch Equation. Multi-reference Case* . . . . .	226
10.4	Problems with the Bethe–Salpeter Equation . . . . .	228
<b>11</b>	<b>Analytical Treatment of the Bethe–Salpeter Equation . . . . .</b>	<b>231</b>
11.1	Helium Fine Structure . . . . .	231
11.2	The Approach of Sucher . . . . .	232
11.3	Perturbation Expansion of the BS Equation . . . . .	237
11.4	Diagrammatic Representation . . . . .	239
11.5	Comparison with the Numerical Approach . . . . .	241
<b>12</b>	<b>Regularization and Renormalization . . . . .</b>	<b>243</b>
12.1	The Free-Electron QED . . . . .	243
12.1.1	The Free-Electron Propagator . . . . .	243
12.1.2	The Free-Electron Self-Energy . . . . .	245
12.1.3	The Free-Electron Vertex Correction . . . . .	247
12.2	Renormalization Process . . . . .	248
12.2.1	Mass Renormalization . . . . .	249
12.2.2	Charge Renormalization . . . . .	251
12.3	Bound-State Renormalization. Cut-Off Procedures . . . . .	255
12.3.1	Mass Renormalization . . . . .	255
12.3.2	Evaluation of the Mass Term . . . . .	256
12.3.3	Bethe’s Nonrelativistic Treatment . . . . .	257
12.3.4	Brown-Langer-Schaefer Regularization . . . . .	259
12.3.5	Partial-Wave Regularization . . . . .	262
12.4	Dimensional Regularization in Feynman Gauge* . . . . .	264
12.4.1	Evaluation of the Renormalized Free-Electron Self-Energy in Feynman Gauge . . . . .	264
12.4.2	Free-Electron Vertex Correction in Feynman Gauge . . . . .	268
12.5	Dimensional Regularization in Coulomb Gauge . . . . .	270
12.5.1	Free-Electron Self-Energy in the Coulomb Gauge . . . . .	270

## Part IV Dynamical Processes with Bound States

<b>13 Dynamical Bound-State Processes . . . . .</b>	<b>277</b>
13.1 Optical Theorem for Free and Bound Particles. . . . .	278
13.1.1 Scattering of Free Particles, Optical Theorem. . . . .	278
13.1.2 Optical Theorem for Bound Particles . . . . .	279
13.2 Atomic Transition Between Bound States . . . . .	280
13.2.1 Self-Energy Insertion on the Incoming Line. . . . .	282
13.2.2 Self-Energy Insertion on the Outgoing Line. . . . .	284
13.2.3 Vertex Correction. . . . .	285
13.3 Radiative Recombination. . . . .	286
13.3.1 Lowest . . . . .	287
13.3.2 Self-Energy Insertion on the Bound State . . . . .	288
13.3.3 Vertex Correction. . . . .	289
13.3.4 Self-Energy Insertion on the Free-Electron State. . . . .	290
13.3.5 Scattering Amplitude . . . . .	291
13.3.6 Photoionization . . . . .	293
<b>14 Summary and Conclusions . . . . .</b>	<b>295</b>
<b>Appendix A: Notations and Definitions. . . . .</b>	<b>297</b>
<b>Appendix B: Second Quantization . . . . .</b>	<b>309</b>
<b>Appendix C: Representations of States and Operators . . . . .</b>	<b>315</b>
<b>Appendix D: Dirac Equation and the Momentum Representation . . . . .</b>	<b>321</b>
<b>Appendix E: Lagrangian Field Theory. . . . .</b>	<b>331</b>
<b>Appendix F: Semiclassical Theory of Radiation . . . . .</b>	<b>337</b>
<b>Appendix G: Covariant Theory of Quantum Electro Dynamics. . . . .</b>	<b>353</b>
<b>Appendix H: Feynman Diagrams and Feynman Amplitude. . . . .</b>	<b>365</b>
<b>Appendix I: Evaluation Rules for Time-Ordered Diagrams. . . . .</b>	<b>371</b>
<b>Appendix J: Some Integrals. . . . .</b>	<b>379</b>
<b>Appendix K: Unit Systems and Dimensional Analysis. . . . .</b>	<b>385</b>
<b>References . . . . .</b>	<b>391</b>
<b>Index . . . . .</b>	<b>403</b>



# Acronyms

CCA	Coupled-cluster approach
CEO	Covariant evolution operator
GML	Gell-Mann–Low relation
HP	Heisenberg picture
IP	Interaction picture
LDE	Linked-diagram expansion
MBPT	Many-body perturbation theory
MSC	Model-space contribution
NVPA	No-virtual-pair approximation
PWR	Partial-wave regularization
QED	Quantum electrodynamics
SCF	Self-consistent field
SI	International unit system
SP	Schrödinger picture

# Chapter 1

## Introduction

### 1.1 Standard Many-Body Perturbation Theory

The quantum-mechanical treatment of many-electron systems, based on the Schrödinger equation and the Coulomb interaction between the electrons, was developed shortly after the advent of quantum mechanics, particularly by John Slater in the late 1920s and early 1930s [230]. Self-consistent-field (SCF) schemes were early developed by Slater, Hartree, Fock and others.<sup>1</sup> Perturbative schemes for quantum-mechanical system, based on the Rayleigh–Schrödinger and Brillouin–Wigner schemes, were developed in the 1930s and 1940s, leading to the important *linked-diagram expansion*, introduced by Brueckner [40] and Goldstone [78] in the 1950s, primarily for nuclear applications. That scheme was in the 1960s and 1970s also applied to electronic systems [104] and extended to degenerate and quasi-degenerate energy levels (“multi-reference systems”) [34, 117]. The next step in this development was the introduction of “*all-order methods*” of *coupled-cluster* type, where certain effects are taken to all orders of the perturbation expansion (see [246]). This represents the last—and probably final—major step of the development of a non-relativistic many-body perturbation theory (MBPT).<sup>2</sup>

The first step towards a relativistic treatment of many-electron systems was taken in the early 1930s by Gregory Breit [35], extending works made somewhat earlier by J.A. Gaunt [73]. Physically, the Gaunt interaction represents the magnetic interaction between the electrons, which is a purely relativistic effect. Breit augmented this treatment by including the leading retardation effect, due to the fact that the Coulomb interaction is not instantaneous, which is an effect of the same order.

---

<sup>1</sup>For a review of the SCF methods the reader is referred to the book by Ch. Froese-Fischer [71].

<sup>2</sup>By MBPT we understand here perturbative methods based upon the Rayleigh–Schrödinger perturbation scheme and the linked-diagram expansion. To that group we also include non-perturbative schemes, like the coupled-cluster approach (CCA), which are based upon the same formalism.

A proper relativistic theory should be *Lorentz covariant*, like the Dirac single-electron theory.<sup>3</sup> The Dirac equation for the individual electrons together with the instantaneous Coulomb and Breit interactions between the electrons represent for a many-electron system all effects up to order  $\alpha^2$  H(artree atomic units) or  $\alpha^4 m_e c^2$ .<sup>4</sup> This procedure, however, is NOT Lorentz covariant, and the instantaneous Breit interaction can only be treated to first-order in perturbation theory, unless projection operators are introduced to prevent the intermediate states from falling into the “Dirac sea” of negative-energy states, as discussed early by Brown and Ravenhall [39] and later by Joe Sucher [238]. The latter approach has been successfully employed for a long time in relativistic many-body calculations and is known as the *no-virtual-pair approximation* (NVPA).

A fully covariant relativistic many-body theory requires a field-theoretical approach, i.e., the use of *quantum electrodynamics* (QED). In principle, there is no sharp distinction between relativity and QED, but conventionally we shall refer to effects beyond the no-virtual-pair approximation as QED effects. This includes “*non-radiative*” effects (retardation and virtual electron-positron pairs) as well as “*radiative*” effects (self-energy, vacuum polarization, vertex correction). The systematic treatment of these effects requires a covariant approach, where the QED effects are included in the wave function and hence can be treated on the same footing as the electron-electron interaction. It is the main purpose of the present book to formulate the foundations of such a unified MBPT-QED procedure.

## 1.2 Quantum Electrodynamics

Already in the 1930s deviations were observed between the results of precision spectroscopy and the Dirac theory for simple atomic systems, primarily the hydrogen atom. Originally, this deviation was expected to be due to *vacuum polarization*, i.e., spontaneous creation of electron-positron pairs in the vacuum, but this effect turned out to be too small and even of the wrong sign. An alternative explanation was the *electron self-energy*, i.e., the emission and absorption of a virtual photon on the same electron—another effect that is not included in the Dirac theory. Early attempts to calculate this effect, however, were unsuccessful, due to singularities (infinities) in the mathematical expressions.

The first experimental observation of a clear-cut deviation from the Dirac theory was the detection in 1947 by Lamb and Retherford of the so-called *Lamb shift* [116],

---

<sup>3</sup>A physical quantity (scalar, vector, tensor) is said to be Lorentz covariant, if it transforms according to a representation of the Lorentz group. (Only a scalar is invariant under a that transformation.) An equation or a theory, like the theory of relativity or Maxwell’s theory of electromagnetism, is said to be Lorentz covariant, if it can be expressed entirely in terms of covariant quantities (see, for instance, the books of Bjorken and Drell [21, 22]).

<sup>4</sup> $\alpha$  is the fine-structure constant  $\approx 1/137$  and  $m_e c^2$  is the electron rest energy (see Appendix K).

namely the shift between the  $2s$  and  $2p_{1/2}$  levels in atomic hydrogen, levels that are exactly degenerate in the Dirac theory [58, 59]. In the same year Hans Bethe was able to explain the shift by a non-relativistic calculation, eliminating the singularity of the self-energy by means of a *renormalization process* [19]. At about the same time Kusch and Foley observed that the magnetic  $g$ -factor of the free electron deviates slightly but significantly from the Dirac value  $-2$  [110, 111]. These observations led to the development of the modern form of the quantum-electrodynamic theory by Feynman, Schwinger, Dyson, Tomanaga and others by which the deviations from the Dirac theory could be explained with good accuracy [63, 68, 69, 224, 244].<sup>5</sup>

The original theory of QED was applied to free electrons. During the last four to five decades several methods have been developed for numerical calculation of QED effects in *bound* electronic states. The scattering-matrix or *S-matrix formulation*, originally developed for dealing with the scattering of free particles, was made applicable also to bound states by Joe Sucher [236], and the numerical procedure was refined in the 1970s particularly by Peter Mohr [153]. During the last two decades the method has been extensively used in studies of highly charged ions in order to test the QED theory under extreme conditions, works that have been pioneered by Mohr and Soff (for a review, see [159]).

The *Green's function* is one of the most important tools in mathematical physics with applications in essentially all branches of physics.<sup>6</sup> During the 1990s the method was adopted to bound-state QED problems by Shabaev et al. [226]. This procedure is referred to as the *two-time Green's function* and has recently been extensively applied to highly-charged ions by the St Petersburg group.

During the first decade of this century another procedure for numerical QED calculations was developed by the Gothenburg atomic theory group, first termed the *Covariant evolution-operator* method [130], which was applied to the fine structure and other energy-level separations of heliumlike ions. This can be combined with electron correlation to arbitrary order, and we then refer to this procedure as the *Green's-operator method*. This represents a step towards a fully covariant treatment of many-electron systems and formally equivalent to the *Bethe–Salpeter equation* (see below).

### 1.3 Bethe–Salpeter Equation

The first completely covariant treatment of a bound-state problem was presented in 1951 by Salpeter and Bethe [20, 213] and by Gell-Mann and Low [74]. The two-particle Bethe–Salpeter (BS) equation contains in principle the complete relativistic and interelectronic interaction, i.e., all kinds of electron-correlation and QED effects.

---

<sup>5</sup>For the history of the development of the QED theory the reader is referred to the authoritative review by Silvan Schweber [221].

<sup>6</sup>For a comprehensive account of the applications, particularly in condensed-matter physics, the reader is referred to the book by Gerald Mahan [140].

The BS equation is associated with several fundamental problems, which were discussed in the early days, particularly by Dyson [64], Goldstein [77], Wick [251] and Cutkosky [53]. Dyson found that the question of relativistic quantum mechanics is “*full of obscurities and unsolved problems*” and that “*the physical meaning of the 4-dimensional wave function is quite unclear*”. It seems that some of these problems still remain.

The BS equation is based upon field theory, and there is no direct connection to the Hamiltonian approach of quantum mechanics. The solution of the field-theoretical BS equation leads to a four-dimensional wave function with individual times for the two particles. This is not in accordance with the standard quantum-mechanical picture, which has a single time variable also for many-particle systems. The additional time variable leads sometimes to “*abnormal solutions*” with no counterparts in non-relativistic quantum mechanics, as discussed particularly by Nakanishi [172] and Namyslowski [173].

Much effort has been devoted to simplifying the BS equation by reducing it to a three-dimensional equation, in analogy with the standard quantum-mechanical equations (for reviews, see [32, 49]). Salpeter [212] derived early an “*instantaneous*” approximation, neglecting retardation, which led to a relativistically exact three-dimensional equation, similar to—but not exactly equal to—the Breit equation. More sophisticated is the so-called *quasi-potential approximation*, introduced by Todorov [242], frequently used in scattering problems. Here, a three-dimensional Schrödinger-type equation is derived with an **energy-dependent** potential, deduced from scattering theory. Sazdjian [216, 217] was able to separate the BS equation into a three-dimensional equation of Schrödinger type and one equation for the relative time of the two particles, serving as a perturbation—an approach that is claimed to be exactly equivalent to the original BS equation. This approach establishes a definitive link between the Hamiltonian relativistic quantum mechanics and field theory. Connell [49] further developed the quasi-potential approximation of Todorov by introducing series of corrections, a procedure that also is claimed to be formally equivalent to the original BS equation.

Caswell and Lepage [42] applied the quasi-potential method to evaluate the hyperfine structure of muonium and positronium to the order  $\alpha^6 m_e c^2$  by combining analytical and perturbative approaches. Grotch and Yennie [32, 83] have applied the method to evaluate higher-order nuclear corrections to the energy levels of the hydrogen atom, and Adkins and Fell [3, 4] have applied it to positronium.

A vast literature on the Bethe–Salpeter equation, its fundamental problems and its applications, has been gathered over the years since the original equation appeared. Most applications are performed in the strong-coupling case (QCD), where the fundamental problems of the equation are more pronounced. The interested reader is here referred to some reviews of the field, where numerous references to original works can be found [82, 172, 173, 178, 217].

## 1.4 Helium Atom. Analytical Approach

An approach to solve the BS equation, known as the *external-potential approach*, was first developed by Sucher [235, 237] in order to evaluate the lowest-order QED contributions to the ground-state energy of the helium atom, and equivalent results were at the same time also derived by Araki [5]. The electrons are here assumed to move in the field of the (infinitely heavy) atomic nucleus. The relative time of the two electrons is eliminated by integrating over the corresponding energy of the Fourier transform, which leads to a Schrödinger-like equation, as in the quasi-potential-method. The solution of this equation is expanded in terms of a Brillouin–Wigner perturbation series. This work has been further developed and applied by Douglas and Kroll [60] and by Zhang and Drake [259, 263] by considering higher-order terms in the  $\alpha$  and  $Z\alpha$  expansions. This approach, which is reviewed in Chap. 11, can be used for light systems, such as light heliumlike ions, where the power expansions are sufficiently convergent. The QED effects are here evaluated by means of highly correlated wave functions of Hylleraas type, which implies that QED and electron-correlation effects are highly mixed. A related technique, referred to as the *effective Hamiltonian approach*, has been developed and applied to heliumlike systems by Pachucki and Sapirstein [179, 180, 181].

A problem that has been controversial for quite some time is the fine structure of the lowest  $P$  state of the neutral helium atom. The very accurate analytical results of Drake et al. and by Pachucki et al. give results close to the experimental results obtained by Gabrielse and others [258], but there have for quite some time been significant deviations—well outside the estimated limits of error. More recently, Pachucki and Yerokhin have by means of improved calculations shown that the controversy has been resolved [182, 183, 184, 185].

## 1.5 Field-Theoretical Approach to Many-Body Perturbation Theory

The methods mentioned for numerical QED calculations can for practical reasons be used only to evaluate one- and two-photon exchange in a complete way. This implies that the electron correlation can only be treated to lowest order. This might be sufficiently accurate for highly charged systems, where the QED effects dominate over the electron correlation, but is usually quite insufficient for lighter systems, where the situation is different.

In the numerical procedures for standard (relativistic) MBPT the electron correlation can be evaluated effectively to essentially all orders by techniques of coupled-cluster type. QED effects can here be included only as first-order energy corrections, a technique applied particularly by the Notre-Dame group [195]. To treat electron correlation, relativity and QED in a unified manner would require a field-theoretical many-body approach from the start.

The methods developed for QED calculations are all based upon field-theory. Of these methods, the covariant-evolution-operator method, has the advantage that it has a structure that is quite akin to that of standard MBPT. Contrary to the other methods it can be used to evaluate perturbations to the **wave function**—not only to the energy. Then it can serve as a basis for a unified field-theoretical many-body approach, where the dominating QED effects can be evaluated order for order together with the Coulomb interaction. This leads to a procedure for the combination of QED and electron correlation. This is the approach that will be described in the present book and represents the direction of research presently being pursued by the Gothenburg atomic theory group.

(It should be mentioned that a related idea was proposed by Leonard Rosenberg more than 20 years ago [203], namely of including Coulomb interactions in the QED Hamiltonian.)

The covariant evolution operator can be singular, as the standard evolution operator of non-relativistic quantum mechanics, but the singularities can be eliminated in a similar way as the corresponding singularities of the Green's function. The regular part of the covariant evolution operator is the *Green's operator*, which can be regarded as an extension of the Green's-function concept and shown to serve as a link between field theory and standard many-body perturbation theory. The perturbation used in this procedure represents the interaction between the electromagnetic field and the individual electrons. This implies that the equations operate in an extended *photonic Fock space* with variable number of photons.

The strategy is here to combine a single retarded photon with numerous Coulomb interactions. As long as no virtual pairs are involved, this can be performed iteratively. In this way the dominating QED effects can—for the first time—be treated in the same manner as standard many-body perturbations. For practical reasons only a single retarded photon can be included in each iteration at present time, but due to the iterations this corresponds to the most important (“reducible”) effects also in higher orders [132]. When extended to (“irreducible”) interactions of multi-photon type, this would lead for two-particle systems to the *Bethe–Salpeter equation*, and in the multi-reference case to an extension of this equation, referred to as the *Bethe–Salpeter–Bloch equation* [131].

In the first edition we dealt with the combination of electron correlation and **non-radiative** QED effects, mainly retardation and virtual electron-positron pairs, based upon the PhD thesis of Daniel Hedendahl in the Gothenburg group. In the meantime, similar calculations have been performed for **radiative** effects (electron self-energy and vertex correction) by Johan Holmberg in his thesis of the same group, and his main results are included in the present second edition.

In combining QED with electron correlation it has been found advantageous to work in the *Coulomb gauge*. In the Feynman gauge there are enormous cancellations between various QED effects, which is not the case in the Coulomb gauge, making the calculations in the latter gauge much more stable. This has the consequence, as is demonstrated in Chap. 9, that it is practically impossible to carry calculations involving radiative effects beyond second order using the Feynman gauge. With the Coulomb gauge, on the other hand, reliable results could here be obtained.

Furthermore, in this gauge one can, for instance, include the instantaneous Breit interaction, which in other gauges, like the Feynman gauge, would correspond to multiple transverse photons. Although this gauge is *non-covariant* in contrast to, for instance, the simpler Feynman gauge, it can be argued that the deviation from a fully covariant treatment will have negligible effect in practical applications when handled properly. This makes it possible to mix a larger number of Coulomb interactions with the retarded-photon interactions, which is expected to lead to the same ultimate result as a fully covariant approach but with faster convergence rate due to the dominating role of the Coulomb interaction.

The procedure can also be extended to systems with more than two electrons, and due to the complete compatibility between the standard and the extended procedures, the QED effects need only be included where they are expected to be most significant.

In principle, also the procedure outlined here leads to *individual times* for the particles involved, consistent with the full Bethe–Salpeter equation but not with the standard quantum-mechanical picture. We shall mainly work in the *equal-time approximation* here, and we shall not analyze effects beyond this approximation in any detail. It is expected that—if existing—any such effect would be extremely small for electronic systems.

## 1.6 Dynamical Processes

The first edition of the book dealt only with *static processes*, i.e., structure calculations. In recent time experiments on *dynamical processes* have become increasingly important in various parts of physics and chemistry. The standard theoretical procedure for dealing with such processes is the S-matrix formalism. In evaluating QED effects for such systems, where bound states are involved, intermediate model-space states will appear, which will lead to singularities that cannot be handled with the S-matrix formalism. However, these singularities are of the same kind as those appearing in structure calculations, which has the consequence that the methods developed for QED calculations for structure calculations, such as the covariant evolution operator method, work perfectly well also for dynamical processes. This is demonstrated in Part IV of the second edition for the case of transition rates and radiative recombination. Experiments are presently being performed to detect QED effects in such processes. These effects are presently on the verge of being detectable experimentally.



**Part I**  
**Basics. Standard Many-body**  
**Perturbation Theory**

# Chapter 2

## Time-Independent Formalism

In this first part of the book we shall review some basics of quantum mechanics and the many-body theory for bound electronic systems that will form the foundations for the following treatment. This material can also be found in several standard text books. The time-independent formalism is summarized in the present chapter<sup>1</sup> and the time-dependent formalism in the following one.

### 2.1 First Quantization

First quantization is the term for the elementary treatment of quantized systems, where the particles of the system are treated quantum-mechanically, for instance, in terms of Schrödinger wave functions, while the surrounding fields are treated classically.

#### 2.1.1 *De Broglie's Relations*

As an introduction to the quantum mechanics we shall derive the Schrödinger equation from the classical relations of De Broglie.

According to Planck-Einstein's quantum theory the electromagnetic radiation is associated with particle-like *photons* with the energy ( $E$ ) and momentum ( $p$ ) given by the relations

---

<sup>1</sup>This chapter is essentially a short summary of the second part of the book *Atomic Many-Body Theory* by Lindgren and Morrison [124], and the reader who is not well familiar with the subject is recommended to consult that book.

$$\begin{cases} E = h\nu = \omega\hbar \\ p = h/\lambda = \hbar k, \end{cases} \quad (2.1)$$

where  $\hbar = h/2\pi$ ,  $h$  being Planck's constant (see further Appendix K),  $\nu$  the cyclic frequency of the radiation (cycles/second) and  $\omega = 2\pi\nu$  the angular frequency (radians/second).  $\lambda = c/\nu$  ( $c$  being the velocity of light in vacuum) is the wavelength of the radiation and  $k = 2\pi/\lambda$  the wave number.

De Broglie assumed that the relations (2.1) for photons would hold also for material particles, like electrons. Non-relativistically, we have for a free electron in one dimension

$$E = \frac{p^2}{2m_e} \quad \text{or} \quad \hbar\omega = \frac{\hbar^2 k^2}{2m_e}, \quad (2.2)$$

where  $m_e$  is the mass of the electron.

De Broglie assumed that a particle could be represented by a *wave packet*

$$\chi(t, x) = \int dk a(k) e^{i(kx - \omega t)}. \quad (2.3)$$

The relation (2.2) then leads to the one-dimensional wave equation for a free electron

$$i\hbar \frac{\partial \chi(t, x)}{\partial t} = -\frac{\hbar^2}{2m_e} \frac{\partial^2 \chi(t, x)}{\partial x^2}, \quad (2.4)$$

which is the Schrödinger equation for a free particle. This can be obtained from the first of the relations (2.2) by means of the substitutions

$$E \rightarrow i\hbar \frac{\partial}{\partial t} \quad p \rightarrow -i\hbar \frac{\partial}{\partial x}. \quad (2.5)$$

### 2.1.2 The Schrödinger Equation

We can generalize the treatment above to an electron in three dimensions in an external field,  $v_{\text{ext}}(\mathbf{x})$ , for which the energy Hamiltonian is

$$E = H = \frac{\mathbf{p}^2}{2m_e} + v_{\text{ext}}(\mathbf{x}). \quad (2.6)$$

Generalizing the substitutions above to<sup>2</sup>

$$\mathbf{p} \rightarrow \hat{\mathbf{p}} = -i\hbar\nabla \quad \text{and} \quad \mathbf{x} \rightarrow \hat{\mathbf{x}} = \mathbf{x}, \quad (2.7)$$

---

<sup>2</sup>Initially, we shall use the 'hat' symbol to indicate an *operator*, but later we shall use this symbol only when the operator character needs to be emphasized.

where  $\nabla$  is the vector gradient operator (see Appendix A.1), leads to the *Hamilton operator*

$$\hat{H} = \frac{\hat{\mathbf{p}}^2}{2m_e} + v_{\text{ext}}(\mathbf{x}) = -\frac{\hbar^2}{2m_e} \nabla^2 + v_{\text{ext}}(\mathbf{x}) \quad (2.8)$$

and to the *Schrödinger equation for a single electron*

$$\boxed{i\hbar \frac{\partial}{\partial t} \chi(t, \mathbf{x}) = \hat{H} \chi(t, \mathbf{x}) = \left( -\frac{\hbar^2}{2m_e} \nabla^2 + v_{\text{ext}}(x) \right) \chi(t, \mathbf{x}).} \quad (2.9)$$

For an  $N$ -electron system the Schrödinger equation becomes correspondingly<sup>3</sup>

$$i\hbar \frac{\partial}{\partial t} \chi(t; \mathbf{x}_1, \mathbf{x}_2, \dots, \mathbf{x}_N) = \hat{H} \chi(t; \mathbf{x}_1, \mathbf{x}_2, \dots, \mathbf{x}_N), \quad (2.10)$$

where we assume the Hamiltonian to be of the form  $\hat{H} = \hat{H}_1 + \hat{H}_2$  (see Appendix (B.19))<sup>4</sup>

$$\begin{aligned} \hat{H}_1 &= \sum_{n=1}^N \left( -\frac{\hbar^2}{2m_e} \nabla_n^2 + v_{\text{ext}}(\mathbf{x}_n) \right) =: \sum_{n=1}^N \hat{h}_1(n) \\ \hat{H}_2 &= \sum_{m < n}^N \frac{e^2}{4\pi\epsilon_0 r_{mn}} =: \sum_{m < n}^N \hat{h}_2(m, n). \end{aligned} \quad (2.11)$$

Here,  $r_{mn}$  is the interelectronic distance,  $r_{mn} = |\mathbf{x}_m - \mathbf{x}_n|$  and  $v_{\text{ext}}$  represents the external (essentially nuclear) energy potential.

Generally, the quantum-mechanical operators  $\hat{A}$ ,  $\hat{B}$  that represent the corresponding classical quantities  $A$ ,  $B$  in the Hamilton formulation (see Appendix E) should satisfy the *quantization condition*

$$[\hat{A}, \hat{B}] = \hat{A}\hat{B} - \hat{B}\hat{A} = i\hbar\{A, B\}, \quad (2.12)$$

where the square bracket (with a comma) represents the *commutator* and the curly bracket the *Poisson bracket* (E.10). For *conjugate momenta*, like the coordinate vector  $\mathbf{x}$  and the momentum vector  $\mathbf{p}$ , the Poisson bracket equals unity, and, the quantization conditions for the corresponding operators become

$$[\hat{x}, \hat{p}_x] = [\hat{y}, \hat{p}_y] = [\hat{z}, \hat{p}_z] = i\hbar, \quad (2.13)$$

which is consistent with the substitutions (2.7).

<sup>3</sup>Note that according to the quantum-mechanical picture the wave function has a *single time* also for a many-electron system. This question will be discussed further in later chapters.

<sup>4</sup>The symbol “=:” indicates that this is a definition.

We shall be mainly concerned with *stationary, bound states of electronic systems*, for which the wave function can be separated into a time function and a space function

$$\chi(t; \mathbf{x}_1, \dots, \mathbf{x}_N) = F(t) \Psi(\mathbf{x}_1, \mathbf{x}_2, \dots, \mathbf{x}_N).$$

As shown in standard text books, this leads to a separation into two equations, one for the time part and one for the space part. The time equation becomes

$$i\hbar \frac{\partial}{\partial t} F(t) = E F(t)$$

with the solution

$$F(t) \propto e^{-iEt/\hbar}$$

and the space part is the standard *time-independent Schrödinger equation*

$$\boxed{\hat{H}\Psi(\mathbf{x}_1, \dots, \mathbf{x}_N) = E(\Psi(\mathbf{x}_1, \dots, \mathbf{x}_N))}. \quad (2.14)$$

Thus, for *stationary states* the time-dependent wave function is of the form

$$\chi(t; \mathbf{x}_1, \dots, \mathbf{x}_N) = e^{-iEt/\hbar} \Psi(\mathbf{x}_1, \dots, \mathbf{x}_N). \quad (2.15)$$

The separation constant  $E$  is interpreted as the energy of the state.

## 2.2 Second Quantization

### 2.2.1 Schrödinger Equation in Second Quantization\*

In the following, we shall consistently base our treatment upon *second quantization*, which implies that also the particles and fields are quantized and expressed in terms of (creation- and absorption) field operators (see Appendices B and C). Here, we shall first derive the second-quantized form of the time-dependent Schrödinger equation (SE) (2.9), which reads

$$\boxed{i\hbar \frac{\partial}{\partial t} |\chi(t)\rangle = H |\chi(t)\rangle}. \quad (2.16)$$

With the partitioning (2.11), the operator becomes in second quantization (B.12)

$$\hat{H} = c_i^\dagger \langle i|h_1|j\rangle c_j + \frac{1}{2} c_i^\dagger c_j^\dagger \langle ij|h_2|kl\rangle c_l c_k \quad (2.17)$$

and the state is expressed as a vector (C.4). Equation (2.16) is by no means obvious, and we shall here indicate the proof. (The proof follows largely that given by Fetter and Walecka [67, Chap. 1].)

For the sake of concretization we consider a two-electron system. With the coordinate representation (C.19) of the state vector

$$\chi(x_1, x_2) = \langle \mathbf{x}_1, \mathbf{x}_2 | \chi(t) \rangle \quad (2.18)$$

the SE (2.16) becomes

$$i\hbar \frac{\partial}{\partial t} \langle \mathbf{x}_1, \mathbf{x}_2 | \chi(t) \rangle = \langle \mathbf{x}_1, \mathbf{x}_2 | H | \chi(t) \rangle. \quad (2.19)$$

We consider first the effect of the one-body part of the Hamiltonian (2.17) operating on the wave function (2.18), and we shall show that this is equivalent to operating with the second-quantized form of the operator (B.19)

$$\hat{H} = c_i^\dagger \langle i | h_1 | j \rangle c_j \quad (2.20)$$

on the state vector  $|\chi(t)\rangle$ .

We start by expanding the state vector in terms of straight products of single-electron state vectors ( $t_1 = t_2 = t$ )

$$|\chi(t)\rangle = a_{kl}(t) |k\rangle |l\rangle \quad (2.21)$$

( $a_{kl} = -a_{lk}$ ). The coordinate representation of this relation is

$$\chi(x_1, x_2) = \langle \mathbf{x}_1, \mathbf{x}_2 | \chi(t) \rangle = a_{kl}(t) \langle \mathbf{x}_1 | k \rangle \langle \mathbf{x}_2 | l \rangle. \quad (2.22)$$

We now operate with the single-particle operator (2.20) on the state vector expansion (2.21)

$$\hat{H}_1 |\chi(t)\rangle = c_i^\dagger \langle i | h_1 | j \rangle c_j a_{kl}(t) |k\rangle |l\rangle. \quad (2.23)$$

For  $j = k$  the electron in position 1 is annihilated in the state  $k$  and replaced by an electron in the state  $i$ , yielding

$$\langle i | h_1 | k \rangle a_{kl}(t) |i\rangle |l\rangle.$$

The coordinate representation of this relation becomes

$$\langle \mathbf{x}_1 | i \rangle \langle i | h_1 | k \rangle a_{kl}(t) \langle \mathbf{x}_2 | l \rangle = \langle \mathbf{x}_1 | h_1 | k \rangle a_{kl}(t) \langle \mathbf{x}_2 | l \rangle,$$

using the resolution of the identity (C.12). The right-hand side of (2.23) can also be expressed

$$h_1(\mathbf{x}_1) \phi_k(\mathbf{x}_1) \phi_l(\mathbf{x}_2) a_{kl}(t) = h_1(\mathbf{x}_1) \chi(x_1, x_2).$$

Together with the case  $j = l$  this leads to

$$\langle \mathbf{x}_1, \mathbf{x}_2 | H_1 | \chi(t) \rangle = (h_1(\mathbf{x}_1) + h_1(\mathbf{x}_2)) \chi(x_1, x_2) = H_1 \chi(x_1, x_2).$$

Thus, we have shown the important relation

$$\langle \mathbf{x}_1, \mathbf{x}_2 | H_1 | \chi(t) \rangle = H_1 \chi(x_1, x_2). \quad (2.24)$$

A similar relation can be derived for the two-body part of the Hamiltonian, which implies that

$$\langle \mathbf{x}_1, \mathbf{x}_2 | H | \chi(t) \rangle = H \chi(x_1, x_2) \quad (2.25)$$

and from the relation (2.19)

$$i\hbar \frac{\partial}{\partial t} \langle \mathbf{x}_1, \mathbf{x}_2 | \chi(t) \rangle = \langle \mathbf{x}_1, \mathbf{x}_2 | H | \chi(t) \rangle. \quad (2.26)$$

This is the coordinate representation of the Schrödinger equation (2.16), which is thus verified. It should be observed that (2.16) does not contain any space coordinates. The treatment is here performed for the two-electron case, but it can easily be extended to the general case.

## 2.2.2 Particle-Hole Formalism. Normal Order and Contraction

In the *particle-hole formalism* we separate the single-particle states into *particle and hole states*, a division that is to some extent arbitrary. Normally, core states (closed-shell states) are treated as hole states and virtual and valence states as particle states, but sometimes it might be advantageous to treat some closed-shell states as valence states or some valence states as hole states. (All states of one (sub) shell must be treated either as particles or holes.)

If time increases from right to left, the creation/annihilation operators are said to be *time ordered*. Time ordering can be achieved by using the *Wick time-ordering operator*, which for fermions reads

$$T[A(t_1)B(t_2)] = \begin{cases} A(t_1)B(t_2) & (t_1 > t_2) \\ -B(t_2)A(t_1) & (t_1 < t_2) \end{cases}. \quad (2.27)$$

The case  $t_1 = t_2$  will be discussed later.

The creation/annihilation operators are said to be in **normal order**, if the particle-creation and hole-annihilation operators appear to the left of the particle-annihilation and hole-creation operators

$$c_p^\dagger c_p c_h c_h^\dagger, \quad (2.28)$$

where  $p, h$  stand for particle/hole states.

- A **contraction** of two operators is defined as the **difference between the time-ordered and the normal-ordered products**,

$$\boxed{xy} = T[xy] - N[xy]. \quad (2.29)$$

In the following we shall use **curly brackets to denote the normal product** [118]

$$N[xy] \equiv \{xy\}. \quad (2.30)$$

From these definitions it follows that the non-vanishing contractions of the *electron-field operators* (B.28) are

$$\begin{aligned} \overbrace{\hat{\psi}_+(x_1)\hat{\psi}_+^\dagger(x_2)} &= -\overbrace{\hat{\psi}_+^\dagger(x_2)\hat{\psi}_+(x_1)} = \begin{cases} \phi_p(\mathbf{x}_1)\phi_p^\dagger(\mathbf{x}_2) e^{-i\varepsilon_p(t_1-t_2)/\hbar} & t_1 > t_2 \\ 0 & t_1 < t_2 \end{cases} \\ \overbrace{\hat{\psi}_-(x_1)\hat{\psi}_-^\dagger(x_2)} &= -\overbrace{\hat{\psi}_-^\dagger(x_2)\hat{\psi}_-(x_1)} = \begin{cases} 0 & t_1 > t_2 \\ -\phi_h(\mathbf{x}_1)\phi_h^\dagger(\mathbf{x}_2) e^{-i\varepsilon_h(t_1-t_2)/\hbar} & t_1 < t_2 \end{cases}. \end{aligned} \quad (2.31)$$

Here,  $\hat{\psi}_\pm$  represents the positive-/negative-energy part of the spectrum, respectively, and  $\phi_p$  and  $\phi_h$  denote particle (positive-energy) and hole (negative-energy) states, respectively.

### 2.2.3 Wick's Theorem

The handling of operators in second quantization is greatly simplified by *Wick's theorem* [250] (for an introduction, see, for instance, Fetter and Walecka [67, Sect. 8] or Lindgren and Morrison [124, Chap. 11]), which states that a product of creation and annihilation operators  $\hat{A}$  can be written as the normal product plus all single, double ... contractions with the uncontracted operators in normal form, or symbolically

$$\hat{A} = \{\hat{A}\} + \overbrace{\{\hat{A}\}}. \quad (2.32)$$

A particularly useful form of Wick's theorem is the following. *If  $\hat{A}$  and  $\hat{B}$  are operators in normal form, then the product is equal to the normal product plus all normal-ordered contractions between  $\hat{A}$  and  $\hat{B}$* , or formally

$$\boxed{\hat{A}\hat{B}} = \{\hat{A}\hat{B}\} + \overbrace{\{\hat{A}\hat{B}\}}. \quad (2.33)$$

With this formulation there are no further contractions within the operators to be multiplied. This forms the basic rule for the graphical representation of the operators and operator relations to be discussed below.



## 2.3 Time-Independent Many-Body Perturbation Theory

### 2.3.1 Bloch Equation

Here, we shall summarize the most important concepts of standard time-independent many-body perturbation theory (MBPT) as a background for the further treatment. (For more details the reader is referred to designated books, like Lindgren-Morrison, *Atomic Many-Body Theory* [124].)

We are considering a number of stationary electronic states,  $|\Psi^\alpha\rangle$  ( $\alpha = 1 \cdots d$ ), termed *target states*, that satisfy the Schrödinger equation

$$H|\Psi^\alpha\rangle = E^\alpha|\Psi^\alpha\rangle \quad (\alpha = 1 \cdots d). \quad (2.34)$$

For each target state there exists an “approximate” or **model state**,  $|\Psi_0^\alpha\rangle$  ( $\alpha = 1 \cdots d$ ), which is more easily accessible and which forms the starting point for the perturbative treatment. We assume that the model states are linearly independent and that they span a **model space**. The *projection operator* for the model space is denoted  $P$  and that for the complementary or *orthogonal space* by  $Q$ , which together form the *identity operator*

$$P + Q = I. \quad (2.35)$$

A **wave operator** is introduced—also known as the Møller operator [162]—which transforms the model states back to the exact states,

$$|\Psi^\alpha\rangle = \Omega|\Psi_0^\alpha\rangle \quad (\alpha = 1 \cdots d), \quad (2.36)$$

and this operator is the same for all states under consideration.

We define an **effective Hamiltonian** with the property that *operating on a model function it generates the corresponding exact energy*

$$H_{\text{eff}}|\Psi_0^\alpha\rangle = E^\alpha|\Psi_0^\alpha\rangle \quad (\alpha = 1 \cdots d) \quad (2.37)$$

with the eigenvectors representing the model states. Operating on this equation with  $\Omega$  from the left, using the definition (2.36), yields

$$\Omega H_{\text{eff}}|\Psi_0^\alpha\rangle = E^\alpha|\Psi^\alpha\rangle, \quad (2.38)$$

which we compare with the Schrödinger equation (2.34)

$$H\Omega|\Psi_0^\alpha\rangle = E^\alpha|\Psi^\alpha\rangle. \quad (2.39)$$

Since this relation holds for each state of the model space, we have the important operator relation

$$\boxed{\Omega H_{\text{eff}} P = H \Omega P}, \quad (2.40)$$

which is known as the **generalized Bloch equation**.

The form above of the Bloch equation is valid independently on the choice of normalization. In the following, we shall mainly work with the **intermediate normalization** (IN), which implies

$$\langle \Psi_0^\alpha | \Psi^\alpha \rangle = 1, \quad (2.41a)$$

$$|\Psi_0^\alpha\rangle = P |\Psi^\alpha\rangle \quad (\alpha = 1 \cdots d). \quad (2.41b)$$

Then we have after projecting the Schrödinger equation onto the model space

$$P H \Omega |\Psi_0^\alpha\rangle = E^\alpha |\Psi_0^\alpha\rangle, \quad (2.42)$$

and we find that the effective Hamiltonian (2.37) becomes in IN

$$\boxed{H_{\text{eff}} = P H \Omega P}. \quad (2.43)$$

Normally, the multi-dimensional or multi-reference model space is applied in connection with *valence universality*, implying that the same operators are used for different stages of ionization (see further Sect. 2.5).

### 2.3.2 Partitioning of the Hamiltonian

For electrons moving in an external (nuclear) potential,  $v_{\text{ext}}$ , the single-electron (Schrödinger) Hamiltonian (2.8) is

$$h_S = -\frac{\hbar^2}{2m_e} \nabla^2 + v_{\text{ext}}. \quad (2.44)$$

The corresponding Schrödinger equation

$$h_S \phi_i(\mathbf{x}) = \varepsilon_i \phi_i(\mathbf{x}) \quad (2.45)$$

generates a complete spectrum of functions, which can form the basis for numerical calculations. This is known to as the *Furry picture*. These single-electron functions are normally referred to as (single-electron) *orbitals*—or *spin-orbitals*, if a spin eigenfunction is adhered. Degenerate orbitals (with the same eigenvalue) form an *electron shell*.

The Hamiltonian for a many-electron system (2.11) is

$$H = \sum_n^N \left( -\frac{\hbar^2}{2m_e} \nabla^2 + v_{\text{ext}} \right)_n + \sum_{n < m}^N \frac{e^2}{4\pi\epsilon_0 r_{nm}}, \quad (2.46)$$

where the last term represents the interelectronic interaction. For the perturbation treatment we separate the many-electron Hamiltonian into

$$H = H_0 + V, \quad (2.47)$$

where  $H_0$  a *model Hamiltonian* that is a sum of single-electron Hamiltonians

$$H_0 = \sum_n^N \left( -\frac{\hbar^2}{2m_e} \nabla^2 + v_{\text{ext}} + u \right)_n =: \sum_n^N h_0(n), \quad (2.48)$$

and  $V$  is a *perturbation*

$$V = -\sum_n^N u_n + \sum_{n < m}^N \frac{e^2}{4\pi\epsilon_0 r_{nm}}. \quad (2.49)$$

The potential  $u$  is optional and used primarily to improve the convergence properties of the perturbation expansion.

The *antisymmetrized*  $N$ -electron eigenfunctions of  $H_0$  can be expressed as determinantal products of single-electron orbitals (see Appendix B)

$$\begin{aligned} H_0 \Phi_A(\mathbf{x}_1, \mathbf{x}_2 \cdots \mathbf{x}_N) &= E_0^A \Phi_A(\mathbf{x}_1, \mathbf{x}_2 \cdots \mathbf{x}_N) \\ \Phi_A(\mathbf{x}_1, \mathbf{x}_2 \cdots \mathbf{x}_N) &= 1/\sqrt{N!} \mathcal{A}\{\phi_1(\mathbf{x}_1)\phi_2(\mathbf{x}_2) \cdots \phi_N(\mathbf{x}_N)\}, \end{aligned} \quad (2.50)$$

where  $\mathcal{A}$  is an antisymmetrizing operator. The determinants are referred to as *Slater determinants* and constitute our basis functions. The eigenvalues are given by

$$E_0 = \sum_{n=1}^N \varepsilon_n, \quad (2.51)$$

summed over the spin-orbitals of the determinant.

Degenerate determinants form a *configuration*. The model space is supposed to be formed by one or several configurations that can have different energies. We distinguish between three kinds of orbitals

- *core orbitals*, present in all determinants of the model space
- *valence orbitals*, present in some determinants of the model space
- *virtual orbitals*, not present in any determinants of the model space.

**The model space is said to be complete, if it contains all configurations that can be formed by distributing the valence electrons among the valence orbitals in all possible ways.** In the following we shall normally assume this to be the case.

With the partitioning (2.47), the Bloch equation above can be expressed

$$\boxed{(\Omega H_{\text{eff}} - H_0 \Omega) P = V \Omega P.} \quad (2.52)$$

With  $H_0$  of the form (2.48) it commutes with the projection operator  $P$ . Then we find that

$$H_{\text{eff}} = P H_0 P + P V \Omega P, \quad (2.53)$$

and we shall refer to the second term as the **effective interaction**

$$\boxed{W = P V \Omega P.} \quad (2.54)$$

- The partitioning leads to the commonly used form of the **generalized Bloch equation** [113, 117, 124]

$$\boxed{[\Omega, H_0] P = Q(V \Omega - \Omega W) P,} \quad (2.55)$$

which is frequently used as the basis for many-body perturbation theory (MBPT) in atomic or molecular applications. The last term appears only for open-shell systems with unfilled valence shell(s) and is graphically represented by so-called **folded** or **backwards** diagrams, first introduced by Brandow in nuclear physics [34] and by Sandars [214] (see further below).

If the model space is completely degenerate with a single energy  $E_0$ , the general Bloch equation reduces to its original form, derived in the late 1950s by Claude Bloch [24, 25],

$$(E_0 - H_0) \Omega P = V \Omega P - \Omega W. \quad (2.56)$$

This equation can be used to generate the standard *Rayleigh-Schrödinger* perturbation expansion, found in many text books.

The generalized Bloch equation (2.55) is valid for a general model space, which can contain different zeroth-order energy levels. Using such an **extended model space**, represents usually a convenient way of treating very closely spaced or **quasi-degenerate** unperturbed energy levels, a phenomenon that otherwise can lead to serious convergence problems. This can be illustrated by the relativistic calculation of the fine structure of heliumlike ions, where a one-dimensional model space leads to convergence problems for light elements, a problem that can normally be remedied in a straightforward way by means of the extended model space [146, 195]. But the extended model space can also lead to problems, due to so-called *intruder states*, as will be further discussed below.

With an extended model space we can separate the projection operator into the corresponding energy components<sup>5</sup>

$$P = \sum_{\mathcal{E}} P_{\mathcal{E}}; \quad H_0 P_{\mathcal{E}} = \mathcal{E} P_{\mathcal{E}}. \quad (2.57)$$

Operating with the general Bloch equation (2.55) on a particular component, then yields

$$(\mathcal{E} - H_0)\Omega P_{\mathcal{E}} = Q(V\Omega - \Omega W)P_{\mathcal{E}}, \quad (2.58)$$

where  $Q$  is still given by (2.35),

$$Q = 1 - P. \quad (2.59)$$

Expanding the wave operator order by order

$$\Omega = 1 + \Omega^{(1)} + \Omega^{(2)} + \dots \quad (2.60)$$

leads to the recursive formula

$$(\mathcal{E} - H_0)\Omega^{(n)}P_{\mathcal{E}} = Q(V\Omega^{(n-1)} - (\Omega W)^{(n)})P_{\mathcal{E}} \quad (2.61)$$

or

$$\Omega^{(n)}P_{\mathcal{E}} = \Gamma_Q(\mathcal{E})(V\Omega^{(n-1)} - (\Omega W)^{(n)})P_{\mathcal{E}}, \quad (2.62)$$

where

$$W^{(k)} = P V \Omega^{(k-1)} P. \quad (2.63)$$

Here,

$$\Gamma(\mathcal{E}) = \frac{1}{\mathcal{E} - H_0} \quad (2.64)$$

and

$$\Gamma_Q(\mathcal{E}) = Q\Gamma(\mathcal{E}) \quad (2.65)$$

are known as the **resolvent** and the **reduced resolvent**, respectively [138].

The recursive formula (2.62) can generate a *generalized form of the Rayleigh-Schrödinger perturbation expansion* (see [124, Chap.9]), valid also for a *quasi-degenerate model space*. We see from the form of the resolvent that in each new order of the perturbation expansion there is a denominator equal to the energy difference between the initial and final states. This leads to the **Goldstone rules** in the evaluation of the time-ordered diagrams to be consider in the following section.

---

<sup>5</sup>In the case of an extended model space, we shall normally use the symbol  $\mathcal{E}$  for the different energies of the model space.

Even if the perturbation is energy independent, we see that the wave operator and effective interaction will still generally be energy dependent, due to the energy dependence of the resolvent. In first order we have

$$\Omega^{(1)}P_{\mathcal{E}} = \Gamma_Q(\mathcal{E})VP_{\mathcal{E}} \quad (2.66)$$

and in second order

$$\Omega^{(2)}(\mathcal{E})P_{\mathcal{E}} = \Gamma_Q(\mathcal{E})\left(V\Omega^{(1)}(\mathcal{E}) - \Omega^{(1)}(\mathcal{E}')P_{\mathcal{E}'}W^{(1)}\right)P_{\mathcal{E}}, \quad (2.67)$$

where  $W^{(1)} = PVP$ . Note that the wave operator in the last term operates on the projection operator  $P_{\mathcal{E}'}$  and therefore depends on the corresponding energy  $\mathcal{E}'$ . We now have

$$\begin{aligned} \frac{\delta\Omega^{(1)}(\mathcal{E})}{\delta\mathcal{E}} &= \frac{\delta\Gamma_Q(\mathcal{E})}{\delta\mathcal{E}}V = \frac{\Gamma_Q(\mathcal{E}') - \Gamma_Q(\mathcal{E})}{\mathcal{E}' - \mathcal{E}}V = -\Gamma_Q(\mathcal{E})\Gamma_Q(\mathcal{E}')V \\ &= -\Gamma_Q(\mathcal{E})\Omega^{(1)}(\mathcal{E}'), \end{aligned} \quad (2.68)$$

and we note that the last folded term in (2.67) has a *double denominator*. We can express the second-order Bloch equation as

$$\boxed{\Omega^{(2)}(\mathcal{E})P_{\mathcal{E}} = \Gamma_Q(\mathcal{E})VP_{\mathcal{E}}\Omega^{(1)}(\mathcal{E})P_{\mathcal{E}} + \frac{\delta\Omega^{(1)}(\mathcal{E})}{\delta\mathcal{E}}W^{(1)}(\mathcal{E})P_{\mathcal{E}}.} \quad (2.69)$$

In the limit of complete degeneracy space the difference ratio goes over into a partial derivative. We shall show in later chapters that the second-order expression above holds also when the perturbation is energy dependent (6.114).

## 2.4 Graphical Representation

In this section we shall briefly describe a way of representing the perturbation expansion graphically. (For further details, the reader is referred to the book by Lindgren and Morrison [124].)

### 2.4.1 Goldstone Diagrams

The Rayleigh-Schrödinger perturbation expansion can be conveniently represented in terms of diagrams by means of second quantization (see above and Appendix B).

The perturbation (2.49) becomes in second quantization

$$\hat{V} = c_i^\dagger c_j \langle i|f|j \rangle + \frac{1}{2} c_i^\dagger c_j^\dagger c_l c_k \langle ij|g|kl \rangle, \quad (2.70)$$

where  $f$  is the negative potential  $f = -u$  and  $g$  is the Coulomb interaction between the electrons. When some of the states are hole states, the expression (2.70) is not in normal order. By normal ordering the expression, zero-, one- and two-body operators will appear [124, Eq. 11.39]

$$V = V_0 + V_1 + V_2, \quad (2.71)$$

where

$$\begin{aligned} V_0 &= \sum_i^{\text{hole}} \langle i|f|i \rangle + \frac{1}{2} \sum_{ij}^{\text{hole}} [\langle ij|g|kl \rangle - \langle ji|g|kl \rangle] \\ V_1 &= \{c_i^\dagger c_j\} \langle i|V_{\text{eff}}|j \rangle \\ V_2 &= \frac{1}{2} \{c_i^\dagger c_j^\dagger c_l c_k\} \langle ij|g|kl \rangle. \end{aligned} \quad (2.72)$$

In the one- and two-body parts the summation is performed over *all* orbitals. Here,

$$\langle i|V_{\text{eff}}|j \rangle = \langle i|f|j \rangle + \sum_k^{\text{hole}} [\langle ik|g|jk \rangle - \langle ki|g|jk \rangle] \quad (2.73)$$

is known as the *effective potential interaction* and can be represented graphically as shown in Fig. 2.3. The summation term represents the *Hartree-Fock potential*

$$\langle i|v_{\text{HF}}|j \rangle = \sum_k^{\text{hole}} [\langle ik|g|jk \rangle - \langle ki|g|jk \rangle], \quad (2.74)$$

where the first term is a “*direct*” integral and the second term an “*exchange*” integral. In the *Hartree-Fock model* we have  $u = v_{\text{HF}}$ , and the *effective potential vanishes* [124].

We can now represent the perturbation (2.72) by the **normal-ordered diagrams** in Fig. 2.1. The zero- and one-body parts are shown in more detail in Figs. 2.2 and 2.3. In our diagrams the dotted line with the cross represents the potential interaction,  $f = -u$ , and the dotted line between the electrons the Coulomb interaction,  $g = e^2/4\pi\epsilon_0 r_{12}$ . We use here a simplified version of Goldstone diagrams. Each free vertical line at the top (bottom) represents an electron creation (absorption) operator but normally we do not distinguish between the different kinds of orbitals (core, valence and virtual) as done traditionally. There is a summation of internal lines over all orbitals of the same category. We use generally **heavy lines** to indicate

$$V = V_0 + \begin{array}{c} j \\ \uparrow \\ \text{---} \text{---} \otimes \\ \uparrow \\ i \end{array} + \begin{array}{c} i \\ \uparrow \\ \text{---} \text{---} \\ \uparrow \\ k \end{array} \quad \begin{array}{c} \uparrow \\ j \\ \uparrow \\ l \end{array}$$

**Fig. 2.1** Graphical representation the effective-potential interaction (2.72). The *heavy lines* represent the orbitals in the Furry picture. The *dotted line with the cross* represents the potential  $-u$  and the *dotted, horizontal lines* the Coulomb interaction. The zero-body and one-body parts of the interaction are depicted in Figs. 2.2 and 2.3, respectively

$$V_0 = \begin{array}{c} i \\ \uparrow \\ \text{---} \text{---} \otimes \\ \uparrow \\ i \end{array} + \begin{array}{c} k \\ \uparrow \\ \text{---} \text{---} \\ \uparrow \\ k \end{array} \quad \begin{array}{c} l \\ \uparrow \\ \text{---} \text{---} \\ \uparrow \\ l \end{array} + \begin{array}{c} k \\ \uparrow \\ \text{---} \text{---} \\ \uparrow \\ l \end{array}$$

**Fig. 2.2** Graphical representation of the zero-body part of the effective-potential interaction (2.72). The orbitals are summed over all core/hole states

$$\begin{array}{c} i \\ \uparrow \\ V_{\text{eff}} \\ \uparrow \\ j \end{array} \otimes = \begin{array}{c} i \\ \uparrow \\ \text{---} \text{---} \otimes \\ \uparrow \\ j \end{array} + \begin{array}{c} i \\ \uparrow \\ \text{---} \text{---} \text{---} \text{---} \\ \uparrow \\ i \end{array} + \begin{array}{c} i \\ \uparrow \\ \text{---} \text{---} \text{---} \text{---} \\ \uparrow \\ j \end{array}$$

**Fig. 2.3** Graphical representation of the effective-potential interaction (2.73). For the closed orbital lines (with no free end) there is a summation over the core/hole states. The last two diagrams represent the ‘‘Hartree-Fock’’ potential, and the entire effective-potential interaction vanishes when HF orbitals are used

that the orbitals are generated in an external (nuclear) potential, i.e., the *bound-state representation* or *Furry picture*.

By means of Wick’s theorem we can now normal order the right-hand side (r.h.s.) of the perturbation expansion of the Bloch equation (2.62), and

- **each resulting normal-ordered term will be represented by a diagram.**

The first-order wave operator (2.66)

$$\Omega^{(1)} P_{\mathcal{E}} = \Gamma_Q(\mathcal{E}) V P_{\mathcal{E}} = \Gamma_Q(\mathcal{E}) (V_1 + V_2) P_{\mathcal{E}} \tag{2.75}$$

becomes in second quantization (2.72)

$$\Omega^{(1)} P_{\mathcal{E}} = Q \left[ \{c_i^\dagger c_j\} \frac{\langle i | V_{\text{eff}} | j \rangle}{\varepsilon_j - \varepsilon_i} + \frac{1}{2} \{c_i^\dagger c_j^\dagger c_l c_k\} \frac{\langle ij | g | kl \rangle}{\varepsilon_k + \varepsilon_l - \varepsilon_i - \varepsilon_j} \right] P_{\mathcal{E}}. \tag{2.76}$$

This can be represented in the same way as the open part ( $V_1 + V_2$ ) of the perturbation (2.70) (Fig. 2.1), if we include the extra energy denominator according to the Goldstone rules, summarized below.



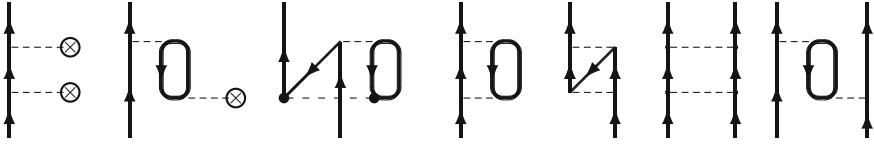


**Fig. 2.4** Examples of second-order wave-operator diagrams, excluding folded diagrams

In second order we have from (2.67), using Wick's theorem (2.33),

$$\Omega^{(2)} P_{\mathcal{E}} = \Gamma_Q(\mathcal{E}) \left( \{V \Omega_{\mathcal{E}}^{(1)}\} + \overbrace{\{V \Omega_{\mathcal{E}}^{(1)}\}} - \{\Omega_{\mathcal{E}}^{(1)} P_{\mathcal{E}'} V_{\text{eff}}\} - \overbrace{\{\Omega_{\mathcal{E}'}^{(1)} P_{\mathcal{E}'} V_{\text{eff}}\}} \right) P_{\mathcal{E}}, \quad (2.77)$$

where the hook represents a contraction. The first, uncontracted term is represented by combinations of the diagrams in Fig. 2.1, such as

$$(2.78)$$

considered as a single diagram. This diagram can be of two types.

- **If both disconnected parts are open, the diagram is referred to as linked.**<sup>6</sup> **If, on the other hand, at least one of them is closed, the diagram is referred to as unlinked.**

In the unlinked part of the second term in (2.77) the closed part represents  $V_{\text{eff}}$ , and since the order of the operators in the normal product is immaterial, this unlinked diagram appears also in the third term and is therefore eliminated. The last, contracted term survives and represents the “folded” term. Here, the wave operator depends on the energy ( $\mathcal{E}'$ ) of the intermediate state, which might differ from the energy of the initial state ( $\mathcal{E}$ ). We can then express the second-order wave operator by

$$\Omega^{(2)} P_{\mathcal{E}} = \Gamma_Q(\mathcal{E}) \left( V \Omega_{\mathcal{E}}^{(1)} - \Omega_{\mathcal{E}'}^{(1)} P_{\mathcal{E}'} V_{\text{eff}} \right)_{\text{linked}} P_{\mathcal{E}}, \quad (2.79)$$

where only linked diagrams are maintained (see Fig. 2.4).

The diagrams in Fig. 2.4 are second-order *time-ordered Goldstone diagrams*. In these diagrams, time is supposed to run from the bottom (although the formalism is here time independent). The diagrams are evaluated by the **standard Goldstone rules** with a denominator after each interaction equal to the energy difference between

<sup>6</sup>A **closed** diagram has the initial as well as the final state in the model space. Such a diagram can—in the case of complete model space—have no other free lines than valence lines. A diagram that is not **closed** is said to be **open**.

the (model-space) state at the bottom and that directly after the interaction (see Appendix I and [124, Sect. 12.4]). (In later chapters we shall mainly use *Feynman diagrams*, which contain all possible time orderings between the interactions.)

## 2.4.2 Linked-Diagram Expansion

### 2.4.2.1 Complete Model Space

Written more explicitly, the second-order wave operator (2.79) becomes

$$\Omega^{(2)} P_{\mathcal{E}} = \left( \Gamma_Q(\mathcal{E}) V \Gamma_Q(\mathcal{E}) V - \Gamma_Q(\mathcal{E}) \Gamma_Q(\mathcal{E}') V P_{\mathcal{E}'} V \right)_{\text{linked}} P_{\mathcal{E}}. \quad (2.80)$$

Here, the second term has a *double resolvent* (double denominator, which might contain different model-space energies), and it is traditionally drawn in a “folded” way, as shown in the left diagram below (see, for instance, [124, Sect. 13.3])

$$(2.81)$$

The reason for drawing the diagram folded in this way is that the two pieces—before and after the fold—should be evaluated with their denominators independently. In the general case, by considering all possible time-orderings between the two pieces, together with the Goldstone evaluation rules, it can be shown that the denominators do *factorize*. In a relativistic treatment, which we shall employ for the rest of this book, the treatment is most conveniently based upon Feynman diagrams, which automatically contain all possible time-orderings, and then it is more natural to draw the diagram straight, as shown in the second diagram above. Factorization then follows directly. The double bar indicates that the diagram is “folded” with a double denominator in the upper part—one denominator with the energy of the initial state and one with that of the intermediate model-space state. The second-order wave operator can then be illustrated as shown in Fig. 2.5. Note that there is a minus sign associated with the folded diagram.

The general ladder diagram (Fig. 2.5) may contain a (quasi)singularity, when the intermediate state lies in the model space and is (quasi)degenerate with the initial state. This singularity is automatically eliminated in the Bloch equation and leads to the folded term. Later, in Sect. 6.8 we shall discuss this kind of singularity in more detail in connection with energy-dependent interactions, and then we shall refer to the finite remainder as the **model-space contribution** (MSC).

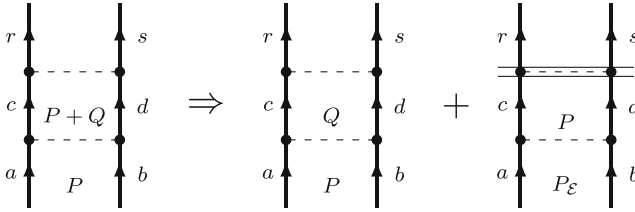


**Fig. 2.5** Removing the singularity from a ladder diagram leads to finite remainder, represented by a “folded” diagram (last). The *double bar* represents a double denominator (with a factor of  $-1$ )

We have seen that the so-called unlinked diagrams are eliminated in the second-order wave operator (2.79). When the model space is “*complete*” (see definition above), it can be shown that unlinked diagrams disappear in all orders of perturbation theory. This is the *linked-cluster or linked-diagram theorem* (LDE), first demonstrated in the 1950s by Brueckner [40] and Goldstone [78] for a degenerate model space. It holds also for a complete quasi-degenerate model space, as was first shown by Brandow [34], using a double perturbation expansion. This was demonstrated more directly by Lindgren [117] by means of the generalized Bloch equation (2.55), and the result can then be formulated<sup>7</sup>

$$\boxed{[\Omega, H_0]P = (V\Omega P - \Omega W)_{\text{linked}}P.} \quad (2.82)$$

This equation is a convenient basis for many-body perturbation theory, as developed, for instance, in [124]. It will also constitute a fundament of the theory developed in the present book.

### 2.4.2.2 Incomplete Model Spaces

When the model space is *incomplete*, i.e., does not contain all configurations that can be formed by the valence orbitals, the expansion is not necessarily completely linked. As first shown by Mukherjee [125, 166], the linked-diagram theorem can still be shown to hold, if the normalization condition (2.41a) is abandoned. As will be discussed later, a complete model space often has the disadvantage of so-called *intruder states*, which destroy the convergence. Then also other means of circumventing this problem will be briefly discussed.

<sup>7</sup>The Rayleigh-Schrödinger and the linked-diagram expansions have the advantage compared to, for instance, the Brillouin-Wigner expansion, that they are *size-extensive*, which implies that the energy of a system increases linearly with the size of the system. This idea was actually behind the discovery of the linked-diagram theorem by Brueckner [40], who found that the so-called unlinked diagrams have a non-physical non-linear energy dependence and therefore must be eliminated in the complete expansion. The concept of size extensivity should not be confused with the term *size consistency*, introduced by People [197, 198], which implies that the *wave function* separates correctly when a molecule dissociates. The Rayleigh-Schrödinger or linked-diagram expansions are generally **not** size consistent. The coupled-cluster approach (to be discussed below), on the other hand, does have this property in addition to the property of size extensivity.

## 2.5 All-Order Methods. Coupled-Cluster Approach

### 2.5.1 Pair Correlation

Instead of solving the Bloch equation order by order, it is often more efficient to solve it iteratively. By separating the second-quantized wave operator into normal-ordered zero-, one-, two-,...body parts

$$\Omega = \Omega_0 + \Omega_1 + \Omega_2 + \dots \quad (2.83)$$

with

$$\begin{cases} \Omega_1 = \{c_i^\dagger c_j\} x_j^i \\ \Omega_2 = \frac{1}{2} \{c_i^\dagger c_j^\dagger c_l c_k\} x_{kl}^{ij} \\ \text{etc.} \end{cases} \quad (2.84)$$

the Bloch equation can be separated into the following coupled  $n$ -particle equations

$$\begin{aligned} [\Omega_1, H_0]P &= (V\Omega - \Omega W)_{\text{linked}, 1} P \\ [\Omega_2, H_0]P &= (V\Omega - \Omega W)_{\text{linked}, 2} P \end{aligned} \quad (2.85)$$

etc., where

$$W = PV\Omega P \quad (2.86)$$

is the effective interaction.

Usually, the two-body operator dominates heavily, since it contains the important pair correlation between the electrons. Therefore, a good approximation for many cases is

$$\Omega \approx 1 + \Omega_1 + \Omega_2, \quad (2.87)$$

which yields

$$\begin{aligned} [\Omega_1, H_0]P &= (V_1 + V\Omega_1 + V\Omega_2 - \Omega_1 W_1)_{\text{linked}, 1} P \\ [\Omega_2, H_0]P &= (V_2 + V\Omega_1 + V\Omega_2 - \Omega_1 W_2 - \Omega_2 W_1 - \Omega_2 W_2)_{\text{linked}, 2} P, \end{aligned} \quad (2.88)$$

where

$$\begin{aligned} W_1 &= (V_1 + V_1\Omega_1)_{\text{closed}, 1} \\ W_2 &= (V_2 + V\Omega_1 + V\Omega_2)_{\text{closed}, 2}. \end{aligned} \quad (2.89)$$

We see here that the equations are coupled, so that  $\Omega_1$  appears in the equation of  $\Omega_2$  and vice versa. This approach is known as the *pair-correlation approach*. Solving these coupled equations self consistently, is equivalent to a perturbation expansion—including one- and two-body effects—to essentially all orders. It should be noted, though, that each iteration does not correspond to a certain order of the perturbative expansion.

As a simple illustration we consider the simplified pair-correlation approach

$$\Omega = \Omega_2, \quad (2.90)$$

omitting single excitations. (This would be exact for a two-electron system using hydrogenic basis functions, in which case there are no core orbitals, but is a good approximation also in other cases.) The equation for  $\Omega_2$  is

$$[\Omega_2, H_0]P = (V + V\Omega_2 - \Omega_2 W_2)_{\text{linked}, 2} P. \quad (2.91)$$

Operating on an initial two-electron state of energy  $\mathcal{E}$ , the solution can be expressed

$$\Omega_2 P_{\mathcal{E}} = \Gamma_Q(\mathcal{E})(V + V\Omega_2 - \Omega_2 W_2)_{\text{linked}} P_{\mathcal{E}}. \quad (2.92)$$

Solving this iteratively, leads to

$$\Omega_2^{(1)} P_{\mathcal{E}} = \Gamma_Q(\mathcal{E})V P_{\mathcal{E}}, \quad (2.93)$$

$$\begin{aligned} \Omega_2^{(2)} P_{\mathcal{E}} &= \Gamma_Q(\mathcal{E})\left(V\Omega_2^{(1)} - \Omega_2^{(1)} P_{\mathcal{E}'} W_2^{(1)}\right) P_{\mathcal{E}} \\ &= \Gamma_Q(\mathcal{E})V\Gamma_Q(\mathcal{E})V P_{\mathcal{E}} - \Gamma_Q(\mathcal{E})\Gamma_Q(\mathcal{E}')V P_{\mathcal{E}'} V P_{\mathcal{E}}, \\ &\text{etc.} \end{aligned} \quad (2.94)$$

where all terms are assumed to be linked. This leads to the “*ladder sequence*”, illustrated in Fig. 2.6. Note that in the expression above, all energies of the first term depend on the initial state, while in the folded term the wave operator depends on the energy of the intermediate state ( $\mathcal{E}'$ ) (c.f., the “*dot product*”, introduced in Sect. 6.8).

Operating with  $\Omega_2$  in (2.84) on the initial state  $|ab\rangle$ , leads to the *pair function*

$$\Omega_2|ab\rangle = x_{ab}^{rs}|rs\rangle = \rho_{ab}(x_1, x_2), \quad (2.95)$$

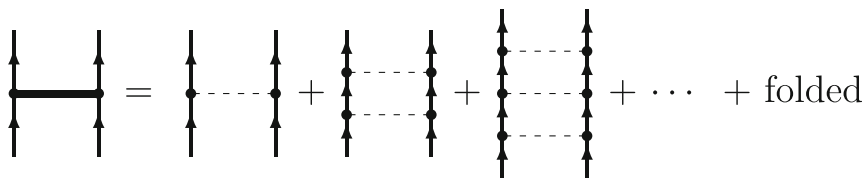
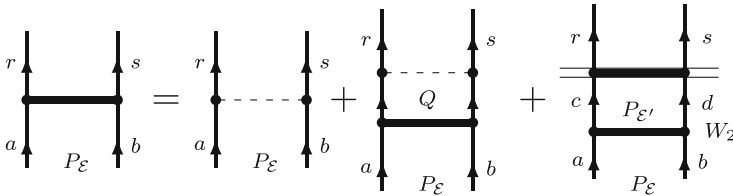


Fig. 2.6 Graphical representation of the pair function (2.96)



**Fig. 2.7** Graphical representation of the self-consistent pair equation (2.99). The last diagram represents the “folded” term  $-\Omega_2 W_2$ . The *double line* represents the double denominator (double resolvent)

which inserted in (2.88) leads to the pair equation

$$\begin{aligned} & (\varepsilon_a + \varepsilon_b - h_0(1) - h_0(2)) \rho_{ab}(x_1, x_2) \\ &= \left( |rs\rangle \langle rs| V |ab\rangle + |rs\rangle \langle rs| V | \rho_{ab}\rangle - | \rho_{cd}\rangle \langle cd| W_2 |ab\rangle \right)_{\text{linked}}. \end{aligned} \quad (2.96)$$

(For simplicity we work with straight product functions—not antisymmetrized—in which case we sum over all combinations of  $r, s$  (without the factor of  $1/2$ ) with  $x_{ab}^{rs} = -x_{ab}^{sr}$ .)

We can also express the pair function as

$$| \rho_{ab}\rangle = \Gamma_Q(\mathcal{E}) I^{\text{Pair}} |ab\rangle, \quad (2.97)$$

where  $\Gamma_Q(\mathcal{E})$  is the reduced resolvent (2.65) and  $\mathcal{E}$  is the energy of the initial state  $|ab\rangle$ .  $I^{\text{Pair}}$  represents the ladder sequence of Coulomb interactions (including folded terms), corresponding to the heavy line in Fig. 2.6. Including the resolvent (final denominator) then leads to the pair function  $| \rho_{ab}\rangle$ . The effective interaction  $W_2$  can be expressed as

$$W_2 = P_{\mathcal{E}'} I^{\text{Pair}} P_{\mathcal{E}}, \quad (2.98)$$

which can be represented by the same diagrams as in Fig. 2.6 (with no final denominator), if the final state (with energy  $\mathcal{E}'$ ) lies in the model space. The pair function (2.92) can now be expressed

$$\Gamma_Q(\mathcal{E}) I^{\text{Pair}} P_{\mathcal{E}} = \Gamma_Q(\mathcal{E}) \left( V + V \Gamma_Q(\mathcal{E}) I^{\text{Pair}} - \Gamma_Q(\mathcal{E}') I^{\text{Pair}} P_{\mathcal{E}'} I^{\text{Pair}} P_{\mathcal{E}} \right) P_{\mathcal{E}}. \quad (2.99)$$

This relation can be represented graphically as shown in Fig. 2.7.

### 2.5.2 Exponential Ansatz: Coupled-Cluster Approach

A particularly effective form of the all-order approach is the *Exponential Ansatz* or *Coupled-Cluster Approach* (CCA), first developed in nuclear physics by Hubbard,

Coster and Kümmel [50, 51, 90, 107, 108]. It was introduced into quantum chemistry by Čížek [47] and has been extensively used during the last decades. (For more details the reader is referred to a recent book “*Recent Progress in Coupled Cluster Methods*” [246], which reviews the development of the methods since the start.) The CCA is a non-linear approach, and the linear all-order approach (2.85), discussed above, is sometimes inadvertently referred to as “*linear CCA*”(!)—a term that should be avoided.

In the exponential Ansatz the wave operator is expressed in the form of an exponential

$$\Omega = e^S = 1 + S + \frac{1}{2}S^2 + \frac{1}{3!}S^3 + \dots, \quad (2.100)$$

$S$  being the *cluster operator* (in chemical literature normally denoted by  $T$ ). It can then be shown that for a degenerate model space the cluster operator is represented by *connected* diagrams only.<sup>8</sup> This implies that the linked but disconnected diagrams of the wave operator are here represented by the higher powers in the expansion of the exponential.

For *open-shell systems* (with unfilled valence shell) it is convenient to represent the Ansatz in the *normal-ordered form*, introduced by Lindgren [118, 124],

$$\Omega = \{e^S\} = 1 + S + \frac{1}{2}\{S^2\} + \frac{1}{3!}\{S^3\} + \dots. \quad (2.101)$$

This form has the advantage that unwanted contractions between the cluster operators are avoided. The cluster operator is completely connected also in this case, if the model space is complete [118], which can be formulated by means of the Bloch equation

$$\boxed{[S, H_0]P = Q(V\Omega P - \Omega W)_{\text{conn}}}. \quad (2.102)$$

It has been analyzed in detail by Lindgren and Mukherjee under what conditions the cluster operator is connected also for an incomplete model space [125].

Expanding the cluster operator in analogy with the wave-operator expansion (2.83) in terms on one-, two-...body operators,

$$S = S_1 + S_2 + S_3 + \dots \quad (2.103)$$

yields

$$\Omega = \{e^S\} = 1 + S_1 + S_2 + \frac{1}{2}\{S_1^2\} + \{S_1 S_2\} + \frac{1}{2}\{S_2^2\} + \frac{1}{2}\{S_1^2 S_2\} + \frac{1}{3!}\{S_1^3\} + \dots. \quad (2.104)$$

---

<sup>8</sup>The distinction between *linked* and *connected* diagrams should be noted. A linked diagram can be disconnected, if all parts are *open*, as defined in Sect. 2.4.

With the approximation

$$S = S_1 + S_2 \quad (2.105)$$

the cluster operators satisfy the *coupled Bloch equations*

$$\begin{aligned} [S_1, H_0]P &= (V\Omega - \Omega W)_{\text{conn}, 1} P \\ [S_2, H_0]P &= (V\Omega - \Omega W)_{\text{conn}, 2} P, \end{aligned} \quad (2.106)$$

illustrated in analogy with Fig. 2.7 in Fig. 2.8. These equations lead to one- and two-particle equations, analogous to the pair equation given above (2.96). Also these equations have to be solved *iteratively*, and we observe that they are *coupled*, as are the corresponding equations (2.88) for the full wave operator.

The normal-ordered scheme is usually combined with a *complete model space*—or complete active space (CAS)—and the *valence universality*. This means that the parameters of the expansion are the same for different stages of ionization. This approach is usually referred to as *Fock-space coupled-cluster* (FSCC). It is advantageous in calculating energy differences between different ionization stages, like ionization energy and affinities. A severe disadvantage is that it might lead to problems due to *intruder states* to be discussed further below.

For atomic systems with essentially *spherical symmetry* the cluster equations can be separated into angular and radial parts, where the former can be treated analytically and only the radial part has to be solved numerically (see, for instance, [125, Chap. 15]). For molecular systems, on the other hand, analytical basis-set functions of Slater or Gaussian types are normally used to solve the coupled-cluster equations, as described in numerous articles in the field.

As mentioned, the advantage of the normal ordering of the exponential Ansatz is that a number of unwanted contractions between open-shell operators is avoided. More recently, Mukherjee has shown that certain valence-shell contractions are actually desired, particularly when valence holes and strong relaxation are involved [95]. He then introduced a modified normal ordering

$$\Omega = \{\{\exp(S)\}\}, \quad (2.107)$$

where contractions involving passive (spectator) valence lines are reintroduced compared to the original normal ordering.

### 2.5.3 Various Models for Coupled-Cluster Calculations. *Intruder-State Problem*

The early forms of coupled-cluster models were of *single-reference* type (SRCC) with a one-dimensional (closed-shell) model space. In the last few decades various



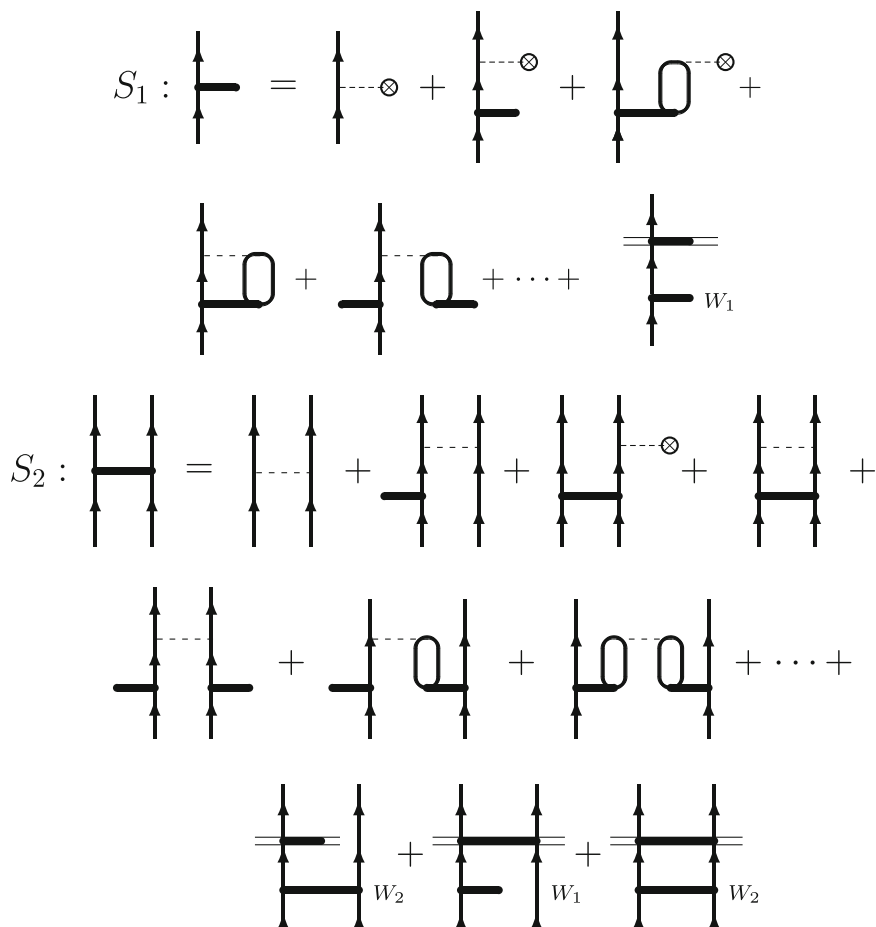


**Fig. 2.8** Diagrammatic representation of the equations for the cluster operators  $S_1$  and  $S_2$  (2.106). The circle with a cross represents the “effective potential” in Fig. 2.3. The second diagram in the second row and the diagrams in the fourth row are examples of coupled-cluster diagrams. The last diagram in the second row and the three diagrams in the last row are folded diagrams, where the double line represents a double denominator (c.f. Fig. 2.7)

versions of *multi-reference* (MRCC) models with multi-dimensional model space have appeared (for reviews, see e.g., [14, 125, 168]). These are essentially two major types, known as *valence-universal* multi-reference (VU-MRCC) [118, 167] and *state-universal* multi-reference (SU-MRCC) [98, 99] methods, respectively. In the valence-universal methods the same cluster operators are being used for different ionization states and therefore particularly useful for calculating ionization energies and affinities. In the state-universal methods specific operators are used for a particular ionization stage and particularly used when different states of the same ionization are considered or in the molecular case for studying potential energy surfaces (PES).

A serious problem that can appear in MBPT with a multi-reference model space is what is known as the “*intruder-state-problem*”. This appears when a state outside the model space—of the same symmetry as the state under consideration—has a perturbed energy between those of the same symmetry originating from the model space. This will destroy the convergence of the perturbation expansion. This problem was first observed in nuclear physics [218], but it was early observed also in atomic physics for the beryllium atom [207]. Here, the ground state is  $1s^2 2s^2 \ ^1S$ , and the excited state  $1s^2 2p^2 \ ^1S$  has a low unperturbed energy, while the true state lies close to the  $2s$  ionization limit. This implies that when the perturbation is gradually turned on, a large number of “outside” states,  $1s^2 2s \ ns$ , will cross the energy of the  $1s^2 2p^2 \ ^1S$  state, and there will be no convergence beyond the crossing point.

The convergence problem due to intruders is particularly serious in perturbation theory, when the states are expanded order-by-order from the unperturbed ones. In the coupled-cluster approach, which in principle is *non-perturbative*, it might be possible to find a self-consistent solution of the coupled equations without reference to any perturbative expansion. It was first shown by Jankowski and Malinowski [93, 94, 142] that it was in fact possible to find a solution to the beryllium problem with a complete model space. Lindroth and Mårtensson [136] solved the same problem by means of *complex rotation*.

Several other methods have been developed to reduce the intruder-state problem. One way is to reduce the model space and make it *incomplete*. As mentioned, the linked character of the diagram expansion could here still be maintained by abandoning the intermediate normalization (2.41a) [125, 166].

Another approach to avoid or reduce the intruder-state problem is to apply an *intermediate-effective Hamiltonian*, a procedure developed by the Toulouse group (Malrieu, Durand et al.) in the mid 1980s [62]. Here, only a limited number of roots of the secular equation are being looked for. A modified approach of the method has been developed by Meissner and Malinowski [147] and applied to the above-mentioned beryllium case.

A way to avoid the intruder problem completely is to study one single state at the time, the so-called *state-specific multi-reference* (SS-MRCC) approach [141]. This approach can be regarded as an extreme of the intermediate-Hamiltonian approach and is frequently used particularly for studying potential-energy surfaces.

Another alternative to the Fock-space or valence-universal approach is the so-called *Similarity-Transformed Equation-of-Motion* approach (ST-EOM), which makes it possible to study a large number of excited states simultaneously [175, 176]. This approach is also free of intruders.

All the coupled-cluster approaches can also be applied in the relativistic formalism, although applications are here still quite limited. We shall return briefly to this problem in Chap. 8.

## 2.6 Relativistic MBPT. No-Virtual-Pair Approximation

In setting up a Hamiltonian for relativistic quantum mechanics it may be tempting to replace the single-electron Schrödinger Hamiltonian in the many-body Hamiltonian (2.11) by the Dirac Hamiltonian (see Appendix D)

$$h_D = c\boldsymbol{\alpha} \cdot \hat{\mathbf{p}} + \beta mc^2 + v_{\text{ext}}, \quad (2.108)$$

which with the Coulomb interaction between the electrons

$$V_C = \sum_{i < j}^N \frac{e^2}{4\pi\epsilon_0 r_{ij}} \quad (2.109)$$

yields the *Dirac–Coulomb Hamiltonian*

$$H_{DC} = \sum_{i=1}^N h_D(i) + V_C. \quad (2.110)$$

This Hamiltonian, however, has several serious shortcomings. Firstly, it is not bound from below, because nothing prevents the electrons from falling into the “*Dirac sea*” of negative-energy electron states. A many-electron state with a mixture of negative-energy and positive-energy electron states can then be accidentally degenerate with a state with only positive-energy states—a phenomenon known as the *Brown-Ravenhall disease* [39]. In Chap. 6 we shall derive a field-theoretical many-body Hamiltonian that will be used in the further development. In this model there is no “Dirac sea”, but the negative-energy states correspond to the creation of *positron states*, which are highly excited. Then there can be no Brown-Ravenhall effect.

Within the conventional many-body treatment the Brown-Ravenhall effect can be circumvented by means of projection operators [238], which exclude negative-energy states, leading to the *projected Dirac–Coulomb Hamiltonian*

$$H_{DC\text{proj}} = \Lambda_+ \left[ \sum_{i=1}^N h_D(i) + V_C \right] \Lambda_+. \quad (2.111)$$

Including also the *instantaneous Breit interaction* (see Appendix F)

$$V_B = -\frac{e^2}{8\pi\epsilon_0} \sum_{i < j} \left[ \frac{\boldsymbol{\alpha}_i \cdot \boldsymbol{\alpha}_j}{r_{ij}} + \frac{(\boldsymbol{\alpha}_i \cdot \mathbf{r}_{ij})(\boldsymbol{\alpha}_j \cdot \mathbf{r}_{ij})}{r_{ij}^3} \right], \quad (2.112)$$

where  $\boldsymbol{\alpha}_i$  is the Dirac alpha matrix vector for particle  $i$  (see Appendix D), leads to the *projected Dirac–Coulomb–Breit Hamiltonian*

$$H_{\text{NVPA}} = \Lambda_+ \left[ \sum_{i=1}^N h_D(i) + V_C + V_B \right] \Lambda_+, \quad (2.113)$$

which is known as the **No-Virtual-Pair Approximation** (NVPA). Graphical representation of the instantaneous Breit interaction is shown in Fig. 4.5.

With the partitioning (2.47)

$$H = H_0 + V \quad (2.114)$$

we choose the model Hamiltonian to be

$$H_0 = \sum_i^N (h_D + u)_i =: \sum_i^N h_0(i) \quad (2.115)$$

and the perturbation

$$V = - \sum_i^N u(i) + V_C + V_B. \quad (2.116)$$

The Dirac–Coulomb and Dirac–Coulomb–Breit Hamiltonians, which are valid only in the *Coulomb gauge* (see Appendix G.2), have been extensively used in relativistic MBPT calculations and particularly in self-consistent-field calculations of *Dirac-Fock* type. In the latter type of calculations the projection operators can often be left out, since the boundary conditions usually excludes negative-energy solutions (see the book by I.P. Grant for a modern review [79]). Several reviews on relativistic effects in chemical systems has been published by Pekka Pyykkö [200].

NVPA is a good approximation for many purposes, and it includes all effects to order  $\alpha^2 H$ , but it is *not Lorentz covariant* (see definition in the Introduction). In later chapters we shall consider a more rigorous many-body Hamiltonian, based upon field theory.

### 2.6.1 QED Effects

As mentioned, we shall refer to effects beyond the NVPA as *QED effects*, although this separation is to some extent arbitrary. These effects are of two kinds

- *non-radiative effects*, representing effects due to negative-energy states and to retardation of the Breit interaction, shown in the upper line of Fig. 2.9. These effects are also referred to as the *Araki-Sucher* effects [5, 235, 237] and
- *radiative effects*, represented by the lower line of Fig. 2.9, which are “true” quantum-electrodynamical effects due to the electron self-energy (first diagram), vacuum polarization (next two diagrams) or vertex correction (last diagram) (see further Chap. 4).

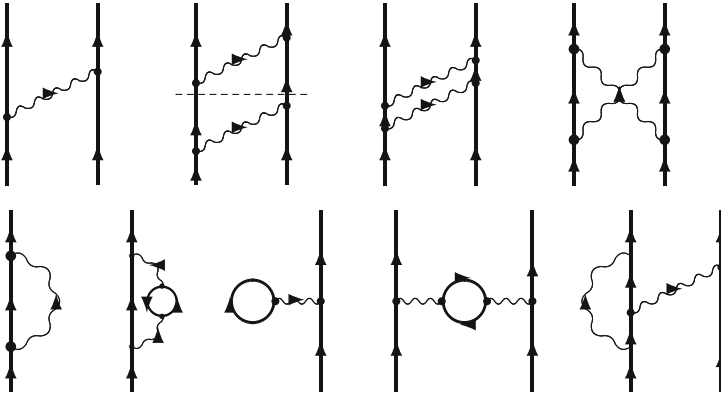


**Fig. 2.9** Non-radiative (*upper line*) and radiative (*lower line*) “QED effects”. These diagrams are *Feynman diagrams*, where the orbital lines can represent particle as well as hole or anti-particle states (see further Chap. 4). The second diagram in the first row is reducible (there is an intermediate time with no photon), while the remaining ones are irreducible

The QED effects can also be separated into *reducible* and *irreducible* effects, where a reducible effect is represented by a diagram that can be separated into two legitimate diagrams by a horizontal cut, such as the second non-radiative diagram in Fig. 2.9. Remaining diagrams are irreducible.<sup>9</sup>

## 2.7 Some Numerical Results of Standard MBPT and CC Calculations, Applied to Atoms

In the book *Atomic Many-Body Theory* [124, Sect. 15.5] a brief summary is given of the situation in the late 1970s concerning the numerical application of many-body perturbation theories. Most effective at that time to handle the electron-correlation problem were various pair-correlation approaches, based on works of Kelly [104], Meyer [148], Sinanoglu [229], Nesbet [174], Kutzelnigg [112] and others. Coupled-cluster methods were available at that time but still relatively undeveloped. Also methods of treating open shells and the quasi-degenerate problem, using the extended model space [117] (2.55), were available but not particularly well-known.

In the three decades that have followed, a dramatic development regarding numerical implementations has taken place. All-order methods, in particular, coupled-cluster methods, have been developed to a stage of “almost perfection”. Also the open-shell

<sup>9</sup>It should be noted that this definition leads to different classification, depending on the effects studied. If only the energy or the effective Hamiltonian is studied, then a diagram would be reducible if it contains an intermediate model-space state. If, on the other hand, also the wave function or wave operator is studied, then the diagram would be reducible if there is an intermediate state free from photons.

techniques have been further developed and are now routinely used. Here, two main lines have emerged, based upon *multi-reference* or *single-reference states*. The latter technique has been developed mainly to circumvent the *intruder problem*, although there are methods of dealing with this problem also in the multi-reference case, as was briefly mentioned above. We shall in no way try to review this immense field here but limit ourselves to some comments concerning developments that are most relevant for the theme of this book. (We refer to the previously mentioned book, edited by Čárský et al. [246], for more details.) We also call attention to a comprehensive review of all-order relativistic atomic calculations that has recently been published by Safronova and Johnson [204].

The coupled-cluster approach was early applied to various molecular systems, particularly by Čížek, Paldus and coworkers in the Waterloo group [186, 187]. Extensions of the method and extensive calculations have been performed by Bartlett and his collaborators at Gainesville [15, 199]. The paper by Purvis and Bartlett [199], together with the simultaneous publication by People et al. [196], represent the first applications of CCA with both single and double excitations (CCSD). Bartlett et al. have later extended the technique to include part of triples, CCSD(T), and quadruples, CCSD(TQ), techniques that are now widely spread.

In molecular calculations functional basis sets of Slater or Gaussian type are normally used. For atomic systems, on the other hand, it is normally preferable to use numerical integration of the radial coordinates. Such techniques have been developed and applied particularly by the groups at Notre Dame, Gothenburg and Tel Aviv.

The Notre-Dame group has for a long time performed relativistic many-body calculations on atomic systems by applying and further developed the *spline technique* with piece-wise polynomial fitting [100]. This was first used for calculations to second-order (third order in energy) of the helium atom and the sodium isoelectronic sequence [101]. The method was then extended by Blundell et al. [31] to an all-order technique (linear with singles and doubles) and applied to the Li atom and the  $\text{Be}^+$  ion and by Plante et al. [195] to a sequence of heliumlike ions. In Table 2.1 we reproduce from the latter work the contributions to the ground-state ionization energies due to (a) all-order Coulomb interactions, (b) same with one instantaneous Breit interaction, (c) same with TWO instantaneous Breit interactions, (d) first-order

**Table 2.1** Contributions to the ground-state ionization energies of heliumlike ions

Z	Coulomb	Breit	Double Breit	QED	Total
10	43.962	0.010708	0.000048	-0.004610	43.946
20	188.636	0.096696	0.000433	-0.054905	168.485
40	792.126	0.83482	0.00409	-0.57860	790.717
60	1855.119	2.97236	0.01528	-2.22984	1849.832
80	3472.330	7.51789	0.03914	-5.89519	3458.965
100	5841.499	16.0999	0.0836	-12.9704	5812.513

From [195] (in Hartrees)

**Table 2.2** Binding energies of the two lowest states of the lithium atom (in  $\mu\text{H}$ )

Lithium atom			
	$2^2S$	$2^2P$	References
Expt'l	198 159	130 246	
Hartree-Fock	196 304	128 637	
LSD	198 159	130 219	Blundell et al. [31]
CCSD	198 154	130 221	Lindgren [119]
CCSD	198 139	130 171	Eliav et al. [65]

**Table 2.3** Correlation energy of some low-lying states of the sodium atom (in  $\mu\text{H}$ ) (from [205])

Sodium atom					
	$3^2S$	$3^2P_{1/2}$	$3^2P_{3/2}$	$4^2S$	References
Expt'l	6 825	2121	2110	1415	
LSD	6 835	2118	2108	1418	Safronova et al. [205]
CCSD	6 458				Salomonson-Ynnerman [211]
CCSD	6 385				Eliav et al. [65]
CCSD(T)	6 840				Salomonson-Ynnerman [211]

QED contribution (from [61]), (e) total ionization energy. Later, the Notre-Dame group, partly together with Safronova, has extended the technique to full relativistic CCSD, including also some triples, CCSD(T), and applied it extensively to various atomic and ionic systems [139, 204] (see Tables 2.2 and 2.3).

The Gothenburg group developed numerical non-relativistic all-order and coupled-cluster approaches in the late 1970s and early 1980s. Ann-Marie Mårtensson (Pendrill) [145] developed an all-order pair program (LD)—linear with doubles without coupled clusters—based upon the first-order pair program developed by Morrison [72, 164], and first applied it to the helium atom. This technique was later converted into a coupled-cluster program with doubles (CCD) by Salomonson [129] and applied to various atomic systems. It was also applied to open-shell systems [165, 207]—in the second paper (concerning the beryllium atom) the famous *intruder problem*, mentioned above, was probably observed for the first time in an atomic system. The procedure of the Gothenburg group was also early extended to include singles and applied by Lindgren in 1985 [119] (see Table 2.2) and later by Salomonson et al. [208, 211] (see Tables 2.3 and 2.4).

A *relativistic* version of the linear all-order pair program (LD) was developed by Eva Lindroth [135], and applied to the helium atom. This was extended to a relativistic coupled-cluster program by Salomonson and Öster, who also developed a new numerical, highly accurate technique, referred to as the *discretization technique* [209]. This technique was early applied relativistically as well non-relativistically to a number of atomic systems [208, 211] and is used also in all later works of the group.

**Table 2.4** Correlation energy of the ground state of the beryllium atom and the negative lithium ion (in  $\mu\text{H}$ ) (from [41])

Beryllium atom and negative lithium ion			
	Be	Li <sup>-</sup>	References
CCD	-92.960	-71.148	Bukowski et al. [41]
CCD	-92.961	71.266	Salomonson-Öster [208]
CCSD	-93.665	72.015	Bukowski et al. [41]
CCSD	-93.667	72.142	Salomonson-Öster [208]

In Tables 2.2, 2.3 and 2.4 we have compared some all-order calculations for the lithium, sodium, and beryllium atoms as well as for the Li<sup>-</sup> ion. The calculations on Be and Li<sup>-</sup> demonstrate clearly the importance of single excitations in this case. The results for sodium show the importance of triple excitations in this case. (The results by Safronova et al. is probably fortuitous, indicating that effects of non-linear coupled-cluster terms and triples accidentally cancel.) The accurate results from numerical integrations by Salomonson et al. are sometimes used as benchmarks for testing calculations with finite basis sets [41].

The Tel-Aviv group has applied the relativistic coupled-cluster technique with singles and doubles (CCSD) particularly to very heavy atoms and simple molecules (see, for instance, the review article by Kaldor and Eliav [103], as well as Tables 2.2 and 2.3).



# Chapter 3

## Time-Dependent Formalism

In the present chapter we shall summarize the fundamentals of time-dependent perturbation theory. Apart from the last part (Chap. 13), we shall be concerned only with **stationary** problems in this book. Nevertheless, we shall find it convenient to apply time-dependent methods. We restrict ourselves in the present chapter to the *non-relativistic formalism* and return to the relativistic one in later chapters.

### 3.1 Transition Rate

A general time-dependent single-particle state can be expanded in stationary states as

$$|\chi(t, \mathbf{r})\rangle = \sum_k c_k(t) |\Psi_k(\mathbf{r})\rangle e^{-i\omega_k t}, \quad (3.1)$$

where  $\omega_k = E_k/\hbar$ . Inserted into the time-dependent Schrödinger equation (2.9) yields with  $H = H_0 + V(t)$

$$\sum_k \left( i\hbar \frac{dc_k(t)}{dt} - c_k V(t) \right) \Psi_k(\mathbf{r}) e^{-i\omega_k t} = 0, \quad (3.2)$$

and

$$\frac{dc_k(t)}{dt} = -\frac{i}{\hbar} \sum_k c_k(t) \langle l|V(t)|k\rangle e^{i\omega_{lk}}, \quad (3.3)$$

where  $|l\rangle = \Psi_l(\mathbf{r})$  etc. and  $\omega_{lk} = \omega_l - \omega_k$ . If the state is  $|0\rangle = \Psi_0$  at  $t_0$ , then in first order

$$c_k(t) = -\frac{i}{\hbar} \int_0^t dt' \langle l|V(t')|0\rangle e^{i\omega_{l0}t'}. \quad (3.4)$$

If the perturbation is *harmonic*,

$$V(t) = F e^{-i\omega t}, \quad (3.5)$$

then

$$c_l(t) = -\frac{i}{\hbar} \langle l | F | 0 \rangle \int_0^t dt' e^{i(\omega_{l0} - \omega)t'}. \quad (3.6)$$

$|c_k(t)|^2$  is the probability that the state at time  $t$  after a measurement will be in the stationary state  $\Psi_l$ .

The *transition rate* to the state  $l$  is defined

$$R_l(\omega) = \lim_{t \rightarrow \infty} \frac{d}{dt} |c_l(t)|^2 = \frac{1}{\hbar^2} |\langle l | F | 0 \rangle|^2 F(x), \quad (3.7)$$

where  $x = \omega_{l0} - \omega$  and

$$F(x) = \lim_{t \rightarrow \infty} \frac{d}{dt} \left| \int_0^t dt' e^{ixt'} \right|^2. \quad (3.8)$$

From (A.16) in Appendix A it follows that

$$\lim_{t \rightarrow \infty} \int_0^t dt' e^{ixt'} = \pi \delta(x),$$

which yields  $F(x) = 2\pi \delta(x)$  and the transition rate

$$\boxed{R_l(\omega) = 2\pi \delta(\omega_{l0} - \omega) |\langle l | F | 0 \rangle|^2 / \hbar^2.} \quad (3.9)$$

## 3.2 Evolution Operator

It follows from the Schrödinger equation (2.16) that the state vector evolves in time according to

$$|\chi_S(t)\rangle = e^{-iH(t-t_0)/\hbar} |\chi_S(t_0)\rangle. \quad (3.10)$$

This is known as the *Schrödinger picture* (SP), indicated by the subscript “S”. In another representation, known as the *interaction picture* (IP) (see Appendix B, B.23) the Hamiltonian is partitioned according to (2.47),  $H = H_0 + V$ , and the state vectors and the operators are transformed according to

$$|\chi_I(t)\rangle = e^{iH_0 t/\hbar} |\chi_S(t)\rangle; \quad \mathcal{O}_I(t) = e^{iH_0 t/\hbar} \mathcal{O}_S e^{-iH_0 t/\hbar}. \quad (3.11)$$

This implies that the state vectors are normally much more slowly varying with time, and most of the time dependence is instead transferred to the operators that are normally time independent in SP.

The Schrödinger equation is in IP transformed to

$$\boxed{i\hbar \frac{\partial}{\partial t} |\chi_I(t)\rangle = V_I(t) |\chi_I(t)\rangle} \quad (3.12)$$

with the solution

$$|\chi_I(t)\rangle = |\chi_I(t_0)\rangle - \frac{i}{\hbar} \int_{t_0}^t dt_1 V_I(t_1) |\chi_I(t_1)\rangle. \quad (3.13)$$

$V_I(t)$  is the perturbation in the interaction picture, which is assumed to be *time independent in the Schrödinger picture*.

For a *stationary state* of energy  $E$  the time dependence (2.15) is  $e^{-iEt/\hbar}$ . It then follows that the state in the IP is of the form

$$|\chi_I(t)\rangle = e^{-it(E-H_0)/\hbar} |\chi_I(t=0)\rangle. \quad (3.14)$$

The *time-evolution operator* in IP,  $U_I(t, t_0)$ , is defined by the relation<sup>1</sup>

$$\boxed{|\chi_I(t)\rangle = U_I(t, t_0) |\chi_I(t_0)\rangle \quad (t > t_0).} \quad (3.15)$$

Evidently, we then have

$$U_I(t, t) = 1 \quad (3.16)$$

$$U_I(t, t_1) U_I(t_1, t_2) = U_I(t, t_2). \quad (3.17)$$

From the relation (3.10) it follows that the corresponding evolution operator in SP is

$$U_S(t, t_0) = e^{-iH(t-t_0)/\hbar}. \quad (3.18)$$

Transforming (3.11) to IP then yields<sup>2</sup>

$$U_I(t, t_0) = e^{iH_0t/\hbar} e^{-iH(t-t_0)/\hbar} e^{-iH_0t_0/\hbar}. \quad (3.19)$$

---

<sup>1</sup>The evolution operator does not preserve the intermediate normalization, and, furthermore, when bound states are involved, it may contain singularities that are eliminated by the normalization constant (see further below).

<sup>2</sup>It should be noted that generally  $e^{iH_0t/\hbar} e^{-iHt/\hbar} \neq e^{-iVt/\hbar}$ , since the operators do not necessarily commute.

This evolution operator satisfies the differential equation

$$\boxed{i\hbar \frac{\partial}{\partial t} U_1(t, t_0) = V_1(t) U_1(t, t_0)}, \quad (3.20)$$

which leads to the expansion<sup>3</sup>

$$\begin{aligned} U(t, t_0) &= 1 - \frac{i}{\hbar} \int_{t_0}^t dt_1 V(t_1) U(t_1, t_0) \\ &= 1 - \frac{i}{\hbar} \int_{t_0}^t dt_1 V(t_1) + \left(\frac{-i}{\hbar}\right)^2 \int_{t_0}^t dt_1 V(t_1) \int_{t_0}^{t_1} dt_2 V(t_2) U(t_2, t_0) \end{aligned} \quad (3.21)$$

etc. By extending all integrations from  $t_0$  to  $t$ , this can be expressed [67, Fig. 6.1]

$$U(t, t_0) = 1 - \frac{i}{\hbar} \int_{t_0}^t dt_1 V(t_1) + \frac{1}{2} \left(\frac{-i}{\hbar}\right)^2 \int_{t_0}^t dt_1 \int_{t_0}^t dt_2 T[V(t_1)V(t_2)] U(t_2, t_0), \quad (3.22)$$

where  $T$  is the *time-ordering operator*, which orders the operators after decreasing time (without any sign change). This leads to the expansion

$$\begin{aligned} U_1(t, t_0) &= -\frac{i}{\hbar} \int_{t_0}^t dt_1 V(t_1) \\ U_2(t, t_0) &= \frac{1}{2} \left(\frac{-i}{\hbar}\right)^2 \int_{t_0}^t dt_1 \int_{t_0}^t dt_2 T[V(t_1) V(t_2)] \end{aligned} \quad (3.23)$$

etc., which can be generalized to [67, Eq. 6.23], [92, Eqs. 4–56]

$$U(t, t_0) = \sum_{n=0}^{\infty} \frac{1}{n!} \left(\frac{-i}{\hbar}\right)^n \int_{t_0}^t dt_1 \dots \int_{t_0}^t dt_n T[V(t_1) \dots V(t_n)]. \quad (3.24)$$

(We have here included the term  $n = 0$  to replace the unity.)

We introduce the *Hamiltonian density*  $\mathcal{H}(x)$  by

$$V(t) = \int d^3\mathbf{x} \mathcal{H}(t, \mathbf{x}). \quad (3.25)$$

We do not have to specify the perturbation at this point, but we shall later assume that it is given by the interaction between the electrons (of charge  $-e$ ) and the

---

<sup>3</sup>The zeroth-order component is conventionally chosen to be unity. Unless specified otherwise, we shall in the following assume that the evolution operators always are expressed in IP and leave out the subscript  $\mathbb{1}$ .

electromagnetic radiation field (see Appendix E.3)

$$\boxed{\mathcal{H}(x) = -\hat{\psi}^\dagger(x) e c \alpha^\mu A_\mu(x) \hat{\psi}(x)}. \quad (3.26)$$

Here,  $\alpha^\mu$  is the Dirac operator (see Appendix D) and  $A_\mu$  is the covariant radiation field operator (Appendix G.2)

$$A_\mu(x) = \sqrt{\frac{\hbar}{2\epsilon_0\omega V}} \sum_{kr} \varepsilon_{\mu r} [a_{kr}^\dagger e^{ikx} + a_{kr} e^{-ikx}]. \quad (3.27)$$

The Hamiltonian density is time independent in the Schrödinger picture (see Sect. 6.7).

The evolution operator (3.24) can now be expressed

$$\boxed{U(t, t_0) = \sum_{n=0}^{\infty} \frac{1}{n!} \left(\frac{-i}{c\hbar}\right)^n \int_{t_0}^t dx_1^4 \dots \int_{t_0}^t dx_n^4 T[\mathcal{H}(x_1) \dots \mathcal{H}(x_n)]}. \quad (3.28)$$

The factor of  $c$  in the denominator is due to the fact that we now use the integration variable  $x_0 = ct$ . The integrations are performed over all space and over time as indicated. Alternatively, this can be expressed

$$U(t, t_0) = T \left[ \exp \left( \frac{-i}{c\hbar} \int_{t_0}^t d^4x \mathcal{H}(x) \right) \right]. \quad (3.29)$$

The evolution operator can be represented graphically by means of Goldstone diagrams in the same way as the wave operator, discussed previously. As a simple example, we consider the first-order interaction with a time-independent energy-potential interaction  $v(\mathbf{x})$ . In second quantization the evolution operator becomes

$$U^{(1)}(t, t_0) = -\frac{i}{\hbar} \int_{t_0}^t dt c_r^\dagger \langle r | v(\mathbf{x}_1) | a \rangle c_a \quad (3.30)$$

or after summing over the states

$$U^{(1)}(t, t_0) = -\frac{i}{\hbar} \int_{t_0}^t dt_1 \int d^3\mathbf{x}_1 \hat{\psi}^\dagger(x_1) v(\mathbf{x}_1) \hat{\psi}(x_1), \quad (3.31)$$

which is illustrated in Fig. 3.1 (left).

The two-body interaction can be given by a *contraction* of two perturbations (3.26), corresponding to the exchange of one virtual photon,  $v(x_1, x_2)$ , as will be further discussed in Chap. 4. The corresponding, second-order evolution operator then becomes (Fig. 3.1, right)

**Fig. 3.1** Graphical representation of the evolution operator for first-order potential interaction and single-photon exchange

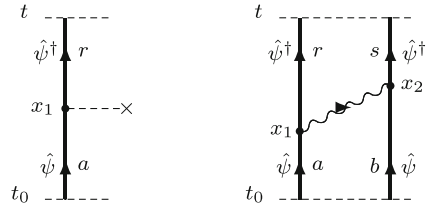
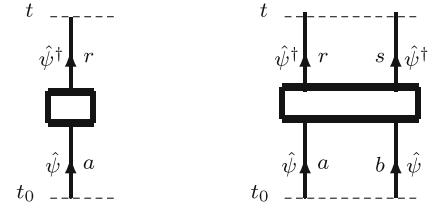


**Fig. 3.2** Schematic graphical representation of the connected one- and two-body parts of the evolution operator



$$U^{(2)}(t, t_0) = \frac{1}{2} \left( \frac{-i}{\hbar} \right)^2 \iint_{t_0}^t dt_1 dt_2 \iint d^3 \mathbf{x}_1 d^3 \mathbf{x}_2 \hat{\psi}^\dagger(x_1) \hat{\psi}^\dagger(x_2) v(x_1, x_2) \hat{\psi}(x_2) \hat{\psi}(x_1). \quad (3.32)$$

In higher orders the operator can have connected as well as disconnected parts and can be separated into zero-, one-, two-,...body parts. The connected one- and two-body pieces are schematically illustrated in Fig. 3.2. Expressions with uncontracted photons fall in an *extended photonic Fock space*, as will be further discussed in later chapters.

### 3.3 Adiabatic Damping. Gell-Mann–Low Theorem

For the mathematical treatment we shall find it convenient to apply an “*adiabatic damping*” to the perturbation,

$$V(t) \rightarrow V(t) e^{-\gamma|t|}, \quad (3.33)$$

where  $\gamma$  is a small, positive number, which implies that

$$H \rightarrow H_0 \text{ as } t \rightarrow \pm\infty. \quad (3.34)$$

The expansion (3.28) then becomes

$$U_\gamma(t, t_0) = \sum_{n=0}^{\infty} \frac{1}{n!} \left( \frac{-i}{c\hbar} \right)^n \times \int_{t_0}^t dx_1^4 \dots \int_{t_0}^t dx_n^4 T[\mathcal{H}(x_1) \dots \mathcal{H}(x_n)] e^{-\gamma(|t_1| + |t_2| + \dots + |t_n|)}. \quad (3.35)$$

The damping is adiabatically ‘switched off’ at the end of the calculation. The evolution operator satisfies now the equation (3.20)

$$i\hbar \frac{\partial}{\partial t} U_\gamma(t, t_0) = (V(t) \mp i\gamma) U_\gamma(t, t_0), \quad (3.36)$$

where the upper sign is valid for  $t > 0$ .

### 3.3.1 Gell-Mann–Low Theorem

The damped perturbation (3.33) vanishes, when  $\gamma t \rightarrow \pm\infty$ , and the perturbed (target) state vector approaches in these limits an eigenstate of  $H_0$ ,

$$|\chi_{I_\gamma}(t)\rangle \Rightarrow |\Phi\rangle, \quad (3.37)$$

which we call the *parent state*. Gell-Mann and Low have shown that for  $t = 0$  and in the limit  $\gamma \rightarrow 0$ , the state vector<sup>4</sup>

$$\boxed{\lim_{\gamma \rightarrow 0} |\chi_{I_\gamma}(0)\rangle = \lim_{\gamma \rightarrow 0} \frac{U_\gamma(0, -\infty)|\Phi\rangle}{\langle\Phi|U_\gamma(0, -\infty)|\Phi\rangle} =: |\Psi\rangle} \quad (3.38)$$

is a solution of the time-independent Schrödinger equation

$$(H_0 + V)|\Psi\rangle = E|\Psi\rangle, \quad (3.39)$$

where  $H_0$  is the model Hamiltonian (2.48) without the perturbation. Here,

$$E = E_0 + i\hbar\gamma\lambda \frac{\langle\Phi|\frac{\partial}{\partial\lambda}U_\gamma(0, -\infty)|\Phi\rangle}{\langle\Phi|U_\gamma(0, -\infty)|\Phi\rangle}. \quad (3.40)$$

This is the famous **Gell-Mann–Low theorem** (GML) [74], [67, p. 61], [220, p. 336], which represents one of the fundamentals of the theory presented here. The perturbation,  $V$ , must in the limit  $\gamma \rightarrow 0$  be **time-independent in the Schrödinger picture**, as is the case with the perturbation (3.26).

---

<sup>4</sup>Here, the numerator and the denominator might be singular in the limit, and it is important that the **ratio** is formed **before** the limit is taken.

### 3.4 Extended Model Space. The Generalized Gell-Mann–Low Relation

The original Gell-Mann–Low theorem (3.38) is valid only in the single-reference case (one-dimensional model space). The time-dependent MBPT was in the 1960s and 1970s further developed by several groups [36, 102, 109, 163, 177, 243], mainly in connection with nuclear calculations. We shall extend this treatment here and prove a generalization of the Gell-Mann–Low theorem for an arbitrary model space. This treatment follows mainly that performed in [130] (see also [67, Sect. 6]).

We choose the parent states to be the (normalized) limits of the target states for finite  $\gamma$  as  $t \rightarrow -\infty$ , as introduced by Tolmachev [243],

$$|\Phi^\alpha\rangle = N^\alpha \lim_{t \rightarrow -\infty} |\chi^\alpha\rangle_\gamma \quad (\alpha = 1, 2, \dots, d), \quad (3.41)$$

where  $N^\alpha$  is a normalization constant. The parent functions are then eigenfunctions of  $H_0$ ,

$$H_0 |\Phi^\alpha\rangle = E_0^\alpha |\Phi^\alpha\rangle, \quad (3.42)$$

but generally we do not know which eigenvalue a specific target state will converge to.

In analogy with the single-reference case (3.38) we construct the state

$$|\Psi_\gamma^\alpha\rangle = \frac{U_\gamma(0, -\infty) |\Phi^\alpha\rangle}{\langle \Psi_0^\alpha | U_\gamma(0, -\infty) | \Phi^\alpha \rangle}, \quad (3.43)$$

which is normalized in the intermediate normalization,  $\langle \Psi_0^\alpha | \Psi^\alpha \rangle = 1$ .

We shall now demonstrate that this state is in the limit  $\gamma \rightarrow 0$  an eigenstate of the time-independent Hamiltonian of the system for all values of  $\alpha$ ,

$$(H_0 + V) |\Psi^\alpha\rangle = E^\alpha |\Psi^\alpha\rangle \quad (\alpha = 1, 2, \dots, d). \quad (3.44)$$

- This is a **generalization of the original Gell-Mann–Low relation (3.38)**, and it **holds also for a quasi-degenerate model space with several energy levels** [130].

In order to prove the theorem, we consider one term in the expansion (3.35), recalling that the interactions are expressed in IP,

$$U_\gamma^{(n)}(t, -\infty) = \frac{1}{n!} \left( \frac{-i}{\hbar} \right)^n \int_{-\infty}^t dt_n \int_{-\infty}^{t_n} dt_{n-1} \cdots \int_{-\infty}^{t_2} dt_1 T[V_1(t_n) V_1(t_{n-1}) \cdots] e^{\gamma(t_1 + t_2 + \dots + t_n)}. \quad (3.45)$$

(As long as  $t$  does not approach  $+\infty$ , we can leave out the absolute signs in the damping factor.) Using the identity



$$[H_0, ABC \cdots] = [H_0, A] BC \cdots + A[H_0, B] C \cdots + \cdots,$$

we obtain, noting that  $V_I(t) = e^{itH_0/\hbar} V_S e^{-itH_0/\hbar}$ ,

$$\frac{\partial V_I(t)}{\partial t} = i[H_0, V_I(t)] \quad (3.46)$$

provided that  $V_S$ , the perturbation in the Schrödinger picture, is time independent. This leads to

$$[H_0, V_I(t_n) V_I(t_{n-1}) \cdots] = -i\hbar \left( \frac{\partial}{\partial t_n} + \frac{\partial}{\partial t_{n-1}} + \cdots \right) V_I(t_n) V_I(t_{n-1}) \cdots \quad (3.47)$$

and

$$\begin{aligned} [H_0, U_\gamma^{(n)}(t, -\infty)] &= -\frac{1}{n!} \left( \frac{-i}{\hbar} \right)^{(n-1)} \int_{-\infty}^t dt_n \int_{-\infty}^{t_n} dt_{n-1} \cdots \\ &\quad \times T \left[ \left( \frac{\partial}{\partial t_n} + \frac{\partial}{\partial t_{n-1}} + \cdots \right) V_I(t_n) V_I(t_{n-1}) \cdots \right] e^{\gamma(t_1+t_2+\cdots+t_n)}. \end{aligned}$$

When integrating by parts, each term gives the same contribution, yielding

$$[H_0, U_\gamma^{(n)}(t, -\infty)] = -V_I(t) U_\gamma^{(n-1)}(t, -\infty) + i\hbar n\gamma U_\gamma^{(n)}(t, -\infty), \quad (3.48)$$

where the last term originates from derivating the damping term. Introducing an order parameter,  $\lambda$ ,

$$H = H_0 + \lambda V(t), \quad (3.49)$$

the result can be expressed

$$[H_0, U_\gamma(t, -\infty)] = -V_I(t) U_\gamma(t, -\infty) + i\hbar\gamma\lambda \frac{\partial}{\partial \lambda} U_\gamma(t, -\infty). \quad (3.50)$$

By operating with the commutator on the parent function (3.41), utilizing the fact that the parent state  $\Phi^\alpha$  is an eigenstate of  $H_0$ , we obtain for  $t = 0$

$$\left( H_0 - E_0^\alpha + V \right) U_\gamma(0, -\infty) |\Phi^\alpha\rangle = i\hbar\gamma\lambda \frac{\partial}{\partial \lambda} U_\gamma(0, -\infty) |\Phi^\alpha\rangle, \quad (3.51)$$

where  $V = V_I(0)$  or with the state (3.43)

$$(H_0 + V - E_0^\alpha) |\Psi_\gamma^\alpha\rangle = i\hbar\gamma\lambda \frac{\frac{\partial}{\partial \lambda} U_\gamma(0, -\infty) |\Phi^\alpha\rangle}{\langle \Psi_0^\alpha | U_\gamma(0, -\infty) | \Phi^\alpha \rangle}. \quad (3.52)$$

(Note that at  $t = 0$  the Schrödinger and interaction pictures are identical.) We note from the relation (3.43), that

$$\begin{aligned} \frac{\partial}{\partial \lambda} |\Psi_\gamma^\alpha\rangle &= \frac{\partial}{\partial \lambda} \frac{U_\gamma(0, -\infty) |\Phi^\alpha\rangle}{\langle \Psi_0^\alpha | U_\gamma(0, -\infty) | \Phi^\alpha \rangle} = \frac{\frac{\partial}{\partial \lambda} U_\gamma(0, -\infty) |\Phi^\alpha\rangle}{\langle \Psi_0^\alpha | U_\gamma(0, -\infty) | \Phi^\alpha \rangle} \\ &\quad - \frac{\langle \Psi_0^\alpha | \frac{\partial}{\partial \lambda} U_\gamma(0, -\infty) | \Phi^\alpha \rangle}{\langle \Psi_0^\alpha | U_\gamma(0, -\infty) | \Phi^\alpha \rangle} \frac{U_\gamma(0, -\infty) |\Psi_0^\alpha\rangle}{\langle \Psi_0^\alpha | U_\gamma(0, -\infty) | \Phi^\alpha \rangle}. \end{aligned} \quad (3.53)$$

Therefore, the r.h.s. of (3.52) can be expressed

$$i\hbar\gamma\lambda \frac{\frac{\partial}{\partial \lambda} U_\gamma(0, -\infty) |\Phi^\alpha\rangle}{\langle \Psi_0^\alpha | U_\gamma(0, -\infty) | \Phi^\alpha \rangle} = \Delta E_\gamma^\alpha |\Psi_\gamma^\alpha\rangle + i\gamma\lambda \frac{\partial}{\partial \lambda} |\Psi_\gamma^\alpha\rangle,$$

where

$$\Delta E_\gamma^\alpha = i\hbar\gamma\lambda \frac{\langle \Psi_0^\alpha | \frac{\partial}{\partial \lambda} U_\gamma(0, -\infty) | \Phi^\alpha \rangle}{\langle \Psi_0^\alpha | U_\gamma(0, -\infty) | \Phi^\alpha \rangle},$$

and this yields

$$(H_0 + V - E_0^\alpha - \Delta E_\gamma^\alpha) |\Psi_\gamma^\alpha\rangle = i\hbar\gamma\lambda \frac{\partial}{\partial \lambda} |\Psi_\gamma^\alpha\rangle. \quad (3.54)$$

Provided that the perturbation expansion of  $|\Psi_\gamma^\alpha\rangle$  converges, the r.h.s. will vanish as  $\gamma \rightarrow 0$ . Then *the generalized Gell-Mann–Low (GML) relation* reads

$$\boxed{|\Psi^\alpha\rangle = \lim_{\gamma \rightarrow 0} |\Psi_\gamma^\alpha\rangle = \lim_{\gamma \rightarrow 0} \frac{U_\gamma(0, -\infty) |\Phi^\alpha\rangle}{\langle \Psi_0^\alpha | U_\gamma(0, -\infty) | \Phi^\alpha \rangle}.} \quad (3.55)$$

The energy eigenvalue corresponding the Gell-Mann–Low state (3.55) becomes

$$E^\alpha = \lim_{\gamma \rightarrow 0} \left[ E_0^\alpha + i\hbar\gamma\lambda \frac{\langle \Psi_0^\alpha | \frac{\partial}{\partial \lambda} U_\gamma(0, -\infty) | \Phi^\alpha \rangle}{\langle \Psi_0^\alpha | U_\gamma(0, -\infty) | \Phi^\alpha \rangle} \right]. \quad (3.56)$$

This expression is not very useful for evaluating the energy, since the eigenvalue  $E_0^\alpha$  of the parent state is generally not known. The procedure is here used mainly to demonstrate that the functions satisfy the Schrödinger equation. Instead we shall derive an expression for the effective Hamiltonian (2.53), which is the natural tool for a multi-level model space.<sup>5</sup>

---

<sup>5</sup>A necessary condition for the proof of the theorem given here is that the parent state (3.42) is an eigenstate of the model Hamiltonian  $H_0$  (see 3.51). This is in conflict with the statement of Kuo et al. [109], who claim that it is sufficient that this state has a nonzero overlap with the corresponding target state.

In the one-dimensional model space, singularities appear in  $U$  for unlinked terms. In the general multi-dimensional case, singularities can appear also for linked diagrams that have an *intermediate state in the model space*. The remaining diagrams are regular. In addition, so-called *quasi-singularities* can appear—i.e., very large, but finite, contributions—when an intermediate state is *quasi-degeneracy* with the initial state. All singularities and quasi-singularities are eliminated in the ratio (3.55)—in analogy with the original Gell-Mann–Low theorem, although in the general case there is a *finite remainder*, so-called *model-space contribution* (MSC). The elimination of these quasi-singularities represent the major advantage of the procedure using an extended model space. The model-space contributions play a major role in the theory we are constructing here.

**Part II**  
**Bound-State Quantumelectrodynamics:**  
**One- and Two-Photon Exchange**

## Chapter 4

# S-Matrix

In Part I we have considered methods for treating electronic many-body systems within the standard relativistic *Many-Body-Perturbation Theory* (MBPT) and coupled-cluster schemes, in what is known as the *no-virtual-pair approximation* (NVPA). In this second part we shall include effects beyond this approximation, which we refer to as *quantum-electrodynamical (QED) effects*. We concentrate on *bound-state systems*, where the procedure is less developed. We shall describe three methods for numerical calculations of such effects on such systems, developed in the last few decades, which are all based upon field theory.<sup>1</sup>

In the present chapter we introduce the most frequently applied scheme for bound-state QED calculations, namely the *S-matrix formulation*. In this chapter we shall also come into contact with the important question of the choice of gauge. The Maxwell equations are invariant under a certain class of gauge transformations, as shown in Appendix G. So far, practically all QED calculations have been performed using what is known as *covariant gauges*, particularly the Feynman gauge, where the expressions involved are particularly simple. However, for bound-state problems, in combining QED with electron correlation, it is often be more advantageous to use the Coulomb gauge. This is demonstrated, in particular, in connection with numerical applications in Chap. 9. It has been shown by several authors [1, 203] that it is perfectly legitimate use the Coulomb gauge also in QED calculations and that this leads to results that are renormalizable and completely equivalent to those obtained using covariant gauges.

In the next chapter we shall consider the *Green's-function method*, which is frequently used in various fields of physics. In Chap. 6 we shall present the more recently

---

<sup>1</sup>From now on we shall for simplicity set  $\hbar = 1$  but maintain the remaining fundamental constants. In this way our results will be valid in the relativistic or natural unit system as well as in the Hartree atomic unit system. They will also be valid in the cgs unit system, as long as we stay consistently to either the electrostatic or the magnetic version, but they will NOT be valid in the Gaussian system that is a mixture of the two. With our choice it will still be possible to perform a meaningful dimensional analysis (see further Appendix K).

introduced *covariant-evolution operator and Green's-operator method*, which will form the basis for the unified approach we are developing in the chapters that follow.

Unless specified otherwise, we shall continue working in the *Interaction Picture* (IP) (see Sect. 3.2).

## 4.1 Definition of the S-Matrix. Feynman Diagrams

### 4.1.1 General

The *scattering matrix* or *S-matrix* was introduced by John Wheeler [248] and Werner Heisenberg in the 1930s, particularly for studying the scattering processes between elementary particles, primarily free particles. The formalism is not particularly suited for bound-state problems but has in the last few decades been applied also to structure calculations in connection with QED calculations (see, for instance, the review article by Mohr et al. [159] for a modern update). Concerning the application of the S-matrix to **dynamical problems**, see Chap. 13.

The S-matrix relates the initial state of a particle or system of particles,  $\Phi_i = \Phi(t = -\infty)$ , *before* the interaction has taken place, to the final state *after* the interaction is completed,  $\Phi_f = \Phi(t = +\infty)$ ,

$$\Phi(t = +\infty) = S \Phi(t = -\infty). \quad (4.1)$$

We know that the time evolution of the state vector in the interaction picture is governed by the evolution operator (3.15), which leads to the connection

$$S = U(\infty, -\infty). \quad (4.2)$$

This is assumed to hold also relativistically (see, for instance, Bjorken and Drell [22]). With the expansion (3.35) this becomes

$$S = \sum_{n=0}^{\infty} \frac{1}{n!} \left( \frac{-i}{c} \right)^n \int dx_1^4 \dots \int dx_n^4 T[\mathcal{H}(x_1) \dots \mathcal{H}(x_n)] e^{-\gamma(|t_1|+|t_2|+\dots|t_n|)}, \quad (4.3)$$

integrated over all space and time. The zeroth-order component is here equal to unity (c.f., (3.21)).  $x$  is the four-dimensional coordinate vector  $x = (ct, \mathbf{x})$ , which explains the factor of  $c$  in the denominator. The S-matrix is—in contrast to the evolution operator for finite times—*Lorentz covariant* in the limit of vanishing damping (see footnote in the Introduction), which is manifestly demonstrated by its form given here. We shall normally assume that the perturbation density is given by the interaction between the electrons and the electromagnetic radiation field (3.26)

$$\mathcal{H}(x) = -\hat{\psi}^\dagger(x) e c \alpha^\mu A_\mu(x) \hat{\psi}(x). \quad (4.4)$$

This can also be expressed

$$\mathcal{H}(x) = -\bar{\psi}ec\gamma^\mu A_\mu(x)\hat{\psi}(x) = -\bar{\psi}ec\hat{A}(x)\hat{\psi}(x),$$

where  $\bar{\psi} = \hat{\psi}^\dagger\beta$  and  $\gamma^\mu = \beta\alpha^\mu$ , which is the more common notation. In this book, however, we shall base the notations on the use of  $\Psi^\dagger$ , in order to make the formalism more compatible with that of the standard many-body theory. This will have the consequence that some operators, like the electron propagator, will have non-covariant forms. We shall comment upon this when appropriate.

The S-matrix can conveniently be represented by so called *Feynman diagrams*. Feynman has in his famous papers from 1949 [68, 69] developed a set of rules for evaluating the S-matrix for various elementary processes (see Appendix H), and this has formed the basis for much of the developments that followed in quantum electrodynamics and field theory in general (see, for instance, the books by Mandl and Shaw [143, chap. 7] and Peskin and Schroeder [194]). This has also formed the basis for the diagrammatic representation of many-body perturbation theory (MBPT), discussed earlier [124].

In order to represent the S-matrix by means of Feynman diagrams, it has to be transformed into *normal order*, which can be performed by means of Wick's theorem (see Sect. 2.2). This leads to all possible (zero, single, double ...) contractions between the perturbations  $\mathcal{H}$  and to diagrams of the type shown in Fig. 2.9. Each normal-ordered term obtained in this process is represented by a diagram. (Details of this process are found in standard text books, e.g., Fetter and Walecka [67] or Lindgren–Morrison [124].) Below we shall illustrate this by a few simple examples.

### 4.1.2 Bound States

Even if the S-matrix formulation was initially set up for scattering problems for free particles, we shall here be mainly concerned with applications to structure problems for bound-state systems. Since the final time of the scattering process is  $t = +\infty$ , we cannot directly apply the Gell-Mann–Low theorem (3.40 and 3.55). Sucher [236] has, however, modified the Gell-Mann–Low energy formula so that it can be applied also to the S-matrix. With the S-matrix expanded in a perturbation series

$$S = \sum_n S^{(n)} \tag{4.5}$$

the energy shift can be expressed

$$\Delta E = \lim_{\gamma \rightarrow 0} \frac{i\gamma}{2} \frac{\sum_n n \langle \Phi | S^{(n)} | \Phi \rangle}{\langle \Phi | S | \Phi \rangle}. \tag{4.6}$$

This energy formula can also be applied to a *degenerate* multi-state model space—but *not* in the case of *quasi-degeneracy* or any other situation with several distinct energy levels within the model space. Furthermore, in the S-matrix formulation no information can be derived for the corresponding change of the state vector or wave function. For these reasons the S-matrix formulation is not suited as a basis for a unification with many-body perturbation theory, which is our main concern in this book. We shall return to this problem in later chapters.

Before we consider some physical processes, we shall define two very important concepts, namely the *Feynman electron* and *photon propagators* that will be frequently used in the following.

## 4.2 Electron Propagator

The **contraction** between two electron-field operators is defined as *the difference between the time and normal orderings* (see Sect. 2.2)

$$\overbrace{\hat{\psi}(x_1)\hat{\psi}^\dagger(x_2)} = T[\hat{\psi}(x_1)\hat{\psi}^\dagger(x_2)] - N[\hat{\psi}(x_1)\hat{\psi}^\dagger(x_2)]. \quad (4.7)$$

Since the vacuum expectation value vanishes for every normal-ordered product, it follows that *the contraction is equal to the vacuum expectation value of the time-ordered product*<sup>2</sup>

$$\begin{aligned} \overbrace{\hat{\psi}(x_1)\hat{\psi}^\dagger(x_2)} &= \langle 0|T[\hat{\psi}(x_1)\hat{\psi}^\dagger(x_2)]|0\rangle \\ &= \langle 0|\Theta(t_1 - t_2)\hat{\psi}(x_1)\hat{\psi}^\dagger(x_2) - \Theta(t_2 - t_1)\hat{\psi}^\dagger(x_2)\hat{\psi}(x_1)|0\rangle, \end{aligned} \quad (4.8)$$

considering that the electron fields operators are fermions that anticommute.  $\Theta$  is the Heaviside step function (Appendix A, (A.33)).

- **The Feynman electron propagator is defined** (see Fig. 4.1)<sup>3</sup>

$$\overbrace{\hat{\psi}(x_1)\hat{\psi}^\dagger(x_2)} = \langle 0|T[\hat{\psi}(x_1)\hat{\psi}^\dagger(x_2)]|0\rangle =: i S_F(x_1, x_2). \quad (4.9)$$

<sup>2</sup>In field theory the vacuum state is normally the “true” vacuum with no (positive-energy) particles or photons present. In the Dirac picture this implies that the negative-energy states or “hole” states of the “Dirac sea” are filled. In many-body applications without reference to field theory, the “vacuum” is normally a closed-shell state related to the system (finite or infinite) under study, obtained for instance by removing the valence or open-shell single-electron states. Single-electron states present in this vacuum state are referred to as hole states and those not present as virtual or particle states. In our unified approach we shall let hole states include negative-energy (anti-particle) states as well as core states.

<sup>3</sup>Note that we define here the electron propagator, using  $\hat{\psi}^\dagger$  rather than the adjoint field  $\bar{\psi} = \hat{\psi}^\dagger\beta$ , which leads to a non-covariant form of the propagator we denote  $\overline{S}_F$ . The corresponding covariant propagator becomes  $\overline{S}_F = S_F\beta$ .



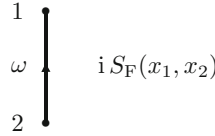


**Fig. 4.1** Graphical representation of the (bound-state) electron propagator. (As before, we shall let *thick vertical lines* represent electron orbitals or propagators in the bound-state representation (Furry picture) and *thin lines* in the free-electron representation

Separating the field operators into particle ( $p$ ) and hole ( $h$ ) parts,  $\hat{\psi} = \hat{\psi}_+ + \hat{\psi}_-$ , above and below the Fermi surface, respectively, it follows that the expression (4.8) is identical to

$$\begin{aligned} & \langle 0 | \Theta(t_1 - t_2) \hat{\psi}_+(x_1) \hat{\psi}_+^\dagger(x_2) - \Theta(t_2 - t_1) \hat{\psi}_-(x_2) \hat{\psi}_-(x_1) | 0 \rangle \\ &= \Theta(t_1 - t_2) \phi_p(x_1) \phi_p^\dagger(x_2) e^{-i\varepsilon_p(t_1-t_2)} - \Theta(t_2 - t_1) \phi_h^\dagger(x_2) \phi_h(x_1) e^{-i\varepsilon_h(t_1-t_2)}, \end{aligned}$$

using the time dependence of the field operators in the interaction picture in Appendix B (B.28).

As will be demonstrated below,

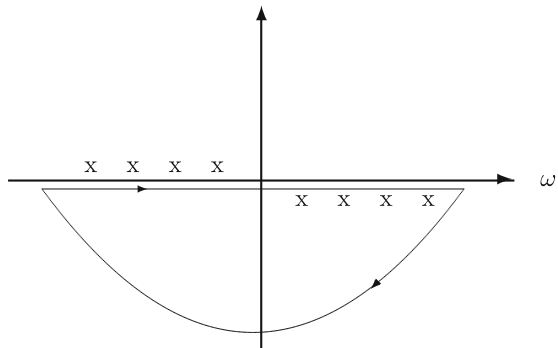
- *the electron propagator can be expressed as a complex integral*

$$S_F(x_1, x_2) = \int \frac{d\omega}{2\pi} \frac{\phi_j(x_1) \phi_j^\dagger(x_2)}{\omega - \varepsilon_j + i\eta \operatorname{sgn}(\varepsilon_j)} e^{-i\omega(t_1-t_2)}, \tag{4.10}$$

where  $\eta$  is a small, positive number.

In order to verify the integral formula (4.10), we first consider the case  $t_1 > t_2$ . Here, the integrand vanishes exponentially as  $\omega \rightarrow -i\infty$ , and we then integrate over the *negative* half-plane, as illustrated in Fig. 4.2. Here, the poles appear at  $\omega = \varepsilon_j$

**Fig. 4.2** Complex integration of the electron propagator (4.10)



when this is positive. The contribution to the integral from this pole is  $-2\pi i$  times the pole value—with the minus sign due to the negative (clockwise) integration—or  $-i\phi_j(\mathbf{x}_1)\phi_j^\dagger(\mathbf{x}_2)e^{-i\varepsilon_j(t_1-t_2)}$ . Similarly, when  $t_1 < t_2$ , we integrate over the *positive* half plane with the result  $+i\phi_j(\mathbf{x}_1)\phi_j^\dagger(\mathbf{x}_2)e^{-i\varepsilon_j(t_1-t_2)}$ , when  $\varepsilon_j$  is negative. It then follows that  $iS_F$ , as defined by the integral, is identical to the time-ordered vacuum expectation (4.8).

- *The Fourier transform of the electron propagator with respect to time is*

$$\boxed{S_F(\omega; \mathbf{x}_1, \mathbf{x}_2) = \frac{\phi_j(\mathbf{x}_1)\phi_j^\dagger(\mathbf{x}_2)}{\omega - \varepsilon_j + i\eta \operatorname{sgn}(\varepsilon_j)},} \quad (4.11)$$

which can be regarded as the *coordinate representation* (see Appendix C)

$$S_F(\omega; \mathbf{x}_1, \mathbf{x}_2) = \langle \mathbf{x}_1 | \hat{S}_F(\omega) | \mathbf{x}_2 \rangle = \frac{\langle \mathbf{x}_1 | j \rangle \langle j | \mathbf{x}_2 \rangle}{\omega - \varepsilon_j + i\eta \operatorname{sgn}(\varepsilon_j)} \quad (4.12)$$

of the operator<sup>4</sup>

$$\hat{S}_F(\omega) = \frac{|j\rangle \langle j|}{\omega - \varepsilon_j (1 - i\eta)}. \quad (4.13)$$

Using the relation (D.52) in Appendix D, this can also be expressed

$$\hat{S}_F(\omega) = \frac{1}{\omega - \hat{h}_D (1 - i\eta)}, \quad (4.14)$$

where  $\hat{h}_D$  is the Dirac Hamiltonian *operator*.

The contraction has so far been defined only for  $t_1 \neq t_2$ . For the bound-state problem it is necessary to consider also *equal-time contractions*. We then define the time-ordering for equal time as

$$T[\psi(x_1)\psi^\dagger(x_2)] = \frac{1}{2} [\psi(x_1)\psi^\dagger(x_2) - \psi^\dagger(x_2)\psi(x_1)] \quad (t_1 = t_2). \quad (4.15)$$

In this case we have

$$\begin{aligned} \overbrace{\psi(x_1)\psi^\dagger(x_2)} &= \langle 0 | T[\psi(x_1)\psi^\dagger(x_2)] | 0 \rangle = \frac{1}{2} \langle 0 | \psi(x_1)\psi^\dagger(x_2) - \psi^\dagger(x_2)\psi(x_1) | 0 \rangle \\ &= \frac{1}{2} \sum_p \phi_p(\mathbf{x}_1)\phi_p^\dagger(\mathbf{x}_2) - \frac{1}{2} \sum_h \phi_h(\mathbf{x}_1)\phi_h^\dagger(\mathbf{x}_2) = \frac{1}{2} \sum_j \operatorname{sgn}(\varepsilon_j)\phi_j(\mathbf{x}_1)\phi_j^\dagger(\mathbf{x}_2), \end{aligned}$$

---

<sup>4</sup>As stated before, we use the ‘hat’ symbol to emphasize that the quantity is an *operator*. In cases where this is obvious, the hat will normally be omitted.

where  $j$  as before runs over particles and holes. This can still be expressed by the integral above, as can be seen from the relation

$$\begin{aligned} \frac{1}{\varepsilon_j - z - i\eta \operatorname{sgn}(\varepsilon_j)} &= \frac{\varepsilon_j - z}{(\varepsilon_j - z)^2 + \eta^2} + \frac{i\eta \operatorname{sgn}(\varepsilon_j)}{(\varepsilon_j - z)^2 + \eta^2} \\ &= \mathcal{P} \frac{1}{\varepsilon_j - z} + i\pi \operatorname{sgn}(\varepsilon_j) \delta(\varepsilon_j - z). \end{aligned} \quad (4.16)$$

$\mathcal{P}$  stands for the *principal-value integration*, which does not contribute here. Therefore, *the electron-propagator expression (4.10) is valid also for equal times.*

### 4.3 Photon Propagator

The exchange of a single photon between the electrons corresponds to a *contraction* (2.29) of two photon-field operators (3.27), defined as in the electron-field case (4.7),

$$\begin{aligned} \overline{A_\mu(x_1)A_\nu(x_2)} &= \langle 0 | T [A_\mu(x_1)A_\nu(x_2)] | 0 \rangle \\ &= \langle 0 | \Theta(t_1 - t_2) A_\mu(x_1) A_\nu(x_2) + \Theta(t_2 - t_1) A_\nu(x_2) A_\mu(x_1) | 0 \rangle \end{aligned} \quad (4.17)$$

(the photon-field operators commute in contrast to the electron-field operators), and in analogy with the electron propagator.

- *the Feynman photon propagator is defined* (see Fig. 4.3)

$$\overline{A_\mu(x_1)A_\nu(x_2)} = \langle 0 | T [A_\mu(x_1)A_\nu(x_2)] | 0 \rangle =: i D_{F\mu\nu}(x_1, x_2). \quad (4.18)$$

We shall also sometimes for convenience use the short-hand notation

$$D_F(x_1, x_2) = \alpha^\mu \alpha^\nu D_{F\mu\nu}(x_1, x_2), \quad (4.19)$$

using the summation convention.

With  $A_\mu = A_\mu^+ + A_\mu^-$  we see that (4.17) is identical to

$$\langle 0 | \Theta(t_1 - t_2) [A_\mu^+(x_1), A_\nu^-(x_2)] + \Theta(t_2 - t_1) [A_\nu^+(x_2), A_\mu^-(x_1)] | 0 \rangle,$$

$$1, \mu \quad \bullet \quad \overset{z}{\rightsquigarrow} \quad \bullet \quad \nu, 2 \quad i D_{F\nu\mu}(x_2, x_1)$$

**Fig. 4.3** Graphical representation of the photon propagator

where the square bracket with a comma between the operators represents the commutator (2.12) and noting that the photon-field operators do commute.

Before evaluating the photon propagator we have to make a choice of gauge (see Appendix G.2). In so-called *covariant gauges* the field components are related by a Lorentz transformation. Most commonly used of the covariant gauges is the *Feynman gauge*, because of its simplicity. In our work with combined QED and electron correlation, however, it will for different reasons, to be discussed later, be more advantageous to use the *non-covariant Coulomb gauge*. We shall demonstrate that this is quite feasible, although not always straightforward.

### 4.3.1 Feynman Gauge

In the *Feynman gauge* we have, using the commutation rule (G.11) in Appendix G,

$$\begin{aligned} [A_\mu^+(x_1), A_\nu^-(x_2)] &= \frac{1}{2\epsilon_0\omega V} \epsilon_{\mu r} \epsilon_{\nu r'} [a_{\mathbf{k}r}, a_{\mathbf{k}'r'}^\dagger] e^{-i(kx_1 - k'x_2)} \\ &= -\frac{1}{2\epsilon_0\omega V} g_{\mu\nu} \delta_{\mathbf{k},\mathbf{k}'} \delta_{r,r'} e^{-ik(x_1 - x_2)}. \end{aligned}$$

With  $kx_1 = k_0x_{10} - \mathbf{k} \cdot \mathbf{x}_1$  and  $k'x_2 = k'_0x_{20} - \mathbf{k}' \cdot \mathbf{x}_2$  ( $x_0 = ct$ ,  $\omega = ck_0$ ) this yields for the vacuum expectation in (4.18)

$$\begin{aligned} &\langle 0|T[A_\mu(x_1)A_\nu(x_2)]|0\rangle \\ &= -\frac{1}{2\epsilon_0ck_0V} g_{\mu\nu} \left[ \Theta(t_1 - t_2) e^{-ik(x_1 - x_2)} + \Theta(t_2 - t_1) e^{ik(x_1 - x_2)} \right] \\ &= -g_{\mu\nu} \sum_{\mathbf{k}} \frac{1}{2\epsilon_0ck_0V} e^{i\mathbf{k} \cdot \mathbf{r}_{12}} \left[ \Theta(t_1 - t_2) e^{-ik_0(x_{10} - x_{20})} + \Theta(t_2 - t_1) e^{ik_0(x_{10} - x_{20})} \right] \end{aligned} \quad (4.20)$$

with  $\mathbf{r}_{12} = \mathbf{x}_1 - \mathbf{x}_2$ . The sign of the exponent  $\mathbf{k} \cdot \mathbf{r}_{12}$  is immaterial.

The expression in the square brackets of (4.20) can in analogy with (4.10) be written as a complex integral

$$\Theta(t_1 - t_2) e^{-ik_0(x_{10} - x_{20})} + \Theta(t_2 - t_1) e^{ik_0(x_{10} - x_{20})} = 2ik_0 \int_{-\infty}^{\infty} \frac{dq}{2\pi} \frac{e^{-iq(x_{10} - x_{20})}}{q^2 - k_0^2 + i\eta}. \quad (4.21)$$

Thus (see Appendix D.2),

$$\begin{aligned} \langle 0|T[A_\mu(x_1)A_\nu(x_2)]|0\rangle &= -ig_{\mu\nu} \frac{1}{\epsilon_0 c V} \sum_{\mathbf{k}} e^{i\mathbf{k}\cdot\mathbf{r}_{12}} \int_{-\infty}^{\infty} \frac{dq}{2\pi} \frac{e^{-iq(x_{10}-x_{20})}}{q^2 - \mathbf{k}^2 + i\eta} \\ &\rightarrow -ig_{\mu\nu} \frac{1}{c\epsilon_0} \int \frac{d^3\mathbf{k}}{(2\pi)^3} e^{i\mathbf{k}\cdot\mathbf{r}_{12}} \int_{-\infty}^{\infty} \frac{dq}{2\pi} \frac{e^{-iq(x_{10}-x_{20})}}{q^2 - \mathbf{k}^2 + i\eta} \end{aligned} \quad (4.22)$$

with  $k_0 = |\mathbf{k}|$ , and the photon propagator (4.18) becomes in the *Feynman gauge* (c.f. Appendix (F.62))

$$\begin{aligned} D_{F\mu\nu}^F(x_1, x_2) &= -\frac{g_{\mu\nu}}{c\epsilon_0} \int \frac{d^3\mathbf{k}}{(2\pi)^3} e^{i\mathbf{k}\cdot\mathbf{r}_{12}} \int_{-\infty}^{\infty} \frac{dq}{2\pi} \frac{e^{-iq(x_{10}-x_{20})}}{q^2 - \mathbf{k}^2 + i\eta} \\ &= -\frac{g_{\mu\nu}}{\epsilon_0} \int \frac{d^3\mathbf{k}}{(2\pi)^3} e^{i\mathbf{k}\cdot\mathbf{r}_{12}} \int_{-\infty}^{\infty} \frac{dz}{2\pi} \frac{e^{-iz(t_1-t_2)}}{z^2 - c^2\mathbf{k}^2 + i\eta}, \end{aligned} \quad (4.23)$$

where  $z = cq$  is the energy parameter. It then follows that

- ***the Fourier transform of the photon propagator with respect to  $x_0 = ct$  becomes in the Feynman gauge***

$$D_{F\mu\nu}^F(q; \mathbf{x}_1, \mathbf{x}_2) = -\frac{g_{\mu\nu}}{c\epsilon_0} \int \frac{d^3\mathbf{k}}{(2\pi)^3} \frac{e^{i\mathbf{k}\cdot\mathbf{r}_{12}}}{q^2 - \mathbf{k}^2 + i\eta} \quad (4.24)$$

and the inverse transformation becomes

$$D_{F\mu\nu}^F(x_1, x_2) = \int \frac{dq}{2\pi} D_{F\mu\nu}^F(q; \mathbf{x}_1, \mathbf{x}_2) e^{-iq(x_{10}-x_{20})}. \quad (4.25)$$

After integration over the angular part (see Appendix J) this becomes

$$D_{F\mu\nu}^F(q; \mathbf{x}_1, \mathbf{x}_2) = -\frac{g_{\mu\nu}}{4\pi^2 c\epsilon_0 r_{12}} \int_0^\infty \frac{2\kappa d\kappa \sin \kappa r_{12}}{q^2 - \kappa^2 + i\eta}, \quad (4.26)$$

where  $\kappa = |\mathbf{k}|$  and  $q = k_0$  is now decoupled from  $|\mathbf{k}|$ .<sup>5</sup> Fourier transforming (4.25) with respect to space, yields

$$D_{F\mu\nu}^F(q; \mathbf{k}) = -\frac{g_{\mu\nu}}{c\epsilon_0} \frac{1}{q^2 - \kappa^2 + i\eta} \quad (4.27)$$

<sup>5</sup>In some literature  $|\mathbf{k}|$  is denoted by  $k$ , but here we introduce a new notation ( $\kappa$ ), reserving  $k$  for the four-dimensional vector, in order to avoid confusion.

or in covariant notation

$$D_{F\mu\nu}^F(k) = -\frac{g_{\mu\nu}}{c\epsilon_0} \frac{1}{k^2 + i\eta}, \quad (4.28)$$

where  $k$  is the four-dimensional momentum vector,  $k^2 = k_0^2 - \mathbf{k}^2$ .

The Fourier transforms with respect to time are similarly

$$\begin{aligned} D_{F\mu\nu}^F(z; \mathbf{x}_1, \mathbf{x}_2) &= -\frac{g_{\mu\nu}}{\epsilon_0} \int \frac{d^3\mathbf{k}}{(2\pi)^3} \frac{e^{i\mathbf{k}\cdot\mathbf{r}_{12}}}{q^2 - \mathbf{k}^2 + i\eta} \\ &= -\frac{g_{\mu\nu}}{4\pi^2\epsilon_0 r_{12}} \int_0^\infty \frac{2\kappa d\kappa \sin \kappa r_{12}}{z^2 - c^2\kappa^2 + i\eta}, \end{aligned} \quad (4.29)$$

$$D_{F\mu\nu}^F(z; \mathbf{k}) = -\frac{g_{\mu\nu}}{\epsilon_0} \frac{1}{z^2 - c^2\kappa^2 + i\eta}, \quad (4.30)$$

which differ from the previous transforms with respect to momentum (4.26) and (4.27) by a factor of  $c$  (see Appendix K.2).  $z = cq$  is the energy parameter. The inverse transformation is here

$$D_{F\mu\nu}^F(x_1, x_2) = \int \frac{dz}{2\pi} D_{F\mu\nu}^F(z; \mathbf{x}_1, \mathbf{x}_2) e^{-iz(t_1-t_2)}. \quad (4.31)$$

### 4.3.2 Coulomb Gauge

Above we have found an expression for the photon propagator in the Feynman gauge, and by means of the formulas for gauge transformation in Appendix G.2 we can derive the corresponding expressions in other gauges.

In the *Coulomb gauge* (G.19) the scalar part ( $\mu\nu = 00$ ) of the photon propagator is

$$D_{F00}^C(k) = \frac{1}{c\epsilon_0 \mathbf{k}^2}. \quad (4.32)$$

Transforming back to 4-dimensional space yields according to (4.23)

$$\begin{aligned} D_{F00}^C(x_1, x_2) &= \frac{1}{c\epsilon_0} \int \frac{d^3\mathbf{k}}{(2\pi)^3} \frac{e^{i\mathbf{k}\cdot\mathbf{r}_{12}}}{\mathbf{k}^2} \int \frac{dk_0}{2\pi} e^{-ik_0(x_{01}-x_{02})} \\ &= \frac{1}{4\pi^2 c\epsilon_0 r_{12}} \int_0^\infty \frac{2\kappa d\kappa \sin \kappa r_{12}}{\kappa^2} \int \frac{dk_0}{2\pi} e^{-ik_0(x_{01}-x_{02})}, \end{aligned}$$

using the relation (J.17). With  $x_0 = ct$  and  $z = ck_0$  this can be expressed

$$D_{F00}^C(x_1, x_2) = \frac{V_C}{e^2 c^2} \int \frac{dz}{2\pi} e^{-iz(t_1 - t_2)}, \quad (4.33)$$

where  $V_C$  is the Coulomb interaction (2.109). With the damping factor the integral tends to a delta function (A.16)

$$D_{F00}^C(x_1, x_2) \Rightarrow \frac{V_C}{e^2 c^2} \delta(t_1 - t_2), \quad (4.34)$$

but we shall normally use the more explicit expression (4.33).

From the relation (4.33) we find that the Fourier transform with respect to time becomes

$$D_{F00}^C(z; \mathbf{x}_1, \mathbf{x}_2) = \frac{1}{4\pi^2 c^2 \epsilon_0 r_{12}} \int_0^\infty \frac{2\kappa d\kappa \sin \kappa r_{12}}{\kappa^2} = \frac{V_C}{e^2 c^2}. \quad (4.35)$$

The vector part of the photon propagator in the Coulomb gauge is according to (G.19) ( $q = k_0$ )

$$D_{Fij}^C(k) = -\frac{1}{c\epsilon_0(k^2 + i\eta)} \left( g_{ij} + \frac{k_i k_j}{\mathbf{k}^2} \right), \quad (4.36)$$

and transformation back to the 3-dimensional space yields

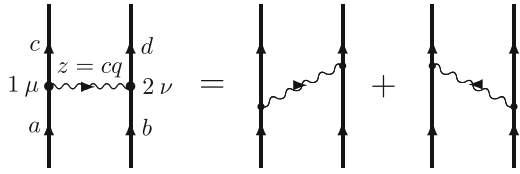
$$\begin{aligned} D_{Fij}^C(q; \mathbf{x}_1, \mathbf{x}_2) &= -\frac{1}{c\epsilon_0} \int \frac{d^3\mathbf{k}}{(2\pi)^3} \frac{e^{i\mathbf{k}\cdot\mathbf{r}_{12}}}{q^2 - \mathbf{k}^2 + i\eta} \left( g_{ij} + \frac{k_i k_j}{\mathbf{k}^2} \right) \\ &= -\frac{1}{c\epsilon_0} \int_0^\infty \frac{2\kappa d\kappa \sin \kappa r_{12}}{q^2 - \kappa^2 + i\eta} \left( g_{ij} + \frac{k_i k_j}{\mathbf{k}^2} \right) \\ &= c D_{Fij}^C(z; \mathbf{x}_1, \mathbf{x}_2) \quad (z = cq). \end{aligned} \quad (4.37)$$

Again, we see that these transformations differ by a factor of  $c$ .

## 4.4 Single-Photon Exchange

We consider now the exchange of a single photon between the electrons, represented by the Feynman diagram in Fig. 4.4 (left). We start with a general covariant gauge, like the Feynman gauge, and consider then the non-covariant Coulomb gauge.

**Fig. 4.4** The Feynman representation of the exchange of a single, virtual photon between two electrons. This contains two time-orderings



#### 4.4.1 Covariant Gauge

The *second-order* S-matrix (4.3) for a single-photon exchange is given by the contraction of the electromagnetic fields

$$S^{(2)} = \frac{1}{2} \left( \frac{-i}{c} \right)^2 \iint d^4x_2 d^4x_1 T \left[ \overbrace{\mathcal{H}(x_2) \mathcal{H}(x_1)} \right] e^{-\gamma(|t_1|+|t_2|)}. \quad (4.38)$$

With the interaction density (4.4) this becomes

$$S^{(2)} = \frac{(ie)^2}{2} \iint d^4x_2 d^4x_1 T \left[ \overbrace{(\psi^\dagger(x) \alpha^\nu A_\nu(x) \psi(x))_2 (\psi^\dagger(x) \alpha^\mu A_\mu(x) \psi(x))_1} \right] e^{-\gamma(|t_1|+|t_2|)}, \quad (4.39)$$

where the contraction between the radiation-field operators yields the photon propagator,  $iD_{F\mu\nu}$  (4.18), or with the short-hand notation (4.19),

$$S^{(2)} = \frac{(ie)^2}{2} \iint d^4x_2 d^4x_1 \psi^\dagger(x_1) \psi^\dagger(x_2) iD_F(x_2, x_1) \psi(x_2) \psi(x_1) e^{-\gamma(|t_1|+|t_2|)}. \quad (4.40)$$

Identification with the second-quantized form (see Appendix B)

$$S^{(2)} = \frac{1}{2} c_c^\dagger c_d^\dagger \langle cd | S^{(2)} | ab \rangle c_b c_a, \quad (4.41)$$

yields a particular matrix element of the  $S^{(2)}$  matrix

$$\begin{aligned} \langle cd | S^{(2)} | ab \rangle &= - \iint d^4x_2 d^4x_1 \phi_c^\dagger(x_1) \phi_d^\dagger(x_2) ie^2 D_F(x_2, x_1) \\ &\quad \times \phi_b(x_2) \phi_a(x_1) e^{-\gamma(|t_1|+|t_2|)} = \int \frac{dz}{2\pi} \langle cd | -ie^2 D_F(z, \mathbf{x}_2, \mathbf{x}_1) | ab \rangle \\ &\quad \times \iint c^2 dt_1 dt_2 e^{-it_1(\varepsilon_a - \varepsilon_c - z)} e^{-it_2(\varepsilon_b - \varepsilon_d + z)} e^{-\gamma(|t_1|+|t_2|)}, \end{aligned} \quad (4.42)$$



using the Fourier transform (4.31). After performing the time integrations (A.18), this becomes

$$\begin{aligned} \langle cd | S^{(2)} | ab \rangle &= \int \frac{dz}{2\pi} \langle cd | -ie^2 c^2 D_F(z, \mathbf{x}_2, \mathbf{x}_1) | ab \rangle \\ &\quad \times 2\pi \Delta_\gamma(\varepsilon_a - z - \varepsilon_c) 2\pi \Delta_\gamma(\varepsilon_b + z - \varepsilon_d). \end{aligned} \quad (4.43)$$

• **We introduce the single-photon interaction**

$$\boxed{I(x_1, x_2) = V_{\text{sp}}(x_1, x_2) = e^2 c^2 \alpha_1^\mu \alpha_2^\nu D_{F\mu\nu}(x_1, x_2) = e^2 c^2 D_F(x_1, x_2)} \quad (4.44)$$

with the Fourier transform with respect to time

$$I(z; \mathbf{x}_1, \mathbf{x}_2) = e^2 c^2 \alpha_1^\mu \alpha_2^\nu D_{F\mu\nu}(z; \mathbf{x}_1, \mathbf{x}_2) = e^2 c^2 D_F(z; \mathbf{x}_1, \mathbf{x}_2), \quad (4.45)$$

which has the form of an energy potential. We shall generally express *the Fourier transform of the interaction with respect to time* as

$$\boxed{I(z; \mathbf{x}_1, \mathbf{x}_2) = e^2 c^2 \alpha_1^\mu \alpha_2^\nu D_{F\mu\nu}(z; \mathbf{x}_1, \mathbf{x}_2) = \int \frac{2c^2 \kappa d\kappa f(\kappa, \mathbf{x}_1, \mathbf{x}_2)}{z^2 - c^2 \kappa^2 + i\eta}}, \quad (4.46)$$

where  $f(\kappa, \mathbf{x}_1, \mathbf{x}_2)$  is a gauge-dependent function. This transform, as well as the function  $f(\kappa, \mathbf{x}_1, \mathbf{x}_2)$ , has the dimension of energy (or  $s^{-1}$  with our convention with  $\hbar = 1$ ).<sup>6</sup>

With the notation above the S-matrix element (4.43) becomes

$$\langle cd | S^{(2)} | ab \rangle = \int \frac{dz}{2\pi} \langle cd | -iI(z) | ab \rangle 2\pi \Delta_\gamma(\varepsilon_a - z - \varepsilon_c) 2\pi \Delta_\gamma(\varepsilon_b + z - \varepsilon_d) \quad (4.47)$$

in agreement with the evaluation rules in Sect. 4.7. In Appendix A.3 it is shown that

$$\begin{aligned} &\int \frac{dz}{2\pi} 2\pi \Delta_\gamma(a - z) 2\pi \Delta_\gamma(b - z) \frac{1}{z^2 - c^2 \kappa^2 + i\eta} \\ &= 2\pi \Delta_{2\gamma}(a - b) \frac{1}{z^2 - c^2 \kappa^2 + i\gamma}, \end{aligned} \quad (4.48)$$

where we observe that the infinitesimally small quantity  $\eta$ , appearing in the propagators in order to indicate the position of the poles, is replaced by the adiabatic damping parameter,  $\gamma$ , which is a finite quantity (that eventually tends to zero). This gives

---

<sup>6</sup>The constants of the expressions can be conveniently checked by dimensional analysis (see Appendix K.2).

$$\langle cd|S^{(2)}|ab\rangle = 2\pi\Delta_{2\gamma}(\varepsilon_a + \varepsilon_b - \varepsilon_c - \varepsilon_d)\langle cd|-iI(z)|ab\rangle \quad (4.49)$$

with  $z = cq = \varepsilon_a - \varepsilon_c$ . This can also be expressed

$$\langle cd|S^{(2)}|ab\rangle \Rightarrow 2\pi\Delta_{2\gamma}(E_{\text{in}} - E_{\text{out}})\langle cd|-iI(z)|ab\rangle, \quad (4.50)$$

where  $E_{\text{in}}$  and  $E_{\text{out}}$  are the incoming and outgoing energies, respectively. Using the Sucher energy formula (4.6) and the relation (A.20)

$$\lim_{\gamma \rightarrow 0} 2\pi\gamma\Delta_{2\gamma}(x) = \delta_{x,0}, \quad (4.51)$$

the corresponding energy shift becomes

$$\Delta E^{(1)} = \delta_{E_{\text{in}}, E_{\text{out}}}\langle cd|I(z)|ab\rangle. \quad (4.52)$$

Assuming that  $\Phi_{\text{out}} = \Phi_{\text{in}} = \Phi$  is the antisymmetrized state

$$|\Phi\rangle = |\{ab\}\rangle = \frac{1}{\sqrt{2}}[|ab\rangle - |ba\rangle]$$

the *first-order energy shift* becomes

$$\Delta E = \langle \Phi|I(z)|\Phi\rangle = \langle ab|I(z)|ab\rangle - \langle ba|I(z)|ab\rangle, \quad (4.53)$$

which is consistent with the *interpretation of the interaction  $I(z)$  as an equivalent energy-dependent perturbing potential*.

We have seen here that *the time integration—in the limit  $\gamma \rightarrow 0$ —leads to*

- **energy conservation at each vertex with the propagator energy parameters treated as energies.**

Due to the energy conservation of the scattering process, only diagonal (“on-the-energy-shell”) matrix elements are obtained from the analysis of the S-matrix. Therefore, the technique cannot be used for studying quasi-degenerate states by means of the extended-model-space technique (see Sect. 2.3). *Off-diagonal elements* needed for this approach cannot be evaluated by the S-matrix formalism but can be obtained by means of the Green’s-operator technique, described in Chap. 6, which represents an extension of the formalism.

From the above we see that in the S-matrix we shall insert

- **for single-photon exchange** (see Sect. 4.7)

$$-iI(z; \mathbf{x}_1, \mathbf{x}_2) = -ie^2c^2\alpha_1^\mu\alpha_2^\nu D_{F\mu\nu}(z; \mathbf{x}_1, \mathbf{x}_2) = -ie^2c^2D_F(z; \mathbf{x}_1, \mathbf{x}_2).$$

### 4.4.1.1 Feynman Gauge

With the expression (4.29) of the photon propagator in Feynman gauge the corresponding interaction (4.45) becomes ( $z = cq$ )

$$I^F(z; \mathbf{x}_1, \mathbf{x}_2) = -\frac{e^2}{4\pi^2\epsilon_0 r_{12}} \alpha_1^\mu \alpha_{2\mu} \int \frac{2\kappa d\kappa \sin \kappa r_{12}}{q^2 - \kappa^2 + i\eta}. \quad (4.54)$$

The corresponding  $f$  function in (4.46) then becomes

$$f^F(\kappa, \mathbf{x}_1, \mathbf{x}_2) = -\frac{e^2}{4\pi^2\epsilon_0} \alpha_1^\mu \alpha_{2\mu} \frac{\sin \kappa r_{12}}{r_{12}} = -\frac{e^2}{4\pi^2\epsilon_0} (1 - \boldsymbol{\alpha}_1 \cdot \boldsymbol{\alpha}_2) \frac{\sin \kappa r_{12}}{r_{12}}. \quad (4.55)$$

Evaluating the integral in (4.54), using the result in Appendix J, we obtain

$$I^F(z; \mathbf{x}_1, \mathbf{x}_2) = \frac{e^2}{4\pi\epsilon_0 r_{12}} (1 - \boldsymbol{\alpha}_1 \cdot \boldsymbol{\alpha}_2) e^{i|z|r_{12}/c}, \quad (4.56)$$

which agrees with the semiclassical potential (Appendix F.73).

### 4.4.2 Non-covariant Coulomb Gauge

In the Coulomb gauge we separate the interaction into the *instantaneous Coulomb part* and the *time-dependent transverse (Breit) part*,

$$I^C = I_C^C + I_T^C. \quad (4.57)$$

The transverse part of the interaction can be treated in analogy with the covariant gauges. According to (4.44) we have

$$I_T^C(x_1, x_2) = e^2 c^2 \alpha_1^i \alpha_2^j D_{\text{Fij}}^C(x_1, x_2), \quad (4.58)$$

which with (4.37) yields (with  $z = cq$ )

$$\begin{aligned} I_T^C(z; \mathbf{x}_1, \mathbf{x}_2) &= \frac{e^2}{\epsilon_0} \int \frac{d^3\mathbf{k}}{(2\pi)^3} \left( \boldsymbol{\alpha}_1 \cdot \boldsymbol{\alpha}_2 - \frac{(\boldsymbol{\alpha}_1 \cdot \mathbf{k})(\boldsymbol{\alpha}_2 \cdot \mathbf{k})}{k^2} \right) \frac{e^{i\mathbf{k} \cdot \mathbf{r}_{12}}}{q^2 - k^2 + i\eta} \\ &= \frac{e^2}{\epsilon_0} \int \frac{d^3\mathbf{k}}{(2\pi)^3} \left( \boldsymbol{\alpha}_1 \cdot \boldsymbol{\alpha}_2 - \frac{(\boldsymbol{\alpha}_1 \cdot \nabla_1)(\boldsymbol{\alpha}_2 \cdot \nabla_2)}{k^2} \right) \frac{e^{i\mathbf{k} \cdot \mathbf{r}_{12}}}{q^2 - k^2 + i\eta} \\ &= \frac{e^2}{4\pi^2\epsilon_0 r_{12}} \int \frac{2\kappa d\kappa \sin \kappa r_{12}}{q^2 - \kappa^2 + i\eta} \left( \boldsymbol{\alpha}_1 \cdot \boldsymbol{\alpha}_2 - \frac{(\boldsymbol{\alpha}_1 \cdot \nabla_1)(\boldsymbol{\alpha}_2 \cdot \nabla_2)}{\kappa^2} \right), \end{aligned} \quad (4.59)$$

and the corresponding  $f$  function becomes (4.46)

$$f_T^C(\kappa, \mathbf{x}_1, \mathbf{x}_2) = \frac{e^2}{4\pi^2\epsilon_0} \frac{\sin(\kappa r_{12})}{r_{12}} \left[ \boldsymbol{\alpha}_1 \cdot \boldsymbol{\alpha}_2 - \frac{(\boldsymbol{\alpha}_1 \cdot \nabla_1)(\boldsymbol{\alpha}_2 \cdot \nabla_2)}{\kappa^2} \right]. \quad (4.60)$$

Performing the  $\kappa$  integration in (4.59), using the integrals in Appendix J, yields for the transverse (Breit) part

$$I_T^C(z; \mathbf{x}_1, \mathbf{x}_2) = -\frac{e^2}{4\pi\epsilon_0} \left[ \boldsymbol{\alpha}_1 \cdot \boldsymbol{\alpha}_2 \frac{e^{i|z|r_{12}}}{r_{12}} - (\boldsymbol{\alpha}_1 \cdot \nabla_1)(\boldsymbol{\alpha}_2 \cdot \nabla_2) \frac{e^{i|z|r_{12}} - 1}{z^2 r_{12}} \right]. \quad (4.61)$$

This agrees with the semi-classical result obtained in Appendix F.2 (F.54).

The *instantaneous Breit interaction* is obtained by letting  $z \Rightarrow 0$ ,

$$I^{\text{Breit}} = B_{12}^{\text{Inst}} = -\frac{e^2}{4\pi\epsilon_0 r_{12}} \left[ \frac{1}{2} \boldsymbol{\alpha}_1 \cdot \boldsymbol{\alpha}_2 + \frac{(\boldsymbol{\alpha}_1 \cdot \mathbf{r}_{12})(\boldsymbol{\alpha}_1 \cdot \mathbf{r}_{12})}{2r_{12}^2} \right], \quad (4.62)$$

which is the interaction in the Dirac-Coulomb-Breit approximation (NVPA) (2.112) and agrees with the expression derived in Appendix F (F.55). The instantaneous Coulomb and Breit interactions are illustrated in Fig. 4.5.

The (instantaneous) Coulomb part of the interaction becomes, using the relations (4.33) and (4.35),

$$I_C^C(x_1, x_2) = \frac{e^2}{4\pi^2\epsilon_0 r_{12}} \int \frac{2\kappa d\kappa \sin \kappa r_{12}}{\kappa^2} \int \frac{dz}{2\pi} e^{-iz(t_1-t_2)} = V_C \int \frac{dz}{2\pi} e^{-iz(t_1-t_2)} \quad (4.63a)$$

$$I_C^C(z; \mathbf{x}_1, \mathbf{x}_2) = \frac{e^2}{4\pi^2\epsilon_0 r_{12}} \int \frac{2\kappa d\kappa \sin \kappa r_{12}}{\kappa^2} = V_C. \quad (4.63b)$$

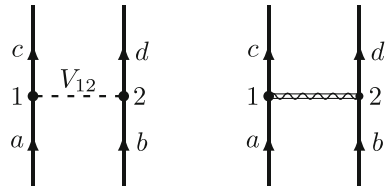
This leads to, using (4.43),

$$\langle cd | S^{(2)} | ab \rangle = \int \frac{dz}{2\pi} \langle cd | -iV_C | ab \rangle 2\pi \Delta_\gamma(\varepsilon_a - z - \varepsilon_c) 2\pi \Delta_\gamma(\varepsilon_b + z - \varepsilon_d)$$

and in analogy with (4.49)

$$\langle cd | S^{(2)} | ab \rangle = \langle cd | -iV_C | ab \rangle \Delta_{2\gamma}(\varepsilon_a + \varepsilon_b - \varepsilon_c - \varepsilon_d).$$

**Fig. 4.5** Instantaneous Coulomb and Breit interactions between the electrons



The Sucher energy formula (4.6) then gives the expected result for the first-order energy shift

$$\Delta E^{(1)} = \delta_{E_{in}, E_{out}} \langle cd | V_C | ab \rangle, \tag{4.64}$$

where, as before,  $E_{in} = \varepsilon_a + \varepsilon_b$  is the initial and  $E_{out} = \varepsilon_c + \varepsilon_d$  is the final energy. Again, this demonstrates that the interaction (4.45) represents an equivalent interaction potential and that the energy is conserved for the scattering or S-matrix.

### 4.4.3 Single-Particle Potential

Finally, we consider in this subsection the simple case of an interaction between a single electron and a time-independent external field,  $A_\mu(\mathbf{x})$  (Fig. 4.6). Here, the scattering amplitude becomes from (4.3) with the interaction density (4.4)

$$S^{(1)} = \int d^4x \hat{\psi}^\dagger(x) ie\alpha^\mu A_\mu(\mathbf{x}) \hat{\psi}(x) e^{-\gamma|t|}. \tag{4.65}$$

In analogy with the previous cases this yields ( $dx_0 = c dt$ )

$$\langle b | S^{(1)} | a \rangle = iec \langle b | \alpha^\mu A_\mu | a \rangle 2\pi \Delta_\gamma(\varepsilon_a - \varepsilon_b). \tag{4.66}$$

with  $A_\mu = (\phi/c, -\mathbf{A})$  according to (F.6) in Appendix F.

Considering a scalar **energy** potential,  $V(\mathbf{x}) = -e\phi(\mathbf{x}) = -ecA_0$ , the S-matrix element becomes

$$\langle b | S^{(1)} | a \rangle = 2\pi \Delta_\gamma(\varepsilon_a - \varepsilon_b) \langle b | -iV | a \rangle. \tag{4.67}$$

The Sucher energy formula (4.6) then yields the expected result

$$\Delta E^{(1)} = \delta_{\varepsilon_a, \varepsilon_b} \langle b | V | a \rangle. \tag{4.68}$$

In the S-matrix we shall insert

- $-iV(\mathbf{x})$  for an energy potential  $V(\mathbf{x})$  (see Sect. 4.7).

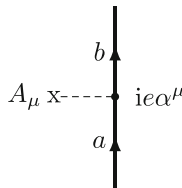


**Fig. 4.6** Diagrammatic representation of the interaction between an electron and an external field. The heavy lines represent electronic states in the bound-interaction picture

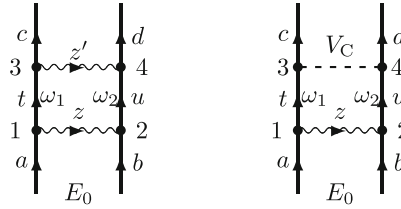


**Fig. 4.7** The Feynman representation of the two-photon exchange. The *left diagram* represents a Coulomb and a transverse photon interaction in Coulomb gauge

## 4.5 Two-Photon Exchange

### 4.5.1 Two-Photon Ladder

We consider next the exchange of two uncrossed photons, illustrated in Fig. 4.7 (left). Again, this is a *Feynman diagram*, which contains all relative time orderings of the times involved, still with the photons uncrossed.

As before, we consider first this problem using a general *covariant gauge*, like the Feynman gauge, and then we shall consider the Coulomb gauge, in particular.

In analogy with the single-photon exchange (4.47), the S-matrix of two non-crossing photons becomes, after contracting also the electron-field operators (4.9),

$$S^{(4)} = \frac{(ie)^4}{4!} \iiint d^4x_1 d^4x_2 d^4x_3 d^4x_4 \hat{\psi}^\dagger(x_3) \hat{\psi}^\dagger(x_4) iD_F(x_4, x_3) \\ \times iS_F(x_3, x_1) iS_F(x_4, x_2) iD_F(x_2, x_1) \hat{\psi}(x_2) \hat{\psi}(x_1) e^{-\gamma(|t_1|+|t_2|+|t_3|+|t_4|)}. \quad (4.69)$$

The vertices can here be permuted in  $4!$  ways, and this leads to 12 equivalent pairs, each pair with two diagrams, related by a reflection in a vertical plane. This leads to<sup>7</sup>

$$S^{(4)} = \frac{(ie)^4}{2} \iiint d^4x_1 d^4x_2 d^4x_3 d^4x_4 \hat{\psi}^\dagger(x_3) \hat{\psi}^\dagger(x_4) iD_F(x_4, x_3) \\ \times iS_F(x_3, x_1) iS_F(x_4, x_2) iD_F(x_2, x_1) \hat{\psi}(x_2) \hat{\psi}(x_1) e^{-\gamma(|t_1|+|t_2|+|t_3|+|t_4|)}. \quad (4.70)$$

This leads in analogy with the single-photon exchange (4.40) to the matrix elements<sup>8</sup>

<sup>7</sup>This factor is consistent with the rule found in many-body theory for time-ordered Goldstone diagrams that there is a factor of  $1/2$  for each possible symmetry operation, like reflexion, that transforms the diagram into itself or to another diagram in the set [124, Sect. 12.4].

<sup>8</sup>We have here an illustration of the general rules for setting up the S-matrix, given in Appendix H, that there is (i) a factor  $iS_F$  for each electron propagator, (ii) a factor  $-iI$  for each single-photon exchange and (iii) a  $\Delta$  factor for each vertex.

$$\begin{aligned}
\langle cd|S^{(4)}|ab\rangle &= \iint \frac{dz}{2\pi} \frac{dz'}{2\pi} \iint \frac{d\omega_1}{2\pi} \frac{d\omega_2}{2\pi} \\
&\times \langle cd|(-i)I(z'; \mathbf{x}_4, \mathbf{x}_3) iS_F(\omega_1; \mathbf{x}_3, \mathbf{x}_1) iS_F(\omega_2; \mathbf{x}_4, \mathbf{x}_2) (-i)I(z; \mathbf{x}_2, \mathbf{x}_1)|ab\rangle \\
&\times 2\pi\Delta_\gamma(\varepsilon_a - z - \omega_1) 2\pi\Delta_\gamma(\varepsilon_b + z - \omega_2) 2\pi\Delta_\gamma(\omega_1 - z' - \varepsilon_c) 2\pi\Delta_\gamma(\omega_2 + z' - \varepsilon_d).
\end{aligned}$$

Integrations over  $\omega_1, \omega_2$  then yield

$$\begin{aligned}
\langle cd|S^{(4)}|ab\rangle &= \iint \frac{dz}{2\pi} \frac{dz'}{2\pi} \langle cd|(-i)I(z'; \mathbf{x}_4, \mathbf{x}_3) iS_F(\varepsilon_a - z; \mathbf{x}_3, \mathbf{x}_1) \\
&\times iS_F(\varepsilon_b + z; \mathbf{x}_4, \mathbf{x}_2) (-i)I(z; \mathbf{x}_2, \mathbf{x}_1)|ab\rangle \\
&\times 2\pi\Delta_{2\gamma}(\varepsilon_a - \varepsilon_c - z - z') 2\pi\Delta_{2\gamma}(\varepsilon_b - \varepsilon_d + z + z'). \quad (4.71)
\end{aligned}$$

(As shown before, the  $\eta$  parameter in the electron propagators should here be replaced by the adiabatic damping parameter  $\gamma$ .) After integration over  $z'$  we have

$$\begin{aligned}
\langle cd|S^{(4)}|ab\rangle &= \int \frac{dz}{2\pi} \langle cd|(-i)I(\varepsilon_a - \varepsilon_c - z; \mathbf{x}_3, \mathbf{x}_4) iS_F(\varepsilon_a - z; \mathbf{x}_3, \mathbf{x}_1) \\
&\times iS_F(\varepsilon_b + z; \mathbf{x}_4, \mathbf{x}_2) (-i)I(z; \mathbf{x}_2, \mathbf{x}_1)|ab\rangle 2\pi\Delta_{4\gamma}(\varepsilon_a + \varepsilon_b - \varepsilon_c - \varepsilon_d). \quad (4.72)
\end{aligned}$$

To evaluate this integral is straightforward but rather tedious, and we shall not perform this here (see, for instance, [126]).

Next, we shall consider the special case, where we have *one instantaneous Coulomb interaction and one transverse-photon interaction* (Fig. 4.7, right), using the **Coulomb gauge**.

Separating the interaction according to (4.57), we now have

$$\begin{aligned}
\langle cd|S^{(4)}|ab\rangle &= \int \frac{dz}{2\pi} \langle cd|(-i)I_C^C(z; \mathbf{x}_4, \mathbf{x}_3) iS_F(\varepsilon_a - z; \mathbf{x}_3, \mathbf{x}_1) \\
&\times iS_F(\varepsilon_b + z; \mathbf{x}_4, \mathbf{x}_2) (-i)I_T^C(z; \mathbf{x}_2, \mathbf{x}_1)|ab\rangle \\
&\times 2\pi\Delta_{2\gamma}(\varepsilon_a - \varepsilon_c - z) 2\pi\Delta_{4\gamma}(\varepsilon_a + \varepsilon_b - \varepsilon_c - \varepsilon_d). \quad (4.73)
\end{aligned}$$

Inserting the expressions for the electron propagators (4.10) and the interaction (4.46), this yields

$$\begin{aligned}
\langle cd|S^{(4)}|ab\rangle &= \langle cd|V_C \int \frac{dz}{2\pi} \frac{|t\rangle\langle t|}{\varepsilon_a - z - \varepsilon_t + i\gamma_t} \frac{|u\rangle\langle u|}{\varepsilon_b + z - \varepsilon_u + i\gamma_u} \\
&\times \int \frac{2\kappa c^2 d\kappa}{z^2 - c^2\kappa^2 + i\eta} f_T^C(\kappa)|ab\rangle 2\pi\Delta_{4\gamma}(\varepsilon_a + \varepsilon_b - \varepsilon_c - \varepsilon_d), \quad (4.74)
\end{aligned}$$

where  $V_C$  is the Coulomb interaction  $f_T^C$  (4.63b) and  $f_T^C$  is given by (4.60). The products of the propagators can be expressed

$$\begin{aligned} & \frac{1}{\varepsilon_a - z - \varepsilon_t + i\gamma_t} \frac{1}{\varepsilon_b + z - \varepsilon_u + i\gamma_u} \\ &= \frac{1}{E_0 - \varepsilon_t - \varepsilon_u} \left[ \frac{1}{\varepsilon_a - z - \varepsilon_t + i\gamma_t} + \frac{1}{\varepsilon_b + z - \varepsilon_u + i\gamma_u} \right] \end{aligned} \quad (4.75)$$

with  $E_0 = \varepsilon_a + \varepsilon_b$ . The poles are here at  $z = \varepsilon_a - \varepsilon_t + i\gamma_t$ ,  $z = \varepsilon_u - \varepsilon_b - i\gamma_u$  and  $z = \pm(c\kappa - i\eta)$ . Integrating the first term over the negative half plane ( $z = c\kappa - i\eta$ ) and the second term over the positive half plane ( $z = -c\kappa + i\eta$ ), yields

$$\begin{aligned} & \langle cd | S^{(4)} | ab \rangle \\ &= -i \langle cd | V_C \frac{|tu\rangle\langle tu|}{E_0 - \varepsilon_t - \varepsilon_u} V_T | ab \rangle 2\pi \Delta_{4\gamma}(E_0 - E_{\text{out}}), \end{aligned} \quad (4.76)$$

where

$$\begin{aligned} \langle tu | V_T | ab \rangle &= \langle tu | \int c \, d\kappa \, f_T^C(\kappa) \\ &\quad \times \left[ \frac{1}{\varepsilon_a - \varepsilon_t - (c\kappa - i\gamma)_t} + \frac{1}{\varepsilon_b - \varepsilon_u - (c\kappa - i\gamma)_u} \right] | ab \rangle \end{aligned} \quad (4.77)$$

is the **transverse-photon potential**. The corresponding energy shift becomes in analogy with the single-photon case (4.53)

$$\Delta E = \langle \Phi | V_C \frac{|tu\rangle\langle tu|}{E_0 - \varepsilon_t - \varepsilon_u} V_T | \Phi \rangle. \quad (4.78)$$

*This holds when particle as well as hole states are involved.*

In principle, the adiabatic damping has to be switched off *simultaneously* at all vertices. If the intermediate state is not degenerate with the initial state, the damping can be switched off at each vertex independently, which leads to energy conservation at each vertex, using the orbital energies of the free lines and the energy parameters of the propagators. The degenerate case, which leads to what is referred to as the *reference-state contribution*, is more complicated to handle [27, 126], and we shall not consider that further here. This kind of contribution is easier to evaluate in the Green's-operator formalism that we shall consider in Chap. 6.

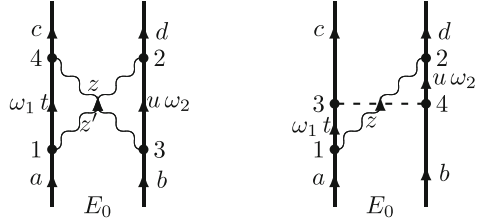
## 4.5.2 Two-Photon Cross\*

For two crossed photons (Fig. 4.8) the S-matrix becomes

$$\begin{aligned} \langle cd | S^{(4)} | ab \rangle &= \iint \frac{dz}{2\pi} \frac{dz'}{2\pi} \iint \frac{d\omega_1}{2\pi} \frac{d\omega_2}{2\pi} \\ &\quad \times \langle cd | (-i)I(z'; \mathbf{x}_4, \mathbf{x}_3) iS_F(\omega_1; \mathbf{x}_4, \mathbf{x}_1) iS_F(\omega_2; \mathbf{x}_2, \mathbf{x}_3) (-i)I(z; \mathbf{x}_2, \mathbf{x}_1) | ab \rangle \\ &\quad \times 2\pi \Delta_\gamma(\varepsilon_a - z - \omega_1) 2\pi \Delta_\gamma(\varepsilon_b - z' - \omega_2) 2\pi \Delta_\gamma(\omega_1 + z' - \varepsilon_c) 2\pi \Delta_\gamma(\omega_2 + z - \varepsilon_d). \end{aligned}$$



**Fig. 4.8** The Feynman representation of the two-photon cross



Integrations over  $\omega_1, \omega_2$  yield

$$\begin{aligned}
 \langle cd|S^{(4)}|ab\rangle &= \iint \frac{dz}{2\pi} \frac{dz'}{2\pi} \langle cd|(-i)I(z'; \mathbf{x}_4, \mathbf{x}_3) iS_F(\varepsilon_a - z; \mathbf{x}_4, \mathbf{x}_1) \\
 &\quad \times iS_F(\varepsilon_b - z'; \mathbf{x}_2, \mathbf{x}_3) (-i)I(z; \mathbf{x}_2, \mathbf{x}_1)|ab\rangle \\
 &\quad \times 2\pi\Delta_{2\gamma}(\varepsilon_a - \varepsilon_c - z + z') 2\pi\Delta_{2\gamma}(\varepsilon_b - \varepsilon_d + z - z'). \quad (4.79)
 \end{aligned}$$

Again, we consider the simpler case with *one Coulomb and one transverse interaction* (Fig. 4.8, right), using the Coulomb gauge. Then the diagonal element becomes

$$\begin{aligned}
 \langle ab|S^{(4)}|ab\rangle &= \langle ab|V_C \int \frac{dz}{2\pi} \frac{|t\rangle\langle t|}{\varepsilon_a - z - \varepsilon_t + i\gamma_t} \frac{|u\rangle\langle u|}{\varepsilon_d - z - \varepsilon_u + i\gamma_u} \\
 &\quad \times \int \frac{2c^2\kappa d\kappa f_T^C(\kappa)}{z^2 - c^2\kappa^2 + i\eta} |ab\rangle 2\pi\Delta_{4\gamma}(0), \quad (4.80)
 \end{aligned}$$

using the fact that  $\varepsilon_a + \varepsilon_b = \varepsilon_c + \varepsilon_d$ . Integration over  $z$  leads in analogy with (4.77) to

$$\langle ab|S^{(4)}|ab\rangle = -i \langle ab|V_C \frac{|tu\rangle\langle tu|}{\varepsilon_a - \varepsilon_d - \varepsilon_t + \varepsilon_u} V_T^X |ab\rangle 2\pi\Delta_{4\gamma}(0), \quad (4.81)$$

where  $V_T^X$  is the potential

$$\begin{aligned}
 &\langle tu|V_T^X|ab\rangle \\
 &= \langle tu| \int c d\kappa f_T^C(\kappa) \left[ \frac{1}{\varepsilon_a - \varepsilon_t - (c\kappa - i\gamma)_t} - \frac{1}{\varepsilon_d - \varepsilon_u - (c\kappa - i\gamma)_u} \right] |ab\rangle. \quad (4.82)
 \end{aligned}$$

If  $\varepsilon_t$  and  $\varepsilon_u$  have the same sign, the denominators in the expression (4.81) can be expressed

$$\frac{1}{\varepsilon_a - \varepsilon_t - (c\kappa - i\gamma)_t} \frac{1}{\varepsilon_d - \varepsilon_u - (c\kappa - i\gamma)_u},$$

which is in agreement with the evaluation rules for time-ordered diagrams, derived in Appendix I.

The two-photon ladder and the two-photon cross have been studied in great detail by means of the S-matrix technique for the ground-state of heliumlike systems by Blundell et al. [27] and by Lindgren et al. [126]. Some numerical results are given in Chap. 7.

*In the S-matrix we shall insert*

- $iS_F$  for *exch electron propagator*.
- $-iI(z; \mathbf{x}_1, \mathbf{x}_2) = -ie^2c^2\alpha_1^\mu\alpha_2^\nu D_{F\mu\nu}(z; \mathbf{x}_1, \mathbf{x}_2) = -ie^2c^2 D_F(z; \mathbf{x}_1, \mathbf{x}_2)$  for each *single-photon exchange*, when integrating over time (see Sect. 4.7).

## 4.6 QED Corrections

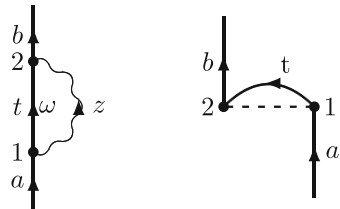
In this section we shall consider how various first-order QED corrections—beyond the no-virtual-pair approximation (see Sect. 2.6)—can be evaluated using the S-matrix formulation. With this formulation only corrections to the energy can be evaluated. In Chap. 6 we shall demonstrate a way of including these effects directly into the wave functions, which makes it possible to incorporate them into the many-body procedure in a more systematic way. Some QED effects contain singularities (divergences), which can be handled by means of *regularization* and *renormalization*, as will be discussed in Chap. 12.

### 4.6.1 Bound-Electron Self-energy

When the photon is emitted from and absorbed on the same electron, we have an effect of the *electron self-energy*, illustrated in Fig. 4.9. This forms the major part of the *Lamb shift*, discovered experimentally by Lamb and Retherford in 1947 [116]. This was the starting point for the development of modern QED (see the book by Schweber [221]). The second most important part of the Lamb shift is the *vacuum polarization*, to be treated below.

We treat first the self-energy and start with a covariant gauge and then consider the non-covariant Coulomb gauge.

**Fig. 4.9** Diagram representing the first-order bound-electron self-energy. The *second diagram* represents the Coulomb part of the self-energy in Coulomb gauge



### 4.6.1.1 Covariant Gauge

For the electron self-energy (Fig. 4.9) we can set up the expression for the S-matrix in analogy with the single-photon exchange (4.40),

$$S_{\text{SE}} = \frac{(ie)^2}{2} \iint d^4x_2 d^4x_1 \psi^\dagger(x_2) iS_{\text{F}}(x_2, x_1) iD_{\text{F}}(x_2, x_1) \psi(x_1) e^{-\gamma(|t_1|+|t_2|)} \quad (4.83)$$

with summation over the internal orbital  $t$ . Considering also the equivalent case with  $1 \leftrightarrow 2$ , the matrix element becomes

$$\begin{aligned} \langle b | S_{\text{SE}} | a \rangle &= \iint \frac{dz}{2\pi} \frac{d\omega}{2\pi} \langle b | iS_{\text{F}}(\omega; \mathbf{x}_2, \mathbf{x}_1) (-i) I(z; \mathbf{x}_2, \mathbf{x}_1) | a \rangle \\ &\quad \times 2\pi \Delta_\gamma(\varepsilon_a - z - \omega) 2\pi \Delta_\gamma(\omega + z - \varepsilon_b) \end{aligned} \quad (4.84)$$

and after integration over  $\omega$

$$\langle b | S_{\text{SE}} | a \rangle = 2\pi \Delta_{2\gamma}(\varepsilon_a - \varepsilon_b) \langle b | \mathcal{M}^{(2)} | a \rangle,$$

where  $\mathcal{M}^{(2)}$  is the second-order *Feynman amplitude* (see Sect. 4.7 and Appendix H),

$$\mathcal{M}^{(2)} = -i\Sigma(\varepsilon_a). \quad (4.85)$$

with

$$\Sigma(\varepsilon_a) = i \int \frac{dz}{2\pi} S_{\text{F}}(\varepsilon_a - z; \mathbf{x}_2, \mathbf{x}_1) I(z; \mathbf{x}_2, \mathbf{x}_1) \quad (4.86)$$

being the *self-energy function*.<sup>9</sup> The Sucher energy formula (4.6) yields the corresponding energy shift

$$\Delta E_{\text{SE}} = \lim_{\gamma \rightarrow 0} \frac{1}{2} i\gamma 2 \langle b | S_{\text{SE}} | a \rangle = \delta_{\varepsilon_a, \varepsilon_b} \langle b | \Sigma(\varepsilon_a) | a \rangle, \quad (4.87)$$

using the relation between the Dirac delta function and the Kronecker delta factor in (A.20) in Appendix A.

With the expressions for the electron propagator (4.10), the bound-state self-energy becomes

$$\begin{aligned} \langle a | \Sigma(\varepsilon_a) | a \rangle &= i \langle a t | \int \frac{dz}{2\pi} \frac{1}{\varepsilon_a - \varepsilon_t - z + i\eta_t} I(z; \mathbf{x}_2, \mathbf{x}_1) | t a \rangle \\ &= i \langle a t | \int \frac{dz}{2\pi} \frac{1}{\varepsilon_a - \varepsilon_t - z + i\eta_t} \int \frac{2c^2 \kappa d\kappa f(\kappa)}{z^2 - c^2 \kappa^2 + i\eta} | t a \rangle. \end{aligned} \quad (4.88)$$

<sup>9</sup>This is non-covariant, due to our conventions, as discussed above. The corresponding covariant form is  $\bar{\Sigma}(\varepsilon_a) = \beta \Sigma(\varepsilon_a)$ , which will be discussed in detail in Chap. 12.

Performing the  $z$  integration, yields

$$\langle a | \Sigma(\varepsilon_a) | a \rangle = \left\langle at \left| \int \frac{c \, d\kappa f(\kappa)}{\varepsilon_a - \varepsilon_t - (c\kappa - i\eta)_t} \right| ta \right\rangle, \quad (4.89)$$

where the  $f$  function defined in (4.46).

In the *Feynman gauge* we have

$$\langle a | \Sigma(\varepsilon_a) | a \rangle = \left\langle at \left| \int \frac{c \, d\kappa f^F(\kappa)}{\varepsilon_a - \varepsilon_t - (c\kappa - i\eta)_t} \right| ta \right\rangle \quad (4.90)$$

and using the function (4.55)

$$\langle a | \Sigma(\varepsilon_a) | a \rangle = -\frac{e^2}{4\pi^2 \varepsilon_0} \left\langle at \left| \frac{\alpha_1^\mu \alpha_{2\mu}}{r_{12}} \int \frac{c \, d\kappa \sin \kappa r_{12}}{\varepsilon_a - \varepsilon_t - (c\kappa - i\eta)_t} \right| ta \right\rangle. \quad (4.91)$$

#### 4.6.1.2 Coulomb Gauge

In the *Coulomb gauge* the *transverse part* can be treated in analogy with the covariant gauge (4.89)

$$\langle a | \Sigma(\varepsilon_a) | a \rangle_{\text{Trans}} = \left\langle at \left| \int \frac{c \, d\kappa f_T^C(\kappa)}{\varepsilon_a - \varepsilon_t - (c\kappa - i\eta)_t} \right| ta \right\rangle \quad (4.92)$$

or with (4.60)

$$\begin{aligned} \langle a | \Sigma(\varepsilon_a) | a \rangle_{\text{Trans}} &= \frac{e^2}{4\pi^2 \varepsilon_0} \left\langle at \left| \frac{1}{r_{12}} \int \frac{c \, d\kappa \sin \kappa r_{12}}{\varepsilon_a - \varepsilon_t - (c\kappa - i\eta)_t} \right. \right. \\ &\quad \left. \left. \times \left[ \boldsymbol{\alpha}_1 \cdot \boldsymbol{\alpha}_2 - \frac{(\boldsymbol{\alpha}_1 \cdot \nabla_1)(\boldsymbol{\alpha}_2 \cdot \nabla_2)}{\kappa^2} \right] \right| ta \right\rangle. \end{aligned} \quad (4.93)$$

For the *Coulomb part* we insert the expression for  $I_C^C$  in (4.63b) into (4.86), yielding

$$\begin{aligned} \Sigma(\varepsilon_a)_{\text{Coul}} &= \frac{ie^2}{4\pi^2 \varepsilon_0 r_{12}} \int \frac{dz}{2\pi} S_F(\varepsilon_a - z; \mathbf{x}_2, \mathbf{x}_1) \int \frac{2\kappa \, d\kappa \sin \kappa r_{12}}{\kappa^2} \\ &= i \int \frac{dz}{2\pi} S_F(\varepsilon_a - z; \mathbf{x}_2, \mathbf{x}_1) V_C \end{aligned} \quad (4.94)$$

and

$$\langle a | \Sigma(\varepsilon_a) | a \rangle_{\text{Coul}} = i \left\langle at \left| \int \frac{dz}{2\pi} \frac{1}{\varepsilon_a - z - \varepsilon_t + i\eta_t} V_C \right| ta \right\rangle. \quad (4.95)$$

The integral can be evaluated as a principal integral (which vanishes) and *half* a pole contribution, yielding the result  $-i \operatorname{sgn}(\varepsilon_t)/2$ . The self-energy then becomes

$$\langle a | \Sigma(\varepsilon_a) | a \rangle_{\text{Coul}} = \frac{1}{2} \operatorname{sgn}(\varepsilon_t) \langle at | V_C | ta \rangle. \quad (4.96)$$

The electron self-energy is *divergent* and has to be renormalized, as will be discussed in Chap. 12. Some numerical results, using the Feynman gauge, are given in Chap. 7.

- **In the S-matrix we shall insert  $-i\Sigma(\varepsilon)$  for each electron self-energy** (see Sect. 4.7).

### 4.6.2 Vertex Correction

The vertex correction, shown in Fig. 4.10, is a correction to the single-potential interaction in Fig. 4.6, and the S-matrix becomes in analogy with the self-energy, using (4.67),

$$\begin{aligned} \langle b | S_{\text{VC}} | a \rangle &= \iint \frac{dz}{2\pi} \frac{d\omega}{2\pi} \\ &\times \sum_{t,u} \int d\mathbf{x}_3 \langle bt | iS_{\text{F}}(\omega; \mathbf{x}_2, \mathbf{x}_3) (-i)V(\mathbf{x}_3) iS_{\text{F}}(\omega; \mathbf{x}_3, \mathbf{x}_1) (-i)I(z; \mathbf{x}_2, \mathbf{x}_1) | ua \rangle \\ &\times 2\pi\Delta_\gamma(\varepsilon_a - z - \omega) 2\pi\Delta_\gamma(\omega + z - \varepsilon_b), \end{aligned} \quad (4.97)$$

where the matrix element involves integration over  $\mathbf{x}_1, \mathbf{x}_2$ . (compare (4.67)). After integration over  $\omega$  this becomes (compare (4.86))

$$\langle b | S_{\text{VC}} | a \rangle = 2\pi\Delta_{2\gamma}(\varepsilon_a - \varepsilon_b) \langle bt | -i\Lambda^0(\varepsilon_a, \varepsilon_a, \mathbf{x}_3)V(\mathbf{x}_3) | ua \rangle \quad (4.98)$$

with integration over  $\mathbf{x}_3$ . Here,

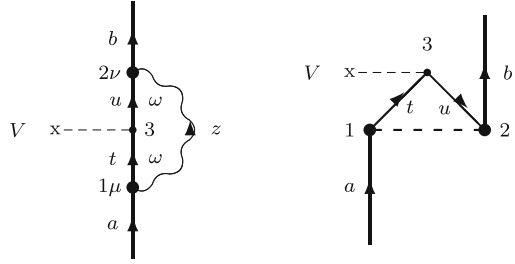
$$\Lambda^0(\varepsilon_a, \varepsilon_a, \mathbf{x}_3) = i \int \frac{dz}{2\pi} S_{\text{F}}(\varepsilon_a - z; \mathbf{x}_2, \mathbf{x}_3) S_{\text{F}}(\varepsilon_a - z; \mathbf{x}_3, \mathbf{x}_1) I(z; \mathbf{x}_2, \mathbf{x}_1) \quad (4.99)$$

with integration over  $\mathbf{x}_1, \mathbf{x}_2$  and summation over  $t, u$ . This is the first-order *vertex-correction function* for a scalar-potential interaction.<sup>10</sup>

---

<sup>10</sup>In the first edition of this book the vertex function was defined with the opposite sign. The new definition is more logical and has the consequence that in the S matrix the vertex correction should be represented by  $-\Lambda$  in analogy with other similar insertions (see further below).

**Fig. 4.10** Diagram representing the first-order vertex correction



The vertex-correction function is divergent, and can be expressed

$$\Lambda^0 = L + \Lambda_{\text{ren}}^0, \tag{4.100}$$

where  $L$  is a divergent constant and  $\Lambda_{\text{ren}}^0$  is the finite, renormalized vertex function. This is further discussed in Chap. 12.

### 4.6.2.1 Covariant Gauge

With the expression for the electron and the photon propagators in a covariant gauge ((4.11) and (4.46)) we have, leaving out the space coordinates,

$$\begin{aligned} \Lambda^0(\varepsilon_a, \varepsilon_a) &= i \int \frac{dz}{2\pi} \frac{1}{\varepsilon_a - \varepsilon_u - z + i\eta_u} \frac{1}{\varepsilon_a - \varepsilon_t - z + i\eta_t} \int \frac{2c^2 \kappa d\kappa f(\kappa)}{z^2 - c^2 \kappa^2 + i\eta} \\ &= \int \frac{c d\kappa f(\kappa)}{(\varepsilon_a - \varepsilon_u - c\kappa + i\eta)(\varepsilon_a - \varepsilon_t - c\kappa + i\eta)}, \end{aligned} \tag{4.101}$$

assuming *positive* intermediate states. The corresponding expressions of the particular gauge is obtained by inserting the expression for  $f(k)$  in that gauge.

Comparing with the self-energy (4.89), we find for the *diagonal part*,  $t = u$ , what is known as

- *the Ward identity* (see also Chap. 12)

$$\frac{\partial}{\partial \varepsilon_a} \Sigma(\varepsilon_a) = -\Lambda^0(\varepsilon_a, \varepsilon_a). \tag{4.102}$$

### 4.6.2.2 Coulomb Gauge

The transverse part in Coulomb gauge is analogous to the expression in the covariant gauge, using the corresponding  $f$  function. For the Coulomb part we insert the Coulomb interaction (4.63b) in expression (4.99), yielding

$$\begin{aligned} \Lambda^0(\varepsilon_a, \varepsilon_a) &= i \left\langle u \left| \int \frac{dz}{2\pi} \frac{1}{\varepsilon_a - \varepsilon_u - z + i\eta_u} \frac{1}{\varepsilon_a - \varepsilon_t - z + i\eta_t} V_C \right| t \right\rangle \\ &= \left\langle u \left| \operatorname{sgn}(\varepsilon_t) \frac{V_C}{\varepsilon_t - \varepsilon_u} \right| t \right\rangle, \end{aligned} \tag{4.103}$$

provided  $\varepsilon_t$  and  $\varepsilon_u$  have different sign. If  $\varepsilon_t = \varepsilon_u$  this becomes singular, which is consistent with the Ward identity, since the energy derivative of the self-energy also becomes singular (see further Chap. 12).

- *In the S-matrix we shall insert  $-i\Lambda^0(\varepsilon, \varepsilon')$  for each scalar vertex correction* (see Sect. 4.7).

### 4.6.3 Vacuum Polarization

The field near the atomic nucleus can give rise to a “*polarization effect*” in the form of the creation of electron-positron pairs, an effect referred to as the *vacuum polarization*. The first-order effect, illustrated in Fig. 4.11, forms together with the first-order self-energy (Fig. 4.9) the leading contributions to the *Lamb shift*.

In order to set up the S-matrix for the leading vacuum polarization (first diagram in Fig. 4.11), we go back to the relation (4.39) for single-photon exchange

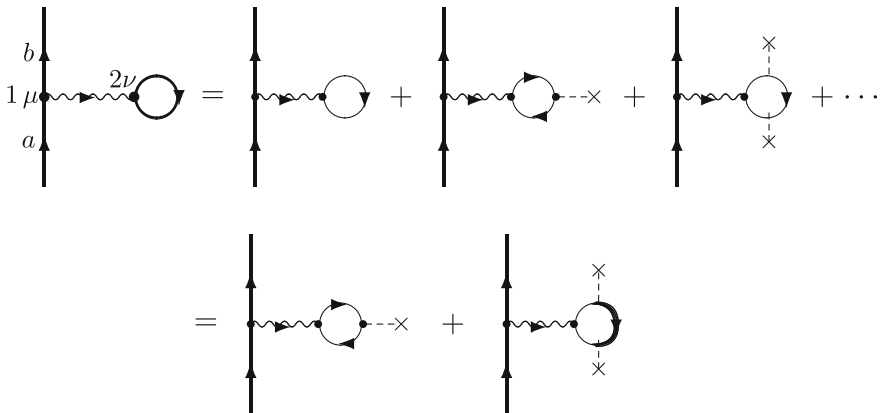


**Fig. 4.11** Diagram representing the first-order vacuum polarization according to (4.109). The closed loop contains summation over **all** orbitals (particles and holes). The *first and third diagrams* on the r.h.s. of the first row vanish due to Furry’s theorem (see text). The *first diagram* in the *second row* represents the Uehling part and the final diagrams the Wichmann–Kroll part. The *heavy lines* represent the *bound-state* orbital or propagator and the *thin lines* the *free-electron* propagator

$$- \iint d^4x_2 d^4x_1 T \left[ \overbrace{(\psi^\dagger(x) e \alpha^\nu A_\nu(x) \psi(x))_2 (\psi^\dagger(x) e \alpha^\mu A_\mu(x) \psi(x))_1} \right] e^{-\gamma(|t_1|+|t_2|)},$$

leaving out the factor of 1/2, since we can interchange 1 and 2. The contraction between the creation and absorption electron-field operators at vertex 2 represents the closed orbital loop. Explicitly, writing out the spinor components, we have at this vertex

$$\overbrace{\psi_\sigma^\dagger(x_2) e \alpha_{\sigma\tau}^\nu A_\nu(x_2) \psi_\tau(x_2)} = \text{Tr} \left[ \overbrace{\psi^\dagger(x_2) e \alpha^\nu A_\nu(x_2) \psi(x_2)} \right],$$

where “Tr” stands for the *trace* of the matrix, i.e., the sum of the diagonal elements. The contraction leads here to  $-iS_F(x_2, x_2)$  (note order between the field operators). We then have the S-matrix element

$$-e^2 \iint d^4x_2 d^4x_1 i \alpha_1^\mu D_{F\nu\mu}(x_2, x_1) \text{Tr} \left[ \alpha_2^\nu (-i) S_F(x_2, x_2) \right] e^{-\gamma(|t_1|+|t_2|)}.$$

With the Fourier transforms  $S_F(\omega; \mathbf{x}_2, \mathbf{x}_2)$  and  $D_{F\nu\mu}(z; \mathbf{x}_2, \mathbf{x}_1)$  the time dependence is

$$e^{-i t_1 (\varepsilon_b - \varepsilon_a - z) - \gamma |t_1|} e^{-i t_2 (\omega - \omega + z) - \gamma |t_2|},$$

and this leads after time integrations to the S-matrix element

$$\begin{aligned} \langle b | S_{SE}^{(2)} | a \rangle &= -2\pi \Delta_\gamma(\varepsilon_a - \varepsilon_b - z) 2\pi \Delta_\gamma(\omega - \omega + z) \\ &\times e^2 \iint \frac{d\omega}{2\pi} \frac{dz}{2\pi} \langle b | \alpha_1^\mu D_{F\nu\mu}(z; \mathbf{x}_2, \mathbf{x}_1) \text{Tr} \left[ \alpha_2^\nu S_F(\omega; \mathbf{x}_2, \mathbf{x}_2) \right] | a \rangle \end{aligned} \quad (4.104)$$

and in the limit  $\gamma \rightarrow 0$ , using the relation (A.32) in Appendix A,

$$\begin{aligned} \langle b | S_{SE}^{(2)} | a \rangle &= -2\pi \Delta_{2\gamma}(\varepsilon_a - \varepsilon_b) \\ &\times e^2 \int \frac{d\omega}{2\pi} \langle b | \alpha_1^\mu D_{F\nu\mu}(0; \mathbf{x}_2, \mathbf{x}_1) \text{Tr} \left[ \alpha_2^\nu S_F(\omega; \mathbf{x}_2, \mathbf{x}_2) \right] | a \rangle. \end{aligned} \quad (4.105)$$

According to Sucher’s energy formula (4.6) we have in second order

$$\Delta E = \lim_{\gamma \rightarrow 0} i\gamma \langle \Phi | S^{(2)} | \Phi \rangle, \quad (4.106)$$

and using the relation (A.20)

$$\begin{aligned} \Delta E &= -i\delta(\varepsilon_a, \varepsilon_b) \\ &\times e^2 \int \frac{d\omega}{2\pi} \langle b | \alpha_1^\mu D_{F\nu\mu}(0; \mathbf{x}_2, \mathbf{x}_1) \text{Tr} \left[ \alpha_2^\nu S_F(\omega; \mathbf{x}_2, \mathbf{x}_2) \right] | a \rangle. \end{aligned} \quad (4.107)$$



It can furthermore be shown that only  $\nu = 0$ , i.e.,  $\alpha^\nu = 1$  will contribute here [190]. The vacuum-polarization contribution is divergent and has to be renormalized, which in this case turns out to be not too difficult (see below).

The bound-state electron propagator,  $S_F(\omega)$ , is in operator form (4.14)

$$\hat{S}_F(\omega) = \frac{1}{\omega - \hat{h}_{\text{bau}}(1 - i\eta)}. \quad (4.108)$$

Expressing the Dirac Hamiltonian for an electron in an external (nuclear) potential  $v_{\text{ext}}$  as  $\hat{h}_{\text{bau}} = \hat{h}_{\text{free}} + v_{\text{ext}}$ , where  $\hat{h}_{\text{free}}$  is the free-electron Hamiltonian, the propagator (4.108) can be expanded as

$$\begin{aligned} \frac{1}{z - \hat{h}_{\text{bau}}(1 - i\eta)} &= \frac{1}{z - \hat{h}_{\text{free}}(1 - i\eta)} + \frac{1}{z - \hat{h}_{\text{free}}(1 - i\eta)} V \frac{1}{z - \hat{h}_{\text{free}}(1 - i\eta)} \\ &\quad + \frac{1}{z - \hat{h}_{\text{free}}(1 - i\eta)} V \frac{1}{z - \hat{h}_{\text{free}}(1 - i\eta)} V \frac{1}{z - \hat{h}_{\text{free}}(1 - i\eta)} + \dots \\ &= \frac{1}{z - \hat{h}_{\text{free}}(1 - i\eta)} + \frac{1}{z - \hat{h}_{\text{free}}(1 - i\eta)} V \frac{1}{z - \hat{h}_{\text{free}}(1 - i\eta)} \\ &\quad + \frac{1}{z - \hat{h}_{\text{free}}(1 - i\eta)} V \frac{1}{z - \hat{h}_{\text{bau}}(1 - i\eta)} V \frac{1}{z - \hat{h}_{\text{free}}(1 - i\eta)}, \end{aligned} \quad (4.109)$$

which leads to the expansion illustrated in Fig. 4.11.

The first and third diagrams on the r.h.s. in the first row in Fig. 4.11 vanish due to “Furry’s theorem”. According to this theorem, a diagram will vanish if it contains a free-electron loop with an *odd number of vertices* [143, Sect. 9.1]. The first diagram in the second row represents the *Uehling part* [245], and the second part is the so-called *Wichmann–Kroll* [249] part. The Uehling part is *divergent*, but Uehling was already in 1934 able to handle this divergence and derive an analytic expression for the renormalized potential. The Wichmann–Kroll part is finite and has to be evaluated numerically.

Both the Uehling and the Wichmann–Kroll effects can be expressed in terms of single-particle potentials that can be added to the external potential, used to generate the single particle spectrum, and in this way the effects can be automatically included in the calculations to arbitrary order (see, for instance, Persson et al. [190]). In Table 4.1 we show the result of some accurate vacuum-polarization calculations. The diagrams above for the vacuum-polarization and the self-energy can be compared with the corresponding many-body diagrams, discussed in Sect. 2.4 (Fig. 2.3). In the MBPT case the internal line represent core orbitals only, while in the present case they can represent **all orbitals**—particle as well as hole states.

**Table 4.1** Vacuum-polarization effects in the ground state of some hydrogenlike systems (in eV) (from Persson et al. [190])

36Kr	Uehling Wichmann–Kroll	−1.35682 0.01550
54Xe	Uehling Wichmann–Kroll	−7.3250 0.1695
70Yb	Uehling Wichmann–Kroll	−23.4016 0.8283
92U	Uehling Wichmann–Kroll	−93.5868 4.9863

### 4.6.4 Photon Self-energy

The interaction between the photon and the electron-positron fields can give rise to another form of *vacuum polarization*, illustrated in Fig. 4.12. The S-matrix for this process can be obtained from that of single-photon exchange (4.40) by replacing  $-ie^2\alpha_1^\mu D_{F\nu\mu}(x_1, x_2)\alpha_2^\nu$  by

$$\iint d^4x_3 d^4x_4 (-ie^2)\alpha_1^\mu D_{F\mu\sigma}(x_1, x_3) i\Pi^{\sigma\tau}(x_3, x_4) (-ie^2) D_{F\tau\nu}(x_4, x_2)\alpha_2^\nu, \tag{4.110}$$

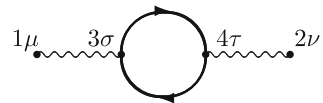
where

$$\begin{aligned} i\Pi^{\sigma\tau}(x_3, x_4) &= \alpha_3^\sigma \underbrace{\hat{\psi}^\dagger(x_3)\hat{\psi}(x_3)\hat{\psi}^\dagger(x_4)\hat{\psi}(x_4)} \alpha_4^\tau = \alpha_3^\sigma \underbrace{\hat{\psi}(x_3)\hat{\psi}^\dagger(x_4)} \underbrace{\hat{\psi}^\dagger(x_3)\hat{\psi}(x_4)} \alpha_4^\tau \\ &= -\text{Tr}[\alpha_3^\sigma iS_F(x_3, x_4) iS_F(x_4, x_3)\alpha_4^\tau] \end{aligned} \tag{4.111}$$

is the *first-order polarization tensor* [143, Eqs. (7.22), (9.5)]. The contractions lead here to the *trace* as in the previous case, and there is also here a minus sign due to the closed loop.

The photon self-energy is (charge) divergent and requires a *renormalization*, as is discussed further in Chap. 12, and after the renormalization there is a *finite remainder*.

**Fig. 4.12** Diagram representing the first-order photon self-energy



## 4.7 Feynman Diagrams for the S-Matrix. Feynman Amplitude

### 4.7.1 Feynman Diagrams

We have in this chapter constructed S-matrix expressions for a number of Feynman diagrams, and we summarize here the rules that can be deduced for this construction. We also define the so-called *Feynman amplitude*, introduced by Richard Feynman in his original works on quantum-field theory, which we shall find convenient to use also in other procedures to be discussed later. These rules are also summarized in Appendix H.

The S-matrix is given by (3.35 and 4.3)

$$S = \sum_{n=0}^{\infty} \left( \frac{-i}{c} \right)^n \frac{1}{n!} \int dx_1^4 \dots \int dx_n^4 T[\mathcal{H}(x_1) \dots \mathcal{H}(x_n)] e^{-\gamma(|t_1|+|t_2|+\dots+|t_n|)}$$

with the interaction density (4.4)

$$\mathcal{H}(x) = -\hat{\psi}^\dagger(x) e c \alpha^\mu A_\mu(x) \hat{\psi}(x).$$

This leads to the following rules for the *S-matrix*: There is

- an electron-field creation/absorption operator,  $\hat{\psi}^\dagger/\hat{\psi}$ , for each outgoing/incoming *electron orbital*;
- $ie c \alpha^\mu$  at each vertex;
- $i S_F(x_1, x_2)$  for each *electron propagator* (4.9 and 4.11);
- $i D_{F\nu\mu}$  for each *photon propagator* (4.18);
- at each vertex a factor of  $2\pi \Delta_\gamma(arg)$ , where *arg* is the sum of all incoming energy parameters minus the some of all outgoing ones;
- a factor of  $-1$  and a trace symbol for each closed orbital loop.

This leads to, after integrating over time,

- $-iI(z; \mathbf{x}_1, \mathbf{x}_2)$  for each a *single-photon interaction* (4.44);
- $-iV(\mathbf{x})$  for each *energy-potential interaction*  $V(\mathbf{x})$ ;
- $-i\Sigma$  for each *electron self-energy* (4.86 and 4.91);
- $-i\Lambda^0$  for each *scalar vertex-correction* (4.99 and 4.101);

### 4.7.2 Feynman Amplitude. Energy Diagram

- For an irreducible S-matrix diagram (no internal model-space state) with  $n$  vertices,  $S^{(n)}$ , the *Feynman amplitude*,  $\mathcal{M}^{(n)}$ , is defined by (using (A.18) in Appendix A)

$$\langle cd|S^{(n)}|ab\rangle = 2\pi\delta(E_{\text{in}} - E_{\text{out}})\langle cd|\mathcal{M}^{(n)}|ab\rangle = \lim_{\gamma\rightarrow 0} 2\pi\Delta_{n\gamma}(E_{\text{in}} - E_{\text{out}})\langle cd|\mathcal{M}^{(n)}|ab\rangle, \quad (4.112)$$

where  $E_{\text{in}}$ ,  $E_{\text{out}}$  are the incoming and outgoing energies, respectively (see further Appendix H)

- The energy shift is given by the Sucher formula (4.6)

$$\frac{1}{2} \lim_{\gamma\rightarrow 0} i\gamma n \langle cd|S^{(n)}|ab\rangle \quad (4.113)$$

(no denominator, when the diagram is irreducible). This yields in each order with (A.21)

$$\boxed{\Delta E = \delta_{E_{\text{in}}, E_{\text{out}}} \langle cd|i\mathcal{M}^{(n)}|ab\rangle}. \quad (4.114)$$

# Chapter 5

## Green's Functions

The *Green's function* is an important tool with applications in classical as well as quantum physics (for an introduction, see, particularly the book by Fetter and Walecka [67, Chap.3] and also the book by Mahan [140]). More recently it has been applied also to quantum electrodynamics, particularly by Shabaev et al. [226]. As a background we shall first consider the classical Green's function.

### 5.1 Classical Green's Function

The classical *Green's function*,  $G(x, x_0)$ , can be defined so that it describes the propagation of a wave from one space-time point  $x_0 = (t_0, \mathbf{x}_0)$  to another space-time point  $x = (t, \mathbf{x})$ , known as the Huygens' principle (see, for instance the book by Bjorken and Dell [22, Sect. 6.2])

$$\chi(x) = \int d^3\mathbf{x}_0 G(x, x_0) \chi(x_0). \quad (5.1)$$

The *retarded* Green's function is defined as the part of the function  $G(x, x_0)$  for which  $t > t_0$

$$G_+(x, x_0) = \Theta(t - t_0) G(x, x_0), \quad (5.2)$$

where  $\Theta(t)$  is the Heaviside step function (Appendix A.33), which implies

$$\Theta(t - t_0) \chi(x) = \int d^3\mathbf{x}_0 G_+(x, x_0) \chi(x_0). \quad (5.3)$$

We assume now that the function  $\chi(x)$  satisfies a differential equation of Schrödinger type

$$\left(i\frac{\partial}{\partial t} - H(x)\right)\chi(x) = 0. \quad (5.4)$$

Operating with the bracket on (5.3), yields

$$i\delta(t - t_0)\chi(x) = \int d^3x_0 \left(i\frac{\partial}{\partial t} - H(x)\right) G_+(x, x_0)\chi(x_0),$$

using the relation (A.35) in Appendix A, which implies that

- *the retarded Green's function satisfies the differential equation*

$$\boxed{\left(i\frac{\partial}{\partial t} - H(x)\right) G_+(x, x_0) = i\delta^4(x - x_0)} \quad (5.5)$$

—a relation often taken as the definition of the (mathematical) Green's function.

The Green's function can be used for solving inhomogeneous differential equations. If we have

$$\left(i\frac{\partial}{\partial t} - H(x)\right)\Psi(x) = f(x), \quad (5.6)$$

then the solution can be expressed

$$\Psi(x) = \int dx' G_+(x', x) f(x'). \quad (5.7)$$

## 5.2 Field-Theoretical Green's Function—Closed-Shell Case

### 5.2.1 Definition of the Field-Theoretical Green's Function

- *In the closed-shell case the field-theoretical single-particle Green's function can be defined [67]<sup>1</sup>*

$$G(x, x_0) = \frac{\langle 0_{\text{H}} | T[\hat{\psi}_{\text{H}}(x)\hat{\psi}_{\text{H}}^\dagger(x_0)] | 0_{\text{H}} \rangle}{\langle 0_{\text{H}} | 0_{\text{H}} \rangle}, \quad (5.8)$$

where  $T$  is the *Wick time-ordering operator* (2.27) and  $\hat{\psi}_{\text{H}}$ ,  $\hat{\psi}_{\text{H}}^\dagger$  are the electron-field operators in the Heisenberg representation (HP) (B.27). The state  $|0_{\text{H}}\rangle$  is the

---

<sup>1</sup>Different definitions of the field-theoretical Green's function are used in the literature. The definition used here agrees with that of Itzykson and Zuber [92], while that of Fetter and Walecka [67] differs by a factor of  $i$ .

“vacuum in the Heisenberg representation”, i.e., the state in the Heisenberg representation with no particles or holes. In a “closed-shell state” the single reference or model state is identical to the vacuum state (see Sect. 2.3).

The Heisenberg vacuum is time independent and equal to the corresponding vacuum state in the interaction picture at  $t = 0$ , i.e.,

$$|0_H\rangle = U(0, -\infty)|0\rangle, \quad (5.9)$$

where  $U(t, t_0)$  is the evolution operator (3.15) and  $|0\rangle$  is the unperturbed vacuum or the IP vacuum as  $t \rightarrow -\infty$  (c.f. 3.37).

Using the relation between the electron-field operators in HP and IP (B.25)

$$\hat{\psi}_H(x) = U(0, t) \hat{\psi}(x) U(t, 0), \quad (5.10)$$

we can transform the Green's function (5.8) to the interaction picture

$$G(x, x_0) = \frac{\langle 0|U(\infty, 0) T \left[ U(0, t) \hat{\psi}(x) U(t, 0) U(0, t_0) \hat{\psi}^\dagger(x_0) U(t_0, 0) \right] U(0, -\infty)|0\rangle}{\langle 0|U(\infty, -\infty)|0\rangle}. \quad (5.11)$$

For  $t > t_0$  the numerator becomes

$$\langle 0|U(\infty, t) \hat{\psi}(x) U(t, t_0) \hat{\psi}^\dagger(x_0) U(t_0, -\infty)|0\rangle \quad (5.12a)$$

and for  $t < t_0$

$$\langle 0|U(\infty, t_0) \hat{\psi}^\dagger(x_0) U(t_0, t) \hat{\psi}(x) U(t, -\infty)|0\rangle, \quad (5.12b)$$

using the relation (3.17). From the expansion (3.24) we obtain the identity

$$\begin{aligned} U(t, t_0) &= \sum_{\nu=0}^{\infty} \frac{(-i)^\nu}{\nu!} \int_{t_0}^t dt_1 \dots \int_{t_0}^t dt_\nu T [V(t_1) \dots V(t_\nu)] e^{-\gamma(|t_1|+|t_2|+\dots)} \\ &= \sum_{n=0}^{\infty} \frac{(-i)^n}{n!} \int_{t_1}^t dt_1 \dots \int_{t_1}^t dt_n T [V(t_1) \dots V(t_n)] e^{-\gamma(|t_1|+|t_2|+\dots)} \\ &\quad \times \sum_{m=0}^{\infty} \frac{(-i)^m}{m!} \int_{t_0}^{t_1} dt_1 \dots \int_{t_0}^{t_1} dt_m T [V(t_1) \dots V(t_m) e^{-\gamma(|t_1|+|t_2|+\dots)}], \end{aligned} \quad (5.13)$$

where we have included the unity as the zeroth-order term in the summation. If we concentrate on the  $\nu$ :th term of the first sum, we have the identity (leaving out the damping factor)

$$\begin{aligned} & \frac{1}{\nu!} \int_{t_0}^t dt_1 \dots \int_{t_0}^t dt_\nu T [V(t_1) \dots V(t_\nu)] \\ &= \sum_{m+n=\nu} \frac{1}{m!n!} \int_{t_1}^t dt_1 \dots \int_{t_1}^t dt_n T [\dots] \int_{t_0}^{t_1} dt_1 \dots \int_{t_0}^{t_1} dt_m T [\dots]. \end{aligned} \quad (5.14)$$

We can now apply this identity to the first part of the numerator (5.12a),  $U(\infty, t) \hat{\psi}(x) U(t, t_0)$ . The interaction times of  $U(\infty, t)$ ,  $\hat{\psi}(x)$  and  $U(t, t_0)$  are time ordered, and hence the result can be expressed

$$\frac{1}{\nu!} \int_{t_0}^{\infty} dt_1 \dots \int_{t_0}^{\infty} dt_\nu T [V(t_1) \dots V(t_\nu) \hat{\psi}(x)]. \quad (5.15)$$

The same procedure can be applied to the rest of the expression (5.12a) as well as to the other time ordering (5.12b). With the perturbation (3.25) the numerator of the single-particle Green's function (5.11) then becomes [67, Eq. 8.9]

$$\begin{aligned} \langle 0_H | T [\hat{\psi}_H(x) \hat{\psi}_H^\dagger(x_0)] | 0_H \rangle &= \sum_{n=0}^{\infty} \frac{1}{n!} \left( \frac{-i}{c} \right)^n \int d^4x_1 \dots \int d^4x_n \\ &\quad \times \langle 0 | T [\hat{\psi}(x) \mathcal{H}(x_1) \dots \mathcal{H}(x_n) \hat{\psi}^\dagger(x_0)] | 0 \rangle e^{-\gamma(|t_1|+|t_2|+\dots)} \end{aligned} \quad (5.16)$$

with integrations over all *internal* times. In transforming the time-ordering to normal ordering by means of Wick's theorem, only *fully contracted* terms remain, since the vacuum expectation of any normal-ordered expression vanishes (see Sect. 2.2).

The denominator in (5.8) becomes, using the relation (5.9),

$$\langle 0_H | 0_H \rangle = \langle 0 | U(\infty, -\infty) | 0 \rangle = \langle 0 | S | 0 \rangle,$$

where  $S$  is the S-matrix (4.2). Then

- ***the Green's function can be expressed***

$$G(x, x_0) = \frac{\langle 0_H | T [\hat{\psi}_H(x) \hat{\psi}_H^\dagger(x_0)] | 0_H \rangle}{\langle 0 | S | 0 \rangle}. \quad (5.17)$$

We see that this expansion is very similar to that of the S-matrix (4.3), the main difference being the two additional electron-field operators. Therefore,

- ***the Green's function can also be expressed as***

$$G(x, x_0) = \frac{\langle 0 | T [\hat{\psi}(x) U(\infty, -\infty) \hat{\psi}^\dagger(x_0)] | 0 \rangle}{\langle 0 | S | 0 \rangle}, \quad (5.18)$$



where the time-ordered product is connected to form a one-body operator. This leads to

$$G(x, x_0) = \frac{1}{\langle 0|S|0\rangle} \sum_{n=0}^{\infty} \frac{1}{n!} \left(\frac{-i}{c}\right)^n \int d^4x_1 \dots \int d^4x_n \\ \times \langle 0|T \left[ \hat{\psi}(x) \mathcal{H}(x_1) \dots \mathcal{H}(x_n) \hat{\psi}^\dagger(x_0) \right] |0\rangle e^{-\gamma(|t_1|+|t_2|+\dots)}. \quad (5.19)$$

The Green's function is like the S-matrix *Lorentz covariant* (in the limit of vanishing damping).

The two-particle Green's function is defined in an analogous way

$$G(x, x'; x_0, x'_0) = \frac{\langle 0|T \left[ \hat{\psi}_H(x) \hat{\psi}_H(x') \hat{\psi}_H^\dagger(x'_0) \hat{\psi}_H^\dagger(x_0) \right] |0\rangle}{\langle 0|S|0\rangle}, \quad (5.20)$$

and transforming to the interaction picture, leads similarly to

$$G(x, x'; x_0, x'_0) = \frac{1}{\langle 0|S|0\rangle} \sum_{n=0}^{\infty} \frac{1}{n!} \left(\frac{-i}{c}\right)^n \int d^4x_1 \dots \int d^4x_n \\ \times \langle 0|T \left[ \hat{\psi}(x) \hat{\psi}(x') \mathcal{H}(x_1) \dots \mathcal{H}(x_n) \hat{\psi}^\dagger(x'_0) \hat{\psi}^\dagger(x_0) \right] |0\rangle e^{-\gamma(|t_1|+|t_2|+\dots)} \quad (5.21)$$

and analogously in the general many-particle case.

Contracting the electron-field operators has the consequence that in the diagrammatic representation *all free ends are electron propagators*.

Note that the coordinates are here four-dimensional space-time coordinates, which implies that the particles have *individual initial and final times*. This is in contrast to the quantum-mechanical wave function or state vector, which has the same time for all particles. We shall discuss this question further below.

We can transform the time-ordered products above to normal-ordered ones by means of Wick's theorem (see Sect. 2.2.3). Since normal-ordered products do not contribute to the vacuum expectation value, it follows that only fully contracted terms contribute to the Green's function. The contractions between the electron-field operators and the interaction operators lead to *electron propagators* ( $S_F$ ) (4.9) on the in- and outgoing lines as well as all internal lines (see Fig. 5.1).<sup>2</sup> This allows time to run in both directions and *both particle and hole states can be involved*.

---

<sup>2</sup>In our notations, an orbital line between heavy dots always represents an electron propagator.

**Fig. 5.1** Graphical representation of the one- and two-particle Green's function. The orbital lines between dots represent electron propagators

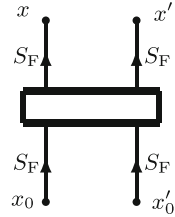
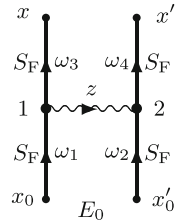


**Fig. 5.2** Green's function for single-photon exchange



### 5.2.2 Single-Photon Exchange

The Green's function for single-photon exchange in Fig. 5.2 can be constructed in close analogy to that of the corresponding S-matrix in Sect. 4.4,

$$G(x, x', x_0, x'_0) = \iint d^4x_2 d^4x_1 iS_F(x, x_1) iS_F(x', x_2) \times (-i)e^2 D_F(x_2, x_1) iS_F(x_1, x_0) iS_F(x_2, x'_0) e^{-\gamma(|t_1|+|t_2|)}. \quad (5.22)$$

With the transforms (4.10) and (4.31) this becomes after integrating over the internal times (using the relation A.20)

$$G(x, x', x_0, x'_0) = e^{-it\omega_3} e^{-it'\omega_4} e^{it_0\omega_1} e^{it'_0\omega_2} \times \iint d^3x_1 d^3x_2 \iint \frac{d\omega_3}{2\pi} \frac{d\omega_4}{2\pi} \iint \frac{d\omega_1}{2\pi} \frac{d\omega_2}{2\pi} \int \frac{dz}{2\pi} iS_F(\omega_3; \mathbf{x}, \mathbf{x}_1) \times iS_F(\omega_4; \mathbf{x}', \mathbf{x}_2) (-i)e^2 D_F(z; \mathbf{x}_2, \mathbf{x}_1) iS_F(\omega_1; \mathbf{x}_1, \mathbf{x}_0) \times iS_F(\omega_2; \mathbf{x}_2, \mathbf{x}'_0) 2\pi\Delta_\gamma(\omega_1 - z - \omega_3) 2\pi\Delta_\gamma(\omega_2 + z - \omega_4). \quad (5.23)$$

In the *equal-time approximation*, where the particles have the same initial and final times ( $t = t'$  and  $t_0 = t'_0$ ), the external time dependence becomes  $e^{-it(\omega_3+\omega_4)} e^{it_0(\omega_1+\omega_2)}$ . In the limit  $\gamma \rightarrow 0$  we have after  $z$ -integration  $\omega_1 + \omega_2 = \omega_3 + \omega_4$ , and if we consider the diagram as a part of a ladder, this is equal to the initial energy  $E_0$ .

*We define the Feynman amplitude for the Green's function as the function with the external time dependence removed.* This gives

$$G(x, x', x_0, x'_0) = \mathcal{M}_{\text{sp}}(\mathbf{x}, \mathbf{x}'; \mathbf{x}_0, \mathbf{x}'_0) e^{-i(t-t_0)E_0} \quad (5.24)$$

and

$$\begin{aligned} \mathcal{M}_{\text{sp}}(\mathbf{x}, \mathbf{x}'; \mathbf{x}_0, \mathbf{x}'_0) &= \iint d^3x_1 d^3x_2 \iint \frac{d\omega_3}{2\pi} \frac{d\omega_4}{2\pi} \iint \frac{d\omega_1}{2\pi} \frac{d\omega_2}{2\pi} \\ &\times iS_{\text{F}}(\omega_3; \mathbf{x}, \mathbf{x}_1) iS_{\text{F}}(\omega_4; \mathbf{x}', \mathbf{x}_2) (-i)I(\omega_1 - \omega_3; \mathbf{x}_2, \mathbf{x}_1) iS_{\text{F}}(\omega_1; \mathbf{x}_1, \mathbf{x}_0) \\ &\times iS_{\text{F}}(\omega_2; \mathbf{x}_2, \mathbf{x}'_0) 2\pi\Delta_{2\gamma}(\omega_1 + \omega_2 - \omega_3 - \omega_4), \end{aligned} \quad (5.25)$$

using the definition (4.44).

**The Feynman amplitude is the same as for the S-matrix and can be evaluated by means of the rules given above (Sect. 4.7).**

### 5.2.3 Fourier Transform of the Green's Function

#### 5.2.3.1 Single-Particle Green's Function

Assuming the Heisenberg vacuum state  $|0_{\text{H}}\rangle$  to be normalized, the single-particle Green's function (5.8) becomes

$$\begin{aligned} G(x, x_0) &= \langle 0_{\text{H}} | T \left[ \hat{\psi}_{\text{H}}(x) \hat{\psi}_{\text{H}}^\dagger(x_0) \right] | 0_{\text{H}} \rangle \\ &= \Theta(t - t_0) \langle 0_{\text{H}} | \hat{\psi}_{\text{H}}(x) \hat{\psi}_{\text{H}}^\dagger(x_0) | 0_{\text{H}} \rangle - \Theta(t_0 - t) \langle 0_{\text{H}} | \hat{\psi}_{\text{H}}^\dagger(x_0) \hat{\psi}_{\text{H}}(x) | 0_{\text{H}} \rangle. \end{aligned} \quad (5.26)$$

The retarded part (5.2) is then, using the relation (B.27) in Appendix B,

$$\begin{aligned} G_+(x, x_0) &= \langle 0_{\text{H}} | \hat{\psi}_{\text{H}}(x) \hat{\psi}_{\text{H}}^\dagger(x_0) | 0_{\text{H}} \rangle \\ &= \langle 0_{\text{H}} | \left( e^{iHt} \hat{\psi}_{\text{S}}(\mathbf{x}) e^{-iHt} \right) \left( e^{iHt_0} \hat{\psi}_{\text{S}}^\dagger(\mathbf{x}_0) e^{-iHt_0} \right) | 0_{\text{H}} \rangle. \end{aligned} \quad (5.27)$$

Inserting between the field operators a complete set of positive-energy eigenstates of the second-quantized Hamiltonian  $H$  (2.17), corresponding to the  $(N + 1)$ -particle system

$$H |n\rangle = E_n |n\rangle, \quad (5.28)$$

yields the *Lehmann representation*

$$G_+(x, x_0) = \sum_n \langle 0_{\text{H}} | e^{iHt} \hat{\psi}_{\text{S}}(x) | n \rangle e^{-iE_n(t-t_0)} \langle n | \hat{\psi}_{\text{S}}^\dagger(x_0) e^{-iHt} | 0_{\text{H}} \rangle. \quad (5.29)$$

summed over the intermediate states of the  $(N + 1)$  system. The ground state as well as the inserted intermediate states are eigenstates of the Hamiltonian  $H$ , and setting the energy of the former to zero, this yields

$$G_+(x, x_0) = \sum_n \langle 0_H | \hat{\psi}_S(x) | n \rangle e^{-iE_n(t-t_0)} \langle n | \hat{\psi}_S^\dagger(x_0) | 0_H \rangle. \quad (5.30)$$

Performing a Fourier transform of the Green's function, including the *adiabatic damping*  $e^{-\gamma\tau}$  (see Sect. 3.3), yields ( $\tau = t - t_0 > 0$ )

$$G_+(E; \mathbf{x}, \mathbf{x}_0) = \int_0^\infty d\tau e^{iE\tau} G_+(\tau, \mathbf{x}, \mathbf{x}_0) = i \frac{\langle 0_H | \hat{\psi}_S(\mathbf{x}) | n \rangle \langle n | \hat{\psi}_S^\dagger(\mathbf{x}_0) | 0_H \rangle}{E - E_n + i\gamma}, \quad (5.31)$$

using

$$\int_0^\infty dt e^{i\alpha t} e^{-\gamma t} = \frac{i}{\alpha + i\gamma}. \quad (5.32)$$

Analogous results are obtained for the *advanced* part ( $t < t_0$ ) of the Green's function, corresponding to a *hole* in the initial system.

The expression  $\langle 0_H | \hat{\psi}_S(\mathbf{x}) | n \rangle$  represents a state  $\Psi_n(\mathbf{x})$  of the  $(N + 1)$  system in the Schrödinger picture, and an equivalent expression of

- ***the Fourier transform of the Green's function becomes***

$$G_+(E; \mathbf{x}, \mathbf{x}_0) = i \sum_n \frac{\Psi_n(\mathbf{x}) \Psi_n^*(\mathbf{x}_0)}{E - E_n + i\gamma}. \quad (5.33)$$

This implies that

- ***the poles of the retarded/advanced single-particle Green's function represent the true energies of the vacuum plus/minus one particle, relative to the vacuum state.***

In order to show that the definition (5.8) of the Green's function is compatible with the classical definition (5.1) and (5.5), we form the reverse transformation

$$G_+(x, x_0) = G_+(\tau, \mathbf{x}, \mathbf{x}_0) = \int \frac{dE}{2\pi} e^{-iE\tau} i \sum_n \frac{\Psi_n(\mathbf{x}) \Psi_n^*(\mathbf{x}_0)}{E - E_n + i\gamma}. \quad (5.34)$$

We then find that

$$\left( i \frac{\partial}{\partial t} - H(x) \right) G_+(x, x_0) = \int \frac{dE}{2\pi} e^{-iE\tau} i \sum_n \frac{E - E_n}{E - E_n + i\gamma} \Psi_n(\mathbf{x}) \Psi_n^*(\mathbf{x}_0). \quad (5.35)$$

Letting  $\gamma \rightarrow 0$  and using the closure property (C.27)

$$\sum_n \Psi_n(\mathbf{x}) \Psi_n^*(\mathbf{x}_0) = \delta^3(\mathbf{x} - \mathbf{x}_0)$$

and the integral

$$\int \frac{dE}{2\pi} e^{-iE\tau} = \delta(\tau) = \delta(t - t_0)$$

we confirm that the retarded part of the Green's function (5.8) satisfies the relation (5.5)

$$\left( i \frac{\partial}{\partial t} - H(x) \right) G_+(x, x_0) = i\delta^4(x - x_0). \quad (5.36)$$

### 5.2.3.2 Electron Propagator

We consider now the zeroth-order single-particle Green's function (5.19)

$$G_0(x, x_0) = \langle 0 | T[\hat{\psi}(x)\hat{\psi}^\dagger(x_0)] | 0 \rangle, \quad (5.37)$$

where the vacuum and the field operators are expressed in the interaction picture. Then we find that

- **the single-particle Green's function is identical to the Feynman electron propagator (4.9) times the imaginary unit  $i$**

$$G_0(x, x_0) \equiv iS_F(x, x_0). \quad (5.38)$$

The retarded operator can be transformed in analogy with the Lehmann representation above

$$G_{0+}(x, x_0) = \sum_n \langle 0_H | \hat{\psi}_S(x) | n^0 \rangle e^{-iE_n^0(t-t_0)} \langle n^0 | \hat{\psi}_S^\dagger(x_0) | 0_H \rangle, \quad (5.39)$$

where  $|n^0\rangle$  are eigenstates of the zeroth-order Hamiltonian for the  $(N + 1)$ -particle system (B.22)

$$H_0 |n^0\rangle = E_n^0 |n^0\rangle,$$

and  $E_n^0$  are the energies relative the vacuum. Performing the time integration, yields the Fourier transform

$$G_{0+}(\mathbf{x}, \mathbf{x}_0, E) = i \sum_n \frac{\langle \mathbf{x} | n^0 \rangle \langle n^0 | \mathbf{x}_0 \rangle}{E - E_n^0 + i\gamma}. \quad (5.40)$$

The corresponding advanced function becomes

$$G_{0-}(\mathbf{x}, \mathbf{x}_0, E) = -i \sum_n \frac{\langle \mathbf{x} | n^0 \rangle \langle n^0 | \mathbf{x}_0 \rangle}{E - E_n^0 - i\gamma}. \quad (5.41)$$

Both of these results can be expressed by means of a complex integral

$$G_0(x, x_0) = iS_F(x, x_0) = i \int \frac{dE}{2\pi} \frac{\langle \mathbf{x} | n^0 \rangle \langle n^0 | \mathbf{x}_0 \rangle}{E - E_n^0 + i\gamma_n} e^{-iE(t-t_0)}, \quad (5.42)$$

where  $\gamma_n$  has the same sign as  $E_n^0$ , i.e., positive for particle states and negative for hole or antiparticle states.

The zeroth-order Green's function or electron propagator can also be expressed in operator form as

$$\hat{G}_0(E) = i\hat{S}_F(E) = \frac{i}{E - H_0 \pm i\gamma}. \quad (5.43)$$

### 5.2.3.3 Two-Particle Green's Function in the Equal-Time Approximation

Setting the initial and final times equal for the two particles,  $t = t'$  and  $t_0 = t'_0$ , the retarded two-particle Green's function (5.20) becomes

$$\begin{aligned} G_+(x, x'; x_0, x'_0) &= \langle 0_H | \hat{\psi}_H(x) \hat{\psi}_H(x') \hat{\psi}_H^\dagger(x'_0) \hat{\psi}_H^\dagger(x_0) | 0_H \rangle \\ &= \langle 0_H | \left( e^{iHt} \hat{\psi}_S(\mathbf{x}) \hat{\psi}_S(\mathbf{x}') e^{-iHt} \right) \left( e^{iHt_0} \hat{\psi}_S^\dagger(\mathbf{x}'_0) \hat{\psi}_S^\dagger(\mathbf{x}_0) e^{-iHt_0} \right) | 0_H \rangle. \end{aligned} \quad (5.44)$$

We introduce a complete set of two-particle states (5.28), which leads to the Lehmann representation

$$G_+(x, x'; x_0, x'_0) = \sum_n \langle 0_H | \hat{\psi}_S(x) \hat{\psi}_S(x') | n \rangle e^{-iE_n(t-t_0)} \langle n | \hat{\psi}_S^\dagger(x'_0) \hat{\psi}_S^\dagger(x_0) | 0_H \rangle \quad (5.45)$$

with the Fourier transform

$$G_+(E; \mathbf{x}, \mathbf{x}'; \mathbf{x}_0, \mathbf{x}'_0) = \sum_n \frac{\langle 0_H | \hat{\psi}_S(\mathbf{x}) \hat{\psi}_S(\mathbf{x}') | n \rangle \langle n | \hat{\psi}_S^\dagger(\mathbf{x}'_0) \hat{\psi}_S^\dagger(\mathbf{x}_0) | 0_H \rangle}{E - E_n \pm i\gamma} \quad (5.46)$$

with the upper (lower) sign for the retarded (advanced) function. Here,  $\langle n | \hat{\psi}_S^\dagger(\mathbf{x}_0) \hat{\psi}_S^\dagger(\mathbf{x}'_0) | 0_H \rangle$  represents a two-particle state  $\Psi_n(\mathbf{x}, \mathbf{x}')$  in the Schrödinger picture, which yields the Fourier transform

$$G_+(E; \mathbf{x}, \mathbf{x}'; \mathbf{x}_0, \mathbf{x}'_0) = i \sum_n \frac{\Psi_n(\mathbf{x}, \mathbf{x}') \Psi_n^*(\mathbf{x}_0, \mathbf{x}'_0)}{E - E_n \pm i\gamma}. \quad (5.47)$$

This implies that also in this case the poles of the Green's function represent the exact eigenvalues of the system, relative to the vacuum. Note that this holds in the many-particle case only in the *equal-time approximation*, where there is only a single time coordinate  $\tau = t - t_0$ .









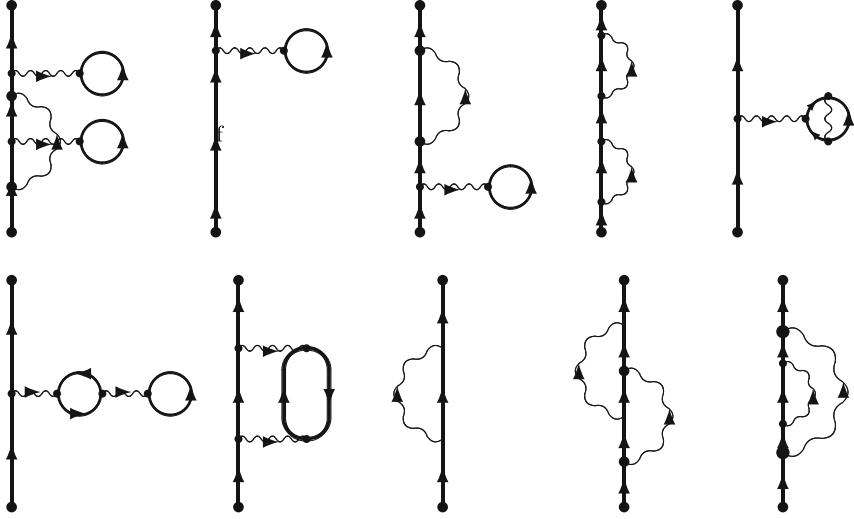


**Fig. 5.3** Second-order connected diagrams of the one-body Green's function, assuming a two-body interaction

We denote these diagrams by  $S_{\text{cl}}^{(2)} = \langle 0|S^{(2)}|0\rangle$ . In addition, we have the free electron-field operators, which combine to the zeroth-order Green's function  $G_0$ . Therefore, we can express the corresponding GF diagrams as  $G_0 S_{\text{cl}}^{(2)}$ .

Next, we consider the case where one of the interactions in (5.59) is closed by itself, while the remaining part is connected. This leads to disconnected diagrams, where the disconnected part is the closed first order (5.55) and the connected part is identical to the connected first-order diagrams in (5.56), which we can express the disconnected diagram as  $G_C^{(1)} S_{\text{cl}}^{(1)}$ .

Finally, we have the case where all diagram parts are completely connected, shown in Fig. 5.3, which we denote by  $G_C^{(2)}$ .

Going to third order, we find similarly that we can have  $G_0 = G^{(0)}$  combined with the closed diagrams  $S_{\text{cl}}^{(3)}$ ,  $G_C^{(1)}$  combined with  $S_{\text{cl}}^{(2)}$ ,  $G_C^{(2)}$  combined with  $S_{\text{cl}}^{(1)}$  and finally completely connected  $G_C^{(3)}$  diagrams. This leads to the sequence

$$\begin{cases} G^{(0)} \\ G_C^{(1)} + G^{(0)} S_{\text{cl}}^{(1)} \\ G_C^{(2)} + G_C^{(1)} S_{\text{cl}}^{(1)} + G^{(0)} S_{\text{cl}}^{(2)} \\ G_C^{(3)} + G_C^{(2)} S_{\text{cl}}^{(1)} + G_C^{(1)} S_{\text{cl}}^{(2)} + G^{(0)} S_{\text{cl}}^{(3)} \\ \text{etc.} \end{cases}$$

which summarizes to

$$(G^{(0)} + G_C^{(1)} + G_C^{(2)} + \dots)(1 + S_{\text{cl}}^{(1)} + S_{\text{cl}}^{(2)} + \dots) = (G_0 + G_C)(1 + S_{\text{cl}}), \quad (5.62)$$

where  $G_C$  represents all connected diagrams of the numerator of the GF expression (5.21) and  $S_{cl}$  represents all closed  $S$  diagrams. But the last factor is the vacuum expectation of the  $S$  matrix to all orders

$$\langle 0|S|0\rangle = 1 + S_{cl}, \tag{5.63}$$

which implies that this is cancelled by the denominator in the definition (5.8). Hence,

- **the single-particle Green's function can in the close-shell case be represented by completely connected diagrams**

$$iG(x, x_0) = \left[ \sum_{n=0}^{\infty} \frac{1}{n!} \left(\frac{-1}{c^2}\right)^n \int \dots \int d^4x_1 \dots d^4x_{2n} \times \langle 0|T \left[ \hat{\psi}(x) \mathcal{H}(x_1, x_2) \dots \mathcal{H}(x_{2n-1}, x_{2n}) \hat{\psi}^\dagger(x_0) \right] |0\rangle \right]_{\text{conn}}. \tag{5.64}$$

This can also be expressed

$$G(x, x_0) = \langle 0_H | T [\hat{\psi}_H(x) \hat{\psi}_H^\dagger(x_0)] | 0_H \rangle_{\text{conn}}. \tag{5.65}$$

The connectedness of the Green's function can also be shown in a somewhat different way. If we remove the two electron-field operators and the denominator from the Green's function expansion (5.19), then we retrieve the vacuum expectation of the  $S$ -matrix (4.3),  $\langle 0|S|0\rangle$ . Therefore, if the field operators are connected to each other and the interactions among themselves, the result (after including the denominator) is simply the zeroth-order Green's function  $iG^{(0)}$ . If the field operators are connected to one of the interactions, they form the connected first-order Green's function  $iG_{\text{conn}}^{(1)}$  and the remaining interactions again form  $\langle 0|S|0\rangle$ . Continuing the process leads to

$$G = G^{(0)} + G_{\text{conn}}^{(1)} + G_{\text{conn}}^{(2)} + \dots, \tag{5.66}$$

which proves that the *single-particle Green's function is entirely connected*.

### 5.3.1.1 One-Body Interaction

We shall now consider the case when we in addition to the two-body interaction have a one-body interaction of potential typ

$$\bullet \text{---} \text{wavy line} \text{---} \times \tag{5.67}$$

The graphical representation can then be constructed in the same way as before, and we then find in first order the additional diagrams

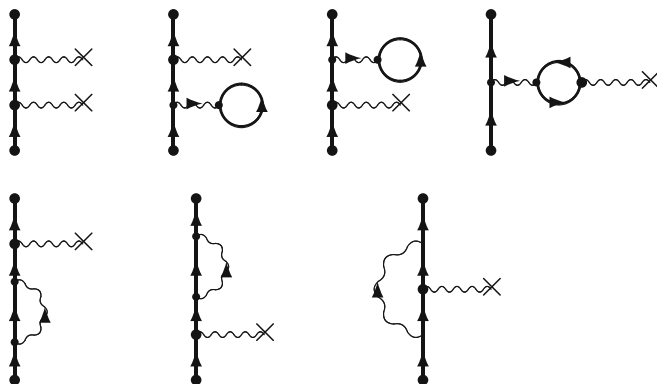


**Fig. 5.4** Additional second-order diagrams of the single-particle Green's function—in addition to those in Fig. 5.3—with a combination of one- and two-body interaction

(5.68)

The first diagram is unconnected, and the closed part is a part of  $\langle 0|S|0\rangle$  and hence this diagram is eliminated by the denominator of (5.19), as before. It is not difficult to show that the single-particle Green's function is represented by connected diagrams only, when we have a mixture of one- and two-body interactions. The additional connected diagrams in second order are shown in Fig. 5.4.

### 5.3.2 Many-Particle Green's Function

We now turn to the two-particle Green's function (5.21). The zeroth-order Green's function is in analogy with the one-particle function (5.49) represented by

$$G_0(x, x'; x_0, x'_0) = \begin{array}{c} x \bullet \\ | \\ x_0 \bullet \end{array} \begin{array}{c} x' \bullet \\ | \\ x'_0 \bullet \end{array} = iS_F(x, x_0) iS_F(x', x'_0) \tag{5.69}$$

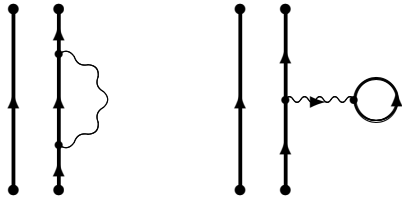
or a product of two Feynman electron propagators.

As mentioned before, the (initial and final) times of the two particles in principle can be different, although we shall in most applications assume that they are equal, as will be further discussed in the following.

In first order we have in analogy with the single-particle case (5.53)

$$\langle 0 | T [ \begin{array}{c} \bullet \quad \bullet \\ | \quad | \\ \bullet \quad \bullet \\ \text{---} \text{---} \text{---} \text{---} \text{---} \text{---} \\ \bullet \quad \bullet \\ | \quad | \\ \bullet \quad \bullet \end{array} ] | 0 \rangle \tag{5.70}$$

This can lead to disconnected diagrams, composed of the zeroth-order function (5.69) and the closed first-order diagrams (5.55). Another type of disconnected diagrams is the combination of zeroth-order single-particle GF and the connected first-order GF



$$\tag{5.71}$$

It should be noted that both parts are here considered as *open* (not closed).<sup>3</sup> Finally, we can have an open two-particle diagram



$$\tag{5.72}$$

In second order we can have the zeroth-order two-particle Green's function, combined with second-order closed diagrams,  $S_{cl}^{(2)}$ , and connected first-order diagrams combined with first-order closed diagrams,  $S_{cl}^{(1)}$ . In addition, we can have disconnected diagrams with two open first-order single-particle diagrams (5.56).

Continuing this process leads formally to the same result as in the single-particle case (5.62)—the diagrams with a disconnected closed part are eliminated by the denominator. Formally, the diagrams can still be disconnected, like (5.71), since there is a disconnected zeroth-order Green's function part. We shall refer to such diagrams as *linked* in analogy with the situation in MBPT (Sect. 2.4). The result is then expressed

<sup>3</sup>Generally, a diagram is considered closed if it has no free lines/propagators, like the diagrams in (5.60) and (5.61), while an open diagram has at least one pair of free lines, like those in Fig. 5.3. An operator or a function represented by a closed/open diagram is said to be closed/open.

$$\begin{aligned}
G(x, x'; x_0, x'_0) &= \left[ \sum_{n=0}^{\infty} \frac{1}{n!} \left( \frac{-1}{c^2} \right)^n \int d^4x_1 \dots \int d^4x_{2n} \right. \\
&\quad \left. \times \langle 0|T \left[ \hat{\psi}(x) \hat{\psi}(x') v(x_1, x_2) \dots v(x_{2n-1}, x_{2n}) \hat{\psi}^\dagger(x'_0) \hat{\psi}^\dagger(x_0) \right] |0 \rangle \right]_{\text{linked}}, \quad (5.73)
\end{aligned}$$

a result that can easily be extended to the general many-particle case.

The two-body interactions used here correspond to two contracted interactions of the type (4.4). Uncontracted interactions of this kind cannot contribute to the Green's function, since this is a vacuum expectation. Therefore, the results above can in the single-particle case also be expressed

$$\begin{aligned}
G(x, x_0) &= \sum_{n=0}^{\infty} \frac{1}{n!} \left( \frac{-i}{c} \right)^n \int d^4x_1 \dots \int d^4x_n \\
&\quad \times \langle 0|T \left[ \hat{\psi}(x) \mathcal{H}(x_1) \dots \mathcal{H}(x_n) \hat{\psi}^\dagger(x_0) \right] |0 \rangle_{\text{conn}}, \quad (5.74)
\end{aligned}$$

including even- as well as odd-order terms, and similarly in the many-particle case. This can also be expressed

$$\boxed{G(x, x_0) = \langle 0_{\text{H}} | T [\hat{\psi}_{\text{H}}(x) \hat{\psi}_{\text{H}}^\dagger(x_0)] | 0_{\text{H}} \rangle_{\text{conn}}.} \quad (5.75)$$

and in the two-particle case

$$\boxed{G(x, x'; x_0, x'_0) = \langle 0_{\text{H}} | T [\hat{\psi}_{\text{H}}(x) \hat{\psi}_{\text{H}}^\dagger(x') \hat{\psi}_{\text{H}}(x'_0) \hat{\psi}_{\text{H}}^\dagger(x_0)] | 0_{\text{H}} \rangle_{\text{linked}}} \quad (5.76)$$

The linked character of the Green's function can also in the two-particle case be shown as we did at the end on the single-particle section. If all interactions of the expansion (5.21) are connected among themselves, they form the vacuum expectation value of the S-matrix, cancelling the denominator, and the electron-field operators form the two-body zeroth-order Green's function  $G_2^{(0)}$ . If one pair of field operators are internally connected, then the remaining part is identical to the single-particle Green's function  $G_1$ , which has been shown to be connected. The result  $G_1^{(0)} G_1$  is *disconnected* but since both parts are open, this is *linked* with the convention we use. If one pair of field operators are connected to some of the interactions and the other pair to the remaining ones, the result is  $G_1 G_1$ , which is also disconnected but linked. Finally, all field operators can be connected to the interactions, which leads to the connected two-particle Green's function  $G_{2,\text{conn}}$ . The remaining interactions form  $\langle 0|S|0 \rangle$ , cancelling the denominator, and the result becomes  $G_{2,\text{conn}}$ . In summary, the two-particle Green's function becomes

$$G_2 = G_2^{(0)} + G_{1,\text{conn}} G_{1,\text{conn}} + G_{2,\text{conn}}, \quad (5.77)$$

which can be disconnected but linked. This argument can easily be generalized, implying that

- *the many-particle Green's function in the closed-shell case is linked.*

### 5.3.3 Self-Energy. Dyson Equation

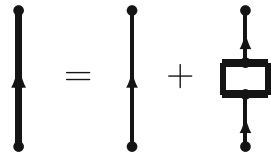
All diagrams of the one-particle Green's function can be expressed in the form

$$G(x, x_0) = G_0(x, x_0) + \iint d^4x_1 d^4x_2 G_0(x, x_1) (-i)\Sigma(x_1, x_2) G_0(x_2, x_0), \tag{5.78}$$

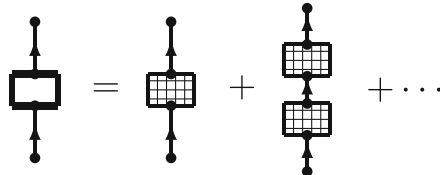
where  $\Sigma(x_2, x_1)$  represents the self-energy. This can be represented as shown in Fig. 5.5, i.e., as the zeroth-order Green's function plus all self-energy diagrams.

Some of the second-order self-energy diagrams in Figs. 5.3 and 5.4 have the form of two first-order diagrams, connected by a zeroth-order GF. All diagrams of that kind can be represented as a sequence of *proper self-energy diagrams*,  $\Sigma^*$ , which have the property that they cannot be separated into lower-order diagrams by cutting a single line. This leads to the expansion of the total self-energy shown in Fig. 5.6, where the crossed box represents the proper self-energy. The single-particle Green's function can then be represented as shown in Fig. 5.7, which corresponds to the *Dyson equation for the single-particle Green's function*.

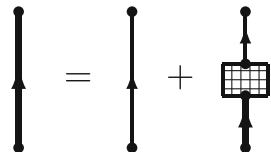
**Fig. 5.5** The single-particle Green's function expressed in terms of the self-energy



**Fig. 5.6** Expansion of the total self-energy in terms of proper self-energies. The *crossed box* represents the proper self-energy  $\Sigma^*$



**Fig. 5.7** Graphical representation of the Dyson equation for the single-particle Green's function (5.79), using the proper self-energy  $\Sigma^*$



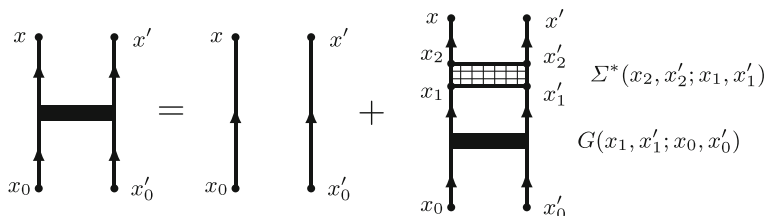


**Fig. 5.8** Graphical representation of the Dyson equation for the two-particle Green's function (5.80). The *crossed box* represents the proper two-particle self-energy

$$G(x, x_0) = G_0(x, x_0) + \iint d^4x_1 d^4x_2 G_0(x, x_2) (-i) \Sigma^*(x_2, x_1) G(x_1, x_0). \quad (5.79)$$

Similarly, the Dyson equation for two-particle Green's function becomes

$$\begin{aligned} G(x, x'; x_0, x'_0) &= G_0(x, x'; x_0, x'_0) \\ &+ \iiint d^4x_1 d^4x_2 d^4x'_1 d^4x'_2 G_0(x, x'; x_2, x'_2) (-i) \\ &\times \Sigma^*(x_2, x'_2; x_1, x'_1) G(x_1, x'_1; x_0, x'_0). \end{aligned} \quad (5.80)$$

This equation is illustrated in Fig. 5.8, where the crossed box represents the proper two-particle self-energy. This is equivalent to the Bethe–Salpeter equation, discussed in Sect. 8.3 and Chap. 10.

### 5.3.4 Numerical Illustration

Here, we shall illustrate the application of the Green's-function technique for many-body calculation by the electron affinity of the calcium atom (Table 5.1). The negative calcium ion is a very delicate system, with a very feeble binding energy, and it has

**Table 5.1** Electron affinity of Ca atom (in meV)

	$4p_{1/2}$	$4p_{3/2}$	Reference
Theory	19	-13	Salomonson [210]
Theory	22	-18	Avgoustoglou [12]
Theory	49	-18	Dzuba [12]
Expt'l	24, 55	-19.73	Petrinin (1996)
Expt'l	18, 4		Walter [247]
Expt'l	17, 5		Nadeau [171]



been quite difficult to determine this quantity experimentally as well as theoretically. It is only recently that it has been possible to obtain reasonable agreement.

The calculation of Salomonson et al. is performed by means of the Green's-function method, that of Dzuba et al. by many-body perturbation theory and that of Avgoustoglou by all-order pair-correlation method.

## 5.4 Field-Theoretical Green's Function—Open-Shell Case\*

In this section we shall indicate how the Green's-function concept could be extended to the open-shell case, when the model states are separated from the vacuum state. It is recommended that Chap. 6 is first studied, where the treatment is more akin to the normal situation in MBPT, discussed in Sect. 2.3. We shall leave out most details here and refer to the treatment of the covariant evolution operator and the Green's operator, which is quite equivalent. In the present section we shall in particular look into the special approach due to Shabaev [226].

### 5.4.1 Definition of the Open-Shell Green's Function

In the general open-shell case singularities of the Green's function can appear also for connected diagrams, as in the covariant evolution operator (see below). If we consider a sequence of ladder diagrams of single-photon exchange,  $V$ , as discussed in the next chapter (Fig. 6.5), considering only particle states (no-pair), the Feynman amplitude for the Green's function is the same as for the covariant evolution operator (6.35) with no model-space states,

$$\mathcal{M} = 1 + \Gamma_Q(E_0) V(E_0) + \Gamma_Q(E_0) V(E_0) \Gamma_Q(E_0) V(E_0) + \dots, \quad (5.81)$$

where

$$\Gamma_Q(E_0) = \frac{Q}{E_0 - H_0 + i\gamma} = \frac{|rs\rangle\langle rs|}{E_0 - \varepsilon_r - \varepsilon_s + i\gamma}$$

is the reduced resolvent (2.65) and  $E_0$  is the energy parameter (of the Fourier transform) of the Green's function. The GF becomes singular, when there is an intermediate state  $|rs\rangle$  of energy  $E_0$ . Including the residuals after removing the singularities (model-space contributions), leads as shown below (6.167) to a shift of the energy parameter,  $E_0 \rightarrow E = E_0 + \Delta E$ ,

$$\mathcal{M} = 1 + \Gamma_Q(E) V(E) + \Gamma_Q(E) V(E) \Gamma_Q(E) V(E) + \dots. \quad (5.82)$$

This is a Brillouin-Wigner perturbation expansion, and it can be summed to

$$\mathcal{M} = \frac{1}{E - H + i\gamma} = \frac{|n\rangle\langle n|}{E - E_n + i\gamma} \quad (5.83)$$

with  $H = H_0 + V(E)$  and  $|n\rangle$  represents the exact eigenstates of the system with the energy  $E_n$ . This agrees with the Fourier transform of the GF derived above (5.33), demonstrating that the transform has poles at the exact energies. Consequently, this holds also in the open-shell case.

The Green's-function technique yields information only about the energy of the system. This is in contrast to the *Green's-operator formalism*, to be treated in the next chapter, which can give information also about the wave function or state vector of the system under study.

### 5.4.2 Two-Time Green's Function of Shabaev

The use of the Green's-function technique for atomic calculations has been further developed by Shabaev et al. [226] under the name of the “*two-time Green's function*” (which is equivalent to the equal-time approximation, discussed above). This technique is also applicable to degenerate and quasi-degenerate energy states, and we shall outline its principles here.

We return to the *extended-model* concept, discussed in Sect. 2.3. Given are a number of eigenstates (target states) of the many-body Hamiltonian

$$H|\Psi^\alpha\rangle = E^\alpha|\Psi^\alpha\rangle \quad (\alpha = 1 \cdots d). \quad (5.84)$$

The corresponding model states are in intermediate normalization the projections on the model space

$$|\Psi_0^\alpha\rangle = P|\Psi^\alpha\rangle \quad (\alpha = 1 \cdots d). \quad (5.85)$$

The model states are generally *non-orthogonal*, and following Shabaev we introduce a “dual set”  $\{|\tilde{\Psi}_0^\beta\rangle\}$ , defined by

$$|\tilde{\Psi}_0^\beta\rangle\langle\Psi_0^\alpha| = |\Psi_0^\beta\rangle\langle\tilde{\Psi}_0^\alpha| = \delta_{\alpha,\beta}. \quad (5.86)$$

Then the standard projection operator becomes

$$P = \sum_{\beta \in D} |\tilde{\Psi}_0^\beta\rangle\langle\Psi_0^\beta| = \sum_{\beta \in D} |\Psi_0^\beta\rangle\langle\tilde{\Psi}_0^\beta| \quad (5.87)$$

with the summation performed over the model space  $D$ . We also define a alternative projection operator as

$$\mathcal{P} = \sum_{\beta \in D} |\Psi_0^\beta\rangle\langle\tilde{\Psi}_0^\beta| \quad \mathcal{P}^{-1} = \sum_{\beta} |\tilde{\Psi}_0^\beta\rangle\langle\Psi_0^\beta|. \quad (5.88)$$

Then

$$\mathcal{P}|\tilde{\Psi}_0^\alpha\rangle = |\Psi_0^\alpha\rangle \quad \text{and} \quad \mathcal{P}^{-1}|\Psi_0^\alpha\rangle = |\tilde{\Psi}_0^\alpha\rangle. \quad (5.89)$$

The Fourier transform of the retarded Green's function is generally (5.33)

$$G_+(E; \mathbf{x}, \mathbf{x}_0) = i \sum_n \frac{\langle \mathbf{x} | \Psi_n \rangle \langle \Psi_n | \mathbf{x}_0 \rangle}{E - E_n + i\gamma}, \quad (5.90)$$

where we let  $\mathbf{x}, \mathbf{x}_0$  represent the space coordinates of all outgoing/incoming particles. It then follows that

$$\oint_{\Gamma_n} dE G_+(E; \mathbf{x}, \mathbf{x}_0) = -2\pi \langle \mathbf{x} | \Psi_n \rangle \langle \Psi_n | \mathbf{x}_0 \rangle \quad (5.91)$$

and

$$\oint_{\Gamma_n} E dE G_+(E; \mathbf{x}, \mathbf{x}_0) = -2\pi \langle \mathbf{x} | \Psi_n \rangle E_n \langle \Psi_n | \mathbf{x}_0 \rangle, \quad (5.92)$$

where  $\Gamma_n$  is a closed contour, encircled in the positive direction and containing the single target energy  $E_n$  and no other pole. (This holds if all poles are distinct. In the case of degeneracy we can assume that an artificial interaction is introduced that lifts the degeneracy, an interaction that finally is adiabatically switched off.) This yields the relation [226, Eq. (44)]

$$E_n = \frac{\oint_{\Gamma_n} E dE G_+(E; \mathbf{x}, \mathbf{x}_0)}{\oint_{\Gamma_n} dE G_+(E; \mathbf{x}, \mathbf{x}_0)}. \quad (5.93)$$

Following Shabaev, we also introduce a “projected” Green's function by

$$g_+(E; \mathbf{x}, \mathbf{x}_0) = i \sum_{\beta \in D} \frac{\langle \mathbf{x} | \Psi_0^\beta \rangle \langle \Psi_0^\beta | \mathbf{x}_0 \rangle}{E - E^\beta + i\gamma}, \quad (5.94)$$

which is the coordinate representation (see Appendix C.3) of the corresponding operator

$$\hat{g}_+(E) = i \sum_{\beta \in D} \frac{|\Psi_0^\beta\rangle \langle \Psi_0^\beta|}{E - E^\beta + i\gamma} = i \sum_{\beta \in D} \frac{P |\Psi^\beta\rangle \langle \Psi^\beta| P}{E - E^\beta + i\gamma}, \quad (5.95)$$

operating only within the model space.

The effective Hamiltonian (2.53) is defined by

$$H_{\text{eff}} |\Psi_0^\alpha\rangle = E^\alpha |\Psi_0^\alpha\rangle$$

and we can then express this operator as

$$H_{\text{eff}} = \sum_{\beta \in D} |\Psi_0^\beta\rangle E^\beta \langle \tilde{\Psi}_0^\beta| = \mathcal{H}_{\text{eff}} \mathcal{P}^{-1}, \quad (5.96)$$

where

$$\mathcal{H}_{\text{eff}} = \sum_{\beta \in D} |\Psi_0^\beta\rangle E^\beta \langle \Psi_0^\beta|. \quad (5.97)$$

From the definition (5.94) it follows that

$$\mathcal{H}_{\text{eff}} = -\frac{1}{2\pi} \oint E \, dE \, g_+(E), \quad (5.98)$$

where the integration contour contains the energies of all target states. As before, we assume that the poles are distinct.

Expanding the effective Hamiltonian (5.96) order-by-order leads to

$$H_{\text{eff}} = \mathcal{H}_{\text{eff}}^{(0)} + \mathcal{H}_{\text{eff}}^{(1)} - \mathcal{H}_{\text{eff}}^{(0)} \mathcal{P}^{(1)} + \dots \quad (5.99)$$

The first-order operator  $\mathcal{H}_{\text{eff}}^{(1)}$  becomes

$$\mathcal{H}_{\text{eff}}^{(1)} = -\frac{1}{2\pi} \oint E \, dE \, g_+^{(0)}(E), \quad (5.100)$$

where

$$g_+^{(0)}(E; \mathbf{x}, \mathbf{x}_0) = i \sum_{\beta \in D} \frac{\langle \mathbf{x} | \Psi_0^\beta \rangle \langle \Psi_0^\beta | \mathbf{x}_0 \rangle}{E - E^\beta + i\gamma}. \quad (5.101)$$

The effective Hamiltonian above is *non-hermitian*, as in the MBPT treatment in Sect. 2.3. It can also be given a hermitian form [226], but we shall maintain the non-hermitian form here, since it makes the formalism simpler and the analogy with the later treatments more transparent.

### 5.4.3 Single-Photon Exchange

We shall now apply the two-time Greens function above to the case of single-photon exchange between the electrons, discussed above (Fig. 5.2). We shall evaluate the contribution to the effective Hamiltonian in the general quasi-degenerate case. In the equal-time approximation the (first-order) Green's function (5.25) is given by

$$G^{(1)}(x, x', x_0, x'_0) = \mathcal{M}_{\text{sp}}^{(1)}(\mathbf{x}, \mathbf{x}'; \mathbf{x}_0, \mathbf{x}'_0) e^{-it(\omega_3 + \omega_4)} e^{it_0(\omega_1 + \omega_2)} \quad (5.102)$$

and the first-order Feynman amplitude is given by (5.23)

$$\begin{aligned}
\mathcal{M}_{\text{sp}}^{(1)}(\mathbf{x}, \mathbf{x}'; \mathbf{x}_0, \mathbf{x}'_0) &= -i \iint \frac{d\omega_3}{2\pi} \frac{d\omega_4}{2\pi} \iint \frac{d\omega_1}{2\pi} \frac{d\omega_2}{2\pi} \\
&\times S_{\text{F}}(\omega_3; \mathbf{x}, \mathbf{x}_1) S_{\text{F}}(\omega_4; \mathbf{x}', \mathbf{x}_2) I(\omega_1 - \omega_3; \mathbf{x}_2, \mathbf{x}_1) \\
&\times S_{\text{F}}(\omega_1; \mathbf{x}_1, \mathbf{x}_0) S_{\text{F}}(\omega_2; \mathbf{x}_2, \mathbf{x}'_0) 2\pi \Delta_{2\gamma}(\omega_1 + \omega_2 - \omega_3 - \omega_4)
\end{aligned} \tag{5.103}$$

after integrations over  $z$ .

The Fourier transform of the Green's function with respect to  $t$  and  $t_0$  is

$$\begin{aligned}
G^{(1)}(E', E) &= \iint \frac{dt}{2\pi} \frac{dt_0}{2\pi} e^{iE't} e^{iEt_0} G^{(1)}(x, x', x_0, x'_0) \\
&= \Delta_{\gamma}(E' - \omega_3 - \omega_4) \Delta_{\gamma}(E - \omega_1 - \omega_2) \mathcal{M}_{\text{sp}}^{(1)}(\mathbf{x}, \mathbf{x}'; \mathbf{x}_0, \mathbf{x}'_0)
\end{aligned} \tag{5.104}$$

or

$$\begin{aligned}
G^{(1)}(E', E) &= -i \iint \frac{d\omega_3}{2\pi} \frac{d\omega_1}{2\pi} \\
&\times S_{\text{F}}(\omega_3; \mathbf{x}, \mathbf{x}_1) S_{\text{F}}(E' - \omega_3; \mathbf{x}', \mathbf{x}_2) I(\omega_1 - \omega_3; \mathbf{x}_2, \mathbf{x}_1) \\
&\times S_{\text{F}}(\omega_1; \mathbf{x}_1, \mathbf{x}_0) S_{\text{F}}(E - \omega_1; \mathbf{x}_2, \mathbf{x}'_0) 2\pi \Delta_{2\gamma}(E' - E)
\end{aligned} \tag{5.105}$$

after integrations over  $\omega_2, \omega_4$ . With the expression for the electron propagator (4.12) the matrix element of the Green's function becomes

$$\begin{aligned}
\langle rs | G^{(1)}(E', E) | tu \rangle &= \langle rs | \iint \frac{d\omega_3}{2\pi} \frac{d\omega_1}{2\pi} \\
&\times \frac{1}{\omega_3 - \varepsilon_r + i\gamma_u} \frac{1}{E' - \omega_3 - \varepsilon_s + i\gamma_s} I(\omega_1 - \omega_3) \\
&\times \frac{1}{\omega_1 - \varepsilon_t + i\gamma_t} \frac{1}{E - \omega_1 - \varepsilon_u + i\gamma_u} | tu \rangle 2\pi \Delta_{2\gamma}(E' - E).
\end{aligned} \tag{5.106}$$

With  $|rs\rangle$  and  $|tu\rangle$  in the model space, this is the same as the matrix element of the projected Green's function (5.94), considering only poles corresponding to the relevant target states. We define the single-energy Fourier transform by

$$G(E) = \int \frac{dE'}{2\pi} G(E', E), \tag{5.107}$$

which yields

$$\begin{aligned}
 \langle rs | G^{(1)}(E) | tu \rangle &= -i \langle rs | \iint \frac{d\omega_3}{2\pi} \frac{d\omega_1}{2\pi} I(\omega_1 - \omega_3) \\
 &\quad \times \frac{1}{E - \varepsilon_r - \varepsilon_s} \left[ \frac{1}{\omega_3 - \varepsilon_r + i\gamma_r} + \frac{1}{E - \omega_3 - \varepsilon_s + i\gamma_s} \right] \\
 &\quad \times \frac{1}{E - \varepsilon_t - \varepsilon_u} \left[ \frac{1}{\omega_1 - \varepsilon_t + i\gamma_t} + \frac{1}{E - \omega_1 - \varepsilon_u + i\gamma_u} \right] | tu \rangle.
 \end{aligned} \tag{5.108}$$

We assume here that the initial and final states lie in the model space with all single-particle states involved being particle states. The relevant poles are here

$$E = \varepsilon_t + \varepsilon_u = E_{\text{in}} \quad \text{and} \quad E = \varepsilon_r + \varepsilon_s = E_{\text{out}}.$$

The contribution of the first pole is

$$\begin{aligned}
 &\frac{-i}{2\pi i} \langle rs | \iint \frac{d\omega_3}{2\pi} \frac{d\omega_1}{2\pi} I(\omega_1 - \omega_3) \\
 &\quad \times \frac{E_{\text{in}}}{E_{\text{in}} - E_{\text{out}}} \left[ \frac{1}{\omega_3 - \varepsilon_r + i\gamma} + \frac{1}{E_{\text{in}} - \omega_3 - \varepsilon_s + i\gamma} \right] \\
 &\quad \times \left[ \frac{1}{\omega_1 - \varepsilon_t + i\gamma} + \frac{1}{E_{\text{in}} - \omega_1 - \varepsilon_u + i\gamma} \right] | tu \rangle.
 \end{aligned} \tag{5.109}$$

The last bracket yields  $-2\pi i \Delta_\gamma(\omega_1 - \varepsilon_t)$ , and integration over  $\omega_1$  yields

$$\begin{aligned}
 &i \langle rs | \int \omega_3 I(\varepsilon_t - \omega_3) \\
 &\quad \times \frac{E_{\text{in}}}{E_{\text{in}} - E_{\text{out}}} \left[ \frac{1}{\omega_3 - \varepsilon_r + i\gamma} + \frac{1}{E_{\text{in}} - \omega_3 - \varepsilon_s + i\gamma} \right] | tu \rangle.
 \end{aligned} \tag{5.110}$$

Similarly the other pole yields

$$\begin{aligned}
 &i \langle rs | \int \frac{d\omega_1}{2\pi} I(\omega_1 - \varepsilon_r) \\
 &\quad \times \frac{E_{\text{out}}}{E_{\text{in}} - E_{\text{out}}} \left[ \frac{1}{\omega_1 - \varepsilon_t + i\gamma} + \frac{1}{E_{\text{out}} - \omega_1 - \varepsilon_u + i\gamma} \right] | tu \rangle
 \end{aligned} \tag{5.111}$$

The matrix element of  $\mathcal{P}^{(1)}$  is similar with  $E_{\text{in}}$  and  $E_{\text{out}}$  in the numerator removed. The matrix element of  $\mathcal{H}_{\text{eff}}^{(0)} \mathcal{P}^{(1)}$  is obtained by multiplying by  $E_{\text{out}}$ , and the first-order contribution then becomes

$$\begin{aligned} \langle rs | H_{\text{eff}}^{(1)} | tu \rangle &= i \langle rs | \int \frac{d\omega_3}{2\pi} I(\varepsilon_t - \omega_3) \\ &\times \left[ \frac{1}{\omega_3 - \varepsilon_r + i\gamma} + \frac{1}{E_{\text{in}} - \omega_3 - \varepsilon_s + i\gamma} \right] | tu \rangle. \end{aligned} \quad (5.112)$$

The photon interaction is in the Feynman gauge given by (4.46)

$$I(q; \mathbf{x}_1, \mathbf{x}_2) = \int \frac{2c^2 \kappa d\kappa f^F(\kappa; \mathbf{x}_1, \mathbf{x}_2)}{q^2 - c^2 \kappa^2 + i\eta} \quad (5.113)$$

with  $f^F$  given by (4.55). This gives

$$I(\varepsilon_t - \omega_3) = \int \frac{2c^2 \kappa d\kappa f^F(\kappa; \mathbf{x}_1, \mathbf{x}_2)}{(\varepsilon_t - \omega_3)^2 - c^2 \kappa^2 + i\eta} \quad (5.114)$$

with the poles at  $\omega_3 = \varepsilon_t \pm (-i\eta)$ . Integrating the relation (5.112) over  $\omega_3$  then yields

$$\langle rs | H_{\text{eff}}^{(1)} | tu \rangle = \langle rs | \int cd\kappa f^F \left[ \frac{1}{\varepsilon_t - \varepsilon_r - (\kappa - i\eta)} + \frac{1}{\varepsilon_u - \varepsilon_s - (\kappa - i\eta)} \right] | tu \rangle. \quad (5.115)$$

This agrees with the result obtained with the Green's-operator method in the next chapter (6.23). The latter result is more general, since it is valid also when the initial and/or final states lie in the complementary  $Q$  space, in which case the result contributes to the wave function or wave operator.

In contrast to the S-matrix formulation the Green's-function method is applicable also when the initial and final states have different energies, which makes it possible to evaluate the effective Hamiltonian in the case of an extended model space and to handle the quasi-degenerate situation.

The two-time Green's function has in recent years been successfully applied to numerous highly charged ionic systems by Shabaev, Artemyev et al. of the St. Petersburg group for calculating two-photon radiative effects, fine structure separations and g-factors of hydrogenic systems [6, 9, 252, 254]. Some numerical results are given in Chap. 7.

## Chapter 6

# The Covariant Evolution Operator and the Green's-Operator Method

The third method we shall consider for numerical QED calculations on bound states is the Covariant-Evolution operator (CEO), developed during the last decade by the Gothenburg group [130, 131, 132]. This procedure is based upon the non-relativistic time-evolution operator, discussed in Chap. 3, but made relativistically covariant in order to be applicable in relativistic calculations. This method has the advantage over the two methods discussed previously, the S-matrix procedure and the Green's-function procedure, that it can be used perturbatively, and the perturbations can be included in the **wave function**—not only added to the energy. It then forms a convenient basis for a *covariant relativistic many-body perturbation procedure*, where electron correlation and quantum electrodynamics are systematically combined. For two-electron systems this is fully compatible with the *Bethe–Salpeter equation*. This question will be the main topic for the rest of the book.

### 6.1 Definition of the Covariant Evolution Operator

In the standard time-evolution operator (3.15),  $U(t, t_0)$ , time is assumed to evolve only *forwards* in the positive direction, which implies that  $t \geq t_0$ . Internally, time may run also *backwards* in the negative direction, which in the Feynman/Stückelberg interpretation [69, 234] represents the propagation of *hole or antiparticle states* with negative energy. However, all internal times ( $t_i$ ) are limited to the interval  $t_i \in [t, t_0]$ , and therefore this operator is **not covariant**.

In the S-matrix (4.2) the initial and final times are  $t_0 = -\infty$  and  $t = +\infty$ , respectively, which implies that the internal integrations do run over **all times**, making the concept *Lorentz covariant*.<sup>1</sup>

In order to make the time-evolution operator generally applicable for relativistic calculations, all internal integrations have to run over **all times**. This can be achieved

---

<sup>1</sup>See footnote in the Introduction.



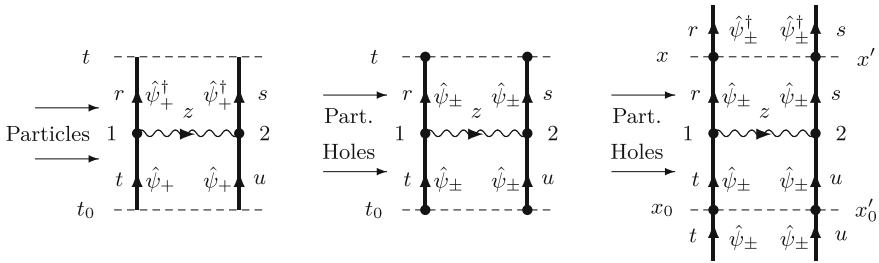


**Fig. 6.1** Comparison between the standard evolution operator, the Green's function and the covariant evolution operator for single-photon exchange in the equal-time approximation

by inserting electron propagators on the free lines and letting all vertices run over all times. This leads to what is referred to as the **covariant evolution operator** (CEO), introduced by Lindgren, Salomonson and coworkers in the early 2000s [120, 123, 130, 131, 132].

The CEO is, as well as the S-matrix and the Green's function, a *field-theoretical concept*, and the perturbative expansions of these objects are quite similar. Since the integrations are performed over all times, these objects are normally represented by *Feynman diagrams* instead of time-ordered *Goldstone diagrams*, discussed earlier (Sect. 2.4).

The evolution operator contains generally (quasi)singularities, when it is unlinked or when an intermediate state lies in the model space. Later in this chapter we shall see how these singularities can be removed for the CEO, leading to what we refer to as the **Green's operator**, since it is quite analogous to the Green's *function*, which is also free of singularities.

As mentioned, the covariant perturbation expansion we shall formulate here leads for two-particle systems ultimately to the full **Bethe–Salpeter (BS) equation** [131]. In principle, the BS equation has separate time variables for the individual particles, which makes it manifestly covariant. This is, in principle, also the case for the CEO and the Green's operator as well as for the Green's function. In most applications, however, times are equalized, so that the objects depend only on a single—initial and final—time, which is known as the **equal-time approximation**. This makes the procedure in line with the standard quantum-mechanical picture, where the wave function has a single time variable,  $\Psi(t, x_1, x_2 \dots)$ , but the covariance is then partly lost. (This issue was discussed at some length in the Introduction.) Here, we shall mainly work with this approximation in order to be able to combine the procedure with the standard many-body perturbation theory.

As a first illustration we consider the single-photon exchange with the standard evolution operator (Fig. 6.1, left), the Green's function (middle) and the CEO (right). In the standard evolution operator only *particle states* (positive-energy states) are involved in the lines in and out. Therefore, this operator is NOT Lorentz covariant. In the Green's function there are electron propagators on the free lines, involving *particle as well as hole states* (positive- and negative-energy states), and the internal

times can flow in both directions between  $-\infty$  and  $+\infty$ , which makes the concept covariant. In the CEO electron propagators are inserted as well as electron-field operators on the free lines of the standard evolution operator with integration over the space coordinates. We can then see the CEO as the Green's function with electron-field operators attached to the free ends. This makes the CEO into an **operator**, while the Green's function is a **function**.

- We generally define the *Covariant Evolution Operator* (CEO) in the single-particle case by the one-body operator<sup>2</sup>

$$U_{\text{Cov}}^1(t, t_0) = \iint d^3\mathbf{x} d^3\mathbf{x}_0 \hat{\psi}^\dagger(x) \langle 0_{\text{H}} | T[\hat{\psi}_{\text{H}}(x) \hat{\psi}_{\text{H}}^\dagger(x_0)] | 0_{\text{H}} \rangle \hat{\psi}(x_0). \quad (6.1)$$

We use here the same vacuum expectation in the Heisenberg representation as in the definition of the Green's function (5.8) with two additional electron-field operators,  $\hat{\psi}^\dagger(x)$  and  $\hat{\psi}(x_0)$ , with space integrations over  $\mathbf{x}$ ,  $\mathbf{x}_0$ . In contrast to the Green's function, we shall assume here that the number of photons does not need to be conserved. When this number is conserved, the vacuum expectation is a number and represents the corresponding Green's function (the norm is here unity). The space integration makes the electron-field operators attached to this function, as illustrated in Fig. 6.2, left (c.f. Fig. 5.1, left).

- In analogy with the expression (5.18) for the Green's function, we can also express the one-body covariant evolution operator as

$$U_{\text{Cov}}^1(t, t_0) = \iint d^3\mathbf{x} d^3\mathbf{x}_0 \hat{\psi}^\dagger(x) \langle 0 | T[\hat{\psi}(x) U^1(\infty, -\infty) \hat{\psi}^\dagger(x_0)] | 0 \rangle \hat{\psi}(x_0). \quad (6.2)$$

- In expanding the S-matrix (see 5.16), we obtain

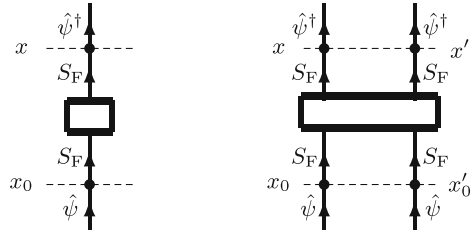
$$U_{\text{Cov}}^1(t, t_0) = \sum_{n=0}^{\infty} \frac{1}{n!} \iint d^3\mathbf{x} d^3\mathbf{x}_0 \left(\frac{-i}{c}\right)^n \int d^4x_1 \cdots \int d^4x_n \\ \times \hat{\psi}^\dagger(x) \langle 0 | T[\hat{\psi}(x) \mathcal{H}(x_1) \cdots \mathcal{H}(x_n) \hat{\psi}^\dagger(x_0)] | 0 \rangle \hat{\psi}(x_0) e^{-\gamma(|t_1| + |t_2| \cdots)}, \quad (6.3)$$

where the operators are connected to form a one-body operator.

- Similarly, the two-particle CEO becomes—in analogy with the corresponding Green's function (5.21) and Fig. 5.1 (right)—

<sup>2</sup>An “*n*-body operator” is an operator with  $n$  pairs of creation/absorption operators (for particles), while an “*m*-particle” function or operator is an object of  $m$  particles outside our vacuum. In principle,  $n$  can take any value  $n \leq m$ , although we shall normally assume that  $n = m$ .

**Fig. 6.2** One- and two-particle covariant evolution operators



$$\begin{aligned}
 U_{\text{Cov}}^2(t, t'; t_0, t'_0) &= \sum_{n=0}^{\infty} \frac{1}{n!} \iiint d^3x d^3x' d^3x_0 d^3x'_0 \left(\frac{-i}{c}\right)^n \int d^4x_1 \cdots \int d^4x_n \\
 &\times \hat{\psi}^\dagger(x) \hat{\psi}^\dagger(x') \langle 0 | T \left[ \hat{\psi}(x) \hat{\psi}(x') \mathcal{H}(x_1) \cdots \mathcal{H}(x_n) \hat{\psi}^\dagger(x'_0) \hat{\psi}^\dagger(x_0) \right] | 0 \rangle \\
 &\times \hat{\psi}(x'_0) \hat{\psi}(x_0) e^{-\gamma(|t_1|+|t_2|+\cdots)}, \tag{6.4}
 \end{aligned}$$

connected to form a two-body operator.

We see here that in the graphical representation each free end has an electron propagator with an electron-field operator attached to it (c.f. Fig. 5.1).

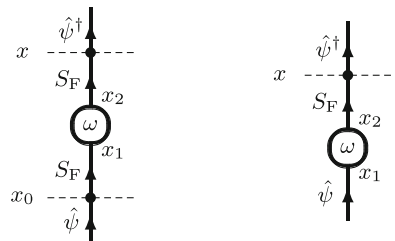
### 6.2 Lowest-Order Single-Particle Covariant Evolution Operator

We consider now the single-particle covariant evolution operator (6.3) in lowest order, represented by the first diagram in Fig. 6.3. It is given by the expression

$$\begin{aligned}
 U_{\text{Cov}}^1(t, t_0) &= \left(\frac{-i}{c}\right)^2 \iint d^3x d^3x_0 \hat{\psi}^\dagger(x) \hat{\psi}(x) \iint d^4x_1 d^4x_2 \\
 &\times \mathcal{H}(x_1) \mathcal{H}(x_2) \langle 0 | T \left[ \hat{\psi}(x) \hat{\psi}(x') \mathcal{H}(x_1) \cdots \mathcal{H}(x_n) \hat{\psi}^\dagger(x'_0) \hat{\psi}^\dagger(x_0) \right] | 0 \rangle \\
 &\times \hat{\psi}^\dagger(x_0) \hat{\psi}(x_0) e^{-\gamma(|t_1|+|t_2|)}, \tag{6.5}
 \end{aligned}$$

connected to form a one-body operator (cf., Eq. 4.39). The factor of 1/2 is eliminated by considering only one of the permutations of the vertices 1 and 2. We assume that we have a perturbation  $V(x_1, x_2)$  of the self-energy type with no external lines, defined by

**Fig. 6.3** First-order single-particle CEO. In the diagram to the *right* it is assumed that the initial time  $t_0 \rightarrow -\infty$



$$\mathcal{H}(x_1)\mathcal{H}(x_2) = \hat{\psi}^\dagger(x_1) iV(x_1, x_2)\hat{\psi}(x_2). \quad (6.6)$$

This gives

$$U_{\text{Cov}}^1(t, t_0) = \frac{1}{c^2} \iint d^3\mathbf{x} d^3\mathbf{x}_0 \hat{\psi}^\dagger(x) \times \left\{ \iint d^4x_1 d^4x_2 iS_F(x, x_2) (-i)V(x_2, x_1) iS_F(x_1, x_0) e^{-\gamma(|t_1|+|t_2|)} \right\} \hat{\psi}(x_0). \quad (6.7)$$

The expression in the curly brackets is the corresponding Green's function (5.19) (the denominator does not contribute in first- order). The CEO contains additional electron creation/annihilation operators and integration over the space coordinates at the initial and final times.

When the initial state is unperturbed, it implies with the adiabatic damping (Sect. 3.3) that the initial time  $t_0 \rightarrow -\infty$ . From the definition of the electron propagator (4.8) it can be shown that, as  $t_0 \rightarrow -\infty$ ,

$$\int d^3\mathbf{x}_0 iS_F(x, x_0) \hat{\psi}(x_0) \Rightarrow \hat{\psi}(x), \quad (6.8)$$

when the incoming state is a particle state. Therefore, we can leave out the propagator on the incoming line, as illustrated in the second diagram in Fig. 6.3, corresponding to the expression

$$U_{\text{Cov}}^1(t, -\infty) = \frac{1}{c^2} \int d^3\mathbf{x} \hat{\psi}^\dagger(x) \times \left\{ \iint d^4x_1 d^4x_2 iS_F(x, x_2) (-i)V(x_2, x_1); e^{-\gamma(|t_1|+|t_2|)} \right\} \hat{\psi}(x_1). \quad (6.9)$$

The matrix elements become

$$\begin{aligned} \langle r | U_{\text{Cov}}^1(t, -\infty) | a \rangle &= e^{i\varepsilon_r} \iint dt_1 dt_2 \langle r | iS_F(x, x_2) (-i)V(x_2, x_1) | a \rangle \\ &\quad \times e^{-it_1\varepsilon_a} e^{-\gamma(|t_1|+|t_2|)} \\ &= e^{i\varepsilon_r(\varepsilon_r - \omega_1)} \iint dt_1 dt_2 \iint \frac{d\omega}{2\pi} \frac{d\omega_1}{2\pi} \\ &\quad \times \langle r | iS_F(\omega_1, \mathbf{x}, x_2) (-i)V(\omega, \mathbf{x}_2, \mathbf{x}_1) | a \rangle \\ &\quad \times e^{-it_1(\varepsilon_a - \omega)} e^{-it_2(\omega - \omega_1)} e^{-\gamma(|t_1|+|t_2|)}. \end{aligned} \quad (6.10)$$

The electron propagator has the time dependence  $e^{-i\omega_1(t-t_2)}$  (4.10) and the perturbation is assumed to have a similar dependence,  $e^{-i\omega(t_2-t_1)}$ . Integration over the times leads to  $2\pi\Delta_\gamma(\omega - \omega_1)$  and  $2\pi\Delta_\gamma(\varepsilon_a - \omega)$  (see Appendix A.3), and the integrations

over the omegas in the limit  $\gamma \rightarrow 0$  yield  $\omega = \omega_1 = \varepsilon_a$ . The space integrations are incorporated in the matrix element and  $d^4x = c d^3x dt$ .

The result can then be expressed

$$U_{\text{Cov}}^1(t, -\infty)|a\rangle = e^{-it(\varepsilon_a - \varepsilon_r)} |r\rangle \langle r| iS_F(\varepsilon_a) (-i)V(\varepsilon_a) |a\rangle, \tag{6.11}$$

leaving out the space coordinates.  $\varepsilon_a$  is the initial energy that we shall denote  $E_0$ , and  $\varepsilon_r$  can be replaced by the zeroth-order Hamiltonian  $H_0$ , operating on the final state  $|r\rangle$ , yielding

$$U_{\text{Cov}}^1(t, -\infty)|a\rangle = e^{-it(E_0 - H_0)} |r\rangle \langle r| \mathcal{M}^1(E_0) |a\rangle. \tag{6.12}$$

$\mathcal{M}^1(E_0)$  is the *Feynman amplitude* for the first-order single-particle CEO (c.f. 5.23)

$$\langle r| \mathcal{M}^1 |a\rangle = \langle r| iS_F(E_0) (-i)V(E_0) |a\rangle. \tag{6.13}$$

This is consistent with the S-matrix result (4.67) and in agreement with the Feynman rules given in Appendix H.

### 6.3 Single-Photon Exchange in the Covariant-Evolution-Operator Formalism

We shall now consider the exchange of a single photon between the electrons in the covariant-evolution-operator formalism. We consider here a general *covariant gauge* (see Sect. 4.3), like the Feynman gauge, and we shall later consider the non-covariant Coulomb gauge.

The CEO for the exchange of a single photon, when the initial times  $t_0, t'_0 \rightarrow -\infty$  is represented by diagrams in Fig. 6.4. In analogy with the single-particle case (6.9) it is given by the expression

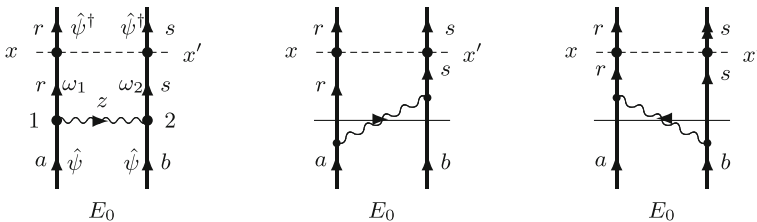


**Fig. 6.4** The evolution-operator diagram for single-photon exchange

$$\begin{aligned}
U_{\text{sp}}(t, t'; -\infty) &= \iint d^3\mathbf{x} d^3\mathbf{x}' \hat{\psi}^\dagger(\mathbf{x}) \hat{\psi}^\dagger(\mathbf{x}') \\
&\times \left\{ \frac{1}{2} \iint d^4x_1 d^4x_2 iS_{\text{F}}(x, x_1) iS_{\text{F}}(x', x_2) \right. \\
&\quad \left. (-i)e^2 D_{\text{F}}(x_2, x_1) e^{-\gamma(|t_1|+|t_2|)} \right\} \hat{\psi}(x_2) \hat{\psi}(x_1), \quad (6.14)
\end{aligned}$$

where  $D_{\text{F}}$  is given by (4.19). Considering only one permutation of the vertices, the factor of 1/2 is, as before, eliminated. This leads to the matrix element

$$\begin{aligned}
\langle rs | U_{\text{sp}}(t, t'; -\infty) | ab \rangle &= e^{i(t\varepsilon_r + t'\varepsilon_s)} \iint dt_1 dt_2 \langle rs | iS_{\text{F}}(x, x_1) \\
&\quad \times iS_{\text{F}}(x', x_2) (-i)e^2 c^2 D_{\text{F}}(x_2, x_1) | ab \rangle \\
&\quad \times e^{-i(t_1\varepsilon_a + t_2\varepsilon_b)} e^{-\gamma(|t_1|+|t_2|)}. \quad (6.15)
\end{aligned}$$

Introducing the Fourier transforms  $S_{\text{F}}(\omega_1; \mathbf{x}, \mathbf{x}_1)$  och  $S_{\text{F}}(\omega_2; \mathbf{x}', \mathbf{x}_2)$  and applying the *equal-time approximation* ( $t = t'$ ), the initial time dependence becomes  $e^{-it(\omega_1 + \omega_2 - \varepsilon_r - \varepsilon_s)}$ . Since in the limit  $\gamma \rightarrow 0$   $\omega_1 + \omega_2 = \varepsilon_a + \varepsilon_b = E_0$  is the *initial* energy and  $\varepsilon_r + \varepsilon_s$  is the *final* energy, we have in this limit

$$\langle rs | U_{\text{sp}}(t, -\infty) | ab \rangle = e^{-it(E_0 - \varepsilon_r - \varepsilon_s)} \langle rs | \mathcal{M}_{\text{sp}} | ab \rangle \quad (6.16)$$

or

$$U_{\text{sp}}(t, -\infty) | ab \rangle = e^{-it(E_0 - H_0)} | rs \rangle \langle rs | \mathcal{M}_{\text{sp}} | ab \rangle, \quad (6.17)$$

where  $\mathcal{M}_{\text{sp}}$  represents the Feynman amplitude in analogy with the single-particle case (6.12). This yields

$$\begin{aligned}
\langle rs | \mathcal{M}_{\text{sp}} | ab \rangle &= \left\langle rs \left| \iint \frac{d\omega_1}{2\pi} \frac{d\omega_2}{2\pi} \int \frac{dz}{2\pi} iS_{\text{F}}(\omega_1; \mathbf{x}, \mathbf{x}_1) iS_{\text{F}}(\omega_2; \mathbf{x}', \mathbf{x}_2) \right. \right. \\
&\quad \left. \left. \times (-i)I(z; \mathbf{x}_2, \mathbf{x}_1) 2\pi\Delta_\gamma(\varepsilon_a - z - \omega_1) 2\pi\Delta_\gamma(\varepsilon_b + z - \omega_2) \right| ab \right\rangle, \quad (6.18)
\end{aligned}$$

where  $I$  represents the single-photon interaction (4.44). After integration over  $\omega_1, \omega_2$  this becomes in the limit  $\gamma \rightarrow 0$

$$\langle rs | \mathcal{M}_{\text{sp}} | ab \rangle = \left\langle rs \left| \int \frac{dz}{2\pi} iS_{\text{F}}(\varepsilon_a - z) iS_{\text{F}}(\varepsilon_b + z) (-i)I(z) \right| ab \right\rangle, \quad (6.19)$$

again leaving out the space coordinates.

***This demonstrates that the Feynman amplitude for the evolution operator is the same as for the S-matrix and for the Green's function and can be evaluated by the same rules, given in Appendix H.***

Inserting the expressions for the propagator (4.10) and the interaction (4.46), then yields

$$\begin{aligned} & \langle rs | \mathcal{M}_{\text{sp}} | ab \rangle \\ &= \left\langle rs \left| i \int \frac{dz}{2\pi} \frac{1}{\varepsilon_a - z - \varepsilon_r + i\gamma_r} \frac{1}{\varepsilon_b + z - \varepsilon_s + i\gamma_s} \int \frac{2c^2 \kappa d\kappa f(\kappa)}{z^2 - c^2 \kappa^2 + i\eta} \right| ab \right\rangle. \end{aligned} \quad (6.20)$$

With the identity (4.75), this can be expressed

$$\langle rs | \mathcal{M}_{\text{sp}} | ab \rangle = \frac{1}{E_0 - \varepsilon_r - \varepsilon_s} \langle rs | V_{\text{sp}} | ab \rangle \quad (6.21)$$

or

$$\mathcal{M}_{\text{sp}}(\mathbf{x}, \mathbf{x}') | ab \rangle = \frac{1}{E_0 - H_0} V_{\text{sp}} | ab \rangle, \quad (6.22)$$

where  $V_{\text{sp}}$  is the potential for single-photon exchange (4.77),

$$\begin{aligned} & \langle rs | V_{\text{sp}} | ab \rangle \\ &= \left\langle rs \left| \int_0^\infty c d\kappa f(\kappa) \left[ \frac{1}{\varepsilon_a - \varepsilon_r - (c\kappa - i\gamma)_r} + \frac{1}{\varepsilon_b - \varepsilon_s - (c\kappa - i\gamma)_s} \right] \right| ab \right\rangle. \end{aligned} \quad (6.23)$$

The evolution operator (6.17) then becomes

$$\boxed{U_{\text{sp}}(t, -\infty) | ab \rangle = \frac{e^{-it(E_0 - H_0)}}{E_0 - H_0} V_{\text{sp}} | ab \rangle.} \quad (6.24)$$

**The results above hold in any covariant gauge, like the Feynman gauge. They do hold also for the transverse part in the Coulomb gauge** by using the transverse part of the  $f$  function (4.60).

The result (6.23) is identical to the Green's-function result (5.115), when the final state,  $|rs\rangle$ , lies in the model space. **In the covariant-evolution-operator case the final state can also lie in the complementary  $Q$  space, in which case the evolution operator contributes to the wave function/operator.**

The covariant-evolution-operator result (6.23) can be represented by means of two time-ordered Feynman diagrams, as shown in Fig. 6.4. We then see formally that the denominators are given essentially by the *Goldstone rules* of standard many-body perturbation theory [66, Sect. 12.4], i.e., *the unperturbed energy minus the energies of the orbital lines cut by a horizontal line, in the present case including also  $-c\kappa$*

cutting the photon line<sup>3</sup>, provided that we interpret the photon exchange as composed of TWO perturbations (see further Sect. 6.7 and Chap. 9).

When the initial and final states have the same energy, the potential (6.23) above becomes

$$\langle cd|V_{\text{sp}}|ab\rangle = \left\langle cd \left| \int_0^\infty \frac{2\kappa d\kappa f(\kappa)}{q^2 - \kappa^2 + i\gamma} \right| ab \right\rangle, \quad (6.25)$$

where  $cq = \varepsilon_a - \varepsilon_c = \varepsilon_d - \varepsilon_b$ , which is the energy-conservative S-matrix result (4.46 and 4.52).

We have seen here that the covariant evolution operator for single-photon exchange has the time dependence  $e^{-it(E_0-H_0)}$ , which differs from that of the non-relativistic evolution operator (3.20). We shall return to this question at the end of this chapter.

## 6.4 Ladder Diagrams

By generalizing the treatment in the two previous sections, we can construct the covariant evolution operator for a “ladder diagram”, i.e., a sequence of interactions that are *reducible* in the sense that it can be separated into legitimate CEO diagrams. We consider first a second-order one-body ladder, illustrated to the left in Fig. 6.5. In analogy with (6.9) we have

$$U(t; -\infty) = \frac{1}{c^4} \int d^3\mathbf{x} \hat{\psi}^\dagger(x) \iiint d^4x_1 d^4x_2 d^4x_3 d^4x_4 iS_F(x, x_4) (-i) V(x_4, x_3) \\ \times iS_F(x_3, x_2) (-i) V(x_2, x_1) e^{-\gamma(|t_1|+|t_2|+|t_3|+|t_4|)} \hat{\psi}(x_1), \quad (6.26)$$

where  $V$  is the potential interaction (6.6), previously used. Fourier transforming the operators and integrating of the times and the energy parameters, we find that all parameters become equal to the initial energy  $\varepsilon_a$ , and

$$\langle r|U(t; -\infty)|a\rangle = e^{-it(\varepsilon_a - \varepsilon_r)} \langle r|\mathcal{M}|a\rangle, \quad (6.27)$$

where  $\mathcal{M}$  is the Feynman amplitude

$$\langle r|\mathcal{M}|a\rangle = \langle r|iS_F(\varepsilon_a)(-i)V(\varepsilon_a)iS_F(\varepsilon_a)(-i)V(\varepsilon_a)|a\rangle. \quad (6.28)$$

All space integrations are included in the matrix element. The electron propagator can be expressed (4.14)

---

<sup>3</sup>It should be observed that a Goldstone diagram is generally distinct from a “time-ordered Feynman diagram”, as is further analyzed in Appendix I.



$$S_F(\varepsilon_a) = \frac{|i\rangle\langle i|}{\varepsilon_a - \varepsilon_i} = \frac{1}{\varepsilon_a - \hat{h}_D}, \quad (6.29)$$

which is identical to resolvent operator (2.64).

We assume now that we operate on a general model space that might contain several energies. Operating on a part with energy  $\mathcal{E}$ , with projection operator  $P_{\mathcal{E}}$ , we have

$$U(t; -\infty)P_{\mathcal{E}} = e^{-it(\mathcal{E}-H_0)}\mathcal{M}P_{\mathcal{E}} \quad (6.30)$$

with

$$\mathcal{M}P_{\mathcal{E}} = iS_F(\mathcal{E})(-i)V(\mathcal{E})iS_F(\mathcal{E})(-i)V(\mathcal{E})P_{\mathcal{E}} = \Gamma(\mathcal{E})V(\mathcal{E})\Gamma(\mathcal{E})V(\mathcal{E})P_{\mathcal{E}} \quad (6.31)$$

and

$$S_F(\mathcal{E}) = \Gamma(\mathcal{E}) = \frac{1}{\mathcal{E} - H_0}. \quad (6.32)$$

In a similar way one finds that the two-photon ladder to the right in Fig. 6.5 yields

$$\mathcal{M}P_{\mathcal{E}} = \Gamma(\mathcal{E})V_{\text{sp}}(\mathcal{E})\Gamma(\mathcal{E})V_{\text{sp}}(\mathcal{E})P_{\mathcal{E}}, \quad (6.33)$$

where the potential is given by (6.23) and illustrated in Fig. 6.6

$$\begin{aligned} & \langle rs|V_{\text{sp}}(\mathcal{E})|tu\rangle \\ &= \langle rs|\int_0^\infty c \, d\kappa f(\kappa) \left[ \frac{1}{\mathcal{E} - \varepsilon_r - \varepsilon_u - (c\kappa - i\gamma)_r} + \frac{1}{\mathcal{E} - \varepsilon_t - \varepsilon_s - (c\kappa - i\gamma)_s} \right] |tu\rangle. \end{aligned} \quad (6.34)$$

This potential depends on the energy ( $\mathcal{E}$ ) of the initial state.

The procedure can be generalized to a sequence of arbitrary interactions

$$\mathcal{M}P_{\mathcal{E}} = [1 + \Gamma(\mathcal{E})V(\mathcal{E}) + \Gamma(\mathcal{E})V(\mathcal{E})\Gamma(\mathcal{E})V(\mathcal{E}) + \dots]P_{\mathcal{E}}, \quad (6.35)$$

and the corresponding part of the evolution operator is according to (6.17)

$$U(t, -\infty)P_{\mathcal{E}} = e^{-it(\mathcal{E}-H_0)}[1 + \Gamma(\mathcal{E})V(\mathcal{E}) + \Gamma(\mathcal{E})V(\mathcal{E})\Gamma(\mathcal{E})V(\mathcal{E}) + \dots]P_{\mathcal{E}}. \quad (6.36)$$

**Fig. 6.5** Second-order ladder diagrams (6.33)

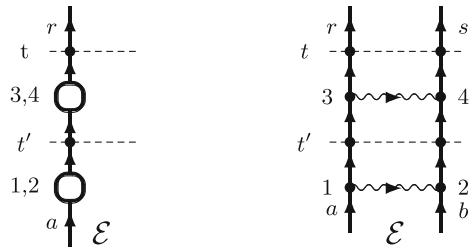
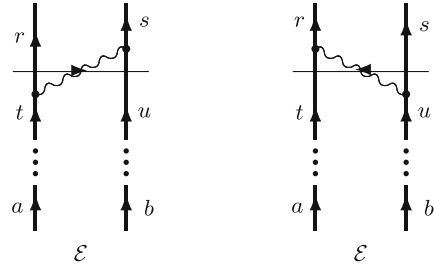


**Fig. 6.6** The single-photon exchange as a part of a ladder diagram. This depends on the energy of the initial state



This evolution operator can be singular due to intermediate **and/or** final model-space states, and the singularities can be eliminated by means of counterterms, leading to **model-space contributions, MSC**, to be discussed below. The evolution operator **without** any model-space states becomes<sup>4</sup>

$$U_0(t, -\infty) P_{\mathcal{E}} = e^{-ir(\mathcal{E}-H_0)} [1 + \Gamma_Q(\mathcal{E}) V(\mathcal{E}) + \Gamma_Q(\mathcal{E}) V(\mathcal{E}) \Gamma_Q(\mathcal{E}) V(\mathcal{E}) + \dots] P_{\mathcal{E}}, \tag{6.37}$$

where  $\Gamma_Q(\mathcal{E}) = Q\Gamma(\mathcal{E})$  is the reduced resolvent (2.65).

It should be observed that

- **in the equal-time approximation the interactions and the resolvents as well as the time factor of the ladder without MSC all depend on the energy of the initial, unperturbed state.**

The MSC will affect the energy parameter of the interaction as well as that of the time factor, as will be demonstrated below.

We have seen that **the Covariant Evolution Operator can be evaluated by means of the standard Feynman rules, like the S-matrix and the Green's function** (see Sect. 4.7 and Appendix H). We also see the **close analogy with the standard MBPT** in Chap. 2 (see also [124]). This is the **basis for employing the CEO in combining MBPT and QED**, to be discussed in the following chapters.

## 6.5 Multi-Photon Exchange

### 6.5.1 General

We shall now briefly consider the general case of multi-photon exchange. We can describe this by means of a general many-body potential, which we can separate into one-, two-,.... body parts,

$$V = V_1 + V_2 + V_3 + \dots \tag{6.38}$$

<sup>4</sup>In the covariant formalism we need a time dependence also on the zeroth-order component (see 6.96), in contrast to the standard evolution operator (3.21).

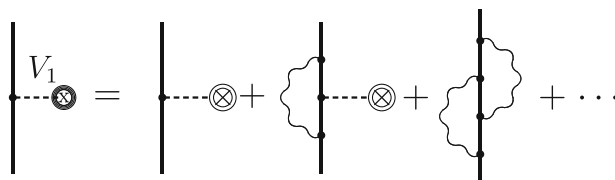


**Fig. 6.7** Graphical representation of the one-body part of the effective potential (6.38), containing the one-body potential in Fig. 6.8 as well as irreducible one-body potential diagrams, including radiative effects

and which contains all **irreducible** interactions, defined in Sect. 2.6.1. By iterating such a potential, also all **reducible** interactions will be generated, making the expansion complete. In Figs. 6.7 and 6.9 we illustrate the one- and two-body parts of this potential, including radiative effects—vacuum polarization, self-energy, vertex correction (see Sect. 2.6)—which, of course, have to be properly renormalized (see Chap. 12).

The one-body potential contains an effective-potential interaction (Fig. 6.8) in analogy to that in ordinary MBPT (2.73). In the effective potential here, however, the internal lines can be hole lines as well as particle lines. This implies that the second diagram on the r.h.s. in Fig. 6.8 contains the direct Hartree–Fock potential as well as the radiative effect of vacuum polarization and the last diagram the exchange part of the HF potential as well as the electron self-energy (both radiative effects properly renormalized). All heavy lines here represent orbitals in the external (nuclear) potential, which implies that the vacuum polarization contains the Uehling potential [245] (see Sect. 4.6) as well as the Wichmann–Kroll [249] correction, discussed earlier in Sect. 4.6.

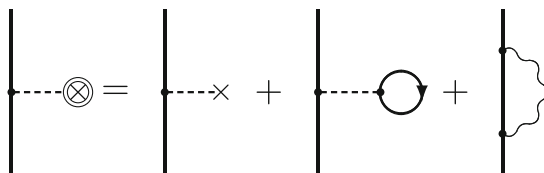


**Fig. 6.8** Graphical representation of the “extended” effective potential interaction. This is analogous to the effective potential in Fig. 2.3, but the *internal lines* represent here **all** orbitals (particles as well as holes). This implies that the last two diagrams include the (renormalized) vacuum polarization and self-energy

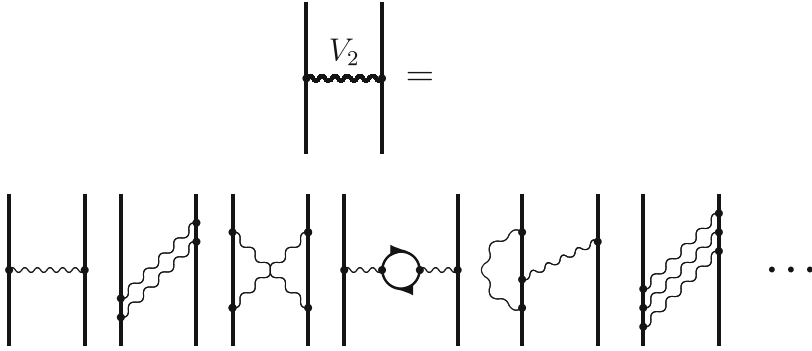


**Fig. 6.9** The two-body part of the effective potential (6.38) contains all irreducible two-body potential diagrams

### 6.5.2 Irreducible Two-Photon Exchange\*

We consider next the general two-photon exchange, illustrated in Fig. 6.10, still assuming the equal-time approximation and unperturbed initial state.

#### 6.5.2.1 Uncrossing Photons

Generalizing the result for single-photon exchange, we find that the *kernel* of the first (ladder)diagram becomes (see the rules in Sect. 4.7 and Appendix H)

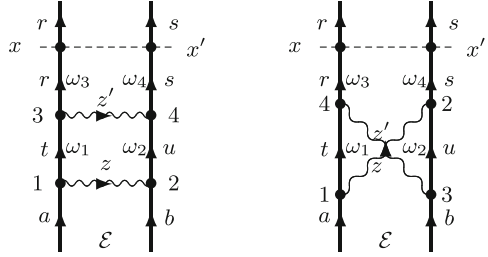
$$\begin{aligned}
 & iS_F(x, x_3) iS_F(x', x_4) (-i)e^2 D_F(x_4, x_3) iS_F(x_3, x_1) \\
 & iS_F(x_4, x_2) (-i)e^2 D_F(x_2, x_1).
 \end{aligned}
 \tag{6.39}$$

This leads to the Feynman amplitude in analogy with (6.18)

$$\begin{aligned}
 \mathcal{M}_{\text{sp}}(\mathbf{x}, \mathbf{x}'; \mathbf{x}_0, \mathbf{x}'_0) = & \iiint \frac{d\omega_1}{2\pi} \frac{d\omega_2}{2\pi} \frac{d\omega_3}{2\pi} \frac{d\omega_4}{2\pi} \iint \frac{dz}{2\pi} \frac{dz'}{2\pi} iS_F(\omega_3; \mathbf{x}, \mathbf{x}_3) \\
 & \times iS_F(\omega_4; \mathbf{x}', \mathbf{x}_4) (-i)I(z'; \mathbf{x}_4, \mathbf{x}_3) iS_F(\omega_1; \mathbf{x}_3, \mathbf{x}_1) iS_F(\omega_2; \mathbf{x}_4, \mathbf{x}_2) \\
 & \times (-i)I(z; \mathbf{x}_2, \mathbf{x}_1) 2\pi\Delta_\gamma(\varepsilon_a - \omega_1 - z) 2\pi\Delta_\gamma(\varepsilon_b - \omega_2 + z) \\
 & \times 2\pi\Delta_\gamma(\omega_1 - z' - \omega_3) 2\pi\Delta_\gamma(\omega_2 + z' - \omega_4).
 \end{aligned}
 \tag{6.40}$$

Integration over  $\omega_1, \omega_2$  leads to

**Fig. 6.10** Covariant-evolution-operator diagrams for two-photon ladder and “cross”



$$\begin{aligned}
 \mathcal{M}_{\text{sp}}(\mathbf{x}, \mathbf{x}') &= \iint \frac{d\omega_3}{2\pi} \frac{d\omega_4}{2\pi} \iint \frac{dz}{2\pi} \frac{dz'}{2\pi} iS_{\text{F}}(\omega_3; \mathbf{x}, \mathbf{x}_3) iS_{\text{F}}(\omega_4; \mathbf{x}', \mathbf{x}_4) \\
 &\quad \times (-i)I(z'; \mathbf{x}_4, \mathbf{x}_3) iS_{\text{F}}(\varepsilon_a - z; \mathbf{x}_3, \mathbf{x}_1) iS_{\text{F}}(\varepsilon_b + z; \mathbf{x}_4, \mathbf{x}_2) \\
 &\quad \times (-i)I(z; \mathbf{x}_2, \mathbf{x}_1) 2\pi\Delta_{2\gamma}(\varepsilon_a - z - z' - \omega_3) 2\pi\Delta_{2\gamma}(\varepsilon_b + z + z' - \omega_4)
 \end{aligned} \tag{6.41}$$

and over  $\omega_3, \omega_4$

$$\begin{aligned}
 \mathcal{M}_{\text{sp}}(\mathbf{x}, \mathbf{x}') &= \iint \frac{dz}{2\pi} \frac{dz'}{2\pi} iS_{\text{F}}(\varepsilon_a - z - z'; \mathbf{x}, \mathbf{x}_3) iS_{\text{F}}(\varepsilon_b + z + z'; \mathbf{x}', \mathbf{x}_4) \\
 &\quad \times (-i)I(z'; \mathbf{x}_4, \mathbf{x}_3) iS_{\text{F}}(\varepsilon_a - z; \mathbf{x}_3, \mathbf{x}_1) iS_{\text{F}}(\varepsilon_b + z; \mathbf{x}_4, \mathbf{x}_2) \\
 &\quad \times (-i)I(z; \mathbf{x}_2, \mathbf{x}_1).
 \end{aligned} \tag{6.42}$$

Integration over  $z'$  leads to the denominators

$$\frac{1}{\mathcal{E} - \varepsilon_r - \varepsilon_s} \left[ \frac{1}{\varepsilon_a - \varepsilon_r - z - (c\kappa'_r - i\gamma)_r} + \frac{1}{\varepsilon_b - \varepsilon_s + z - (c\kappa'_s - i\gamma)_s} \right],$$

and the remaining part of the integrand is

$$\frac{1}{\mathcal{E} - \varepsilon_t - \varepsilon_u} \left[ \frac{1}{\varepsilon_a - \varepsilon_t - z + i\gamma_t} + \frac{1}{\varepsilon_b + z + i\gamma_u} \right] \frac{1}{z^2 - c^2\kappa^2 + i\eta}.$$

### 6.5.2.2 Crossing Photons

For the crossed-photon exchange in Fig. 6.10 (right) the corresponding result is

$$\begin{aligned}
 \mathcal{M}_{\text{sp}}(\mathbf{x}, \mathbf{x}'; \mathbf{x}_0, \mathbf{x}'_0) &= \iiint \frac{d\omega_1}{2\pi} \frac{d\omega_2}{2\pi} \frac{d\omega_3}{2\pi} \frac{d\omega_4}{2\pi} \iint \frac{dz}{2\pi} \frac{dz'}{2\pi} iS_{\text{F}}(\omega_3; \mathbf{x}, \mathbf{x}_4) \\
 &\quad \times iS_{\text{F}}(\omega_4; \mathbf{x}', \mathbf{x}_2) (-i)I(z'; \mathbf{x}_4, \mathbf{x}_3) iS_{\text{F}}(\omega_1; \mathbf{x}_4, \mathbf{x}_1) iS_{\text{F}}(\omega_2; \mathbf{x}_2, \mathbf{x}_3) \\
 &\quad \times (-i)I(z; \mathbf{x}_2, \mathbf{x}_1) 2\pi\Delta_{\gamma}(\varepsilon_a - \omega_1 - z) 2\pi\Delta_{\gamma}(\varepsilon_b - \omega_2 - z') \\
 &\quad \times 2\pi\Delta_{\gamma}(\omega_1 - z' - \omega_3) 2\pi\Delta_{\gamma}(\omega_2 + z - \omega_4).
 \end{aligned} \tag{6.43}$$

Integration over the omegas yields

$$\begin{aligned} \mathcal{M}_{\text{sp}}(\mathbf{x}, \mathbf{x}') &= \iint \frac{dz}{2\pi} \frac{dz'}{2\pi} iS_{\text{F}}(\varepsilon_a + z' - z; \mathbf{x}, \mathbf{x}_4) iS_{\text{F}}(\varepsilon_b + z - z'; \mathbf{x}', \mathbf{x}_2) \\ &\quad \times (-i)I(z'; \mathbf{x}_4, \mathbf{x}_3) iS_{\text{F}}(\varepsilon_a - z; \mathbf{x}_4, \mathbf{x}_1) \\ &\quad \times iS_{\text{F}}(\varepsilon_b - z; \mathbf{x}_2, \mathbf{x}_3) (-i)I(z; \mathbf{x}_2, \mathbf{x}_1). \end{aligned} \quad (6.44)$$

Integration over  $z'$  leads to the denominators

$$\frac{1}{\mathcal{E} - \varepsilon_r - \varepsilon_s} \left[ \frac{1}{\varepsilon_a - \varepsilon_r - z - (c\kappa' - i\gamma)_r} + \frac{1}{\varepsilon_b - \varepsilon_s + z - (c\kappa' - i\gamma)_s} \right],$$

and the remaining part of the integrand is

$$\frac{1}{\varepsilon_a - \varepsilon_t - z + i\gamma_t} \frac{1}{\varepsilon_b - \varepsilon_u - z + i\gamma_u} \frac{1}{z^2 - c^2\kappa^2 + i\eta}.$$

To evaluate the integrals above is quite complicated, but they are considered in detail in [130, Appendix A2] and in the Ph.D. thesis of Björn Åsén [10]. The two-photon effects have been evaluated for heliumlike ions, and some results are shown in the following chapter.

### 6.5.3 Potential with Radiative Parts

Two-photon potentials with self-energy and vacuum-polarization insertions can also be evaluated in the Green's-operator formalism, as discussed in [130]. We shall not consider this any further here, but return to these effects in connection with the many-body-QED procedure in Chap. 8.

## 6.6 Relativistic Form of the Gell-Mann–Low Theorem

We have in Chap. 3 considered the non-relativistic form of the Gell-Mann–Low theorem, and we now extend this to the relativistic formalism. This theorem plays a fundamental role in the formalism we are developing here.

We start with

- **a conjecture that the time evolution of the relativistic state vector is governed by the CEO in the equal-time approximation** (in the interaction picture), in analogy with the situation in the non-relativistic case (3.15) (c.f. [22, Sect. 6.4]),

$$\boxed{|\chi_{\text{Rel}}^\alpha(t)\rangle \propto U_{\text{Cov}}(t, t_0) |\chi_{\text{Rel}}^\alpha(t_0)\rangle.} \quad (6.45)$$

(The evolution operator does not conserve the intermediate normalization.) We shall later demonstrate that this conjecture is consistent with the standard quantum-mechanical picture (6.170) (see also 10.13).

It can now be shown as in the non-relativistic case in Sect. 3.4 that the conjecture above leads to a

- **relativistic form of the Gell-Mann–Low theorem for a general quasi-degenerate model space**<sup>5</sup>

$$\boxed{|\chi_{\text{Rel}}^{\alpha}(0)\rangle = |\Psi_{\text{Rel}}^{\alpha}\rangle = \lim_{\gamma \rightarrow 0} \frac{U_{\text{Cov}}(0, -\infty) |\Phi_{\text{Rel}}^{\alpha}\rangle}{\langle \Psi_{0\text{Rel}}^{\alpha} | U_{\text{Cov}}(0, -\infty) |\Phi_{\text{Rel}}^{\alpha}\rangle}}, \quad (6.46)$$

which is quite analogous to the non-relativistic theorem (3.55). Here,  $|\Phi_{\text{Rel}}^{\alpha}\rangle$  is, as before, the *parent state* (3.41), i.e., the limit of the corresponding target state, as the perturbation is adiabatically turned off,

$$|\Phi_{\text{Rel}}^{\alpha}\rangle = N^{\alpha} \lim_{t \rightarrow -\infty} |\chi_{\text{Rel}}^{\alpha}(t)\rangle. \quad (6.47)$$

( $N^{\alpha}$  is a normalization constant) and  $|\Psi_{0\text{Rel}}^{\alpha}\rangle = P|\Psi_{\text{Rel}}^{\alpha}\rangle$  is the (intermediately normalized) model state.

- The state vector  $|\Psi_{\text{Rel}}^{\alpha}\rangle$  satisfies a **relativistic eigenvalue equation**, analogous to the non-relativistic (Schrödinger-like) **Gell-Mann–Low equation** (3.44),

$$\boxed{(H_0 + V_F) |\Psi_{\text{Rel}}^{\alpha}\rangle = E^{\alpha} |\Psi_{\text{Rel}}^{\alpha}\rangle}, \quad (6.48)$$

where  $V_F$  is the perturbation, used in generating the evolution operator (see 6.52).

In proving the relativistic form of the GML theorem, we observe that the covariant evolution operator differs from the corresponding non-relativistic operator mainly by the addition of pairs of electron-field operators. It then follows that the commutator of  $H_0$  with the covariant operator is the same as with the nonrelativistic operator, which implies that the proof in Sect. 3.4 can be used also in the covariant case.

A condition for the GML theorem to hold is, as in the non-relativistic case, that **the perturbation is time-independent in the Schrödinger picture** (apart from damping), which is the case here.

## 6.7 Field-Theoretical Many-Body Hamiltonian in the Photonic Fock Space

In the unified procedure we are developing here we shall mainly apply the Coulomb gauge, which is most appropriate for the combined MBPT-QED calculations (see, in particular, Chap. 9). (That it is quite possible to use the Coulomb gauge in QED

---

<sup>5</sup>As pointed out before, the numerator and denominator might here be separately singular in the limit, and only the **ratio** is regular.

calculation has been demonstrated among others by Adkins [1], Rosenberg [203] and others.) In this gauge we separate the interaction between the electrons in the *instantaneous Coulomb interaction* and the *transverse interaction*, with the Coulomb part being (2.109)

$$V_C = \sum_{i < j}^N \frac{e^2}{4\pi\epsilon_0 r_{ij}}. \quad (6.49)$$

The exchange of a virtual transverse photon between the electrons is represented by TWO perturbations of the one-body perturbation

$$v_T(t) = \int d^3\mathbf{x} \mathcal{H}(t, \mathbf{x}) \quad (6.50)$$

with the perturbation density given by (4.4),

$$\mathcal{H}(x) = \mathcal{H}(t, \mathbf{x}) = -\hat{\psi}^\dagger(x) e c \alpha^\mu A_\mu(x) \hat{\psi}(x) \quad (6.51)$$

with  $A_\mu$  being the quantized, transverse radiation field (see Appendix F.2). The total perturbation is then

$$\boxed{V_F = V_C + v_T}. \quad (6.52)$$

The perturbation (6.51) represents the emission/absorption of a photon. Therefore, with this perturbation the GML equation works in a *photonic Fock space*<sup>6</sup>, where the number of photons is not preserved. This perturbation is time-independent in the Schrödinger picture, as required for the GML relation (see B.16 and G.2). (This is clearly demonstrated also by the form of the interaction given in Sect. 8.1.2.)

The model many-body Hamiltonian we shall apply is primarily a sum of Dirac single-electron Hamiltonians in an external (nuclear) field (Furry picture) (2.108)

$$h_D = c \boldsymbol{\alpha} \cdot \hat{\mathbf{p}} + \beta m c^2 + v_{\text{ext}}. \quad (6.53)$$

(As before, we may include an optional potential,  $u$ , in the model Hamiltonian (2.48)—and subtract the same quantity in the perturbation—in order to improve the convergence rate for many-electron systems.)

However, since the number of photons is no longer constant in the space we work in, we have to include in the model Hamiltonian also the radiation field,  $H_{\text{Rad}}$  (see Appendices G.12 and B.20), yielding

$$H_0 = \sum h_D + H_{\text{Rad}}. \quad (6.54)$$

---

<sup>6</sup>Also the Fock space is a form of Hilbert space, and therefore we shall refer to the Hilbert space with a constant number of photons as the *restricted (Hilbert) space* and the space with a variable number of photons as the (extended) *photonic Fock space* (see Appendix A.2).



The *full field-theoretical many-body Hamiltonian* will then be

$$\boxed{H = H_0 + V_F = H_0 + V_C + v_T}, \quad (6.55)$$

sometimes also referred to as the *many-body Dirac Hamiltonian*. This leads with the GML relation (6.48) to the corresponding *Fock-space many-body equation*<sup>7</sup>

$$\boxed{H\Psi = E\Psi}. \quad (6.56)$$

In comparing our many-body Dirac Hamiltonian with the Coulomb-Dirac-Breit Hamiltonian of standard MBPT (2.113), we see that we have included the radiation field,  $H_{\text{Rad}}$ , and replaced the instantaneous Breit interaction with the transverse field interaction,  $v_T$ , in addition to removing the projection operators.

Using second quantization (see Appendices B and E),

- ***the field-theoretical many-body Hamiltonian in the photonic Fock space*** (6.55) becomes in the *Coulomb gauge*

$$\boxed{H = \int d^3\mathbf{x} \hat{\psi}^\dagger(x) \left( c \boldsymbol{\alpha} \cdot \hat{\mathbf{p}} + \beta mc^2 + v_{\text{ext}}(x) - e c \alpha^\mu A_\mu(x) \right) \hat{\psi}(x) + H_{\text{Rad}} + \frac{1}{2} \iint d^3\mathbf{x}_1 d^3\mathbf{x}_2 \hat{\psi}^\dagger(x_1) \hat{\psi}^\dagger(x_2) \frac{e^2}{4\pi\epsilon_0 r_{12}} \hat{\psi}(x_2) \hat{\psi}(x_1)}, \quad (6.57)}$$

where  $v_{\text{ext}}(x)$  is the external (nuclear) field of the electrons (Furry picture). In the Coulomb gauge the operator  $A_\mu(x)$  represents only the **transverse** part of the radiation field.

- ***By treating the Coulomb and the transverse photon interactions separately, a formal departure is made from a fully covariant treatment. However, this procedure is, when performed properly, in practice equivalent to the use of a fully covariant gauge.***

In a *covariant gauge* the entire electron-electron interaction is expressed by means of the field term and the Coulomb part is left out. We define the *covariant wave-operator* in analogy with the non-relativistic case (2.36)<sup>8</sup>

$$|\Psi^\alpha\rangle = \Omega_{\text{Cov}} |\Psi_0^\alpha\rangle \quad (\alpha = 1 \dots d) \quad (6.58)$$

but now acting in the extended photonic Fock space. The Gell-Mann–Low relation (6.48) can then be expressed

<sup>7</sup>This equation is not completely covariant, because it has a single time, in accordance with the established quantum-mechanical picture. This is the *equal-time approximation*, mentioned above and further discussed later. In addition, a complete covariant treatment would require that also the interaction between the electrons and the nucleus is treated in a covariant way by means of the exchange of virtual photons (see, for instance, [227]).

<sup>8</sup>In the following we shall leave out the subscript “Rel”.

$$(H_0 + V_F) \Omega_{\text{Cov}} |\Psi_0^\alpha\rangle = E^\alpha \Omega_{\text{Cov}} |\Psi_0^\alpha\rangle. \quad (6.59)$$

The *effective Hamiltonian* is defined as before (2.37),

$$H_{\text{eff}} |\Psi_0^\alpha\rangle = E^\alpha |\Psi_0^\alpha\rangle,$$

which leads to

$$H_{\text{eff}} = P(H_0 + V_F)\Omega_{\text{Cov}}P. \quad (6.60)$$

The *covariant effective interaction* is defined

$$W = H_{\text{eff}} - PH_0P, \quad (6.61)$$

yielding

$$W|\Psi_0^\alpha\rangle = (E^\alpha - E_0^\alpha)|\Psi_0^\alpha\rangle \quad (6.62)$$

and

$$\boxed{W = PV_F\Omega_{\text{Cov}}P.} \quad (6.63)$$

This is a ***Fock-space relation***, where the number of photons is not conserved. The corresponding relation in the restricted space without uncontracted photons will be given in Sect. 6.11 (6.174).

The many-body Fock-space relation (6.56) can be solved iteratively in the same way as the corresponding standard many-body equation, as long as no virtual pairs are involved. (In the case such pairs are present, the perturbations have to be evaluated by other means, as will be discussed particularly in Chap. 8.) This is the basic principle of the covariant relativistic many-body perturbation procedure we shall develop in this book. How this can be accomplished will be discussed in the following. First, we shall introduce the important concept of the *Green's operator*.

## 6.8 Green's Operator

### 6.8.1 Definition

The vacuum expectation used to define the Green's function (5.8) contains singularities in the form of unlinked diagrams, where the disconnected closed part represents the vacuum expectation of the S-matrix. This is a *number*, and it then follows that the singularities can be eliminated by dividing by this number. For the covariant evolution operator (CEO) (6.1) the situation is more complex, since this is an *operator*, and the disconnected parts will also in general be operators. Therefore, we shall here proceed in a somewhat different manner. This will lead to a more general concept, valid also in the multi-reference case (quasi-degeneracy).

As mentioned earlier,

- we shall refer to the **regular part of the Covariant-Evolution Operator as the Green's operator**—in the single-particle case denoted  $\mathcal{G}(t, t_0)$ —due to its great similarity with the Green's function. We define the single-particle Green's operator by the relation<sup>9</sup>

$$\boxed{U(t, t_0)P = \mathcal{G}(t, t_0) \cdot PU(0, t_0)P}, \quad (6.64)$$

where  $P$  is the projection operator for the model space, and analogously in the many-particle case. Below we shall demonstrate that this definition leads to an operator that is *regular*.

The *heavy dot* in the definition of the Green's operator implies that the operator acts on the **intermediate** model space state at the position of the dot.

The definition above implies that **the interactions and the resolvents to the left of the dot depend on the energy of the model-space state at the position of the dot**. If we operate to the right on the part of the model space  $P_{\mathcal{E}}$  of energy  $\mathcal{E}$  and the intermediate model-space state lies in the part  $P_{\mathcal{E}'}$  of energy  $\mathcal{E}'$ , we can express the two kinds of products as

$$\left\{ \begin{array}{l} \overbrace{AP_{\mathcal{E}'}BP_{\mathcal{E}}} = \overbrace{A(\mathcal{E})P_{\mathcal{E}'}B(\mathcal{E})P_{\mathcal{E}}} \\ \overbrace{A \cdot P_{\mathcal{E}'}BP_{\mathcal{E}}} = \overbrace{A(\mathcal{E}')P_{\mathcal{E}'}B(\mathcal{E})P_{\mathcal{E}}} \end{array} \right. \quad (6.65)$$

with the energy parameter of  $A$  equal to  $\mathcal{E}$  in the first case and to  $\mathcal{E}'$  in the second case. By the hooks we indicate that the operators must be connected by at least one contraction. We shall soon see the implication of this definition.

### 6.8.2 Relation Between the Green's Operator and Many-Body Perturbation Procedures

From the conjecture (6.45) and the definition (6.64) we have (leaving out the damping)

$$|\chi^{\alpha}(t)\rangle = N_{\alpha}U(t, -\infty)|\Phi^{\alpha}\rangle = N_{\alpha}\mathcal{G}(t, -\infty) \cdot PU(0, -\infty)P|\Phi^{\alpha}\rangle, \quad (6.66)$$

where  $N_{\alpha}$  is the normalization constant

$$N_{\alpha} = \frac{1}{\langle \Psi_0^{\alpha} | U(0, -\infty) | \Phi^{\alpha} \rangle}, \quad (6.67)$$

<sup>9</sup>The Green's operator is closely related—but not quite identical—to the *reduced covariant evolution operator*, previously introduced by the Gothenburg group [130].

making the state vector intermediately normalized for  $t = 0$ . Here,  $|\Phi^\alpha\rangle$  is the parent state (6.47), and  $|\Psi^\alpha\rangle = N_\alpha U(0, -\infty)|\Phi^\alpha\rangle$  is the target state (for  $t = 0$ ). The model state is

$$|\Psi_0^\alpha\rangle = P|\Psi^\alpha\rangle = N_\alpha P U(0, -\infty)|\Phi^\alpha\rangle.$$

This leads directly to

- the relation

$$\boxed{|\chi^\alpha(t)\rangle = \mathcal{G}(t, -\infty)|\Psi_0^\alpha\rangle}, \quad (6.68)$$

which implies that *the time dependence of the relativistic state vector is governed by the Green's operator*.

- Therefore, *the Green's operator can be regarded as a time-dependent wave operator*.
- For the time  $t = 0$  we have the *covariant analogue of the standard wave operator of MBPT* (2.36)

$$|\chi^\alpha(0)\rangle = |\Psi^\alpha\rangle = \Omega_{\text{Cov}}|\Psi_0^\alpha\rangle \quad (6.69)$$

with

$$\boxed{\Omega_{\text{Cov}} = \mathcal{G}(0, -\infty)}. \quad (6.70)$$

It follows directly from the definition (6.64) that

$$P\mathcal{G}(0, -\infty)P = P, \quad (6.71)$$

and the relation above can also be expressed

$$\boxed{\Omega_{\text{Cov}} = 1 + Q\mathcal{G}(0, -\infty)}. \quad (6.72)$$

We note here that it is important that the Green's operator is defined with the dot product (6.64). The definition of the wave operator (2.36) can be expressed

$$|\Psi^\alpha\rangle = \Omega_{\text{Cov}} \cdot P|\Psi^\alpha\rangle = \Omega_{\text{Cov}} \cdot P U(0, -\infty)|\Phi^\alpha\rangle, \quad (6.73)$$

indicating that the energy parameter of the wave operator depends on the intermediate model-space state.

We shall now derive a general relation between the *covariant effective interaction* (6.63) and the Green's operator. Assuming that the time dependence of the relativistic state vector is the same as that of the non-relativistic one (2.15) (which will be verified in Sect. 6.11), i.e., in the interaction picture

$$|\chi^\alpha(t)\rangle = e^{-it(E^\alpha - H_0)}|\chi^\alpha(0)\rangle = e^{-it(E^\alpha - H_0)}|\Psi^\alpha\rangle, \quad (6.74)$$

or

$$i\frac{\partial}{\partial t}|\chi^\alpha(t)\rangle = (E^\alpha - H_0)|\chi^\alpha(t)\rangle, \quad (6.75)$$

we obtain with the relation (6.68) for the time  $t = 0$

$$i\left(\frac{\partial}{\partial t} |\chi^\alpha(t)\rangle\right)_{t=0} = i\left(\frac{\partial}{\partial t} \mathcal{G}(t, -\infty)\right)_{t=0} |\Psi_0^\alpha\rangle = (E^\alpha - H_0)|\Psi^\alpha\rangle. \quad (6.76)$$

Here, the rhs becomes, using the GML relation (6.48) and the wave-operator relation (6.69),

$$(H - H_0)|\Psi^\alpha\rangle = V_F|\Psi^\alpha\rangle = V_F\Omega_{\text{Cov}}|\Psi_0^\alpha\rangle. \quad (6.77)$$

This relation holds for all model states, which leads us to the important operator relation for the entire model space

$$\boxed{\mathcal{R}P = i\left(\frac{\partial}{\partial t} \mathcal{G}(t, -\infty)\right)_{t=0} P = V_F\Omega_{\text{Cov}}P,} \quad (6.78)$$

referred to as the **reaction operator**. Projecting this onto the model space, yields according to the relation (6.63)

- *the covariant relativistic effective intercation*

$$\boxed{W = P\mathcal{R}P = PV_F\Omega_{\text{Cov}}P = P\left(i\frac{\partial}{\partial t} \mathcal{G}(t, -\infty)\right)_{t=0} P.} \quad (6.79)$$

This is a relation in the *photonic Fock space*, to be compared with the corresponding relation in the restricted space (6.174).

Our procedure here is based upon quantum-field theory, and the Green's operator can be regarded as a *field-theoretical extension of the traditional wave-operator concept* of MBPT, and it serves as a *connection between field theory and MBPT*.

### 6.8.2.1 Fourier Transform of the Green's Operator

Generalizing the results in Sect. 6.2, we find that the single-particle Green's operator can generally be written in the form

$$\mathcal{G}(t, -\infty) = \int d^3\mathbf{x} \int d^4x_1 \hat{\psi}^\dagger(x) iS_F(x, x_1) (-i)\hat{\mathcal{R}}\hat{\psi}(x_1), \quad (6.80)$$

where  $\hat{\mathcal{R}}$  is an insertion of self-energy type (see Fig. 6.3). This holds for the perturbed part of the Green's operator with at least one interaction, excluding the zeroth-order part,  $\mathcal{G}^{(0)}$  (6.96), with no interaction. Operating on a part of the model space of energy  $\mathcal{E}$ , this becomes in operator form

$$\mathcal{G}(t, -\infty) P_{\mathcal{E}} = e^{-it(\mathcal{E}-H_0)} iS_F(\mathcal{E}) (-i)\hat{\mathcal{R}}P_{\mathcal{E}} = e^{-it(\mathcal{E}-H_0)} \frac{1}{\mathcal{E} - H_0} \hat{\mathcal{R}}P_{\mathcal{E}}, \quad (6.81)$$

where

$$\frac{1}{\mathcal{E} - H_0} \hat{\mathcal{R}} P_{\mathcal{E}} = \mathcal{M} P_{\mathcal{E}} \quad (6.82)$$

is the Feynman amplitude. Applying the formula (6.78), we find that the operator  $\hat{\mathcal{R}}$  is identical to the *reaction operator*  $\mathcal{R}$ .

The perturbed Green's operator (6.81) is of the form

$$\mathcal{G}(t, -\infty) = e^{-it(\mathcal{E} - H_0)} \mathcal{M} P_{\mathcal{E}} \quad (6.83)$$

and the *Fourier transform* becomes

$$\mathcal{G}(E) P_{\mathcal{E}} = \int dt e^{iEt} \mathcal{G}(t, -\infty) P_{\mathcal{E}} \quad (6.84)$$

or

$$\boxed{\mathcal{G}(E) P_{\mathcal{E}} = 2\pi \delta(E - \mathcal{E} + H_0) \mathcal{M} P_{\mathcal{E}}.} \quad (6.85)$$

It then follows that

$$\int \frac{dE}{2\pi} E \mathcal{G}(E) = (\mathcal{E} - H_0) \mathcal{M} = \mathcal{R}, \quad (6.86)$$

which can be compared with the relation (5.98) for the Green's function.

### 6.8.2.2 The Green's Operator for Infinite Initial and Final Times

We have so far considered the Green's operator for infinite negative initial time and **finite final times**. The Green's operator for infinite initial and final times has interesting properties that we shall now explore.

Letting the **final** time be  $t \rightarrow +\infty$ , we have in analogy with (6.8)

$$\int d^3\mathbf{x} \hat{\psi}^\dagger(x) iS_F(x, x_1) \Rightarrow \hat{\psi}^\dagger(x_1). \quad (6.87)$$

We then get from (6.80) for the perturbed part

$$\mathcal{G}(\infty, -\infty) = \int d^4x_1 \hat{\psi}^\dagger(x_1) (-i)\mathcal{R} \hat{\psi}(x_1) \quad (6.88)$$

and

$$\langle b | i\mathcal{G}(\infty, -\infty) | a \rangle = \int dt_1 e^{-it_1(\varepsilon_a - \varepsilon_b)} \langle b | \mathcal{R} | a \rangle.$$

Integration over the time leads to energy conservation

$$\langle b | i\mathcal{G}(\infty, -\infty) | a \rangle = 2\pi\delta(\varepsilon_a - \varepsilon_b) \langle b | \mathcal{R} | a \rangle. \quad (6.89)$$

By means of the relation (6.79) we then obtain the important relation

$$\boxed{Pi\mathcal{G}(\infty, -\infty)P = 2\pi\delta(E_{\text{in}} - E_{\text{out}})W}, \quad (6.90)$$

where  $W = H_{\text{eff}} - PH_0P$  is the effective interaction (6.61). (The zeroth-order component is here excluded from the Green's operator.) Thus, we see that *the Green's operator for infinite initial and final times is closely related to the effective Hamiltonian*. We shall find this property quite useful in dealing with dynamical processes in Chap. 13.

If there are no intermediate model-space states, then the perturbed part of  $\mathcal{G}(\infty, -\infty)$  is identical to the corresponding part of the evolution operator  $U(\infty, -\infty)$  and hence also of the S-matrix (4.2). We then have the corresponding relation in the free-electron case,

$$\boxed{PiSP = 2\pi\delta(E_{\text{in}} - E_{\text{out}})W}, \quad (6.91)$$

where only the perturbed part of the S-matrix with at least one interaction appears.

## 6.9 Model-Space Contribution

*The model-space contributions* (MCS), i.e., the contributions due to model-space states in the expansion of the evolution operator, play an important role in the theory we are here developing. They lead to singularities, and we shall now demonstrate how these singularities can be eliminated in the general multi-reference case. We assume that the initial time is  $t_0 = -\infty$ . We also work in the *equal-time approximation*, where all final times are the same.

In general, we still operate in the extended *photonic Fock space*, where the number of free photons is not conserved. We initially consider single-photon exchanges and shall later consider multi-photon irreducible interactions.

We start by expanding the relation (6.64) order by order, using the fact that  $U^{(0)}(0)P = P$ . We assume that the model space can have different energies, and we start from a particular energy,  $\mathcal{E}$ , and assume that a possible intermediate model-space state has the energy  $\mathcal{E}'$

$$\begin{aligned} U^{(0)}(t, \mathcal{E})P_{\mathcal{E}} &= \mathcal{G}^{(0)}(t, \mathcal{E})P_{\mathcal{E}} \\ U^{(1)}(t, \mathcal{E})P_{\mathcal{E}} &= \mathcal{G}^{(1)}(t, \mathcal{E})P_{\mathcal{E}} + \mathcal{G}^{(0)}(t, \mathcal{E}') \cdot P_{\mathcal{E}'}U^{(1)}(0)P_{\mathcal{E}} \\ U^{(2)}(t, \mathcal{E})P_{\mathcal{E}} &= \mathcal{G}^{(2)}(t, \mathcal{E})P_{\mathcal{E}} + \mathcal{G}^{(1)}(t, \mathcal{E}') \cdot P_{\mathcal{E}'}U^{(1)}(0)P_{\mathcal{E}} + \mathcal{G}^{(0)}(t, \mathcal{E}') \cdot PU^{(2)}(0)P_{\mathcal{E}} \\ U^{(3)}(t, \mathcal{E})P_{\mathcal{E}} &= \mathcal{G}^{(3)}(t, \mathcal{E})P_{\mathcal{E}} + \mathcal{G}^{(2)}(t, \mathcal{E}') \cdot P_{\mathcal{E}'}U^{(1)}(0)P_{\mathcal{E}} + \mathcal{G}^{(1)}(t, \mathcal{E}') \cdot PU^{(2)}(0)P_{\mathcal{E}} \\ &\quad + \mathcal{G}^{(0)}(t, \mathcal{E}') \cdot PU^{(3)}(0)P_{\mathcal{E}} \end{aligned} \quad (6.92)$$

etc. (For clarity, we insert the energy parameter in the operator symbol, which should not be confused with the Fourier transform (6.85), discussed above.)

Solving the equations (6.92) for the Green's operator, we then have

$$\begin{aligned}
 \mathcal{G}^{(0)}(t, \mathcal{E})P_{\mathcal{E}} &= U^{(0)}(t, \mathcal{E})P_{\mathcal{E}} \\
 \mathcal{G}^{(1)}(t, \mathcal{E})P_{\mathcal{E}} &= U^{(1)}(t, \mathcal{E})P_{\mathcal{E}} - \mathcal{G}^{(0)}(t, \mathcal{E}')P_{\mathcal{E}'}U^{(1)}(0, \mathcal{E})P_{\mathcal{E}} \\
 \mathcal{G}^{(2)}(t, \mathcal{E})P_{\mathcal{E}} &= U^{(2)}(t, \mathcal{E})P_{\mathcal{E}} - \mathcal{G}^{(0)}(t, \mathcal{E}')P_{\mathcal{E}'}U^{(2)}(0, \mathcal{E})P_{\mathcal{E}} - \mathcal{G}^{(1)}(t, \mathcal{E}')P_{\mathcal{E}'}U^{(1)}(0, \mathcal{E})P_{\mathcal{E}} \\
 \mathcal{G}^{(3)}(t, \mathcal{E})P_{\mathcal{E}} &= U^{(3)}(t, \mathcal{E})P_{\mathcal{E}} - \mathcal{G}^{(0)}(t, \mathcal{E}')P_{\mathcal{E}'}U^{(3)}(0, \mathcal{E})P_{\mathcal{E}} - \mathcal{G}^{(1)}(t, \mathcal{E}')P_{\mathcal{E}'}U^{(2)}(0, \mathcal{E})P_{\mathcal{E}} \\
 &\quad - \mathcal{G}^{(2)}(t, \mathcal{E}')P_{\mathcal{E}'}U^{(1)}(0, \mathcal{E})P_{\mathcal{E}}
 \end{aligned} \tag{6.93}$$

etc., which can be summarized as

$$\mathcal{G}(t, \mathcal{E})P_{\mathcal{E}} = U(t, \mathcal{E})P_{\mathcal{E}} - \mathcal{G}(t, \mathcal{E}')P_{\mathcal{E}'}[U(0, \mathcal{E}) - 1]P_{\mathcal{E}}. \tag{6.94}$$

We shall demonstrate that the negative terms above, referred to as *counterterms*, will remove the singularities of the evolution operator.

It follows directly from the definition of the dot product above that the singularities due to *disconnected* parts are exactly eliminated by the counterterms. Therefore, we need only consider the *connected* (ladder) part, and we consider a fully contracted two-body diagram as an illustration (Fig. 6.5). It is sufficient for our present purpose to consider only positive intermediate states, as in (6.35).

### 6.9.1 Lowest Orders

From (6.36) it follows that the evolution operator can be expressed

$$U(t, \mathcal{E})P_{\mathcal{E}} = e^{-it(\mathcal{E}-H_0)} U(0, \mathcal{E})P_{\mathcal{E}} = \mathcal{G}^{(0)}(t, \mathcal{E})U(0, \mathcal{E})P_{\mathcal{E}}, \tag{6.95}$$

where the zeroth-order evolution operator is

$$U^{(0)}(t, \mathcal{E}) = \mathcal{G}^{(0)}(t, \mathcal{E}) = e^{-it(\mathcal{E}-H_0)}, \tag{6.96}$$

which is also the zeroth-order Green's operator.<sup>10</sup>

The **first-order** evolution operator becomes

$$U(t, \mathcal{E})^{(1)}P_{\mathcal{E}} = \mathcal{G}^{(0)}(t, \mathcal{E})U^{(1)}(0, \mathcal{E})P_{\mathcal{E}}. \tag{6.97}$$

Including the counterterm (6.93), gives the first-order Green's operator

$$\mathcal{G}^{(1)}(t, \mathcal{E})P_{\mathcal{E}} = \mathcal{G}^{(0)}(t, \mathcal{E})(P_{\mathcal{E}'} + Q)U^{(1)}(0, \mathcal{E})P_{\mathcal{E}} - \mathcal{G}^{(0)}(t, \mathcal{E}')P_{\mathcal{E}'}U^{(1)}(0, \mathcal{E})P_{\mathcal{E}}, \tag{6.98}$$

<sup>10</sup>Compare footnote in Sect. 6.4.



where we observe that the Green's operator in the counterterm has the energy parameter  $\mathcal{E}'$ .

The terms with intermediate  $P_{\mathcal{E}'}$  become

$$\left(\mathcal{G}^{(0)}(t, \mathcal{E}) - \mathcal{G}^{(0)}(t, \mathcal{E}')\right) P_{\mathcal{E}'} U^{(1)}(0, \mathcal{E}) P_{\mathcal{E}}. \quad (6.99)$$

But

$$P_{\mathcal{E}'} U^{(1)}(0, \mathcal{E}) P_{\mathcal{E}} = P_{\mathcal{E}'} \Gamma(\mathcal{E}) V(\mathcal{E}) P_{\mathcal{E}} = P_{\mathcal{E}'} \frac{1}{\mathcal{E} - H_0} V(\mathcal{E}) P_{\mathcal{E}} = P_{\mathcal{E}'} \frac{V(\mathcal{E})}{\mathcal{E} - \mathcal{E}'} P_{\mathcal{E}}, \quad (6.100)$$

and the terms above become<sup>11</sup>

$$\mathcal{G}_1^{(1)}(t, \mathcal{E}) P_{\mathcal{E}} = \frac{\delta \mathcal{G}^{(0)}(t, \mathcal{E})}{\delta \mathcal{E}} P_{\mathcal{E}'} V(\mathcal{E}) P_{\mathcal{E}}. \quad (6.101)$$

The *difference ratio* is defined

$$\frac{\delta \mathcal{G}^{(0)}(t, \mathcal{E})}{\delta \mathcal{E}} = \frac{\mathcal{G}^{(0)}(t, \mathcal{E}) - \mathcal{G}^{(0)}(t, \mathcal{E}')}{\mathcal{E} - \mathcal{E}'} \Rightarrow \frac{\partial \mathcal{G}^{(0)}(t, \mathcal{E})}{\partial \mathcal{E}}, \quad (6.102)$$

which turns into a derivative at complete degeneracy.

Then we can express the first-order Green's operator as

$$\mathcal{G}^{(1)}(t, \mathcal{E}) P_{\mathcal{E}} = \mathcal{G}^{(0)}(t, \mathcal{E}) \Gamma_Q V P_{\mathcal{E}} + \frac{\delta \mathcal{G}^{(0)}(t, \mathcal{E})}{\delta \mathcal{E}} P_{\mathcal{E}'} V(\mathcal{E}) P_{\mathcal{E}}. \quad (6.103)$$

The elimination process is illustrated in Fig. 6.11.

Applying the formula (6.79) to the first-order Green's operator (6.103), we find that the *first-order effective interaction* becomes<sup>12</sup>

$$W^{(1)} = P_{\mathcal{E}} \left( i \frac{\partial}{\partial t} \mathcal{G}^{(1)}(t, \mathcal{E}) \right)_{t=0} P_{\mathcal{E}} = P_{\mathcal{E}'} V P_{\mathcal{E}} \quad (6.104)$$

This gives

$$\boxed{\mathcal{G}^{(1)}(t, \mathcal{E}) P_{\mathcal{E}} = \mathcal{G}_0^{(1)}(t, \mathcal{E}) P_{\mathcal{E}} + \frac{\delta \mathcal{G}^{(0)}(t, \mathcal{E})}{\delta \mathcal{E}} W^{(1)},} \quad (6.105)$$

<sup>11</sup>We use the convention that the subscript denotes the number of model-space states ("folds"), intermediate or final, and the superscript in brackets the order of perturbation.

<sup>12</sup> $\mathcal{G}^{(0)}(t, \mathcal{E}) = e^{-it(\mathcal{E}-H_0)}$  and  $\mathcal{G}_0(t, \mathcal{E}) P_{\mathcal{E}} = \mathcal{G}^{(0)}(t, \mathcal{E}) U_0(0, \mathcal{E}) P_{\mathcal{E}} = \mathcal{G}^{(0)}(t, \mathcal{E}) (1 + QU_0(0, \mathcal{E})) P_{\mathcal{E}}$ , which gives  $P_{\mathcal{E}'} \left( i \frac{\partial}{\partial t} \mathcal{G}^{(0)}(t, \mathcal{E}) \right)_{t=0} P_{\mathcal{E}} = P_{\mathcal{E}'} \left( i \frac{\partial}{\partial t} \mathcal{G}_0(t, \mathcal{E}) \right)_{t=0} P_{\mathcal{E}} = 0$  and  $P_{\mathcal{E}'} \left( i \frac{\partial}{\partial t} \frac{\delta \mathcal{G}^{(0)}}{\delta \mathcal{E}} \right)_{t=0} P_{\mathcal{E}} = P_{\mathcal{E}'} \left( i \frac{\partial}{\partial t} \frac{\delta \mathcal{G}_0}{\delta \mathcal{E}} \right)_{t=0} P_{\mathcal{E}} = P_{\mathcal{E}'} P_{\mathcal{E}}$ .

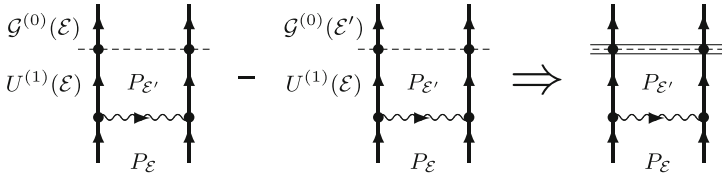


**Fig. 6.11** Illustration of the elimination of singularity of the first-order evolution operator, due to a final model-space state. The *double bar* represents the difference ratio/derivative of the zeroth-order Green’s operator (c.f. Fig. 6.12)

where  $\mathcal{G}_0^{(1)}(t, \mathcal{E})P_{\mathcal{E}} = \mathcal{G}^{(0)}(t, \mathcal{E})\Gamma_Q(\mathcal{E})V P_{\mathcal{E}}$ . The second term in (6.105) lies in the model space, while the first term in lies in the complementary  $Q$  space.

The result (6.104) is the natural result from the viewpoint of standard perturbation theory, but it should be observed that this is based upon the Fock-space relation (6.79) and NOT on the classical relation (2.54)

$$W = PV\Omega P. \tag{6.106}$$

The latter does not hold generally in the photonic Fock space, although it does in this particular case. We shall soon see a case when it does *not* hold.

From (6.96) we have

$$\frac{\partial \mathcal{G}^{(0)}(t, \mathcal{E})}{\partial \mathcal{E}} = -it\mathcal{G}^{(0)}(t, \mathcal{E}) = -it e^{-it(\mathcal{E}-H_0)}, \tag{6.107}$$

which is imaginary and vanishes for  $t = 0$ . This contribution—times the effective interaction—is the first-order correction to the time exponent, as discussed in detail in Sect. 6.11.

In *second order* the Green’s operator without folds becomes identical to the corresponding covariant evolution operator (6.37)

$$\mathcal{G}_0^{(2)}(t, \mathcal{E})P_{\mathcal{E}} = U_0^{(2)}(t, \mathcal{E}) = \mathcal{G}^{(0)}(t, \mathcal{E})\Gamma_Q(\mathcal{E})V(\mathcal{E})\Gamma_Q(\mathcal{E})V(\mathcal{E})P_{\mathcal{E}}. \tag{6.108}$$

If there is only a final model-space state we have in analogy with (6.101)

$$\frac{\delta \mathcal{G}^{(0)}(t, \mathcal{E})}{\delta \mathcal{E}} P_{\mathcal{E}'}V(\mathcal{E})\Gamma_Q(\mathcal{E})V(\mathcal{E})P_{\mathcal{E}}P_{\mathcal{E}}. \tag{6.109}$$

Applying the relation (6.79), we find that the second-order effective interaction without folds becomes

$$W_0^{(2)} = P_{\mathcal{E}}V(\mathcal{E})\Gamma_Q(\mathcal{E})V(\mathcal{E})P_{\mathcal{E}}. \tag{6.110}$$

If there is only an intermediate model-space state, the evolution operator (6.108) becomes

$$\mathcal{G}^{(0)}(t, \mathcal{E}) \Gamma_Q(\mathcal{E}) V(\mathcal{E}) P_{\mathcal{E}'} U^{(1)}(\mathcal{E}) P_{\mathcal{E}} = \mathcal{G}_0^{(1)}(t, \mathcal{E}) P_{\mathcal{E}'} U^{(1)}(\mathcal{E}) P_{\mathcal{E}}. \quad (6.111)$$

Including the counterterm, yields in analogy with the first-order case (6.101)

$$\frac{\delta \mathcal{G}_0^{(1)}(t, \mathcal{E})}{\delta \mathcal{E}} P_{\mathcal{E}'} V(\mathcal{E}) P_{\mathcal{E}}. \quad (6.112)$$

If there is also a final model-space state, we should include the second part of the first-order Green's operator (6.105) and replace  $\mathcal{G}_0^{(1)}$  by the full first-order Green's operator. This gives the entire second-order Green's operator

$$\boxed{\mathcal{G}^{(2)}(t, \mathcal{E}) P_{\mathcal{E}} = \mathcal{G}_0^{(2)}(t, \mathcal{E}) P_{\mathcal{E}} + \frac{\delta \mathcal{G}^{(0)}(t, \mathcal{E})}{\delta \mathcal{E}} W_0^{(2)} + \frac{\delta \mathcal{G}^{(1)}(t, \mathcal{E})}{\delta \mathcal{E}} W^{(1)}}. \quad (6.113)$$

Here, the first term represents the part without model-space states, the second term that with only a final model-space state and the last term that with an intermediate and possible also a final model-space state.

The second-order elimination process, due to an intermediate model-space state, is illustrated in Fig. 6.12, and the corresponding part of the Green's operator is illustrated in Fig. 6.13. This process is quite analogous to the appearance of *folded diagram*, discussed in connection with standard MBPT (2.81) but yields, in addition, a derivative of the energy-dependent potential (see below). Since we are here dealing with Feynman diagrams, it is more logical to draw the "folded" part straight, indicating the position of the "fold" by a double bar from which the denominators of the upper part are to be evaluated. (The elimination process in first-order has no analogy in standard MBPT, since there final model-space states do not appear in the wave function.)

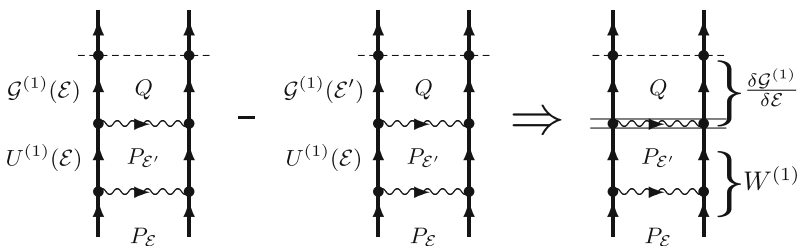


**Fig. 6.12** Elimination of the singularity of the second-order evolution operator, due to an intermediate model-space state. This leads to a residual contribution that corresponds to the folded diagram in standard many-body perturbation theory (Fig. 2.5) but contains, in addition, a derivative of the energy-dependent potential. Furthermore, there can be a singularity at the final state, as in first order (see Fig. 6.11)

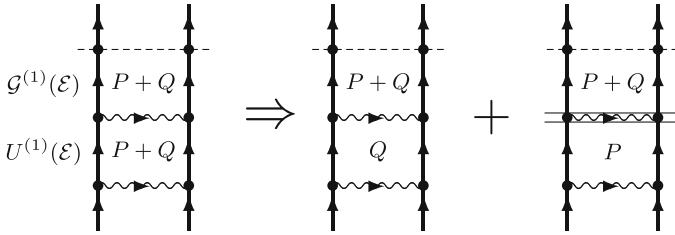


**Fig. 6.13** Elimination of the singularity of the second-order evolution operator due to an intermediate model-space state

For  $t = 0$  we have from (6.113)

$$Q\mathcal{G}^{(2)}(0, \mathcal{E})P_{\mathcal{E}} = \Gamma_Q(\mathcal{E})V(\mathcal{E})\Gamma_Q(\mathcal{E})V(\mathcal{E})P_{\mathcal{E}} + Q\frac{\delta\mathcal{G}^{(1)}(t, \mathcal{E}', \mathcal{E})}{\delta\mathcal{E}}P_{\mathcal{E}}W^{(1)}P_{\mathcal{E}}, \tag{6.114}$$

which is quite analogous to the corresponding second-order wave operator in ordinary time-independent perturbation theory (2.69). The only difference is here that the derivative of the first-order Green’s operator leads in addition to the standard folded term to a term with the energy-derivative of the interaction. This term is sometimes referred to as the *reference-state contribution* [159], but here we shall refer to both terms as the **model-space contribution** (MSC), which is more appropriate in the general multi-reference case.

From the second-order expression (6.113) we obtain, using the expression for the covariant effective interaction (6.79), the second-order effective interaction<sup>13</sup>

$$W^{(2)} = W_0^{(2)} + \frac{\delta W^{(1)}}{\delta\mathcal{E}}W^{(1)}. \tag{6.115}$$

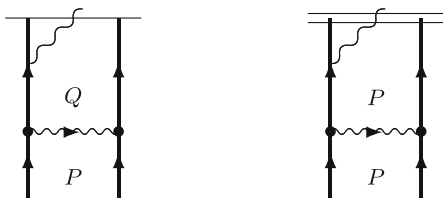
We note here that there is a model-space contribution (second term), which has no analogy in the classical energy-independent formalism (6.106). Since the wave operator beyond zeroth order lies in the  $Q$  space, there can be no MSC in the standard second-order effective interaction. This is an example, when the classical and the field-theoretical (Fock-space) treatments lead to different results.

The Fock-space result can be understood in the following way. The first-order interaction can be looked upon as illustrated in Fig. 6.14 (see Sect. 8.1.2). Considering the case with two retarded photons, the wave operator can be represented by the two diagrams below

<sup>13</sup>From the previous footnote we have  $P_{\mathcal{E}''}i\frac{\partial}{\partial t}\left(\frac{\delta\mathcal{G}^{(1)}}{\delta\mathcal{E}}\right)_{t=0}P_{\mathcal{E}'}W^{(1)}P_{\mathcal{E}} = P_{\mathcal{E}''}i\frac{\partial}{\partial t}\left(\frac{\delta\mathcal{G}_0^{(1)}(t, \mathcal{E}')}{\delta\mathcal{E}} + \frac{\delta^2\mathcal{G}^{(0)}(t, \mathcal{E}')}{\delta\mathcal{E}^2}W^{(1)} + \frac{\delta\mathcal{G}^{(0)}(t, \mathcal{E}')}{\delta\mathcal{E}}\frac{\delta W^{(1)}}{\delta\mathcal{E}}\right)_{t=0}P_{\mathcal{E}'}W^{(1)}P_{\mathcal{E}} = P_{\mathcal{E}''}P_{\mathcal{E}'}W^{(1)}P_{\mathcal{E}} + P_{\mathcal{E}''}\frac{\delta W^{(1)}}{\delta\mathcal{E}}W^{(1)}P_{\mathcal{E}}$ .



**Fig. 6.14** Illustration of the single-photon exchange in Fock space. The first diagram represents the first-order wave operator with an uncontracted photon, which is then contracted by a second interaction to form a full single-photon interaction (*right*)



These diagrams represent the wave operator in the photonic Fock space with the intermediate state in  $Q$  and  $P$  spaces, respectively. In the first diagram there is an energy denominator that yields the energy dependence and in the second diagram a double denominator that yields the energy derivative. Closing these parts by the second part of the single-photon interaction (6.52), yields the two contributions in (6.115).

We have assumed so far that in the ladder *all interactions are identical*. **If the interactions are different**, some precaution is required. We see in the second-order expression that the differential/derivative in the last term should refer to the **SECOND** interaction, while if we treat this in an order-by-order fashion we would get the differential of the **FIRST** interaction. If the interactions are in order  $V_1$  and  $V_2$ , then last term above becomes

$$\frac{\delta(\Gamma_Q V_2)}{\delta \mathcal{E}} P_{\mathcal{E}} V_1 P_{\mathcal{E}}, \quad (6.116)$$

(leaving out the arguments). This issue will be further discussed below.

## 6.9.2 All Orders\*

The procedure performed above can be generalized to all orders of perturbation theory. The treatment here follows mainly those of [131, 132] but is more general.

We consider first an evolution operator in the form (6.37) with a general energy-dependent interaction,  $V(\mathcal{E})$ , and with all **intermediate and final** model-space states removed,

$$U_0(t, \mathcal{E})P_{\mathcal{E}} = \mathcal{G}^{(0)}(t, \mathcal{E}) \left( 1 + \Gamma_Q(\mathcal{E})V(\mathcal{E}) + \Gamma_Q(\mathcal{E})V(\mathcal{E})\Gamma_Q(\mathcal{E})V(\mathcal{E}) + \dots \right) P_{\mathcal{E}}, \quad (6.117)$$

with  $\mathcal{G}^{(0)}(t, \mathcal{E})$  given by (6.96). This also represents the Green's operator with no model-space states,  $\mathcal{G}_0(t, \mathcal{E})$ .

The evolution operator with **exactly one intermediate or final** model-space state (or “fold”) can be expressed

$$U_1(t, \mathcal{E}) = \mathcal{G}_0(t, \mathcal{E}')P_{\mathcal{E}'} \left( U_0(0, \mathcal{E}) - 1 \right) P_{\mathcal{E}} \quad (6.118)$$

and the corresponding counter term (6.94)

$$\mathcal{G}_0(t, \mathcal{E}')P_{\mathcal{E}'} \left( U_0(0, \mathcal{E}) - 1 \right) P_{\mathcal{E}}, \quad (6.119)$$

where the parameter of the first operator is now the energy of the intermediate state. This leads to the Green's operator with exactly one fold

$$\mathcal{G}_1(t, \mathcal{E}) = \frac{\delta \mathcal{G}_0(t, \mathcal{E})}{\delta \mathcal{E}} P_{\mathcal{E}'} W_0 P_{\mathcal{E}}, \quad (6.120)$$

where

$$\boxed{W_0(\mathcal{E})P_{\mathcal{E}} = P \left( V(\mathcal{E}) + V(\mathcal{E})\Gamma_Q(\mathcal{E})V(\mathcal{E}) + \dots \right) P_{\mathcal{E}}} \quad (6.121)$$

in analogy with the low-order cases.<sup>14</sup>

The Green's operator with just a **final fold** is obtained by replacing  $\mathcal{G}_0$  (the all-order operator without folds) by the zeroth-order operator,  $\mathcal{G}^{(0)}$ ,

$$\frac{\delta \mathcal{G}^{(0)}(t, \mathcal{E})}{\delta \mathcal{E}} P_{\mathcal{E}'} W_0 P_{\mathcal{E}}. \quad (6.122)$$

<sup>14</sup>The rules for differentiating are as follows

$$\begin{aligned} \frac{\delta \mathcal{G}}{\delta \mathcal{E}} &= \frac{\mathcal{G}_{\mathcal{E}} - \mathcal{G}_{\mathcal{E}'}}{\mathcal{E} - \mathcal{E}'}; & \frac{\delta}{\delta \mathcal{E}} \left( \frac{\delta \mathcal{G}}{\delta \mathcal{E}} V \right) &= \frac{\left( \frac{\delta \mathcal{G}}{\delta \mathcal{E}} \right)_{\mathcal{E}} V_{\mathcal{E}} - \left( \frac{\delta \mathcal{G}}{\delta \mathcal{E}} \right)_{\mathcal{E}'} V_{\mathcal{E}'}}{\mathcal{E} - \mathcal{E}'} \\ &= \frac{\left( \frac{\delta \mathcal{G}}{\delta \mathcal{E}} \right)_{\mathcal{E}} V_{\mathcal{E}} - \left( \frac{\delta \mathcal{G}}{\delta \mathcal{E}} \right)_{\mathcal{E}'} V_{\mathcal{E}'} + \left( \frac{\delta \mathcal{G}}{\delta \mathcal{E}} \right)_{\mathcal{E}'} V_{\mathcal{E}} - \left( \frac{\delta \mathcal{G}}{\delta \mathcal{E}} \right)_{\mathcal{E}'} V_{\mathcal{E}'}}{\mathcal{E} - \mathcal{E}'} = \frac{\delta^2 \mathcal{G}}{\delta \mathcal{E}^2} V + \frac{\delta \mathcal{G}}{\delta \mathcal{E}} \frac{\delta V}{\delta \mathcal{E}} \\ \frac{\delta}{\delta \mathcal{E}} V^2 &= \frac{\delta}{\delta \mathcal{E}} V_{\mathcal{E}''} V_{\mathcal{E}} = V_{\mathcal{E}''} \frac{V_{\mathcal{E}} - V_{\mathcal{E}'}}{\mathcal{E} - \mathcal{E}'} = V \frac{\delta V}{\delta \mathcal{E}}. \end{aligned}$$

This can be generalized to

$$\frac{\delta^n (AB)}{\delta \mathcal{E}^n} = \sum_{m=0}^n \frac{\delta^m A}{\delta \mathcal{E}^m} \frac{\delta^{n-m} B}{\delta \mathcal{E}^{n-m}}$$

(see further [132, Appendix B]).

Applying here the formula (6.79), demonstrates that  $W_0$  is the *all-order effective interaction without folds*, extending the relations (6.104) and (6.110),

The evolution operator with **two folds** can be expressed in analogy with (6.118)

$$U_2(t, \mathcal{E}) P_{\mathcal{E}} = \mathcal{G}_0(t, \mathcal{E}) P_{\mathcal{E}'} \left( U_0(0, \mathcal{E}) - 1 \right) P_{\mathcal{E}'} \left( U_0(0, \mathcal{E}) - 1 \right) P_{\mathcal{E}}. \quad (6.123)$$

The two leftmost factors represent the first-order expression (6.118), and after eliminating the singularity, we can replace this by the operator (6.101), yielding the Green's operator with **two folds** (intermediate and/or final)

$$\mathcal{G}_2(t, \mathcal{E}) = \frac{\delta \mathcal{G}_1(t, \mathcal{E}')}{\delta \mathcal{E}'} P_{\mathcal{E}'} W_0(\mathcal{E}) P_{\mathcal{E}}.$$

Continuing this process leads to

$$\mathcal{G}_n(t, \mathcal{E}) = \frac{\delta \mathcal{G}_{n-1}(t, \mathcal{E}')}{\delta \mathcal{E}'} P_{\mathcal{E}'} W_0(\mathcal{E}) P_{\mathcal{E}}, \quad (6.124)$$

and

$$\begin{aligned} \mathcal{G}(t, \mathcal{E}) P_{\mathcal{E}} &= \left( \mathcal{G}_0(t, \mathcal{E}) + \mathcal{G}_1(t, \mathcal{E}) + \mathcal{G}_2(t, \mathcal{E}) + \dots \right) P_{\mathcal{E}} \\ &= \left[ \mathcal{G}_0(t, \mathcal{E}) + \left( \frac{\delta \mathcal{G}_0(t, \mathcal{E})}{\delta \mathcal{E}} + \frac{\delta \mathcal{G}_1(t, \mathcal{E})}{\delta \mathcal{E}} + \dots \right) W_0 \right] P_{\mathcal{E}} \end{aligned}$$

or

$$\boxed{\mathcal{G}(t, \mathcal{E}) P_{\mathcal{E}} = \mathcal{G}_0(t, \mathcal{E}) P_{\mathcal{E}} + \frac{\delta \mathcal{G}(t, \mathcal{E})}{\delta \mathcal{E}} W_0 P_{\mathcal{E}}.} \quad (6.125)$$

Here, the last term represents all intermediate/final folds due to model-space states. This relation is *valid for the entire model space* and it is consistent with [132, Eq. (54)] but more general. The expressions given here are *valid for all times* and for the final state in  $P$  as well as  $Q$  spaces. The corresponding wave-operator relation is obtained by setting  $t = 0$ .

If we apply the relation (6.79) to the relation (6.125), we find the corresponding relation for the effective interaction

$$\boxed{W = W_0 + \frac{\delta W}{\delta \mathcal{E}} W_0,} \quad (6.126)$$

where  $W_0$  represents the effective interaction **without** model-space contributions and  $W$  the **full interaction**, including such contributions (MSC).<sup>15</sup>

<sup>15</sup>  $\frac{\delta \mathcal{G}}{\delta \mathcal{E}} = \frac{\delta \mathcal{G}^{(0)}}{\delta \mathcal{E}} + \frac{\delta \mathcal{G}^{(1)}}{\delta \mathcal{E}} + \dots$ ;  $P_{\mathcal{E}} \left( i \frac{\partial}{\partial t} \mathcal{G}_0(t, \mathcal{E}) \right)_{t=0} P_{\mathcal{E}} = 0$ ;  $P_{\mathcal{E}} \left( i \frac{\partial}{\partial t} \frac{\delta \mathcal{G}^{(0)}}{\delta \mathcal{E}} \right)_{t=0} P_{\mathcal{E}} = 1$ ;  
 $P_{\mathcal{E}} \left( i \frac{\partial}{\partial t} \frac{\delta \mathcal{G}^{(1)}}{\delta \mathcal{E}} \right)_{t=0} P_{\mathcal{E}} = P_{\mathcal{E}} i \frac{\partial}{\partial t} \frac{\delta}{\delta \mathcal{E}} \left( \frac{\delta \mathcal{G}^{(0)}}{\delta \mathcal{E}} W^{(1)} \right)_{t=0} P_{\mathcal{E}} = \frac{\delta W^{(1)}}{\delta \mathcal{E}}$ ;

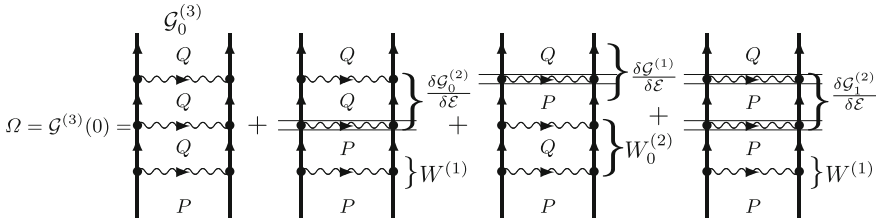


**Fig. 6.15** Graphical representation of the open part of the third-order Green's operator (6.127)

The third-order Green's operator becomes, using the formula (6.125),

$$\begin{aligned} \mathcal{G}^{(3)} &= \mathcal{G}_0^{(3)} + \frac{\delta \mathcal{G}^{(2)}}{\delta \mathcal{E}} W^{(1)} + \frac{\delta \mathcal{G}^{(1)}}{\delta \mathcal{E}} W_0^{(2)} + \frac{\delta \mathcal{G}^{(0)}}{\delta \mathcal{E}} W_0^{(3)} \\ &= \mathcal{G}_0^{(3)} + \frac{\delta \mathcal{G}_0^{(2)}}{\delta \mathcal{E}} W^{(1)} + \frac{\delta \mathcal{G}_1^{(2)}}{\delta \mathcal{E}} W^{(1)} + \frac{\delta \mathcal{G}^{(1)}}{\delta \mathcal{E}} W_0^{(2)} + \frac{\delta \mathcal{G}^{(0)}}{\delta \mathcal{E}} W_0^{(3)}. \end{aligned} \quad (6.127)$$

Here,  $W_0^{(n)}$  represents the effective interaction of order  $n$  without intermediate model-space states. The last term does not contribute to the wave operator at  $t = 0$ . That part, going into the  $Q$  space is illustrated in Fig. 6.15.

We can find an alternative expression for the folded term in (6.125) by considering

$$\mathcal{G} = \mathcal{G}_0 + \mathcal{G}_1 + \mathcal{G}_2 + \cdots,$$

where  $\mathcal{G}_m$  represents the Green's operator with exactly  $m$  (intermediate or final) model-state states. From the relation (6.124) we find

$$\begin{aligned} \mathcal{G}_1 &= \frac{\delta \mathcal{G}_0}{\delta \mathcal{E}} W_0 \\ \mathcal{G}_2 &= \frac{\delta \mathcal{G}_1}{\delta \mathcal{E}} W_0 = \frac{\delta}{\delta \mathcal{E}} \left( \frac{\delta \mathcal{G}_0}{\delta \mathcal{E}} W_0 \right) W_0 = \frac{\delta^2 \mathcal{G}_0}{\delta \mathcal{E}^2} W_0^2 + \frac{\delta \mathcal{G}_0}{\delta \mathcal{E}} \frac{\delta W_0}{\delta \mathcal{E}} W_0 \\ &= \frac{\delta^2 \mathcal{G}_0}{\delta \mathcal{E}^2} W_0^2 + \frac{\delta \mathcal{G}_0}{\delta \mathcal{E}} W_1. \end{aligned} \quad (6.128)$$

$W_n$  represents the effective interaction with exactly  $n$  folds, and it follows from (6.126) that

$$W_n = \frac{\delta W_{n-1}}{\delta \mathcal{E}} W_0. \quad (6.129)$$

---


$$\begin{aligned} P_{\mathcal{E}} i \frac{\partial}{\partial t} \left( \frac{\delta \mathcal{G}^{(2)}}{\delta \mathcal{E}} \right)_{t=0} P_{\mathcal{E}} &= P_{\mathcal{E}} i \frac{\partial}{\partial t} \left( \frac{\delta \mathcal{G}^{(0)}}{\delta \mathcal{E}} \frac{\delta W_0^{(2)}}{\delta \mathcal{E}} \right)_{t=0} P_{\mathcal{E}} \\ &+ P_{\mathcal{E}} i \frac{\partial}{\partial t} \left( \frac{\delta^2 \mathcal{G}^{(1)}}{\delta \mathcal{E}^2} W^{(1)} + \frac{\delta \mathcal{G}^{(1)}}{\delta \mathcal{E}} \frac{\delta W^{(1)}}{\delta \mathcal{E}} \right)_{t=0} P_{\mathcal{E}} = \frac{\delta W_0^{(2)}}{\delta \mathcal{E}} + \frac{\delta^2 W^{(1)}}{\delta \mathcal{E}^2} W^{(1)} + \frac{\delta W^{(1)}}{\delta \mathcal{E}} \\ &= \frac{\delta W_0^{(2)}}{\delta \mathcal{E}} + \frac{\delta W_1^{(2)}}{\delta \mathcal{E}} = \frac{\delta W^{(2)}}{\delta \mathcal{E}} \Rightarrow P_{\mathcal{E}} i \frac{\partial}{\partial t} \left( \frac{\delta \mathcal{G}}{\delta \mathcal{E}} \right)_{t=0} P_{\mathcal{E}} = 1 + \frac{\delta W^{(1)}}{\delta \mathcal{E}} + \frac{\delta W^{(2)}}{\delta \mathcal{E}} + \cdots = 1 + \frac{\delta W}{\delta \mathcal{E}}. \end{aligned}$$



Similarly,

$$\mathcal{G}_3 = \frac{\delta \mathcal{G}_2}{\delta \mathcal{E}} W_0 = \frac{\delta^3 \mathcal{G}_0}{\delta \mathcal{E}^3} W_0^3 + \frac{\delta^2 \mathcal{G}_0}{\delta \mathcal{E}^2} \frac{\delta W_0}{\delta \mathcal{E}} W_0^2 + \frac{\delta^2 \mathcal{G}_0}{\delta \mathcal{E}^2} W_1 W_0 + \frac{\delta \mathcal{G}_0}{\delta \mathcal{E}} \frac{\delta W_1}{\delta \mathcal{E}} W_0$$

or

$$\mathcal{G}_3 = \frac{\delta^3 \mathcal{G}_0}{\delta \mathcal{E}^3} W_0^3 + \frac{\delta^2 \mathcal{G}_0}{\delta \mathcal{E}^2} 2W_1 W_0 + \frac{\delta \mathcal{G}_0}{\delta \mathcal{E}} W_2.$$

Summing this sequence, leads to

$$\begin{aligned} \mathcal{G} &= \mathcal{G}_0 + \frac{\delta \mathcal{G}_0}{\delta \mathcal{E}} (W_0 + W_1 + W_2 + \dots) \\ &+ \frac{\delta^2 \mathcal{G}_0}{\delta \mathcal{E}^2} (W_0^2 + 2W_0 W_1 + \dots) + \frac{\delta^3 \mathcal{G}_0}{\delta \mathcal{E}^3} (W_0^3 + \dots) + \dots \end{aligned} \quad (6.130)$$

It can be shown by induction [131] that this leads to

$$\mathcal{G} = \mathcal{G}_0 + \sum_{n=1}^{\infty} \frac{\delta^n \mathcal{G}_0}{\delta \mathcal{E}^n} (W_0 + W_1 + W_2 + \dots)^n. \quad (6.131)$$

Here,

$$W = W_0 + W_1 + W_2 + \dots \quad (6.132)$$

is the total effective interaction, yielding

$$\boxed{\mathcal{G}(t, \mathcal{E}) P_{\mathcal{E}} = \mathcal{G}_0(t, \mathcal{E}) P_{\mathcal{E}} + \sum_{n=1}^{\infty} \frac{\delta^n \mathcal{G}_0(t, \mathcal{E})}{\delta \mathcal{E}^n} W^n P_{\mathcal{E}}.} \quad (6.133)$$

This relation is consistent with the results in [131, Eq. (100)] and [132, Eq. 61], where more details of the derivations are given. As the previous relation (6.125), it is **valid for all times** and with the final state in  $Q$  as well as  $P$  space. In case the interactions are different, *the derivatives should be taken of the latest interactions*.

We can find a corresponding equation for the effective interaction by expanding (6.126) order-by order,

$$W^{(2)} = W_0^{(2)} + \frac{\delta W^{(1)}}{\delta \mathcal{E}} W^{(1)}; \quad (6.134)$$

$$W^{(3)} = W_0^{(3)} + \frac{\delta W^{(2)}}{\delta \mathcal{E}} W^{(1)} + \frac{\delta W^{(1)}}{\delta \mathcal{E}} W_0^{(2)}. \quad (6.135)$$

From this sequence we can derive the analogue of (6.133) for the effective interaction

$$\boxed{W(\mathcal{E}) P_{\mathcal{E}} = W_0(\mathcal{E}) P_{\mathcal{E}} + \sum_{n=1}^{\infty} \frac{\delta^n W_0(\mathcal{E})}{\delta \mathcal{E}^n} W^n P_{\mathcal{E}}.} \quad (6.136)$$

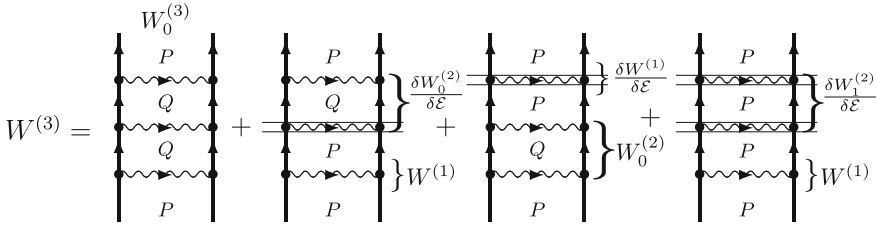


**Fig. 6.16** Graphical representation of the third-order effective interaction (6.137)

This gives

$$W^{(3)} = W_0^{(3)} + \frac{\delta W_0^{(2)}}{\delta \mathcal{E}} W^{(1)} + \frac{\delta W^{(1)}}{\delta \mathcal{E}} W^{(2)} + \frac{\delta^2 W^{(1)}}{\delta \mathcal{E}^2} (W^{(1)})^2, \quad (6.137)$$

which can easily be shown to be identical to the previous result (6.135). This is illustrated in Fig. 6.16 (compare Fig. 6.15).

The treatment here can, in principle, be generalized by replacing the single-photon potential by the complete irreducible multi-photon exchange potential (6.38) in Fig. 6.9.

### 6.9.2.1 Regularity and Linkedness of the Green's Operator

It follows from the treatment here that the counterterms eliminate all singularities so that *the Green's operator is completely regular at all times*.

It also follows that all parts of the expansions above are linked, so this demonstrates that

- *the Green's operator is completely linked also in the multi-reference case.*
- The *linkedness of the single-particle Green's operator* can be expressed, using (6.3),

$$\mathcal{G}(t, t_0) = \left[ \sum_{n=0}^{\infty} \frac{1}{n!} \iint d^3x d^3x_0 \left(\frac{-i}{c}\right)^n \int d^4x_1 \dots \int d^4x_n \right. \\ \left. \times \left\langle 0 \left| \hat{\psi}^\dagger(x) T \left[ \hat{\psi}(x) \mathcal{H}(x_1) \dots \mathcal{H}(x_n) \hat{\psi}^\dagger(x_0) \right] \hat{\psi}(x_2) \right| 0 \right\rangle e^{-\gamma(|t_1|+|t_2|+\dots)} \right]_{\text{linked+folded}} \quad (6.138)$$

and similarly in the many-particle case.

- This represents a *field-theoretical extension of the linked-diagram theorem of standard many-body perturbation theory* (2.82).

## 6.10 Bloch Equation for Green's Operator\*

We now want to transform the general expression above for the Green's operator into a general Bloch-type of equation (2.55) that, in principle, can be solved iteratively (self-consistently). *Iterations can be performed, only if the in- and outgoing states contain only particle states of positive energy (no holes)*. Therefore, we assume this to be the case. If we have an interaction with hole states in or out, we can apply a Coulomb interaction, so that all in- and outgoing states are particle states, as will be discussed further in later chapters.

We work for the moment in the *restricted Hilbert space* with complete single-photon (or multi-photon) interactions.

We want to have an equation of the form

$$[\mathcal{G}^{(n)}, H_0]P = V\mathcal{G}^{(n-1)}P + \text{folded} \quad (6.139)$$

or

$$\mathcal{G}^{(n)}P_{\mathcal{E}} = \Gamma_Q \left( V\mathcal{G}^{(n-1)} + \text{folded} \right) P_{\mathcal{E}}, \quad (6.140)$$

where  $V$  is the *latest* interaction.

We start from the relation (6.125),

$$\mathcal{G}_0 = \mathcal{G}^{(0)} + \frac{\delta \mathcal{G}}{\delta \mathcal{E}} W_0, \quad (6.141)$$

where

$$\mathcal{G} = \mathcal{G}_0 + \mathcal{G}_1 + \mathcal{G}_2 + \dots$$

Here,

$$\mathcal{G}_0 = \mathcal{G}^{(0)}(1 + \Gamma_Q V + \Gamma_Q V \Gamma_Q V + \dots), \quad (6.142)$$

and  $\mathcal{G}_m$  is the Green's operator with exactly  $m$  intermediate/final folds (model-space states),

$$\mathcal{G}_m = \frac{\delta \mathcal{G}_{m-1}}{\delta \mathcal{E}} W_0. \quad (6.143)$$

Similarly, the total effective interaction is (6.132)

$$W = W_0 + W_1 + W_2 + \dots, \quad (6.144)$$

where  $W_m$  is the effective interaction (6.129) with  $m$  folds and

$$W_m = \frac{\delta W_{m-1}}{\delta \mathcal{E}} W_0. \quad (6.145)$$

The folded contribution of order  $n > 0$  is according to (6.140)

$$\begin{aligned} \mathcal{G}^{(n)} - \Gamma_Q V \mathcal{G}^{(n-1)} &= \mathcal{G}_0^{(n)} + \mathcal{G}_1^{(n)} + \mathcal{G}_2^{(n)} + \dots \\ - \Gamma_Q V \mathcal{G}_0^{(n-1)} - \Gamma_Q V \mathcal{G}_1^{(n-1)} - \Gamma_Q V \mathcal{G}_2^{(n-1)} - \dots \end{aligned} \quad (6.146)$$

In the case of no folds we have

$$\mathcal{G}_0^{(n)} - \Gamma_Q V \mathcal{G}_0^{(n-1)} = 0. \quad (6.147)$$

In the case of a single fold we have

$$\Delta_1 = \mathcal{G}_1^{(n)} - \Gamma_Q V \mathcal{G}_1^{(n-1)} = \left( \frac{\delta \mathcal{G}_0}{\delta \mathcal{E}} W_0 \right)^{(n)} - \Gamma_Q V \left( \frac{\delta \mathcal{G}_0}{\delta \mathcal{E}} W_0 \right)^{(n-1)}.$$

Here, all terms cancel except those where the last factor of  $\Gamma_Q V$  is being differentiated in the first part of  $\Delta_1$ . Those terms do not appear in the second part of the difference.

We then have

$$\Delta_1 = \left( \frac{\delta^* \mathcal{G}_0}{\delta \mathcal{E}} W_0 \right)^{(n)}, \quad (6.148)$$

where we have introduced the notation  $\delta^*$ , with the asterisk indicating that the **differentiation applies only to the last interaction**,  $\Gamma_Q V$ , including the associated resolvent,<sup>16</sup>

$$\frac{\delta^*(\Gamma_Q V_a \Gamma_Q V_b \dots)}{\delta \mathcal{E}} = \frac{\delta(\Gamma_Q V_a)}{\delta \mathcal{E}} \Gamma_Q V_b \dots \quad (6.150)$$

and, in addition, differentiation of  $\mathcal{G}^{(0)}$  in case there is no  $\Gamma_Q V$  factor.<sup>17</sup>

In the case of **two** folds we have from (6.146), using (6.143),

$$\begin{aligned} \Delta_2 &= \mathcal{G}_2^{(n)} - \Gamma_Q V \mathcal{G}_2^{(n-1)} = \left( \frac{\delta \mathcal{G}_1}{\delta \mathcal{E}} W_0 \right)^{(n)} - \Gamma_Q V \left( \frac{\delta \mathcal{G}_1}{\delta \mathcal{E}} W_0 \right)^{(n-1)} \\ &= \left[ \frac{\delta}{\delta \mathcal{E}} \left( \frac{\delta \mathcal{G}_0}{\delta \mathcal{E}} W_0 \right) W_0 \right]^{(n)} - \Gamma_Q V \left[ \frac{\delta}{\delta \mathcal{E}} \left( \frac{\delta \mathcal{G}_0}{\delta \mathcal{E}} W_0 \right) W_0 \right]^{(n-1)} \\ &= \left[ \frac{\delta^2 \mathcal{G}_0}{\delta \mathcal{E}^2} (W_0)^2 \right]^{(n)} - \Gamma_Q V \left[ \frac{\delta^2 \mathcal{G}_0}{\delta \mathcal{E}^2} (W_0)^2 \right]^{(n-1)} \end{aligned}$$

<sup>16</sup>Distinguishing the various interactions, we can write

$$\begin{aligned} \mathcal{G}_0 &= \mathcal{G}^{(0)} (1 + \Gamma_Q V_1 + \Gamma_Q V_1 \Gamma_Q V_2 + \dots); & \Delta_1 &= \left[ \frac{\delta \mathcal{G}_0}{\delta \mathcal{E}} - \Gamma_Q V_1 \frac{\delta \mathcal{G}_0}{\delta \mathcal{E}} \right] W_0 \\ &= \left[ \frac{\delta \mathcal{G}^{(0)}}{\delta \mathcal{E}} + \mathcal{G}_0 \frac{\delta(\Gamma_Q V_1)}{\delta \mathcal{E}} (1 + \Gamma_Q V_2 + \dots) \right] W_0 =: \frac{\delta^* \mathcal{G}_0}{\delta \mathcal{E}} W_0; \end{aligned} \quad (6.149)$$

<sup>17</sup>It should be noted that an irreducible multi-photon potential is here regarded as a single interaction.

$$+ \left[ \frac{\delta \mathcal{G}_0}{\delta \mathcal{E}} W_1 \right]^{(n)} - \Gamma_Q V \left[ \frac{\delta \mathcal{G}_0}{\delta \mathcal{E}} W_1 \right]^{(n-1)}.$$

With the convention above we can express the double folds<sup>18</sup>

$$\Delta_2 = \left( \frac{\delta^* \mathcal{G}_0}{\delta \mathcal{E}} W_1 \right)^{(n)} + \left( \frac{\delta^* \mathcal{G}_1}{\delta \mathcal{E}} W_0 \right)^{(n)},$$

where, according to (6.145),

$$W_1 = \frac{\delta W_0}{\delta \mathcal{E}} W_0. \quad (6.152)$$

Continuing this process leads to the total folded contribution

$$\left( \frac{\delta^* \mathcal{G}_0}{\delta \mathcal{E}} + \frac{\delta^* \mathcal{G}_1}{\delta \mathcal{E}} + \dots + \dots \right) (W_0 + W_1 + \dots) = \frac{\delta^* \mathcal{G}}{\delta \mathcal{E}} W.$$

We then have *the generalized Bloch equation* for an *arbitrary energy-dependent interaction* (V)

$$\boxed{\mathcal{G} = \mathcal{G}^{(0)} + \Gamma_Q V \mathcal{G} + \frac{\delta^* \mathcal{G}}{\delta \mathcal{E}} W,} \quad (6.153)$$

where  $W$  is given by (6.144) and *the asterisk represents derivation with respect to the last interaction  $\Gamma_Q V$  and with respect to  $\mathcal{G}^{(0)}$  when no factor of  $\Gamma_Q V$  is present.*<sup>19</sup>

This equation is **valid also when the interactions are different**, and then it should be interpreted as ( $n > 0$ )

---

18

$$\begin{aligned} \left[ \frac{\delta^2 \mathcal{G}_0}{\delta \mathcal{E}^2} - \Gamma_Q V_1 \frac{\delta^2 \mathcal{G}_0}{\delta \mathcal{E}^2} \right] (W_0)^2 &= \left[ \frac{\delta^2 \mathcal{G}^{(0)}}{\delta \mathcal{E}^2} + \frac{\delta \mathcal{G}^{(0)}}{\delta \mathcal{E}} \frac{\delta(\Gamma_Q V_1)}{\delta \mathcal{E}} (1 + \Gamma_Q V_2 + \dots) \right. \\ &\quad \left. + \mathcal{G}^{(0)} \frac{\delta^2(\Gamma_Q V_1)}{\delta \mathcal{E}^2} (1 + \Gamma_Q V_2 + \dots) + \mathcal{G}^{(0)} \frac{\delta(\Gamma_Q V_1)}{\delta \mathcal{E}} \frac{\delta(\Gamma_Q V_2)}{\delta \mathcal{E}} \right. \\ &\quad \left. \times (1 + \Gamma_Q V_3 + \dots) + \dots \right] (W_0)^2 \\ &= \frac{\delta}{\delta \mathcal{E}} \left( \frac{\delta^* \mathcal{G}_0}{\delta \mathcal{E}} \right) (W_0)^2 =: \frac{\delta^* \mathcal{G}_1}{\delta \mathcal{E}} W_0. \end{aligned} \quad (151)$$

19

$$\frac{\delta^* \mathcal{G}}{\delta \mathcal{E}} = \frac{\delta^* \mathcal{G}_0}{\delta \mathcal{E}} + \frac{\delta^* \mathcal{G}_1}{\delta \mathcal{E}} + \frac{\delta^* \mathcal{G}_2}{\delta \mathcal{E}} + \dots \quad (6.154)$$

$$\frac{\delta^* \mathcal{G}_0}{\delta \mathcal{E}} = \frac{\delta \mathcal{G}^{(0)}}{\delta \mathcal{E}} + \frac{\delta \Gamma_Q V}{\delta \mathcal{E}} \mathcal{G}_0 \quad \text{and} \quad \frac{\delta^* \mathcal{G}_n}{\delta \mathcal{E}} = \frac{\delta}{\delta \mathcal{E}} \left( \frac{\delta^* \mathcal{G}_{n-1}}{\delta \mathcal{E}} \right) W_0, \quad (6.155)$$

$$\mathcal{G}^{(n)} = \Gamma_Q V_n \mathcal{G}^{(n-1)} + \sum_{m=1}^{n-1} \frac{\delta^* \mathcal{G}^{(m)}}{\delta \mathcal{E}} W^{(n-m)}, \quad (6.156)$$

where  $V_n$  is the last interaction and the operator  $\mathcal{G}^{(m)}$  is formed by the  $m$  last interactions and  $W^{(n-m)}$  by the  $(n-m)$  first ones.

We can check the formula (6.153) in second order, where it yields

$$\mathcal{G}^{(2)} = \Gamma_Q V \mathcal{G}^{(1)} + \frac{\delta \mathcal{G}^{(0)}}{\delta \mathcal{E}} W^{(2)} + \frac{\delta^* \mathcal{G}^{(1)}}{\delta \mathcal{E}} W^{(1)}. \quad (6.157)$$

With

$$\mathcal{G}^{(1)} = \mathcal{G}^{(0)} \Gamma_Q V + \frac{\delta \mathcal{G}^{(0)}}{\delta \mathcal{E}} W^{(1)} \quad (6.158)$$

from (6.105) and

$$\frac{\delta^* \mathcal{G}^{(1)}}{\delta \mathcal{E}} = \mathcal{G}^{(0)} \frac{\delta \Gamma_Q V}{\delta \mathcal{E}} + \frac{\delta^2 \mathcal{G}^{(0)}}{\delta \mathcal{E}^2} W^{(1)} \quad (6.159)$$

this becomes

$$\mathcal{G}^{(2)} = \mathcal{G}_0^{(2)} + \Gamma_Q V \frac{\delta \mathcal{G}^{(0)}}{\delta \mathcal{E}} W^{(1)} + \frac{\delta \mathcal{G}^{(0)}}{\delta \mathcal{E}} W^{(2)} + \mathcal{G}^{(0)} \frac{\delta \Gamma_Q V}{\delta \mathcal{E}} W^{(1)} + \frac{\delta^2 \mathcal{G}^{(0)}}{\delta \mathcal{E}^2} (W^{(1)})^2, \quad (6.160)$$

which can easily be shown to be identical to (6.113). For  $t = 0$  this becomes

$$\Omega^{(2)} = \mathcal{G}^{(2)}(0) = \Gamma_Q V \Gamma_Q V + \frac{\delta(\Gamma_Q V)}{\delta \mathcal{E}} W^{(1)}, \quad (6.161)$$

which goes over into the second-order wave operator OS standard MBPT, when the perturbation is energy independent (2.69).

We can see that in the case of energy-independent interactions the Bloch equation (6.153) generally reduces to the standard Bloch equation (2.55), since

$$\frac{\delta^* \mathcal{G}}{\delta \mathcal{E}} = -\Gamma_Q \mathcal{G}. \quad (6.162)$$

The similarity between the Bloch equations for the Green's operator and the standard MBPT wave operator demonstrates that the perturbation expansion based upon the CEO or Green's function is completely compatible with the standard procedure. Therefore it can serve as a convenient basis for a **unified procedure**, where QED and Coulomb interactions can, in principle, be mixed arbitrarily.

## 6.11 Time Dependence of the Green's Operator. Connection to the Bethe–Salpeter Equation\*

### 6.11.1 Single-Reference Model Space

Operating with the relation (6.133) on a model function,  $\Psi_0$ , of energy  $E_0$ , yields

$$\mathcal{G}(t, E_0)|\Psi_0\rangle = \left[ \mathcal{G}_0(t, \mathcal{E}) + \sum_{n=1}^{\infty} \frac{\delta^n \mathcal{G}_0(t, \mathcal{E})}{\delta \mathcal{E}^n} (\Delta E)^n \right]_{\mathcal{E}=E_0} |\Psi_0\rangle, \quad (6.163)$$

where  $\mathcal{G}_0$  is the Green's operator without model-space states (6.117) and  $\mathcal{G}$  is the full Green's operator, including model-space contributions (MSC). We have here used the fact (6.62) that

$$W|\Psi_0\rangle = (E - E_0)|\Psi_0\rangle = \Delta E|\Psi_0\rangle. \quad (6.164)$$

The expansion (6.163) is a Taylor series with the effect of shifting the energy parameter from the unperturbed energy,  $E_0$ , to the fully perturbed energy,  $E$ . Hence, the result can be expressed

$$\boxed{\mathcal{G}(t, E_0)|\Psi_0\rangle = \mathcal{G}_0(t, E)|\Psi_0\rangle}. \quad (6.165)$$

This implies that the sum in (6.133), representing

- *the model-space contributions (MSC) to all orders, has the effect of shifting the energy parameter from the model energy  $E_0$  to the target energy  $E$ .*

From the relation (6.37) we have the Green's operator for the ladder *without MSC* in the present case

$$\begin{aligned} \mathcal{G}_0(t, E_0)|\Psi_0\rangle &= e^{-it(E_0-H_0)} \\ &\times \left[ 1 + \Gamma_Q(E_0) V(E_0) + \Gamma_Q(E_0) V(E_0) \Gamma_Q(E_0) V(E_0) + \dots \right] |\Psi_0\rangle. \end{aligned} \quad (6.166)$$

The result (6.165) then implies that the Green's operator **with** model-space contributions becomes

$$\begin{aligned} \mathcal{G}(t, E_0)|\Psi_0\rangle &= \mathcal{G}_0(t, E)|\Psi_0\rangle = e^{-it(E-H_0)} \\ &\times \left[ 1 + \Gamma_Q(E) V(E) + \Gamma_Q(E) V(E) \Gamma_Q(E) V(E) + \dots \right] |\Psi_0\rangle, \end{aligned} \quad (6.167)$$

- *shifting also the energy parameter of the time dependence*, which is a consequence of the fact that the zeroth-order Green's operator,  $\mathcal{G}^{(0)}$  (6.96), is also being modified by the expansion (6.133).

This leads to

$$i \frac{\partial}{\partial t} \mathcal{G}(t, E_0) |\Psi_0\rangle = (E - H_0) \mathcal{G}(t, E_0) |\Psi_0\rangle \quad (6.168)$$

and with (6.70) to

$$\left( i \frac{\partial}{\partial t} \mathcal{G}(t, E_0) \right)_{t=0} |\Psi_0\rangle = (E - H_0) \Omega |\Psi_0\rangle, \quad (6.169)$$

results that are consistent with those in Sect. 6.8.2.

The time dependence of the Green's operator is according to the relation (6.68) the same as that of the relativistic state vector. It then follows from the relation (6.167) that the time-dependence of the state vector is (in the interaction picture)

$$|\chi(t)\rangle = e^{-it(E-H_0)} |\Psi\rangle, \quad (6.170)$$

consistent with the assumption (6.74) and with the elementary quantum-mechanical result ((2.15) and (3.11)).

Setting the time  $t = 0$  in (6.167), yields with the identity (6.70),  $\Omega |\Psi_0\rangle = \mathcal{G}(0, E_0) |\Psi_0\rangle$ , the corresponding relation for the wave operator

$$|\Psi\rangle = \Omega |\Psi_0\rangle = \left[ 1 + \Gamma_Q(E) V(E) + \Gamma_Q(E) V(E) \Gamma_Q(E) V(E) + \dots \right] |\Psi_0\rangle, \quad (6.171)$$

which is the generalized form of the *Brillouin–Wigner expansion* of the wave operator.

From the relation (6.121) we have the effective interaction without folds

$$W_0(E_0) |\Psi_0\rangle = P \left( V(E_0) + V(E_0) \Gamma_Q(E_0) V(E_0) + \dots \right) |\Psi_0\rangle. \quad (6.172)$$

It can be shown in the same way as for the wave function that inclusion of the MSC (folds) leads to the replacement  $E_0 \rightarrow E$  and to the expression for the full effective interaction (6.132)

$$W |\Psi_0\rangle = W_0(E) |\Psi_0\rangle = P \left( V(E) + V(E) \Gamma_Q(E) V(E) + \dots \right) |\Psi_0\rangle, \quad (6.173)$$

which is the generalized *Brillouin–Wigner expansion* of the effective interaction. This can also be expressed

$$\boxed{W |\Psi_0\rangle = P V(E) \Omega |\Psi_0\rangle}, \quad (6.174)$$

using the expression (6.171) for the wave operator. Note that the energy parameter of the interaction is here the **full energy**. From the relation (6.174) and the expression (6.79) for the effective interaction we have the alternative expression



$$W|\Psi_0\rangle = P(E - H_0)\Omega|\Psi_0\rangle. \quad (6.175)$$

Equation (6.174) is an expression for the effective interaction in the restricted Hilbert space with no uncontracted photons, equivalent to the photonic-Fock-space relation (6.63). This is analogous to the MBPT result (2.54), but now the perturbation is **energy dependent**.

It should be noted that the expression above contains the *full energy* of the target state in question. If we look at the first term in (6.173), we can expand the energy perturbatively

$$PV(E)P = PV(E_0)P + P\frac{\delta V(E)}{\delta E}\Delta EP + \dots \quad (6.176)$$

The second term is consistent with the folded term in (6.115). Again we see that *the shift in the energy parameter is due to the model-space contributions*. This illustrates the fact that *the expressions above with the full energy parameter acting in the restricted space with no uncontracted photons are equivalent to the Fock-space relations with the unperturbed parameter*, discussed earlier in the chapter.

From the relation (6.171) we have

$$\begin{aligned} Q(E - H_0)\Omega|\Psi_0\rangle &= Q(E - H_0)\left[1 + \Gamma_Q(E)V(E) + \Gamma_Q(E)V(E)\Gamma_Q(E)V(E) + \dots\right]|\Psi_0\rangle \\ &= Q\left[V(E) + V(E)\Gamma_Q(E)V(E) + \dots\right]|\Psi_0\rangle = QV(E)\Omega|\Psi_0\rangle, \end{aligned}$$

using the fact that the resolvent is  $\Gamma_Q(E) = Q/(E - H_0)$ . Combining this with (6.174) and (6.175), leads to the Schrödinger-like equation in the restricted space

$$\boxed{\left(H_0 + V(E)\right)|\Psi\rangle = E|\Psi\rangle} \quad (6.177)$$

and an *energy-dependent Hamilton operator*

$$\boxed{H = H_0 + V(E)}. \quad (6.178)$$

These relations can be compared with the corresponding GML relations (6.48 and 6.55) in the photonic Fock space. The equation (6.177) is identical to the effective-potential form of the *Bethe-Salpeter equation* (10.20).

It should be observed that the Hamiltonian (6.178) in the restricted Hilbert space is derived starting from the Gell-Mann-Low relation (6.55) in the photonic Fock space without any further assumptions.

As before, we can generalize this treatment by replacing the single-photon potential  $V$  by the *irreducible multi-photon potential* in Fig. 6.9.

### 6.11.2 Multi-reference Model Space

We shall now investigate the time dependence of the Green's operator in a general, quasi-degenerate model space. We start from the relation (6.133)

$$\mathcal{G}(t, \mathcal{E})P_{\mathcal{E}} = \mathcal{G}_0(t, \mathcal{E})P_{\mathcal{E}} + \sum_{n=1}^{\infty} \frac{\delta^n \mathcal{G}_0(t, \mathcal{E})}{\delta \mathcal{E}^n} W^n P_{\mathcal{E}}, \quad (6.179)$$

valid in the general multi-reference (quasi-degenerate) case. As before,  $P_{\mathcal{E}}$  is the part of the model space with energy  $\mathcal{E}$  and  $W$  is given by (6.79). This can formally be expressed as a relation, valid in the entire model space,

$$\mathcal{G}(t, H_0^*)P = \mathcal{G}_0(t, H_0^*)P + \sum_{n=1}^{\infty} \frac{\delta^n \mathcal{G}_0(t, H_0^*)}{\delta (H_0^*)^n} (W^*)^n P. \quad (6.180)$$

where the symbol  $A^*$  implies that the operator  $A$  operates directly on the model-space state to the right. Thus,  $H_0^* B P_{\mathcal{E}} = \mathcal{E} B P_{\mathcal{E}} = B H_0^* P_{\mathcal{E}}$ . Similarly,  $H_{\text{eff}}^* B |\Psi_0^\alpha\rangle = E^\alpha B |\Psi_0^\alpha\rangle = B H_{\text{eff}}^* |\Psi_0^\alpha\rangle$ .

From (6.62) we have

$$W |\Psi_0^\alpha\rangle = P(E^\alpha - H_0) |\Psi_0^\alpha\rangle \quad (6.181)$$

or in operator form

$$W^* = H_{\text{eff}}^* - P H_0^* P. \quad (6.182)$$

Then the expansion (6.180) leads in analogy with (6.133) to

$$\boxed{\mathcal{G}(t, H_0^*) P = \mathcal{G}_0(t, H_{\text{eff}}^*) P.} \quad (6.183)$$

From (6.166) we have

$$\begin{aligned} \mathcal{G}_0(t, \mathcal{E})P_{\mathcal{E}} &= e^{-it(\mathcal{E}-H_0)} \\ &\times \left[ 1 + \Gamma_{\mathcal{Q}}(\mathcal{E}) V(\mathcal{E}) + \Gamma_{\mathcal{Q}}(\mathcal{E}) V(\mathcal{E}) \Gamma_{\mathcal{Q}}(\mathcal{E}) V(\mathcal{E}) + \dots \right] P_{\mathcal{E}} \end{aligned} \quad (6.184)$$

or generally

$$\begin{aligned} \mathcal{G}_0(t, H_0^*)P &= e^{-it(H_0^*-H_0)} \\ &\times \left[ 1 + \Gamma_{\mathcal{Q}}(H_0^*) V(H_0^*) + \Gamma_{\mathcal{Q}}(H_0^*) V(H_0^*) \Gamma_{\mathcal{Q}}(H_0^*) V(H_0^*) + \dots \right] P. \end{aligned} \quad (6.185)$$

This leads in analogy with (6.167) to

$$\begin{aligned} \mathcal{G}(t, H_0^*)P &= \mathcal{G}_0(t, H_{\text{eff}}^*)P = e^{-it(H_{\text{eff}}^* - H_0)} \left[ 1 + \Gamma_Q(H_{\text{eff}}^*) V(H_{\text{eff}}^*) \right. \\ &\quad \left. + \Gamma_Q(H_{\text{eff}}^*) V(H_{\text{eff}}^*) \Gamma_Q(H_{\text{eff}}^*) V(H_{\text{eff}}^*) + \dots \right] P. \end{aligned} \quad (6.186)$$

From this we conclude that

- *the general time dependence of the Green's operator* is given by

$$\boxed{i \frac{\partial}{\partial t} \mathcal{G}(t, H_0^*)P = (H_{\text{eff}}^* - H_0) \mathcal{G}(t, H_0^*)P.} \quad (6.187)$$

Using  $P\mathcal{G}(0, H_0^*)P = P\Omega P = P$ , this gives with (6.182)

$$P \left( i \frac{\partial}{\partial t} \mathcal{G}(t, H_0^*) \right)_{t=0} P = P(H_{\text{eff}}^* - H_0) \mathcal{G}(0, H_0^*)P = W^*, \quad (6.188)$$

which is the expected result.

In analogy with (6.174) we have

$$W^* = PV(H_{\text{eff}}^*)\Omega P \quad (6.189)$$

and similarly in analogy with (6.178) the generalized Hamilton operator

$$H = H_0 + V(H_{\text{eff}}^*). \quad (6.190)$$

and the Schrödinger-like equation

$$\boxed{\left( H_0 + V(H_{\text{eff}}^*) \right) |\Psi^\alpha\rangle = E^\alpha |\Psi^\alpha\rangle.} \quad (6.191)$$

This agrees with the equation derived in [131, Eq. 133]. When the potential is the complete irreducible multi-photon potential, this is equivalent to the **Bethe-Salpeter-Bloch equation**, discussed in Chap. 10 (10.30).

# Chapter 7

## Examples of Numerical Calculations of One- and Two-Photon QED Effects

In this chapter we shall give some numerical illustrations of the three QED methods described in Part II, the S-matrix, the two-time Green's-function and the covariant evolution operator (CEO) methods, applied to evaluation of one- and two-photon exchange. Effects beyond that level will be discussed in the following chapters.

### 7.1 S-Matrix

#### 7.1.1 Electron Self-energy of Hydrogenlike Ions

In the early days of quantum electrodynamics the effects were calculated analytically, applying a double expansion in  $\alpha$  and  $Z\alpha$ . For high nuclear charge,  $Z$ , such an expansion does not work well, and it is preferable to perform the evaluation numerically to all orders of  $Z\alpha$ . The first numerical evaluations of the electron self-energy on heavy, many-electron atoms were performed by Brown et al. in the late 1950s [38] and by Desiderio and Johnson in 1971 [56], applying a scheme devised by Brown et al. [37] (see Sect. 12.3).

An improved method for self-energy calculations, applicable also for lighter systems, was developed and successfully applied to hydrogenlike ions by Peter Mohr [149, 154, 156–158]. The energy shift due to the first-order electron self-energy is conventionally expressed as

$$\Delta E = \frac{\alpha}{\pi} \frac{(Z\alpha)^4}{n^3} F(Z\alpha) mc^2, \quad (7.1)$$

where  $n$  is the main quantum number. The function  $F(Z\alpha)$  is evaluated numerically, and some results are given in Table 7.1.

**Table 7.1** The  $F(Z\alpha)$  function for the ground state of hydrogenlike mercury

Reference	$F(Z\alpha)$
Desiderio and Johnson [56]	1.48
Mohr [153]	1.5032(6)
Blundell and Snyderman [28]	1.5031(3)
Mohr [149]	1.5027775(4)

To perform accurate self-energy calculations numerically for low  $Z$  is complicated due to slow convergence. Mohr has estimated the first-order Lamb shift (self-energy + vacuum polarization) by means of elaborate extrapolation from heavier elements and obtained the value 1057.864(14) MHz for the  $2s - 2p_{1/2}$  shift in neutral hydrogen [156], in excellent agreement with the best experimental value at the time, 1057.893(20) MHz. More recently, Jentschura, Mohr and Soff [96] have extended the method of Mohr in order to calculate directly the self-energy of light elements down to hydrogen with extremely high accuracy. Accurate calculations have also been performed for highly excited states [97].

The original method of Mohr was limited to point-like nuclei but was extended to finite nuclei in a work with Gerhard Soff [161]. An alternative method also applicable to finite nuclei has been devised by Blundell and Snyderman [28, 29].

### 7.1.2 Lamb Shift of Hydrogenlike Uranium

In high-energy accelerators, like that at GSI in Darmstadt, Germany, highly charged ions up to hydrogenlike uranium can be produced. For such systems the QED effects are quite large, and accurate comparison between experimental and theoretical results can here serve as an important test of the QED theory in extremely strong electromagnetic fields—a test that has never been performed before.

The first experimental determination of the Lamb-shift in hydrogenlike uranium was made by the GSI group (Stöhlker, Mokler et al.) in 1993 [233]. The result was 429(23) eV, a result that has gradually been improved by the group, and the most recent value is 460.2(4.6) eV [232]. The shift is here defined as the experimental binding energy compared to the Dirac theory for a *point nucleus*, implying that it includes also the effect of the finite nuclear size. In Table 7.2 we show the various contributions to the theoretical value. The self-energy contribution was evaluated by Mohr [149] and the finite-nuclear-size effect by Mohr and Soff [161]. The vacuum-polarization, including the Wichmann–Kroll correction (see Sect. 4.6.3), was evaluated by Persson et al. [190]. The second-order QED effects, represented by the diagrams in Fig. 7.1, have also been evaluated. Most of the reducible part was evaluated by Persson et al. [189]. The last two irreducible two-loop diagrams are much more elaborate to calculate and have only recently been fully evaluated by Yerokhin et al. [256]<sup>1</sup>

<sup>1</sup>See Sect. 2.6.

**Table 7.2** Ground-state Lamb shift of hydrogenlike uranium (in eV, mainly from [159])

Correction	Value	Reference
Nuclear size	198.82	
First-order self-energy	355,05	[149, 161]
Vacuum polarization	-88.59	[190]
Second-order effects	-1.57	
Nuclear recoil	0.46	
Nuclear polarization	-0.20	
Total theory	463.95	
Experimental	460.2 (4,6)	

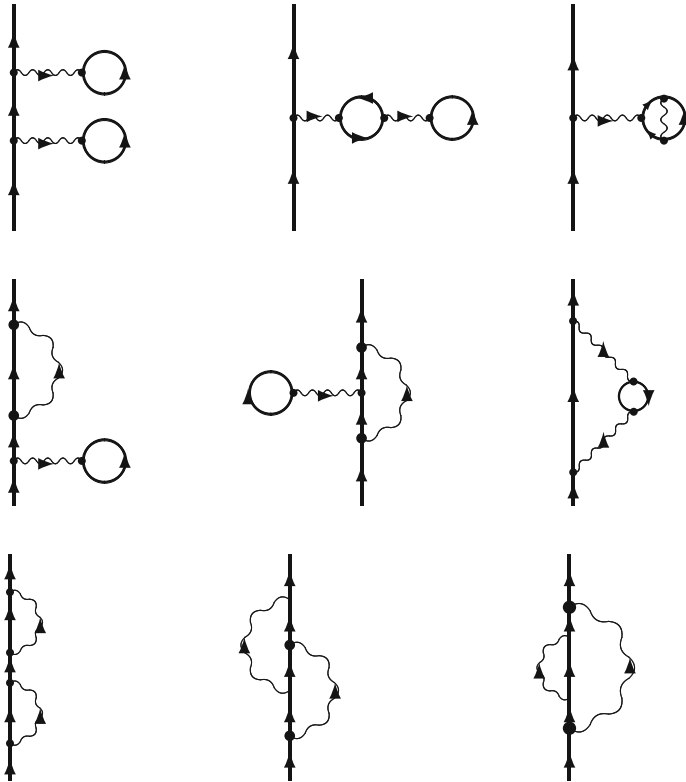


**Fig. 7.1** Second-order contributions to the Lamb shift of hydrogenlike ions (c.f. Fig. 5.3)

The main uncertainty of the theoretical calculation on hydrogenlike uranium stems from the finite-nuclear-size effect, which represents almost half of the entire shift from the Dirac point-nuclear value. Even if the experimental accuracy would be significantly improved, it will hardly be possible to test with any reasonable accuracy

the second-order QED effects, which are only about one percent of the nuclear-size effect. For that reason other systems, like lithium-like ions, seem more promising for testing such effects.

### 7.1.3 *Lamb Shift of Lithiumlike Uranium*

The  $2s - 2p_{1/2}$  Lamb shift of lithiumlike uranium was measured at the Berkeley HILAC accelerator by Schweppe et al. in 1991 [222]. The first theoretical evaluations of the self-energy was performed by Cheng et al. [46] and the complete first-order shift, including vacuum polarization by Blundell [26], Lindgren et al. [128], and Persson et al. [189], the latter calculation including also some reducible second-order QED effects. Later, more complete calculations were performed by Yerokhin et al. [254]. The results are summarized in Table 7.3.

In lithiumlike systems the nuclear-size effect is considerably smaller than in the corresponding hydrogenlike system and can be more easily accounted for. The second-order QED effects in Li-like uranium are of the same order as the present uncertainties in theory and experiment, and with some improvement these effects can be tested. Therefore, systems of this kind seem to have the potential for the most accurate test of high-field QED at the moment.

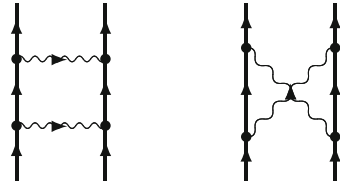
### 7.1.4 *Two-Photon Non-radiative Exchange in Heliumlike Ions*

Accurate S-matrix calculations of the *non-radiative* two-photon exchange for heliumlike ions (ladder and cross), corresponding to the Feynman diagrams in Fig. 7.2, have been performed by Blundell et al. [27] and by Lindgren et al. [126]. The

**Table 7.3**  $2s - 2p_{1/2}$  Lamb shift of lithiumlike uranium (in eV)

Correction	[26]	[189]	[254]
Relativistic MBPT	322.41	322.32	322.10
1. Order self-energy	-53.94	-54.32	
1. Order vacuum polarization	(12.56)	12.56	
1. Order self-energy + vac. pol.	-41.38	-41.76	-41.77
2. Order self-energy + vac. pol.		0.03	0.17
Nuclear recoil	(0.10)	(-0.08)	-0.07
Nuclear polarization	(0.10)	(0.03)	-0.07
Total theory	280.83(10)	280.54(15)	280.48(20)
Experimental	280.59(9)		

**Fig. 7.2** Feynman diagrams representing the two-photon exchange (ladder and cross) for heliumlike ions



results are illustrated in Fig. 7.3 (taken from [126]). In the figure the contributions are displayed *versus* the nuclear charge, relative to the zeroth-order non-relativistic ionization energy,  $Z^2/2$  (in atomic Hartree units). The vertical scale is logarithmic, so that  $-1$  corresponds to  $\alpha$ ,  $-2$  to  $\alpha^2$  etc.

For low  $Z$  the first-order Coulomb interaction is proportional to  $Z$ , the first-order Breit interaction to  $Z^3\alpha^2$ , and the first-order Lamb shift to  $Z^4\alpha^3$ . For high  $Z$  we can replace  $Z\alpha$  by unity, and then after dividing by  $Z^2$ , all first-order effects tend to  $\alpha$  as  $Z$  increases, as is clearly seen in the top picture of Fig. 7.3 (see also Fig. 9.1 and Table 9.1).

An additional Coulomb interaction reduces the effect for small  $Z$  by a factor of  $Z$ . Therefore, the Coulomb–Coulomb interaction, i.e., the leading electron correlation, is in first order independent of  $Z$  and the Coulomb–Breit interaction proportional to  $Z^2\alpha^2$ . The screened Lamb shift is proportional to  $Z^3\alpha^3$  and the second-order Breit interaction (in the no-pair approximation) to  $Z^4\alpha^4$ . After division with  $Z^2$ , we see (second picture of Fig. 7.3) that all second-order effects tend to  $\alpha^2$ .

The third picture in Fig. 7.3 shows the effect of the retarded Coulomb–Breit and Breit–Breit interactions without and with virtual pairs. For low  $Z$  these effects are one order of  $\alpha$  smaller than the corresponding unretarded interactions with no virtual pairs, while for high  $Z$  they tend—rather slowly—to the same  $\alpha^2$  limit. It is notable that for the Coulomb–Breit interactions the retardation and virtual pairs have nearly the same effect but with opposite sign. For the Breit–Breit interactions the effects of single and double pairs have opposite sign and the total effect changes its sign around  $Z = 40$ .

More recently, Mohr and Sapirstein have performed S-matrix calculations also on the excited states of heliumlike ions and compared with second-order MBPT calculations in order to determine the effect of non-radiative QED, retardation and virtual pairs [160], and some results are shown in Table 7.4.

### 7.1.5 *Electron Correlation and QED Calculations on Ground States of Heliumlike Ions*

The two-electron effect on the ground-state energy of some heliumlike ions has been measured by Marrs et al. at Livermore Nat. Lab. by comparing the ionization energies of the corresponding heliumlike and hydrogenlike ions [144]. (The larger effect due to single-electron Lamb shift is eliminated in this type of experiment.)



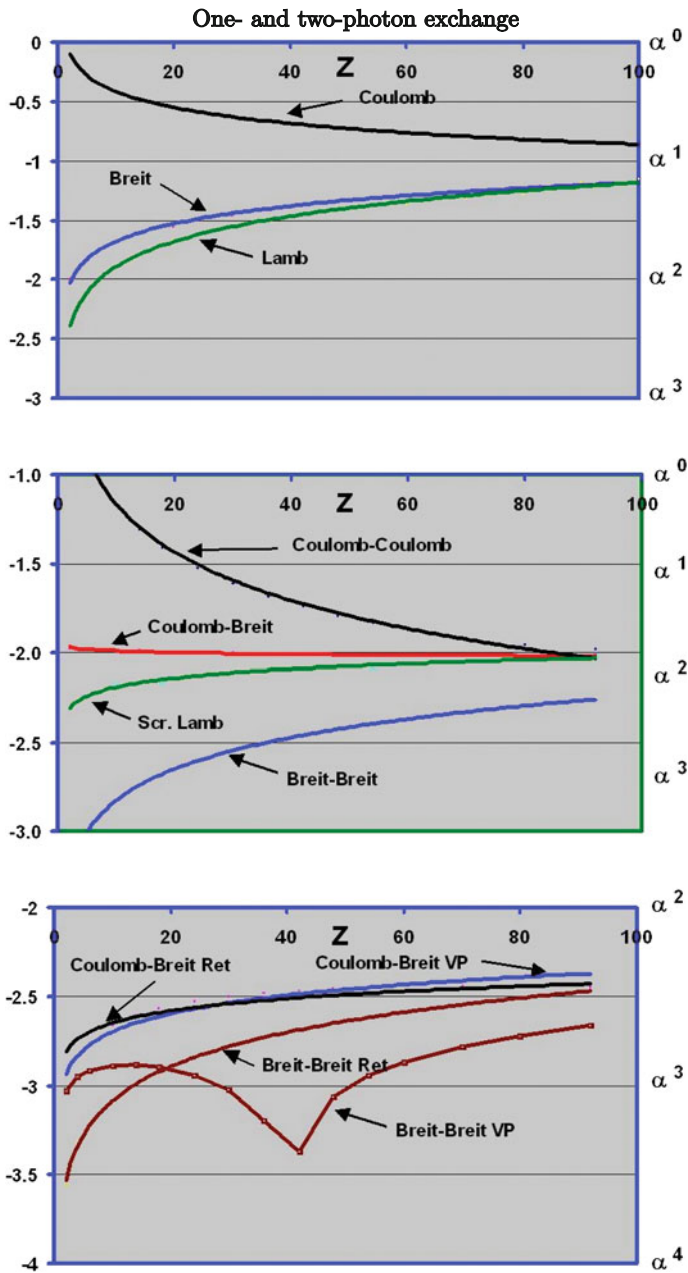


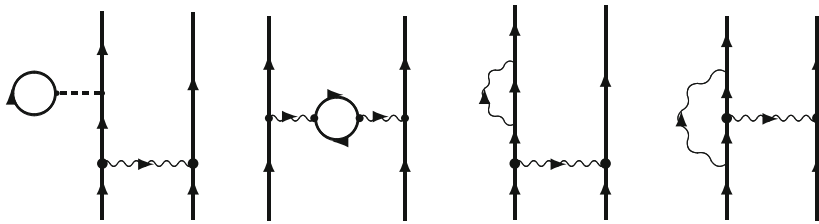
**Fig. 7.3** Various contributions to the ground-state energy of He-like ions. The *top picture* represents the first-order contributions, the *middle picture* the second-order contributions in the NVPA as well as the screened Lamb shift, and the *bottom picture* contributions due to retardation and virtual pairs. The values are normalized to the non-relativistic ionization energy, and the scale is logarithmic (powers of the fine-structure constant  $\alpha$ )

**Table 7.4** Two-photon effects on some excited states of heliumlike ions (in  $\mu\text{Hartree}$ , from [160])

Z		$2^3S_1$	$2^3P_0$	$2^3P_2$
30	MBPT	-49 541	-88 752	-75 352
	QED	-8.7	145	77.6
50	MBPT	-53 762	-123 159	-79 949
	QED	64	1340	767
80	MBPT	-66 954	-251 982	-93
	QED	966	9586	5482

**Table 7.5** Two-electron effects on the ground-state energy of heliumlike ions (in eV, from [192])

Z	Plante et al.	Indelicato et al.	Drake	Persson et al.	Expt'l
32	562.0	562.1	562.1	562.0	$562.5 \pm 1.5$
54	1028.4	1028.2	1028.8	1028.2	$1027.2 \pm 3.5$
66	1372.2	1336.5	1338.2	1336.6	$1341.6 \pm 4.3$
74	1574.8	1573.6	1576.6	1573.9	$1568 \pm 15$
83		1880.8	1886.3	1881.5	$1876 \pm 14$

**Fig. 7.4** Feynman diagrams representing the two-electron screened vacuum polarization and self-energy

Persson et al. [192] have calculated the two-electron contribution by adding to the all-order MBPT result the effect of two-photon QED (see Fig. 7.4), using dimensional regularization (see Chap. 12). The results are compared with the experimental results as well as with other theoretical estimates in Table 7.5. The results of Drake were obtained by expanding relativistic and QED effects in powers of  $\alpha$  and  $Z\alpha$ , using Hylleraas-type of wave functions [61]. The calculations of Plante et al. were made by means of relativistic MBPT and adding first-order QED corrections taken from the work of Drake [195], and the calculations of Indelicato et al. were made by means of multi-configurational Dirac-Fock with an estimate of the Lamb shift [91]. The agreement between experiments and theory is quite good, although the experimental accuracy is not good enough to test the QED parts, which lie in the range 1–5 eV. The agreement between the various theoretical results is also very good—only the results of Drake are somewhat off for the heaviest elements, which is due to the shortcoming of the power expansion.

### 7.1.6 *g*-Factor of Hydrogenlike Ions. Mass of the Free Electron

The Zeeman splitting of hydrogenlike ions in a magnetic field is another good test of QED effects in highly charged ions. The lowest-order contributions to this effect are represented by the Feynman diagrams in Fig. 7.5.

The bound-electron *g*-factor can be expanded as [193]

$$g_J = -2 \left\{ \frac{1}{3} \left[ 1 + 2\sqrt{1 - (Z\alpha)^2} \right] 1 + \frac{\alpha}{\pi} \left( \frac{1}{2} + \frac{(Z\alpha)^2}{12} + \dots \right) \right\}, \quad (7.2)$$

where  $Z$  is the nuclear charge. The first term represents the relativistic value with a correction from the Dirac value of order  $\alpha^2$ . The second term, proportional to  $\alpha$  is the leading QED correction, known as the *Schwinger correction*, and the following term, proportional to  $\alpha^3$ , is the next-order QED correction, first evaluated by Grotch [84].

Numerical calculations to all orders in  $Z\alpha$  have been performed by Blundell et al. [30] (only self-energy part, (b, c) in Fig. 7.5) and by the Gothenburg group [18, 193] (incl. the vacuum polarization (d, e)). The results are displayed in Fig. 7.6, showing the comparison between the Grotch term (the leading QED correction beyond the Schwinger correction) and the numerical result. (The common factor of  $2\alpha/\pi$  has been left out.) The vacuum-polarization data include the Wichmann-Kroll correction in addition to the Uehling correction, and both sets of data include the Breit screening in addition to the Coulomb one. More accurate calculations have later been performed by the St Petersburg group, including also two-loop corrections and the nuclear recoil [255, 257].

The *g*-factors of hydrogenlike ions have been measured with high accuracy by the Mainz group, using an ion trap of Penning type [16, 85]. The accuracy of the experimental and theoretical determinations is so high that the main uncertainty is due to the experimental mass of the electron. Some accurate data for H-like carbon are shown in Table 7.6. By fitting the theoretical and experimental values, a value of the

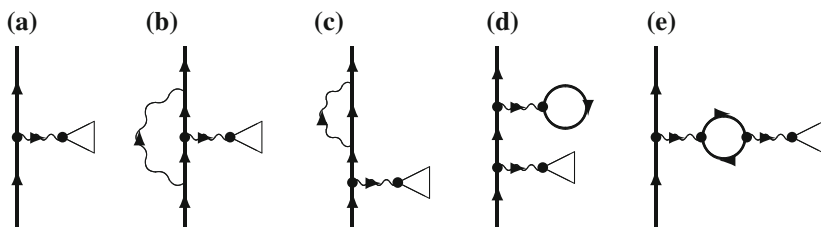


**Fig. 7.5** Feynman diagrams representing the lowest-order contributions to the Zeeman effect of hydrogenlike ions. Diagrams (b) and (c) represent the leading self-energy correction to the first-order effect (a) and (d) and (e) the leading vacuum-polarization correction

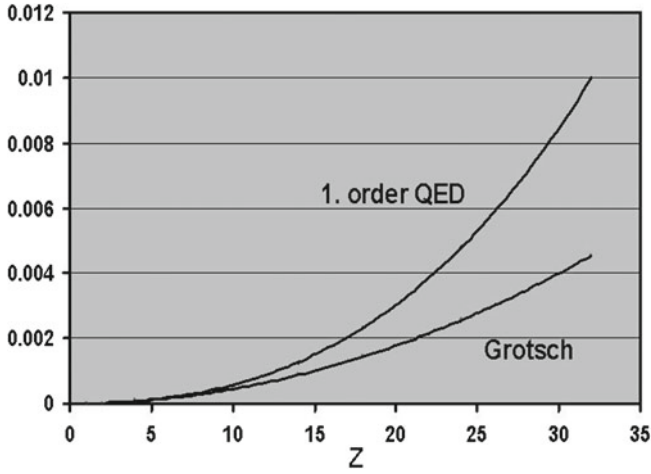


**Fig. 7.6** The full first-order, numerically evaluated, QED correction to the  $g_j$  value of hydrogenlike ions, compared with the leading analytical (Grotsch) term (7.2). Both results are first-order in  $\alpha$  but the numerical result is all order in  $Z\alpha$ , while the Grotsch result contains only the leading term (from [193]). A common factor  $2\alpha/\pi$  is left out

**Table 7.6** Theoretical contributions to the g-factor of hydrogenlike carbon (mainly from [17])

Correction	Value
Dirac theory	1.998 721 3544
Finite nuclear-size corr.	+0.000 000 0004
Nuclear recoil	+0.000 000 0876
Free-electron QED, first order	+0.002 322 8195
Free-electron QED, higher orders	+0.000 003 5151
<b>Bound-electron QED, first order</b>	<b>+0.000 000 8442</b>
Bound-electron QED, higher orders	-0.000 000 0011
Total theory	2.001 041 5899

electron mass (in atomic mass units)  $m_e = 0.0005485799093(3)$ , is deduced from the carbon experiment and the value  $m_e = 0.0005485799092(5)$  from a similar experiment on oxygen [16]. These results are four times more accurate than the previously accepted value,  $m_e = 0.0005485799110(12)$  [152]. The new value is now included in the latest adjustments of the fundamental constants [150, 151].

## 7.2 Two-Time Green's-Function and the Covariant Evolution Operator Method, Applied to He-Like Ions

The two-time Green's function and the covariant evolution operator (CEO) methods have the important advantage over the S-matrix formulation that they can be applied also to *quasi-degenerate* energy levels. As a first illustration we consider here the evaluation of some fine-structure separations of the lowest  $P$  state of heliumlike ions, shown Table 7.7. The calculations of Plante et al. [195] are relativistic many-body calculations in the NVPA scheme (see Sect. 2.6) with first-order QED-energy corrections, taken from the work of Drake [61]. The calculations by Åsén et al. [10, 123], were performed with the newly developed CEO method, described in the previous chapter. This was the first numerical evaluation of (non-radiative) QED effects on quasi-degenerate energy levels. It can be noted that the energy of the  $1s2p^3P_1$  state, which a linear combination of the closely spaced states  $1s2p_{1/2}$  and  $1s2p_{1/3}$ , could not be evaluated by the S-matrix formulation due to the close degeneracy (see, for instance, the above-mentioned work of Mohr and Sapirstein [160]). Later, calculations have also been performed on these systems by the St Petersburg group, using the two-time-Green's-function method [9], where also the radiative parts are evaluated numerically.

The accuracy of the experimental fine-structure results is in most cases not sufficient to test the second-order corrections evaluated by Åsén and Artemyev. One exception is the case of Fluorine ( $Z = 9$ ), where the accuracy seems to be sufficient to test even higher-order QED effects. At present theory cannot match the experimental accuracy here, but this might form a good testing ground for the new combined QED-correlation procedure, discussed in the following chapters.

As a second illustration we consider some laser and X-ray transition energies for He-like ions in Table 7.8. The transition  $1s2s^1S_0 - 1s2p^3P_1$  for He-like silicon has been measured extremely accurately by Myers et al. [57]. Corresponding calculations have been performed by Artemyev et al. [9], using the two-time Green's function and Plante et al. [195], using relativistic MBPT with first-order QED correction. Here, it can be seen that the experiment is at least two orders of magnitude more accurate than the theoretical estimates. Also here the combined higher-order MBPT-QED corrections are expected to be significant.

In the same table we show a comparison between experimental and theoretical values for some the X-ray transition  $1s^2^1S_0 \rightarrow 1s2p^1P_1$ . The experimental values are taken from [9], for  $Z = 23$  and 26 the weighted average of two experimental results is taken. The experimental value for  $Z = 22$  (Ti) is taken from Chantler [43]. The agreement between the two theoretical results is excellent. The agreement between theory and experiments is in most cases also quite good, but in a few cases discrepancies up to three standard deviations. It is argued whether this is accidental or not [43], as will be further discussed in Chap. 9.

**Table 7.7** The  $1s2p^3P$  fine structure of He-like ions (values for  $Z = 2, 3$  given in MHz and the remaining ones in  $\mu\text{Hartree}$ )

Z	$^3P_1 - ^3P_0$	$^3P_2 - ^3P_0$	$^3P_2 - ^3P_1$	Ref. expt <sup>1</sup>	Ref. theory
2	29616.95166(70)		2291.17759(51)	Gabrielse et al. [258]	
	29616.9527(10)			Giusfred et al. [76]	
	29616.9509(9)			Hessels et al. [75]	
3	29616.9523(17)		2291.17753(35)	Hessels et al. [33]	Pachuecki et al. [184]
	155704.27(66)		2291.1789(17)		
			-62678.41(65)	Riis et al. [202]	
9	155703.4(1,5)		-62678.46(98)	Clarke et al. [48]	
	701(10)	5064(8)	-62679.4(5)		Drake et al. [61]
	680	5050	<b>4364.517(6)</b>	Myers et al. [169]	
10	681	5045	4362(5)		Drake et al. [61]
	690	5050	4364		Plante et al. [195]
	1371(7)	8458(2)	7087(8)		Åsén et al. [10, 130]
	1361(6)	8455(6)	7094(8)	Curd et al. [52]	
12	1370	8469	7099		Drake et al. [61]
	1370	8460	7090		Plante et al. [195]
	3789(26)	20069(9)	16280(27)		Åsén et al. [123]
	3796(7)			Curd et al. [52]	
14	3778(10)	20046(10)	16268(13)	Myers et al. [170]	
	3796	20072	16276		Drake et al. [61]
	3800,1	20071			Plante et al. [195]
		40707(9)			Artemyev et al. [9]
14	8108(23)	40708(23)	32601(33)	Curd et al. [52]	
	8094	40707	32613		Drake et al. [61]
		40712			Plante et al. [195]
					Artemyev et al. [9]

(continued)

Table 7.7 (continued)

$Z$	${}^3P_1 - {}^3P_0$	${}^3P_2 - {}^3P_0$	${}^3P_2 - {}^3P_1$	Ref. expt'l	Ref. theory
18		124960(30)		Kukla et al. [106]	
		124810(60)			Drake et al. [61]
	23692	124942	101250		Plante et al. [195]
	23790	124940	101150		Åsén et al. [123]
		124945(3)			Artemyev et al. [9]

**Table 7.8** Comparison between theory and experiments for some transition energies of heliumlike ions

$1s2s\ ^1S_0 - 1s2p\ ^3P_1$ (in $\text{cm}^{-1}$ )			
Z	Myers et al.	Plante et al.	Experimental
14	<b>7230.585(6)</b>	7229(2)	7231.1
$1s^2\ ^1S_0 \rightarrow 1s2p\ ^1P_1$ (in eV)			
Z	Artemyev et al.	Plante et al.	Experimental
16	2460.629	2460.628	2460.649(9)
18	3159.582	3159.580	3159.553(38)
19	3510.462(1)	3510.459	3510.58(12)
21	4315.412(1)	4315.409	4315.54(15)
22	4749.644(1)	4749.639	4749.85(7)
23	5205.165(1)	5205.154	5205.15(12)
24	5682.068(1)	5682.061	5682.32(40)
26	6700.435(1)	6700.423	6700.80(15)
32	10280.218(3)	10280.185	10280.70(22)

**Table 7.9** Two-photon calculations on the  $1s2s\ ^1S$ ,  $^3S$  states of heliumlike ions (in  $\mu\text{Hartree}$ , first two columns from Åsén et al. [11], last column from Mohr and Sapirstein [160])

Z		$2\ ^3S_0$	$2\ ^3S_1$	$2\ ^3S_1$
10	MBPT	-116 005	-47 638	
	QED	6.2	-1.2	
18	MBPT	-119 381	-48 158	
	QED	3.8	4.6	
30	MBPT	-128 349	-49 542	-49 541
	QED	93	6.9	8.7
60	MBPT	-177 732	-57 025	-57 023
	QED	2358	216	224

The CEO method has also been applied by Åsén et al. [10, 11] to evaluate the two-photon diagrams in Fig. 7.2 for the first excited  $S$  states of some heliumlike ions. The results are compared with relativistic MBPT results, in order to determine the non-radiative QED effects, as in Table 7.4. The results are shown in Table 7.9, where comparison is also made with some results of Mohr and Sapirstein [160].



**Part III**  
**Unification of Many-Body**  
**Perturbation Theory**  
**and Quantum Electrodynamics**

## Chapter 8

# Beyond Two-Photon Exchange: Combination of Quantum Electrodynamics and Electron Correlation

In Part I we have considered some standard methods for many-body calculations on electronic systems. These methods are well developed and can treat dominating electron-correlation effects to essentially all orders of perturbation theory. In Part II we have considered three different methods for numerical QED calculations on bound electronic systems, which have been successfully applied to various problems. The latter methods are, however, in practice limited to *one- and two-photon exchange*, implying that electron correlation can only be treated in lowest order. For many systems the electron correlation is of great importance, and in order to be able to evaluate the QED effects accurately, it may be necessary to take into account also how *the quantum-electrodynamical effects are affected by electron correlation*. This implies going beyond second order and requires that new methods have to be developed.

One of the three methods discussed for QED calculations, the covariant evolution operator (CEO) method, has the advantage over the other two that it can also deal with perturbations of the **wave function**, not only of the energy. It can be used in a perturbative way and therefore forms a suitable basis for a combined QED-MBPT procedure, as we shall demonstrate in this third part. When all effects are considered, this is equivalent to the *relativistically covariant Bethe–Salpeter equation*, valid also in the multi-reference case and referred here to as the *Bethe–Salpeter–Bloch equation*.

In this work we shall apply the *equal-time approximation*, discussed in Chap. 6. Furthermore, it is important to work with the *Coulomb gauge*, particularly when radiative QED effects are involved, as will be demonstrated in connection with the numerical results, presented in the following chapter.

## 8.1 Non-radiative QED Effects, Combined with Electron Correlation

We shall first treat the non-radiative QED effects—the retardation and the virtual electron-positron pairs—to see how they can be combined with electron correlation.

### 8.1.1 Single-Photon Exchange with Virtual Pairs

In the treatment of single-photon exchange in Chap. 6 the incoming state was assumed to be unperturbed. We shall now generalize this treatment and allow the incoming state to be perturbed, involving *particle as well as hole states*.

To start with, we shall work in the standard Hilbert space, assuming that the interactions are complete, and we shall return to the Fock-space case in the following section.

With the Coulomb gauge the total interaction is according to (4.57) separated into a *Coulomb and a transverse part* (see Fig. 8.1)

$$I^C = I_C^C + I_T^C. \tag{8.1}$$

The corresponding single-photon interaction is similarly separated into

$$V_{sp} = V_C + V_T. \tag{8.2}$$

We start with the transverse part and consider the Coulomb part later.

#### 8.1.1.1 Transverse Part

The kernel of the transverse part of the single-photon exchange in Coulomb gauge is in analogy with (6.18) given by (Fig. 8.2)

$$i S_F(x, x_1) i S_F(x', x_2) (-i) I_T^C(x_2, x_1) i S_F(x_1, x_0) i S_F(x_2, x'_0) e^{-\gamma(|l_1|+|l_2|)}. \tag{8.3}$$

**Fig. 8.1** In the Coulomb gauge the single-photon exchange is separated into a Coulomb and a transverse (Breit) part

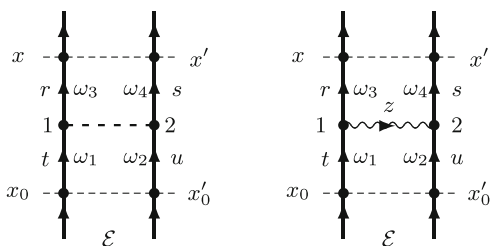
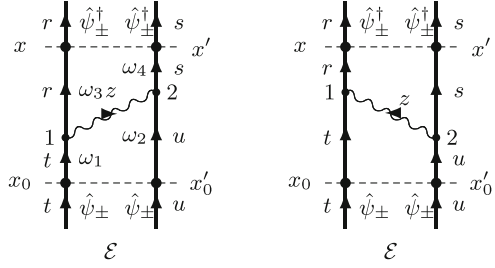


**Fig. 8.2** Time-ordered evolution-operator diagrams for single-photon exchange, transverse part



The external time dependence is (with the notations in the figure) in the *equal-time approximation* in analogy with the previous case (6.16)

$$e^{-it(\omega_3+\omega_4-\varepsilon_r-\varepsilon_s)} e^{it_0(\omega_1+\omega_2-\varepsilon_r-\varepsilon_u)}.$$

As before, we can argue that in the limit  $\gamma \rightarrow 0$   $\omega_1 + \omega_2 = \omega_3 + \omega_4 = \mathcal{E}$ , i.e., equal to the initial energy ( $\mathcal{E}$ ), and the time dependence becomes

$$e^{-it(\mathcal{E}-\varepsilon_r-\varepsilon_s)} e^{it_0(\mathcal{E}-\varepsilon_r-\varepsilon_u)}.$$

We then have the relation

$$U_T(t, t_0) = e^{-it(\mathcal{E}-H_0)} \mathcal{M}_T e^{it_0(\mathcal{E}-H_0)}, \tag{8.4}$$

where  $\mathcal{M}_T$  is the corresponding *Feynman amplitude*, defined as before (6.17). This yields

$$\begin{aligned} \mathcal{M}_T(\mathbf{x}, \mathbf{x}'; \mathbf{x}_0, \mathbf{x}'_0) &= \frac{1}{2} \iiint \frac{d\omega_1}{2\pi} \frac{d\omega_2}{2\pi} \frac{d\omega_3}{2\pi} \frac{d\omega_4}{2\pi} \int \frac{dz}{2\pi} iS_F(\omega_3; \mathbf{x}, \mathbf{x}_1) \\ &\times iS_F(\omega_4; \mathbf{x}', \mathbf{x}_2) (-i)I_T^C(z; \mathbf{x}_2, \mathbf{x}_1) iS_F(\omega_1; \mathbf{x}_1, \mathbf{x}_0) iS_F(\omega_2; \mathbf{x}_2, \mathbf{x}'_0) \\ &\times 2\pi\Delta_\gamma(\omega_1 - z - \omega_3) 2\pi\Delta_\gamma(\omega_2 + z - \omega_4), \end{aligned} \tag{8.5}$$

leaving out the internal space integrations. (The factor of 1/2 is, as before, eliminated when considering a particular permutation of the vertices.)

After integrations over  $\omega_2, \omega_3, \omega_4$ , the amplitude becomes

$$\begin{aligned} \mathcal{M}_T(\mathbf{x}, \mathbf{x}', \mathbf{x}_0, \mathbf{x}'_0) &= \frac{1}{2} \iint \frac{d\omega_1}{2\pi} \frac{dz}{2\pi} iS_F(\omega_1 - z; \mathbf{x}, \mathbf{x}_1) iS_F(\mathcal{E} - \omega_1 + z; \mathbf{x}', \mathbf{x}_2) \\ &\times (-i)I_T^C(z; \mathbf{x}_2, \mathbf{x}_1) iS_F(\omega_1; \mathbf{x}_1, \mathbf{x}_0) iS_F(\mathcal{E} - \omega_1; \mathbf{x}_2, \mathbf{x}'_0). \end{aligned} \tag{8.6}$$

Inserting the expressions for the electron propagator (4.10) and the interaction (4.46), a specific matrix element becomes

$$\begin{aligned} \langle rs | \mathcal{M}_T | ab \rangle &= \left\langle rs \left| -i \int \frac{d\omega_1}{2\pi} \int \frac{dz}{2\pi} \frac{1}{\omega_1 - z - \varepsilon_r + i\gamma_r} \frac{1}{\mathcal{E} - \omega_1 + z - \varepsilon_s + i\gamma_s} \right. \right. \\ &\quad \left. \left. \times \frac{1}{\omega_1 - \varepsilon_t + i\gamma_t} \frac{1}{\mathcal{E} - \omega_1 - \varepsilon_u + i\gamma_u} \int \frac{2c^2 \kappa d\kappa f_T^C(\kappa)}{z^2 - c^2 \kappa^2 + i\eta} \right| ab \right\rangle, \end{aligned} \quad (8.7)$$

where  $f_T^C$  is the transverse part of the  $f$  function in Coulomb gauge (4.60). Integration over  $z$  now yields—in analogy with the treatment in Chap. 6—

$$\mathcal{M}_T = (-i)^2 \int \frac{d\omega_1}{2\pi} \int c d\kappa f_T^C(\kappa)$$

times the propagator expressions

$$\frac{1}{\mathcal{E} - \varepsilon_r - \varepsilon_s} \left[ \frac{1}{\omega_1 - \varepsilon_r - (c\kappa - i\gamma)_r} + \frac{1}{\mathcal{E} - \omega_1 - \varepsilon_s - (c\kappa - i\gamma)_s} \right]$$

and

$$\frac{1}{\mathcal{E} - \varepsilon_t - \varepsilon_u} \left[ \frac{1}{\omega_1 - \varepsilon_t + i\gamma_t} + \frac{1}{\mathcal{E} - \omega_1 - \varepsilon_u + i\gamma_u} \right].$$

We have now *four combinations* that contribute depending on the sign of the orbital energies (after integration over  $\omega_1$ ):

$$\begin{aligned} \text{sgn}(\varepsilon_r) \neq \text{sgn}(\varepsilon_t) &: \frac{\text{sgn}(\varepsilon_t)}{\varepsilon_t - \varepsilon_r - (c\kappa - i\gamma)_r} \\ \text{sgn}(\varepsilon_s) = \text{sgn}(\varepsilon_t) &: \frac{\text{sgn}(\varepsilon_t)}{\mathcal{E} - \varepsilon_t - \varepsilon_s - (c\kappa - i\gamma)_s} \\ \text{sgn}(\varepsilon_u) = \text{sgn}(\varepsilon_r) &: \frac{\text{sgn}(\varepsilon_u)}{\mathcal{E} - \varepsilon_r - \varepsilon_u - (c\kappa - i\gamma)_r} \\ \text{sgn}(\varepsilon_u) \neq \text{sgn}(\varepsilon_s) &: \frac{\text{sgn}(\varepsilon_u)}{\varepsilon_u - \varepsilon_s - (c\kappa - i\gamma)_s} \end{aligned} \quad (8.8)$$

times  $(-i)$ .

The *Feynman amplitude* for the transverse part of the single-photon exchange now becomes

$$\mathcal{M}_T = \Gamma(\mathcal{E}) iV_T(\mathcal{E}) \Gamma(\mathcal{E}), \quad (8.9)$$

where  $\Gamma(\mathcal{E})$  is the resolvent (2.64). This yields for the present process

$$\boxed{\langle rs | \mathcal{M}_T(\mathcal{E}) | tu \rangle = \frac{i}{\mathcal{E} - \varepsilon_r - \varepsilon_s} \langle rs | V_T(\mathcal{E}) | tu \rangle \frac{1}{\mathcal{E} - \varepsilon_t - \varepsilon_u}}, \quad (8.10)$$

where  $V_T(\mathcal{E})$  is now the *generalized transverse-photon potential*

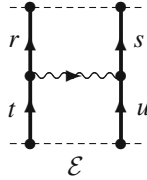
$$\langle rs | V_T(\mathcal{E}) | tu \rangle = \langle rs | \int c d\kappa f_T^C(\kappa) \left[ \pm \frac{t_{\pm} r_{\mp}}{\varepsilon_t - \varepsilon_r \pm c\kappa} \pm \frac{t_{\pm} s_{\pm}}{\mathcal{E} - \varepsilon_t - \varepsilon_s \mp c\kappa} \pm \frac{u_{\pm} r_{\pm}}{\mathcal{E} - \varepsilon_r - \varepsilon_u \mp c\kappa} \pm \frac{u_{\pm} s_{\mp}}{\varepsilon_u - \varepsilon_s \pm c\kappa} \right] | tu \rangle. \quad (8.11)$$

Here,  $t_{\pm}$  etc. represent *projection operators* for particle/hole states, respectively. The upper or lower sign should be used consistently in each term, inclusive the sign in the front, but all combinations of upper and lower signs in the four term should be used, corresponding to the 16 time-ordered combinations, shown in Fig. 8.3.

*It should be noted that the expression above is valid also for the entire interaction in any covariant gauge, using the appropriate  $f$  function.*

We shall now illustrate the potential (8.11) by giving explicit expressions in a few cases. In the next subsection we shall see how these combinations can be evaluated in a more systematic way.

### No virtual pairs



The potential becomes here

$$\langle rs | V_T(\mathcal{E}) | tu \rangle = \langle rs | \int c d\kappa f_T^C(\kappa) \times \left[ \frac{1}{\mathcal{E} - \varepsilon_r - \varepsilon_u - c\kappa} + \frac{1}{\mathcal{E} - \varepsilon_t - \varepsilon_s - c\kappa} \right] | tu \rangle, \quad (8.12)$$

and the Feynman amplitude agrees with the previous result (6.23). This agrees with the result of the evaluation of the corresponding time-ordered diagram according to the rules of Appendix I.

### Single hole in ( $t$ )

The potential becomes here

$$\langle rs | V_T(\mathcal{E}) | tu \rangle = \langle rs | \int c d\kappa f_T^C(\kappa) \times \left[ \frac{-1}{\varepsilon_t - \varepsilon_r - c\kappa} + \frac{1}{\mathcal{E} - \varepsilon_r - \varepsilon_u - c\kappa} \right] | tu \rangle, \quad (8.13)$$

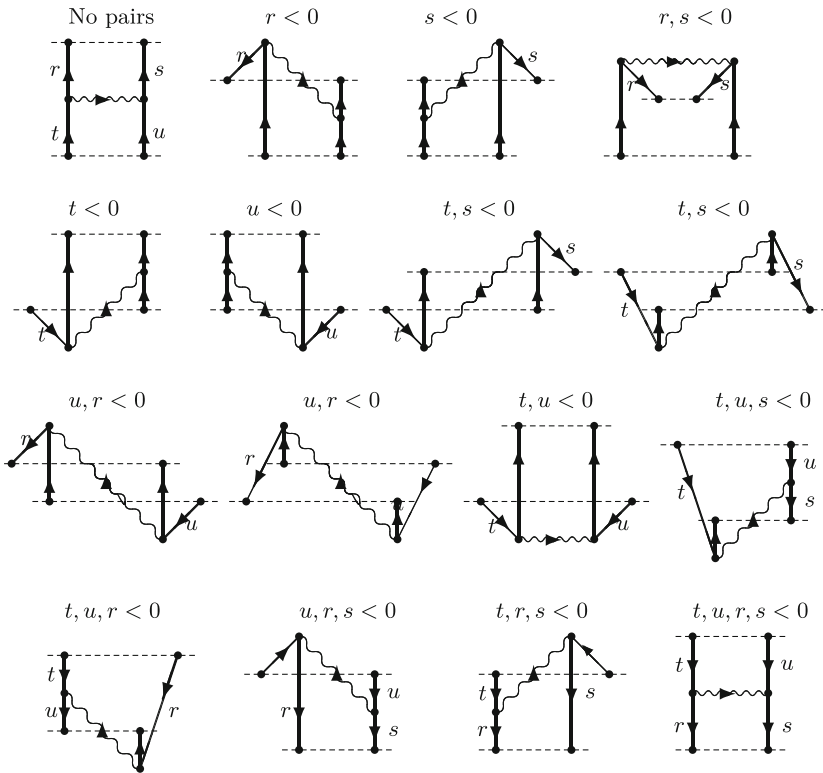
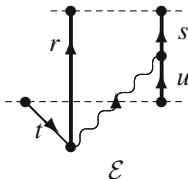


**Fig. 8.3** All 16 time-ordered diagrams corresponding to the transverse single-photon exchange given by (8.11)



which can also be expressed

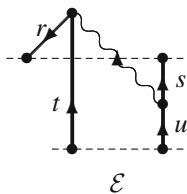
$$\begin{aligned}
 \langle rs | V_T(\mathcal{E}) | tu \rangle &= -(\mathcal{E} - \varepsilon_t - \varepsilon_u) \\
 &\times \langle rs | \int c \, d\kappa f_T^C(\kappa) \frac{1}{\varepsilon_t - \varepsilon_r - c\kappa} \frac{1}{\mathcal{E} - \varepsilon_r - \varepsilon_u - c\kappa} | tu \rangle, \quad (8.14)
 \end{aligned}$$

and the denominators of the Feynman amplitude become

$$-\frac{1}{\mathcal{E} - \varepsilon_r - \varepsilon_s} \frac{1}{\varepsilon_t - \varepsilon_r - c\kappa} \frac{1}{\mathcal{E} - \varepsilon_r - \varepsilon_u - c\kappa}. \quad (8.15)$$

This agrees with the evaluation rules of Appendix I. We see here that one of the resolvents in (8.9) can be singular (“Brown–Ravenhall effect”), which is eliminated by the potential.

**Single hole out ( $r$ )**



The potential (8.11) becomes

$$\begin{aligned} \langle rs | V_T(\mathcal{E}) | tu \rangle &= \langle rs | \int c \, d\kappa f_T^C(\kappa) \\ &\quad \times \left[ \frac{1}{\varepsilon_t - \varepsilon_r + c\kappa} + \frac{1}{\mathcal{E} - \varepsilon_t - \varepsilon_s - c\kappa} \right] | tu \rangle. \end{aligned} \quad (8.16)$$

The denominators can here be expressed

$$(\mathcal{E} - \varepsilon_r - \varepsilon_s) \frac{1}{\varepsilon_t - \varepsilon_r + c\kappa} \frac{1}{\mathcal{E} - \varepsilon_t - \varepsilon_s - c\kappa}, \quad (8.17)$$

and the denominators of the Feynman amplitude becomes

$$\frac{1}{\varepsilon_t - \varepsilon_r + c\kappa} \frac{1}{\mathcal{E} - \varepsilon_t - \varepsilon_s - c\kappa} \frac{1}{\mathcal{E} - \varepsilon_t - \varepsilon_u - c\kappa}, \quad (8.18)$$

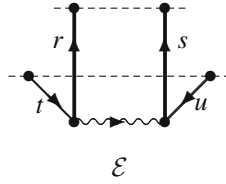
which agrees with the evaluation rules of Appendix I.

**Double hole in  $t, u$**

The potential (8.11) is here

$$\begin{aligned} \langle rs | V_T(\mathcal{E}) | tu \rangle &= \langle rs | \int c \, d\kappa f_T^C(\kappa) \\ &\quad \times \left[ \frac{-1}{\varepsilon_t - \varepsilon_r - c\kappa} + \frac{-1}{\varepsilon_u - \varepsilon_s - c\kappa} \right] | tu \rangle, \end{aligned} \quad (8.19)$$





and the denominators of the Feynman amplitude become

$$\frac{-1}{\mathcal{E} - \varepsilon_r - \varepsilon_s} \left[ \frac{1}{\varepsilon_t - \varepsilon_r - c\kappa} + \frac{1}{\varepsilon_u - \varepsilon_s - c\kappa} \right] \frac{1}{\mathcal{E} - \varepsilon_t - \varepsilon_u}. \tag{8.20}$$

We shall demonstrate explicitly here that this agrees with the evaluation rules of Appendix I. With one time-ordering  $t_{34} > t_2 > t > -\infty$  and  $\infty > t_{34} > t_2$  the time integrations yield

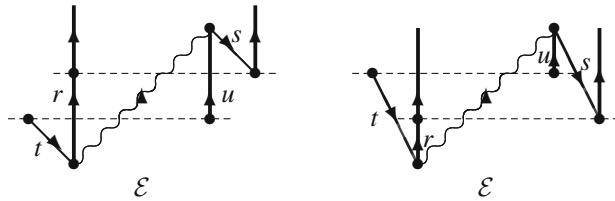
$$(-i)^3 \int_{t_{34}}^{-\infty} dt_2 e^{-id_2 t_2} \int_{t_2}^{\infty} dt_{34} e^{-id_{34} t_{34}} \int_{t_2}^{-\infty} dt_1 e^{-id_1 t_1}. \tag{8.21}$$

Together with the alternative time ordering  $1 \leftrightarrow 2$  this becomes

$$\frac{-1}{d_{1234} d_{34}} \left[ \frac{1}{d_1} + \frac{1}{d_2} \right] \tag{8.22}$$

with the notations of Appendix I, which is identical to the result (8.20). Note that this is NOT in agreement with the standard Goldstone rules of MBPT [124].

**Single hole in and out (t, s)**



The potential (8.11) yields

$$\begin{aligned} \langle rs | V_T(\mathcal{E}) | tu \rangle = & \langle rs | \int c d\kappa f_T^C(\kappa) \left[ \frac{-1}{\varepsilon_t - \varepsilon_r - c\kappa} \right. \\ & \left. + \frac{-1}{\mathcal{E} - \varepsilon_t - \varepsilon_s + c\kappa} + \frac{1}{\mathcal{E} - \varepsilon_u - \varepsilon_r - c\kappa} + \frac{1}{\varepsilon_u - \varepsilon_s + c\kappa} \right] | tu \rangle. \end{aligned} \tag{8.23}$$

Using the notations of Appendix I,

$$\begin{aligned}
 d_1 &= \varepsilon_t - \varepsilon_r - c\kappa; & d_2 &= \varepsilon_u - \varepsilon_s + c\kappa; & d_3 &= \varepsilon_a - \varepsilon_t - c\kappa; \\
 d_4 &= \varepsilon_b - \varepsilon_u + c\kappa; & d_{34} &= \mathcal{E} - \varepsilon_t - \varepsilon_u; \\
 d_{134} &= \mathcal{E} - \varepsilon_r - \varepsilon_u - c\kappa; & d_{234} &= \mathcal{E} - \varepsilon_t - \varepsilon_s + c\kappa; & d_{1234} &= \mathcal{E} - \varepsilon_r - \varepsilon_s,
 \end{aligned}$$

the bracket above becomes

$$-\frac{1}{d_1} - \frac{1}{d_{234}} + \frac{1}{d_2} + \frac{1}{d_{134}} = \frac{d_{1234}d_{34}}{d_{134}d_{234}} \left[ \frac{1}{d_2} - \frac{1}{d_1} \right], \tag{8.24}$$

and the denominators of the Feynman amplitude (8.10)

$$\frac{1}{d_{134}d_{234}} \left[ \frac{1}{d_2} - \frac{1}{d_1} \right] = \frac{1}{d_1d_2} \left[ \frac{1}{d_{134}} - \frac{1}{d_{234}} \right], \tag{8.25}$$

which agrees with the rules of Appendix I.

### 8.1.1.2 Coulomb Interaction

The Coulomb part of the interaction is obtained in a similar way (see Fig. 8.4). In analogy with (8.5) we now have

$$\mathcal{M}_C = \frac{1}{2} \iint \frac{d\omega_1}{2\pi} \frac{d\omega_3}{2\pi} \int \frac{dz}{2\pi} iS_F(\omega_1) iS_F(E_0 - \omega_1) (-i)I_C^C iS_F(\omega_3) iS_F(E_0 - \omega_3),$$

leaving out the space coordinates. After  $z$  integration, using (4.63b), and with the explicit form of the propagators this leads to

$$\begin{aligned}
 \langle rs | \mathcal{M}_C | ab \rangle &= \langle rs | -i \iint \frac{d\omega_1}{2\pi} \frac{d\omega_3}{2\pi} \frac{1}{\omega_1 - \varepsilon_r + i\gamma_r} \frac{1}{E_0 - \omega_1 - \varepsilon_s + i\gamma_s} \\
 &\quad \times V_C \frac{1}{\omega_3 - \varepsilon_t + i\gamma_t} \frac{1}{E_0 - \omega_3 - \varepsilon_u + i\gamma_u} | ab \rangle \\
 &= \langle rs | \pm \frac{i}{E_0 - \varepsilon_r - \varepsilon_s} V_C \frac{1}{E_0 - \varepsilon_t - \varepsilon_u} | ab \rangle, \tag{8.26}
 \end{aligned}$$

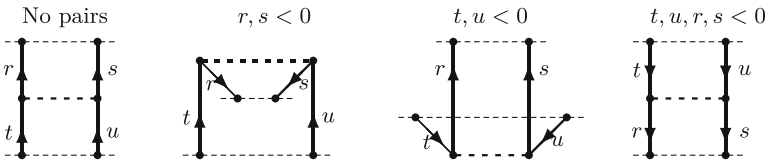


Fig. 8.4 Same as Fig. 8.3 for the Coulomb interaction

where  $V_C$  is the Coulomb interaction (2.109). Here, the plus sign is used if  $\text{sgn}(\varepsilon_t) = \text{sgn}(\varepsilon_u) = \text{sgn}(\varepsilon_r) = \text{sgn}(\varepsilon_s)$  and the minus sign if  $\text{sgn}(\varepsilon_t) = \text{sgn}(\varepsilon_u) \neq \text{sgn}(\varepsilon_r) = \text{sgn}(\varepsilon_s)$ .

### 8.1.2 Fock-Space Treatment

We shall now see how the general single-photon potential (8.11) can be evaluated in a systematic way by working in the *photonic Fock space*. We shall also be able to evaluate the potential with one or several crossing Coulomb interactions. This part follows largely the presentation in [132] and the PhD thesis of Daniel Hedendahl [86].

We have seen earlier that with the perturbation (6.51)

$$\mathcal{H}(x) = \mathcal{H}(t, \mathbf{x}) = -\hat{\psi}^\dagger(x) e c \alpha^\mu A_\mu(x) \hat{\psi}(x) \quad (8.27)$$

the wave function partly lies in an *extended photonic Fock space*, where the number of photons is no longer conserved. According to the Gell-Mann–Low theorem we have a Schrödinger-like equation (6.48) in that space

$$(H_0 + V_F)|\Psi^\alpha\rangle = E^\alpha|\Psi^\alpha\rangle, \quad (8.28)$$

where  $V_F$  is the perturbation (6.52) with the Coulomb and the transverse Fock-space parts,  $V_F = V_C + v_T$ .

In working in the extended space with uncontracted perturbations it is necessary to include in the model Hamiltonian ( $H_0$ ) also the energy operator of the photon field (6.54)

$$H_0 = H_0 + c\kappa a_i^\dagger(\mathbf{k}) a_i(\mathbf{k}), \quad (8.29)$$

where  $\kappa = |\mathbf{k}|$ .

The wave operator is, as before, given by the Green's operator at  $t = 0$  (6.70), which may now contain uncontracted photon terms,

$$|\Psi^\alpha\rangle = \Omega|\Psi_0^\alpha\rangle. \quad (8.30)$$

$|\Psi_0^\alpha\rangle = P|\Psi^\alpha\rangle$  is the corresponding model state, which lies entirely within the restricted space with no uncontracted photons.

The expression for single transverse-photon exchange is given by (6.34)

$$\begin{aligned} & \langle rs | V_{\text{sp}} | tu \rangle \\ &= \langle rs | \int_0^\infty c \, d\kappa f(\kappa) \left[ \frac{1}{\mathcal{E} - \varepsilon_r - \varepsilon_u - (c\kappa - i\gamma)_r} + \frac{1}{\mathcal{E} - \varepsilon_s - \varepsilon_t - (c\kappa - i\gamma)_s} \right] | tu \rangle. \end{aligned} \quad (8.31)$$

In the Coulomb gauge these expressions involve the functions  $f_T^C$ , given by (4.60)

$$f_T^C(\kappa) = \frac{e^2}{4\pi^2\epsilon_0} \left[ \boldsymbol{\alpha}_1 \cdot \boldsymbol{\alpha}_2 \frac{\sin(\kappa r_{12})}{r_{12}} - (\boldsymbol{\alpha}_1 \cdot \nabla_1) (\boldsymbol{\alpha}_2 \cdot \nabla_2) \frac{\sin(\kappa r_{12})}{\kappa^2 r_{12}} \right]. \quad (8.32)$$

By means of the expansion theorem

$$\frac{\sin \kappa r_{12}}{\kappa r_{12}} = \sum_{l=0}^{\infty} (2l+1) j_l(\kappa r_1) j_l(\kappa r_2) \mathbf{C}^l(1) \cdot \mathbf{C}^l(2), \quad (8.33)$$

where  $j_l(\kappa r)$  are radial Bessel functions and  $\mathbf{C}^l$  vector spherical harmonics [124], we can express the function  $f_T^C$  as a sum of products of single-electron operators [132, App. A]

$$f_T^C(\kappa) = \sum_{l=0}^{\infty} [V_G^l(\kappa r_1) \cdot V_G^l(\kappa r_2) + V_{sr}^l(\kappa r_1) \cdot V_{sr}^l(\kappa r_2)], \quad (8.34)$$

where

$$V_G^l(\kappa r) = \frac{e}{2\pi\sqrt{\epsilon_0}} \sqrt{\kappa(2l+1)} j_l(\kappa r) \boldsymbol{\alpha} \mathbf{C}^l, \quad (8.35a)$$

$$V_{sr}^l(\kappa r) = \frac{e}{2\pi\sqrt{\epsilon_0}} \sqrt{\frac{\kappa}{2l+1}} \left[ \sqrt{(l+1)(2l+3)} j_{l+1}(\kappa r) \{\boldsymbol{\alpha} \mathbf{C}^{l+1}\}^l + \sqrt{l(2l-1)} j_{l-1}(\kappa r) \{\boldsymbol{\alpha} \mathbf{C}^{l-1}\}^l \right]. \quad (8.35b)$$

In (8.32) the first term represents the *Gaunt interaction* and the second term the *scalar retardation*, which together form the Breit interaction (see Appendix F.2). The terms in the expansion—which are all time independent in the Schrödinger picture—will together with the Coulomb interaction ( $V_C = e^2/4\pi r_{12}$ ) form the **time-independent** perturbation

$$V_F = V_C + V_G^l(\kappa r) + V_{sr}^l(\kappa r). \quad (8.36)$$

### 8.1.2.1 Transverse-Photon Potential

We consider now the general transverse-photon exchange treated above (8.11), combined with Coulomb interactions. We consider first the case where no virtual pairs are present.

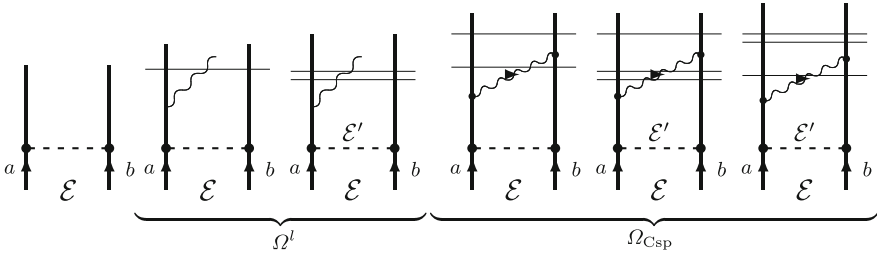


**Fig. 8.5** Expansion of the equation (8.38) in the photonic Fock space, no virtual pairs, leading to single-photon exchange, including folded diagrams. The *second* and *third diagrams* represent  $\Omega^l$  in (8.38) and the *last three diagrams* the full single-photon exchange with one Coulomb interaction,  $\Omega_{\text{Csp}}$  in (8.39)

We consider first a single Coulomb perturbation

$$\Omega^{(1)}P_{\mathcal{E}} = \Gamma_Q(\mathcal{E})V_C P_{\mathcal{E}}, \tag{8.37}$$

where  $P_{\mathcal{E}}$  is the projection operator for a sector of the model space of energy  $\mathcal{E}$ . Then we perturb this by one of the  $V^l$  terms (8.34), representing part of the transverse interaction, using the generalized Bloch equation (6.156)<sup>1</sup> (here,  $\mathcal{G}^{(1)} = \Gamma_Q V^l$ ),

$$\begin{aligned} \Omega^l P_{\mathcal{E}} &= \Gamma_Q(\mathcal{E})V^l \Omega^{(1)}P_{\mathcal{E}} + \frac{\delta(\Gamma_Q V^l)}{\delta \mathcal{E}} W^{(1)} \\ &= \Gamma_Q(\mathcal{E})V^l \Omega^{(1)}P_{\mathcal{E}} - \Gamma_Q(\mathcal{E})\Gamma_Q(\mathcal{E}')V^l W^{(1)} \end{aligned} \tag{8.38}$$

with  $W^{(1)} = P_{\mathcal{E}'}V_C P_{\mathcal{E}}$ . Here,

$$\Gamma_Q(\mathcal{E}) = \frac{Q}{\mathcal{E} - \varepsilon_r - \varepsilon_u - c\kappa}$$

is the reduced resolvent (2.65), which contains the term  $-c\kappa$  due to the crossing photon (8.29).

The first term in (8.38) with a single denominator (resolvent) yields part of the potential (6.23), and the second term with the energy derivative or a **double** denominator represents the folded or model-space contribution. These terms correspond to the second and third diagrams in the Fig. 8.5. We have here indicated by a single line the single denominator and by the double line the double denominator.

We complete the single-photon exchange (+Coulomb) between the electrons by adding a second perturbation  $V^l$  to (8.38) (with somewhat simplified notations),

$$\Omega_{\text{Csp}} = \Gamma_Q V^l \Omega^l - \Gamma_Q \Omega_{\text{sp}} W^{(1)}$$

<sup>1</sup>Even if the perturbations used here are energy independent, we shall find it convenient to use the more general formalism.

$$\Omega_{\text{Csp}} = \Gamma_Q \underbrace{V^l \Gamma_Q V^l}_{\text{folded}} \Omega^{(1)} - \Gamma_Q \underbrace{V^l \Gamma_Q \Gamma_Q V^l}_{\text{folded}} W^{(1)} - \Gamma_Q \underbrace{\Gamma_Q V^l \Gamma_Q V^l}_{\text{folded}} W^{(1)}, \quad (8.39)$$

omitting multiple folds. These terms are illustrated by the last three diagrams of Fig. 8.5.

There is no derivative term here as in (8.38), since the intermediate state between the  $V^l$  perturbations lies in the  $Q$  space (photonic Fock space). On the other hand, there is a standard folded term  $-\Gamma_Q \Omega_{\text{sp}} W^{(1)}$ , last term in (8.39).

Summing over  $\kappa$  and  $l$ , considering photon emission from both electrons and including the Gaunt as well as the scalar-retardation parts (8.34), then  $V^l \Gamma_Q V^l$  corresponds to the single-photon exchange potential  $V_{\text{sp}}$  (8.31) and  $-V^l \Gamma_Q \Gamma_Q V^l$  to the energy derivative of that potential. The last term in (8.39) represents the standard folded term  $-\Gamma_Q \Omega W$ . This can also be expressed

$$\begin{aligned} \Omega_{\text{Csp}} &= \Gamma_Q V_{\text{sp}} \Omega^{(1)} + \Gamma_Q \frac{\delta V_{\text{sp}}}{\delta \mathcal{E}} W^{(1)} - \Gamma_Q \Gamma_Q V_{\text{sp}} W^{(1)} \\ &= \Gamma_Q V_{\text{sp}} \Omega^{(1)} + \frac{\delta(\Gamma_Q V_{\text{sp}})}{\delta \mathcal{E}} W^{(1)}, \end{aligned} \quad (8.40)$$

which is consistent with the Bloch equation (6.156).

We see that

- *the energy dependence of the single-photon-exchange potential is generated by a single energy denominator and the energy derivative (difference ratio) by a double denominator (folded contribution).*

### 8.1.2.2 Crossing Coulomb Interactions. No Virtual Pairs

After the first interaction  $V^l$  (8.38) it is possible to add one or more Coulomb interactions, **before** closing the photon interaction, yielding

$$\Omega_C^l = \Gamma_Q V_C \Omega^l, \quad (8.41)$$

corresponding to the first two diagrams in Fig. 8.6. Again, there is no MSC here, since the intermediate state lies in the Fock space. Closing the photon by a second  $V^l$  interaction, gives rise to the retarded photon exchange with a crossing Coulomb interaction

$$\Omega_{\text{spC}} = \Gamma_Q V^l \Omega_C^l = \Gamma_Q V^l \Gamma_Q V_C \Omega^l. \quad (8.42)$$

This corresponds to the last two diagrams in the figure.

Inserting the expression for  $\Omega^l$  (8.38), the expression above becomes

$$\Omega_{\text{spC}} = \Gamma_Q V^l \Gamma_Q V_C \left[ \Gamma_Q V^l \Omega^{(1)} - \Gamma_Q \Gamma_Q V^l W^{(1)} \right]. \quad (8.43)$$

In a similar way several Coulomb interactions could be inserted.

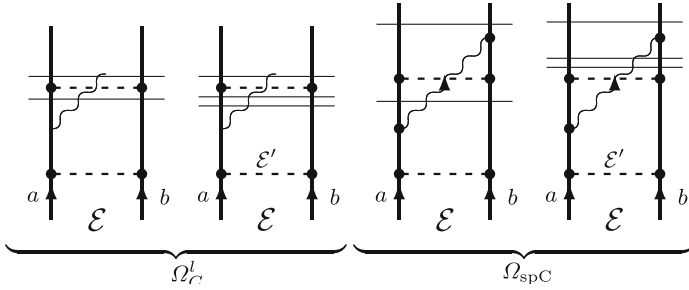
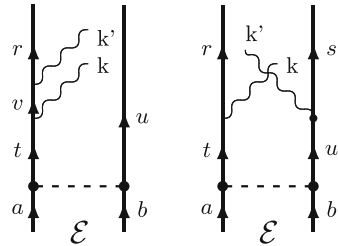


**Fig. 8.6** Perturbing with one or several Coulomb interactions before closing the retarded interaction gives rise to a retarded photon interaction with Coulomb crossings. The *first two diagrams* represent  $\Omega_C^l$  in (8.41) and the last two  $\Omega_{spC}$  in (8.42)

**Fig. 8.7** By emitting several photons before closing the first one can give rise to irreducible multi-photon exchange



A second perturbation  $V^l$  can also be applied without contracting the first one, leading to diagrams indicated by the second and third diagrams in Fig. 8.7, but this is beyond the approximation of single-transverse-photon we are concerned with here.

**8.1.2.3 Crossing Coulomb Interactions. Virtual Pairs**

*Illustration.* The iterative procedure of the previous subsection works well in the no-pair situation, when the repeated single-photon exchange leads to *reducible* diagrams of ladder type, which means that they can be separated into legitimate diagrams.

In the presence of virtual pairs we have to use a different procedure. We consider now a first-order Coulomb wave function with a single hole out (Fig. 8.8a), perturbed by the general potential  $V_T$  (8.11), including virtual pairs,

$$\Omega_{sp} = \Gamma_Q V_T \Omega^{(1)} + \frac{\delta(\Gamma_Q V_T)}{\delta \mathcal{E}} \Omega^{(1)} W. \tag{8.44}$$

To generate the first term we perturb  $\Omega^{(1)}$  by the first part  $V^l$  of the transverse photon (8.34), represented by diagram (b). Closing with a second  $V^l$  perturbation,

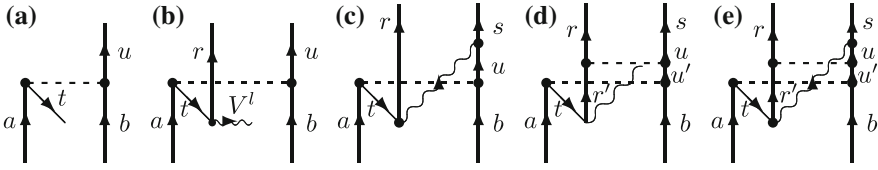


**Fig. 8.8** Generating a photon interaction with crossing Coulomb in the presence of a virtual pair

the relevant part of  $V_T$  with a hole out is given by (8.13), yielding for the first term, represented by diagram (c),

$$\Omega_{\text{sp}} = \frac{1}{\mathcal{E} - \varepsilon_r - \varepsilon_s} \left[ -\frac{\langle s_+ | V^l | u_+ \rangle \langle r_+ | V^l | t_- \rangle}{\varepsilon_t - \varepsilon_r - c\kappa} + \frac{\langle s_+ | V^l | u_+ \rangle \langle r_+ | V^l | t_- \rangle}{\mathcal{E} - \varepsilon_r - \varepsilon_u - c\kappa} \right] \langle t_- u_+ | V_C | ab \rangle. \quad (8.45)$$

This can be compared with the corresponding no-pair expression (8.43). In the expression above the resolvents are replaced by the denominators from the potential (8.11).

Before closing the photon, we can apply a Coulomb interaction, as in the previous case. This is illustrated in the last two diagram in the figure and corresponds to

$$\Omega_{\text{sp}} = -\frac{1}{\mathcal{E} - \varepsilon_r - \varepsilon_s} \frac{\langle s_+ | V^l | u_+ \rangle \langle r_+ u_+ | V_C | r'_+ u'_+ \rangle \langle r'_+ | V^l | t_- \rangle}{(\mathcal{E} - \varepsilon_r - \varepsilon_u - c\kappa)(\mathcal{E} - \varepsilon'_r - \varepsilon'_u - c\kappa)(\varepsilon_t - \varepsilon_r - c\kappa)} \times \langle t_- u'_+ | V_C | ab \rangle. \quad (8.46)$$

It can be remarked that there seems to be a crossing Coulomb interaction also in figure (c), before applying the last Coulomb. But this Coulomb is applied **before** the transverse-photon transmission has started and therefore not really a “crossing”. In fact, these interactions are separable in time and therefore **reducible** in the sense we use the word here. The second Coulomb, on the other hand, is applied while the photon is “in the air”, and therefore is a crossing in a strict sense.

**Full treatment.** We shall now generalize the treatment above and consider all 16 combinations of the single-photon exchange (8.11) (see Fig. 8.3), essentially in a single shot.

Inserting the full potential (8.11), we have

$$\Omega_{\text{sp}} = \frac{\langle r | V^l | t \rangle \langle s | V^l | u \rangle \langle tu | V_C | ab \rangle}{\mathcal{E} - \varepsilon_r - \varepsilon_s} \times \left[ \pm \frac{t_{\pm} r_{\mp}}{\varepsilon_t - \varepsilon_r \pm c\kappa} \pm \frac{t_{\pm} s_{\pm}}{\mathcal{E} - \varepsilon_t - \varepsilon_s \mp c\kappa} \pm \frac{u_{\pm} r_{\pm}}{\mathcal{E} - \varepsilon_r - \varepsilon_u \mp c\kappa} \pm \frac{u_{\pm} s_{\mp}}{\varepsilon_u - \varepsilon_s \pm c\kappa} \right]. \quad (8.47)$$

This can be evaluated in the following way. We first construct a matrix representing the matrix element  $\langle r | V^l | t \rangle$ , separated into four blocks, depending on particle/hole



**Fig. 8.9** The matrix elements  $\langle r|V_1|t\rangle$ , separated according particle/hole in/out

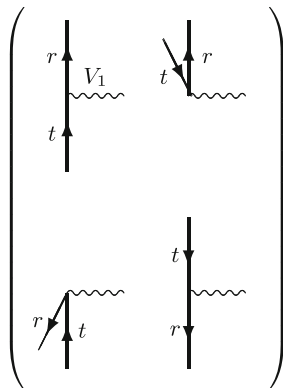


**Fig. 8.10** Coulomb matrix element separated into four blocks, according particle/hole in/out

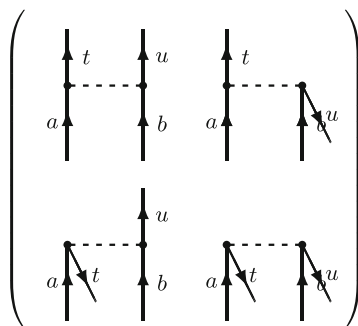
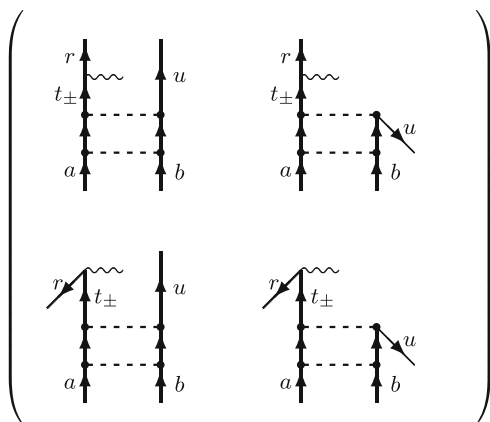


**Fig. 8.11** Result of multiplying the matrices in Figs. 8.10 and 8.9. The  $t$  line represents particle as well as hole states



in/out, as shown in Fig. 8.9. This will be multiplied by a similar matrix representing the Coulomb matrix  $\langle tu|V_C|ab\rangle$  in Fig. 8.10 with the result shown in Fig. 8.11.

Multiplying the resulting matrix by a matrix representing  $\langle s|V^I|u\rangle$  yields the final matrix in Fig. 8.12. We have here also indicated the denominators in (8.47). “A–B” in the upper left corner indicates that the denominator is +A and –B when  $t$  is a

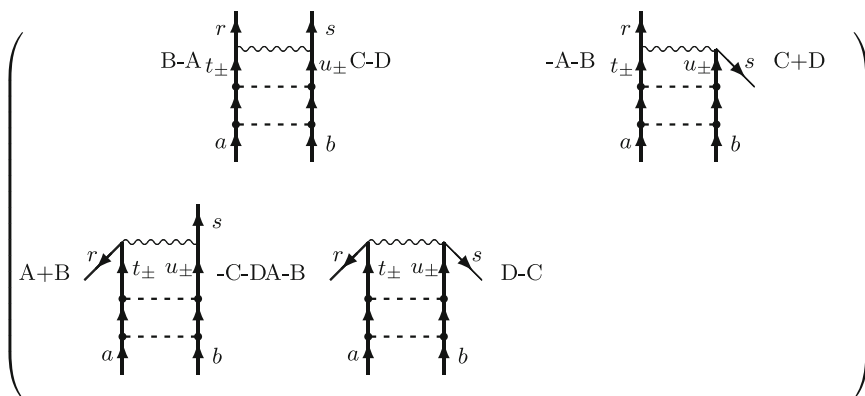


**Fig. 8.12** Result of multiplying the matrices in Figs. 8.10 and 8.9. The  $t$  line represents particle as well as hole states

particle and a hole, respectively. “ $-A -B$ ” in the upper right corner indicates that the denominators are  $-A$  as well as  $-B$ , when  $t$  is a hole and no denominator when a particle. ( $A, B, C, D$  represent the four denominators in the general potential.)

The terms can also be determined from the following table:

- r particle:** t hole  $-A$ ; u particle  $+C$
- r hole:** t particle  $+A$ ; u hole  $-C$
- s particle:** t particle  $+B$ ; u hole  $-D$
- s hole:** t hole  $-B$ ; u particle  $+D$

It is possible also in the general case to insert crossing Coulomb interactions, as indicated in the illustration (8.46). This is the case when the orbitals  $u$  and  $r$  or  $t$  and  $s$  are of the same kind (particle or hole). It is relatively straightforward when either of these pairs are particle states, and this case is also likely to be the more important. When  $u$  and  $r$  are both particle states, there will be an additional Coulomb matrix element and a denominator of C-type, as in the illustration above (8.46). The situation is similar when  $t$  and  $s$  are both particle states.

The derivative of the potential can be obtained as before, remembering that only the resolvents are energy dependent.

### 8.1.3 Continued Iteration. Combination of Non-radiative QED with Electron Correlation

In many applications we want to have an expression for the wave operator in the form of a Bloch equation, where we start from a wave operator,  $\Omega_1$ , of energy-independent interactions, such as the Coulomb pair function with  $t = 0$  (see Fig. 2.6),

$$\Omega_1 = 1 + \Gamma_Q V_C + \Gamma_Q V_C \Gamma_Q V_C + \dots + \text{folded}, \tag{8.48}$$

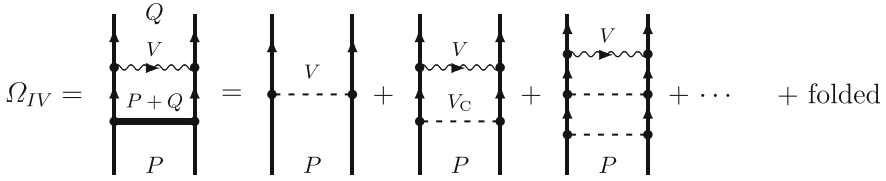


**Fig. 8.13** A single energy-dependent interaction is added to a pair function of energy-independent interactions in Fig. 2.6. The final state is here in the  $Q$  space and the state immediately before the last interaction can be in the  $P$  or  $Q$  space

and then add a single energy-dependent interaction,  $V$ . The continued inclusion of Coulomb interactions can then be made iteratively, as long as no negative-energy states are involved.

We assume that the final state of the pair function lies in the complementary  $Q$  space as illustrated in Fig. 8.13.

The Bloch equation (6.153) is then of the form

$$\mathcal{G} = \Gamma_Q V \Omega_1 + \frac{\delta^* \mathcal{G}}{\delta \mathcal{E}} W_1, \quad (8.49)$$

where  $W_1$  is the effective interaction, due to the pair function,

$$W_1 = P V_C \Omega_1 P. \quad (8.50)$$

The order-by-order expansion yields

$$\mathcal{G}^{(1)} = \Omega_1^{(1)} + \frac{\delta \mathcal{G}^{(0)}}{\delta \mathcal{E}} W_1^{(1)} = \Gamma_Q V_C + \frac{\delta \mathcal{G}^{(0)}}{\delta \mathcal{E}} W_1^{(1)}; \quad (8.51)$$

$$\begin{aligned} \mathcal{G}^{(2)} &= \Gamma_Q V \Omega_1^{(1)} + \frac{\delta \mathcal{G}^{(0)}}{\delta \mathcal{E}} W_1^{(2)} + \frac{\delta^* \mathcal{G}^{(1)}}{\delta \mathcal{E}} W_1^{(1)} \\ &= \Gamma_Q V \Gamma_Q V_C + \frac{\delta \mathcal{G}^{(0)}}{\delta \mathcal{E}} W_1^{(2)} + \frac{\delta \Gamma_Q V}{\delta \mathcal{E}} W_1^{(1)} + \frac{\delta^2 \mathcal{G}^{(0)}}{\delta \mathcal{E}^2} (W_1^{(1)})^2; \end{aligned} \quad (8.52)$$

$$\begin{aligned} \mathcal{G}^{(3)} &= \Gamma_Q V \Omega_1^{(2)} + \frac{\delta \mathcal{G}^{(0)}}{\delta \mathcal{E}} W_1^{(3)} + \frac{\delta^* \mathcal{G}^{(1)}}{\delta \mathcal{E}} W_1^{(2)} + \frac{\delta^* \mathcal{G}^{(2)}}{\delta \mathcal{E}} W_1^{(1)} \\ &= \Gamma_Q V \Omega_1^{(2)} + \frac{\delta \mathcal{G}^{(0)}}{\delta \mathcal{E}} W_1^{(3)} + \frac{\delta \Gamma_Q V}{\delta \mathcal{E}} W_1^{(2)} + 2 \frac{\delta^2 \mathcal{G}^{(0)}}{\delta \mathcal{E}^2} W_1^{(1)} W_1^{(2)} \\ &\quad + \frac{\delta \Gamma_Q V}{\delta \mathcal{E}} \Gamma_Q V_C W_1^{(1)} + \frac{\delta^2 \Gamma_Q V}{\delta \mathcal{E}^2} (W_1^{(1)})^2 + \frac{\delta^3 \mathcal{G}^{(0)}}{\delta \mathcal{E}^3} (W_1^{(1)})^3. \end{aligned} \quad (8.53)$$

$\Omega_1$  and  $W_1$  contain only energy-independent interactions with all possible folds. The energy derivatives of  $\mathcal{G}^{(0)}$  (6.107) vanish for  $t = 0$ , which implies that these terms do not contribute to the wave operator (6.70),  $\Omega = \mathcal{G}(t = 0)$ . (The first time derivative, on the other hand, does contribute to the effective interaction (6.79).)

The third-order wave operator becomes

$$\Omega^{(3)} = \Gamma_Q V \Omega_1^{(2)} + \frac{\delta \Gamma_Q V}{\delta \mathcal{E}} W_1^{(2)} + \frac{\delta \Gamma_Q V}{\delta \mathcal{E}} \Gamma_Q V_C W_1^{(1)} + \frac{\delta^2 \Gamma_Q V}{\delta \mathcal{E}^2} (W_1^{(1)})^2, \quad (8.54)$$

which agrees with the previous result (6.127) (Fig. 6.15). This can be generalized to

$$\Omega = 1 + \Gamma_Q V \Omega_1 + \sum_{m=1} \frac{\delta^m (\Gamma_Q V)}{\delta \mathcal{E}^m} \Omega_1 W_1^m. \quad (8.55)$$

This is a generalization of the first-order result (8.44). Note that the wave operator  $\Omega_1$  contains the unity (8.48), which implies that there can be a model-space contribution (folded term) directly after the Coulomb interactions, as indicated in Fig. 8.13.

We can understand the appearance of the sequence of difference ratios above in the following way. Each model-space contribution (MSC) should contain a differentiation of all the following interactions. In  $\Omega_1$  the last interaction is not involved, and therefore a differentiation of  $\Gamma_Q V$  for each model-space state in  $\Omega_1$  is required.

Next, we consider the corresponding case for the *effective interaction*, i.e., when the final state lies in the model space, as illustrated in Fig. 8.14 (left).

From the relations (6.134) and (6.137) we have

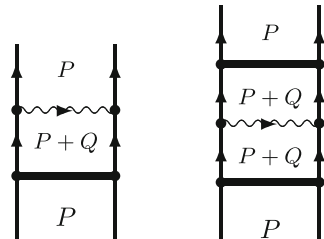
$$W^{(2)} = W_0^{(2)} + \frac{\delta W^{(1)}}{\delta \mathcal{E}} W^{(1)}; \quad (8.56)$$

$$W^{(3)} = W_0^{(3)} + \frac{\delta W_0^{(2)}}{\delta \mathcal{E}} W^{(1)} + \frac{\delta W^{(1)}}{\delta \mathcal{E}} W^{(2)} + \frac{\delta^2 W^{(1)}}{\delta \mathcal{E}^2} (W^{(1)})^2 \quad (8.57)$$

(see Fig. 6.16). Here,

$$W_0^{(2)} = PV \Gamma_Q V_C P = PV \Omega_1^{(1)} P,$$

**Fig. 8.14** The effective interaction, (8.61), corresponding to the Green’s operator in Fig. 8.13 (left) and after continued Coulomb iterations *right*



and

$$W_0^{(3)} = PV\Gamma_Q V_C \Gamma_Q V_C P = PV\Omega_{I_0}^{(2)} P, \quad (8.58)$$

where  $\Omega_{I_0}^{(2)}$  is the second-order pair function without model-space state. The second term in (8.57) is

$$\frac{\delta W_0^{(2)}}{\delta \mathcal{E}} W^{(1)} = P \frac{\delta V}{\delta \mathcal{E}} \Omega_1^{(1)} W^{(1)} + PV \frac{\delta \Gamma_Q V_C}{\delta \mathcal{E}} W^{(1)}. \quad (8.59)$$

The last term can be expressed  $PV\Omega_{I_1}^{(2)}P$ , i.e., the second-order pair function with one fold, which together with (8.58) forms the expression  $PV\Omega_1^{(2)}P$ , where  $\Omega_1^{(2)}$  is the entire second-order wave operator (with and without folds). The third-order effective interaction can then be expressed

$$W^{(3)} = PV\Omega^{(2)}P + P \frac{\delta V}{\delta \mathcal{E}} \Omega_1^{(1)} W^{(1)} + P \frac{\delta V}{\delta \mathcal{E}} W^{(2)} + P \frac{\delta^2 V}{\delta \mathcal{E}^2} (W^{(1)})^2, \quad (8.60)$$

which in analogy with (8.55) can be generalized to

$$W = PV\Omega_1 P + P \sum \frac{\delta^m V}{\delta \mathcal{E}^m} \Omega_1 W^m. \quad (8.61)$$

This is illustrated in Fig. 8.14 (left). Also here we observe that there can be a model-space contribution (fold) directly after the pair function.

Finally, we can add additional energy-independent interactions perturbatively, as long as no virtual pairs are involved, as illustrated to the right in Fig. 8.14. We can use the standard Bloch equation in this iteration procedure (Sect. 2.3.1).

The energy-dependent potential is here assumed to be the retarded electrostatic interaction between the electrons, which can include *crossing energy-independent interactions* as well as *virtual pairs*, as shown above and demonstrated numerically in [86] (see Chap. 9). As shown above (8.8), it is also possible to include the **combination** of crossing energy-independent interactions and virtual pairs, although this has not yet been implemented.

In the next section we shall discuss the similar treatment of radiative effects, electron self-energy and vertex correction.

## 8.2 Radiative QED Effects, Combined with Electron Correlation

We shall now analyze how the **radiative** QED corrections—electron self-energy, vertex correction and vacuum polarization—can be treated within the Green’s-operator formalism and combined with the electron correlation—in analogy with the non-

radiative interactions, treated in the previous section. We consider a two-electron system and start with the second-order cases with a single Coulomb interaction, i.e., first-order screened self-energy and lowest-order vertex correction. These are both singular, but we shall see that the singularities cancel. Details of the renormalization process are described in Chap. 12.

### 8.2.1 Two-Electron Screened Self-Energy and Vertex Correction in Lowest Order

We consider first the first-order Coulomb screened self-energy and vertex correction for He-like systems, illustrated in Fig. 8.15. We start with assuming the final state lies in the model space, i.e., considering the effective interaction.

The bound-state self-energy can be expanded into a *zero-potential, one-potential and many-potential parts* (see Fig. 8.16)

$$\Sigma^{\text{bou}} = \Sigma_{\text{zp}}^{\text{free}} + \Sigma_{\text{op}}^{\text{free}} + \Sigma_{\text{mp}}^{\text{free}}. \tag{8.62}$$

The potential used is that of the generating Dirac equation for the bound orbitals, normally the nuclear potential,  $V_{\text{nuc}}$ . The free-electron (zero-potential) self-energy

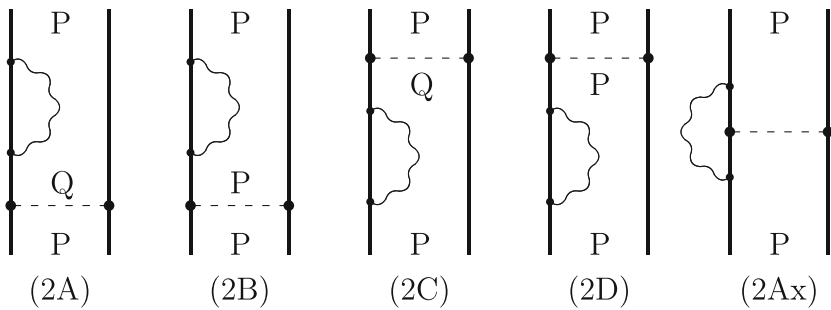


**Fig. 8.15** Second-order Coulomb screened self-energy and vertex correction for He-like systems. Diagrams (2B) and (2Ax) are divergent

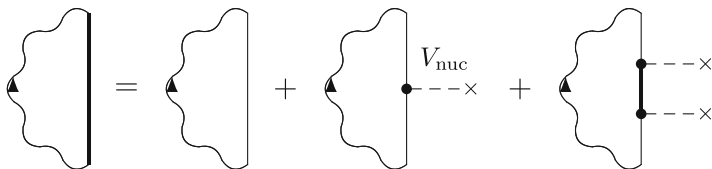


**Fig. 8.16** Expanding the bound-state self-energy into zero-, one-, and many-potential terms. The *heavy vertical lines* represent the bound-state orbitals, generated in an extern (nuclear) potential, and the *thin lines* represent free-electron states

can be expressed (12.37)

$$\Sigma^{\text{free}}(\omega, \mathbf{p}) = \Sigma_{\text{zp}}^{\text{free}} = \beta A + B(\alpha^\mu p_\mu c - \beta mc^2) + \beta C(\alpha^\mu p_\mu c - \beta mc^2)^2, \quad (8.63)$$

where  $A = \delta mc^2$  is the mass counterterm, employed in the mass renormalization, the second term represents the charge divergence and the third term is the finite renormalized free-electron self-energy,  $\Sigma_{\text{ren}}^{\text{free}}$ .<sup>2</sup> The divergence lies entirely in the zero-potential or free-electron part.

The scalar vertex-correction parameter is expressed (4.100)

$$\Lambda^0 = L + \Lambda_{\text{ren}}^0, \quad (8.64)$$

where  $\Lambda^0$  is the unrenormalized vertex-correction parameter (4.98 and 12.42),  $\Lambda_{\text{ren}}^0$  the renormalized one, and  $L$  is the divergence constant. Also here, the divergence lies entirely in the free-electron part, and hence

$$\Lambda^{0,\text{free}} = L + \Lambda_{\text{ren}}^{0,\text{free}}. \quad (8.65)$$

The one-potential part of the bound-state self-energy becomes

$$\Sigma_{\text{op}}^{\text{free}}(\omega, \mathbf{p}) = \Lambda^{0,\text{free}} V_{\text{nuc}} = (L + \Lambda_{\text{ren}}^{0,\text{free}}) V_{\text{nuc}}. \quad (8.66)$$

The mass-renormalized bound-state self-energy then becomes, after including also the many-potential part in (8.62),

$$\Sigma_{\text{massren}}^{\text{bou}} = \Sigma = B(\alpha^\mu p_\mu c - \beta mc^2) + \Sigma_{\text{ren}}^{\text{free}} + (L + \Lambda_{\text{ren}}^{0,\text{free}}) V_{\text{nuc}} + \Sigma_{\text{mp}}^{\text{free}}. \quad (8.67)$$

In this chapter we shall in the following always understand that the bound-state self-energy is mass-renormalized, and we denote that simply by  $\Sigma$ .

It follows from the Ward identity (4.102) that

$$\boxed{B = -L}. \quad (8.68)$$

Our bound-state orbitals satisfy the Dirac equation (D.43)

$$H_{\text{D}}|a\rangle = \left[ -c\alpha^\mu(\hat{p}_\mu + eA_\mu) + \beta m_e c^2 \right] |a\rangle = 0. \quad (8.69)$$

Therefore, when operating on such an orbital, we can replace the bracket in the first term in (8.67) by  $-ec\alpha^\mu A_\mu$ , which for the scalar potential,  $V_{\text{nuc}}$ , becomes (D.42)

<sup>2</sup>This differs from the conventional expression found in most textbooks by a factor of  $\beta$ , due to the fact that we base our formalism on  $\Psi^\dagger$  rather than on  $\bar{\Psi} = \Psi^\dagger \beta$ . Multiplying the expression (8.63) by  $\beta$ , yields

$$\Sigma^{\bar{\text{free}}} = \beta \Sigma^{\text{free}} = A + B(\not{p} - mc^2) + C(\not{p} - mc^2)^2,$$

which is the expression commonly used.

$$-e c A_0 = -e \phi(x) = V_{\text{nuc}}.$$

With  $B = -L$  it then follows that the (charge) divergent parts of (8.67) vanish, and (8.67) becomes

$$\Sigma_{\text{ren}}^{\text{bou}} = \Sigma_{\text{ren}} = \Sigma_{\text{ren}}^{\text{free}} + \Lambda_{\text{ren}}^{0,\text{free}} V_{\text{nuc}} + \Sigma_{\text{mp}}^{\text{free}}. \quad (8.70)$$

For the energy derivative of the mass-renormalized bound-state self-energy (8.67) we have

$$\frac{\delta \Sigma}{\delta \mathcal{E}} = B + \frac{\delta \Sigma_{\text{ren}}^{\text{free}}}{\delta \mathcal{E}} + \frac{\delta \Lambda_{\text{ren}}^{0,\text{free}}}{\delta \mathcal{E}} V_{\text{nuc}} + \frac{\delta \Sigma_{\text{mp}}^{\text{free}}}{\delta \mathcal{E}} = B + \frac{\delta \Sigma_{\text{ren}}}{\delta \mathcal{E}}, \quad (8.71)$$

using  $\mathcal{E} = p_0 c$  and  $\alpha_0 = 1$ .

The power expansion of the effective interaction can be generated from the general equation (6.126)

$$W = W_0 + \frac{\delta W}{\delta \mathcal{E}} W_0, \quad (8.72)$$

where  $W_0$  represents the operator without intermediate model-space states. In second-order this becomes

$$W^{(2)} = W_0^{(2)} + W_1^{(2)} = W_0^{(2)} + \frac{\delta W^{(1)}}{\delta \mathcal{E}} W^{(1)}. \quad (8.73)$$

For the first-order Coulomb screened self-energy with an intermediate  $Q$  state, diagram (2A) in Fig. 8.15, there is no model-space contribution. This part is represented by the first term in (8.73), which becomes

$$W_0^{(2)} \Rightarrow \langle P | \Sigma \Gamma_Q V_C | P \rangle = \langle P | \Sigma_{\text{ren}} \Gamma_Q V_C | P \rangle, \quad (8.74)$$

where  $\Sigma_{\text{ren}}$  is the renormalized bound-state self-energy (8.71) and  $V_C$  is the Coulomb interaction. This diagram is obviously regular.

With an intermediate model-space state, diagram (2B), we have a model-space contribution (MSC), corresponding to the second term in (8.73),

$$\frac{\delta W^{(1)}}{\delta \mathcal{E}} W^{(1)} \Rightarrow \langle P | \frac{\delta \Sigma}{\delta \mathcal{E}} | P \rangle W^{(1)}, \quad (8.75)$$

where  $W^{(1)}$  at the bottom is  $\langle P | V_C | P \rangle$  and the self-energy derivative is given in (8.70). This has the singularity  $BW^{(1)}$ .

The diagram (2C) yields the same result as (2A).

The diagram (2D) corresponds to

$$\frac{\delta W^{(1)}}{\delta \mathcal{E}} W^{(1)} \Rightarrow \langle P | \frac{\delta W^{(1)}}{\delta \mathcal{E}} | P \rangle \langle P | \Sigma | P \rangle, \quad (8.76)$$



which vanishes, since the Coulomb interaction is energy independent.

The first-order vertex correction, diagram (2Ax), becomes

$$\langle P | \Lambda^0 V_C | P \rangle = \langle P | (L + \Lambda_{\text{ren}}^0) V_C | P \rangle, \tag{8.77}$$

using the relation (8.64). This has the singularity

$$\langle P | L V_C | P \rangle = L W^{(1)}.$$

It follows from the Ward identity (8.68), that **the singularity in the self-energy and vertex diagrams exactly cancel in second order**. The remaining finite parts of the self-energy (2B) and the vertex correction (2Ax) then become

$$\left\langle P \left| \frac{\delta \Sigma_{\text{ren}}}{\delta \mathcal{E}} \right| P \right\rangle W^{(1)} + \left\langle P \left| \Lambda_{\text{ren}}^0 V_C \right| P \right\rangle. \tag{8.78}$$

Due to the Ward identity we have

$$\Lambda_{\text{ren}}^0 = - \frac{\delta \Sigma_{\text{ren}}}{\delta \mathcal{E}}. \tag{8.79}$$

### 8.2.2 All Orders

We now generalize the treatment above to the case with a pair function with an arbitrary number of Coulomb interactions (8.48) as input (see Fig. 8.17)

$$\Omega_1 = 1 + \Gamma_Q V_C + \Gamma_Q V_C \Gamma_Q V_C + \dots + \text{folded}. \tag{8.80}$$

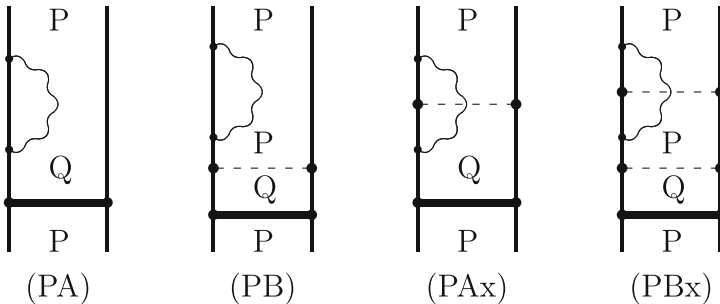


**Fig. 8.17** Self-energy and vertex correction for He-like systems screened by a pair function with an arbitrary number of Coulomb interactions. The diagrams (PB) and (PAx) are divergent

We can now apply the formula (8.61), yielding

$$W = P\Sigma\Omega_1P + P\frac{\delta\Sigma}{\delta\mathcal{E}}\Omega_1W_1 + P\frac{\delta^2\Sigma}{\delta\mathcal{E}^2}\Omega_1W_1^2 + \dots \quad (8.81)$$

Here,  $W_1$  is the effective interaction associated with the Coulomb pair function (8.50)

$$W_1 = PV_C\Omega_1P,$$

which includes the model-space contributions of the pair function. The corresponding equation for the vertex correction is obtained by replacing  $\Sigma$  by  $\Lambda^0V_C$ .

When there is a  $Q$  state directly before the self-energy, we have diagram (PA)

$$W = P\Sigma Q\Omega_1P, \quad (8.82)$$

which is regular.

When there is a  $P$  state directly before the self-energy, we have from (8.81) (diagram PB)

$$P\frac{\delta\Sigma}{\delta\mathcal{E}}W_1 + P\frac{\delta^2\Sigma}{\delta\mathcal{E}^2}W_1^2 + \dots \quad (8.83)$$

The first term has the singularity  $BW_1$ .

The vertex correction with a  $Q$  state directly before the correction, diagram (PAx), becomes

$$P\Lambda^0V_CQ\Omega_1P + P\frac{\delta(\Lambda^0V_C)}{\delta\mathcal{E}}Q\Omega_1W_1 + \dots \quad (8.84)$$

This has a singularity  $LW_1$  that cancels that of the divergent self-energy diagram. The finite remaining part of the vertex diagram is

$$W_{VxQ} = P\Lambda_{\text{ren}}^0V_CQ\Omega_1P + P\frac{\delta\Lambda_{\text{ren}}^0}{\delta\mathcal{E}}V_CQ\Omega_1W_1 + \dots \quad (8.85)$$

The vertex correction with a  $P$  state directly before the correction, diagram (PBx), becomes

$$W_{VxP} = P\frac{\delta\Lambda^0}{\delta\mathcal{E}}V_CW_1 + \dots = P\frac{\delta\Lambda_{\text{ren}}^0}{\delta\mathcal{E}}V_CW_1 + \dots, \quad (8.86)$$

which is regular.

Possible model-space states within the pair function will lead to additional singularities, which all cancel.

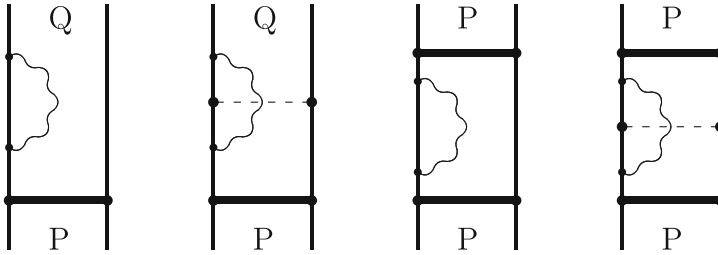


**Fig. 8.18** All-order screened self-energy and vertex correction for He-like systems

### 8.2.3 Continued Coulomb Iterations

We can also have additional Coulomb interactions after the self-energy/vertex correction in analogy with the situation discussed in Sect. 8.1.3 and illustrated in Fig. 8.18. We then start with diagrams with the final state in the  $Q$  space, representing a wave operator, as illustrated in the first two diagrams in Fig. 8.18. Then the Coulomb iterations can be continued, as in the previous case (Sect. 8.1.3), yielding the complete electron correlation, as shown in the last two diagrams of the figure.

It is expected that the singularities should cancel each other in each order of the perturbation, but we have not been able to show this explicitly beyond second order.

## 8.3 Higher-Order QED. Connection to the Bethe–Salpeter Equation. Coupled-Cluster-QED

In the two last sections we have demonstrated how the electron correlation to all orders can be combined in a systematic way with **first-order** non-radiative and radiative QED interactions, respectively.<sup>3</sup> **Reducible** multi-photon effects can be included in the wave operator or Green's operator by means of iterations, as will be discussed in the present section. For practical reasons, it is not possible, for the time being, to treat **irreducible**, multi-photon QED effects in the same manner. The procedure will eventually lead to the Bethe–Salpeter equation that has been previously discussed in Sect. 6.11 and will be treated in more detail in Chaps. 10 and 11.

<sup>3</sup>As mentioned, the terms “reducible” and “irreducible” are used differently if dealing with open wave-operator diagrams or closed effective-operator diagrams (see Sect. 2.6.1).

### 8.3.1 General QED (Single-Transverse-Photon) Potential

In principle, we can include all perturbations we have treated so far in a formal “QED potential”,

$$V^{\text{STP}} = V_C + V_T + V_{\text{TC}} + V_{\text{SE}} + V_{\text{Vx}}, \quad (8.87)$$

as illustrated in Fig. 8.19, containing

- Coulomb interaction ( $V_C$ )
- Transverse photon with virtual pairs ( $V_T$ )
- Transverse photon with virtual pairs and crossing Coulomb interactions ( $V_{\text{TC}}$ )
- Self-energy insertions ( $V_{\text{SE}}$ )
- Vertex corrections ( $V_{\text{Vx}}$ )
- Vacuum polarization.

Such a potential could then be used perturbatively in the same way as ordinary potentials, when no virtual pairs are involved, which represents the dominating part (c.f., Sect. 8.1.1). As before, we restrict ourselves here to first-order interactions, involving a **single transverse photon**. As mentioned, multi-photon interactions could not be handled in this way at present. The process with a single transverse photon, on the other hand, is feasible and expected to be quite accurate, as will be demonstrated in the following chapter.

If the potential has hole states in or out, we add additional Coulomb interactions, so that *all in- and outgoing states are particle states*, illustrated in Fig. 8.20. Then it will be possible to use the potential iteratively.

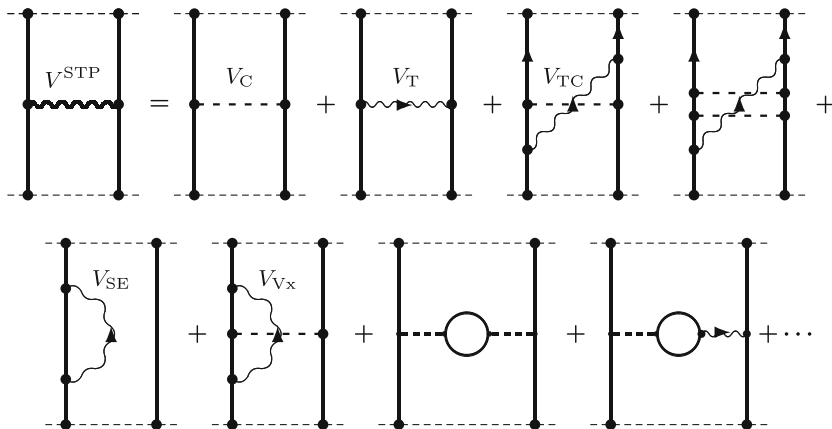


**Fig. 8.19** Feynman diagrams representing the *single-transverse-photon potential* (8.87). We assume that the electron vacuum polarization is included in the orbitals. When there are hole states in and out, we assume that additional Coulomb interaction are inserted, so that only particle states appear in and out (see Fig. 8.20)

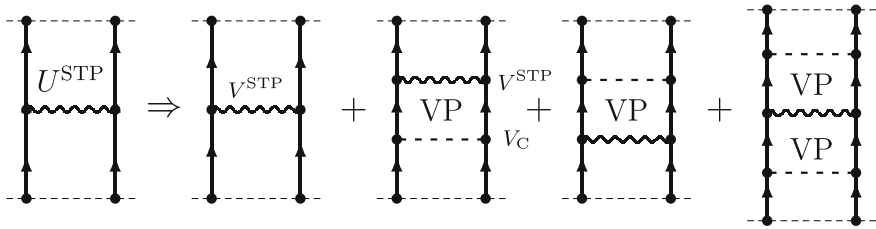


**Fig. 8.20** Illustration of the modified potential (8.87), which can be iterated. It has only positive-energy states in and out and is free from the Brown–Ravenhall effect

The general QED potential can be combined with electron correlation by applying Coulomb interactions before and after the QED potential, using the general equations (8.55 and 8.61), in the same way as the retarded potential in Sect. 8.1.3, illustrated in Fig. 8.14.

### 8.3.2 Iterating the QED Potential. Connection to the Bethe–Salpeter Equation

We shall now see how the general single-transverse-photon potential (8.87) can be combined with the standard MBPT procedure, leading to a unified relativistic MBPT-QED procedure, which ultimately corresponds to the famous Bethe–Salpeter equation.

#### Iterating the Potential

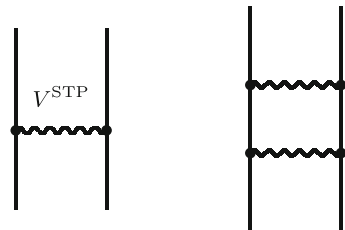
The single-photon potential (8.87) can be iterated, thereby generating *reducible multi-photon exchange* (see Sect. 2.6.1), as illustrated in Fig. 8.21.

The continued iterations can be expressed by means of the generalized Bloch equation (6.153)

$$\Omega = 1 + \Gamma_Q V^{STP} \Omega + \frac{\delta^* \Omega}{\delta \mathcal{E}} W, \tag{8.88}$$

which can be represented by the Dyson-type equation in Fig. 8.22. This is analogous to the equation in Fig. 10.4 in Chap. 10, representing the *Bethe–Salpeter–*

**Fig. 8.21** Iteration of the potential leads to a reducible diagrams



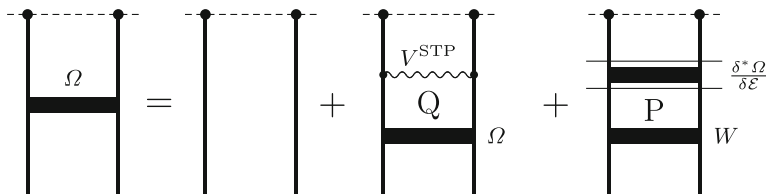


**Fig. 8.22** Dyson-type equation, representing of the Bloch equation (8.88). The last diagram represents the “folded” term, i.e., the last term of the equation

**Bloch equation** (which is a generalization of the standard Bethe–Salpeter equation to a general, multi-reference model space. (Compare also the corresponding Green’s-function diagram in Fig. 5.8.)

The procedure discussed here represents the complete treatment of the single-transverse-photon potential (8.87) and represents the dominating part of the QED effects. In order to get further, also *irreducible* combinations of transverse interactions should be included (see Fig. 6.9). This would correspond to the **full Bethe–Salpeter–Bloch equation**—so far without singles. The missing singles can in principle be generated by applying the coupled-cluster procedure, discussed in the next section.

In the next section we shall describe how the QED potential (8.87) can be used in a **coupled-cluster expansion**, in analogy with the standard procedure of MBPT, described in Sect. 2.5. Then also single-particle effects can be included in a systematic way, and the procedure would be even closer to the **complete Bethe–Salpeter–Bloch procedure**. This approach will also make it possible to apply the procedure to more than two electrons.

It should be noted that the procedure discussed in the previous section with a single QED potential with electron correlation normally leads to a good result much faster than the full BS equation, where all effects are carried to high order.

The Bethe–Salpeter equation will be further analyzed in Chap. 10 and the renormalization procedure will be discussed in Chap. 12.

### 8.3.3 Coupled-Cluster-QED Expansion

With the interactions derived above we can construct an effective *QED-Coupled-Cluster procedure* in analogy with that employed in standard MBPT, described in Sect. 2.5 (see [133]). Considering the singles-and-doubles approximation (2.105)

$$S = S_1 + S_2, \quad (8.89)$$

the MBPT/CC equations are illustrated in Fig. 2.8. In order to obtain the corresponding equations with the covariant potential in Chap. 6, we make the replacements illustrated in Fig. 8.23, which leads to the equations, illustrated in Fig. 8.24.

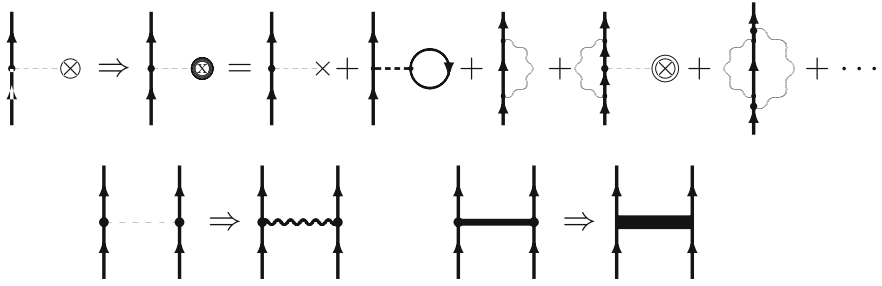


**Fig. 8.23** Replacements to be made in the CC equations in Fig. 2.8 in order to generate the corresponding CC-QED equations (c.f. Figs. 6.7 and 6.8). The wavy line in the *second row* represents the modified potential *USTP* with only particle states in and out

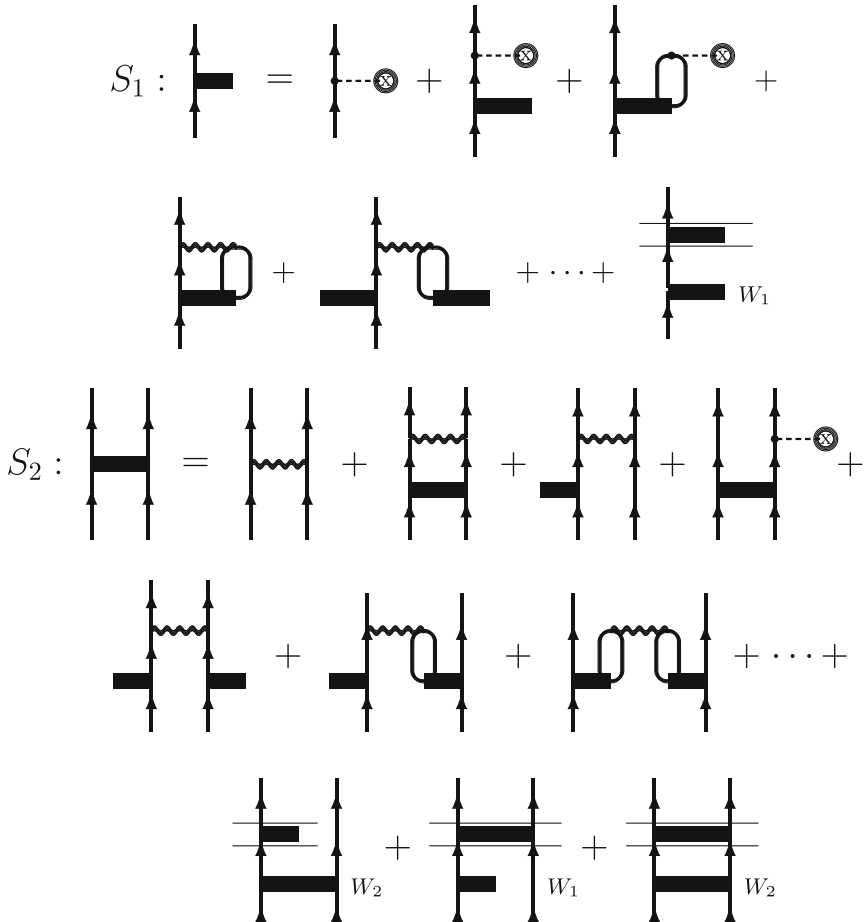


**Fig. 8.24** Diagrammatic representation of the QED-coupled-cluster equations for the operators  $S_1$  and  $S_2$ . The *second diagram* in the *second row* and the diagrams in the *fourth row* are examples of coupled-cluster diagrams. The last diagram in the *second row* and the *three diagrams* in the *last row* represent folded terms (c.f. the corresponding standard CC equations in Fig. 2.8)

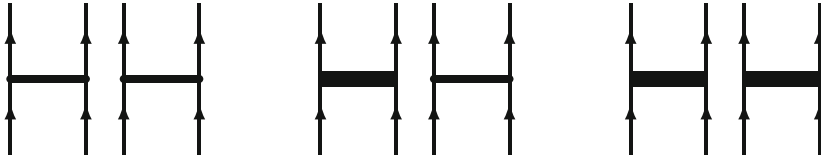


**Fig. 8.25** Diagrammatic representing of the QED-coupled-cluster term  $\frac{1}{2} S_2^2$  with standard pair functions (*left*) and one and two inserted QED pair function, defined in Fig. 8.22, (*right*)

The CC-QED procedure can also be applied to systems with more than two electrons. For instance, if we consider the simple approximation (2.101)

$$\Omega = 1 + S_2 + \frac{1}{2}\{S_2^2\},$$

then we will have in addition to the pair function also the coupled-cluster term, illustrated in Fig. 8.25 (left). Here, one or both of the pair functions can be replaced by the QED pair function in Fig. 8.22 (right) in order to insert QED effects on this level. In addition, of course, single-particle clusters can be included, as in the two-particle case discussed above (Fig. 8.23).

*We can summarize the results obtained here in the following way:*

- *When all one- and two-particle effects are included, the Green’s-operator-QED procedure is fully compatible with the two-particle Bethe–Salpeter(-Bloch) equation—including singles.*
- *The advantage of the Green’s-operator-QED procedure is—thanks to the complete compatibility with the standard MBPT procedure—that the QED potentials need to be included only in cases where the effect is expected to be sufficiently important.*

*The procedure described here is based on the use of the Coulomb gauge (6.57), and therefore not strictly covariant. As mentioned, however, in practice it is equivalent to a fully covariant procedure, and, furthermore, it seems to be the only feasible way for the time being of treating effects beyond two-photon exchange in a systematic fashion (see the following chapter, where numerical results of the procedure are presented).*



# Chapter 9

## Numerical Results of Combined MBPT-QED Calculations Beyond Second Order

In this chapter we reproduce some numerical results recently published by the Gothenburg group of the combined procedure of quantum electrodynamics and electron correlation for heliumlike ions [89]. This goes beyond the two-photon results presented in Chap. 7.

### 9.1 Non-radiative QED Effects in Combination with Electron Correlation

#### 9.1.1 Two-Photon Exchange

In Chap. 7 (Fig. 7.3) we showed the results of two-photon-exchange calculations for the ground-state of heliumlike ions, including crossing photons and virtual electron-positron pairs, using the S-matrix formulation. In Table 9.1 we compare these results with those obtained by Hedendahl et al. [86] in testing the new Green's-operator (GO) method, described in the previous chapters. In the first numerical column "NVPA" represents "No-virtual-Pair-Approximation" (see Sect. 2.6), i.e., the unretarded approximation without virtual pairs, and the following two columns the effect of retardation with no virtual pairs and the effect of virtual pairs with no crossing Coulomb interactions, respectively. The agreement, which is found to be very good, is also displayed in Fig. 9.1, where the solid lines represent the old S-matrix results and the red squares those of the new covariant method. As before, the scale is logarithmic and the norm is the non-relativistic ionization energy.

The old S-matrix calculations were made with the Feynman gauge, while in the new covariant calculations the Coulomb gauge was used. The reason for the latter choice is that these calculations will later be extended to higher orders, and then it is more effective to use the Coulomb gauge.

**Table 9.1** Comparison between two-photon non-radiative effects for He-like ions ground states, evaluated with the S-matrix (see Fig. 7.3) and the Green's-operator (GO) method, described in Chap. 6, from Hedendahl [86] (see Fig. 9.1, in  $\mu$ Hartree)

Z	Method	Coul.-Breit NVPA	Coul.-Breit. Retard.	VP Coul.Breit Uncrossed.
6	S-matrix	-1054.2	31.4	-10.1
6	GO	-1054.9	31.5	-10.0
10	S-matrix	-2870.4	122.3	-45.9
10	GO	-2871.0	122.4	-45.9
14	S-matrix	-5515	293.0	-121.5
14	GO	-5517	292.8	-121.2
18	S-matrix	-8947	553.1	-247.3
18	GO	-8950	553.3	-248.2
30	S-matrix	-23629	1909.2	-1008
30	GO	-23632	1909.9	-1010

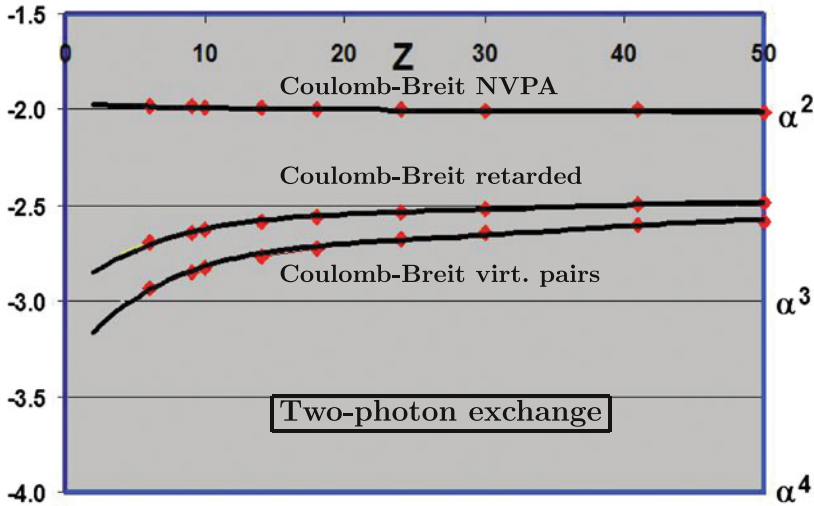


**Fig. 9.1** Comparison of some two-photon exchange contributions for the ground-state of some heliumlike ions—Coulomb-Breit NVPA, Coulomb-Breit retardation, and Coulomb-Breit virtual pairs, no correlation, obtained by S-matrix calculations (see Fig. 7.3) (*heavy lines*) and by means of the Green's-operator (GO) procedure (*squares*), described in this chapter (see Table 9.1, c.f. Fig. 7.3 in Chap. 7) (from [86])

### 9.1.2 Non-radiative Effects. Beyond Two-Photon Exchange

In this section we present results of calculations for some He-like ions of the combination of **non-radiative** QED effects (retardation and virtual pairs) and electron

correlation, *beyond two-photon effects*, as described in Sect. 8.1.3. The results of the calculations, shown in Table 9.2 and displayed in Fig. 9.2, are taken from [86]. For comparison, the effect of two-photon exchange, taken from Chap. 7, is given in the first five columns.

The top line of the Fig. 9.2, representing the Coulomb-Breit interaction with correlation *without* virtual pairs, includes the instantaneous Breit interaction (2.112) in addition to the retardation part. The former part lies within the no-virtual-pair approximation (NVPA) and is therefore NOT a QED effect with the definition given in Sect. 2.6.1. In order to obtain the pure QED effect, the instantaneous part is subtracted, represented by the second line from the top and shown in the sixth numerical column in Table 9.2. The next line represents the same effect with Coulomb crossings, and shown in the following column of the table. The correlational effect of virtual pairs (only non-crossing) is represented by the bottom line of the figure and shown in the last column of the table.

The combination of retardation and virtual pairs is evaluated by the generalized potential (8.11). The effect of crossing Coulomb interactions, with and without virtual pairs, is evaluated as described in Sect. 8.1.2. The corresponding Feynman diagrams are shown at the bottom of the figure (see also Figs. 9.3 and 9.4).

In the Fig. 9.2 we have for comparison also indicated the effect due to doubly retarded two-photon interactions (thin black line), estimated from the S-matrix results. This comparison demonstrates the important result that—starting from single-photon exchange—*for light and medium-heavy elements the effect of electron correlation in combination with a single retarded photon is much more important than a second retarded photon.*

**Table 9.2** The non-radiative QED effects (retardation and virtual pairs) for the ground state of He-like ions, calculated by Hedendahl [86] (see also Fig. 9.2)

Z	Two-photon					Correlation		
	Coul.-Coul	Coulomb-Breit		Breit-Breit		NVP retard.		Virt. pairs
	Virt.pairs	NVP ret.	Virt.p.	NVP ret	Virt.p.	Non-cross	Crossing	Non-cross
10	0.69	3.32	-2.74	0.35	-0.92	-1.1	0.5	0.2
14	1.78	7.97	-7.11	1.07	-1.82	-1.9	0.9	0.4
18	3.57	15.05	-14.2	2.48	-2.82	-2.7	1.3	0.6
24	7.86	30.5	-30.9	6.54	-4.03	-4.2	2.1	0.9
30	14.3	51.9	-55.4	13.9	-4.21	-5.7	2.9	1.3
42	34.8	112.0	-128.8	43.4	+1.51	-9.0	5.0	2.0
50	55	164				-11.5	6.5	2.4

The first five columns represent the effect of two-photon exchange and the remaining ones the effect of correlation, beyond two-photon exchange (in meV)

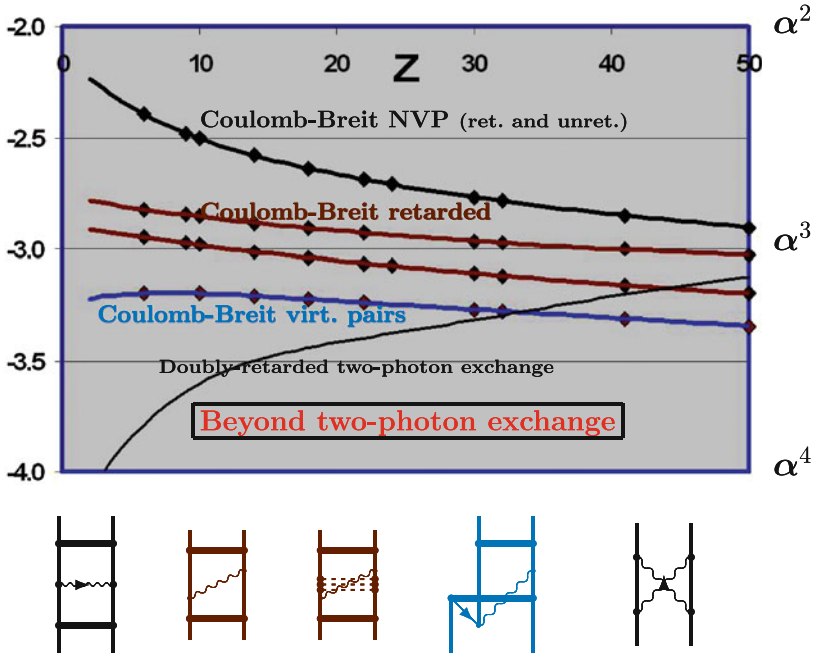


**Fig. 9.2** The effect of electron correlation beyond two-photon exchange for the ground-state of heliumlike ions—Coulomb-Breit NVPA, Coulomb-Breit retardation with and without Coulomb crossings, and Coulomb-Breit virtual pairs, all WITH electron correlation (see Table 9.2, c.f. Fig. 9.1) (from [86]). For comparison the effect of pure retarded two-photon exchange without additional correlation is also indicated

**Fig. 9.3** Retarded transverse interaction with electron correlation and with one and several Coulomb crossings

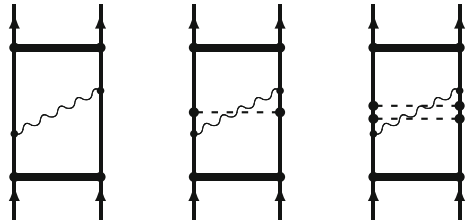
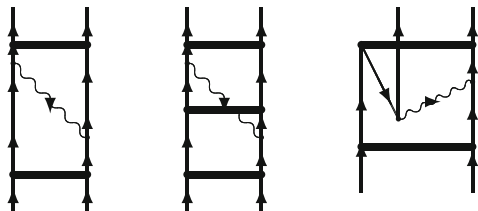


**Fig. 9.4** Diagrams representing the combination of non-radiative QED perturbation (retardation, virtual pair) and electron correlation, evaluated by Hedendahl [86]



## 9.2 Radiative QED Effects in Combination with Electron Correlation. Coulomb Gauge

Next, we consider the numerical evaluation of **radiative** QED effects (electron self-energy, vacuum polarization and vertex correction) in combination with electron correlation.

Until recently, all calculations of radiative QED effects have been performed with the Feynman gauge, or some other covariant gauge, like the Jennie gauge (see App. G). But the use of the non-covariant Coulomb gauge has definite advantages, particularly when radiative QED effects are combined with electron correlation, as we shall now demonstrate.

The use of the Coulomb gauge in evaluating radiative QED effects is more complicated than using the Feynman gauge, but a working procedure has recently been developed by Hedendahl and Holmberg of the Gothenburg group [87, 88] by means of dimensional regularization, based upon the works of Adkins [1, 2] (see Chap. 12). The procedure was first tested on the ground state of hydrogen like systems, as will be demonstrated below.

The electron propagator of the bound-state self-energy operator can be expanded into the free-electron propagator (zero-potential term) and a single-potential and a many-potential term, as illustrated in Fig. 8.16 in the previous chapter. The potential is here that of the Dirac equation, generating the bound-state orbitals. The zero-potential and single-potential parts are singular and can be regularized, using dimensional regularization, as described in Chap. 12. The many-potential term is finite and can be evaluated by subtracting the zero- and one-potential terms from the bound-state self-energy, using the partial-wave expansion.

The calculations of Hedendahl and Holmberg were performed in the Coulomb as well as the Feynman gauge, and the results are expressed by means of the function

$$\Delta E^{SE} = \frac{\alpha}{\pi} (Z\alpha)^4 mc^2 F(Z\alpha). \quad (9.1)$$

The results are shown in Table 9.3, where the gauge invariance is clearly demonstrated. It is interesting to note that the numerical accuracy is considerably higher in the Coulomb gauge. The reason for this is that the many-potential term, where the main numerical uncertainty originates from, is considerably smaller in that gauge (see [87] for further details).

### 9.2.1 Radiative Effects. Two-Photon Effects

The two-photon radiative effects (screened electron self-energy and vacuum-polarization as well as vertex correction) were evaluated for heliumlike ions in the late 1990's in the Feynman gauge by Sunnergren in his Ph.D. thesis at Gothenburg university, using the S-matrix formalism [239], and at about the same time by the

St Petersburg group [8, 253], using the two-time Green’s function. This involves the effects, illustrated in Fig. 7.4. The results of the calculations are shown in Table 9.4. The agreement between the two calculations is excellent.

The two-photon electron self-energy and vertex correction have more recently been evaluated using the Coulomb as well as the Feynman gauge by Holmberg et al. [89], and the results are shown in Table 9.5. For simplicity, these calculations contain only Coulomb screening, while the results in Table 9.4 contain also Breit screening. (The effect of Breit screening can be estimated by comparing the second-order results.) The results in Table 9.5 are separated into “irreducible part”, i.e., the self-energy without the model-space contribution (MSC), referred to as “wavefunction contribution”, and the “reducible part” (MSC) together with the vertex correction. The latter two contributions have singularities (charge divergence) that cancel each other and are therefore taken together. (Individually, they are not well-defined.) In addition, the irreducible part is separated into the zero-, one- and many-potential contributions (see Fig. 8.16), and the MSC and vertex contributions are

**Table 9.3** Values of the function  $F(Z\alpha)$  in (9.1) for the self-energy of the ground state of hydrogenlike ions (from Hedendahl and Holmberg [87])

Z	Coulomb gauge	Feynman gauge
18	3.444 043(9)	3.444 04(3)
26	2.783 762(3)	2.783 77(1)
36	2.279 314(2)	2.279 316(7)
54	1.181 866 2(6)	1.781 868(3)
66	1.604 461 5(4)	1.604 462(2)
82	1.487 258 4(4)	1.487 259(1)
92	1.472 424 1(4)	1.472 425(1)

**Table 9.4** Two-photon vacuum polarization and electron-self-energy contributions to the of ground-state energy of some heliumlike ions, using the Feynman gauge (in eV)

Z	Vacuum pol.		Self-energy	
	Sunnergren	Artemyev	Sunnergren	Yerokhin
18	0.0072		-0.1116	
24	0.0173		-0.2278	
32	0.0427	0.0427	-0.4659	-0.4659
44	0.1226		-1.0490	
54	0.255	0.0255	-1.815	-1.815
66	0.557	0.557	-3.224	-3.223
74	0.908	0.908	-4.590	-4.590
83	1.549	1.550	-6.726	-6.726
92	2.630	2.630	-9.781	-9.780

(From Sunnergren [239], Yerokhin et al. [253], and Artemyev et al. [8])

**Table 9.5** Two-photon electron self-energy and vertex correction for the ground state of He-like ions, using the Coulomb and Feynman gauges, from Holmberg et al. [89] (in meV)

Z	Wave-function contribution				MSC, Vertex			Total SE
	Zero-pot.	One-pot.	Many-pot.	Total wf	Zero-pot	Beyond	Tot.MSC,Vx	
<b>Coulomb gauge</b>								
14	-64.7(7)	2.70(2)	5.583(4)	-56.4(7)	-4.22 (2)	-0.57(1)	-4.79(3)	<b>-61.2(7)</b>
18	-115.8(7)	0.441(4)	11.111(5)	-104.2(7)	-8.58(4)	-1.07(2)	-9.65(6)	<b>-113.8(8)</b>
24	-221.4(6)	-11.1(1)	24.059(7)	-208.4(7)	-19.10(8)	-2.16(4)	-21.3(1)	<b>-229.7(8)</b>
30	-360.4(4)	-37.0(4)	43.33(1)	-354.1(8)	-35.3(2)	-3.71(6)	-39.0(3)	<b>-393(1)</b>
50	-1046.1(1)	-307(3)	162.4(9)	-1191(4)	-142.0(2)	-15.2(3)	-157.2(6)	<b>-1348(5)</b>
<b>Feynman gauge</b>								
14	1498.3(7)	-1149.2(1)	-396.1(1)	-46.9(7)	139.8(2)	-153.9(5)	-14.1(6)	<b>-61(1)</b>
18	1620.8(6)	-1218.2(1)	-489.6(1)	-86.9(6)	165.7(2)	-192.2(6)	-26.5(7)	<b>-113(1)</b>
24	1722.3(3)	-1279.4(1)	-617.1(1)	-174.1(4)	192.2(2)	-246.9(8)	-54.7(10)	<b>-229(1)</b>
30	1758.4(1)	-1322.1(1)	-733.10(1)	-296.8(1)	203.7(2)	-299(1)	-95.3(10)	<b>-392(1)</b>
50	1650.9(7)	-1572.5(1)	-1088.9(1)	-1010.5(9)	130.2(2)	-473(2)	-342(2)	<b>1352(3)</b>

separated into the zero-potential part and “Beyond”, i.e., the remaining one- and many-potential parts.

When all effects are included, the result should be gauge independent, as is also found to be the case numerically to a high degree of accuracy. It is very striking to compare the individual contributions in the two gauges. In the Feynman gauge there are very large cancellations between the various contributions, which is not at all the case in the Coulomb gauge. In the Coulomb gauge, the irreducible part represents about 90% of the total effect, and the reducible part of the self-energy together with the vertex correction the remaining 10%. In the Feynman gauge the relations are quite different. This has important consequences for the higher-order calculations.

### 9.2.2 Radiative Effects. Beyond Two-Photon Exchange

The combination of radiative QED effects and electron correlation, beyond two-photon exchange, has been discussed in Sect. 8.2. Some numerical results, obtained in the Coulomb gauge by Holmberg et al. [89] for the ground state of He-like ions are given in Table 9.6.

The complete numerical evaluation of the model-space contributions of the self-energy and the vertex correction are prohibitively time consuming beyond second order in any gauge. Only the irreducible part and the zero-potential part of the remaining pieces are manageable and have been calculated. In second order it was found that in the Coulomb gauge these parts represented the entire effect within a few percent. It is reasonable to assume that something similar will hold also in higher orders. This yields the results given in Table 9.6. The results using the Feynman gauge, on the other hand, look quite different, and it is not possible to obtain any reasonable results without a complete calculation. In the approximation shown in the table the Feynman-gauge results behave quite “unphysically”, decreasing with increasing nuclear charge and being of the “wrong” sign.

***The conclusion is that it in going beyond second order, sensible results can at present only be obtained using the Coulomb gauge.***

The effect beyond two-photon exchange discussed here is the combined effect of electron self-energy and electron correlation, here confined to multiple instantaneous Coulomb interactions with no virtual pairs. Effects beyond that represent higher-order effects that should be quite small compared to the main correlational effect. Therefore, the results given here can be expected to approximate well *all effects* beyond two-photon exchange.

The effect of high-order vacuum polarization has also been evaluated by Holmberg et al. [89] and found to be an order smaller than the corresponding self-energy effects, as is the case also in lower orders.



**Table 9.6** Correlational effects on the radiative QED for the ground state of He-like ions, beyond two-photon exchange, from Holmberg et al. [89], c.f., Table 9.5 (in meV)

Z	Irreducible part				Zero-potential		Total
	Zero-pot.	One-pot.	Many-pot.	Total wf	MSC	Vertex	Estimated
<b>Coulomb gauge</b>							
14	3.47(3)	-0.0275(2)	-0.451(3)	2.99(4)	0.87	-0.63	<b>3.23(4)</b>
18	4.79(2)	0.143(1)	-0.691(4)	4.24(3)	1.16	-0.73	<b>4.67(3)</b>
24	6.77(2)	0.585(6)	-1.104(6)	6.25(3)	1.54	-0.76	<b>7.03(3)</b>
30	8.702(8)	1.22(1)	-1.569(9)	8.36(3)	1.82	-0.61	<b>9.57(3)</b>
50	14.82(1)	5.17(5)	-3.30(2)	16.69(7)	2.15	1.10	<b>20.0(1)</b>
<b>Feynman gauge</b>							
14	-164.82(3)	71.80(3)	12.17(1)	-80.85(6)	-30.7	66.5	-45
18	-142.39(2)	59.7(5)	11.57(1)	-71.1(5)	-24.3	54.2	-41
24	-118.48(1)	47.8(4)	10.79(2)	-59.9(4)	-17.6	41.6	-36
30	-101.51(1)	40.2(1)	10.25(1)	-51.1(1)	-13.0	33.2	-31
50	-69.6(1)	29.9(1)	19.3(1)	-20.5(1)	-4.9	19.4	-6

### 9.3 Comparison with Experiments

Extensive high-accuracy calculations of the X-ray energies of highly-charged heliumlike ions have been performed by Artemyev et al. using the two-time Green’s function [9], as well as by Plante et al. using the relativistic MBPT with first-order QED corrections to the energy [195]. The agreement with experiments is in most cases quite good, but Chantler et al. claim that there are significant discrepancies [43, 44]—for medium-heavy elements up to the order of 100 meV. The calculations of Artemyev et al. are of second order with an estimate of higher-order effects, while those of Plante et al. include correlational effects (but no QED) beyond second order. One question is, therefore, if the claimed discrepancies could be due to omitted higher-order effects.

In Table 9.7 we compare the estimated higher-order effects of Artemyev et al. [9] with those third-order effects recently calculated by Holmberg et al. [89]. (The results of Table 9.6 are here reduced by about 20% to take into account the fact that negative-energy states are not included.) We can see that the higher -order effects are underestimated by Artemyev et al. particularly for heavier elements. Nevertheless, the effects are much too small to be responsible to the discrepancies claimed by Chantler.

The findings of Chantler et al. have recently been challenged by Kubiček et al. [105], who found excellent agreement between their experiments and the above-mentioned second-order calculations. These results are consistent with the conclusions drawn above.

**Table 9.7** Comparison between the higher-order QED effects for the ground states of He-like ions, calculated by Holmberg et al. [89], and those estimated by Artemyev et al. [9] (in meV)

Z	Holmberg 2015 (calc)	Artemyev 2005 (est'd)
14	1.8(2)	0.8
18	2.8(3)	0.9
24	4.0(5)	
30	5.6(8)	-0.2
50	11(2)	-7.7(50)

## 9.4 Outlook

The results presented above represent the effect of one transverse photon in combination with electron correlation of high order. Results of several transverse photons, namely so-called **reducible** effects (see Sect. 8.3), combined with electron correlation can also be evaluated. The effect of **irreducible** QED effects with correlation, which can be expected to be extremely small in most cases, is on the other hand beyond reach for the moment, but the effect can be estimated by replacing the transverse photons beyond the first one by *instantaneous* Breit interactions (2.112).

The calculations performed so far with the procedure described here concern the ground states of heliumlike ions. By extending the calculations to excited states, it will be possible to make detailed comparison with experimental data. For instance, very accurate data exist for some heliumlike ions, as shown in Table 7.7. In some of these cases the experimental results are at least two orders of magnitude more accurate than the best theoretical estimates made so far. In such cases it might in not too distant a future be possible for the first time to observe QED effects also beyond second order.

# Chapter 10

## The Bethe–Salpeter Equation

In this chapter we discuss the *Bethe–Salpeter equation* and its relation to the procedure we have developed so far. We shall start by summarizing the original derivations of the equation by Bethe and Salpeter and by Gell-Mann and Low, which represented the first rigorous covariant treatments of the *bound-state* problem. We shall demonstrate that this field-theoretical treatment is completely compatible with the presentation made here. The treatments of Bethe and Salpeter and of Gell-Mann and Low concern the single-reference situation, while our procedure is more general. Later in this chapter we extend the Bethe–Salpeter equation to the multi-reference case, which will lead to what we refer to as the *Bethe–Salpeter–Bloch equation* in analogy with corresponding equation in MBPT.

### 10.1 The Original Derivations of the Bethe–Salpeter Equation

The original derivations of the Bethe–Salpeter equation by Salpeter and Bethe [213] and by Gell-Mann and Low [74] were based upon procedures developed in the late 1940s for the relativistic treatment of the scattering of two or more particles by Feynman [68, 69], Schwinger [223, 224], Tomanaga [244] and others, and we shall here summarize their derivations.

#### 10.1.1 Derivation by Salpeter and Bethe

Salpeter and Bethe [213] start their derivation from the Feynman formalism of the scattering problem [68, 69], illustrated in terms of Feynman graphs. A Feynman diagram represents in Feynman’s terminology the “*amplitude function*” or “*kernel*” for the scattering process, which in the case of two-particle scattering, denoted

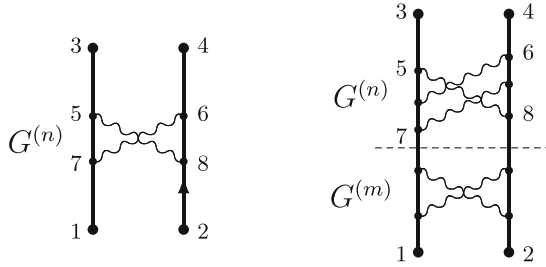


**Fig. 10.1** Examples of Feynman graphs representing scattering amplitudes in (10.1) and (10.2) of the Salpeter–Bethe paper [213]. The first diagram is irreducible, while the second is reducible, since it can be separated into two allowed diagrams by a *horizontal cut*

$K(3, 4; 1, 2)$ , is the probability amplitude for one particle propagating from one space-time point  $x_1$  to another  $x_3$  and the other particle from space-time  $x_2$  to  $x_4$ . For the process involving one irreducible graph  $G^{(n)}$ , i.e., a graph that cannot be separated into two simpler graphs, as illustrated in Fig. 10.1 (left part), the kernel is given by (in Feynman’s notations)

$$K^{(n)}(3, 4; 1, 2) = -i \iiint\!\!\!\int d\tau_5 \dots d\tau_8 K_{+a}(3, 5)K_{+b}(4, 6) \times G^{(n)}(5, 6; 7, 8) K_{+a}(7, 1)K_{+b}(8, 2), \tag{10.1}$$

where  $K_{+a}, K_{+b}$  represent free-particle propagators (positive-energy part). For a process involving *two* irreducible graphs, the kernel illustrated in the right part of the figure becomes

$$K^{(n,m)}(3, 4; 1, 2) = -i \iiint\!\!\!\int d\tau_5 \dots d\tau_8 K_{+a}(3, 5)K_{+b}(4, 6) \times G^{(n)}(5, 6; 7, 8) K^{(m)}(7, 8; 1, 2). \tag{10.2}$$

This leads to the sequence illustrated in Fig. 10.2, where  $G^*$  represents the sum of *all irreducible two-particle self-energy graphs*. From this Salpeter and Bethe arrived at an integral equation for the total kernel

$$K(3, 4; 1, 2) = K_{+a}(3, 1)K_{+b}(4, 2) - i \iiint\!\!\!\int d\tau_5 \dots d\tau_8 K_{+a}(3, 5)K_{+b}(4, 6) \times G^*(5, 6; 7, 8) K(7, 8; 1, 2). \tag{10.3}$$

This is the equation for the two-particle Greens function (5.80) in the form of a *Dyson equation*, in our notations written as

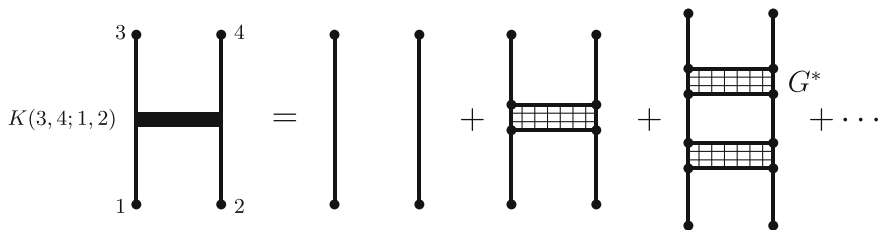


**Fig. 10.2** Graphical representation of the expansion of the Feynman kernel in terms of irreducible graphs

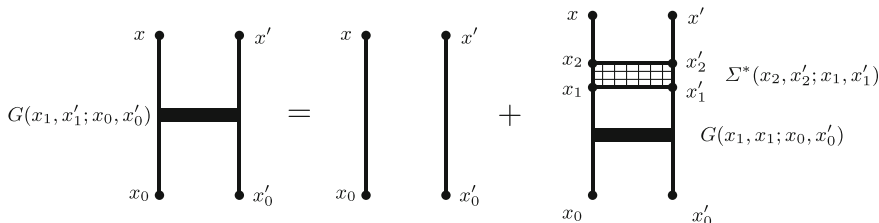


**Fig. 10.3** Graphical representation of the integral equation (10.3) for the Feynman kernel of Salpeter and Bethe—identical to the Dyson equation for the two-particle Green’s function (Fig. 5.8)

$$G(x, x'; x_0, x'_0) = G_0(x, x'; x_0, x'_0) + \iiint\!\!\!\int d^4x_1 d^4x_2 d^4x'_1 d^4x'_2 \times G_0(x, x'; x_2, x'_2) (-i) \Sigma^*(x_2, x'_2; x_1, x'_1) G(x_1, x'_1; x_0, x'_0) \tag{10.4}$$

and depicted in Fig. 10.3 (see also Fig. 5.8). Note that the two-particle kernel  $K$  in the terminology of Feynman and Salpeter–Bethe corresponds to our Green’s function  $G$ , and the irreducible interaction  $G^*$  corresponds to our proper self-energy  $\Sigma^*$ . The proper (or irreducible) self-energy is identical to the irreducible two-particle potential in Fig. 6.9. Furthermore, the electron propagators are in the Feynman–Salpeter–Bethe treatment free-particle propagators. Note that the intermediate lines in Fig. 10.3 represent a Green’s function, where the singularities are eliminated.

Salpeter and Bethe then argued that a similar equation could be set up for the *bound-state wave function*. Since the free lines of the diagrams in the Feynman formulation represent free particles, they concluded that the first (inhomogeneous) term on the r.h.s. could not contribute, as the bound-state wave function cannot contain any free-particle component. This leads in their notations to the *homogeneous* equation

$$\Psi(3, 4) = -i \iiint\!\!\!\int d\tau_5 \dots d\tau_8 K_{+a}(3, 5) K_{+b}(4, 6) G^*(5, 6; 7, 8) \Psi(7, 8). \tag{10.5}$$

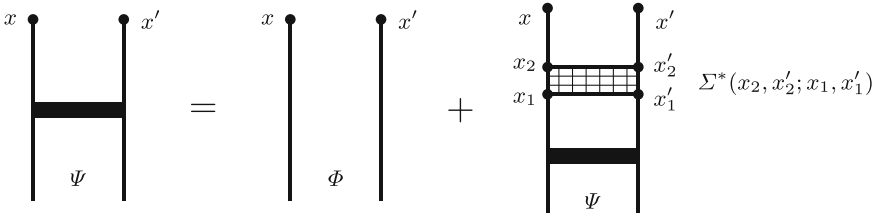


**Fig. 10.4** Graphical representation of the *inhomogeneous* Bethe–Salpeter equation (10.6).  $\Sigma^*$  represents the proper self-energy, which contains all irreducible interaction graphs and is identical to the irreducible two-particle potential in Fig. 6.9. This equation can be compared with that represented in Fig. 8.22, valid also in the multi-reference case

This is the famous *Bethe–Salpeter equation*. In the *Furry picture* we use here, where the basis single-electron states are generated in an external (nuclear) potential, the inhomogeneous term does survive, and the equation becomes in our notations

$$\Psi(x, x') = \Phi(x, x') + \iiint\!\!\!\int d^4x_1 d^4x_2 d^4x'_1 d^4x'_2 \times G_0(x, x'; x_2, x'_2) (-i) \Sigma^*(x_2, x'_2; x_1, x'_1) \Psi(x_1, x'_1). \tag{10.6}$$

This is the *inhomogeneous Bethe–Salpeter equation* we shall use, and it is graphically depicted in Fig. 10.4.

### 10.1.2 Derivation by Gell-Mann and Low

The derivation of Gell-Mann and Low [74] starts from the “*Feynman two-body kernel*”, used in the definition of the Green’s function (5.20) (in their slightly modified notations),

$$K(x_1, x_2; x_3, x_4) = \langle \Psi_0 | T[\hat{\psi}_H(x_1) \hat{\psi}_H(x_2) \hat{\psi}_H^\dagger(x_4) \hat{\psi}_H^\dagger(x_3)] | \Psi_0 \rangle. \tag{10.7}$$

$T$  is the time-ordering operator (2.27) and  $\hat{\psi}_H, \hat{\psi}_H^\dagger$  are the particle-field operators in the Heisenberg representation.  $\Psi_0$  is the vacuum (ground state) of the interacting system in the *Heisenberg picture*,  $|0_H\rangle$ .

In an Appendix of the same paper Gell-Mann and Low derive a relation between the interacting ( $\Psi_0$ ) and the non-interacting ( $\Phi_0$ ) vacuum states (both in the interaction picture)

$$c\Psi_0 = \frac{U(0, -\infty)\Phi_0}{\langle \Phi_0 | U(0, -\infty) | \Phi_0 \rangle}, \tag{10.8}$$

which is the famous *Gell-Mann–Low theorem* (3.38), discussed previously. Here,  $c$  is a normalization constant (equal to unity in the intermediate normalization that we use). This can be eliminated by considering

$$1 = \langle \Psi_0 | \Psi_0 \rangle = \frac{\langle \Phi_0 | U(\infty, -\infty) | \Phi_0 \rangle}{c^2 \langle \Phi_0 | U(\infty, 0) | \Phi_0 \rangle \langle \Phi_0 | U(0, -\infty) | \Phi_0 \rangle}. \quad (10.9)$$

Inserting the expression (10.8) into the kernel (10.7), utilizing the relation (10.9), yields

$$K(x_1, x_2; x_3, x_4) = \frac{\langle \Phi_0 | U(\infty, 0) T[\hat{\psi}_H(x_1) \hat{\psi}_H(x_2) \hat{\psi}_H^\dagger(x_4) \hat{\psi}_H^\dagger(x_3)] U(0, -\infty) | \Phi_0 \rangle}{\langle \Phi_0 | U(\infty, -\infty) | \Phi_0 \rangle}, \quad (10.10)$$

which is equivalent to the field-theoretical definition of the Green's function  $G(x_1, x_2; x_3, x_4)$  in (5.20).

Gell-Mann and Low then conclude that expanding the expression above in a perturbation series leads to the two-body kernel of Feynman in terms of Feynman diagrams, as we have performed in Chap. 5. This is identical to the expansion given by Salpeter and Bethe, and hence leads also to the integral equation (10.3). Gell-Mann and Low then use the same arguments as Salpeter and Bethe to set up the Bethe–Salpeter equation (10.5) for the wave function. In addition, they argue that *single-particle self-energy parts* can easily be included by modifying the single-particle propagators.

The derivation of Gell-Mann and Low, which starts from the field-theoretical definition of the Green's function, has a firm field-theoretical basis. This is true, in principle, also of the derivation of Salpeter and Bethe, which is based upon Feynman diagrams for scattering of field-theoretical origin.

In the next subsection we shall see how the Bethe–Salpeter equation can be motivated from the graphical form of the Dyson equation in Fig. 10.3.

### 10.1.3 Analysis of the Derivations of the Bethe–Salpeter Equation

We can understand the Bethe–Salpeter equation graphically, if we let the Dyson equation in Fig. 10.3 act on the zeroth-order state,  $\Phi(x_0, x'_0)$ , which we represent by two vertical lines without interaction. (The treatment can easily be extended to the situation, where the model function is a linear combination of straight products.) From the relation (6.8) we see that the electron propagator acting on an electron-field operator (with space integration) shifts the coordinates of the operator. Therefore, acting with the zeroth-order Green's function on the model function, shifts the coordinates of the function according to

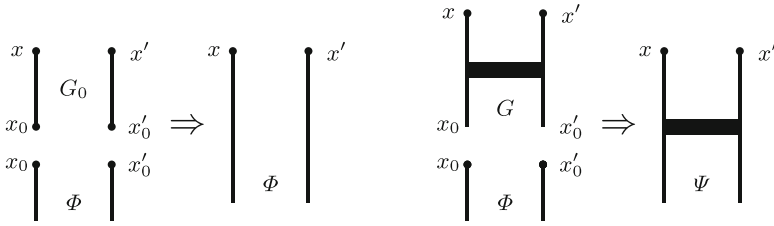


**Fig. 10.5** Graphical illustration of (10.11) and (10.12)

$$\Phi(x, x') = \iint d^3\mathbf{x}_0 d^3\mathbf{x}'_0 G_0(x, x'; x_0, x'_0) \Phi(x_0, x'_0). \tag{10.11}$$

This is illustrated in Fig. 10.5 (left) and corresponds to the first diagram on the rhs of Fig. 10.4. Similarly, operating with the *full* Green’s function in Fig. 10.5 on the model function leads to

$$\Psi(x, x') = \iint d^3\mathbf{x}_0 d^3\mathbf{x}'_0 G(x, x'; x_0, x'_0) \Phi(x_0, x'_0), \tag{10.12}$$

illustrated in Fig. 10.5 (right). Then the entire equation (10.6), illustrated in Fig. 10.4, is reproduced.

The equation (10.12) is consistent with the definition of the classical Green’s function (5.1), which propagates a wave function from one space-time point to another pair—in our case from one *pair* of space-time point to another. This equation can also be expressed as an **operator equation**

$$|\Psi(t, t')\rangle = \mathcal{G}(t, t'; t_0, t'_0) |\Psi(t_0, t'_0)\rangle, \tag{10.13}$$

where  $\mathcal{G}$  is the *Green’s operator*, introduced in Sect. 6.8. The coordinate representation of this equation

$$\langle \mathbf{x}, \mathbf{x}' | \Psi(t, t') \rangle = \langle \mathbf{x}, \mathbf{x}' | \mathcal{G}(t, t'; t_0, t'_0) | \mathbf{x}_0, \mathbf{x}'_0 \rangle \langle \mathbf{x}_0, \mathbf{x}'_0 | \Psi(t_0, t'_0) \rangle \tag{10.14}$$

is identical to (10.12).

This implies that

- *the Green’s function is the coordinate representation of the Green’s operator* and that
- *the four-times Green’s operator represents the time propagation of the two-particle Bethe–Salpeter state vector.*

In the equal-time approximation this is consistent with our previous result (6.68) and with our conjecture (6.45).

It is of interest to compare the Bethe–Salpeter equation (10.6), depicted in Fig. 10.4, with the Dyson equation for the combined QED-electron-correlation



effects in Fig. 8.22. If in the latter more and more effects are included in the QED potential, then the Coulomb interactions, represented by the standard pair function, become insignificant. Then this equation is identical to the Bethe–Salpeter equation. To solve the original BS equation iteratively, however, is extremely tedious and often very slowly converging, due to the dominating Coulomb interaction. As mentioned in the previous chapter, the QED-correlation equation is expected to be a faster road to reach the same goal. One- and two-photon exchange in the QED potential will very likely yield extremely good results, while such effects in the BS equation will often be quite insufficient, due to the often dominating Coulomb interaction (c.f. the discussion about the QED methods in Part II).

## 10.2 Quasi- and Effective-Potential Approximations. Single-Reference Case

In the equal-time approximation, where we equalize the (outgoing) times of the two particles in the Bethe–Salpeter equation (10.6), we can make a Fourier transformation of it with a single energy parameter as in the treatment of the single-particle Green’s function in Sect. 5.2.3. The  $Q$  part, falling outside the model space, then leads to

$$Q \Psi(E) = Q G_0(E) (-i) \Sigma^*(E) \Psi(E), \quad (10.15)$$

leaving out the space coordinates and integrations.

Replacing the zeroth-order Green’s function with the resolvent (5.43)

$$G_0(E) = \frac{i}{E - H_0}, \quad (10.16)$$

we obtain

$$Q(E - H_0) \Psi(E) = Q \Sigma^*(E) \Psi(E). \quad (10.17)$$

If we identify the proper self-energy with the generalized potential (8.11)

$$V(E) = \Sigma^*(E), \quad (10.18)$$

the equation above leads together with the relation (6.174)

$$P(H - H_0)\Omega\Psi(E) = PV(E)\Psi(E) \quad (10.19)$$

to

- *the effective-potential form of the Bethe–Salpeter equation*

$$\boxed{(E - H_0)|\Psi\rangle = V(E)|\Psi\rangle}, \quad (10.20)$$

frequently used in various applications. This equation was also derived above, using the Green's operator only (6.177).

The equation (10.20) can also be expressed

$$|\Psi\rangle = |\Psi_0\rangle + \frac{Q}{E - H_0} V(E)|\Psi\rangle, \quad (10.21)$$

where  $\Psi_0$  is the model state  $\Psi_0 = P\Psi$ . This is equivalent to the *Lippmann-Schwinger equation* [137], frequently used in scattering theory. Formally, (10.20) can also be expressed in the form of the time-independent Schrödinger equation

$$H\Psi = E\Psi, \quad (10.22)$$

where  $H$  is the *energy-dependent* Hamiltonian

$$H(E) = H_0 + V(E). \quad (10.23)$$

The equation (10.20) operates entirely in the restricted Hilbert space with constant number of photons. This can be related to the equivalent equation (6.48), derived by means of the Gell-Mann–Low theorem, which operates in the *photonic Fock space*. We can then regard the equation above as the *projection of the Fock-space equation onto the restricted space*.

### 10.3 Bethe–Salpeter–Bloch Equation. Multi-reference Case\*

We can extend the treatment above to the general multi-reference case. From the expression (6.167), using the fact that the Green's operator at time  $t = 0$  is identical to the wave operator (6.70), we have in the *single-reference case (one-dimensional) model space*

$$|\Psi\rangle = \Omega|\Psi_0\rangle = \left[1 + \Gamma_Q(E) V(E) + \Gamma_Q(E) V(E)\Gamma_Q(E) V(E) + \dots\right] |\Psi_0\rangle, \quad (10.24)$$

where  $|\Psi_0\rangle$  is the model state,  $|\Psi_0\rangle = P|\Psi\rangle$ , and

$$\Gamma_Q(E) = \frac{Q}{E - H_0}$$

is the reduced resolvent (2.65).

Operating on (10.24) from the left with  $Q(E - H_0)$  now yields

$$Q(E - H_0)|\Psi\rangle = QV(E)|\Psi\rangle, \quad (10.25)$$

which is identical to (10.17) with the identification (10.18).

For a *general multi-dimensional (quasi-degenerate) model space* we have similarly

$$Q(E^\alpha - H_0)|\Psi^\alpha\rangle = QV(E^\alpha)|\Psi^\alpha\rangle \quad (10.26)$$

and

$$P(E^\alpha - H_0)|\Psi^\alpha\rangle = PV(E^\alpha)|\Psi^\alpha\rangle. \quad (10.27)$$

This leads to

$$(E^\alpha - H_0)|\Psi^\alpha\rangle = V(E^\alpha)|\Psi^\alpha\rangle \quad (10.28)$$

or in operator form

$$(H_{\text{eff}}^* - H_0)\Omega P = V(H_{\text{eff}}^*)\Omega P, \quad (10.29)$$

using the notations introduced in Sect. 6.11. But

$$H_{\text{eff}}^*\Omega P = \Omega H_{\text{eff}} P = \Omega H_0 P + \Omega W,$$

which yields the commutator relation

$$\boxed{[\Omega, H_0] P = V(H_{\text{eff}}^*)\Omega P - \Omega P W,} \quad (10.30)$$

where according to (6.189)  $W = PV(H_{\text{eff}}^*)\Omega P$ . Here, the energy parameter of  $V(H_{\text{eff}}^*)$  is given by the model-space state to the far right, while the energy parameter of  $\Omega$  of the folded term depends on the intermediate model-space state (see footnote in Sect. 6.8). This equation is valid in the general *multi-reference (quasi-degenerate) situation* and represents an extension of the effective-potential form (10.20) of the Bethe–Salpeter equation. Due to its close resemblance with the standard Bloch equation of MBPT (2.55), we refer to it as the *Bethe–Salpeter–Bloch equation*. This is equivalent to the generalized Bethe–Salpeter equation, derived in Chap. 6 (6.191).

In analogy with the MBPT treatment in section (2.5), we can separate the BS–Bloch equation into

$$\begin{aligned} [\Omega_1, H_0] P &= (V(H_{\text{eff}}^*)\Omega P - \Omega P W(H_0^*) P)_{\text{linked},1} \\ [\Omega_2, H_0] P &= (V(H_{\text{eff}}^*)\Omega P - \Omega P W(H_0^*) P)_{\text{linked},2} \end{aligned} \quad (10.31)$$

etc. It should be noted that the potential operator  $V(H_{\text{eff}}^*)$  is an operator or matrix where each element is an operator/matrix. In the first iteration we set  $H_{\text{eff}} = H_0$  and in the next iteration  $H_{\text{eff}} = H_0 + W^{(1)}$  etc. Continued iterations correspond to the

sum term in the expression (6.133), representing the model-space contributions. The two-particle BS-Bloch equation above is an extension of the ordinary pair equation, discussed in Sect. 2.5 (Fig. 2.6).

The Bethe–Salpeter–Bloch equation leads to a perturbation expansion of Rayleigh–Schrödinger or linked-diagram type, analogous to the that of standard MBPT expansions. It differs from the standard Bloch equation by the fact that the Coulomb interaction is replaced by all irreducible multi-photon interactions.

Solving the BS-Bloch equation (10.30) is NOT equivalent to solving the single-state equation for a number of states. The Bloch equation (10.30) leads to a Rayleigh/Schrödinger/linked-diagram expansion with folded terms that is *size extensive*. The single-state equation (10.20), on the other hand, leads to a Brillouin–Wigner expansion (see footnote in Sect. 2.4), that is **not** size extensive.

Due to the very complicate form of the potential of the Bethe–Salpeter–Bloch equation, it is very difficult to handle this equation in its full extent. In the previous chapters we have considered a simpler way of achieving essentially the same goal.

## 10.4 Problems with the Bethe–Salpeter Equation

There are several fundamental problems with the Bethe–Salpeter equation and with relativistic quantum mechanics in general, as briefly mentioned in the Introduction. Dyson says in his 1953 paper [64] that this is a subject “*full of obscurities and unsolved problems*”. The question concerns the relation between the *three-dimensional* and the *four-dimensional* wave functions. In standard quantum mechanics the three-dimensional wave function describes the system at a particular time, while the four-dimensional two-particle wave function describes the probability amplitude for finding particle one at a certain position at a certain time and particle two at another position at another time etc. The latter view is that of the Bethe–Salpeter equation, and Dyson establishes a connection between the two views. The main problem is here the individual times associated with the particles involved, the physical meaning of which is not completely understood. This problem was further analyzed by Wick [251] and Cutkoski [53] and others. The relative time of the particles leads to a number of anomalous or spurious states—states which do not have non-relativistic counterparts. This problem was analyzed in detail in 1965 by Nakanishi [172], and the situation was summarized in 1997 in a comprehensive paper by Namyslowski [173].

The Bethe–Salpeter equation was originally set up for the bound-state problem involving nucleons, such as the ground state of the deuteron. The equation has lately been extensively used for scattering problems in quantum chromodynamics, quark–quark/antiquark scattering. The equation has also been used for a long time in high-accuracy works on simple atomic systems, such as positronium, muonium, hydrogen and heliumlike ions. The problems with the BS equation, associated with the relative time, are most pronounced at strong coupling and assumed to be negligible in atomic physics, due to the very weak coupling. One important question is, of course, whether this is true also in the very high accuracy that is achieved in recent time.

To attack the BS equation directly is very complicated, and for that reason various approximations and alternative schemes have been developed. The most obvious approximation is to eliminate the relative time of the particles, the *equal-time approximation* or *external-potential approach*. The first application of this technique seems to have been made in the thesis of Sucher in the late 1950s [235, 237] for the evaluation of the leading QED corrections to the energy levels of the helium atom. This work has been extended by Douglas and Kroll [60] and by Drake et al. [259, 262], as will be further discussed in the Chap. 11. Another early application of an effective-potential approach was that of Grotch and Yennie [83] to obtain high-order effects of the nuclear recoil on the energy levels of atomic hydrogen. They derived an “*effective potential*” from scattering theory and applied that in a Schrödinger-like equation. A similar approach was applied to strongly interacting nucleons in the same year by Gross [81], assuming one of the particles was “on the mass shell”. Related techniques have been applied to bound-state QED problems among others by Caswell and Lepage [42] and by Bodwin et al. [32]. A more formal derivation of a “quasi-potential” method for scattering as well as bound-state problems was made by Todorov [242], starting from the Lippmann–Schwinger scattering theory [137].

Several attempts have been made to correct for the equal-time approximation. Sazdjian [216, 217] has converted the BSE into *two* equations, one for the relative time and one eigenvalue equation of Schrödinger type. Connell [49] has developed a series of approximations, which ultimately are claimed to lead to the exact BSE. The approaches were primarily intended for strong interactions, but Connell tested the method on QED problems.

# Chapter 11

## Analytical Treatment of the Bethe–Salpeter Equation

### 11.1 Helium Fine Structure

The leading contributions to the helium fine structure beyond the first-order relativistic contribution (NVPA, see, Sect. 2.6) were first derived in 1957 by Araki [5] and Sucher [235, 237], starting from the Bethe–Salpeter (BS) equation [213] and including the non-relativistic as well as the relativistic momentum regions. Following the approach of Sucher et al., Douglas and Kroll [60] have derived all terms of order  $\alpha^4 H(\text{artree})$ ,<sup>1</sup> where no contributions in the relativistic region were found. The same approach was later used by Zhang [259, 264] to derive corrections of order  $\alpha^5 \log \alpha H$  and of order  $\alpha^5 H$  in the non-relativistic region and recoil corrections to order  $\alpha^4 m/M H$  (see also [261]). Later some additional effects of order  $\alpha^5 H$  due to relativistic momenta were found by Zhang and Drake [263]. The radiative parts are treated more rigorously by Zhang in a separate paper [260]. Using a different approach, Pachucki and Sapirstein [181] have derived all contributions of order  $\alpha^5 H$  and reported some disagreement with the early results of Zhang [259].<sup>2</sup>

We shall here follow the approach of Sucher in his thesis [237]. This is based directly on the BS equation, which makes it possible to identify the contributions in terms of Feynman diagrams and therefore to compare them with the results obtained in the previous chapters. This approach of Sucher is closely followed by Douglas and Kroll [60] and by Zhang [259], and we shall in our presentation make frequent references to the corresponding equations of Sucher (S), Douglas and Kroll (DK), and Zhang (Z).

---

<sup>1</sup> $H(\text{artree})$  is the energy unit of the *Hartree atomic unit system* (see Appendix K.1). In the relativistic unit system the energy unit is  $mc^2 = \alpha^{-2}H$ .

<sup>2</sup>The present chapter is largely based upon the paper [121].

## 11.2 The Approach of Sucher

The treatment of Sucher starts from the Bethe–Salpeter equation (10.5), which in our notations (10.6) reads, leaving out the inhomogeneous term (S 1.1, DK 2.5),

$$\begin{aligned} \Psi(x, x') = & \iiint\!\!\!\int d^4x_1 d^4x_2 d^4x'_1 d^4x'_2 \\ & \times G'_0(x, x'; x_2, x'_2) (-i) \Sigma^*(x_2, x'_2; x_1, x'_1) \Psi(x_1, x'_1). \end{aligned} \quad (11.1)$$

$G'_0$  is the zeroth-order two-particle Green's function, dressed with all kinds of single-particle self-energies.  $\Sigma^*$  is identical to the irreducible potential  $V$  (Fig. 6.9). The undressed zeroth-order Green's function is, using the relation (5.38),

$$G_0(x, x'; x_2, x'_2) = G_0(x, x_2) G_0(x', x'_2) = iS_F(x, x_2) iS_F(x', x'_2) \quad (11.2)$$

and the corresponding dressed function is then

$$G'_0(x, x'; x_2, x'_2) = G(x, x_2) G(x', x'_2) = iS'_F(x, x_2) iS'_F(x', x'_2), \quad (11.3)$$

where  $G$  is the full single-particle Green's function, generated in the field of the nucleus (Furry representation) (see Fig. 5.1) and  $S'_F$  the correspondingly dressed electron propagator. The Green's functions satisfy the relation (5.36) (S 1.5)

$$\left( i \frac{\partial}{\partial t} - h_1 \right) G(x, x_0) = i\delta^4(x - x_0), \quad (11.4)$$

which leads to (S 1.6, DK 2.19)

$$\begin{aligned} \left( i \frac{\partial}{\partial t} - h_1 \right) \left( i \frac{\partial}{\partial t'} - h_2 \right) \Psi(x, x') = & i \iiint\!\!\!\int d^4x_1 d^4x_2 d^4x'_1 d^4x'_2 \\ & \times \delta^4(x - x_2) \delta^4(x' - x'_2) \Sigma^*(x_2, x'_2; x_1, x'_1) \Psi(x_1, x'_1) \\ = & i \iint d^4x_1 d^4x'_1 \Sigma^*(x, x'; x_1, x'_1) \Psi(x_1, x'_1), \end{aligned} \quad (11.5)$$

where  $h_{1,2}$  are the Dirac single-electron Hamiltonians for electron 1 and 2.

We assume that the wave function is of the form

$$\Psi(x, x') = \Psi(T, \tau, \mathbf{x}, \mathbf{x}') = e^{-iET} \Psi(\tau, \mathbf{x}, \mathbf{x}'), \quad (11.6)$$

where  $T = (t + t')/2$  is the average time and  $\tau = t - t'$  is the *relative time*. Then

$$i \frac{\partial}{\partial t} \Psi(x, x') = \left( E/2 + i \frac{\partial}{\partial \tau} \right) \Psi(x, x')$$

$$i \frac{\partial}{\partial t'} \Psi(x, x') = \left( E/2 - i \frac{\partial}{\partial \tau} \right) \Psi(x, x'),$$

leading to (S 1.9, DK 2.23)

$$\begin{aligned} & \left( E/2 + i \frac{\partial}{\partial \tau} - h_1 \right) \left( E/2 - i \frac{\partial}{\partial \tau} - h_2 \right) \Psi(\tau, x, x') \\ &= i \int d\tau_1 \iint d^3 \mathbf{x}_1 d^3 \mathbf{x}'_1 \Sigma^*(\tau, \mathbf{x}, \mathbf{x}'; \tau_1, \mathbf{x}_1, \mathbf{x}'_1) \Psi(\tau_1, \mathbf{x}_1, \mathbf{x}'_1), \end{aligned} \quad (11.7)$$

leaving out the average time.

Sucher then transfers to the momentum representation, but we shall here still work in the coordinate representation with a Fourier transform only of the time variables.

We define the Fourier transform with respect to time

$$F(\epsilon) = \int d\tau e^{i\epsilon\tau} F(\tau) \quad (11.8)$$

and the inverse transformation

$$F(\tau) = \int \frac{d\epsilon}{2\pi} e^{-i\epsilon\tau} F(\epsilon). \quad (11.9)$$

Fourier transforming (11.7) with respect to  $\tau$ , yields

$$\begin{aligned} & (E/2 + \epsilon - h_1) (E/2 - \epsilon - h_2) \Psi(\epsilon, \mathbf{x}_1, \mathbf{x}'_1) \\ &= i \int d\tau_1 \iint d^3 \mathbf{x}_1 d^3 \mathbf{x}'_1 \Sigma^*(\epsilon, \mathbf{x}, \mathbf{x}'; \tau_1, \mathbf{x}_1, \mathbf{x}'_1) \Psi(\tau_1, \mathbf{x}_1, \mathbf{x}'_1). \end{aligned} \quad (11.10)$$

Performing the Fourier transform of the rhs with respect to  $\tau_1$ , yields

$$\begin{aligned} & \int d\tau_1 \iint \frac{d\epsilon'_1}{2\pi} \frac{d\epsilon_1}{2\pi} e^{-i\epsilon'_1\tau_1} e^{-i\epsilon_1\tau_1} \Sigma^*(\epsilon, \mathbf{x}, \mathbf{x}'; \epsilon'_1, \mathbf{x}_1, \mathbf{x}'_1) \Psi(\epsilon_1, \mathbf{x}_1, \mathbf{x}'_1) \\ &= \iint \frac{d\epsilon'_1}{2\pi} \frac{d\epsilon_1}{2\pi} 2\pi \delta(\epsilon_1 + \epsilon'_1) \Sigma^*(\epsilon, \mathbf{x}, \mathbf{x}'; \epsilon'_1, \mathbf{x}_1, \mathbf{x}'_1) \Psi(\epsilon_1, \mathbf{x}_1, \mathbf{x}'_1) \end{aligned} \quad (11.11)$$

or (S 1.16)

$$\begin{aligned} & (E/2 + \epsilon - h_1) (E/2 - \epsilon - h_2) \Psi(\epsilon, \mathbf{x}_1, \mathbf{x}'_1) \\ &= i \int \frac{d\epsilon_1}{2\pi} \iint d^3 \mathbf{x}_1 d^3 \mathbf{x}'_1 \Sigma^*(\epsilon, \mathbf{x}, \mathbf{x}'; -\epsilon_1, \mathbf{x}_1, \mathbf{x}'_1) \Psi(\epsilon_1, \mathbf{x}_1, \mathbf{x}'_1). \end{aligned} \quad (11.12)$$

Following Sucher, we express the relation (11.10) in operator form

$$\hat{\mathcal{F}} |\Psi\rangle = \hat{g} |\Psi\rangle. \quad (11.13)$$



The operator  $\hat{\mathcal{F}}$  has the (diagonal) coordinate representation

$$\langle \epsilon, \mathbf{x}, \mathbf{x}' | \mathcal{F} | \epsilon, \mathbf{x}, \mathbf{x}' \rangle = (E/2 + \epsilon - h_1) (E/2 - \epsilon - h_2) \quad (11.14)$$

and the operator  $\hat{g}$  has the (non-diagonal) representation

$$\langle \epsilon, \mathbf{x}, \mathbf{x}' | \hat{g} | \epsilon_1, \mathbf{x}_1, \mathbf{x}'_1 \rangle = \frac{i}{2\pi} \langle \epsilon, \mathbf{x}, \mathbf{x}' | \hat{\Sigma}^* | \epsilon_1, \mathbf{x}_1, \mathbf{x}'_1 \rangle. \quad (11.15)$$

We expand the interaction into

$$\hat{g} = \hat{g}_c + \hat{g}_\Delta, \quad (11.16)$$

where  $\hat{g}_c$  represents the Columbic part of  $\hat{g}$

$$\hat{g}_c = \frac{i}{2\pi} \hat{I}_c \quad (11.17)$$

and  $\hat{I}_c$  is the Coulomb interaction with the (diagonal) coordinate representation

$$\langle \epsilon, \mathbf{x}, \mathbf{x}' | \hat{I}_c | \epsilon, \mathbf{x}, \mathbf{x}' \rangle = \frac{e^2}{4\pi|x - x_1|}. \quad (11.18)$$

$\hat{g}_\Delta$  represents the remaining part of  $\hat{g}$

$$\hat{g}_\Delta = \hat{g}_T + g_{T \times c} + \hat{g}_{T \times c^2} + \hat{g}_{T \times T} + \dots + \hat{g}^{\text{rad}}, \quad (11.19)$$

where  $\hat{g}_T$  represents a single transverse photon,  $\hat{g}_{T \times c}$  and  $\hat{g}_{T \times c^2}$  a transverse photon with one and two crossing Coulomb interactions, respectively,  $\hat{g}_{T \times T}$  with two irreducible transverse photons, and finally  $\hat{g}^{\text{rad}}$  all radiative corrections. This corresponds to the diagrams shown in Fig. 11.1

With the decomposition (11.16) the relation (11.13) becomes (S 1.30, DK 3.6)

$$|\Psi\rangle = \left( \hat{\mathcal{F}} - \hat{g}_\Delta \right)^{-1} \hat{g}_c |\Psi\rangle \quad (11.20)$$

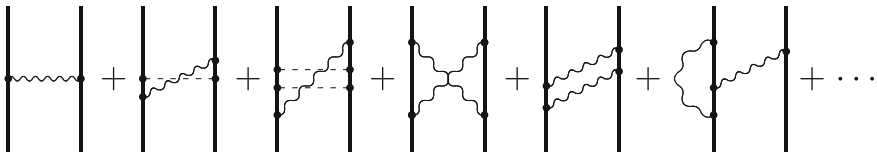


Fig. 11.1 Diagrammatic representation of the approximation in (11.19), used by Sucher

with the coordinate representation

$$\langle \epsilon, \mathbf{x}, \mathbf{x}' | \Psi \rangle = \langle \epsilon, \mathbf{x}, \mathbf{x}' | \left( \hat{\mathcal{F}} - \hat{g}_\Delta \right)^{-1} | \epsilon_2, \mathbf{x}_2, \mathbf{x}'_2 \rangle \langle \epsilon_2, \mathbf{x}_2, \mathbf{x}'_2 | \hat{g}_c | \epsilon_1, \mathbf{x}_1, \mathbf{x}'_1 \rangle \langle \epsilon_1, \mathbf{x}_1, \mathbf{x}'_1 | \Psi \rangle \quad (11.21)$$

or noting that the representation of  $\hat{g}_c$  is diagonal

$$\langle \epsilon, \mathbf{x}, \mathbf{x}' | \Psi \rangle = \langle \epsilon, \mathbf{x}, \mathbf{x}' | \left( \hat{\mathcal{F}} - \hat{g}_\Delta \right)^{-1} | \epsilon_1, \mathbf{x}_1, \mathbf{x}'_1 \rangle \hat{g}_c \langle \epsilon_1, \mathbf{x}_1, \mathbf{x}'_1 | \Psi \rangle. \quad (11.22)$$

Sucher defines the *equal-time wave function* (S 1.32, DK 3.8)

$$\Phi(\mathbf{x}, \mathbf{x}') = \int d\epsilon \Psi(\epsilon, \mathbf{x}, \mathbf{x}') \quad (11.23)$$

or in operator form

$$|\Phi\rangle = |\epsilon\rangle \langle \epsilon | \Psi \rangle, \quad (11.24)$$

which gives with (11.22)

$$\langle \epsilon, \mathbf{x}, \mathbf{x}' | \Psi \rangle = \langle \epsilon, \mathbf{x}, \mathbf{x}' | \left( \hat{\mathcal{F}} - \hat{g}_\Delta \right)^{-1} | \mathbf{x}_1, \mathbf{x}'_1 \rangle \hat{g}_c \langle \mathbf{x}_1, \mathbf{x}'_1 | \Phi \rangle. \quad (11.25)$$

Summing over  $\epsilon$  with the replacement (11.17), this can be expressed (S 1.34)

$$\boxed{|\Phi\rangle = i \int \frac{d\epsilon}{2\pi} \left( \hat{\mathcal{F}} - \hat{g}_\Delta \right)^{-1} \hat{I}_c |\Phi\rangle.} \quad (11.26)$$

Using the identity (S 1.35, DK 3.11)

$$(A - B)^{-1} \equiv A^{-1} + A^{-1}B(A - B)^{-1}, \quad (11.27)$$

the BSE (11.26) becomes (DK 3.12)

$$|\Phi\rangle = i \int \frac{d\epsilon}{2\pi} \left[ \hat{\mathcal{F}}^{-1} + \hat{\mathcal{F}}^{-1} \hat{g}_\Delta (\hat{\mathcal{F}} - \hat{g}_\Delta)^{-1} \right] \hat{I}_c |\Phi\rangle. \quad (11.28)$$

The inverse of the operator  $OF$  is

$$\hat{\mathcal{F}}^{-1} = \frac{1}{E/2 + \epsilon - \hat{h}_1} \frac{1}{E/2 - \epsilon - \hat{h}_2}, \quad (11.29)$$

which is a product of electron propagators in operator form (4.14)

$$\hat{\mathcal{F}}^{-1} = \hat{S}_F(E/2 + \epsilon) \hat{S}_F(E/2 - \epsilon). \quad (11.30)$$

In the coordinate representation (4.12)

$$S_F(\omega; \mathbf{x}, \mathbf{x}_0) = \frac{\langle \mathbf{x}|j\rangle \langle j|\mathbf{x}_0\rangle}{\omega - \epsilon_j + i\eta \operatorname{sgn}(\epsilon_j)} = \frac{\langle \mathbf{x}|j\rangle \langle j|\mathbf{x}_0\rangle}{\omega - \epsilon_j + i\eta} \Lambda_+ + \frac{\langle \mathbf{x}|j\rangle \langle j|\mathbf{x}_0\rangle}{\omega - \epsilon_j - i\eta} \Lambda_-. \quad (11.31)$$

Integration over  $\epsilon$  then yields (S 1.44, DK 3.24)

$$\int \frac{d\epsilon}{2\pi} \mathcal{F}^{-1} = -i \frac{\langle x, x'|rs\rangle \langle rs|x_0, x'_0\rangle}{E - \epsilon_r - \epsilon_s} (\Lambda_{++} - \Lambda_{--}), \quad (11.32)$$

which is also the negative of the Fourier transform of the zeroth-order Green's function  $-G_0(E; \mathbf{x}, \mathbf{x}_0; \mathbf{x}', \mathbf{x}'_0)$ , or in operator form

$$\int \frac{d\epsilon}{2\pi} \hat{\mathcal{F}}^{-1} = -G_0(E) = -\frac{i}{E - \hat{h}_1 - \hat{h}_2} (\Lambda_{++} - \Lambda_{--}). \quad (11.33)$$

Equation (11.28) then becomes (S 1.47, DK 3.26)<sup>3</sup>

$$\left[ h_1 + h_2 + (\Lambda_{++} - \Lambda_{--}) I_c + D i \int \frac{d\epsilon}{2\pi} \mathcal{F}^{-1} g_\Delta (\mathcal{F} - g_\Delta)^{-1} I_c \right] \Phi = E \Phi, \quad (11.34)$$

where

$$D = E - h_1 - h_2. \quad (11.35)$$

This is the starting point for the further analysis.

The operator on the lhs can be written in the form  $H_c + H_\Delta$ , where

$$H_c = h_1 + h_2 + \Lambda_{++} I_c \Lambda_{++} \quad (11.36)$$

is the Hamiltonian of the *no-(virtual)-pair Dirac-Coulomb equation* (Z 16)

$$H_c \Psi_c = E_c \Psi_c \quad (11.37)$$

and

$$H_\Delta = \Lambda_{++} I_c (1 - \Lambda_{++}) - \Lambda_{--} I_c + D i \int \frac{d\epsilon}{2\pi} \mathcal{F}^{-1} g_\Delta (\mathcal{F} - g_\Delta)^{-1} I_c = H_{\Delta 1} + H_{\Delta 2} \quad (11.38)$$

<sup>3</sup>In the following we leave out the hat symbol on the operators.

is the *remaining* “QED part” (S 2.3, DK 3.29, Z 17). The first part  $H_{\Delta 1}$  represents virtual pairs due to the Coulomb interaction and the second part effects of transverse photons (Breit interaction).

In order to include electron self-energy and vacuum polarizations, the electron propagators (5.37) are replaced by propagators with self-energy insertions  $\Sigma(\epsilon)$ , properly renormalized (DK 2.10),

$$S'(\epsilon) = \frac{|r\rangle\langle r|}{\epsilon - \epsilon_r + \beta\Sigma(\epsilon) + i\eta_r}. \quad (11.39)$$

Also renormalized photon self-energies have to be inserted into the photon lines.

### 11.3 Perturbation Expansion of the BS Equation

The effect of the QED Hamiltonian (11.38) can be expanded perturbatively, using the Brillouin–Wigner perturbation theory,

$$\Delta E = E - E_c = \langle \Psi_c | V + V\Gamma V + V\Gamma V\Gamma V + \dots | \Psi_c \rangle = \langle \Psi_c | \frac{V}{1 - \Gamma V} | \Psi_c \rangle, \quad (11.40)$$

where  $\Gamma$  is the reduced resolvent (2.65)

$$\Gamma = \Gamma_Q(E) = \frac{Q}{E - H_c} = \frac{1 - |\Psi_c\rangle\langle\Psi_c|}{E - H_c} = \frac{1 - |\Psi_c\rangle\langle\Psi_c|}{D_c} \quad (11.41)$$

with

$$D_c = E - H_c. \quad (11.42)$$

The unperturbed wave function is in our case one solution of the no-pair Dirac-Coulomb equation (11.37),  $\Psi_c$ , and we can assume that the perturbation is expanded in other eigenfunctions of  $H_c$ .  $Q$  is the projection operator that excludes the state  $\Psi_c$  (assuming no degeneracy). This leads to the expansion (S 2 19–21, DK 3.43, Z 28)

$$\Delta E^{(1)} = \langle \Psi_c | H_{\Delta} | \Psi_c \rangle, \quad (11.43a)$$

$$\Delta E^{(2)} = \langle \Psi_c | H_{\Delta} \Gamma H_{\Delta} | \Psi_c \rangle, \quad (11.43b)$$

$$\Delta E^{(3)} = \langle \Psi_c | H_{\Delta} \Gamma H_{\Delta} \Gamma H_{\Delta} | \Psi_c \rangle, \quad (11.43c)$$

etc.

Since  $\Lambda_{++}|\Psi_c\rangle = |\Psi_c\rangle$  and  $\Lambda_{--}|\Psi_c\rangle = 0$ , it follows that  $\langle\Psi_c|H_{\Delta 1}|\Psi_c\rangle \equiv 0$ , and the first-order correction becomes (DK 3.44)

$$\Delta E^{(1)} = \langle\Psi_c|H_{\Delta 2}|\Psi_c\rangle = \langle\Psi_c|D i \int \frac{d\epsilon}{2\pi} \mathcal{F}^{-1} J \mathcal{F}^{-1} I_c |\Psi_c\rangle \quad (11.44)$$

and (DK 3.45)

$$J = g_\Delta (1 - \mathcal{F}^{-1} g_\Delta)^{-1}. \quad (11.45)$$

The second-order corrections are (DK 3.46)<sup>4</sup>

$$\Delta E_a^{(2)} = \langle\Psi_c|H_{\Delta 1} \Gamma H_{\Delta 1}|\Psi_c\rangle = -\langle\Psi_c|I_c \Lambda_{--} \Gamma \Lambda_{--} I_c |\Psi_c\rangle, \quad (11.46a)$$

$$\Delta E_b^{(2)} = \langle\Psi_c|H_{\Delta 1} \Gamma H_{\Delta 2}|\Psi_c\rangle = \langle\Psi_c|I_c \Lambda_{--} D \Gamma i \int \frac{d\epsilon}{2\pi} \mathcal{F}^{-1} J \mathcal{F}^{-1} I_c |\Psi_c\rangle, \quad (11.46b)$$

$$\Delta E_c^{(2)} = \langle\Psi_c|H_{\Delta 2} \Gamma H_{\Delta 1}|\Psi_c\rangle = \langle\Psi_c|D i \int \frac{d\epsilon}{2\pi} \mathcal{F}^{-1} J \mathcal{F}^{-1} I_c \Gamma \Lambda_{--} I_c |\Psi_c\rangle, \quad (11.46c)$$

$$\begin{aligned} \Delta E_d^{(2)} &= \langle\Psi_c|H_{\Delta 2} \Gamma H_{\Delta 2}|\Psi_c\rangle \\ &= \langle\Psi_c|D i \int \frac{d\epsilon}{2\pi} \mathcal{F}^{-1} J \mathcal{F}^{-1} I_c \Gamma D i \int \frac{d\epsilon}{2\pi} \mathcal{F}^{-1} J \mathcal{F}^{-1} I_c |\Psi_c\rangle. \end{aligned} \quad (11.46d)$$

These formulas can be simplified, noting that

$$\Lambda_{--} \Gamma D = \Lambda_{--} \frac{Q}{E - H_c} (E - h_1 - h_2), \quad (11.47)$$

which, using the relation (11.42), becomes (DK 3.41)

$$\Lambda_{--} \Gamma D = \Lambda_{--} \left( 1 + \frac{\Lambda_{++} I_c \Lambda_{++}}{E - H_c} \right) = \Lambda. \quad (11.48)$$

According to DK  $\Delta E_a^{(2)}$ ,  $\Delta E_c^{(2)}$  and  $\Delta E^{(3)}$  do not contribute to the fs in order  $\alpha^4$  (Hartree). This holds also in the next order according to Zhang, but  $\Delta E^{(3)}$  will contribute to the singlet energy in that order. In the relativistic momentum region the second-order part  $\Delta E_a^{(2)}$  contributes to the energy already in order  $\alpha^3$  H and to the fine structure in order  $\alpha^5$  H [259, p. 1256].

Using the relation (11.42), we have  $E_c - H_c = D_c - \Lambda_{++} D_c \Lambda_{++}$ , and the no-pair equation (11.37) can be written (DK 3.51)

$$(D_c - \Lambda_{++} I_c) \Psi_c = 0. \quad (11.49)$$

<sup>4</sup>Note that the two  $I_c$  in (11.46a) are missing from [60, Eq. 3.46]. Equation (11.46b) agrees with [259, Eq. 30] but not with [60], where the factor  $I_c \mathcal{L}_{++}$  should be removed.

Then the second-order correction  $\Delta E_b^{(2)}$  (11.46b) can be expressed

$$\Delta E_b^{(2)} = \langle \Psi_c | (I_c - D_c) i \int \frac{d\epsilon}{2\pi} \mathcal{F}^{-1} J \mathcal{F}^{-1} I_c | \Psi_c \rangle. \quad (11.50)$$

This can be combined with the first-order correction  $\Delta E^{(1)}$  (11.44), yielding

$$\langle \Psi_c | (I_c + \Delta E) i \int \frac{d\epsilon}{2\pi} \mathcal{F}^{-1} J \mathcal{F}^{-1} I_c | \Psi_c \rangle \quad (11.51)$$

with

$$\Delta E = E - E_c = D - D_c. \quad (11.52)$$

Here, the  $\Delta E$  term differs in sign from (DK 3.54) and (Z 37).

The reason for the discrepancy between our result here and those of DK and Z, seems to be that the latter make the replacement (DK 3.48)

$$\mathcal{F}^{-1} = S_1 S_2 \equiv (S_1 + S_2) (S_1^{-1} + S_2^{-1})^{-1} = \frac{S_1 + S_2}{E - h_1 - h_2} = D^{-1} (S_1 + S_2), \quad (11.53)$$

which follows from (11.30), and then approximate  $D$  with  $D_c$  in the second-order expression.

## 11.4 Diagrammatic Representation

To continue we make the expansion (DK 3.45, Z 32)

$$J = g_\Delta (1 - \mathcal{F}^{-1} g_\Delta)^{-1} = g_\Delta + g_\Delta \mathcal{F}^{-1} g_\Delta + \dots, \quad (11.54)$$

where the first term represents *irreducible* terms and the remaining ones are *reducible*. Furthermore, we make the separation (DK 3.53, Z 12)

$$g_\Delta = g_T + \Delta g, \quad (11.55)$$

where  $g_T$  represents the interaction of a single transverse photon and  $\Delta g$  the irreducible multi-photon exchange of (11.19). The first-order expression (11.44) becomes

$$\Delta E^{(1)} = \langle \Psi_c | D i \int \frac{d\epsilon}{2\pi} \mathcal{F}^{-1} [g_T + g_T \mathcal{F}^{-1} g_T + \Delta g + \dots] \mathcal{F}^{-1} I_c | \Psi_c \rangle, \quad (11.56)$$

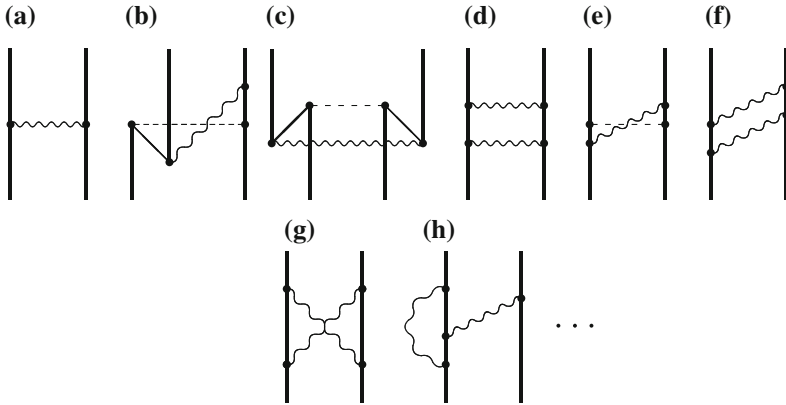


**Fig. 11.2** Diagrammatic representation of the first-order expression (11.56)

and the leading terms are illustrated in Fig. 11.2. The first term can be expanded in no-pair and virtual-pair terms (a–c)

$$\Delta E^{(1)} = \langle \Psi_c | D i \int \frac{d\epsilon}{2\pi} \mathcal{F}^{-1} g_T \mathcal{F}^{-1} (\Lambda_{++} + \Lambda_{+-} + \Lambda_{-+} + \Lambda_{--}) I_c | \Psi_c \rangle. \quad (11.57)$$

The second term in (11.56) represents in lowest order two *reducible* transverse photons (d) and the third term *irreducible* (inclusive radiative) multi-photon part, (e–h). Similarly, the second-order expressions above become

$$\Delta E_a^{(2)} = -\langle \Psi_c | I_c \Lambda_{--} \Gamma \Lambda_{--} I_c | \Psi_c \rangle, \quad (11.58a)$$

$$\Delta E_b^{(2)} = \langle \Psi_c | I_c \Lambda_{--} i \int \frac{d\epsilon}{2\pi} \mathcal{F}^{-1} [g_T + g_T \mathcal{F}^{-1} g_T + \Delta g + \dots] \mathcal{F}^{-1} I_c | \Psi_c \rangle, \quad (11.58b)$$

$$\Delta E_c^{(2)} = \langle \Psi_c | i \int \frac{d\epsilon}{2\pi} \mathcal{F}^{-1} [g_T + g_T \mathcal{F}^{-1} g_T + \Delta g + \dots] \mathcal{F}^{-1} I_c \Lambda_{--} I_c | \Psi_c \rangle, \quad (11.58c)$$

$$\Delta E_d^{(2)} = \langle \Psi_c | D i \int \frac{d\epsilon}{2\pi} \mathcal{F}^{-1} [g_T + \dots] \mathcal{F}^{-1} I_c \Gamma D i \int \frac{d\epsilon}{2\pi} \mathcal{F}^{-1} [g_T + \dots] \mathcal{F}^{-1} I_c | \Psi_c \rangle. \quad (11.58d)$$

This is illustrated in Fig. 11.3. The first second-order contribution (11.58a) represents two Coulomb interactions with double pair (Fig. 11.3a) and the next contribution (11.58b) in lowest order a transverse photon and a Coulomb interaction with double pair (b). The third contribution represents in lowest order one transverse photon and two Coulomb interactions with a double pair (c). The last term represents two *reducible* transverse photons with at least one Coulomb interaction (d).

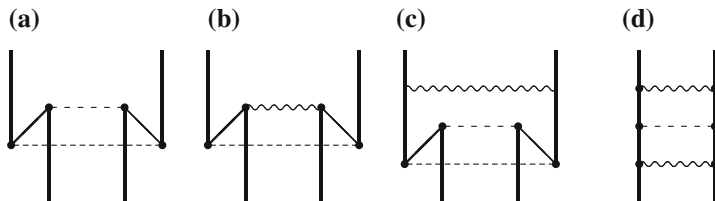


Fig. 11.3 Diagrammatic representation of the second-order expressions (11.58a–11.58d)

### 11.5 Comparison with the Numerical Approach

In previous chapters we have described an approach that has recently been developed by the Gothenburg group and that is largely equivalent to solving the Bethe–Salpeter equation numerically. Numerical results were presented in Chap. 9. This procedure is based upon the covariant-evolution-operator approach and the Green’s-operator technique, described previously, and to a large extent upon the numerical techniques developed by the group and applied to numerous atomic systems (see Sect. 2.7). This new technique has the advantage over the analytical approach that all relativistic effects are automatically included in the procedure. This simplifies the handling appreciably, and it corresponds to the treatment of the entire Sect. 4 of Douglas and Kroll [60] or to Sect. 7 in the paper of Zhang [259].

The numerical technique can handle one retarded photon with arbitrary number of crossing Coulomb interactions together with virtual electron-positron pairs as well as first-order radiative QED effects. This corresponds to most of the terms  $g_T + g_{T \times c} + g_{T \times c^2} + \dots$  of the expansion in (11.19) and to the numerous formulas of Sect. 5 of Douglas-Kroll and of Sect. 4 of Zhang.

Also part of the multi-photon effect can be treated numerically by iterating reducible interactions with a single transverse photon, corresponding to the operator  $g_T \mathcal{F} g_T$  in the formulas above with crossing Coulomb interactions. These effects are treated in Sect. 6 of Douglas and Kroll. The irreducible interaction with several transverse photons cannot be treated at present with the numerical technique, but this can be approximated with one retarded and one or several unretarded photons (instantaneous Breit).



# Chapter 12

## Regularization and Renormalization

(See, for instance, Mandl and Shaw [143, Chap. 9] and Peskin and Schroeder [194, Chap. 7].)

In the previous chapters we have evaluated some radiative effects in the S-matrix (Chap. 4) and Green's-operator formalisms (Chap. 8). In the present chapter we shall discuss the important processes of renormalization and regularization in some detail.

Many integrals appearing in QED are divergent, and these divergences can be removed by replacing the bare electron mass and charge by the corresponding *physical* quantities. Since infinities are involved, this process of *renormalization* is a delicate matter. In order to do this properly, the integrals first have to be *regularized*, which implies that the integrals are modified so that they become finite. This has to be done so that the process is gauge-independent. After the renormalization, the regularization modification is removed. Several regularization schemes have been developed, and we shall consider some of them in this chapter. If done properly, the way of regularization should have no effect on the final result.

### 12.1 The Free-Electron QED

#### 12.1.1 The Free-Electron Propagator

The wave functions for free electrons are given by (D.28) in Appendix D

$$\begin{cases} x\phi_{p_+}(x) = (2\pi)^{-3/2} u_+(\mathbf{p}) e^{i\mathbf{p}\cdot\mathbf{x}} e^{-iE_p t} \\ \phi_{p_-}(x) = (2\pi)^{-3/2} u_-(\mathbf{p}) e^{i\mathbf{p}\cdot\mathbf{x}} e^{iE_p t} \end{cases}, \quad (12.1)$$

where  $\mathbf{p}$  is the momentum vector and  $p_+$  represents positive-energy states ( $r = 1, 2$ ) and  $p_-$  negative-energy states ( $r = 3, 4$ ).  $E_p = cp_0 = \sqrt{c^2\mathbf{p}^2 + m^2c^4}$ . The coordinate representation of the free-electron propagator (4.10) then becomes

$$\langle x_1 | \hat{S}_F^{\text{free}} | x_2 \rangle = \int \frac{d\omega}{2\pi} \sum_{\mathbf{p}, r} \frac{\phi_{\mathbf{p}, r}(\mathbf{x}_1) \phi_{\mathbf{p}, r}^\dagger(\mathbf{x}_2)}{\omega - \varepsilon_p^{\text{free}}(1 - i\eta)} e^{-i\omega(t_1 - t_2)}, \quad (12.2)$$

where  $\varepsilon_p^{\text{free}}$  is the energy eigenvalue of the free-electron function ( $E_p = |\varepsilon_p^{\text{free}}|$ ). The Fourier transform with respect to time then becomes

$$\begin{aligned} \langle x_1 | \hat{S}_F^{\text{free}} | x_2 \rangle &= \sum_{\mathbf{p}, r} \frac{\phi_{\mathbf{p}, r}(\mathbf{x}_1) \phi_{\mathbf{p}, r}^\dagger(\mathbf{x}_2)}{\omega - \varepsilon_p^{\text{free}}(1 - i\eta)} \Rightarrow \\ &= \int \frac{d^3\mathbf{p}}{(2\pi)^3} \sum_r u_r(\mathbf{p}) u_r^\dagger(\mathbf{p}) \frac{e^{i\mathbf{p}\cdot(\mathbf{x}_1 - \mathbf{x}_2)}}{\omega - \varepsilon_p^{\text{free}}(1 - i\eta)} \\ &= \int \frac{d^3\mathbf{p}}{(2\pi)^3} \left[ u_+(\mathbf{p}) u_+^\dagger(\mathbf{p}) \frac{1}{\omega - E_{\mathbf{p}}(1 - i\eta)} \right. \\ &\quad \left. + u_-(\mathbf{p}) u_-^\dagger(\mathbf{p}) \frac{1}{\omega + E_{\mathbf{p}}(1 - i\eta)} \right] e^{i\mathbf{p}\cdot(\mathbf{x}_1 - \mathbf{x}_2)}. \end{aligned}$$

The square bracket above is the Fourier transform of the propagator, and using the relations (D.38, D.39), this becomes<sup>1</sup>

$$\begin{aligned} S_F^{\text{free}}(\omega, \mathbf{p}) &= \frac{1}{2} \left[ \frac{1}{\omega - E_{\mathbf{p}}(1 - i\eta)} + \frac{1}{\omega + E_{\mathbf{p}}(1 - i\eta)} \right] \\ &\quad + \frac{\boldsymbol{\alpha} \cdot \mathbf{p} + \beta mc}{2p_0} \left[ \frac{1}{\omega - E_{\mathbf{p}}(1 - i\eta)} - \frac{1}{\omega + E_{\mathbf{p}}(1 - i\eta)} \right] \\ &= \frac{\omega + c \boldsymbol{\alpha} \cdot \mathbf{p} + \beta mc^2}{\omega^2 - E_p^2 + i\eta} = \frac{\omega + c \boldsymbol{\alpha} \cdot \mathbf{p} + \beta mc^2}{\omega^2 - (c^2\mathbf{p}^2 + m^2c^4)(1 - i\eta)} \\ &= \frac{1}{\omega - (c \boldsymbol{\alpha} \cdot \mathbf{p} + \beta mc^2)(1 - i\eta)} \end{aligned} \quad (12.3)$$

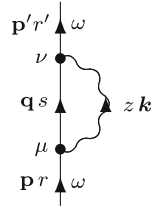
with  $E_p^2 = c^2p_0^2 = c^2\mathbf{p}^2 + m^2c^4$  and  $\boldsymbol{\alpha}\beta = -\beta\boldsymbol{\alpha}$ . This can also be expressed

$$S_F^{\text{free}}(\omega, \mathbf{p}) = \frac{1}{\omega - h_D^{\text{free}}(\mathbf{p})(1 - i\eta)}, \quad (12.4)$$

where  $h_D^{\text{free}}(\mathbf{p})$  is the momentum representation of the free-electron Dirac Hamiltonian operator,  $\hat{h}_D^{\text{free}}(\hat{\mathbf{p}})$ , (D.21).

<sup>1</sup>In the following we shall for simplicity denote the electron physical mass by  $m$  instead of  $m_e$ .

**Fig. 12.1** Diagram representing the first-order free-electron self-energy



Formally, we can write (12.3) in a covariant four-component form with  $\omega = cp_0$  and with  $cp_0$  disconnected from  $E_p = \sqrt{c^2\mathbf{p}^2 + m^2c^4}$ —known as *off the mass-shell*. Then we have

$$cS_F^{\text{free}}(\omega, \mathbf{p}) = \frac{1}{p_0 - \boldsymbol{\alpha} \cdot \mathbf{p} - \beta mc} = \frac{p_0 + \boldsymbol{\alpha} \cdot \mathbf{p} + \beta mc}{p_0^2 - (\mathbf{p}^2 + m^2c^2)(1 - i\eta)} = \frac{(\not{p} + mc)\beta}{p^2 - m^2c^2}$$

or

$$\boxed{\overline{S}_F^{\text{free}}(p) = cS_F^{\text{free}}(\omega, \mathbf{p})\beta = S_F^{\text{free}}(p)\beta = \frac{1}{\not{p} - mc + i\eta}} \quad (12.5)$$

with  $\not{p} = \gamma_\sigma p^\sigma = \beta\alpha_\sigma p^\sigma = \beta(p_0 - \boldsymbol{\alpha} \cdot \mathbf{p}) = (p_0 + \boldsymbol{\alpha} \cdot \mathbf{p})\beta$  (see Appendix D). (Note, that the two transforms differ by a factor of  $c$ .)<sup>2</sup>

### 12.1.2 The Free-Electron Self-Energy

The S-matrix for the first-order free-electron self-energy (Fig. 12.1) is obtained from (4.84), (4.44) with the momentum functions (12.1) after time integrations

$$S^{(2)}(\omega; \mathbf{p}', r', \mathbf{p}, r) = e^2c^2 \int \frac{dz}{2\pi} \iint d^3\mathbf{x} d^3\mathbf{x}' u_r^\dagger(\mathbf{p}') e^{-i\mathbf{p}' \cdot \mathbf{x}'} \times \alpha^{\nu'} iS_F^{\text{free}}(\omega - z; \mathbf{x}', \mathbf{x}) \alpha^\mu u_r(\mathbf{p}) e^{i\mathbf{p} \cdot \mathbf{x}} iD_{F\mu\nu}(z, \mathbf{x}' - \mathbf{x}). \quad (12.6)$$

The relation between the momentum and coordinate representations are

$$S_F^{\text{free}}(\omega; \mathbf{x}', \mathbf{x}) = \int \frac{d^3\mathbf{q}}{(2\pi)^3} S_F^{\text{free}}(\omega, \mathbf{q}) e^{i\mathbf{q} \cdot (\mathbf{x}' - \mathbf{x})} \quad (12.7)$$

$$D_{F\nu\mu}(z; \mathbf{x}', \mathbf{x}) = \int \frac{d^3\mathbf{k}}{(2\pi)^3} D_{F\nu\mu}^{\text{free}}(z, \mathbf{k}) e^{i\mathbf{k} \cdot (\mathbf{x}' - \mathbf{x})}. \quad (12.8)$$

<sup>2</sup>Here,  $S_F^{\text{free}}(p)$  is the *non-covariant* electron propagator, defined by means of  $\Psi^\dagger$  in the formulas (4.9), while  $\overline{S}_F^{\text{free}}(p)$  is the corresponding *covariant* expression, defined by means of  $\overline{\Psi} = \Psi^\dagger\beta$ .

Integration over the space coordinates then yields

$$S^{(2)}(\omega; \mathbf{p}', r', \mathbf{p}, r) = e^2 c^2 \int \frac{d^3 \mathbf{q}}{(2\pi)^3} \int \frac{d^3 \mathbf{k}}{(2\pi)^3} \delta^3(\mathbf{p} - \mathbf{q} - \mathbf{k}) \delta^3(\mathbf{p}' - \mathbf{q} - \mathbf{k}) \\ \times u_{r'}^\dagger(\mathbf{p}') \int \frac{dz}{2\pi} \alpha^\nu S_F^{\text{free}}(\omega - z, \mathbf{k}) \alpha^\mu D_{F\nu\mu}^{\text{free}}(z, \mathbf{k}) u_r(\mathbf{p}) \quad (12.9)$$

and integration over  $\mathbf{q}$

$$S^{(2)}(\omega; \mathbf{p}', r', \mathbf{p}, r) = \delta^3(\mathbf{p}' - \mathbf{p}) u_{r'}^\dagger(\mathbf{p}') (-i) \Sigma^{\text{free}}(\omega, \mathbf{p}) u_r(\mathbf{p}), \quad (12.10)$$

where

$$\Sigma^{\text{free}}(\omega, \mathbf{p}) = ie^2 c^2 \int \frac{dz}{2\pi} \int \frac{d^3 k}{(2\pi)^3} \alpha^\nu S_F^{\text{free}}(\omega - z, \mathbf{k}) \alpha^\mu D_{F\nu\mu}^{\text{free}}(z, \mathbf{k}). \quad (12.11)$$

In the *covariant form* we have, using  $z = ck_0$ ,

$$\Sigma^{\text{free}}(p) = ie^2 c^2 \int \frac{d^4 k}{(2\pi)^4} \alpha^\nu S_F^{\text{free}}(p - k) \alpha^\mu D_{F\nu\mu}(k), \quad (12.12)$$

which is the *free-electron self-energy function*. With the covariant form (12.5) of the free-electron propagator this yields in terms of gamma matrices ( $\gamma^\nu = \beta\alpha^\nu$ )

$$\bar{\Sigma}^{\text{free}}(p) = \beta \Sigma^{\text{free}}(p) = ie^2 c^2 \int \frac{d^4 k}{(2\pi)^4} \gamma^\nu \frac{1}{\not{p} - \not{k} - mc + i\eta} \gamma^\mu D_{F\nu\mu}(k). \quad (12.13)$$

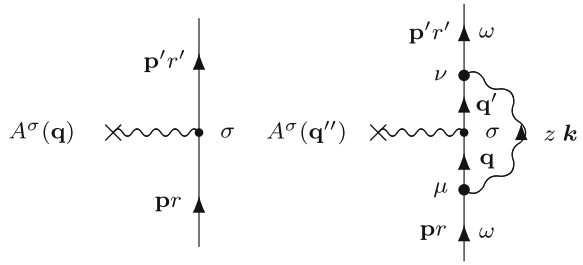
This can also be expressed

$$\bar{\Sigma}^{\text{free}}(p) = \beta \Sigma^{\text{free}}(p) = ie^2 c^2 \int \frac{d^4 k}{(2\pi)^4} \gamma^\nu \frac{\not{p} - \not{k} + mc}{(p - k)^2 - m^2 c^2 + i\eta} \gamma^\mu D_{F\nu\mu}(k). \quad (12.14)$$

In the *Feynman gauge* we have with the photon propagator (4.28) and the commutation rules in Appendix (D.61)

$$\bar{\Sigma}^{\text{free}}(p) = \beta \Sigma^{\text{free}}(p) = \frac{2ie^2 c}{\epsilon_0} \int \frac{d^4 k}{(2\pi)^4} \frac{\not{p} - \not{k} - 2mc}{(p - k)^2 - m^2 c^2 + i\eta} \frac{1}{k^2 + i\eta}. \quad (12.15)$$

**Fig. 12.2** Diagram representing the first-order free-electron vertex correction



### 12.1.3 The Free-Electron Vertex Correction

We consider first the single interaction with an external energy potential (Appendix D.44)  $-e\alpha_\sigma A^\sigma$  Fig. 12.2 (left). The S-matrix (4.3) is given by

$$S^{(1)}(\omega', \omega; \mathbf{p}'r', \mathbf{p}r, \mathbf{q}) = iec \int d^3\mathbf{x} u_{r'}^\dagger(\mathbf{p}') e^{-i\mathbf{p}'\cdot\mathbf{x}} \alpha^\sigma A_\sigma(\mathbf{x}) u_r(\mathbf{p}) e^{i\mathbf{p}\cdot\mathbf{x}} \quad (12.16)$$

or

$$S^{(1)}(\omega', \omega; \mathbf{p}'r', \mathbf{p}r, \mathbf{q}) = iec \delta^3(\mathbf{p} - \mathbf{p}') u_{r'}^\dagger(\mathbf{p}') \alpha^\sigma A_\sigma(\mathbf{p} - \mathbf{p}') u_r(\mathbf{p}), \quad (12.17)$$

where  $A^\sigma(\mathbf{q})$  is the Fourier transform of  $A^\sigma(\mathbf{x})$ .

The vertex-modified free-electron self-energy diagram in Fig. 12.2 (right) becomes similarly

$$\begin{aligned} S^{(3)}(\omega', \omega; \mathbf{p}'r', \mathbf{p}r) &= (ie)^3 c^2 \int \frac{dz}{2\pi} \iiint d^3\mathbf{x}_1 d^3\mathbf{x}_2 d^3\mathbf{x}_3 u_{r'}^\dagger(\mathbf{p}') e^{-i\mathbf{p}'\cdot\mathbf{x}'} \\ &\times \alpha^\nu iS_F^{\text{free}}(\omega' - z, \mathbf{x}', \mathbf{x}'') \alpha^\sigma A_\sigma(\mathbf{x}'') \alpha^\mu iS_F^{\text{free}}(\omega - z, \mathbf{x}'', \mathbf{x}) u_r(\mathbf{p}) e^{i\mathbf{p}\cdot\mathbf{x}} \\ &\times iD_{F\mu\nu}(z, \mathbf{x}' - \mathbf{x}). \end{aligned} \quad (12.18)$$

In analogy with (12.9) this becomes

$$\begin{aligned} S^{(3)}(\omega', \omega; \mathbf{p}'r', \mathbf{p}r) &= e^3 c^2 \int \frac{d^3\mathbf{q}}{(2\pi)^3} \int \frac{d^3\mathbf{q}'}{(2\pi)^3} \int \frac{d^3\mathbf{q}''}{(2\pi)^3} \int \frac{d^3\mathbf{k}}{(2\pi)^3} u_{r'}^\dagger(\mathbf{p}') \\ &\times \delta^3(\mathbf{p} - \mathbf{q} - \mathbf{k}) \delta^3(\mathbf{p}' - \mathbf{q}' - \mathbf{k}) \delta^3(\mathbf{q} - \mathbf{q}' + \mathbf{q}'') \int \frac{dz}{2\pi} \alpha^\nu S_F^{\text{free}}(\omega' - z, \mathbf{q}') \\ &\times \alpha^\sigma A_\sigma(\mathbf{q}'') \alpha^\mu S_F^{\text{free}}(\omega - z, \mathbf{q}) u_r(\mathbf{p}) D_{F\mu\nu}(z, \mathbf{k}) \end{aligned} \quad (12.19)$$

and after integrations over  $\mathbf{q}$ ,  $\mathbf{q}'$ , and  $\mathbf{q}''$  (c.f. 4.99)

$$S^{(3)}(\omega', \omega; \mathbf{p}'r', \mathbf{p}r) = ie \delta^3(\mathbf{p} - \mathbf{p}') u_{r'}^\dagger(\mathbf{p}') \Lambda^\sigma(\omega', \omega; \mathbf{p}', \mathbf{p}) A_\sigma(\mathbf{p} - \mathbf{p}') u_r(\mathbf{p}), \quad (12.20)$$

where

$$\begin{aligned} \Lambda^\sigma(\omega', \omega; \mathbf{p}', \mathbf{p}) &= ie^2 c^2 \int \frac{dz}{2\pi} \int \frac{d^3\mathbf{k}}{(2\pi)^3} \alpha^\nu S_F^{\text{free}}(\omega' - z, \mathbf{p}' - \mathbf{k}) \\ &\quad \times \alpha^\sigma S_F^{\text{free}}(\omega - z, \mathbf{p} - \mathbf{k}) \alpha^\mu D_{F\nu\mu}(z, \mathbf{k}) \end{aligned} \quad (12.21)$$

is the *vertex correction function*. This can be expressed in analogy with the free-electron case (12.5)

$$\Lambda^\sigma(p', p) = ie^2 c \int \frac{d^4k}{(2\pi)^4} \alpha^\nu S_F^{\text{free}}(p' - k) \alpha^\sigma S_F^{\text{free}}(p - k) \alpha^\mu D_{F\nu\mu}(k)$$

and in covariant form

$$\begin{aligned} \overline{\Lambda^\sigma}(p', p) &= \beta \Lambda^\sigma(p', p) = ie^2 c \int \frac{d^4k}{(2\pi)^4} \gamma_\mu \frac{1}{\not{p}' - \not{k} - mc + i\eta} \gamma^\sigma \\ &\quad \times \frac{1}{\not{p} - \not{k} - mc + i\eta} \gamma^\mu D_{F\nu\mu}(k). \end{aligned} \quad (12.22)$$

In the *Feynman gauge* this becomes

$$\begin{aligned} \overline{\Lambda^\sigma}(p', p) &= \beta \Lambda^\sigma(p', p) = \frac{ie^2}{\epsilon_0} \int \frac{d^4k}{(2\pi)^4} \gamma_\mu \frac{1}{\not{p}' - \not{k} - mc + i\eta} \gamma^\sigma \\ &\quad \times \frac{1}{\not{p} - \not{k} - mc + i\eta} \gamma^\mu \frac{1}{k^2 + i\eta}. \end{aligned} \quad (12.23)$$

Comparing (12.22) with the self-energy function (12.13), we find for  $p = p'$  the **Ward identity** [143, (9.60)] (see 4.102)

$$\boxed{\frac{\partial}{\partial cp^\sigma} \Sigma(p) = -\Lambda_\sigma(p, p).} \quad (12.24)$$

Obviously, this relation holds independently of the gauge.

## 12.2 Renormalization Process

We shall here derive expressions for the mass and charge renormalization in terms of counterterms that can be applied in evaluating the QED effects on bound states. The process of regularization will be treated in the next section.

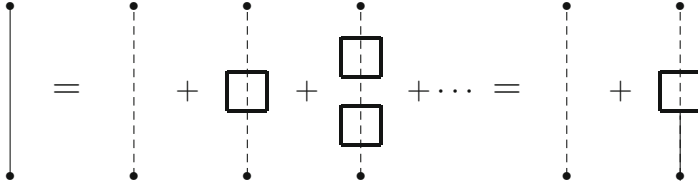


**Fig. 12.3** Dyson equation for the dressed bare-mass electron propagator

### 12.2.1 Mass Renormalization

We consider now a *bare* electron with the mass  $m_0$ . The corresponding free-electron propagator (12.5) is then

$$S_F^{\text{bare}}(\omega, \mathbf{p}) = \frac{1}{\not{p}c - m_0c^2 + i\eta} \beta \tag{12.25}$$

with  $\omega = cp_0$ .

We now “dress” the bare-electron propagator with all kinds of self-energy insertions in the same way as for the bound-electron propagator in Fig. 5.7. This corresponds to the S-matrix in operator form<sup>3</sup>

$$iS_F(\omega, \mathbf{p}) + iS_F(\omega, \mathbf{p})(-i)\Sigma(\omega, \mathbf{p})iS_F(\omega, \mathbf{p}) + \dots = \frac{iS_F(\omega, \mathbf{p})}{1 - \Sigma(\omega, \mathbf{p})S_F(\omega, \mathbf{p})}, \tag{12.26}$$

which leads to

$$S_F^{\text{bare,dressed}}(\omega, \mathbf{p}) = \frac{1}{\not{p}c - m_0c^2 - \beta\Sigma_{\text{bare}}^*(\omega, \mathbf{p}) + i\eta} \beta, \tag{12.27}$$

illustrated in Fig. 12.3. Here, the box represents the *irreducible* or *proper* self-energy insertions,  $\Sigma_{\text{bare}}^*(\omega, \mathbf{p})$ , illustrated in Fig. 12.4. We shall in the following refer to this as the *free-electron self-energy*,  $\Sigma^{\text{free}}(\omega, \mathbf{p})$ ,

$$\Sigma_{\text{bare}}^*(\omega, \mathbf{p}) = \Sigma^{\text{free}}(\omega, \mathbf{p}). \tag{12.28}$$

---

<sup>3</sup>Note that  $\Sigma(\omega, \mathbf{p})$  has the dimension of energy and that the product  $\Sigma(\omega, \mathbf{p})S_F(\omega, \mathbf{p})$  is dimensionfree (see Appendix K).

$$\Sigma^{\text{free}}(p) = \boxed{\text{---}} = \text{---} + \text{---} + \text{---} + \dots$$

**Fig. 12.4** Expansion of the proper self-energy operator for a bare electron

To lowest order the free-electron self-energy is in analogy with (4.86)

$$\Sigma^{\text{free}}(\omega, \mathbf{p}) = i \int \frac{d\omega}{2\pi} S_{\text{F}}^{\text{bare}}(\omega, \mathbf{p}) I^{\text{bare}}(\omega; \mathbf{p}), \quad (12.29)$$

where  $I^{\text{bare}}$  is the interaction (4.44) in the momentum representation with the electronic charge replaced by the bare charge,  $e_0$ .

The bare-electron propagator itself is also associated with a bare-electron charge ( $e_0$ ) at each vertex. The dressing of the electron propagator leads to a modification of the electron mass as well as of the electron charge. One part of the free-electron self-energy is indistinguishable from the mass term in the electron propagator and another part is indistinguishable from the electronic charge, and these parts give rise to the *mass renormalization* and the *charge renormalization*, respectively. The modification of the electron charge is here compensated by a corresponding modification of the vertex (to be discussed below), so that there is no net effect on the electron charge in connection with the electron self-energy. On the other hand, there is a real modification of the electron charge in connection with the modification of the *photon* propagator, as we shall discuss later.

Instead of working with the bare-electron mass and charge with self-energy insertions, we can use the **physical** mass and charge and introduce corresponding *counterterms* (see, for instance, [92, p. 332]). The free-electron propagator with the *physical* electron mass,  $m$ , is (12.5)

$$S_{\text{F}}^{\text{free}}(\omega, \mathbf{p}) = \frac{1}{\not{p} c - mc^2 + i\eta} \beta, \quad (12.30)$$

and it has its poles “**on the mass shell**”,  $\not{p} = mc$  (see Appendix D.33). The dressed propagator (12.27) should have the same pole positions, which leads with

$$m = m_0 + \delta m \quad (12.31)$$

to

$$\boxed{\delta mc^2 = \beta \Sigma^{\text{free}}(\omega, \mathbf{p}) \Big|_{\not{p}=mc}} \quad (12.32)$$

This is the **mass counterterm**. We can now in the dressed operator (12.27) replace  $m_0 c^2$  by

$$mc^2 - \beta \Sigma^{\text{free}}(\omega, \mathbf{p}) \Big|_{\not{p}=mc},$$



which leads to

$$S_F^{\text{free,ren}}(\omega, \mathbf{p}) = \frac{1}{\not{p}c - mc^2 - \beta \Sigma_{\text{ren}}^{\text{free}}(\omega, \mathbf{p}) + i\eta} \beta, \quad (12.33)$$

where

$$\Sigma_{\text{ren}}^{\text{free}}(\omega, \mathbf{p}) = \Sigma^{\text{free}}(\omega, \mathbf{p}) - \Sigma^{\text{free}}(\omega, \mathbf{p}) \Big|_{p/mc}. \quad (12.34)$$

This represents the *mass-renormalization*. Both the free-electron self-energy and the mass counterterms are divergent, while *the renormalized self-energy is finite*.

## 12.2.2 Charge Renormalization

### 12.2.2.1 Electron Self-Energy

The *pole values* (residues) of the dressed bare electron propagator should also be the same as for the physical propagator, including the associated electronic charges. The physical propagator (12.30) with the electronic charge

$$e^2 S_F^{\text{free}}(\omega, \mathbf{p}) = \frac{e^2}{\not{p}c - mc^2 + i\eta} \beta$$

has the pole value  $\beta e^2/c$ . The dressed propagator (12.27) with the bare electron charge is

$$\frac{e_0^2}{\not{p}c - m_0c^2 - \beta \Sigma^{\text{free}}(\omega, \mathbf{p}) + i\eta} \beta = \frac{e_0^2}{\not{p}c - mc^2 - \beta \Sigma_{\text{ren}}^{\text{free}}(\omega, \mathbf{p}) + i\eta} \beta$$

and its pole value at the pole  $\not{p} = mc$  is

$$\lim_{\not{p} \rightarrow mc} \frac{1}{c} \frac{e_0^2 (\not{p} - mc)}{\not{p}c - mc^2 - \beta \Sigma_{\text{ren}}^{\text{free}}(\omega, \mathbf{p}) + i\eta} \beta = \frac{1}{c} \frac{e_0^2}{1 - \beta \frac{\partial}{\partial \not{p}} \Sigma_{\text{ren}}^{\text{free}}(\omega, \mathbf{p}) \Big|_{p/mc} + i\eta} \beta,$$

using l'Hospital's rule. This gives us the relation

$$e^2 = \frac{e_0^2}{1 - \frac{\partial}{\partial c \not{p}} \Sigma_{\text{ren}}^{\text{free}}(\omega, \mathbf{p}) \Big|_{p/mc}} \quad (12.35)$$

or

$$e^2 = e_0^2 \left( 1 + \frac{\partial}{\partial c \not{p}} \Sigma_{\text{ren}}^{\text{free}}(\omega, \mathbf{p}) \Big|_{p/mc} - \dots \right). \quad (12.36)$$

Here, the second term, which is divergent, represents the first-order **charge renormalization**.

The covariant form of the free-electron self-energy, based upon the use of  $\bar{\Psi}$  in the matrix elements is usually expressed as [143, (9.26)]

$$\bar{\Sigma}^{\text{free}}(\omega, \mathbf{p}) = \beta \Sigma^{\text{free}}(\omega, \mathbf{p}) = A + B(\not{p}c - mc^2) + C(\not{p}c - mc^2)^2,$$

which leads to the corresponding non-covariant expression based upon the use of  $\Psi^\dagger$  (see 8.63)

$$\Sigma^{\text{free}}(\omega, \mathbf{p}) = \beta A + B(\alpha^\mu p_\mu c - \beta mc^2) + \beta C(\alpha^\mu p_\mu c - \beta mc^2)^2. \quad (12.37)$$

It then follows that the constant  $A$  is associated to the mass renormalization (12.32),

$$A = \beta \Sigma^{\text{free}}(\omega, \mathbf{p}) \Big|_{p \neq mc} = \delta mc^2 \quad (12.38)$$

and  $B$  with the charge renormalization,

$$B = \frac{\partial}{\partial c p_0} \Sigma^{\text{free}}(\omega, \mathbf{p}) \Big|_{p \neq mc}. \quad (12.39)$$

From (12.36) it follows that for the charge renormalization due to the dressing of the electron propagator becomes

$$e = e_0(1 + B/2 + \dots). \quad (12.40)$$

The constant  $C$  represents the renormalized free-electron self-energy that is finite.

### 12.2.2.2 Vertex Correction

The modification of the vertex function, shown in Fig. 12.2, can be represented by

$$ie_0 \Gamma^\sigma(p, p') = ie_0 \alpha^\sigma + ie_0 \Lambda^\sigma(p, p'), \quad (12.41)$$

where  $e_0$  is the “bare” electron charge. The vertex correction is divergent and can be separated into a divergent part and a renormalized, finite part

$$\Lambda^\sigma(p, p') = L\alpha^\sigma + \Lambda_{\text{ren}}^\sigma(p, p'). \quad (12.42)$$

The divergent vertex part corresponds to a charge renormalization, in first order being

$$e = e_0(1 + \beta L). \quad (12.43)$$

But this should be combined with the charge renormalization due to the dressing of the electron propagators (12.40), which yields

$$e = e_0(1 + \beta L + \beta B), \quad (12.44)$$

since there are two propagators associated with each vertex. Due to the *Ward identity* (12.24), (4.102) we have  $B = -L$  with the consequence that *the charge renormalization due to the electron self-energy and the vertex correction exactly cancel*. This holds also in higher orders.

### 12.2.2.3 Photon Self-Energy

We first transform the first-order photon self-energy (4.110) to the momentum representation, using

$$\begin{aligned} D_{F\nu\mu}(x_1, x_3) &= \int \frac{d^4k}{(2\pi)^4} e^{-ik(x_1-x_3)} D_{F\nu\mu}(k), \\ D_{F\nu\mu}(x_4, x_2) &= \int \frac{d^4k}{(2\pi)^4} e^{-ik'(x_4-x_2)} D_{F\nu\mu}(k'), \\ S_F(x_3, x_4) &= \int \frac{d^4q}{(2\pi)^4} e^{-iq(x_3-x_4)} S_F(q), \\ S_F(x_4, x_3) &= \int \frac{d^4q}{(2\pi)^4} e^{-iq'(x_4-x_3)} S_F(q'). \end{aligned} \quad (12.45)$$

The space integrations over  $x_3$  and  $x_3$  gives rise to the delta functions  $\delta^4(k - q + q')$  and  $\delta^4(k' - q + q')$ , yielding with the bare electron charge  $e_0^2$ ,

$$\begin{aligned} &\int \frac{d^4k}{(2\pi)^4} ie_0^2 \alpha_1^\mu D_{F\nu\mu}(k) i\Pi_{3,4}^{\sigma\tau}(k) ie_0^2 \alpha_2^\nu D_{F\nu\mu}(k), \\ i\Pi_{3,4}^{\sigma\tau}(k) &= \int \frac{d^4q}{(2\pi)^4} \text{Tr}[i\alpha_3^\sigma S_F(q) i\alpha_4^\tau S_F(q-k)]. \end{aligned} \quad (12.46)$$

The photon self-energy represents a modification of the single-photon exchange, illustrated in Fig. 12.5,

$$ie_0^2 D_{F\nu\mu}(k) \Rightarrow ie_0^2 D_{F\nu\mu}(k) + ie_0^2 D_{F\mu\sigma}(k) i\Pi^{\sigma\tau}(k) ie_0^2 D_{F\tau\nu}(k) + \dots \quad (12.47)$$

With the form (4.28) of the photon propagator in the Feynman gauge this becomes

$$\frac{-ie_0^2}{c\epsilon_0} \frac{g_{\mu\nu}}{k^2 + i\eta} \Rightarrow \frac{-ie_0^2}{c\epsilon_0} \frac{g_{\mu\nu}}{k^2 + i\eta} + \frac{-ie_0^2}{c\epsilon_0} \frac{g_{\mu\sigma}}{k^2 + i\eta} i\Pi^{\sigma\tau}(k) \frac{-ie_0^2}{c\epsilon_0} \frac{g_{\tau\nu}}{k^2 + i\eta}. \quad (12.48)$$

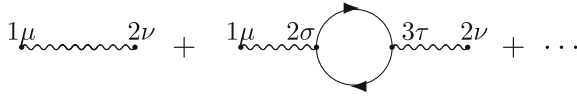


**Fig. 12.5** Diagram representing the first-order vacuum polarization of the single photon (first-order photon self-energy)

From the Lorentz covariance it follows that the polarization tensor must have the form

$$\Pi^{\sigma\tau}(k) = -g^{\sigma\tau}A(k^2) + k^\sigma k^\tau B(k^2), \tag{12.49}$$

and it can be shown that in this case only the second term can contribute [22, p. 155], [143, p. 184]. This reduces the expression above to

$$\begin{aligned} \frac{-ie_0^2}{c\epsilon_0} \frac{g_{\mu\nu}}{k^2 + i\eta} &\Rightarrow \frac{-ie_0^2}{c\epsilon_0} \frac{g_{\mu\nu}}{k^2 + i\eta} \left[ 1 - \frac{e_0^2}{c\epsilon_0} \frac{A(k^2)}{k^2 + i\eta} \right] \\ &\equiv \frac{-ie_0^2}{c\epsilon_0} \frac{g_{\mu\nu}}{k^2 + \left(\frac{e_0^2}{c\epsilon_0}\right)A(k^2) + i\eta}. \end{aligned} \tag{12.50}$$

The expression above represents the modification of the photon propagator due to the photon self-energy. It is infinite and it can be interpreted as a change of the electronic charge—or **charge renormalization**—indexcharge renormalization—in analogy with the mass renormalization treated above.

The photon propagator has a pole at  $k^2 = 0$ , corresponding to the zero photon mass (c.f. the free-electron propagator in (12.5)), and the pole value is proportional to the electron charge squared,  $e_0^2$ . If

$$A(k^2 = 0) = 0, \tag{12.51}$$

then also the modified propagator has a pole at the same place with a pole value proportional to

$$\frac{e_0^2}{1 + \frac{e_0^2}{c\epsilon_0} \frac{dA(k^2)}{dk^2} \Big|_{k^2=0}}. \tag{12.52}$$

This cannot be distinguished from the bare charge and represents the physical electron charge,

$$e^2 = \frac{e_0^2}{1 + \frac{e_0^2}{c\epsilon_0} \frac{dA(k^2)}{dk^2} \Big|_{k^2=0}} \approx e_0^2 \left[ 1 - \frac{e_0^2}{c\epsilon_0} \frac{dA(k^2)}{dk^2} \Big|_{k^2=0} \right], \tag{12.53}$$

which is the charge renormalization.

The polarization tensor may have a finite part that vanishes at  $k^2 = 0$ ,  $\Pi_{\text{ren}}$ , which is the **renormalized photon self-energy**. This is *physically observable*.

### 12.2.2.4 Higher-Order Renormalization

The procedure described above for the first-order renormalization can be extended to higher orders. A second-order procedure has been described by Labzowsky and Mitrushenkov [115] and by Lindgren et al. [127], but we shall not be concerned with that further here.

## 12.3 Bound-State Renormalization. Cut-Off Procedures

Before applying the renormalization procedure, the divergent integrals have to be modified so that they become finite, which is the *regularization procedure*. Details of this process depend strongly on the gauge used. Essentially all QED calculations performed so far have been carried out in the so-called covariant gauges (see Appendix G), preferably the Feynman gauge. As we have mentioned previously, and as will be discussed in more detail in the next chapter, it is essential to be able to perform the calculations in the Coulomb when QED is combined with electron correlation. Therefore, we shall in this chapter consider the renormalization procedures also in the Feynman as well as in the Coulomb gauge.

Several regularization procedures have been developed, and the conceptually simplest ones are the cut-off procedures. The most well-known of these procedures is that of *Pauli-Willars* and another is the so-called *partial-wave regularization*. A more general and more sophisticated procedure is the *dimensional regularization*, which has definite advantages and is frequently used today. We shall consider this process in great detail in the following.

### 12.3.1 Mass Renormalization

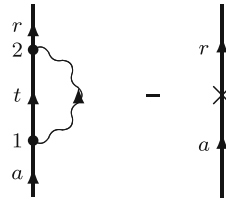
When we express the Dirac Hamiltonian (2.108) with the physical mass

$$\hat{h}_D = c\boldsymbol{\alpha} \cdot \hat{\mathbf{p}} + \beta mc^2 + v_{\text{ext}}, \quad (12.54)$$

we have to include the mass counterterm (12.32) in the perturbation density (6.51)

$$\mathcal{H}(x) = -ec\hat{\psi}^\dagger(x) \alpha^\mu A_\mu(x) \hat{\psi}(x) - \delta mc^2 \hat{\psi}^\dagger(x) \beta \hat{\psi}(x). \quad (12.55)$$

**Fig. 12.6** Diagram representing the renormalization of the first-order self-energy of a bound electron



The bound-electron self-energy operator is given by (4.86)

$$\langle r | \Sigma^{\text{bou}}(\varepsilon_a) | a \rangle = \langle r t | \int \frac{dz}{2\pi} iS_F^{\text{bou}}(\varepsilon_a - z; \mathbf{x}_2, \mathbf{x}_1) I(z; \mathbf{x}_2, \mathbf{x}_1) | t a \rangle, \quad (12.56)$$

and subtracting the corresponding mass-counterterm yields the *renormalized self-energy operator*

$$\langle r | \Sigma_{\text{ren}}^{\text{bou}}(\varepsilon_a) | a \rangle = \langle r | \Sigma^{\text{bou}}(\varepsilon_a) - \beta \delta m c^2 | a \rangle, \quad (12.57)$$

illustrated in Fig. 12.6. Here, both terms contain singularities, which have to be eliminated, which is the regularization process.

In the regularization process due to Pauli and Villars [188], [143, (9.21)], the following replacement is made in the photon propagator

$$\frac{1}{k^2 + i\eta} \Rightarrow \frac{1}{k^2 - \lambda^2 + i\eta} - \frac{1}{k^2 - \Lambda^2 + i\eta}, \quad (12.58)$$

which cuts off the ultraviolet and possible infrared divergence.

### 12.3.2 Evaluation of the Mass Term

(See Mandl and Shaw [143, Sect. 10.2])

On the mass shell,  $\not{p} = mc$ , the free-electron self-energy (12.15) becomes [143, (10.16)]

$$\delta m c^2 = \frac{\beta}{c} [\Sigma^{\text{free}}(p)]_{p=mc} = -i \frac{2e^2}{\epsilon_0} \int \frac{d^4k}{(2\pi)^4} \frac{k + mc}{k^2 - 2pk + i\eta} \frac{1}{k^2 + i\eta}. \quad (12.59)$$

In order to evaluate this integral, we apply the Pauli-Villars regularization scheme, which we can express as

$$\frac{1}{k^2 + i\eta} \Rightarrow \frac{1}{k^2 - \lambda^2 + i\eta} - \frac{1}{k^2 - \Lambda^2 + i\eta} = - \int_{\lambda^2}^{\Lambda^2} \frac{dt}{(k^2 - t + i\eta)^2}. \quad (12.60)$$

By means of the identity (J.4) in Appendix J with  $a = k^2 - t$  and  $b = k^2 - 2pk$  we can express the mass term

$$\delta m c^2 = \frac{4ie^2}{\epsilon_0} \int \frac{d^4k}{(2\pi)^4} \int_{\lambda^2}^{\Lambda^2} dt \int_0^1 dx \frac{(\not{k} + mc)x}{[k^2 - 2pk(1-x) - tx]^3}. \quad (12.61)$$

With the substitutions  $q = -p(1-x)$  and  $s = -tx$  the  $k$  integral becomes, using the integrals (J.8) and (J.9) and  $\not{p} = mc$ ,

$$\int \frac{d^4k}{(2\pi)^4} \frac{(\not{k} + mc)x}{[k^2 + 2qp + s]^3} = \frac{i}{32\pi^2} \frac{mc x(2-x)}{m^2 c^2 (1-x)^2 + tx}, \quad (12.62)$$

yielding

$$\delta m c^2 = \frac{e^2 mc}{8\pi^2 \epsilon_0} \int_0^1 dx (2-x) \ln \frac{\Lambda^2 x + m^2 c^2 (1-x)^2}{\lambda^2 x + m^2 c^2 (1-x)^2}. \quad (12.63)$$

This is logarithmically divergent as  $\Lambda \rightarrow \infty$  with the leading term being

$$\delta m c^2 = \frac{e^2 mc}{8\pi^2 \epsilon_0} \int_0^1 dx (2-x) \left[ \ln \frac{\Lambda^2}{m^2} + \ln \frac{x}{(1-x)^2} \right]. \quad (12.64)$$

To evaluate the second part of the integral we need the following formulas

$$\int dx \ln x = x \ln x - x \quad \int dx x \ln x = \frac{x^2 \ln x}{2} - \frac{x^2}{4}, \quad (12.65)$$

which leads to

$$I = \int_0^1 dx (2-x) \ln \frac{x}{(1-x)^2} = \frac{3}{4}. \quad (12.66)$$

In all unit systems with  $\hbar = 1$  the factor  $e^2/4\pi\epsilon_0 = c\alpha$ , where  $\alpha$  is the fine-structure constant (see Appendix K), and the mass term (12.59) becomes

$$\boxed{\delta m(\Lambda) c^2 = \frac{3\alpha mc^2}{2\pi} \left( \ln \left( \frac{\Lambda}{mc} \right) + \frac{1}{4} \right)}. \quad (12.67)$$

### 12.3.3 Bethe's Nonrelativistic Treatment

Bethe's original non-relativistic treatment of the Lamb shift [19] is of great historical interest, and it also gives some valuable insight into the physical process. Therefore, we shall briefly summarize it here.

From the relation (4.91) we have the bound-state self-energy, using the Feynman gauge (4.55),

$$\langle \mathbf{x}_2 | \Sigma^{\text{bou}}(\varepsilon_a) | \mathbf{x}_1 \rangle = -\frac{e^2 c}{4\pi\epsilon_0 r_{12}} \langle \mathbf{x}_2 | \alpha_\mu | t \rangle \int_0^\infty \frac{d\kappa \sin \kappa r_{12}}{\varepsilon_a - \varepsilon_t - c\kappa \operatorname{sgn} \varepsilon_t} \langle t | \alpha^\mu | \mathbf{x}_1 \rangle, \quad (12.68)$$

where  $r_{12} = |\mathbf{x}_1 - \mathbf{x}_2|$ . For small  $k$  values and positive intermediate states, this reduces to

$$\Sigma^{\text{bou}}(\varepsilon_a) = -\frac{e^2 c}{4\pi^2 \epsilon_0} \alpha_\mu | t \rangle \int_0^\infty \frac{\kappa d\kappa}{\varepsilon_a - \varepsilon_t - c\kappa} \langle t | \alpha^\mu. \quad (12.69)$$

The scalar part of  $\alpha_\mu \alpha^\mu$  cancels in the renormalization, leaving only the vector part to be considered,

$$\Sigma^{\text{bou}}(\varepsilon_a) = \frac{e^2 c}{4\pi^2 \epsilon_0} \boldsymbol{\alpha} | t \rangle \cdot \int_0^\infty \frac{\kappa d\kappa}{\varepsilon_a - \varepsilon_t - c\kappa} \langle t | \boldsymbol{\alpha}. \quad (12.70)$$

The corresponding operator for a *free electron* in the state  $\mathbf{p}_+$  (see Fig. 12.1) is

$$\Sigma^{\text{free}}(\mathbf{p}_+) = \frac{e^2 c}{4\pi^2 \epsilon_0} \boldsymbol{\alpha} | \mathbf{q}_+ \rangle \cdot \int_0^\infty \frac{\kappa d\kappa}{\varepsilon_{\mathbf{p}_+} - \varepsilon_{\mathbf{q}_+} - c\kappa} \langle \mathbf{q}_+ | \boldsymbol{\alpha}, \quad (12.71)$$

restricting the intermediate states to *positive* energies. In the momentum representation this becomes

$$\langle \mathbf{p}'_+ | \Sigma^{\text{free}}(\mathbf{p}_+) | \mathbf{p}_+ \rangle = \frac{e^2 c}{4\pi^2 \epsilon_0} \langle \mathbf{p}'_+ | \boldsymbol{\alpha} | \mathbf{q}_+ \rangle \cdot \int_0^\infty \frac{\kappa d\kappa}{\varepsilon_{\mathbf{p}_+} - \varepsilon_{\mathbf{q}_+} - c\kappa} \langle \mathbf{q}_+ | \boldsymbol{\alpha} | \mathbf{p}_+ \rangle. \quad (12.72)$$

But since  $\boldsymbol{\alpha}$  is diagonal with respect to the momentum, we must have  $\mathbf{q} = \mathbf{p} = \mathbf{p}'$ . Thus,

$$\langle \mathbf{p}'_+ | \Sigma^{\text{free}}(\mathbf{p}_+) | \mathbf{p}_+ \rangle = -\delta_{\mathbf{p}' \cdot \mathbf{p}}^3 \frac{e^2}{4\pi^2 \epsilon_0} |\langle \mathbf{p}_+ | \boldsymbol{\alpha} | \mathbf{p}_+ \rangle|^2 \int_0^\infty d\kappa. \quad (12.73)$$

Obviously, this quantity is infinite. Inserting a set of complete states, this becomes

$$\langle \mathbf{p}'_+ | \Sigma^{\text{free}}(\mathbf{p}_+) | \mathbf{p}_+ \rangle = -\delta_{\mathbf{p}' \cdot \mathbf{p}}^3 \frac{e^2}{4\pi^2 \epsilon_0} \langle \mathbf{p}_+ | \boldsymbol{\alpha} | t \rangle \cdot \langle t | \boldsymbol{\alpha} | \mathbf{p}_+ \rangle \int_0^\infty d\kappa. \quad (12.74)$$

The free-electron self-energy operator can then be expressed

$$\Sigma^{\text{free}}(\mathbf{p}_+) = -\delta_{\mathbf{p}' \cdot \mathbf{p}}^3 \frac{e^2}{4\pi^2 \epsilon_0} \boldsymbol{\alpha} | t \rangle \cdot \int_0^\infty d\kappa \langle t | \boldsymbol{\alpha}, \quad (12.75)$$



which should be subtracted from the bound-electron self-energy operator (12.70). We can assume the intermediate states  $t$  to be identical to those in the bound case. This gives the **renormalized self-energy operator**

$$\Sigma_{\text{ren}}^{\text{bou}}(\varepsilon_a) = \frac{e^2}{4\pi^2\epsilon_0} \boldsymbol{\alpha}|t\rangle \cdot \int_0^\infty d\kappa \frac{\varepsilon_a - \varepsilon_t}{\varepsilon_a - \varepsilon_t - c\kappa} \langle t|\boldsymbol{\alpha}. \quad (12.76)$$

The expectation value of this operator in a bound state  $|a\rangle$  yields the renormalized bound-electron self-energy in this approximation, i.e., the corresponding contribution to the physical **Lamb shift**,

$$\langle a | \Sigma_{\text{ren}}^{\text{bou}}(\varepsilon_a) | a \rangle = \frac{e^2}{4\pi^2\epsilon_0 r_{12}} \langle a|\boldsymbol{\alpha}|t\rangle \cdot \langle t|\boldsymbol{\alpha}|a\rangle \int_0^\infty d\kappa \frac{\varepsilon_a - \varepsilon_t}{\varepsilon_a - \varepsilon_t - c\kappa}. \quad (12.77)$$

This result is derived in a covariant Feynman gauge, where the quantized radiation has transverse as well as longitudinal components. In the Coulomb gauge only the former are quantized. Since all three vector components above yield the same contribution, we will get the result in the Coulomb gauge by multiplying by 2/3. Furthermore, in the non-relativistic limit we have  $\boldsymbol{\alpha} \rightarrow \mathbf{p}/c$ , which leads to

$$\langle a | \Sigma_{\text{ren}}^{\text{bou}}(\varepsilon_a) | a \rangle = \frac{e^2}{6\pi^2 c^2 \epsilon_0 r_{12}} \langle a|\mathbf{p}|t\rangle \cdot \langle t|\mathbf{p}|a\rangle \int_0^\infty d\kappa \frac{\varepsilon_a - \varepsilon_t}{\varepsilon_a - \varepsilon_t - c\kappa}, \quad (12.78)$$

which is essentially the result of Bethe.

Numerically, Bethe obtained the value 1040 MHz for the shift in the first excited state of the hydrogen atom, which is very close to the value 1000 MHz obtained experimentally by Lamb and Retherford. Later, the experimental shift has been determined to be about 1057 MHz. Bethe's results was, of course, partly fortuitous, considering the approximations made. However, it was the first successful performance of a renormalization procedure and represented a breakthrough in the theory of QED.

We can note that the non-relativistic treatment leads to a *linear* divergence of the self-energy, while the relativistic treatment above gives only a *logarithmic* divergence.

### 12.3.4 Brown-Langer-Schaefer Regularization

The bound-state electron propagator can be expanded into a zero-potential term, a one-potential term and a many-potential term

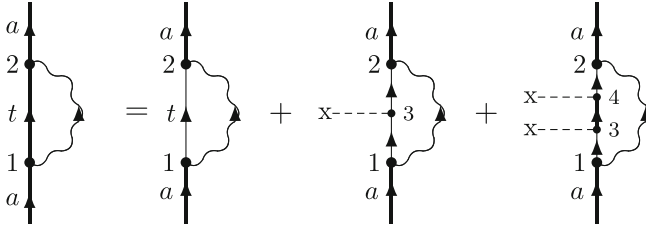


**Fig. 12.7** Expanding the bound-state self-energy in free-electron states according to (4.109)

$$\begin{aligned}
 S_F^{\text{bou}}(\omega, \mathbf{x}_2, \mathbf{x}_1) &= S_F^{\text{free}}(\omega, \mathbf{x}_2, \mathbf{x}_1) \\
 &+ \int d^3\mathbf{x}_3 S_F^{\text{free}}(\omega, \mathbf{x}_2, \mathbf{x}_3) v(\mathbf{x}_3) S_F^{\text{free}}(\omega, \mathbf{x}_3, \mathbf{x}_1) \\
 &+ \int d^3\mathbf{x}_3 d^3\mathbf{x}_4 S_F^{\text{free}}(\omega, \mathbf{x}_2, \mathbf{x}_4) v(\mathbf{x}_4) S_F^{\text{bou}}(\omega, \mathbf{x}_4, \mathbf{x}_3) v(\mathbf{x}_3) S_F^{\text{free}}(\omega, \mathbf{x}_3, \mathbf{x}_1),
 \end{aligned}
 \tag{12.79}$$

which leads to the expansion of the bound-electron self-energy, as illustrated in Fig. 12.7,

$$\begin{aligned}
 \langle a | \Sigma^{\text{bou}}(\varepsilon_a) | a \rangle &= \langle a | \int \frac{dz}{2\pi} S_F^{\text{free}}(\varepsilon_a - z; \mathbf{x}_2, \mathbf{x}_1) I(z; \mathbf{x}_2, \mathbf{x}_1) | ta \rangle \\
 &+ \langle a | \int d^3\mathbf{x}_3 \int \frac{dz}{2\pi} S_F^{\text{free}}(\varepsilon_a - z; \mathbf{x}_2, \mathbf{x}_3) v(\mathbf{x}_3) S_F^{\text{free}}(\varepsilon_a - z; \mathbf{x}_3, \mathbf{x}_1) I(z; \mathbf{x}_2, \mathbf{x}_1) | ta \rangle \\
 &+ \langle a | \int d^3\mathbf{x}_3 d^3\mathbf{x}_4 \int \frac{dz}{2\pi} \int d^3\mathbf{x}_3 d^3\mathbf{x}_4 S_F^{\text{free}}(\omega, \mathbf{x}_2, \mathbf{x}_4) v(\mathbf{x}_4) S_F^{\text{bou}}(\omega, \mathbf{x}_4, \mathbf{x}_3) v(\mathbf{x}_3) \\
 &\times S_F^{\text{free}}(\omega, \mathbf{x}_3, \mathbf{x}_1) I(z; \mathbf{x}_2, \mathbf{x}_1) | ta \rangle,
 \end{aligned}
 \tag{12.80}$$

where  $I(z; \mathbf{x}_2, \mathbf{x}_1)$  represents the single-photon interaction (4.45). We can then express this as

$$\langle a | \Sigma^{\text{bou}}(\varepsilon_a) | a \rangle = \langle a | \Sigma_{\text{free}}(\varepsilon_a) | a \rangle - \langle a | e c A_\sigma A_{\text{free}}^\sigma(\varepsilon_a) | a \rangle + \langle a | \Sigma^{\text{mp}} | a \rangle. \tag{12.81}$$

Here, the first term on the r h s is the average of the free-electron self-energy in the bound state  $|a\rangle$ , the second term a vertex correction (4.99) with  $v(\mathbf{x}) = -e\alpha_\sigma A^\sigma$ , and the last term the “many-potential” term.

We can now use the expansion (12.37) of the free-electron self-energy in (12.81), where the first term ( $A$ ) will be eliminated by the mass-counterterm in (12.57). We are then left with the average of the mass-renormalized free-electron self-energy (12.34), which is still charge divergent. If we separate the vertex operator in a divergent and a renormalized part according to (12.42), it follows from (12.44) that the charge-divergent parts cancel, and we are left with three finite contributions, the mass-renormalized free-electron self-energy (12.34), the many-potential term (12.79) and the finite part of the vertex correction (12.42)

$$\langle r | \Sigma_{\text{ren}}^{\text{bou}}(\varepsilon_a) | a \rangle = \langle r | \Sigma_{\text{ren}}^{\text{free}}(\varepsilon_a) | a \rangle - \langle r | e A_\sigma A_{\text{free,ren}}^\sigma(\varepsilon_a) | a \rangle + \langle r | \Sigma^{\text{mp}} | a \rangle. \quad (12.82)$$

This is the method of Brown, Langer, and Schaefer [37], introduced already in 1959. It was first applied by Brown and Mayers [38] and later by Desidero and Johnson [56], Cheng et al. [45, 46] and others. The problem in applying this expression lies in the many-potential term, but Blundell and Snyderman [28] have devised a method of evaluating this terms numerically with high accuracy (and the remaining terms analytically).

We can also express the renormalized, bound self-energy (12.57) as

$$\langle r | \Sigma_{\text{ren}}^{\text{bou}}(\varepsilon_a) | a \rangle = \left( \langle r | \Sigma^{\text{bou}}(\varepsilon_a) | a \rangle - \langle r | \Sigma^{\text{free}}(\varepsilon_a) | a \rangle \right) + \left( \langle r | \Sigma^{\text{free}}(\varepsilon_a) | a \rangle - \langle r | \beta \delta m c^2 | a \rangle \right), \quad (12.83)$$

where the second term is the renormalized free-electron self-energy (12.34), evaluated between bound states. This is illustrated in Fig. 12.8. The mass term can be evaluated by expanding the bound states in momentum representation

$$\langle r | \beta \delta m c^2 | a \rangle = \langle r | \mathbf{p}', r' \rangle \langle \mathbf{p}', r' | \Sigma^{\text{free}}(\varepsilon_p) | \mathbf{p}, r \rangle \langle \mathbf{p}, r | a \rangle, \quad (12.84)$$

as illustrated in Fig. 12.9. The relation (12.83) can then be written

$$\langle r | \Sigma_{\text{ren}}^{\text{bou}}(\varepsilon_a) | a \rangle = \langle r | \Sigma^{\text{bou}}(\varepsilon_a) - \Sigma^{\text{free}}(\varepsilon_a) | a \rangle + \langle r | \mathbf{p}', r' \rangle \langle \mathbf{p}', r' | \Sigma^{\text{free}}(\varepsilon_a) - \Sigma^{\text{free}}(\varepsilon_p) | \mathbf{p}, r \rangle \langle \mathbf{p}, r | a \rangle, \quad (12.85)$$

where we note that the in the last term the energy parameter of the self-energy operator is equal to the energy of the free particle.

In this way the leading mass-divergence term is eliminated, while the parts are still charge-divergent, but this divergence is cancelled between the parts. The elimination of the mass-renormalization improves the numerical accuracy.

Peter Mohr has developed the method further and included also the one-potential part of the expansion in the two parts, thereby eliminating also the charge divergence. In this way very accurate self-energies have been evaluated for hydrogenic systems [153, 155, 157].

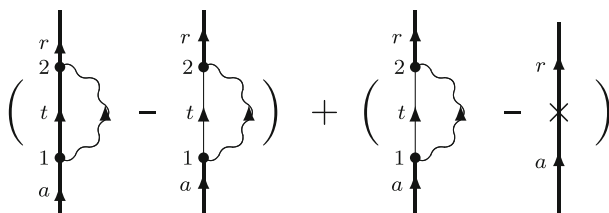
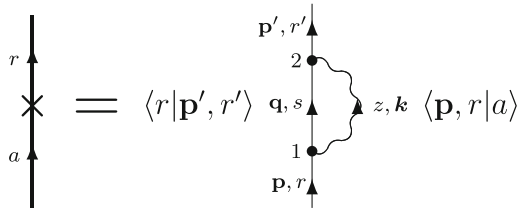


Fig. 12.8 Illustration of the method of Brown, Langer and Schaefer

**Fig. 12.9** Expansion of the mass term in momentum space



### 12.3.5 Partial-Wave Regularization

An alternative scheme for regularizing the electron self-energy is known as the *partial-wave regularization* (PWR), introduced independently by the Gothenburg and Oxford groups [128, 201].

#### 12.3.5.1 Feynman Gauge

Using the expansion (8.33)

$$\frac{\sin \kappa r_{12}}{\kappa r_{12}} = \sum_{l=0}^{\infty} (2l+1) j_l(\kappa r_1) j_l(\kappa r_2) \mathbf{C}^l(1) \cdot \mathbf{C}^l(2), \quad (12.86)$$

the expression (4.91) for the bound-state self-energy in the Feynman gauge can be expressed

$$\Sigma^{\text{bou}}(\varepsilon_a) = -\frac{e^2}{4\pi^2 \varepsilon_0} \sum_{l=0}^{\infty} (2l+1) \int_0^{\infty} c\kappa \, d\kappa \frac{\alpha_{\mu} j_l(\kappa r) \mathbf{C}^l |t\rangle \cdot \langle t | \alpha^{\mu} j_l(\kappa r) \mathbf{C}^l}{\varepsilon_a - \varepsilon_t - c\kappa \operatorname{sgn}(\varepsilon_t)} \quad (12.87)$$

with a summation over the intermediate bound state  $|t\rangle$ . Similarly, for the free electron

$$\Sigma^{\text{free}}(\omega) = -\frac{e^2}{4\pi^2 \varepsilon_0} \sum_{l=0}^{\infty} (2l+1) \int_0^{\infty} c\kappa \, d\kappa \frac{\alpha_{\mu} j_l(\kappa r) \mathbf{C}^l |\mathbf{q}, s\rangle \cdot \langle \mathbf{q}, s | \alpha^{\mu} j_l(\kappa r) \mathbf{C}^l}{\omega - \varepsilon_q - c\kappa \operatorname{sgn}(\varepsilon_q)}, \quad (12.88)$$

summed over free-electron states  $|\mathbf{q}, r\rangle$ . Here,  $\omega$  is the free-running energy parameter and  $\varepsilon_q$  represents the energy of the free-electron state  $|\mathbf{q}, s\rangle$ . *On the mass shell*,  $\omega = \varepsilon_p = \sqrt{c^2 \mathbf{p}^2 + m^2 c^4}$ , this becomes

$$\Sigma^{\text{free}}(\varepsilon_p) = -\frac{e^2}{4\pi^2 \varepsilon_0} \sum_{l=0}^{\infty} (2l+1) \int_0^{\infty} c\kappa \, d\kappa \frac{\alpha_{\mu} j_l(\kappa r) \mathbf{C}^l |\mathbf{q}, s\rangle \cdot \langle \mathbf{q}, s | \alpha^{\mu} j_l(\kappa r) \mathbf{C}^l}{\varepsilon_p - \varepsilon_q - c\kappa \operatorname{sgn}(\varepsilon_q)}. \quad (12.89)$$

The PWR can be combined with the Brown-Langer-Schaefer method discussed above by expanding the remaining terms in (12.83) in a similar way.

The free-electron self-energy is diagonal with respect to the to the momentum  $\mathbf{p}$ , when all partial waves are included, but this is NOT the case for a truncated sum. Furthermore, it has non-diagonal elements with respect to the spinor index  $r$ .

### 12.3.5.2 Coulomb Gauge

In analogy with the Feynman-gauge result (12.87), the *transverse* part of the self-energy in Coulomb gauge becomes

$$\begin{aligned} \Sigma^{\text{bou,trans}}(\varepsilon_a) = & -\frac{e^2}{4\pi^2\varepsilon_0} \sum_{l=0}^{\infty} (2l+1) \int_0^{\infty} c\kappa \, d\kappa \\ & \times \frac{\alpha j_l(\kappa r) \mathbf{C}^l |t\rangle \cdot \langle t | \alpha j_l(\kappa r) \mathbf{C}^l - (\boldsymbol{\alpha} \cdot \nabla) j_l(\kappa r) \mathbf{C}^l |t\rangle \langle t | (\boldsymbol{\alpha} \cdot \nabla) j_l(\kappa r) \mathbf{C}^l / \kappa^2}{\varepsilon_a - \varepsilon_t - c\kappa \operatorname{sgn}(\varepsilon_t)}, \end{aligned} \quad (12.90)$$

using the expression (4.93). The corresponding mass term becomes in analogy with (12.89)

$$\begin{aligned} \Sigma^{\text{free,trans}}(\varepsilon_p) = & -\frac{e^2}{4\pi^2\varepsilon_0} \sum_{l=0}^{\infty} (2l+1) \int_0^{\infty} c\kappa \, d\kappa \\ & \times \frac{\alpha j_l(\kappa r) \mathbf{C}^l | \mathbf{q}, s\rangle \cdot \langle \mathbf{q}, s | \alpha j_l(\kappa r) \mathbf{C}^l - (\boldsymbol{\alpha} \cdot \nabla) j_l(\kappa r) \mathbf{C}^l | \mathbf{q}, s\rangle \langle \mathbf{q}, s | (\boldsymbol{\alpha} \cdot \nabla) j_l(\kappa r) \mathbf{C}^l / \kappa^2}{\varepsilon_p - \varepsilon_{\mathbf{q},s} - c\kappa \operatorname{sgn}(\varepsilon_q)}. \end{aligned} \quad (12.91)$$

The *Coulomb part* in Coulomb gauge is obtained similarly from (4.94)

$$\begin{aligned} \Sigma(\varepsilon_a)^{\text{bou,Coul}} = & \frac{e^2}{8\pi^2\varepsilon_0 r_{12}} \operatorname{sgn}(\varepsilon_t) \\ & \times \sum_{l=0}^{\infty} (2l+1) \int_0^{\infty} 2\kappa \, d\kappa j_l(\kappa r) \mathbf{C}^l |t\rangle \cdot \langle t | j_l(\kappa r) \mathbf{C}^l, \end{aligned} \quad (12.92)$$

using the value  $-i \operatorname{sgn}(\varepsilon_t)/2$  for the integral, and the corresponding mass term

$$\begin{aligned} \Sigma(\varepsilon_a)^{\text{free,Coul}} = & \frac{e^2}{8\pi^2\varepsilon_0 r_{12}} \operatorname{sgn}(\varepsilon_t) \\ & \times \sum_{l=0}^{\infty} (2l+1) \int_0^{\infty} 2\kappa \, d\kappa j_l(\kappa r) \mathbf{C}^l | \mathbf{q}, s\rangle \cdot \langle \mathbf{q}, s | j_l(\kappa r) \mathbf{C}^l. \end{aligned} \quad (12.93)$$

The main advantage of the PWR is that the bound- and free-electron self-energies are calculated in exactly the same way, which improves the numerical accuracy, compared to the standard procedure, where the mass term is evaluated analytically (12.67). Since all terms are here finite, no further regularization is needed. The maximum  $L$  value,  $L_{\max}$ , is increased until sufficient convergence is achieved. This scheme has been successfully applied in a number of cases [128, 201].

It has been shown by Persson, Salomonson, and Sunnergren [191], that the method of PWR gives the correct result in lowest order with an arbitrary number of Coulomb interactions, while a correction term is needed when there is more than one magnetic interaction. This is due to the double summation over partial waves and photon momenta, which is not unique due to the infinities involved.

## 12.4 Dimensional Regularization in Feynman Gauge\*

The most versatile regularization procedure developed so far is the *dimensional regularization*, which is nowadays frequently used in various branches of field theory. In treating the number of dimensions ( $D$ ) as a continuous variable, it can be shown that the integrals of the radiative effects are singular only when  $D$  is an integer. Then by choosing the dimensionality to be  $4 - \epsilon$ , where  $\epsilon$  is a small, positive quantity, the integrals involved will be well-defined and finite. After the renormalization one lets the parameter  $\epsilon \rightarrow 0$ . This method has been found to preserve the gauge invariance and the validity of the Ward identity to all orders. The method was developed mainly by 't Hooft and Veltman in the 1970's [241] (see, for instance, Mandl and Shaw [143, Chap. 10], Peskin and Schroeder [194, Chap. 7] and Snyderman [231]).

### 12.4.1 Evaluation of the Renormalized Free-Electron Self-Energy in Feynman Gauge

We start now from the form (12.14) of the free-electron self-energy in the *Feynman gauge* and the photon propagator in momentum space (4.28)

$$\begin{aligned} \beta \Sigma^{\text{free}}(p) &= ie^2 c^2 \int \frac{d^4 k}{(2\pi)^4} \gamma^\nu \frac{\not{p} - \not{k} + mc}{(p-k)^2 - m^2 c^2 + i\eta} \gamma^\mu D_{F\nu\mu}(k) \\ &= -\frac{ie^2 c}{\epsilon_0} \int \frac{d^4 k}{(2\pi)^4} \gamma^\mu \frac{\not{p} - \not{k} + mc}{(p-k)^2 - m^2 c^2 + i\eta} \gamma^\mu \frac{1}{k^2 + i\eta}. \end{aligned} \quad (12.94)$$

Using the Feynman integral (J.2) (second version) with  $a = k^2$  and  $b = (p - k)^2 - m^2c^2$ , this can be expressed

$$\beta \Sigma^{\text{free}}(p) = -\frac{ie^2c}{\epsilon_0} \int_0^1 dx \int \frac{d^4k}{(2\pi)^4} \frac{\gamma_\mu (\not{p} - \not{k} + mc) \gamma^\mu}{[k^2 + (p^2 - 2pk - m^2c^2)x]^2}. \quad (12.95)$$

We shall now evaluate this integral using *non-integral dimension*  $D = 4 - \epsilon$ ,

$$\begin{aligned} \beta \Sigma^{\text{free}}(p) &= -\frac{ie^2c}{\epsilon_0} \int_0^1 dx \int \frac{d^Dk}{(2\pi)^D} \frac{\gamma_\mu (\not{p} - \not{k} + mc) \gamma^\mu}{[k^2 + (p^2 - 2pk - m^2c^2)x]^2} \\ &= \frac{2ie^2c}{\epsilon_0} \int_0^1 dx \int \frac{d^Dk}{(2\pi)^D} \frac{(1 - \epsilon/2)(\not{p} - \not{k}) - (2 - \epsilon/2) mc}{[k^2 + (p^2 - 2pk - m^2c^2)x]^2} \end{aligned} \quad (12.96)$$

after applying the anti-commutation rules for the gamma matrices in Appendix D.62. With the substitutions  $q = -px$  and  $s = (p^2 - m^2c^2)x$  this becomes

$$\beta \Sigma^{\text{free}}(p) = \frac{2ie^2c}{\epsilon_0} \int_0^1 dx \int \frac{d^Dk}{(2\pi)^D} \frac{(1 - \epsilon/2)(\not{p} - \not{k}) - (2 - \epsilon/2) mc}{[k^2 + 2kq + s]^2}, \quad (12.97)$$

which is of the form of (G.23) and (G.24). This leads to

$$\beta \Sigma^{\text{free}}(p) = -\frac{2e^2c(mc)^{-\epsilon}}{\epsilon_0(4\pi)^{D/2}} \int_0^1 dx \frac{\Gamma(\epsilon/2)}{\Gamma(2)} [(1 - \epsilon/2)(\not{p} - \not{p}x) - (2 - \epsilon/2) mc] \left(\frac{m^2c^2}{w}\right)^{\epsilon/2} \quad (12.98)$$

with  $w = q^2 - s = [m^2c^2 - p^2(1 - x)]x$ . The Gamma function can be expanded as (see Appendix G.4)

$$\Gamma(\epsilon/2) = \frac{2}{\epsilon} - \gamma_E + \dots$$

with  $\gamma_E = 0.5722\dots$  being Euler's constant, and furthermore

$$\begin{aligned} \frac{1}{(4\pi)^{D/2}} &= \frac{1}{(4\pi)^2} \left(1 + \frac{\epsilon}{2} \ln 4\pi + \dots\right) \\ \left(\frac{m^2c^2}{w}\right)^{\epsilon/2} &= 1 - \frac{\epsilon}{2} \ln \left(\frac{w}{m^2c^2}\right) + \dots \end{aligned}$$

This yields

$$\begin{aligned} \frac{\Gamma(\epsilon/2)}{(4\pi)^{D/2}} \left(\frac{m^2 c^2}{w}\right)^{\epsilon/2} &= \frac{1}{4\pi^2} (2/\epsilon - \gamma_E + \dots) \left(1 + \frac{\epsilon}{2} \ln 4\pi + \dots\right) \left(1 - \frac{\epsilon}{2} \ln(w/m^2 c^2) + \dots\right) \\ &= \frac{1}{4\pi^2} \left[\Delta - \ln\left(\frac{w}{m^2 c^2} + \dots\right)\right], \end{aligned} \quad (12.99)$$

where

$$\Delta = \frac{2}{\epsilon} - \gamma_E + \ln 4\pi + \dots \quad (12.100)$$

This leads to

$$\begin{aligned} \beta \Sigma^{\text{free}}(p) &= -2K \left[ \int_0^1 dx (\not{p} - \not{p}x - 2mc) \left[ \Delta - \ln\left(\frac{w}{m^2 c^2} + \dots\right) \right] \right. \\ &\quad \left. - \int_0^1 dx (\not{p} - \not{p}x + mc) \right] \end{aligned} \quad (12.101)$$

with

$$K = \frac{e^2 c}{\epsilon_0 (4\pi)^2} = \frac{c^2 \alpha}{4\pi}. \quad (12.102)$$

We write the denominator in (12.98) as

$$w = m^2 c^2 xX; \quad X = 1 - \frac{p^2}{m^2 c^2} (1-x) = [\rho + (1-\rho)x]$$

with

$$\rho = \frac{m^2 c^2 - p^2}{m^2 c^2}. \quad (12.103)$$

We then express the integral (12.101) as  $2K(A + B + C)$  with

$$\begin{aligned} A &= - \int_0^1 dx (\not{p} - \not{p}x - 2mc) \Delta + \int_0^1 dx (\not{p} - \not{p}x - mc), \\ B &= \int_0^1 dx (\not{p} - \not{p}x - 2mc) \ln x, \\ C &= \int_0^1 dx (\not{p} - \not{p}x - 2mc) \ln [\rho + (1-\rho)x]. \end{aligned}$$



To evaluate this integral we can use the formulas (12.65), yielding

$$\int_0^1 dx \ln(1-x) = -1; \quad \int_0^1 dx x \ln(1-x) = -3/4,$$

$$\int_0^1 dx \ln[\rho + (1-\rho)x] = -1 - \frac{\rho \ln \rho}{1-\rho},$$

$$\int_0^1 dx x \ln[\rho + (1-\rho)x] = \frac{\rho}{(1-\rho)} \left(1 + \frac{\rho \ln \rho}{1-\rho}\right) - \frac{1}{4(1-\rho)^2} (1 + 2\rho^2 \ln \rho - \rho^2),$$

which gives

$$A = -(\not{p}/2 - 2mc) \Delta + (\not{p}/2 - mc),$$

$$B = -3 \not{p}/4 + 2mc,$$

$$\begin{aligned} C &= -\frac{\not{p} \rho}{(1-\rho)} \left(1 + \frac{\rho \ln \rho}{1-\rho}\right) + \frac{\not{p}}{4(1-\rho)^2} (1 + 2\rho^2 \ln \rho - \rho^2) - (\not{p} - 2mc) \left(1 + \frac{\rho \ln \rho}{1-\rho}\right) \\ &= \not{p} \left[ -\frac{1}{(1-\rho)} \left(1 + \frac{\rho \ln \rho}{1-\rho}\right) + \frac{\rho^2 \ln \rho}{2(1-\rho)^2} + \frac{1+\rho}{4(1-\rho)} \right] + 2mc \left(1 + \frac{\rho \ln \rho}{1-\rho}\right). \end{aligned}$$

Subtracting the on-the-mass-shell value ( $\not{p} = mc$ ,  $\rho = 0$ ), yields for the A and B terms

$$(A + B)^{\text{ren}} = -\frac{\not{p} - mc}{2} \left( \Delta + \frac{1}{2} \right).$$

For the C term the on-shell value is  $5mc/4$ , yielding

$$C^{\text{ren}} = -\not{p} \left\{ \frac{\rho(2-\rho) \ln \rho}{2(1-\rho)^2} + \frac{\rho}{(1-\rho)} + \frac{3}{4} \right\} + mc \left\{ \frac{2\rho \ln \rho}{1-\rho} + \frac{3}{4} \right\}.$$

The total *on-shell value* (mass-counter term) becomes

$$\boxed{\delta mc^2 = \frac{mc^2 \alpha}{4\pi} (3\Delta + 4 + \dots)}. \quad (12.104)$$

Collecting all parts we obtain the following expression for the *mass-renormalized free-electron self-energy*

$$\beta \Sigma^{\text{free}}(p) = -\frac{c^2 \alpha}{4\pi} \left[ (\not{p} - mc) \left( \Delta + 2 + \frac{\rho}{1-\rho} + \frac{\rho(2-\rho) \ln \rho}{(1-\rho)^2} \right) + \frac{\rho mc}{1-\rho} \left( 1 - \frac{2-3\rho}{1-\rho} \ln \rho \right) \right] \quad (12.105)$$

with  $\rho = (m^2 c^2 - \not{p}^2)/m^2 c^2$ . This agrees with the result of Snyderman [231, 239]. Here,  $\Delta$  represents the *charge divergence*, which vanishes on the mass-shell,  $\not{p} = mc$ .

### 12.4.2 Free-Electron Vertex Correction in Feynman Gauge

Next, we consider the free-electron vertex correction (12.23)

$$\beta \Lambda^\sigma(p', p) = \frac{ie^2}{\epsilon_0} \int \frac{d^4 k}{(2\pi)^4} \gamma^\mu \frac{\not{p}' - \not{k} + mc}{(p' - k)^2 - m^2 c^2 + i\eta} \gamma^\sigma \times \frac{\not{p} - \not{k} + mc}{(p - k)^2 - m^2 c^2 + i\eta} \gamma^\mu \frac{1}{k^2 + i\eta}. \quad (12.106)$$

The Feynman parametrization (J.4), similar to that in the self-energy case,  $a = k^2$ ,  $b = (k - p)^2 - m^2 c^2$ , and  $c = (k - p')^2 - m^2 c^2$ , yields

$$\beta \Lambda^\sigma(p', p) = \frac{2ie^2}{\epsilon_0} \int_0^1 dx \int_0^{1-x} dy \int \frac{d^4 k}{(2\pi)^4} \times \frac{\gamma_\mu (\not{p}' - \not{k} + mc) \gamma^\sigma (\not{p} - \not{k} + mc) \gamma^\mu}{[k^2 + (p^2 - 2pk - m^2 c^2)x + (p'^2 - 2p'k - m^2 c^2)y]^3}.$$

With  $q = -(px + p'y)$  and  $s = p^2 x + p'^2 y - m^2 c^2(x + y)$  the denominator is of the form  $k^2 + 2kq + s$

$$\begin{aligned} \beta \Lambda^\sigma(p', p) &= \frac{2ie^2}{\epsilon_0} \int_0^1 dx \int_0^{1-x} dy \int \frac{d^D k}{(2\pi)^D} \frac{\gamma_\mu (\not{p}' - \not{k} + mc) \gamma^\sigma (\not{p} - \not{k} + mc) \gamma^\mu}{(k^2 + 2kq + s)^3} \\ &= \frac{2ie^2}{c\epsilon_0} \int_0^1 dx \int_0^{1-x} dy [C_0 + C_1 + C_2], \end{aligned}$$

where the index indicates the power of  $k$  involved,

$$C_0 = \int \frac{d^D k}{(2\pi)^D} \frac{\gamma_\mu(\not{p}' + mc)\gamma_\sigma(\not{p} + mc)\gamma^\mu}{(k^2 + 2kq + s)^3},$$

$$C_1 = \int \frac{d^D k}{(2\pi)^D} \frac{\gamma_\mu(-\not{k})\gamma_\sigma(\not{p} + mc)\gamma^\mu + \gamma_\mu(\not{p}' + mc)\gamma_\sigma(-\not{k})\gamma^\mu}{(k^2 + 2kq + s)^3},$$

$$C_2 = \int \frac{d^D k}{(2\pi)^D} \frac{\gamma_\mu \not{k} \gamma_\sigma \not{k} \gamma^\mu}{(k^2 + 2kq + s)^3}.$$

The coefficients  $C_0$  and  $C_1$  are convergent and we can let  $\epsilon \rightarrow 0$ . With the formula (G.23) ( $n = 3$ ) and the contraction formulas (D.62) we then have

$$C_0 = \frac{i}{(4\pi)^2} \frac{(\not{p} + mc)\gamma_\sigma(\not{p}' + mc)}{w}$$

with

$$w = s - q^2 = s - (px + p'y)^2.$$

Similarly, we have for the numerator in  $C_1$

$$\gamma_\mu(-\not{k})\gamma_\sigma(\not{p} + mc)\gamma^\mu + \gamma_\mu(\not{p}' + mc)\gamma_\sigma(-\not{k})\gamma^\mu = 2(\not{p}\gamma_\sigma \not{k} + \not{k}\gamma_\sigma \not{p}') - 8mck_\sigma$$

and with (G.24)

$$C_1 = \frac{i}{(4\pi)^2} \frac{\not{p}\gamma_\sigma \not{q} + \not{q}\gamma_\sigma \not{p}' - 4mck_\sigma}{w}.$$

The  $C_2$  coefficient is divergent and has to be evaluated with more care. Then the situation is analogous to that of the self-energy (12.98). The numerator becomes

$$\gamma_\mu \not{k} \gamma_\sigma \not{k} \gamma^\mu = -(2 - \epsilon) \not{k} \gamma_\sigma \not{k} - \widetilde{\not{k}} \widetilde{\gamma}_\sigma \widetilde{\not{k}}$$

and

$$C_2 = - \int \frac{d^D k}{(2\pi)^D} \frac{(2 - \epsilon) \not{k} \gamma_\sigma \not{k} + \widetilde{\not{k}} \widetilde{\gamma}_\sigma \widetilde{\not{k}}}{(k^2 + 2kq + s)^3},$$

which can be evaluated with (G.25).

The evaluation of the integrals above is straightforward but rather tedious. The complete result is found in [231].

## 12.5 Dimensional Regularization in Coulomb Gauge

### 12.5.1 Free-Electron Self-Energy in the Coulomb Gauge

For our main purpose of combining MBPT and QED it is important to be able to apply the dimension regularization also in the Coulomb gauge. Analytical expressions for this process have been derived by Adkins [1] and further analyzed by Holmberg [88] (see also [122]).

We start from the expression (12.14)

$$\beta \Sigma^{\text{free}}(p) = ie^2 c^2 \int \frac{d^4 k}{(2\pi)^4} \gamma^\nu \frac{\not{p} - \not{k} + mc}{(p-k)^2 - m^2 c^2 + i\eta} \gamma^\mu D_{F\nu\mu}(k). \quad (12.107)$$

For the photon propagator we use the expressions (4.32) and (4.36)

$$D_{F\mu\nu}^C(k; \mathbf{k}) = \frac{1}{c\epsilon_0} \left[ \frac{\delta_{\mu,0}\delta_{\nu,0}}{\mathbf{k}^2} - \delta_{\mu,i}\delta_{\nu,j} \left( g_{ij} + \frac{k_i k_j}{\mathbf{k}^2} \right) \frac{1}{k^2 + i\eta} \right]. \quad (12.108)$$

The three terms in the propagator correspond to the *Coulomb*, *Gaunt* and *scalar-retardation* parts, respectively, of the interaction (4.59).

The **Coulomb part** of the self-energy becomes

$$\frac{ie^2 c}{\epsilon_0} \int \frac{d^4 k}{(2\pi)^4} \frac{\gamma^0 (\not{p} - \not{k} + mc) \gamma^0}{(p-k)^2 - m^2 c^2 + i\eta} \frac{1}{\mathbf{k}^2 + i\eta} \quad (12.109)$$

$$= \frac{ie^2 c}{\epsilon_0} \int \frac{d^4 k}{(2\pi)^4} \frac{\tilde{p} - \tilde{k} + mc}{(p-k)^2 - m^2 c^2 + i\eta} \frac{1}{\mathbf{k}^2 + i\eta}, \quad (12.110)$$

using the commutation rules in Appendix (D.61). With  $q = -p$  and  $s = p^2 - m^2 c^2$  the denominator is of the form  $k^2 + 2kq + s$  and we can apply the formulas (G.26) and (G.27) without any further substitution ( $n = 1$ ). This gives with  $k^0 \rightarrow q^0 = -p^0$ ,  $k_i \rightarrow q_i y = -p_i y$ ,  $\gamma \cdot \mathbf{k} = -\gamma^i k_i \rightarrow -\gamma \cdot \mathbf{p} y$  and  $w = p^2 y^2 + (1-y) y p_0^2 - (p^2 - m^2 c^2) y$

$$\begin{aligned} & \frac{ie^2 c (mc)^\epsilon}{\epsilon_0} \int \frac{d^D k}{(2\pi)^D} \frac{\tilde{p} - \tilde{k} + mc}{k^2 + 2kq + s + i\eta} \frac{1}{\mathbf{k}^2 + i\eta} \\ &= \frac{e^2 c}{\epsilon_0 (4\pi)^{D/2}} \int_0^1 \frac{dy}{\sqrt{y}} [\gamma \cdot \mathbf{p} (1-y) + mc] \frac{\Gamma(\epsilon/2)}{(w/m^2 c^2)^{\epsilon/2}}. \end{aligned}$$

Using (12.99) this yields the Coulomb contribution

$$K \int_0^1 \frac{dy}{\sqrt{y}} (\gamma \cdot \mathbf{p} (1-y) + mc) (\Delta - \ln(yX))$$

with  $K = e^2 c / (\epsilon_0 (4\pi)^2)$  and  $w = m^2 c^2 y X$ ,  $X = 1 + (\mathbf{p}^2 / m^2 c^2)(1 - y)$ . This leads to

$$K \int_0^1 \frac{dy}{\sqrt{y}} \left( (\boldsymbol{\gamma} \cdot \mathbf{p} (1 - y) + mc) \left( \Delta - \ln y - \ln X \right) \right),$$

and the Coulomb part becomes (times  $K$ )

$$\left( \frac{4}{3} \boldsymbol{\gamma} \cdot \mathbf{p} + 2mc \right) \Delta + \left( \frac{32}{9} \boldsymbol{\gamma} \cdot \mathbf{p} + 4mc \right) - \int_0^1 \frac{dy}{\sqrt{y}} \left( (\boldsymbol{\gamma} \cdot \mathbf{p} (1 - y) + mc) \ln X \right). \quad (12.111)$$

The *Gaunt term* becomes, using (12.107) and the second term of (12.108),

$$-\frac{ie^2 c}{\epsilon_0} \int \frac{d^4 k}{(2\pi)^4} \frac{\gamma_i (\not{p} - \not{k} + mc) \gamma^i}{(p - k)^2 - m^2 c^2 + i\eta} \frac{1}{k^2 + i\eta}. \quad (12.112)$$

The denominator is here the same as in the treatment of the self-energy in the Feynman gauge, and we can use much of the results obtained there.<sup>4</sup>

In analogy with (12.95) we then have

$$\begin{aligned} & -\frac{ie^2 c}{\epsilon_0} \int_0^1 dx \int \frac{d^4 k}{(2\pi)^4} \frac{\gamma_i (\not{p} - \not{k} + mc) \gamma^i}{[k^2 + (p^2 - 2pk - m^2 c^2)x]^2} \\ & = -\frac{ie^2 c}{\epsilon_0} \int_0^1 dx \int \frac{d^4 k}{(2\pi)^4} \frac{(3 - \epsilon)mc - (2 - \epsilon)(\not{p} - \not{k}) - \tilde{p} + \tilde{k}}{[k^2 + (p^2 - 2pk - m^2 c^2)x]^2} \end{aligned} \quad (12.113)$$

after inserting the Feynman integral (J.2) and applying the commutation rules in Appendix (D.62).

With the substitutions  $k \rightarrow -q = px$  and  $s = (p^2 - m^2 c^2)x$  the equation above leads after applying (G.23, G.24) in analogy with (12.98) to

$$\begin{aligned} & -\frac{ie^2 c}{\epsilon_0} \int_0^1 dx \int \frac{d^D k}{(2\pi)^D} \frac{(3 - \epsilon)mc - (2 - \epsilon)(\not{p} - \not{k}) - \tilde{p} + \tilde{k}}{[k^2 + 2kq + s]^2} \\ & = \frac{e^2 c}{\epsilon_0 (4\pi)^{D/2}} \int_0^1 dx \left[ (3 - \epsilon)mc - (2 - \epsilon) \not{p} (1 - x) - \tilde{p} (1 - x) \right] \frac{\Gamma(\epsilon/2)}{(w/\epsilon)^{\epsilon/2}} \\ & = \frac{e^2 c}{\epsilon_0 (4\pi)^{D/2}} \int_0^1 dx \left[ -(1 - x)(3\gamma^0 p_0 - \boldsymbol{\gamma} \cdot \mathbf{p}) + 3mc + \epsilon((1 - x) \not{p} - mc) \right] \frac{\Gamma(\epsilon/2)}{(w/\epsilon)^{\epsilon/2}}, \end{aligned}$$

<sup>4</sup>We use the convention that  $\mu, \nu, \dots$  represent all four components (0,1,2,3), while  $i, j, \dots$  represent the vector part (1,2,3).

where  $w = q^2 - s = p^2 x^2 - (p^2 - m^2 c^2)x = m^2 c^2 x Y$ . This yields (times  $K$ )

$$- \int_0^1 dx \left\{ \left[ (1-x)(3\gamma^0 p_0 - \gamma \cdot \mathbf{p}) - 3mc \right] \left[ \Delta - \ln(xY) \right] - 2((1-x) \not{p} - mc) \right\},$$

using the relation (12.99) and the fact that  $\epsilon \Delta \rightarrow 2$  as  $\epsilon \rightarrow 0$ . Then the **Gaunt part** becomes

$$\boxed{\left[ -\frac{1}{2}(3\gamma^0 p_0 - \gamma \cdot \mathbf{p}) - 3mc \right] \Delta - \frac{5}{4}\gamma^0 p_0 - \frac{1}{4}\gamma \cdot \mathbf{p} + mc + \int_0^1 dx \left[ (1-x)(3\gamma^0 p_0 - \gamma \cdot \mathbf{p}) - 3mc \right] \ln Y.} \quad (12.114)$$

Finally, the **scalar-retardation part** becomes similarly, using the third term of (12.108) and the commutation rules (D.60),

$$\begin{aligned} & - \frac{i e^2 c}{\epsilon_0} \int \frac{d^4 k}{(2\pi)^4} \frac{\gamma^i k_i (\not{p} - \not{k} + mc) \gamma^j k_j}{(p-k)^2 - m^2 c^2 + i\eta} \frac{1}{\mathbf{k}^2} \frac{1}{k^2 + i\eta} \\ &= \frac{i e^2 c}{\epsilon_0} \int \frac{d^4 k}{(2\pi)^4} \frac{\gamma^i k_i \gamma^j k_j (\not{p} - \not{k} - mc) - 2\gamma^i k_i (k^j p_j - k^j k_j)}{(p-k)^2 - m^2 c^2 + i\eta} \frac{1}{\mathbf{k}^2} \frac{1}{k^2 + i\eta} \\ &= - \frac{i e^2 c}{\epsilon_0} \int \frac{d^4 k}{(2\pi)^4} \frac{\not{p} - \tilde{k} - mc + 2\gamma^i k_i k^j p_j / \mathbf{k}^2}{(p-k)^2 - m^2 c^2 + i\eta} \frac{1}{k^2 + i\eta} \end{aligned}$$

with  $\gamma^i k_i \gamma^j k_j = -\mathbf{k}^2 = -k_i k_i$ . With the same substitutions as as in the Gaunt case this becomes

$$- \frac{i e^2 c}{\epsilon_0} \int_0^1 dx \int \frac{d^D k}{(2\pi)^D} \frac{\not{p} - \tilde{k} - mc + 2\gamma^i k_i k^j p_j / \mathbf{k}^2}{[k^2 - 2pkx + (p^2 - m^2 c^2)x]^2}. \quad (12.115)$$

With the substitutions  $k \rightarrow -q = px$  and  $s = (p^2 - m^2)x$  the first part is of the form (G.23) and (G.24) and becomes

$$\frac{e^2 c}{\epsilon_0 (4\pi)^{D/2}} \int_0^1 dx \left[ \not{p} - \tilde{p}x - mc \right] \frac{\Gamma(\epsilon/2)}{w^{\epsilon/2}} \quad (12.116)$$

and with (12.99)

$$K \int_0^1 dx \left[ \not{p} - \tilde{p}x - mc \right] \left( \Delta - \ln(xY) \right) \quad (12.117)$$

with  $K = e^2 c / (\epsilon_0 (4\pi)^2)$  and  $w$  being the same as in the Gaunt case,  $w = q^2 - s = p^2 x^2 - p^2 x + m^2 c^2 x = m^2 c^2 x Y$ .

The second part of (12.115) is of the form (G.28) and becomes ( $k_i k^j \rightarrow q_i q^j y^2 = p_i p^j x^2 y^2$  in first term,  $\rightarrow -\frac{1}{2} g_j^i = -\frac{1}{2} \delta_{ij}$  in second)

$$\begin{aligned}
& K \int_0^1 dx \int_0^1 dy \sqrt{y} \left\{ 2\gamma^i p_i p^j p^j \frac{\Gamma(1 + \epsilon/2)}{w^{1+\epsilon/2}} - \gamma^j p_j \frac{\Gamma(\epsilon/2)}{w^{\epsilon/2}} \right\} \\
& K \int_0^1 dx \int_0^1 dy \sqrt{y} \left\{ \frac{2\gamma^i p_i p^j p_j}{m^2 c^2} \frac{xy}{Z} - \gamma^j p_j (\Delta - \ln(xyZ)) \right\} \\
& = K \int_0^1 dx \int_0^1 dy \sqrt{y} \left\{ \frac{2\boldsymbol{\gamma} \cdot \mathbf{p} \mathbf{p}^2}{m^2 c^2} \frac{xy}{Z} + \boldsymbol{\gamma} \cdot \mathbf{p} (\Delta - \ln(xyZ)) \right\}
\end{aligned}$$

with  $w = xy[-\mathbf{p}^2 xy + p_0^2 x - p^2 + m^2 c^2] = xy[\mathbf{p}^2(1 - xy) - p_0^2(1 - x) + m^2 c^2] = m^2 c^2 Zxy$

Integration by parts of the first term yields (times  $K$ ), noting that  $dZ/dy = -\mathbf{p}^2 x$ ,

$$- \int_0^1 dx \left[ \sqrt{y} y 2\boldsymbol{\gamma} \cdot \mathbf{p} \ln Z \right]_0^1 + 3 \int_0^1 dx \int_0^1 dy \sqrt{y} \boldsymbol{\gamma} \cdot \mathbf{p} \ln Z.$$

The total scalar-retardation part then becomes (with  $Z(y = 1) = Y$ )

$$\begin{aligned}
& \int_0^1 dx [\not{p} - \tilde{p}x - mc] (\Delta - \ln(xY)) - \int_0^1 dx 2\boldsymbol{\gamma} \cdot \mathbf{p} \ln Y \\
& + 3 \int_0^1 dx \int_0^1 dy \sqrt{y} \boldsymbol{\gamma} \cdot \mathbf{p} \ln Z + \int_0^1 dx \int_0^1 dy \sqrt{y} \boldsymbol{\gamma} \cdot \mathbf{p} (\Delta - \ln(xyZ))
\end{aligned}$$

or

$$\begin{aligned}
& \int_0^1 dx (\gamma^0 p_0(1 - x) - \boldsymbol{\gamma} \cdot \mathbf{p}(1 + x) - mc) (\Delta - \ln x) + \int_0^1 dy \sqrt{y} \boldsymbol{\gamma} \cdot \mathbf{p} \Delta \\
& - \int_0^1 dx (\gamma^0 p_0(1 - x) - \boldsymbol{\gamma} \cdot \mathbf{p}(1 - x) - mc) \ln Y \\
& - \int_0^1 dx \int_0^1 dy \sqrt{y} \boldsymbol{\gamma} \cdot \mathbf{p} \ln(xy) + 2 \int_0^1 dx \int_0^1 dy \sqrt{y} \boldsymbol{\gamma} \cdot \mathbf{p} \ln(xy) \\
& - 3 \int_0^1 dx \int_0^1 dy \sqrt{y} \boldsymbol{\gamma} \cdot \mathbf{p} \ln Z,
\end{aligned}$$

which gives<sup>5</sup>

---

<sup>5</sup>

$$\begin{aligned}
\int_0^1 dx \int_0^1 dy \sqrt{y} \ln(xy) &= -\frac{10}{9}; & \int_0^1 dx x \int_0^1 dy \sqrt{y} \ln(xy) &= -\frac{1}{18}; \\
\int_0^1 dx x \int_0^1 dy y \sqrt{y} \ln(xy) &= -\frac{9}{50}
\end{aligned}$$

$$\left(\frac{1}{2}\gamma^0 p_0 - \frac{5}{6}\boldsymbol{\gamma} \cdot \mathbf{p} - mc\right)\Delta + \frac{3}{4}\gamma^0 p_0 - \frac{5}{36}\boldsymbol{\gamma} \cdot \mathbf{p} - mc$$

$$- \int_0^1 dx \left(\gamma^0 p_0(1-x) - \boldsymbol{\gamma} \cdot \mathbf{p}(1-x) - mc\right) \ln Y - 3 \int_0^1 dx \int_0^1 dy \sqrt{y} \boldsymbol{\gamma} \cdot \mathbf{p} \ln Z.$$

Summarizing all contributions yields *the mass-renormalized free-electron self-energy in Coulomb gauge*

$$\beta \Sigma^{\text{free}}(p) = -\frac{c^2 \alpha}{4\pi} \left[ -(\not{p} - mc)\Delta - \frac{1}{2}\gamma^0 p_0 + \frac{19}{6}\boldsymbol{\gamma} \cdot \mathbf{p} - \int_0^1 \frac{dy}{\sqrt{y}} (\boldsymbol{\gamma} \cdot \mathbf{p}(1-y) + mc) \ln X \right. \\ \left. + 2 \int_0^1 dx [(1-x)\not{p} - mc] \ln Y + \int_0^1 dx \int_0^1 dy \sqrt{y} 2\boldsymbol{\gamma} \cdot \mathbf{p} \ln Z \right],$$

(12.118)

where we have subtracted the mass term ( $\not{p} = mc$ ),  $mc(3\Delta + 4)$ . (The expressions for  $X$ ,  $Y$ ,  $Z$  are given in the text.) This is in agreement with the result of Adkins [1].

The treatment of the vertex correction is more complex and will not be reproduced here. Interested readers are referred to the papers by Adkins [2] and Holmberg [88].



**Part IV**  
**Dynamical Processes**  
**with Bound States**

## Chapter 13

# Dynamical Bound-State Processes

So far, we have in this book dealt only with **static** problems, i.e., structure-related problems in atomic and molecular physics. Since the perturbations in QED are energy—or time-dependent, we have developed a time-dependent formalism, but we have so far not studied really time-dependent or **dynamical** processes.

The standard procedure for dealing with dynamical processes for free or unbound particles is the  $S$ -matrix formalism. When bound states are involved, however, this procedure may fail due to possible intermediate model-space states, which might make the  $S$ -matrix singular. In the previous chapters we have learned how to handle this problem in connection with static problems, and we shall now see that the same procedure can be used also in dynamical problems.

In energy calculations for static systems we are mainly concerned with the real part of the effective Hamiltonian. It follows from the so-called *optical theorem* for scattering processes that the scattering cross section is proportional to the **imaginary** part of this operator, which explains why essentially the same procedure can be used in the two—seemingly quite different—cases.

We have also seen in Chap. 6 (Sect. 6.8) that the Green's operator for all times can be regarded as the  $S$ -matrix with all intermediate model-space singularities removed. This implies that this concept is ideal for dealing with dynamical processes, involving bound states, and that the whole machinery developed in the previous chapter can be utilized also in this case. This will be demonstrated in this final part of the main text of the book. The presentation here follows mainly that given recently by the Gothenburg group [134].

Experimental tests are presently being performed at GSI in Darmstadt concerning possible QED effects in dynamical processes [7].

## 13.1 Optical Theorem for Free and Bound Particles

A basic tool for dealing with dynamical processes of various kind is the so-called *optical theorem* for free particles (see, for instance, Peskin and Schroeder [194] (Chap. 7), and we begin this part by deriving this theorem and extend it to the case when also *bound states* are involved.

### 13.1.1 Scattering of Free Particles. Optical Theorem

The amplitude  $\tau$  for a scattering process for free particles from an initial state  $|p\rangle$  to a final state  $\langle q|$  is related to the  $S$ -matrix by

$$\langle q|S|p\rangle = 2\pi i\delta(E_p - E_q)\tau(p \rightarrow q), \quad (13.1)$$

where it is assumed that the  $S$ -matrix contains at least one interaction.

It is convenient to introduce the operators  $T$  and  $T^\dagger$  by

$$S = 1 + iT; \quad S^\dagger = 1 - iT^\dagger, \quad (13.2)$$

where  $^\dagger$  represents hermitean adjoint. The relation (13.1) can then be expressed

$$\langle q|T|p\rangle = 2\pi\delta(E_p - E_q)\tau(p \rightarrow q), \quad (13.3)$$

since the unit part of  $S$  does not contribute.

Since  $S$  is unitary, we have

$$1 = SS^\dagger = 1 + i(T - T^\dagger) + T^\dagger T, \quad (13.4)$$

or

$$-i(T - T^\dagger) = T^\dagger T. \quad (13.5)$$

By considering the diagonal element of this equation and inserting a complete set of intermediate states on the rhs, we have

$$-i\langle p|T - T^\dagger|p\rangle = \sum_q \langle p|T^\dagger|q\rangle \langle q|T|p\rangle = \sum_q \langle q|T|p\rangle^* \langle q|T|p\rangle \quad (13.6)$$

or<sup>1</sup>

$$2\text{Im}\langle p|T|p\rangle = \sum_q \langle q|T|p\rangle^* \langle q|T|p\rangle = \sum_q |\langle q|T|p\rangle|^2. \quad (13.7)$$

---

<sup>1</sup>Note that the imaginary part of a complex number,  $z = x + iy$ , is  $y$ , not  $iy$ , i.e., the imaginary part is a **real** number.

The diagonal element of  $T$  represents the *amplitude of the forward-scattering process*.

With the relation (13.3) we then have the important relation

$$\boxed{2\text{Im}\langle p|T|p\rangle \Rightarrow \sum_q |\langle q|T|p\rangle|^2 = \sum_q \left| 2\pi\delta(E_p - E_q)\tau(p \rightarrow q) \right|^2.} \quad (13.8)$$

This implies that *the imaginary part of the forward scattering amplitude is proportional to the total cross section, which is the optical theorem*.

The forward scattering amplitude becomes imaginary when an intermediate state goes on-shell (degenerate with the initial and final states), and therefore we only have to consider these cases. Cutkosky [194, p. 236] has given the following rules for applying the optical theorem to a Feynman diagram:

- Cut through all diagrams of the forward-scattering amplitude in all possible ways such that the cut propagators can simultaneously be put on shell;
- For each cut, replace  $1/(p^2 - m^2 + i\eta)$  by  $-2\pi i\delta(p^2 - m^2)$  in each propagator and then perform the loop integrals;
- Sum the imaginary contributions for all possible cuts.

### 13.1.2 Optical Theorem for Bound Particles

When bound states are involved in the process, **discrete** intermediate model-space states may appear, which require a special treatment, as we have seen in previous chapters, so-called *model-space contributions* (MSC).

We have seen in Chap. 6 (6.91) that the imaginary unit times the  $S$ -matrix for free particles is closely related to the effective interaction or the effective Hamiltonian. In that relation only the perturbed part of the  $S$ -matrix enters, and with the relation (13.2) we can express this as

$$PTP = -2\pi\delta(E_{\text{in}} - E_{\text{out}})W. \quad (13.9)$$

Then we have

$$P\text{Im}(T)P = 2\pi\delta(E_{\text{in}} - E_{\text{out}})\text{Im}(-H_{\text{eff}}), \quad (13.10)$$

since  $PH_0P$  does not have any imaginary part. The corresponding relation holds for the Green's operator (6.90).

- It then follows that the form

$$2\text{Im}\langle p | -H_{\text{eff}} | p \rangle = \sum_q 2\pi \delta(E_p - E_q) \left| \tau(p \rightarrow q) \right|^2 \quad (13.11)$$

**of the optical theorem is valid for free as well as bound particles.**

The optical theorem in its original form is applicable to the scattering of **free** particles, but by transforming it to a form involving the effective Hamiltonian instead of the  $S$ -matrix, it has a form that will hold also when **bound** states are involved.

In order to evaluate  $2\text{Im}(-H_{\text{eff}})$ , we can use the same Cutkosky rules as before, slightly changed:

- Make a cut in all diagrams of the effective Hamiltonian in all possible ways so that the cut state can be degenerate with the initial and final states;
- For each cut, replace the singularity  $1/(A + i\eta)$  by a principle integral and  $-\pi i\delta(A)$  (cf. (4.16)) and for the possible remaining **discrete** degeneracies evaluate the **model-space contributions**;
- Sum all imaginary contributions.

The optical theorem in the form given here is **not** restricted to scattering problems, but can be applied also to other dynamical processes, like atomic transitions, as will be demonstrated in the following section. In the subsection that then follows we shall consider a scattering problem, radiative recombination.

### 13.2 Atomic Transition Between Bound States

As a first application of the Green's-operator technique to study dynamical processes we calculate the transition probability and transition rate of atomic transitions between two bound states (see Sect. 3.1).

The Feynman diagrams in Fig. 13.1 represent the transition (in lowest order) between two bound states, which can be regarded as a scattering process, where

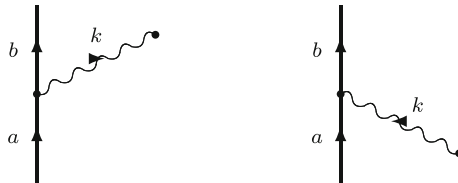
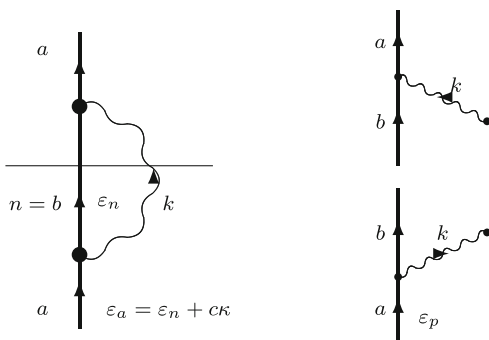


**Fig. 13.1** Lowest-order process in radiative decay (*left*) and photon-induced excitation (*right*). The *solid lines* represent an electron in an initial bound state (**a**) and final bound state (**b**), moving in the nuclear potential. A photon  $k = (c\kappa, -\mathbf{k})$  is emitted

**Fig. 13.2** Applying the optical theorem in lowest order, *left* forward “scattering amplitude”, *right* after the cut



one bound state is transferred to another bound state under the emission (or absorption) of a photon. If the energy of the absorbed photon is large enough, the target may be ionized and the outgoing photon being free (or “quasi-free”). This is the process of *photoionization*, which will be discussed briefly in the next section in connection with the process of *radiative recombination*.

The corresponding “*forward scattering amplitude*” is shown in Fig. 13.2 (left). We assume that the photon-field operators are contracted, but since we shall only be concerned with the imaginary part of the *S*-matrix, we do not have to worry about the singularity and renormalization of the self-energy.

The Green’s operator for all times, which in this case is identical to the *S*-matrix (since there are no model-space contributions, see Chap. 6), is given by means of the Feynman rules for the *S*-matrix (see Appendix H, [143, Chap. 7])

$$\langle a|S|a\rangle = \langle a|\mathcal{G}(\infty, -\infty)|a\rangle = 2\pi\delta(E_{\text{in}} - E_{\text{out}})\langle a|ie\alpha^\mu A_\mu i\Gamma ie\alpha^\nu A_\nu|a\rangle \tag{13.12}$$

or, using the relation (13.9),

$$\langle a|W|a\rangle = \langle a|e\alpha^\mu A_\mu \Gamma e\alpha^\nu A_\nu|a\rangle, \tag{13.13}$$

where  $\Gamma$  is the electron propagator (4.10) or resolvent (2.64)

$$\Gamma = \Gamma(\varepsilon_a) = \frac{|q\rangle\langle q|}{\varepsilon_a - \varepsilon_n - c\kappa + i\eta}, \tag{13.14}$$

$q = (n, k)$  and  $k$  stands for the four-dimensional  $k$  vector  $k = (c\kappa, -\mathbf{k})$ .

The “*forward scattering amplitude*” becomes imaginary only when there is a degeneracy (see the Cutkosky rules above), and we then replace  $1/(A + i\eta)$  by a principle integral and  $-\pi i\delta(A)$ . In the present case we then make the replacement

$$\Gamma \rightarrow \mathcal{P} i\pi\delta(\varepsilon_a - \varepsilon_n - c\kappa), \tag{13.15}$$

i.e., a principal integral and half a pole. This gives

$$\text{Im}\langle a | - H_{\text{eff}} | a \rangle = \pi \delta(\varepsilon_a - \varepsilon_b - c\kappa) \langle a | e c \alpha^\mu A_\mu | q \rangle \langle q | e c \alpha^\mu A_\mu | a \rangle, \quad (13.16)$$

since  $H_0$  does not have any imaginary part, or

$$\boxed{2\text{Im}\langle a | - H_{\text{eff}} | a \rangle = 2\pi \delta(\varepsilon_a - \varepsilon_b - c\kappa) |\langle q | e c \alpha^\mu A_\mu | a \rangle|^2.} \quad (13.17)$$

We assume here that the intermediate state is the degenerate state  $q = (b, k)$ . This degeneracy lies in a *continuum*, since the photon energy is free. Therefore, there is no model-space contribution, which appears only when the degeneracy is a **discrete** state.

The expression (13.17) represents the *decay rate*,  $R_{ab}(\omega)$  (3.9), where  $\omega = c\kappa = \varepsilon_a - \varepsilon_b$ , from the state  $|a\rangle$  to the state  $|b\rangle$ . This relation has been applied by Barberie and Sucher [13] as well as by Sapirstein et al. [215] in studying the decay rate between bound states of hydrogen like ions.

### 13.2.1 Self-Energy Insertion on the Incoming Line

Next, we consider a self-energy insertion on the incoming line of the process in Fig. 13.2. The forward-scattering diagram is given to the left and the situation after a cut at the place indicated to the right. The evolution operator or  $S$ -matrix of the latter becomes after applying the standard Feynman rules

$$\langle a | U | a \rangle = 2\pi \delta(E_{\text{in}} - E_{\text{out}}) \left\langle a \left| i A i \Gamma i A i \Gamma (-i) \Sigma \right| a \right\rangle, \quad (13.18)$$

where  $A = e c \alpha^\mu A_\mu$  and  $\Sigma$  stands for self-energy insertion

$$\Sigma = \Sigma(\varepsilon_a) = \Sigma(\varepsilon_p - c\kappa). \quad (13.19)$$

With the relation (13.9) this becomes

$$\langle a | - W | a \rangle = - \left\langle a \left| A \Gamma A \Gamma \Sigma \right| a \right\rangle. \quad (13.20)$$

The cut indicated in the figure corresponds to the leftmost singularity, when the intermediate state lies in the model space ( $\Gamma_p$ )

$$- \left\langle a \left| A \Gamma_p A \Gamma \Sigma \right| a \right\rangle = - \mathcal{P} + i\pi \delta(\varepsilon_a - \varepsilon_b - c\kappa) \langle a | A | b, k \rangle \langle b, k | A \Gamma \Sigma | a \rangle \quad (13.21)$$

and

$$\langle a | 2\text{Im}(-H_{\text{eff}}) | a \rangle = 2i\pi\delta(\varepsilon_a - \varepsilon_b - c\kappa) \langle a | A | b, k \rangle \langle b, k | A \Gamma \Sigma | a \rangle. \quad (13.22)$$

After the cut *the photon energy is fixed*, and then the other possible bound-state singularity lies in a discrete environment and gives rise to a model-space contribution, as discussed in Chap. 6, involving the derivative of all interactions appearing to the left of the singularity,

$$\langle a | 2\text{Im}(-H_{\text{eff}}) | a \rangle = 2i\pi\delta(\varepsilon_a - \varepsilon_b - c\kappa) \langle a | \frac{\delta}{\delta \mathcal{E}} (A | b, k \rangle \langle b, k | A) | b, k \rangle \langle b, k | \Sigma | a \rangle. \quad (13.23)$$

The other singularity does not correspond to any process where a photon is involved.

There can also be a cut inside the lower self-energy in Fig. 13.3, which corresponds to the inverted process, shown in Fig. 13.4. Then we have instead of (13.22)

$$\langle a | 2\text{Im}(-H_{\text{eff}}) | a \rangle = 2i\pi\delta(\varepsilon_a - \varepsilon_b - c\kappa) \langle a | \Sigma \Gamma A | b, k \rangle \langle b, k | A | a \rangle. \quad (13.24)$$

In this case there is a model-space contribution due to the leftmost singularity, yielding

$$\langle a | 2\text{Im}(-H_{\text{eff}}) | a \rangle = 2i\pi\delta(\varepsilon_a - \varepsilon_b - c\kappa) \langle a | \left( \frac{\delta \Sigma(\mathcal{E})}{\delta \mathcal{E}} \right)_{\mathcal{E}=\varepsilon_a} | a \rangle \langle a | A | b, k \rangle \langle b, k | A | a \rangle. \quad (13.25)$$

**Fig. 13.3** Self-Energy insertion on the incoming line

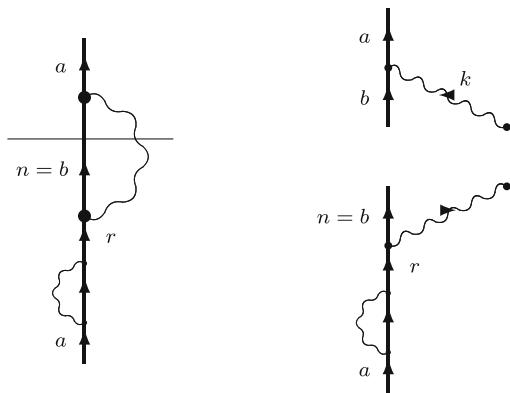
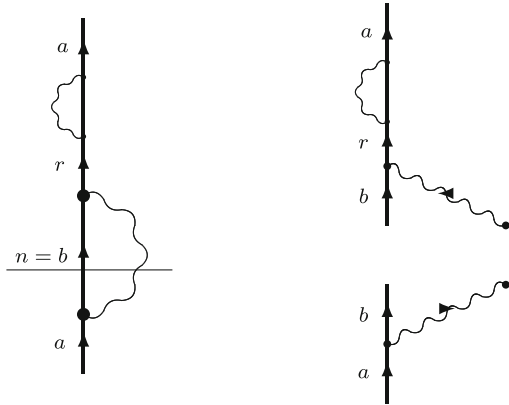




**Fig. 13.4** Inversion of diagram in Fig. 13.3



The non-singular contributions become

$$-\langle a | A \Gamma_P A \Gamma \Sigma | a \rangle = -P + i\pi \delta(\varepsilon_a - \varepsilon_b - c\kappa) \langle a | A | b, k \rangle \langle b, k | A \Gamma_Q \Sigma | a \rangle \quad (13.26)$$

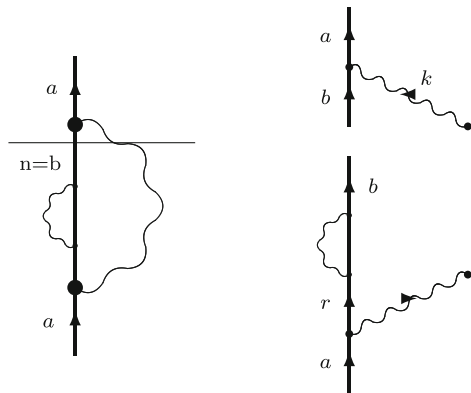
and

$$\langle a | 2\text{Im}(-H_{\text{eff}}) | a \rangle = 2i\pi \delta(\varepsilon_a - \varepsilon_b - c\kappa) \langle a | A | b, k \rangle \langle b, k | A \Gamma_Q \Sigma | a \rangle. \quad (13.27)$$

### 13.2.2 Self-Energy Insertion on the Outgoing Line

The self-energy insertion on the outgoing line is indicated in Fig. 13.5. In applying the optical theorem we can here cut the diagram at two places. Cutting the diagram at the upper singularity (indicated in the figure), yields

**Fig. 13.5** Self-energy insertion on the outgoing line



$$\langle a | 2\text{Im}(-H_{\text{eff}}) | a \rangle = 2i\pi\delta(\varepsilon_a - \varepsilon_b - c\kappa) \langle a | A | b, k \rangle \langle b, k | A \Sigma \Gamma A | a \rangle. \quad (13.28)$$

Here, the model-space contribution becomes

$$\langle a | 2\text{Im}(-H_{\text{eff}}) | a \rangle = 2i\pi\delta(\varepsilon_a - \varepsilon_b - c\kappa) \langle a | \frac{\delta}{\delta \mathcal{E}} \left( A | b, k \rangle \langle b, k | A \Sigma(\mathcal{E}) \right)_{\mathcal{E}=\varepsilon_a} | b, k \rangle \langle b, k | A | a \rangle. \quad (13.29)$$

Cutting the diagram at the lower singularity, yields

$$= 2i\pi\delta(\varepsilon_a - \varepsilon_b - c\kappa) \langle a | A \Gamma \Sigma A | b, k \rangle \langle b, k | A | a \rangle \quad (13.30)$$

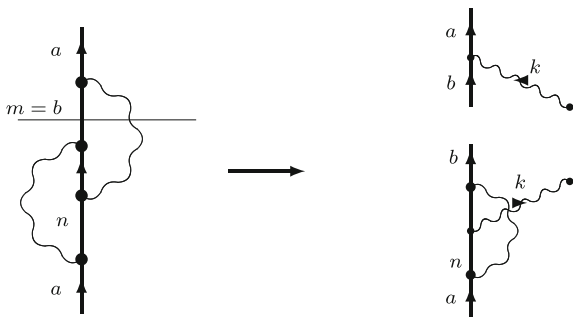
with the model-space contribution

$$\langle a | 2\text{Im}(-H_{\text{eff}}) | a \rangle = 2i\pi\delta(\varepsilon_a - \varepsilon_b - c\kappa) \langle a | \left( \frac{\delta \Sigma(\mathcal{E})}{\delta \mathcal{E}} \right)_{\mathcal{E}=\varepsilon_a} | b, k \rangle \langle b, k | A \Sigma \Gamma A | a \rangle. \quad (13.31)$$

### 13.2.3 Vertex Correction

A vertex correction on the first-order atomic transition in Fig. 13.2 is illustrated in Fig. 13.6 with the cut at the upper singularity. This leads to the  $S$ -matrix

**Fig. 13.6** Vertex correction on the atomic transition



$$\langle a|S|a\rangle = 2\pi\delta(E_{\text{in}} - E_{\text{out}})\langle a| -i\Lambda i\Gamma iA|p\rangle \quad (13.32)$$

with contractions between the field operators.  $\Lambda$  stands for the vertex-correction interaction  $\Lambda = ec\Lambda^\mu A_\mu$  (see Sect. 12.1.3). The corresponding part of the effective interaction becomes

$$\langle a| -W|a\rangle = \langle a|\Lambda\Gamma A|a\rangle. \quad (13.33)$$

A cut at the propagator yields the imaginary part

$$2\text{Im}\langle a| -H_{\text{eff}}|a\rangle = 2\pi\delta(\varepsilon_a - \varepsilon_b - c\kappa)\langle p|\Lambda|b, k\rangle\langle b, k|A|p\rangle. \quad (13.34)$$

There is an inverted diagram, corresponding to the cut at the lower singularity, yielding

$$2\text{Im}\langle a| -H_{\text{eff}}|a\rangle = 2\pi\delta(\varepsilon_a - \varepsilon_b - c\kappa)\langle a|\Lambda|b, k\rangle\langle b, k|A|a\rangle. \quad (13.35)$$

We have now evaluated all first-order QED corrections to the atomic transition between two bound states (Fig. 13.1).

The self-energy that is not cut as well as the vertex correction have to be renormalized, as discussed in Chap. 12. The energy derivative of the self-energy has in addition a charge divergence that is cancelled against the vertex correction, due to the Ward identity (12.24).

The energy derivative of the electron-photon interaction  $A = ec\alpha^\mu A_\mu$  leads to a change in the photon energy due to other perturbations.

### 13.3 Radiative Recombination

As a second application of the Green's-operator technique of a dynamical process we shall study the process of *radiative recombination*, i.e., where a quasi-free electron, moving in the field of an atomic nucleus, will recombine with an ion (or a bare nucleus) under the emission of a photon, as illustrated in Fig. 13.7, a process that has been studied experimentally at the GSI in Darmstadt. It has also been studied theoretically by Shabaev et al. [225, 228], using the two-photon Green's function and by the Gothenburg group, using the Green's and the Green's operators [134].

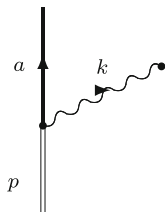


**Fig. 13.7** Lowest-order process in radiative recombination. The *heavy solid line* represents an electron in a bound state and a *thin double-line* a “quasi-free” electron in the continuum, moving in the nuclear potential

Essentially the same procedure can be used in this case as in the previous case with radiative decay, the main difference being that the incoming orbital is “quasi-free”, i.e., an essentially unbound electron moving in an external (nuclear) potential.

### 13.3.1 Lowest

In analogy with (13.13) we have the forward-scattering amplitude in lowest order (see Fig. 13.8)

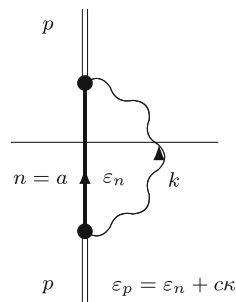
$$\langle p|W|p\rangle = \langle p|e c \alpha^\mu A_\mu \Gamma e c \alpha^\nu A_\nu |p\rangle, \tag{13.36}$$

where  $\Gamma$  is the electron propagator (4.10) or resolvent (2.64)

$$\Gamma = \Gamma(\varepsilon_p) = \frac{|q\rangle\langle q|}{\varepsilon_p - \varepsilon_n - c\kappa + i\eta}, \tag{13.37}$$

and  $p$  represents a quasi-free electronic state (double thin line).

**Fig. 13.8** Applying the optical theorem in lowest order, *left* forward scattering amplitude, *right* after the cut



Instead of (13.16) we now have

$$\langle p|Im(H_{\text{eff}})|p\rangle = -\pi\delta(\varepsilon_p - \varepsilon_n - c\kappa)\langle p|eca^\mu A_\mu|q\rangle\langle q|eca^\nu A_\nu|p\rangle, \quad (13.38)$$

where  $q$  is the degenerate state  $q = (a, k)$ . From the optical theorem the contribution to the forward-scattering amplitude then becomes

$$2\text{Im}\langle p| - H_{\text{eff}}|p\rangle = 2\pi\delta(\varepsilon_p - \varepsilon_a - c\kappa)\langle p|eca^\mu A_\mu|q\rangle\langle q|eca^\mu A_\mu|p\rangle. \quad (13.39)$$

### 13.3.2 Self-Energy Insertion on the Bound State

Next, we consider the case when there is a self-energy insertion in the bound state, for which the forward-scattering amplitude is represented by the Feynman diagram in Fig. 13.9 (cf. Sect. 13.2.2). The evolution operator is given by

$$\langle p|U|p\rangle = 2\pi\delta(E_{\text{in}} - E_{\text{out}})\langle p|iAi\Gamma(-i)\Sigma i\Gamma iA|p\rangle, \quad (13.40)$$

where, as before,  $A$  stands for  $A = eca^\mu A_\mu$  and  $\Sigma$  is the self-energy insertion. The corresponding part of the effective iteration is

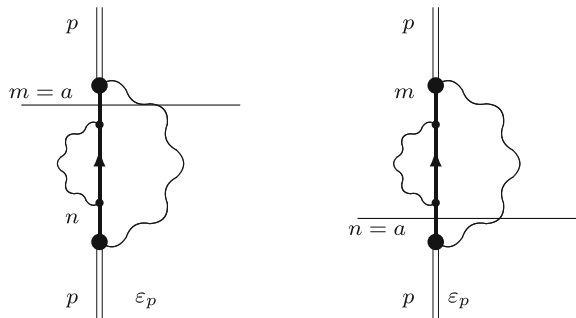
$$\langle p| - W|p\rangle: - \langle p|A\Gamma\Sigma\Gamma A|p\rangle, \quad (13.41)$$

which contains singularities. Applying the Cutkosky rules, we cut the diagram at the two places where it can have a degeneracy, leading to

$$- \langle p|A\Gamma_P\Sigma\Gamma A|p\rangle = -\mathcal{P} + i\pi\delta(\varepsilon_p - \varepsilon_a - c\kappa)\langle p|A|q\rangle\langle q|\Sigma\Gamma A|p\rangle, \quad (13.42)$$

$$- \langle p|A\Gamma\Sigma\Gamma_P A|p\rangle = -\mathcal{P} + i\pi\delta(\varepsilon_p - \varepsilon_a - c\kappa)\langle p|A\Gamma\Sigma|q\rangle\langle q|A|p\rangle. \quad (13.43)$$

**Fig. 13.9** Self-energy on the bound state



The remaining singularities lie in a discrete environment, and hence give rise to a model-space contribution (MSC)

$$- \langle p | A \Gamma_P \Sigma \Gamma A | p \rangle \rightarrow i\pi \delta(\varepsilon_p - \varepsilon_a - c\kappa) \left\langle p \left| \frac{\delta}{\delta \mathcal{E}} (A | q \rangle \langle q | \Sigma (\mathcal{E} - c\kappa))_{\mathcal{E}=\varepsilon_p} | q \rangle \langle q | A \right| p \right\rangle, \tag{13.44}$$

$$- \langle p | A \Gamma \Sigma \Gamma_P A | p \rangle \rightarrow i\pi \delta(\varepsilon_p - \varepsilon_a - c\kappa) \left\langle p \left| \left( \frac{\delta A}{\delta \mathcal{E}} \right)_{\mathcal{E}=\varepsilon_p} | q \rangle \langle q | \Sigma | q \rangle \langle q | A \right| p \right\rangle. \tag{13.45}$$

We then find

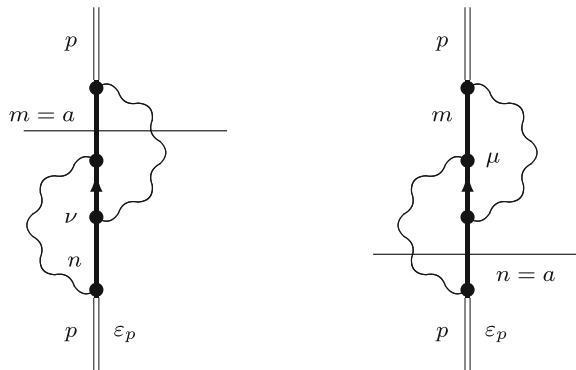
$$\begin{aligned} 2\text{Im} \langle p | - H_{\text{eff}} | p \rangle &= 2\pi \delta(\varepsilon_p - \varepsilon_a - c\kappa) \\ &\times \left\langle p \left| A | q \rangle \langle q | \Sigma \Gamma_Q A + A \Gamma_Q \Sigma | q \rangle \langle q | A + \frac{\delta}{\delta \mathcal{E}} (A | q \rangle \langle q | \Sigma)_{\mathcal{E}=\varepsilon_p} | q \rangle \langle q | A \right. \right. \\ &\left. \left. + \left( \frac{\delta A}{\delta \mathcal{E}} \right)_{\mathcal{E}=\varepsilon_p} | q \rangle \langle q | \Sigma | q \rangle \langle q | A \right| p \right\rangle. \end{aligned} \tag{13.46}$$

### 13.3.3 Vertex Correction

The forward scattering amplitude with a vertex correction is illustrated in Fig. 13.10 and represented by the effective interaction

$$\langle p | U | p \rangle = 2\pi \delta(E_{\text{in}} - E_{\text{out}}) \langle p | i\Lambda i\Gamma iA | p \rangle \quad \text{or} \quad 2\pi \delta(E_{\text{in}} - E_{\text{out}}) \langle p | iA i\Gamma i\Lambda | p \rangle \tag{13.47}$$

**Fig. 13.10** Scattering with a vertex correction



with contractions between the field operators.  $\Lambda$  stands, as before, for the vertex-correction interaction  $\Lambda = ec\Lambda^\mu A_\mu$ . The corresponding part of the effective interaction becomes

$$\langle p| -W|p\rangle = \langle p| -\Lambda \Gamma A|p\rangle \quad \text{or} \quad \langle p| -A \Gamma \Lambda|p\rangle. \quad (13.48)$$

Making a cut at the degeneracy, leads to

$$\langle p| -\Lambda \Gamma_P A|p\rangle = P - i\pi\delta(\varepsilon_p - \varepsilon_a - c\kappa)\langle p| -\Lambda|q\rangle\langle q|A|p\rangle, \quad (13.49)$$

$$\langle p| -A \Gamma_P \Lambda|p\rangle = P - i\pi\delta(\varepsilon_p - \varepsilon_a - c\kappa)\langle p| -A|q\rangle\langle q|\Lambda|p\rangle. \quad (13.50)$$

There are no MSC in this case. This leads to

$$2\text{Im}\langle p| -H_{\text{eff}}|p\rangle = 2i\pi\delta(\varepsilon_p - \varepsilon_a - c\kappa)\left[\langle p|\Lambda|q\rangle\langle q|A|p\rangle + \langle p|A|q\rangle\langle q|\Lambda|p\rangle\right]. \quad (13.51)$$

### 13.3.4 Self-Energy Insertion on the Free-Electron State

When there is a self-energy insertion in the (quasi)free electron state, the forward scattering amplitude is represented by the Feynman diagram in Fig. 13.11 (left), corresponding to the evolution operator

$$\langle p|U|p\rangle = 2\pi\delta(E_{\text{in}} - E_{\text{out}})\langle p|iA i\Gamma iA i\Gamma(-i)\Sigma|p\rangle, \quad (13.52)$$

which leads to

$$\langle p| -W|p\rangle = -\langle p|A\Gamma A\Gamma\Sigma|p\rangle. \quad (13.53)$$

The leftmost singularity corresponds to

$$-\langle p|A\Gamma_P A\Gamma\Sigma|p\rangle = -P + i\pi\delta(\varepsilon_p - \varepsilon_a - c\kappa)\langle p|A|q\rangle\langle q|A\Gamma\Sigma|p\rangle \quad (13.54)$$

and

$$\langle p|2\text{Im}(-H_{\text{eff}})|p\rangle = 2i\pi\delta(\varepsilon_p - \varepsilon_a - c\kappa)\langle p|A|q\rangle\langle q|A\Gamma\Sigma|p\rangle \quad (13.55)$$

The other singularity does not correspond to any process of physical interest. There is no MSC here.

There is also an inverted diagram with a self-energy on the outgoing line. This lead to

$$\begin{aligned} \langle p|2\text{Im}(-H_{\text{eff}})|p\rangle &= 2\pi\delta(\varepsilon_p - c\kappa - \varepsilon_a)\left\langle p\left|A|q\rangle\langle q|A\Gamma\Sigma + \Sigma\Gamma A|q\rangle\langle q|A\right|p\right\rangle \\ &= 2\pi\delta(\varepsilon_p - c\kappa - \varepsilon_a)\left\langle p\left|A|q\rangle\langle q|A\frac{|n\rangle\langle n|}{\varepsilon_p - \varepsilon_n + i\eta}\Sigma + \Sigma\frac{|n\rangle\langle n|}{\varepsilon_p - \varepsilon_n + i\eta}A|q\rangle\langle q|A\right|p\right\rangle. \end{aligned} \tag{13.56}$$

Since the states  $n$  are here **continuous**, the singularity leads to a principal integral and half a pole, of which only the former contributes to the imaginary part.

### 13.3.5 Scattering Amplitude

By summing all contributions of  $2\text{Im}\langle p|\mathcal{T}|p\rangle$  for this particular process, we have according to (13.11)

$$2\text{Im}\langle p| - H_{\text{eff}}|p\rangle = 2\pi\delta(E_p - E_q)|\tau(p \rightarrow q)|^2. \tag{13.57}$$

All contributions above are of the form

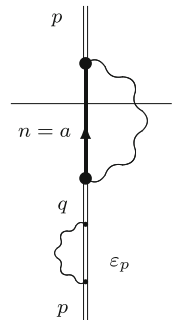
$$2\text{Im}\langle p| - H_{\text{eff}}|p\rangle = 2\pi\delta(E_p - E_q)\langle p|\cdot|p\rangle, \tag{13.58}$$

leading to

$$\langle p|\dots|p\rangle = |\tau(p \rightarrow q)|^2. \tag{13.59}$$

This gives

**Fig. 13.11** Scattering with a self-energy correction on the free electron





$$\begin{aligned}
|\tau(p \rightarrow q)|^2 &= \langle p|A|q\rangle \\
&\times \left\langle q \left| A + \Sigma \Gamma_Q A + \left( \frac{\delta \Sigma}{\delta \mathcal{E}} \right)_{\mathcal{E}=\varepsilon_p} |q\rangle\langle q| A + \Lambda + A \frac{|n\rangle\langle n|}{\varepsilon_p - \varepsilon_n + i\eta} \Sigma \right| p \right\rangle \\
&+ \left\langle p \left| A \Gamma_Q \Sigma + 2 \left( \frac{\delta A}{\delta \mathcal{E}} \right)_{\mathcal{E}=\varepsilon_p} |q\rangle\langle q| \Sigma + \Lambda + \Sigma \frac{|n\rangle\langle n|}{\varepsilon_p - \varepsilon_n + i\eta} A \right| q \right\rangle \langle q|A|p\rangle.
\end{aligned} \tag{13.60}$$

This is of the form

$$|\tau(p \rightarrow q)|^2 = \langle p|A|q\rangle\langle q|A + X|p\rangle + \langle p|Y|q\rangle\langle q|A|p\rangle, \tag{13.61}$$

But since this is a real number, it is also equal to

$$|\tau(p \rightarrow q)|^2 = \langle p|A|q\rangle\langle q|Y^\dagger|p\rangle + \langle p|A + X^\dagger|q\rangle\langle q|A|p\rangle \tag{13.62}$$

and to

$$|\tau(p \rightarrow q)|^2 = \frac{1}{2} \langle p|A|q\rangle\langle q|A + X + Y^\dagger|p\rangle + \frac{1}{2} \langle p|A + X^\dagger + Y|q\rangle\langle q|A|p\rangle. \tag{13.63}$$

This leads to the approximate amplitude

$$\tau(p \rightarrow q) \approx \langle q|A + \frac{1}{2}(X + Y^\dagger)|p\rangle, \tag{13.64}$$

which corresponds to

$$|\tau(p \rightarrow q)|^2 \approx \langle p|A + \frac{1}{2}(X^\dagger + Y)|q\rangle\langle q|A + \frac{1}{2}(X + Y^\dagger)|p\rangle. \tag{13.65}$$

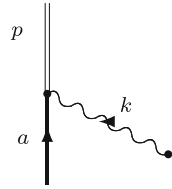
This gives

$$\begin{aligned}
\tau(p \rightarrow q) &\approx \left\langle q \left| A + \Sigma \Gamma_Q A + \Sigma |q\rangle\langle q| \left( \frac{\delta A}{\delta \mathcal{E}} \right)_{\mathcal{E}=\varepsilon_p} \right. \right. \\
&\quad \left. \left. + \frac{1}{2} \left( \frac{\delta \Sigma}{\delta \mathcal{E}} \right)_{\mathcal{E}=\varepsilon_p} |q\rangle\langle q| A + \Lambda + A \frac{|n\rangle\langle n|}{\varepsilon_p - \varepsilon_n + i\eta} \Sigma \right| p \right\rangle.
\end{aligned} \tag{13.66}$$

This result agrees with those of Shabaev et al. [228] and Lindgren et al. [134], in the latter case apart from sign difference for the vertex part, which is due to different sign convention (see Sect. 4.6.2).

The self-energies and vertex corrections that are not affected by the cuts have to be properly renormalized. For the effects affected by the cut the renormalization does not contribute to the imaginary part.

**Fig. 13.12** Lowest-order process in photoionization



It can be noted that the derivative of the self-energy appears only once in the cross-section, which explains the factor of one half in the amplitude. The derivative of the photon energy, on the other hand, appears twice and hence appears with the factor of unity in the amplitude.

The effect of the vacuum polarization is not included here but can be evaluated in very much the same way, and in doing so, we find also here agreement with the result of Shabaev et al.

### 13.3.6 Photoionization

In the process of photoionization an incoming photon interacts with a target atom or molecule, which is being ionized. This is the reverse of the process of radiative recombination, treated in the previous subsection, and the expressions for the various processes can directly be written down (Fig. 13.12).

## Chapter 14

# Summary and Conclusions

The all-order forms of many-body perturbation theory (MBPT), like the coupled-cluster approach (CCA), have been extremely successful in calculations on atomic and in particular on molecular systems. Here, the dominating parts of the electron correlation can be evaluated to essentially all orders of perturbation theory.

A shortcoming, however, of the standard MBPT/CCA procedures is that quantum electrodynamics (QED) can only be included in a very limited fashion (first-order energy). Particularly for highly charged systems, QED effects can be quite important. Certain experimental data on such systems are now several orders of magnitude more accurate than the best available theoretical calculation. In order to account for such data theoretically, it will be necessary to include—among other things—the **combination** of quantum electrodynamics and many-body perturbation theory.

The procedure presented in this book, which is based upon quantum-field theory, describes—for the first time—a road towards a rigorous unification of QED and MBPT. The procedure is based upon the *covariant evolution operator*, which describes the time evolution of the relativistic wave function or state vector.

The covariant evolution operator contains generally singularities that can be eliminated. This leads to the *Green's operator*, which is a generalization of the wave-operator concept in standard many-body theory. The procedure is for two-electron systems fully compatible with the relativistically covariant Bethe–Salpeter equation, but it is more versatile.

The procedure is—in contrast to the standard Bethe–Salpeter equation—applicable to a general multi-reference (quasi-degenerate) model space. It can also be combined with the coupled-cluster approach and is, in principle, applicable to systems with more than two electrons.

In principle, the Green's operator—as well as the Bethe–Salpeter equation—has individual times for the particles involved. Most applications, though, employ the *equal-time approximation*, where the times are equalized, in order to make the procedure consistent with the quantum-mechanical picture.

The Green's operator for time  $t = 0$  corresponds to the *wave operator* used in standard MBPT, and the time derivative at  $t = 0$ , operating within the model space,

to the many-body *effective interaction*. This connects the field-theoretical procedure with the standard MBPT.

The formalism presented here has been tested numerically by the Gothenburg atomic theory group, and in cases where comparison can be made with the more restricted S-matrix formulation, very good agreement is reported.

In order to go beyond two-photon exchange, it is necessary to combine the quantum electrodynamics with electron correlation in a systematic way. When radiative QED effects are involved, it is necessary in such a case to use the Coulomb gauge in order to get sensible results with reasonable efforts, and such calculations have recently been performed. The use of the Coulomb gauge also has other advantages in dealing with QED in combination with electron correlation.

Any experimental verification of the higher-order QED effects beyond second order has not yet been performed, but the experimental accuracy is in several cases so high that such a test would be feasible.

The Green's-operator procedure was primarily developed for evaluating QED effects in **static properties** on bound-state systems. It has turned out, however, that the procedure is equally well applicable to **dynamic problems**, like scattering cross sections and transitions rates. In such cases the standard S-matrix procedure fails due to singularities appearing when internal model-space states are involved, which can be eliminated in the same way as in structure problems. This has recently been applied by the Gothenburg group and corresponding experiments are presently being performed by other groups, and it might in the near future be possible to detect QED effects in such processes.

# Appendix A

## Notations and Definitions

### A.1 Four-Component Vector Notations

A four-dimensional *contravariant vector* is defined<sup>1</sup>

$$x = x^\mu = (x^0, x^1, x^2, x^3) = (x^0, \mathbf{x}) = (ct, \mathbf{x}), \quad (\text{A.1})$$

where  $\mu = 0, 1, 2, 3$  and  $\mathbf{x}$  is the three-dimensional coordinate vector  $\mathbf{x} = (x^1, x^2, x^3) \equiv (x, y, z)$ . The four-dimensional differential is

$$d^4x = cdt - d^3\mathbf{x} \quad \text{and} \quad d^3\mathbf{x} = dx dy dz.$$

A corresponding *covariant vector* is defined

$$x_\mu = (x_0, x_1, x_2, x_3) = g_{\mu\nu}x^\nu = (x_0, -\mathbf{x}) = (ct, -\mathbf{x}), \quad (\text{A.2})$$

which implies that

$$x^0 = x_0 \quad x = -x_i \quad (i = 1, 2, 3). \quad (\text{A.3})$$

$g_{\mu\nu}$  is a *metric tensor*, which can raise the so-called *Lorentz indices* of the vector. Similarly, an analogous tensor can lower the indices

$$x^\mu = g^{\mu\nu}x_\nu. \quad (\text{A.4})$$

These relations hold generally for four-dimensional vectors.

There are various possible choices of the metric tensors, but we shall use the following

---

<sup>1</sup>In all appendices D-M we display complete formulas with all fundamental constants. As before, we employ the Einstein summation rule with summation over repeated indices.

$$g_{\mu\nu} = g^{\mu\nu} = \begin{pmatrix} 1 & 0 & 0 & 0 \\ 0 & -1 & 0 & 0 \\ 0 & 0 & -1 & 0 \\ 0 & 0 & 0 & -1 \end{pmatrix}. \quad (\text{A.5})$$

The four-dimensional *scalar product* is defined as the product of a contravariant and a covariant vector:

$$ab = a^\mu b_\mu = a^0 b_0 - \mathbf{a} \cdot \mathbf{b}, \quad (\text{A.6})$$

where  $\mathbf{a} \cdot \mathbf{b}$  is the three-dimensional scalar product

$$\mathbf{a} \cdot \mathbf{b} = a_x b_x + a_y b_y + a_z b_z.$$

The *covariant* gradient operator is defined as the gradient with respect to a *contravariant* coordinate vector:

$$\partial_\mu = \frac{\partial}{\partial x^\mu} = \left( \frac{1}{c} \frac{\partial}{\partial t}, \nabla \right), \quad (\text{A.7})$$

and the *contravariant* gradient operator analogously

$$\partial^\mu = \frac{\partial}{\partial x_\mu} = \left( \frac{1}{c} \frac{\partial}{\partial t}, -\nabla \right). \quad (\text{A.8})$$

$\nabla$  is the three-dimensional gradient operator

$$\nabla = \frac{\partial}{\partial x} \hat{\mathbf{e}}_x + \frac{\partial}{\partial y} \hat{\mathbf{e}}_y + \frac{\partial}{\partial z} \hat{\mathbf{e}}_z,$$

where  $(\hat{\mathbf{e}}_x, \hat{\mathbf{e}}_y, \hat{\mathbf{e}}_z)$  are unit vectors in the coordinate directions.

The *four-dimensional divergence* is defined

$$\partial_\mu A^\mu = \frac{1}{c} \frac{\partial A^0}{\partial t} + \nabla \cdot \mathbf{A} = \nabla A, \quad (\text{A.9})$$

where  $\nabla \cdot \mathbf{A}$  is the three-dimensional divergence

$$\nabla \cdot \mathbf{A} = \frac{\partial A_x}{\partial x} + \frac{\partial A_y}{\partial y} + \frac{\partial A_z}{\partial z}.$$

The *d'Alembertian operator* is defined

$$\square = \partial^\mu \partial_\mu = \frac{1}{c^2} \frac{\partial^2}{\partial t^2} - \nabla^2 = \nabla^2, \quad (\text{A.10})$$

where

$$\nabla^2 = \Delta = \frac{\partial^2}{\partial x^2} + \frac{\partial^2}{\partial y^2} + \frac{\partial^2}{\partial z^2}$$

is the *Laplacian operator*.

## A.2 Vector Spaces

### *Notations*

$X, Y, ..$  are sets with elements  $x, y, ..$

$x \in X$  means that  $x$  is an element in the set  $X$ .

$\mathbf{N}$  is the set of nonnegative integers.  $\mathbf{R}$  is the set of real numbers.  $\mathbf{C}$  is the set of complex numbers.

$\mathbf{R}^n$  is the set of real  $n$ -dimensional vectors.  $\mathbf{C}^n$  is the set of complex  $n$ -dimensional vectors.

$A \subset X$  means that  $A$  is a subset of  $X$ .

$A \cup B$  is the *union* of  $A$  and  $B$ .  $A \cap B$  is the *Intersection* of  $A$  and  $B$ .

$A = \{x \in X : P\}$  means that  $A$  is the set of all elements  $x$  in  $X$  that satisfy the condition  $P$ .

$f : X \rightarrow Y$  represents a *function* or *operator*, which means that  $f$  maps *uniquely* the elements of  $X$  onto elements of  $Y$ .

A *functional* is a unique mapping  $f : X \rightarrow \mathbf{R}(\mathbf{C})$  of a function space on the space of real (complex) numbers.

The set of arguments  $x \in A$  for which the function  $f : A \rightarrow B$  is defined is the *domain*, and the set of results  $y \in B$  which can be produced is the *range*.

$(a, b)$  is the *open interval*  $\{x \in \mathbf{R} : a < x < b\}$ .  $[a, b]$  is the *closed interval*  $\{x \in \mathbf{R} : a \leq x \leq b\}$ .

*sup* represents the *supremum*, the least upper bound of a set

*inf* represents the *infimum*, the largest lower bound of a set.

### *Basic Definitions*

A real (complex) *vector space* or function space  $X$  is an infinite set of elements,  $x$ , referred to as *points* or *vectors*, which is *closed* under addition,  $x + y = z \in X$ , and under multiplication by a real (complex) number  $c$ ,  $cx = y \in X$ . The continuous functions  $f(x)$  on the interval  $x \in [a, b]$  form a vector space, also with some boundary conditions, like  $f(a) = f(b) = 0$ .

A subset of  $X$  is a *subspace* of  $X$  if it fulfills the criteria for a vector space.

A *norm* of a vector space  $X$  is a function  $p : X \rightarrow [0, \infty]$  with the properties

- (1)  $p(\lambda x) = |\lambda|p(x)$
- (2)  $p(x + y) \leq p(x) + p(y)$  for all real  $\lambda$  ( $\lambda \in \mathbf{R}$ ) and all  $x, y \in X$
- (3) that  $p(x) = 0$  always implies  $x = 0$ .

The norm is written  $p(x) = \|x\|$ . We then have  $\|\lambda x\| = |\lambda| \|x\|$  and  $\|x + y\| \leq \|x\| + \|y\|$  and  $\|x\| = 0 \Rightarrow x = 0$ . If the last condition is not fulfilled, it is a *seminorm*.

A vector space with a norm for all its elements is a *normed space*, denoted  $(X, \|\cdot\|)$ . The continuous functions,  $f(x)$ , on the interval  $[a, b]$  form a normed space by defining a norm, for instance,  $\|f\| = \left[ \int_a^b dt [f(t)]^2 \right]^{1/2}$ . By means of the Cauchy-Schwartz inequality, it can be shown that this satisfies the criteria for a norm [80, p. 93].

If  $f$  is a function  $f : A \rightarrow Y$  and  $A \subset X$ , then  $f$  is defined in the *neighborhood* of  $x_0 \in X$ , if there is an  $\epsilon > 0$  such that the entire sphere  $\{x \in X : \|x - x_0\| < \epsilon\}$  belongs to  $A$  [80, p. 309].

A function/operator  $f : X \rightarrow Y$  is *bounded*, if there exists a number  $C$  such that

$$\sup_{0 \neq x \in X} \left[ \frac{\|fx\|}{\|x\|} \right] = C < \infty.$$

Then  $C = \|f\|$  is the *norm* of  $f$ . Thus,  $\|fx\| \leq \|f\| \|x\|$ .

A function  $f$  is *continuous* at the point  $x_0 \in X$ , if for every  $\delta > 0$  there exists an  $\epsilon > 0$  such that for every member of the set  $x : \|x - x_0\| < \epsilon$  we have  $\|fx - fx_0\| \leq \delta$  [80, p. 139]. This can also be expressed so that  $f$  is continuous at the point  $x_0$ , if and only if  $fx \rightarrow fx_0$  whenever  $x_n \rightarrow x_0$ ,  $\{x_n\}$  being a sequence in  $X$ , meaning that  $fx_n$  converges to  $fx_0$ , if  $x$  converges to  $x_0$  [240, p. 70].

A linear function/operator is continuous if and only if it is bounded [54, p. 22], [80, pp. 197, 213].

A functional  $f : X \rightarrow \mathbf{R}$  is *convex* if

$$f(tx + (t - 1)y) \leq tf(x) + (t - 1)f(y)$$

for all  $x, y \in X$  and  $t \in (0, 1)$ .

A subset  $A \subset X$  is *open*, if for every  $x \in A$  there exists an  $\epsilon > 0$  such that the entire ball  $B_r(x) = \{y \in X \mid \|y - x\| < \epsilon\}$  belongs to  $A$ , i.e.,  $B_r(x) \subset A$  [23, p. 363], [80, p. 98], [240, p. 57].

A *sequence*  $\{x_n\}$ , where  $n$  is an integer ( $n \in \mathbf{N}$ ), is an infinite numbered list of elements in a set or a space. A *subsequence* is a sequence, which is a part of a sequence.

A sequence  $\{x_n \in A\}$  is (strongly) *convergent* towards  $x \in A$ , if and only if for every  $\epsilon > 0$  there exists an  $N$  such that  $\|x_n - x\| < \epsilon$  for all  $n > N$  [80, p. 95, 348].



A sequence is called a *Cauchy sequence* if and only if for every  $\epsilon > 0$  there exists an  $N$  such that  $\|x_n - x_m\| < \epsilon$  for all  $m, n > N$ . If a sequence  $\{x_n\}$  is convergent, then it follows that for  $n, m > N$

$$\|x_m - x_n\| = \|(x_n - x) + (x - x_m)\| \leq \|x_n - x\| + \|x_m - x\| < 2\epsilon$$

which means that a convergent sequence is always a Cauchy sequence. The opposite is not necessarily true, since the point of convergence need not be an element of  $X$  [55, p. 44].

A subset  $A$  of a normed space is termed *compact*, if every infinite sequence of elements in  $A$  has a subsequence, which converges to an element in  $A$ . The closed interval  $[0,1]$  is an example of a compact set, while the open interval  $(0,1)$  is noncompact, since the sequence  $1, 1/2, 1/3\dots$  and all of its subsequences converge to  $0$ , which lies outside the set [240, p. 149]. This sequence satisfies the Cauchy convergence criteria but not the (strong) convergence criteria.

A *dual space* or *adjoint space* of a vector space  $X$ , denoted  $X^*$ , is the space of all functions on  $X$ .

An *inner or scalar product* in a vector space  $X$  is a function  $\langle \cdot, \cdot \rangle : X \times X \rightarrow \mathbf{R}$  with the properties (1)

$$\langle x, \lambda_1 y_1 + \lambda_2 y_2 \rangle = \lambda_1 \langle x, y_1 \rangle + \lambda_2 \langle x, y_2 \rangle, \quad \langle x, y \rangle = \langle y, x \rangle$$

for all  $x, y, y_1, y_2 \in X$  and all  $\lambda_j \in \mathbf{R}$ , and (2)  $\langle x, x \rangle = 0$  only if  $x = 0$ .

## ***Special Spaces***

### **Banach Space**

A *Banach space* is a normed space in which every Cauchy sequence converges to a point in the space.

### **Hilbert Space**

A Banach space with the norm  $\|x\| = +\sqrt{\langle x, x \rangle}$  is called a *Hilbert space* [23, p. 364].

### **Fock Space**

A Fock space is a *Hilbert space*, where the number of particles is variable or unknown.

### A.3 Special Functions

#### *Dirac Delta Function*

We consider the integral

$$\int_{-L/2}^{L/2} dx e^{ikx}. \quad (\text{A.11})$$

Assuming *periodic boundary conditions*,  $e^{-iLx/2} = e^{iLx/2}$ , limits the possible  $k$  values to  $k = k_n = 2\pi n/L$ . Then

$$\frac{1}{L} \int_{-L/2}^{L/2} dx e^{ik_n x} = \delta_{k_n, 0}, \quad (\text{A.12})$$

where  $\delta_{n,m}$  is the *Kronecker delta factor*

$$\delta_{n,m} = \begin{cases} 1 & \text{if } m = n \\ 0 & \text{if } m \neq n \end{cases}. \quad (\text{A.13})$$

If we let  $L \rightarrow \infty$ , then we have to add a ‘*damping factor*’  $e^{-\gamma|x|}$ , where  $\gamma$  is a small positive number, in order to make the integral meaningful,

$$\int \frac{dx}{2\pi} e^{ikx} e^{-\gamma|x|} = \frac{\gamma}{\pi} \frac{1}{k^2 + \gamma^2}, \quad (\text{A.14})$$

which in the limit can be seen as a definition of the Dirac delta function,

$$\lim_{\gamma \rightarrow 0} \int_{-\infty}^{\infty} \frac{dx}{2\pi} e^{ikx} e^{-\gamma|x|} = \lim_{\gamma \rightarrow 0} \frac{\gamma}{\pi} \frac{1}{k^2 + \gamma^2} = \delta(k). \quad (\text{A.15})$$

Formally, we write this relation as

$$\boxed{\int_{-\infty}^{\infty} \frac{dx}{2\pi} e^{ikx} = \delta(k)}. \quad (\text{A.16})$$

Defining a  $\Delta$  function by

$$\boxed{\Delta_{\gamma}(k) = \frac{\gamma}{\pi} \frac{1}{k^2 + \gamma^2}}, \quad (\text{A.17})$$

we then have

$$\boxed{\lim_{\gamma \rightarrow 0} \Delta_{\gamma}(k) = \lim_{\gamma \rightarrow 0} \Delta_{n\gamma}(k) = \delta(k)}. \quad (\text{A.18})$$

The integral over the  $\Delta$  function can easily be found to be equal to unity

$$\int_{-\infty}^{\infty} dk \Delta_{\gamma}(k) = 1, \quad (\text{A.19})$$

using residue calculus, and since it in the limit becomes equal to zero in all points except  $k = 0$ , it satisfies all conditions of the  $\delta$  function.

The  $\Delta$  function also has the following property

$$\lim_{\gamma \rightarrow 0} \pi \gamma \Delta_{\gamma}(k) = \lim_{\gamma \rightarrow 0} \frac{\gamma^2}{k^2 + \gamma^2} = \left\{ \begin{array}{l} 1, \quad k = 0 \\ 0, \quad k \neq 0 \end{array} \right\} = \delta_{k,0}, \quad (\text{A.20})$$

which is the Kronecker delta factor. The same is true for any value of  $n$ ,

$$\lim_{\gamma \rightarrow 0} n \pi \gamma \Delta_{n\gamma}(k) = \delta_{k,0}. \quad (\text{A.21})$$

In three dimensions equation (A.12) goes over into

$$\frac{1}{V} \int_V d^3 \mathbf{x} e^{i \mathbf{k}_n \cdot \mathbf{x}} = \delta^3(\mathbf{k}_n, 0) = \delta(k_{nx}, 0) \delta(k_{ny}, 0) \delta(k_{nz}, 0). \quad (\text{A.22})$$

In the limit where the integration is extended over the entire three-dimensional space, we have in analogy with (A.16)

$$\boxed{\int \frac{d^3 \mathbf{x}}{(2\pi)^3} e^{i \mathbf{k} \cdot \mathbf{x}} = \delta^3(\mathbf{k}).} \quad (\text{A.23})$$

## ***Integrals Over $\Delta$ Functions***

We consider now the integral

$$\begin{aligned} \int_{-\infty}^{\infty} dx \delta(x - a) f(x) &= \lim_{\gamma \rightarrow 0} \int_{-\infty}^{\infty} dx \Delta_{\gamma}(x - a) f(x) \\ &= \frac{1}{2\pi} \lim_{\gamma \rightarrow 0} \int_{-\infty}^{\infty} dx \frac{2\gamma}{(x - a)^2 + \gamma^2} f(x). \end{aligned} \quad (\text{A.24})$$

The integral can be evaluated using residue calculus and leads to

$$\boxed{\int_{-\infty}^{\infty} dx \delta(x - a) f(x) = f(a).} \quad (\text{A.25a})$$

provided the function  $f(x)$  has no poles. In three dimensions we have similarly

$$\int d^3x \delta(\mathbf{x} - \mathbf{x}_0) f(\mathbf{x}) = f(\mathbf{x}_0). \quad (\text{A.25b})$$

integrated over all space.

The relations above are often taken as the definition of the Dirac delta function, but the procedure applied here is more rigorous.

Next, we consider the integral over *two*  $\Delta$  functions

$$\begin{aligned} \int dx \Delta_\gamma(x-a) \Delta_\eta(x-b) &= \frac{1}{(2\pi)^2} \int dx \frac{2\gamma}{(x-a)^2 + \gamma^2} \frac{2\eta}{(x-b)^2 + \eta^2} \\ &= \frac{1}{4\pi^2 i} \int dx \left[ \frac{1}{x-a-i\gamma} - \frac{1}{x-a+i\gamma} \right] \\ &\quad \times \frac{2\eta}{(x-b+i\eta)(x-b-i\eta)} \\ &= \frac{1}{2\pi i} \left[ \frac{1}{b-a-i(\gamma+\eta)} - \frac{1}{b-a+i(\gamma+\eta)} \right] \\ &= \frac{1}{2\pi} \frac{2(\gamma+\eta)}{(a-b)^2 + (\gamma+\eta)^2} \end{aligned} \quad (\text{A.26})$$

after integrating the first term over the negative and the second term over the positive half plane. Thus,

$$\boxed{\int dx \Delta_\gamma(x-a) \Delta_\eta(x-b) = \Delta_{\gamma+\eta}(a-b),} \quad (\text{A.27})$$

and we see that here *the widths of the  $\Delta$  functions are added*.

Now we consider some integrals with the  $\Delta$  functions in combination with electron and photon propagators that are frequently used in the main text.

First, consider the integral with one  $\Delta$  function and an *electron* propagator (4.10)

$$\begin{aligned} \int d\omega \frac{1}{\omega - \varepsilon_j + i\eta} \Delta_\gamma(\varepsilon_a - \omega) &= \int \frac{d\omega}{2\pi} \frac{1}{\omega - \varepsilon_j + i\eta} \frac{2\gamma}{(\varepsilon_a - \omega)^2 + \gamma^2} \\ &= \int \frac{d\omega}{2\pi} \frac{1}{\omega - \varepsilon_j + i\eta} \frac{2\gamma}{(\varepsilon_a - \omega + i\gamma)(\varepsilon_a - \omega - i\gamma)}. \end{aligned}$$

The pole of the propagator yields the contribution  $\Delta_\gamma(\varepsilon_a - \varepsilon_j)$ , which vanishes in the limit  $\gamma \rightarrow 0$ , if  $\varepsilon_a \neq \varepsilon_j$ . Nevertheless, we shall see that this pole has a significant effect on the result.

Integrating above over the *positive* half plane, with the single pole  $\varepsilon_a + i\gamma$ , yields

$$\frac{1}{\varepsilon_a - \varepsilon_j + i\gamma + i\eta},$$

and integrating over the *negative* half plane, with the two poles  $\varepsilon_j - i\eta$ ,  $\varepsilon_a - i\gamma$ , yields

$$-\frac{2i\gamma}{(\varepsilon_a - \varepsilon_j + i\gamma + i\eta)(\varepsilon_a - \varepsilon_j - i\gamma + i\eta)} + \frac{1}{\varepsilon_a - \varepsilon_j - i\gamma + i\eta} = \frac{1}{\varepsilon_a - \varepsilon_j + i\gamma + i\eta},$$

which is identical to the previous result. We observe here that *the pole of the propagator, which has a vanishing contribution in the limit  $\gamma \rightarrow 0$ , has the effect of reversing the sign of the  $i\gamma$  term.*

The  $\gamma$  parameter originates from the adiabatic damping and is small but finite, while the  $\eta$  parameter is infinitely small and only determines the position of the pole of the propagator. Therefore, if they appear together, the  $\gamma$  term dominates, and the  $\eta$  term can be omitted. This yields

$$\boxed{\int d\omega \frac{1}{\omega - \varepsilon_j + i\eta} \Delta_\gamma(\varepsilon_a - \omega) = \frac{1}{\varepsilon_a - \varepsilon_j + i\gamma}}, \quad (\text{A.28})$$

noting that **the  $\eta$  parameter of the propagator is replaced by the damping parameter  $\gamma$ .**

Secondly, we consider the integral with the *photon* propagator (4.31)

$$\begin{aligned} \int d\omega \frac{1}{\omega^2 - \kappa^2 + i\eta} \Delta_\gamma(\varepsilon_a - \omega) &= \frac{1}{2\kappa} \int \frac{d\omega}{2\pi} \left[ \frac{1}{\omega - \kappa + i\eta} - \frac{1}{\omega + \kappa - i\eta} \right] \\ \frac{2\gamma}{(\varepsilon_a - \omega + i\gamma)(\varepsilon_a - \omega - i\gamma)} &= \frac{1}{2\kappa} \left[ \frac{1}{\varepsilon_a + i\gamma - \kappa + i\eta} - \frac{1}{\varepsilon_a - i\gamma + \kappa - i\eta} \right] \\ &= \frac{1}{\varepsilon_a^2 - (\kappa - i\gamma - i\eta)^2} \end{aligned} \quad (\text{A.29})$$

or, neglecting the  $\eta$  term,

$$\boxed{\int d\omega \frac{1}{\omega^2 - \kappa^2 + i\eta} \Delta_\gamma(\varepsilon_a - \omega) = \frac{1}{\varepsilon_a^2 - \kappa^2 + i\gamma}}, \quad (\text{A.30})$$

noting that  $\kappa \geq 0$ .

Finally, we consider the integrals of *two*  $\Delta$  functions and the propagators. With the electron propagator we have

$$\begin{aligned} & \int d\omega \frac{1}{\omega - \varepsilon_j + i\eta} \Delta_\gamma(\varepsilon_a - \omega) \Delta_\gamma(\varepsilon_b - \omega) \\ &= \frac{1}{(2\pi i)^2} \int d\omega \frac{1}{\omega - \varepsilon_j + i\eta} \left[ \frac{1}{\varepsilon_a - \omega - i\gamma} - \frac{1}{\varepsilon_a - \omega + i\gamma} \right] \\ & \quad \times \left[ \frac{1}{\varepsilon_b - \omega - i\gamma} - \frac{1}{\varepsilon_b - \omega + i\gamma} \right]. \end{aligned}$$

Here, three of the combinations with poles on both sides of the real axis contribute, which yields

$$\begin{aligned} & \frac{1}{2\pi i} \left[ \frac{1}{(\varepsilon_b - \varepsilon_j + i\gamma)(\varepsilon_a - \varepsilon_b - 2i\gamma)} + \frac{1}{(\varepsilon_a - \varepsilon_j + i\gamma)(\varepsilon_b - \varepsilon_a - 2i\gamma)} \right. \\ & \quad \left. - \frac{1}{(\varepsilon_a - \varepsilon_j + i\gamma)(\varepsilon_b - \varepsilon_j + i\gamma)} \right]. \end{aligned}$$

The last two terms become

$$\frac{1}{\varepsilon_a - \varepsilon_j + i\gamma} \left[ \frac{1}{\varepsilon_b - \varepsilon_a - 2i\gamma} - \frac{1}{\varepsilon_b - \varepsilon_j + i\gamma} \right] \approx \frac{1}{(\varepsilon_b - \varepsilon_a - 2i\gamma)(\varepsilon_b - \varepsilon_j + i\gamma)},$$

neglecting an imaginary term in the numerator. This leads to

$$\boxed{\int d\omega \frac{1}{\omega - \varepsilon_j + i\eta} \Delta_\gamma(\varepsilon_a - \omega) \Delta_\gamma(\varepsilon_b - \omega) \approx \frac{1}{\varepsilon_a - \varepsilon_j + i\gamma} \Delta_{2\gamma}(\varepsilon_a - \varepsilon_b).} \quad (\text{A.31})$$

Similarly, we find for the photon propagator

$$\boxed{\int d\omega \frac{1}{\omega^2 - \kappa^2 + i\eta} \Delta_\gamma(\varepsilon_a - \omega) \Delta_\gamma(\varepsilon_b - \omega) \approx \frac{1}{\varepsilon_a^2 - \kappa^2 + i\gamma} \Delta_{2\gamma}(\varepsilon_a - \varepsilon_b).} \quad (\text{A.32})$$

*Formally, we can obtain the integral with propagators by replacing the  $\Delta$  function by the corresponding Dirac delta function, noting that we then have to replace the imaginary parameter  $\eta$  in the denominator by the damping factor  $\gamma$ .*

### ***The Heaviside Step Function***

The Heaviside step function is defined

$$\begin{aligned}\Theta(t) &= 1 \quad t' > t \\ &= 0 \quad t' < t.\end{aligned}\tag{A.33}$$

The step function can also be given the integral representation

$$\Theta(t) = i \lim_{\epsilon \rightarrow 0} \int_{-\infty}^{\infty} \frac{d\omega}{2\pi} \frac{e^{-i\omega t}}{\omega + i\epsilon}\tag{A.34}$$

from which we obtain the derivative of the step function

$$\frac{d\Theta(t)}{dt} = \lim_{\epsilon \rightarrow 0} \int_{-\infty}^{\infty} \frac{d\omega}{2\pi} \frac{\omega}{\omega + i\epsilon} e^{-i\omega t} = \delta(t),\tag{A.35}$$

where  $\delta(t)$  is the Dirac delta function.

# Appendix B

## Second Quantization

### B.1 Definitions

(See, for instance, [124, Chap. 11], [220, Chap. 5]). In second quantization—also known as the number representation—a state is represented by a vector (see Appendix C.1)  $|n_1, n_2, \dots\rangle$ , where the numbers represent the number of particles in the particular basis state (which for fermions can be equal only to one or zero).

Second quantization is based upon *annihilation/creation operators*  $c_j/c_j^\dagger$ , which annihilate and create, respectively, a single particle. If we denote by  $|0\rangle$  the vacuum state with no particle, then

$$c_j^\dagger |0\rangle = |j\rangle \tag{B.1}$$

represents a single-particle state. In the coordinate representation (C.19) this corresponds to the wave function

$$\phi_j(\mathbf{x}) = \langle \mathbf{x} | j \rangle, \tag{B.2}$$

satisfying the single-electron Schrödinger or Dirac equation. Obviously, we have

$$c_j |0\rangle = 0. \tag{B.3}$$

For fermions the operators satisfy the *anti-commutation relations*

$$\begin{aligned} \{c_i^\dagger, c_j^\dagger\} &= c_i^\dagger c_j^\dagger + c_j^\dagger c_i^\dagger = 0 \\ \{c_i, c_j\} &= c_i c_j + c_j c_i = 0 \\ \{c_i^\dagger, c_j\} &= c_i^\dagger c_j + c_j c_i^\dagger = \delta_{ij}, \end{aligned} \tag{B.4}$$

where  $\delta_{ij}$  is the Kronecker delta factor (A.13). It then follows that

$$c_i^\dagger c_j^\dagger |0\rangle = -c_j^\dagger c_i^\dagger |0\rangle, \tag{B.5}$$



which means that  $c_i^\dagger c_j^\dagger |0\rangle$  represents an *antisymmetric* two-particle state, which we denote in the following way<sup>2</sup>

$$c_i^\dagger c_j^\dagger |0\rangle = |\{i, j\}\rangle. \quad (\text{B.6})$$

The antisymmetric form is required for fermions by the quantum-mechanical rules. A corresponding bra state is

$$\langle 0|c_l c_k = \langle \{k, l\}|, \quad (\text{B.7})$$

and it then follows that the states are orthonormal.

In the coordinate representation the state above becomes

$$\langle \mathbf{x}_1 \mathbf{x}_2 | \{i, j\}\rangle = \frac{1}{\sqrt{2}} [\phi_i(\mathbf{x}_1) \phi_j(\mathbf{x}_2) - \phi_j(\mathbf{x}_1) \phi_i(\mathbf{x}_2)]. \quad (\text{B.8})$$

Generalizing this to a general many-particle system, leads to an antisymmetric product, known as the *Slater determinant*,

$$\begin{aligned} \langle \mathbf{x}_1, \mathbf{x}_2, \dots, \mathbf{x}_N | c_a^\dagger c_b^\dagger \dots c_N^\dagger |0\rangle &= \frac{1}{\sqrt{N!}} \text{Det}\{a, b, \dots, N\} \\ &= \frac{1}{\sqrt{N!}} \begin{vmatrix} \phi_1(\mathbf{x}_1) & \phi_1(\mathbf{x}_2) & \dots & \phi_1(\mathbf{x}_N) \\ \phi_2(\mathbf{x}_1) & \phi_2(\mathbf{x}_2) & \dots & \phi_2(\mathbf{x}_N) \\ \dots & \dots & \dots & \dots \\ \phi_N(\mathbf{x}_1) & \phi_N(\mathbf{x}_2) & \dots & \phi_N(\mathbf{x}_N) \end{vmatrix}. \end{aligned} \quad (\text{B.9})$$

For an  $N$ -particle system we define one- and two-particle operators by

$$F = \sum_{n=1}^n f_n \quad (\text{B.10})$$

$$G = \sum_{m < n=1}^n g_{mn}, \quad (\text{B.11})$$

respectively, where the  $f_n$  and the  $g_{mn}$  operators are identical, differing only in the particles they operate on. In second quantization these operators can be expressed (see, for instance, [124, Sect. 11.1])<sup>3</sup>

$$\begin{aligned} \hat{F} &= c_i^\dagger \langle i|f|j\rangle c_j \\ \hat{G} &= \frac{1}{2} c_i^\dagger c_j^\dagger \langle ij|g|kl\rangle c_l c_k \end{aligned} \quad (\text{B.12})$$

<sup>2</sup>We shall follow the convention of letting the notation  $|i, j\rangle$  denote a straight product function  $|i, j\rangle = \phi_i(\mathbf{x}_1) \phi_j(\mathbf{x}_2)$ , while  $|\{i, j\}\rangle$  represents an antisymmetric function.

<sup>3</sup>Occasionally, we use a ‘hat’ on the operators to emphasize their second-quantized form. We employ also the Einstein summation rule with summation over all indices that appear twice. Note the order between the annihilation operators.

etc. (note order between the operators in the two-particle case). Here,

$$\begin{aligned}\langle i|f|j\rangle &= \int d^3\mathbf{x}_1 \phi_i^\dagger(x_1) f \phi_j(x_1) \\ \text{bra}ijg|kl\rangle &= \iint d^3\mathbf{x}_1 d^3\mathbf{x}_2 \phi_i^\dagger(x_1) \phi_j^\dagger(x_2) g \phi_k(x_1) \phi_l(x_2).\end{aligned}\quad (\text{B.13})$$

We can check the formulas above by evaluating

$$\begin{aligned}\langle\{cd\}|\hat{G}|\{ab\}\rangle &= \langle\{cd\}|\frac{1}{2}c_i^\dagger c_j^\dagger \langle ij|g|kl\rangle c_l c_k|\{ab\}\rangle \\ &= \frac{1}{2}\langle 0|c_d c_c c_i^\dagger c_j^\dagger \langle ij|g|kl\rangle c_l c_k c_a^\dagger c_b^\dagger|0\rangle.\end{aligned}\quad (\text{B.14})$$

Normal ordering the operators, yields

$$c_l c_k c_a^\dagger c_b^\dagger|0\rangle = \delta_{k,a}\delta_{l,b} - \delta_{l,a}\delta_{k,b}$$

and similarly

$$\langle 0|c_d c_c c_i^\dagger c_j^\dagger = \delta_{i,d}\delta_{j,c} - \delta_{j,c}\delta_{i,d}.$$

Then we have

$$\langle\{cd\}|\hat{G}|\{ab\}\rangle = \langle cd|g|ab\rangle - \langle dc|g|ab\rangle$$

which agrees with the results using determinantal wave functions (see, for instance, [124, Eq. (5.19)])

$$\langle\{cd\}|\hat{G}|\{ab\}\rangle = \frac{1}{2}(\langle cd| - \langle dc|)\hat{G}(|ab\rangle - |ba\rangle).\quad (\text{B.15})$$

We define the **electron field operators** in the *Schrödinger representation* (3.10) by

$$\hat{\psi}_S(\mathbf{x}) = c_j \phi_j(\mathbf{x}); \quad \hat{\psi}_S^\dagger(\mathbf{x}) = c_j^\dagger \phi_j^\dagger(\mathbf{x}).\quad (\text{B.16})$$

Then the second-quantized one-body operator can be expressed

$$\hat{F} = \int d^3\mathbf{x} c_i^\dagger \phi_i^*(x) f c_j \phi_j(x) = \int d^3\mathbf{x} \hat{\psi}_S^\dagger(x) f \hat{\psi}_S(x)\quad (\text{B.17})$$

and similarly with the two-body operator

$$\hat{G} = \frac{1}{2} \iint d^3\mathbf{x}_1 d^3\mathbf{x}_2 \hat{\psi}_S^\dagger(\mathbf{x}_1) \hat{\psi}_S^\dagger(\mathbf{x}_2) g \hat{\psi}_S(\mathbf{x}_2) \hat{\psi}_S(\mathbf{x}_1). \quad (\text{B.18})$$

The non-relativistic Hamiltonian for an  $N$ -electron system (2.11) consists of a single-particle and a two-particle operator

$$\begin{aligned} H_1 &= \sum_{n=1}^N \left( -\frac{\hbar^2}{2m} \nabla_n^2 + v_{\text{ext}}(\mathbf{x}_n) \right) = \sum_{n=1}^N h_1(n) \\ H_2 &= \sum_{m<n}^N \frac{e^2}{4\pi\epsilon_0 r_{mn}} = \sum_{m<n}^N h_2(m, n) \end{aligned} \quad (\text{B.19})$$

and in second quantization this can be expressed

$$\hat{H} = \int d^3\mathbf{x}_1 \hat{\psi}_S^\dagger(\mathbf{x}_1) h_1 \hat{\psi}_S(\mathbf{x}_1) + \frac{1}{2} \iint d^3\mathbf{x}_1 d^3\mathbf{x}_2 \hat{\psi}_S^\dagger(\mathbf{x}_1) \hat{\psi}_S^\dagger(\mathbf{x}_2) h_2 \hat{\psi}_S(\mathbf{x}_2) \hat{\psi}_S(\mathbf{x}_1). \quad (\text{B.20})$$

## B.2 Heisenberg and Interaction Pictures

In an alternative to the Schrödinger picture, the *Heisenberg picture* (HP), the states are time independent and the time-dependence is transferred to the operators,

$$|\Psi_H\rangle = |\Psi_S(t=0)\rangle = e^{i\hat{H}t/\hbar} |\Psi_S(t)\rangle; \quad \hat{O}_H = e^{i\hat{H}t/\hbar} \hat{O}_S e^{-i\hat{H}t/\hbar}. \quad (\text{B.21})$$

In perturbation theory the Hamiltonian is normally partitioned into a *zeroth-order Hamiltonian*  $H_0$  and a *perturbation*  $V$  (2.47),

$$\hat{H} = \hat{H}_0 + \hat{V}. \quad (\text{B.22})$$

We can then define an intermediate picture, known as the *interaction picture* (IP), where, the operators and state vectors are related to those in the Schrödinger picture by

$$|\Psi_1(t)\rangle = e^{i\hat{H}_0 t/\hbar} |\Psi_S(t)\rangle; \quad \hat{O}_1(t) = e^{i\hat{H}_0 t/\hbar} \hat{O}_S e^{-i\hat{H}_0 t/\hbar}. \quad (\text{B.23})$$

The relation between the Heisenberg and the interaction pictures is<sup>4</sup>

$$|\Psi_H\rangle = e^{i\hat{H}t/\hbar} e^{-i\hat{H}_0 t/\hbar} |\Psi_1(t)\rangle; \quad \hat{O}_H(t) = e^{i\hat{H}t/\hbar} e^{-i\hat{H}_0 t/\hbar} \hat{O}_1 e^{i\hat{H}_0 t/\hbar} e^{-i\hat{H}t/\hbar}. \quad (\text{B.24})$$

<sup>4</sup>Note that  $\hat{H}$  and  $\hat{H}_0$  generally do not commute, so that in general  $e^{i\hat{H}t/\hbar} e^{-i\hat{H}_0 t/\hbar} \neq e^{i\hat{V}t/\hbar}$ .

Using the relation (3.18), we then have

$$|\Psi_{\text{H}}\rangle = U(0, t)|\Psi_{\text{I}}(t)\rangle; \quad \hat{O}_{\text{H}}(t) = U(0, t)\hat{O}_{\text{I}}U(t, 0). \quad (\text{B.25})$$

The state vector of time-independent perturbation theory corresponds in all pictures considered here to the time-dependent state vectors with  $t = 0$ ,

$$|\Psi\rangle = |\Psi_{\text{H}}\rangle = |\Psi_{\text{S}}(0)\rangle = |\Psi_{\text{I}}(0)\rangle. \quad (\text{B.26})$$

In the *Heisenberg picture* (B.21) the electron-field operators (B.16) become

$$\hat{\psi}_{\text{H}}(x) = e^{i\hat{H}t/\hbar}\hat{\psi}_{\text{S}}(\mathbf{x})e^{-i\hat{H}t/\hbar}; \quad \hat{\psi}_{\text{H}}^{\dagger}(x) = e^{i\hat{H}t/\hbar}\hat{\psi}_{\text{S}}^{\dagger}(\mathbf{x})e^{-i\hat{H}t/\hbar} \quad (\text{B.27})$$

and in the *interaction picture* (IP) (B.23)

$$\begin{aligned} \hat{\psi}_{\text{I}}(x) &= e^{i\hat{H}_0t/\hbar}\hat{\psi}_{\text{S}}(\mathbf{x})e^{-i\hat{H}_0t/\hbar} = e^{i\hat{H}_0t/\hbar}c_j\phi_j(\mathbf{x})e^{-i\hat{H}_0t/\hbar} \\ &= c_j\phi_j(\mathbf{x})e^{-i\varepsilon_jt/\hbar} = c_j\phi_j(x) \\ \hat{\psi}_{\text{I}}^{\dagger}(x) &= c_j^{\dagger}\phi_j^{\dagger}(\mathbf{x})e^{i\varepsilon_jt/\hbar} = c_j^{\dagger}\phi_j^{\dagger}(x), \end{aligned} \quad (\text{B.28})$$

where  $\phi_j(\mathbf{x})$  is an eigenfunction of  $H_0$ . We also introduce the *time-dependent* creation/annihilations operators in the IP by

$$c_j(t) = c_j e^{-i\varepsilon_jt/\hbar}; \quad c_j^{\dagger}(t/\hbar) = c_j^{\dagger} e^{i\varepsilon_jt/\hbar}, \quad (\text{B.29})$$

which gives

$$\hat{\psi}_{\text{I}}(x) = c_j(t)\phi_j(\mathbf{x}); \quad \hat{\psi}_{\text{I}}^{\dagger}(x) = c_j^{\dagger}(t)\phi_j^{\dagger}(\mathbf{x}). \quad (\text{B.30})$$

From the definition (B.23) we have

$$\frac{\partial}{\partial t}\hat{O}_{\text{I}}(t) = \frac{\partial}{\partial t}\left[e^{i\hat{H}_0t/\hbar}\hat{O}_{\text{S}}e^{-i\hat{H}_0t/\hbar}\right] = \frac{i}{\hbar}[H_0, \hat{O}_{\text{I}}(t)]. \quad (\text{B.31})$$

# Appendix C

## Representations of States and Operators

### C.1 Vector Representation of States

A *state* of a system can be represented by the *wave function* or *Schrödinger function*  $\Psi(x)$ , where  $x$  stands for all (space) coordinates. If we have a complete basis set available in the same *Hilbert space* (see Appendix A.2),  $\{\phi_j(x)\}$ , then we can expand the function as

$$\Psi(x) = a_j \phi_j(x) \tag{C.1}$$

with summation over  $j$  according to the Einstein summation rule. If the basis set is *orthonormal*, implying that the *scalar or inner product* satisfies the relation

$$\langle i|j\rangle = \int dx \phi_j^\dagger \phi_j(x) = \delta_{i,j}, \tag{C.2}$$

then the expansion coefficients are given by the scalar product

$$a_j = \int dx \phi_j^\dagger \Psi(x) = \langle j|\Psi\rangle. \tag{C.3}$$

These numbers form a vector, which is the **vector representation of the state  $\Psi$**  or the **state vector**,

$$|\Psi\rangle = \begin{pmatrix} \langle 1|\Psi\rangle \\ \langle 2|\Psi\rangle \\ \vdots \\ \langle N|\Psi\rangle \end{pmatrix}. \tag{C.4}$$

Note that this is just a set of numbers—no coordinates are involved.  $N$  is here the number of basis states, which may be finite or infinite. [The basis set need not be

numerable and can form a *continuum* in which case the sum over the states is replaced by an integral.] The basis states are represented by unit vectors  $|j\rangle$

$$|1\rangle = \begin{pmatrix} 1 \\ 0 \\ 0 \\ \vdots \\ \vdots \end{pmatrix} \quad |2\rangle = \begin{pmatrix} 0 \\ 1 \\ 0 \\ \vdots \\ \vdots \end{pmatrix} \quad \text{etc.} \quad (\text{C.5})$$

The basis vectors are time independent, and for time-dependent states the time dependence is contained in the coefficients

$$|\Psi(t)\rangle = a_j(t)|j\rangle. \quad (\text{C.6})$$

$|\Psi\rangle$  is a **ket vector**, and for each ket vector there is a corresponding **bra vector**

$$\langle\Psi| = (a_1^*, a_2^*, \dots), \quad (\text{C.7})$$

where the asterisk represents complex conjugate. It follows from (C.1) that

$$a_j^* = \langle\Psi|j\rangle. \quad (\text{C.8})$$

The *scalar product* of two general vectors with expansion coefficients  $a_j$  and  $b_j$ , respectively, becomes

$$\langle\Psi|\Phi\rangle = a_j^* b_j \quad (\text{C.9})$$

with the basis vectors being orthonormal. This is identical to the scalar product of the corresponding vector representations

$$\langle\Psi|\Phi\rangle = (a_1^*, a_2^*, \dots) \begin{pmatrix} b_1 \\ b_2 \\ \vdots \\ \vdots \end{pmatrix}. \quad (\text{C.10})$$

The ket vector (C.4) can be expanded as

$$|\Psi\rangle = |j\rangle\langle j|\Psi\rangle. \quad (\text{C.11})$$

But this holds for any vector in the Hilbert space, and therefore we have the formal relation in that space

$$\boxed{|j\rangle\langle j| \equiv I}, \quad (\text{C.12})$$

where  $I$  is the *identity operator*. This is known as the **resolution of the identity**. Using the expression for the coefficients, the scalar product (C.9) can also be expressed

$$\langle \Psi | \Phi \rangle = \langle \Psi | j \rangle \langle j | \Phi \rangle, \quad (\text{C.13})$$

which becomes obvious, considering the expression for the identity operator.

## C.2 Matrix Representation of Operators

The operators we are dealing with have the property that when acting on a function in our Hilbert space they generate another (or the same) function in that space,

$$\hat{O} \Psi(x) = \Phi(x) \quad (\text{C.14})$$

or with vector notations

$$\hat{O} |\Psi\rangle = |\Phi\rangle. \quad (\text{C.15})$$

Expanding the vectors on the l.h.s according to the above, yields

$$|i\rangle \langle i | \hat{O} | j \rangle \langle j | \Psi \rangle = |\Phi\rangle. \quad (\text{C.16})$$

Obviously, we have the identity

$$\hat{O} \equiv |i\rangle \langle i | \hat{O} | j \rangle \langle j|. \quad (\text{C.17})$$

The numbers  $\langle i | \hat{O} | j \rangle$  are **matrix elements**

$$\langle i | \hat{O} | j \rangle = \int dx \phi_i^\dagger(x) \hat{O} \phi_j(x), \quad (\text{C.18})$$

and they form the **matrix representation of the operator**

$$\hat{O} \Rightarrow \begin{pmatrix} \langle 1 | \hat{O} | 1 \rangle & \langle 1 | \hat{O} | 2 \rangle & \dots \\ \langle 2 | \hat{O} | 1 \rangle & \langle 2 | \hat{O} | 2 \rangle & \dots \\ \dots & \dots & \dots \end{pmatrix}.$$

Standard matrix multiplication rules are used in operations with vector and matrix representations, for instance,

$$\hat{O}|\Psi\rangle = |\Phi\rangle \Rightarrow \begin{pmatrix} \langle 1|\hat{O}|1\rangle & \langle 1|\hat{O}|2\rangle & \cdots \\ \langle 2|\hat{O}|1\rangle & \langle 2|\hat{O}|2\rangle & \cdots \\ \cdots & \cdots & \cdots \end{pmatrix} \cdot \begin{pmatrix} \langle 1|\Psi\rangle \\ \langle 2|\Psi\rangle \\ \vdots \\ \langle N|\Psi\rangle \end{pmatrix} = \begin{pmatrix} \langle 1|\Phi\rangle \\ \langle 2|\Phi\rangle \\ \vdots \\ \langle N|\Phi\rangle \end{pmatrix},$$

where

$$\langle k|\Phi\rangle = \langle k|\hat{O}|j\rangle\langle j|\Phi\rangle,$$

summed over the index  $j$ .

### C.3 Coordinate Representations

#### *Representation of Vectors*

The *coordinate representation* of the ket vector  $|\Psi\rangle$  (C.4) is denoted  $\langle x|\Psi\rangle$ , and this is identical to the corresponding state or (Schrödinger) wave function

$$\langle x|\Psi\rangle \equiv \Psi(x); \quad \langle \Psi|x\rangle \equiv \Psi^\dagger(x). \quad (\text{C.19})$$

This can be regarded as a generalization of the expansion for the expansion coefficients (C.1), where the space coordinates correspond to a continuous set of basis functions.

The basis functions  $\phi_j(x)$  have the coordinate representation  $\langle x|j\rangle$ , and the coordinate representation (C.1) becomes

$$\langle x|\Psi\rangle = a_j \phi_j(x) = a_j \langle x|j\rangle. \quad (\text{C.20})$$

The scalar product between the functions  $\Psi(x)$  and  $\Phi(x)$  is

$$\langle \Psi|\Phi\rangle = \int dx \Psi^\dagger(x) \Phi(x), \quad (\text{C.21})$$

which we can express as

$$\langle \Psi|\Phi\rangle = \int dx \langle \Psi|x\rangle\langle x|\Phi\rangle. \quad (\text{C.22})$$

We shall assume that an *integration is always understood*, when Dirac notations of the kind above are used, i.e.,

$$\langle \Psi|\Phi\rangle = \langle \Psi|x\rangle\langle x|\Phi\rangle, \quad (\text{C.23})$$



in analogy with the summation rule for discrete basis sets. This leads to the formal identity

$$\boxed{|x\rangle\langle x| \equiv I,} \quad (\text{C.24})$$

which is consistent with the corresponding relation (C.12) with a numerable basis set.

### *Closure Property*

From the expansion (C.1) we have

$$\Psi(x) = \int dx' \phi_j^\dagger(x') \Psi(x') \phi_j(x). \quad (\text{C.25})$$

This can be compared with the integration over the Dirac delta function

$$\Psi(x) = \int dx' \delta(x - x') \Psi(x'), \quad (\text{C.26})$$

which leads to the relation known as the **closure property**

$$\boxed{\phi_j^\dagger(x') \phi_j(x) = \delta(x - x')} \quad (\text{C.27})$$

(with summation over  $j$ ). In Dirac notations this becomes

$$\langle x|j\rangle\langle j|x'\rangle = \delta(x - x')$$

or

$$\boxed{\langle x|I|x'\rangle = \delta(x - x'),} \quad (\text{C.28})$$

which implies that **the delta function is the coordinate representation of the identity operator** (C.12). Note that there is *no integration* over the space coordinates here.

### *Representation of Operators*

The coordinate representation of an operator is expressed in analogy with that of a state vector

$$\hat{O} \Rightarrow \langle x|\hat{O}|x'\rangle = \hat{O}(x, x'), \quad (\text{C.29})$$

which is a function of  $x$  and  $x'$ . An operator  $\hat{O}$  acting on a state vector  $|\Psi\rangle$  is represented by

$$\langle x|\hat{O}|\Psi\rangle \Rightarrow \langle x|\hat{O}|x'\rangle\langle x'|\Psi\rangle = \int dx' \hat{O}(x, x') \Psi(x'), \quad (\text{C.30})$$

which is a function of  $x$ .

# Appendix D

## Dirac Equation and the Momentum Representation

### D.1 Dirac Equation

#### *Free Particles*

The standard quantum-mechanical operator representation

$$E \rightarrow \hat{E} = i\hbar \frac{\partial}{\partial t}; \quad \mathbf{p} \rightarrow \hat{\mathbf{p}} = -i\hbar \nabla; \quad \mathbf{x} \rightarrow \hat{\mathbf{x}} = \mathbf{x}, \quad (\text{D.1})$$

where  $E$ ,  $\mathbf{p}$ ,  $\mathbf{x}$  represent the energy, momentum and coordinate vectors and  $\hat{E}$ ,  $\hat{\mathbf{p}}$ ,  $\hat{\mathbf{x}}$  the corresponding quantum-mechanical operators, was early used to obtain the non-relativistic Schrödinger equation (2.9). If we apply the same procedure to the *relativistic* energy relation

$$E^2 = c^2 \mathbf{p}^2 + m_e^2 c^4, \quad (\text{D.2})$$

where  $c$  is the velocity of light in vacuum and  $m_e$  the mass of the electron, this would lead to

$$-\hbar^2 \frac{\partial^2 \psi(x)}{\partial t^2} = \left( c^2 \hat{\mathbf{p}}^2 + m_e^2 c^4 \right) \psi(x), \quad (\text{D.3})$$

which is the *Schrödinger relativistic wave equation*. It is also known as the *Klein-Gordon equation*. In covariant notations (see Appendix A.1) it can be expressed

$$(\hbar^2 \square + m_e^2 c^2) \psi(x) = 0. \quad (\text{D.4})$$

In contrast to the non-relativistic Schrödinger equation (2.9) the Klein-Gordon equation is *non-linear* in the time derivative (energy) and therefore the superposition principle cannot be applied for energies. Furthermore, there is no time-evolution operator, as discussed in Sect. 3.2. In order to obtain an equation that is first order in

the time derivative and still consistent with the energy relation (D.2) and the quantum-mechanical substitutions (D.1), Dirac proposed the form for a free electron<sup>5</sup>

$$\boxed{i\hbar \frac{\partial \psi(x)}{\partial t} = (c\boldsymbol{\alpha} \cdot \hat{\mathbf{p}} + \beta m_e c^2) \psi(x)}, \quad (\text{D.5})$$

where  $\boldsymbol{\alpha}$  and  $\beta$  are constants (but not necessarily pure numbers). This equation is the famous *Dirac equation for a relativistic particle in free space*.

The equivalence with the equation (D.3) requires

$$(c\boldsymbol{\alpha} \cdot \hat{\mathbf{p}} + \beta m_e c^2)(c\boldsymbol{\alpha} \cdot \hat{\mathbf{p}} + \beta m_e c^2) \equiv c^2 \hat{\mathbf{p}}^2 + m_e^2 c^4,$$

which leads to

$$\begin{cases} \alpha_x^2 = \alpha_y^2 = \alpha_z^2 = \beta^2 = 1 \\ \alpha_x \alpha_y + \alpha_y \alpha_x = 0 \quad (\text{cyclic}) \\ \boldsymbol{\alpha} \beta + \beta \boldsymbol{\alpha} = 0, \end{cases} \quad (\text{D.6})$$

where “cyclic” implies that the relation holds for  $x \rightarrow y \rightarrow z \rightarrow x$ .

The solution proposed by Dirac is that  $\boldsymbol{\alpha}$  and  $\beta$  are given by the so-called *Dirac matrices*

$$\boldsymbol{\alpha} = \begin{pmatrix} 0 & \boldsymbol{\sigma} \\ \boldsymbol{\sigma} & 0 \end{pmatrix}; \quad \beta = \begin{pmatrix} 1 & 0 \\ 0 & -1 \end{pmatrix}, \quad (\text{D.7})$$

where  $\boldsymbol{\sigma} = (\sigma_x, \sigma_y, \sigma_z)$  are the *Pauli spin matrices*

$$\sigma_x = \begin{pmatrix} 0 & 1 \\ 1 & 0 \end{pmatrix}; \quad \sigma_y = \begin{pmatrix} 0 & -i \\ i & 0 \end{pmatrix}; \quad \sigma_z = \begin{pmatrix} 1 & 0 \\ 0 & -1 \end{pmatrix}. \quad (\text{D.8})$$

The Dirac matrices anticommute

$$\boldsymbol{\alpha} \beta + \beta \boldsymbol{\alpha} = 0. \quad (\text{D.9})$$

With the covariant four-dimensional momentum vector (A.2)  $p_\mu = (p_0, -\mathbf{p})$ , and the corresponding vector operator in the coordinate representation

$$\hat{p}_\mu = (\hat{p}_0, -\hat{\mathbf{p}}) = \left( \frac{i\hbar}{c} \frac{\partial}{\partial t}, i\hbar \nabla \right), \quad (\text{D.10})$$

the Dirac equation (D.5) becomes

$$(c\hat{p}_0 - c\boldsymbol{\alpha} \cdot \hat{\mathbf{p}} - \beta m_e c^2) \psi(x) = 0. \quad (\text{D.11})$$

---

<sup>5</sup>We use here the “hat” symbol to indicate the momentum operators in the coordinate representation.

With

$$\alpha^\mu = (1, \boldsymbol{\alpha}) \quad (\text{D.12})$$

and  $\alpha^\mu \hat{p}_\mu = \hat{p}_0 - \boldsymbol{\alpha} \cdot \hat{\mathbf{p}}$  we obtain the **covariant form of the Dirac Hamiltonian** for a free-particle

$$\hat{H}_D = -c\alpha^\mu \hat{p}_\mu + \beta m_e^2 c^2 \quad (\text{D.13})$$

and the corresponding Dirac equation

$$(c\alpha^\mu \hat{p}_\mu - \beta m_e c^2) \psi(x) = 0. \quad (\text{D.14})$$

With the *Dirac gamma matrices*

$$\gamma^\mu = \beta \alpha^\mu \quad (\text{D.15})$$

this can also be expressed ( $\beta^2 = 1$ )

$$(\gamma^\mu \hat{p}_\mu - m_e c) \psi(x) = (\hat{\not{p}} - m_e c) \psi(x) = 0, \quad (\text{D.16})$$

where  $\hat{\not{p}}$  is the “*p - slash*” operator

$$\hat{\not{p}} = \gamma^\mu \hat{p}_\mu = \beta \alpha^\mu \hat{p}_\mu = \beta(\hat{p}_0 - \boldsymbol{\alpha} \cdot \hat{\mathbf{p}}). \quad (\text{D.17})$$

Separating the wave function into space and time parts,

$$\psi(x) = \phi_p(\mathbf{x}) e^{-i\varepsilon_p t/\hbar}, \quad (\text{D.18})$$

we have

$$\psi(x) = \hat{p}_0 \phi_p(x) = \frac{\varepsilon_p}{c} \phi_p(x). \quad (\text{D.19})$$

The time-independent part of the Dirac equation (D.5) becomes

$$\hat{h}_D^{\text{free}}(\hat{\mathbf{p}}) \phi_p(\mathbf{x}) = \varepsilon_p \phi_p(\mathbf{x}), \quad (\text{D.20})$$

where

$$\hat{h}_D^{\text{free}} = c\boldsymbol{\alpha} \cdot \hat{\mathbf{p}} + \beta m_e c^2 \quad (\text{D.21})$$

is the corresponding part of the **free-electron Dirac Hamiltonian**. The time-independent part of the Dirac equation can now be expressed

$$\left( \beta \frac{\varepsilon_p}{c} - \beta \boldsymbol{\alpha} \cdot \hat{\mathbf{p}} - m_e c \right) \phi_p(\mathbf{x}) = (\beta \hat{p}_0 - \beta \boldsymbol{\alpha} \cdot \hat{\mathbf{p}} - m_e c) \phi_p(\mathbf{x}) = 0. \quad (\text{D.22})$$

Here,  $\phi_p(\mathbf{x})$  is a four-component wave function, which can be represented by

$$\phi_p(\mathbf{x}) = \frac{1}{\sqrt{V}} u_r(\mathbf{p}) e^{i\mathbf{p}\cdot\mathbf{x}}; \quad \hat{\mathbf{p}} \phi_p(\mathbf{x}) = \mathbf{p} \phi_p(\mathbf{x}). \quad (\text{D.23})$$

$e^{i\mathbf{p}\cdot\mathbf{x}}$  represents a *plane wave*, and  $u_r(\mathbf{p})$  is a four-component vector function of the momentum  $\mathbf{p}$ . For each  $\mathbf{p}$  there are four independent solutions ( $r = 1, 2, 3, 4$ ). The parameter  $p$  in our notations  $\phi_p$  and  $\varepsilon_p$  represents  $\mathbf{p}$  and  $r$  or, more explicitly,

$$\phi_p(\mathbf{x}) = \phi_{\mathbf{p},r}(\mathbf{x}); \quad \varepsilon_p = \varepsilon_{\mathbf{p},r}.$$

With the wave function (D.23) the Dirac equation (D.22) leads to the following equation for the  $u_r(\mathbf{p})$  functions

$$\left( \beta \frac{\varepsilon_p}{c} - \beta \boldsymbol{\alpha} \cdot \mathbf{p} - m_e c \right) u_r(\mathbf{p}) = 0$$

or

$$\begin{pmatrix} \varepsilon_p/c - m_e c & -\boldsymbol{\sigma} \cdot \mathbf{p} \\ \boldsymbol{\sigma} \cdot \mathbf{p} & -\varepsilon_p/c - m_e c \end{pmatrix} u_r(\mathbf{p}) = 0, \quad (\text{D.24})$$

where each element is a  $2 \times 2$  matrix. This eqn has two solutions for each momentum vector  $\mathbf{p}$ :

$$u_+(\mathbf{p}) = N_+ \begin{pmatrix} \varepsilon_p/c + m_e c \\ \boldsymbol{\sigma} \cdot \mathbf{p} \end{pmatrix}; \quad u_-(\mathbf{p}) = N_- \begin{pmatrix} -\boldsymbol{\sigma} \cdot \mathbf{p} \\ -\varepsilon_p/c + m_e c \end{pmatrix} \quad (\text{D.25})$$

corresponding to positive ( $r = 1, 2$ ) and negative ( $r = 3, 4$ ) eigenvalues, respectively. Defining the momentum component  $p_0$ —to be distinguished from the corresponding *operator* component  $\hat{p}_0$  (D.10)—by

$$|\varepsilon_p| = E_p = cp_0; \quad p_0 = \sqrt{\mathbf{p}^2 + m_e^2 c^2}, \quad (\text{D.26})$$

we have

$$u_+(\mathbf{p}) = N_+ \begin{pmatrix} p_0 + m_e c \\ \boldsymbol{\sigma} \cdot \mathbf{p} \end{pmatrix}; \quad u_-(\mathbf{p}) = N_- \begin{pmatrix} -\boldsymbol{\sigma} \cdot \mathbf{p} \\ p_0 + m_e c \end{pmatrix}. \quad (\text{D.27})$$

The corresponding eigenfunctions (D.23) are

$$\phi_{p_+}(x) = \frac{1}{\sqrt{V}} u_+(\mathbf{p}) e^{i\mathbf{p}\cdot\mathbf{x}} e^{-iE_p t/\hbar}; \quad \phi_{p_-}(x) = \frac{1}{\sqrt{V}} u_-(\mathbf{p}) e^{i\mathbf{p}\cdot\mathbf{x}} e^{iE_p t/\hbar}, \quad (\text{D.28})$$

including the time dependence according to (D.18) and (D.26). We note that

$$\begin{cases} \hat{p}_0 \phi_{p_+}(x) = \frac{E_p}{c} \hat{p}_0 \phi_{p_+}(x) = p_0 \phi_{p_+}(x); \\ \hat{p}_0 \phi_{p_-}(x) = -\frac{E_p}{c} \hat{p}_0 \phi_{p_-}(x) = -p_0 \phi_{p_-}(x). \end{cases}$$

The vectors

$$u(\mathbf{p}) = u_+(\mathbf{p}) \quad \text{and} \quad v(\mathbf{p}) = u_-(-\mathbf{p}) = N_- \begin{pmatrix} \boldsymbol{\sigma} \cdot \mathbf{p} \\ p_0 + m_e c \end{pmatrix} \quad (\text{D.29})$$

satisfy the equations

$$(\not{p} - m_e c) u(\mathbf{p}) = 0 \quad \text{and} \quad (\not{p} + m_e c) v(\mathbf{p}) = 0, \quad (\text{D.30})$$

where

$$\not{p} = \beta(p_0 - \boldsymbol{\alpha} \cdot \mathbf{p}) \quad (\text{D.31})$$

is the momentum function—or operator in momentum representation—corresponding to the operator  $\hat{p}$  (D.17) in coordinate space. Note that the negative energy solution corresponds here to the momentum  $-\mathbf{p}$  for the electron (or  $+\mathbf{p}$  for the hole/positron).

It should be observed that in the covariant notation  $p_0$  is normally *disconnected from the energy* (D.26), i.e.,

$$p_0 \neq \sqrt{\mathbf{p}^2 + m_e^2 c^2}. \quad (\text{D.32})$$

This is known as *off the mass shell*. When the relation (D.26) holds, it is referred to as *on the mass shell*, which can also be expressed

$$\boxed{p^2 = p_0^2 - \mathbf{p}^2 = m_e^2 c^2}. \quad (\text{D.33})$$

This is often expressed

$$\boxed{\not{p} = m_e c}, \quad (\text{D.34})$$

which, however, is not a real identity. The corresponding operator relation holds, when operating on an eigenfunction to the Dirac free-particle equation (D.16).

### Normalization

Several different schemes for the normalization of the  $u$  matrices have been used (see, for instance, Mandl and Shaw [143, Chap. 4]). Here, we shall use

$$u_{r'}^\dagger(\mathbf{p}) u_r(\mathbf{p}) = \delta_{r',r}, \quad (\text{D.35})$$

which leads to

$$\begin{aligned} |u_+(\mathbf{p})|^2 &= |N_+|^2 (p_0 + m_e c, \boldsymbol{\sigma} \cdot \mathbf{p}) \begin{pmatrix} p_0 + m_e c \\ \boldsymbol{\sigma} \cdot \mathbf{p} \end{pmatrix} \\ &= |N_+|^2 (p_0 + m_e c)^2 + (\boldsymbol{\sigma} \cdot \mathbf{p})^2 = |N_+|^2 2p_0 (p_0 + m_e c), \end{aligned} \quad (\text{D.36})$$

using  $(\boldsymbol{\sigma} \cdot \mathbf{p})^2 = \mathbf{p}^2 = p_0^2 - m_e^2 c^2$ . This gives

$$N_+ = \frac{1}{\sqrt{2p_0 (p_0 + m_e c)}} \quad (\text{D.37})$$

and the similarly for  $N_-$ .

With the normalization above we have

$$\begin{aligned} u_+(\mathbf{p}) u_+^\dagger(\mathbf{p}) &= |N_+|^2 \begin{pmatrix} p_0 + m_e c \\ \boldsymbol{\sigma} \cdot \mathbf{p} \end{pmatrix} (p_0 + m_e c, \boldsymbol{\sigma} \cdot \mathbf{p}) \\ &= \frac{1}{2p_0} \begin{pmatrix} p_0 + m_e c & \boldsymbol{\sigma} \cdot \mathbf{p} \\ \boldsymbol{\sigma} \cdot \mathbf{p} & p_0 - m_e c \end{pmatrix} = \frac{p_0 + \boldsymbol{\alpha} \cdot \mathbf{p} + \beta m_e c}{2p_0} \end{aligned} \quad (\text{D.38})$$

and similarly

$$u_-(\mathbf{p}) u_-^\dagger(\mathbf{p}) = \frac{p_0 - (\boldsymbol{\alpha} \cdot \mathbf{p} + \beta m_e c)}{2p_0}, \quad (\text{D.39})$$

which gives

$$u_+(\mathbf{p}) u_+^\dagger(\mathbf{p}) + u_-(\mathbf{p}) u_-^\dagger(\mathbf{p}) = I. \quad (\text{D.40})$$

## ***Dirac Equation in an Electromagnetic Field***

Classically, the interaction of an electron with electromagnetic fields is given by the “minimal substitution” (E.15), which in covariant notations can be expressed<sup>6</sup>

$$\hat{p}_\mu \rightarrow \hat{p}_\mu + eA_\mu \quad (\text{D.41})$$

---

<sup>6</sup>In many text books the minimal substitution is expressed as  $\hat{p}_\mu \rightarrow \hat{p}_\mu + \frac{e}{c}A_\mu$ , because a mixed unit system, like the cgs system, is being used. In the SI system—or any other consistent unit system—the substitution has the form given in the text. The correctness of this expression can be checked by means of dimensional analysis (see Appendix K).



with the four-dimensional potential being

$$A_\mu(x) = \left( \frac{\phi(x)}{c}, -\mathbf{A}(x) \right). \quad (\text{D.42})$$

This implies that the Dirac Hamiltonian (D.13) becomes

$$H_D = -c\alpha^\mu (\hat{p}_\mu + eA_\mu) + \beta m_e c^2, \quad (\text{D.43})$$

and that the interaction with the fields is given by the term

$$H_{\text{int}} = -ec\alpha^\mu A_\mu. \quad (\text{D.44})$$

## D.2 Momentum Representation

### *Representation of States*

Above in Sect. C.3 we have considered the coordinate representation of a state vector,  $\phi_a(\mathbf{x}) = \langle \mathbf{x} | a \rangle$ . An alternative is the *momentum representation*, where the state vector is expanded in momentum eigenfunctions. A state  $|a\rangle$  is then represented by  $\phi_a(\mathbf{p}r) = \langle \mathbf{p}r | a \rangle$ , which are the expansion coefficients of the state in momentum eigenfunctions

$$\langle \mathbf{x} | a \rangle = \langle \mathbf{x} | \mathbf{p}r \rangle \langle \mathbf{p}r | a \rangle \quad (\text{D.45})$$

with summations over  $\mathbf{p}$  and  $r$ . The expansion coefficients become

$$\langle \mathbf{p}r | a \rangle = \int d^3\mathbf{x} \langle \mathbf{p}r | \mathbf{x} \rangle \langle \mathbf{x} | a \rangle = \sqrt{\frac{1}{V}} \int d^3\mathbf{x} e^{-i\mathbf{p}\cdot\mathbf{x}} u_r^\dagger(\mathbf{p}) \phi_a(\mathbf{x}). \quad (\text{D.46})$$

In the limit of continuous momenta the sum over  $\mathbf{p}$  is replaced by an integral and  $V$  replaced by  $(2\pi)^3$ .

Note that the *momentum representation is distinct from the Fourier transform*. The latter is defined as

$$\begin{aligned} \langle \mathbf{p} | a \rangle &= u_r(\mathbf{p}) \langle \mathbf{p}r | a \rangle = \sqrt{\frac{1}{V}} \int d^3\mathbf{x} e^{-i\mathbf{p}\cdot\mathbf{x}} \phi_a(\mathbf{x}) \\ &\rightarrow (2\pi)^{-3/2} \int d^3\mathbf{x} e^{-i\mathbf{p}\cdot\mathbf{x}} \phi_a(\mathbf{x}), \end{aligned} \quad (\text{D.47})$$

using the identity (D.40).

In analogy with (C.23) we have

$$\langle a|b\rangle = \langle a|\mathbf{p}, r\rangle \langle \mathbf{p}, r|b\rangle, \quad (\text{D.48})$$

which yields

$$|\mathbf{p}, r\rangle \langle \mathbf{p}, r| \equiv I \quad (\text{D.49})$$

with implicit summation/integration over  $\mathbf{p}$  and summation over  $r$ .

### ***Representation of Operators***

*Coordinate representation* of an operator  $\hat{O}$ :  $O(\mathbf{x}_2, \mathbf{x}_1) = \langle \mathbf{x}_2|\hat{O}|\mathbf{x}_1\rangle$

*Momentum representation* of an operator  $\hat{O}$ :  $O(\mathbf{p}_2 r_2, \mathbf{p}_1 r_1) = \langle \mathbf{p}_2 r_2|\hat{O}|\mathbf{p}_1 r_1\rangle$ . Transformation between the representations

$$\langle \mathbf{p}_2 r_2|\hat{O}|\mathbf{p}_1 r_1\rangle = \iint d^3\mathbf{x}_2 d^3\mathbf{x}_1 \langle \mathbf{p}_2 r_2|\mathbf{x}_2\rangle \langle \mathbf{x}_2|\hat{O}|\mathbf{x}_1\rangle \langle \mathbf{x}_1|\mathbf{p}_1 r_1\rangle. \quad (\text{D.50})$$

The corresponding *Fourier transform* is according to (D.47)

$$u_{r_2}(\mathbf{p}_2) \langle \mathbf{p}_2 r_2|\hat{O}|\mathbf{p}_1 r_1\rangle u_{r_1}^\dagger(\mathbf{p}_1). \quad (\text{D.51})$$

Any operator with a complete set of eigenstates can be expanded as

$$\hat{O} = |j\rangle \varepsilon_j \langle j| \quad \text{where} \quad \hat{O}|j\rangle = \varepsilon_j |j\rangle. \quad (\text{D.52})$$

This gives the coordinate and momentum representations

$$\langle \mathbf{x}_2|\hat{O}|\mathbf{x}_1\rangle = \langle \mathbf{x}_2|j\rangle \varepsilon_j \langle j|\mathbf{x}_1\rangle \quad (\text{D.53a})$$

$$\langle \mathbf{p}_2 r_2|\hat{O}|\mathbf{p}_1 r_1\rangle = \langle \mathbf{p}_2, r_2|j\rangle \varepsilon_j \langle j|\mathbf{p}_1 r_1\rangle. \quad (\text{D.53b})$$

### ***Closure Property for Momentum Functions***

In three dimensions we have the closure property (C.27)

$$\phi_j^\dagger(\mathbf{x}) \phi_j(\mathbf{x}') = \delta^3(\mathbf{x} - \mathbf{x}'), \quad (\text{D.54})$$

and for a continuous set of momentum eigenfunctions this becomes

$$\int d^3\mathbf{p} \phi_{\mathbf{p}r}^\dagger(\mathbf{x}) \phi_{\mathbf{p}r}(\mathbf{x}') = \delta^3(\mathbf{x} - \mathbf{x}') \quad (\text{D.55})$$

with summation over  $r$ . This can also be expressed

$$\langle \mathbf{x} | \mathbf{p} r \rangle \langle \mathbf{p} r | \mathbf{x} \rangle = \delta^3(\mathbf{x} - \mathbf{x}') \quad (\text{D.56})$$

also with integration over  $\mathbf{p}$ . From the closure property (D.54) we have

$$\phi_j^\dagger(\mathbf{p}, r) \phi_j(\mathbf{p}', r') = \delta_{r,r'} \delta^3(\mathbf{p} - \mathbf{p}'), \quad (\text{D.57})$$

which leads to

$$\langle \mathbf{p}, r | j \rangle \langle j | \mathbf{p}', r' \rangle = \delta_{r,r'} \delta^3(\mathbf{p} - \mathbf{p}'). \quad (\text{D.58})$$

### D.3 Relations for the Alpha and Gamma Matrices

From the definition of the alpha matrices and the definitions in Appendix A we find the following useful relations:

$$\begin{aligned} \alpha^\mu \alpha_\mu &= 1 - \alpha^2 = -2 \\ \alpha^\mu \alpha \alpha_\mu &= \alpha \alpha^\mu \alpha_\mu = -2\alpha \\ \alpha^\mu \beta \alpha_\mu &= \beta - \alpha \beta \alpha = 4\beta \\ \alpha^\mu \beta \alpha^\mu &= \beta + \alpha \beta \alpha = -2\beta \\ \alpha^\mu \mathcal{A} \alpha_\mu &= \alpha^\mu \beta \alpha_\sigma A^\sigma \alpha_\mu = 4\mathcal{A} \end{aligned} \quad (\text{D.59})$$

where  $\mathcal{A}$  is defined in (D.17). The gamma matrices satisfy the following anti-commutation rule:

$$\begin{aligned} \gamma^\nu \gamma^\mu + \gamma^\mu \gamma^\nu &= 2g^{\mu\nu} \\ \mathcal{A} \mathcal{B} + \mathcal{B} \mathcal{A} &= 2AB \end{aligned} \quad (\text{D.60})$$

This leads to

$$\begin{aligned} \gamma^\mu \gamma^\nu \gamma_\mu &= -2\gamma_\nu \\ \gamma^\mu \mathcal{A} \gamma_\mu &= -2\mathcal{A} \\ \gamma^\mu \gamma_\mu &= 4 \\ \gamma^\mu \gamma^\nu \gamma_\mu &= -2\gamma_\nu \\ \gamma^\mu \mathcal{A} \gamma_\mu &= -2\mathcal{A} \end{aligned}$$

$$\begin{aligned}
\gamma^0 \gamma_0 &= \gamma^0 \gamma^0 = 1 \\
\gamma^\sigma \gamma^0 &= \gamma^0 \tilde{\gamma}^\sigma \\
\cancel{A} \gamma^0 &= \gamma^0 \tilde{A} \\
\gamma^0 \gamma^\sigma \gamma^0 &= \tilde{\gamma}^\sigma \\
\gamma^0 \cancel{A} \gamma^0 &= \tilde{A} \\
\gamma^0 \gamma^\sigma \gamma^\tau \gamma^0 &= \tilde{\gamma}^\sigma \tilde{\gamma}^\tau \\
\gamma^0 \cancel{A} \cancel{B} \gamma^0 &= \tilde{A} \tilde{B} \\
\gamma^0 \gamma^\beta \gamma^\sigma \gamma^\tau \gamma^0 &= \tilde{\gamma}^\beta \tilde{\gamma}^\sigma \tilde{\gamma}^\tau \\
\gamma^0 \cancel{A} \cancel{B} \cancel{C} \gamma^0 &= \tilde{A} \tilde{B} \tilde{C}
\end{aligned} \tag{D.61}$$

where  $\tilde{A} = \gamma^0 A_0 - \gamma^i A_i = \gamma^0 + \boldsymbol{\gamma} \cdot \mathbf{A}$ .

With the number of dimensions being equal to  $4 - \epsilon$ , to be used in dimensional regularization (see Chap. 12), the relations become

$$\begin{aligned}
\gamma^\mu \gamma_\mu &= 4 - \epsilon \\
\gamma^\mu \gamma^\sigma \gamma_\mu &= -(2 - \epsilon) \gamma^\sigma \\
\gamma^\mu \cancel{A} \gamma_\mu &= -(2 - \epsilon) \cancel{A} \\
\gamma^\mu \gamma^\sigma \gamma^\tau \gamma_\mu &= 4g^{\sigma\tau} - \epsilon \gamma^\sigma \gamma^\tau \\
\gamma^\mu \cancel{A} \cancel{B} \gamma_\mu &= 4AB - \epsilon \cancel{A} \cancel{B} \\
\gamma^\mu \gamma^\beta \gamma^\sigma \gamma^\tau \gamma_\mu &= -2\gamma^\tau \gamma^\sigma \gamma^\beta + \epsilon \gamma^\beta \gamma^\sigma \gamma^\tau \\
\gamma_i \gamma^i &= 3 - \epsilon \\
\gamma_i \gamma^\sigma \gamma^i &= -(2 - \epsilon) \gamma^\sigma - \tilde{\gamma}^\sigma \\
\gamma_i \cancel{A} \gamma^i &= -(2 - \epsilon) \cancel{A} - \tilde{A} \\
\gamma_i \gamma^\sigma \gamma^\tau \gamma^i &= 4g^{\sigma\tau} - \tilde{\gamma}^\sigma \tilde{\gamma}^\tau - \epsilon \gamma^\sigma \gamma^\tau \\
\gamma_i \cancel{A} \cancel{B} \gamma^i &= 4AB - \tilde{A} \tilde{B} - \epsilon \cancel{A} \cancel{B} \\
\gamma_i \gamma^\beta \gamma^\sigma \gamma^\tau \gamma^i &= -2\gamma^\tau \gamma^\sigma \gamma^\beta - \tilde{\gamma}^\beta \tilde{\gamma}^\sigma \tilde{\gamma}^\tau + \epsilon \gamma^\beta \gamma^\sigma \gamma^\tau \\
\gamma_i \cancel{A} \cancel{B} \cancel{C} \gamma^i &= -2\cancel{C} \cancel{B} \cancel{A} - \tilde{A} \tilde{B} \tilde{C} + \epsilon \cancel{A} \cancel{B} \cancel{C}
\end{aligned} \tag{D.62}$$

# Appendix E

## Lagrangian Field Theory

Concerning notations, see Appendix A.

### E.1 Classical Mechanics

In classical mechanics the *Lagrangian function* for a system is defined

$$L = T - V, \tag{E.1}$$

where  $T$  is the kinetic energy and  $V$  the potential energy of the system. Generally, this depends on the coordinates  $q_i$ , the corresponding velocities  $\dot{q}_i = \frac{\partial q_i}{\partial t}$  and possibly explicitly on time (see, for instance, [219, Sect. 23])

$$L(t; q_1, q_2 \dots; \dot{q}_1, \dot{q}_2 \dots). \tag{E.2}$$

The *action* is defined

$$I = \int dt L(t; q_1, q_2 \dots; \dot{q}_1, \dot{q}_2 \dots). \tag{E.3}$$

The *principle of least action* implies that

$$\delta I(q_1, q_2 \dots; \dot{q}_1, \dot{q}_2 \dots) = 0, \tag{E.4}$$

which leads to the *Lagrange equations*

$$\boxed{\frac{d}{dt} \left( \frac{\partial L}{\partial \dot{q}_i} \right) - \frac{\partial L}{\partial q_i} = 0.} \tag{E.5}$$

The Hamilton function can be defined

$$H = p_i \dot{q}_i - L, \quad (\text{E.6})$$

where  $p_i$  is the *canonically conjugate momentum* to the coordinate  $q_i$

$$p_i = \frac{\partial L}{\partial \dot{q}_i}. \quad (\text{E.7})$$

It then follows that

$$\frac{\partial H}{\partial p_i} = \dot{q}_i = \frac{\partial q_i}{\partial t}. \quad (\text{E.8a})$$

Furthermore, from the definitions above and the Lagrange equations we have

$$\boxed{\frac{\partial H}{\partial q_i} = -\dot{p}_i}. \quad (\text{E.8b})$$

These are *Hamilton's canonical equations of motion*.

We consider a general function of time and the coordinates and canonical momenta  $f(t; p_i, q_i)$ . Then the *total derivative* with respect to time becomes

$$\frac{df}{dt} = \frac{\partial f}{\partial t} + \frac{\partial f}{\partial q_i} \frac{\partial q_i}{\partial t} + \frac{\partial f}{\partial p_i} \frac{\partial p_i}{\partial t} = \frac{\partial f}{\partial t} + \frac{\partial f}{\partial q_i} \frac{\partial H}{\partial p_i} - \frac{\partial f}{\partial p_i} \frac{\partial H}{\partial q_i}. \quad (\text{E.9})$$

With the *Poisson bracket* of two functions  $A$  and  $B$ , defined by

$$\boxed{\{A, B\} = \frac{\partial A}{\partial q_i} \frac{\partial B}{\partial p_i} - \frac{\partial B}{\partial q_i} \frac{\partial A}{\partial p_i}} \quad (\text{E.10})$$

the derivative can be expressed

$$\frac{df}{dt} = \frac{\partial f}{\partial t} + \{f, H\}. \quad (\text{E.11})$$

For a single-particle system in one dimension ( $x$ ) the kinetic energy is  $T = p^2/2m$ , where  $m$  is the mass of the particle. This yields

$$L = \frac{p^2}{2m} - V = \frac{mv^2}{2} - V,$$

where  $v = \dot{x}$  is the velocity of the particle. Furthermore,  $p_i \dot{q}_i = p\dot{x} = p^2/m = mv^2$ , yielding with (E.6)

$$H = \frac{p^2}{2m} + V = \frac{mv^2}{2} + V,$$

which is the classical energy expression. The canonically conjugate momentum (E.7) is then

$$p = \frac{\partial L}{\partial \dot{\mathbf{x}}} = \frac{\partial L}{\partial \mathbf{v}} = m\mathbf{v},$$

which is the classical momentum.

### *Electron in External Field*

The Lagrangian for an electron (charge  $-e$ ) in an external field,  $A_\mu = (\phi(\mathbf{x})/c, -\mathbf{A})$ , is [143, p. 25]

$$L(\mathbf{x}, \dot{\mathbf{x}}) = \frac{1}{2} m \dot{\mathbf{x}}^2 - e\mathbf{A} \cdot \dot{\mathbf{x}} + e\phi(\mathbf{x}), \quad (\text{E.12})$$

where the last two terms represent (the negative of) a velocity-dependent potential. The conjugate momentum corresponding to the variable  $\mathbf{x}$  is then according to (E.7)

$$p_i \rightarrow \mathbf{p} = m\dot{\mathbf{x}} - e\mathbf{A}. \quad (\text{E.13})$$

Using the relation (E.6), we get the corresponding Hamilton function

$$H = \mathbf{p} \cdot \dot{\mathbf{x}} - L = \frac{1}{2} m \dot{\mathbf{x}}^2 - e\phi(\mathbf{x}) = \frac{1}{2m} (\mathbf{p} + e\mathbf{A})^2 - e\phi(\mathbf{x}). \quad (\text{E.14})$$

We see that the interaction with the fields  $(\phi, \mathbf{A})$  is obtained by means of the substitutions

$$H \rightarrow H - e\phi(\mathbf{x}) \quad \mathbf{p} \rightarrow \mathbf{p} + e\mathbf{A}, \quad (\text{E.15})$$

known as the *minimal substitutions*.

The corresponding equations of motion can be obtained either from the Lagrange's or Hamilton's equation of motion. We then have

$$\frac{d}{dt} \left( \frac{\partial L}{\partial \dot{q}_i} \right) \rightarrow \frac{d}{dt} (m\dot{\mathbf{x}} - e\mathbf{A})$$

and

$$\frac{\partial L}{\partial q_i} \rightarrow -e\nabla(\mathbf{A} \cdot \dot{\mathbf{x}}) + e\nabla\phi(\mathbf{x}).$$

The same equations are obtained from the Hamilton's equations of motion (E.8b). The **total** time derivative can in analogy with (E.9) be expressed

$$\frac{d}{dt} = \frac{\partial}{\partial t} + \frac{dx}{dt} \frac{\partial}{\partial x} + \dots = \frac{\partial}{\partial t} + \dot{\mathbf{x}} \cdot \nabla,$$

giving

$$\frac{d}{dt}(m\dot{\mathbf{x}} - e\mathbf{A}) = m\ddot{\mathbf{x}} - e\frac{\partial\mathbf{A}}{\partial t} - e(\dot{\mathbf{x}} \cdot \nabla)\mathbf{A}.$$

From the identity

$$\dot{\mathbf{x}} \times (\nabla \times \mathbf{A}) = \nabla(\mathbf{A} \cdot \dot{\mathbf{x}}) - (\dot{\mathbf{x}} \cdot \nabla)\mathbf{A}$$

we then obtain the *equations of the motion*

$$\boxed{m\ddot{\mathbf{x}} = e\nabla\phi(\mathbf{x}) + e\frac{\partial\mathbf{A}}{\partial t} - e\dot{\mathbf{x}} \times (\nabla \times \mathbf{A}) = -e(\mathbf{E} + \mathbf{v} \times \mathbf{B})} \quad (\text{E.16})$$

with  $\mathbf{v} = \dot{\mathbf{x}}$  being the velocity of the electron. This is the classical equations of motion for an electron of charge  $-e$  in an electromagnetic field. The right-hand side is the so-called *Lorentz force* on an electron in a combined electric and magnetic field. This verifies the Lagrangian (E.12).

## E.2 Classical Field Theory

In classical field theory we consider a *Lagrangian density* of the type

$$\mathcal{L} = \mathcal{L}(\phi_r, \partial_\mu\phi_r), \quad (\text{E.17})$$

where  $\phi_r = \phi_r(x)$  represent different fields and

$$\partial_\mu\phi_r = \frac{\partial\phi_r}{\partial x^\mu}. \quad (\text{E.18})$$

The requirement that the *action integral*

$$I = \int d^4x \mathcal{L}(\phi_r, \partial_\mu\phi_r) \quad (\text{E.19})$$

be stationary over a certain volume leads to the *Euler-Lagrange equations*

$$\boxed{\frac{\partial\mathcal{L}}{\partial\phi_r} - \partial_\mu\frac{\partial\mathcal{L}}{\partial(\partial_\mu\phi_r)} = 0.} \quad (\text{E.20})$$

The field conjugate to  $\phi_r(x)$  is

$$\boxed{\pi_r(x) = \frac{\partial\mathcal{L}}{\partial\dot{\phi}_r},} \quad (\text{E.21})$$



where the “dot” represents the time derivative. The *Lagrangian function* is defined

$$L(t) = \int d^3\mathbf{x} \mathcal{L}(\phi_r, \partial_\mu \phi_r). \quad (\text{E.22})$$

The *Hamiltonian density* is defined

$$\mathcal{H}(x) = \pi_r(x) \dot{\phi}_r(x) - \mathcal{L}(\phi_r, \partial_\mu \phi_r). \quad (\text{E.23})$$

In quantized Lagrangian field theory the fields are replaced by *operators*, satisfying the *Heisenberg commutation rules* at equal times [143, Eq. (2.31)]

$$[\hat{\phi}_\mu(x), \hat{\pi}^\nu(x')] = i\hbar \delta_{\mu,\nu} \delta^3(\mathbf{x} - \mathbf{x}') \quad (\text{E.24})$$

with the remaining commutations vanishing. In our applications the quantized field will normally be the electron field in the interaction picture (B.28) or the electromagnetic field (G.2).

### E.3 Dirac Equation in Lagrangian Formalism

From the Dirac equation for a free electron (D.14) we can deduce the corresponding Lagrangian density

$$\mathcal{L}(x) = \hat{\psi}^\dagger(x) (i\hbar c \alpha^\mu \partial_\mu - \beta m_e c^2) \hat{\psi}(x). \quad (\text{E.25})$$

Using the relation (B.17), the space integral over this density yields the corresponding operator

$$L = \int d^3\mathbf{x} \mathcal{L}(x) = i\hbar c \alpha^\mu \partial_\mu - \beta m_e c^2 = c \alpha^\mu p_\mu - \beta m_e c^2 \quad (\text{E.26})$$

(with  $\hat{p}_\mu = i\hbar \partial_\mu$ ) and the corresponding Hamilton operator (E.6)

$$H = -L = -c \alpha^\mu p_\mu + \beta m_e c^2, \quad (\text{E.27})$$

since the fields are time independent. This leads to the Dirac equation for a free electron (D.14).

We can also apply the Euler-Lagrange equations (E.20) on the Lagrangian (E.25), which leads to

$$\partial_\mu \frac{\partial \mathcal{L}}{\partial (\partial_\mu \hat{\psi})} = \partial_\mu (\hat{\psi}^\dagger(x) i\hbar c \alpha^\mu)$$

$$\frac{\partial \mathcal{L}}{\partial \hat{\psi}} = -\hat{\psi}^\dagger(x) \beta m_e c^2$$

and

$$\partial_\mu i\hbar c \alpha^\mu \hat{\psi}^\dagger(x) + \beta m_e c^2 \hat{\psi}^\dagger(x) = 0$$

with the hermitian adjoint

$$(-i\hbar c \alpha^\mu \partial_\mu + \beta m_e c^2) \hat{\psi}(x) = 0, \quad (\text{E.28})$$

which is consistent with the Dirac equation for the free electron.

In the presence of an electromagnetic field we make the *minimal substitution* (D.41)

$$p_\mu \rightarrow p_\mu + eA_\mu(x) \quad \text{or} \quad \partial_\mu \rightarrow \partial_\mu - \frac{ie}{\hbar} A_\mu(x), \quad (\text{E.29})$$

which leads to the *Lagrangian density* in the presence of an electromagnetic field

$$\mathcal{L}(x) = \hat{\psi}^\dagger(x) (c \alpha^\mu p_\mu - \beta m_e c^2 + ec \alpha^\mu A_\mu(x)) \hat{\psi}(x). \quad (\text{E.30})$$

This gives the corresponding *Hamiltonian density*

$$\mathcal{H}(x) = \hat{\psi}^\dagger(x) (-c \alpha^\mu p_\mu + \beta m_e c^2 - ec \alpha^\mu A_\mu(x)) \hat{\psi}(x), \quad (\text{E.31})$$

where the last term represents the *interaction density*

$$\mathcal{H}_{\text{int}}(x) = -\hat{\psi}^\dagger(x) ec \alpha^\mu A_\mu(x) \hat{\psi}(x). \quad (\text{E.32})$$

The corresponding *Hamilton operator* can then be expressed

$$\hat{H} = \int d^3\mathbf{x}_1 \hat{\psi}^\dagger(x_1) (-c \alpha^\mu p_\mu + \beta m_e c^2 - ec \alpha^\mu A_\mu(x)) \hat{\psi}(x_1). \quad (\text{E.33})$$

# Appendix F

## Semiclassical Theory of Radiation

### F.1 Classical Electrodynamics

#### *Maxwell's Equations in Covariant*

The Maxwell equations in vector form are<sup>7</sup>.

$$\nabla \cdot \mathbf{E} = \rho/\epsilon_0 \quad (\text{F.1a})$$

$$\nabla \times \mathbf{B} = \frac{1}{c^2} \frac{\partial \mathbf{E}}{\partial t} + \mu_0 \mathbf{j} \quad (\text{F.1b})$$

$$\nabla \cdot \mathbf{B} = 0 \quad (\text{F.1c})$$

$$\nabla \times \mathbf{E} + \frac{\partial \mathbf{B}}{\partial t} = 0 \quad (\text{F.1d})$$

where  $\rho$  is the electric charge density and  $\mathbf{j}$  the electric current density. Equation (F.1c) gives

$$\mathbf{B} = \nabla \times \mathbf{A} \quad (\text{F.2})$$

where  $\mathbf{A}$  is the *vector potential*. From (F.1d) it follows that the electric field is of the form

$$\mathbf{E} = -\frac{\partial \mathbf{A}}{\partial t} - \nabla \phi \quad (\text{F.3})$$

---

<sup>7</sup>As in the previous Appendices the formulas are here given in a complete form and valid in any consistent unit system, like the SI system (see Appendix K)

where  $\phi$  is the *scalar potential*. The equations (F.1a) and (F.1b) give together with (F.3) and (F.2)

$$\begin{aligned} -\nabla^2\phi - \frac{\partial}{\partial t}\nabla\cdot\mathbf{A} &= \rho/\epsilon_0 = c\mu_0j^0, \\ \left(\nabla^2\mathbf{A} - \frac{1}{c^2}\frac{\partial^2\mathbf{A}}{\partial t^2}\right) - \nabla\left(\nabla\cdot\mathbf{A} + \frac{1}{c^2}\frac{\partial\phi}{\partial t}\right) &= -\mu_0\mathbf{j}, \end{aligned} \quad (\text{F.4})$$

using the vector identity  $\nabla\times(\nabla\times\mathbf{A}) = \nabla(\nabla\cdot\mathbf{A}) - \nabla^2\mathbf{A}$ . Here,  $j^0 = c\rho$  (with  $\epsilon_0\mu_0 = c^{-2}$ ) is the *scalar or “time-like”* part of the four-dimensional current density

$$j = j^\mu = (c\rho, \mathbf{j}), \quad (\text{F.5})$$

where the vector part is the three-dimensional current density  $\mathbf{j}$ . Similarly, the four-dimensional vector potential

$$A^\mu = (\phi/c, \mathbf{A}) \quad A_\mu = (\phi/c, -\mathbf{A}) \quad (\text{F.6})$$

has the scalar part  $\phi/c$  and the vector part  $\mathbf{A}$ . With the d’Alambertian operator (A.10), these equations can be expressed<sup>8</sup>

$$\square\phi - \frac{\partial}{\partial t}(\nabla A) = c\mu_0j^0, \quad (\text{F.7})$$

$$\square A + \nabla(\nabla A) = \mu_0\mathbf{j}, \quad (\text{F.8})$$

which leads to **Maxwell’s equations in covariant form**

$$\boxed{\square A - \nabla(\nabla A) = \mu_0\mathbf{j}} \quad (\text{F.9})$$

or

$$\partial_\nu\partial^\nu A^\mu - \partial^\mu(\partial_\nu A^\nu) = \mu_0j^\mu. \quad (\text{F.10})$$

### Electromagnetic-Field Lagrangian

We introduce the field tensor [143, Eq.5.5]

$$F^{\mu\nu} = \partial^\nu A^\mu - \partial^\mu A^\nu. \quad (\text{F.11})$$

---

<sup>8</sup>Concerning covariant notations, see Appendix A.1.

Then we find for instance

$$F^{01} = \partial^1 A^0 - \partial^0 A^1 = \frac{\partial \phi/c}{\partial x} - \frac{\partial A_x}{\partial ct} = E_x,$$

$$F^{12} = \partial^2 A^1 - \partial^1 A^2 = \frac{\partial A_x}{\partial y} - \frac{\partial A_y}{\partial x} = B_z,$$

etc., leading to the matrix

$$F^{\mu\nu} = \begin{pmatrix} 0 & E_x/c & E_y/c & E_z/c \\ -E_x/c & 0 & B_z & -B_y \\ E_y/c & -B_z & 0 & B_x \\ -E_z & B_x & -B_y & 0 \end{pmatrix}. \quad (\text{F.12})$$

The Maxwell equations (F.10) can now be expressed [143, Eq.5.2]

$$\partial_\nu F^{\mu\nu} = \mu_0 j^\mu, \quad (\text{F.13})$$

using the identity

$$\partial_\nu \partial^\mu A^\mu \equiv \partial^\mu \partial_\nu A^\mu.$$

With  $\phi_r = A_\mu$  the Euler-Lagrange equations (E.20) becomes

$$\boxed{\frac{\partial \mathcal{L}}{\partial A_\mu} - \partial_\nu \frac{\partial \mathcal{L}}{\partial (\partial_\nu A_\mu)} = 0.} \quad (\text{F.14})$$

Using the field tensor (F.11) and the form of the metric tensor (A.5), we have

$$\begin{aligned} F_{\mu\nu} F^{\mu\nu} &= (\partial_\nu A_\mu - \partial_\mu A_\nu)(\partial^\nu A^\mu - \partial^\mu A^\nu) \\ &= (\partial_\nu A_\mu - \partial_\mu A_\nu)(g^{\nu\sigma} \partial_\sigma g^{\mu\pi} A_\pi - g^{\mu\sigma} \partial_\sigma g^{\nu\pi} A_\pi). \end{aligned} \quad (\text{F.15})$$

Here,  $\mu$  and  $\nu$  are running indices that are summed over, and we can replace them with  $\mu'$  and  $\nu'$ , respectively. The derivative with respect to fixed  $\mu$  and  $\nu$  then gives

$$\frac{\partial}{\partial (\partial_\nu A_\mu)} F_{\mu'\nu'} F^{\mu'\nu'} = F^{\mu\nu} - F^{\nu\mu} + F_{\mu'\nu'} g^{\nu'\nu} g^{\mu'\mu} - F_{\nu'\mu'} g^{\mu'\nu} g^{\nu'\mu} = 4F^{\mu\nu}. \quad (\text{F.16})$$

We then find that with the Lagrangian

$$\mathcal{L} = -\frac{1}{4\mu_0} F_{\mu\nu} F^{\mu\nu} - j^\mu A_\mu \quad (\text{F.17})$$

the Euler-Lagrange equations (F.14) lead to the Maxwell equations (F.13).

With the same Lagrangian the conjugate fields (E.21) are

$$\pi^\mu(x) = \frac{\partial \mathcal{L}}{\partial \dot{A}_\mu} = \frac{1}{c} \frac{\partial \mathcal{L}}{\partial (\partial^0 A_\mu)}, \quad (\text{F.18})$$

where the dot represents the time derivative and  $\partial^0 = \frac{\partial}{\partial x_0} = \frac{1}{c} \frac{\partial}{\partial t} = \partial_0$ . Using the relation (F.16), this yields

$$\pi^\mu(x) = -\frac{1}{\mu_0 c} F^{\mu 0}(x). \quad (\text{F.19})$$

The Hamiltonian is given in terms of the Lagrangian by [143, 5.31]

$$H = \int d^3 \mathbf{x} \, sN\{\pi^\mu(x) \dot{A}_\mu(x) - \mathcal{L}\}, \quad (\text{F.20})$$

where  $N\{\}$  represents *normal order* [124, Chap. 11] (see Sect. 2.2).

### Lorenz Condition

The Lorenz condition is<sup>9</sup>

$$\nabla A = \partial_\mu A^\mu = \nabla \cdot \mathbf{A} + \frac{1}{c^2} \frac{\partial \phi}{\partial t} = 0, \quad (\text{F.21})$$

and with this condition the Maxwell equations get the simple form

$$\boxed{\square A = \mu_0 j.} \quad (\text{F.22})$$

Then also the electro-magnetic fields have particularly simple form, given in (G.2).

### Continuity Equation

Operating on Maxwell's equations (F.9) with  $\nabla$  yields:

$$\nabla (\square A) - \nabla \nabla (\nabla A) = \mu_0 \nabla j.$$

Since  $\square = \nabla^2$  and  $\nabla$  commute, this leads to the *continuity equation*

$$\boxed{\nabla j = \partial_\mu j^\mu = 0.} \quad (\text{F.23})$$

---

<sup>9</sup>This condition is named after the Danish physicist Ludvig Lorenz, not to be confused with the more well-known Dutch physicist Hendrik Lorentz (note the different spelling).

## Gauge Invariance

A general gauge transformation is represented by

$$\mathbf{A} \Rightarrow \mathbf{A} + \nabla\Lambda, \quad (\text{F.24})$$

where  $\Lambda$  is an arbitrary scalar.

Inserted into the Maxwell equations (F.9), this yields:

$$\square(\nabla\Lambda) - \nabla(\nabla\nabla\Lambda) = \square(\nabla\Lambda) - \nabla(\square\Lambda) = 0,$$

which shows that **the Maxwell equations are gauge invariant.**

## Coulomb Gauge

### Transverse and Longitudinal Field Components

The vector part of the electromagnetic field can be separated into *transverse* (divergence-free) and *longitudinal* (rotation-free) components

$$\mathbf{A} = \mathbf{A}_\perp + \mathbf{A}_\parallel; \quad \nabla \cdot \mathbf{A}_\perp = 0; \quad \nabla \times \mathbf{A}_\parallel = 0. \quad (\text{F.25})$$

The electric field can be similarly separated

$$\mathbf{E} = \mathbf{E}_\perp + \mathbf{E}_\parallel; \quad \mathbf{E}_\perp = -\frac{\partial \mathbf{A}_\perp}{\partial t}; \quad \mathbf{E}_\parallel = -\frac{\partial \mathbf{A}_\parallel}{\partial t} - \nabla\phi,$$

while the magnetic field has only transverse components due to the relation (F.2). The separated field equations (F.4) then become

$$\nabla^2\phi + \frac{\partial}{\partial t}\nabla \cdot \mathbf{A}_\parallel = -\rho/\epsilon_0, \quad (\text{F.26a})$$

$$\left(\nabla^2\mathbf{A}_\parallel - \frac{1}{c^2}\frac{\partial^2\mathbf{A}_\parallel}{\partial t^2}\right) - \nabla\left(\nabla \cdot \mathbf{A}_\parallel + \frac{1}{c^2}\frac{\partial\phi}{\partial t}\right) = -\mu_0\mathbf{j}_\parallel, \quad (\text{F.26b})$$

$$\left(\nabla^2 - \frac{1}{c^2}\frac{\partial^2}{\partial t^2}\right)\mathbf{A}_\perp = -\mu_0\mathbf{j}_\perp. \quad (\text{F.26c})$$

The longitudinal and the scalar or ‘time-like’ components ( $\mathbf{A}_\parallel, \phi$ ) represent the *instantaneous Coulomb interaction* and the transverse components ( $\mathbf{A}_\perp$ ) represent

retardation of this interaction and all magnetic interactions, as well as the *electromagnetic radiation field* (see Sect. F.2).

The energy of the electromagnetic field is given by

$$\begin{aligned} E_{\text{rad}} &= \frac{1}{2} \int d^3\mathbf{x} \left[ \frac{1}{\mu_0} |\mathbf{B}|^2 + \epsilon_0 |\mathbf{E}|^2 \right] \\ &= \frac{1}{2} \int d^3\mathbf{x} \left[ \frac{1}{\mu_0} |\mathbf{B}|^2 + \epsilon_0 |\mathbf{E}_\perp|^2 \right] + \frac{1}{2} \int d^3\mathbf{x} \epsilon_0 |\mathbf{E}_\parallel|^2. \end{aligned} \quad (\text{F.27})$$

The last term represents the energy of the instantaneous Coulomb field, which is normally already included in the hamiltonian of the system. The first term represents the radiation energy.

Semiclassically, only the transverse part of the field is quantized, while the longitudinal part is treated classically [206, Chaps. 2, 3]. It should be noted that the separation into transverse and longitudinal components is not Lorentz covariant and therefore, strictly speaking, not physically justified, when relativity is taken into account. It can be argued, though, that the separation (as made in the Coulomb gauge) should ultimately lead to the same result as a covariant gauge, when treated properly.

In a fully covariant treatment also the longitudinal component is quantized. The field is then represented by **virtual photons with four directions of polarizations**. A *real photon* can only have *transverse polarizations*.

The *Coulomb gauge* is defined by the condition

$$\nabla \cdot \mathbf{A}(x) = 0. \quad (\text{F.28})$$

Using the Fourier transform

$$A(x) = \int d^4k A(k) e^{-ikx}, \quad (\text{F.29})$$

this condition leads to

$$\frac{\partial A^i}{\partial x^i} = \int d^4k A^i(k) (-i) k_i e^{-ikx} = 0$$

or

$$\mathbf{A}(k) \cdot \mathbf{k} = 0. \quad (\text{F.30})$$

This is also known as the *transversality condition* and implies that there is **no longitudinal component of  $\mathbf{A}$** . Maxwell's equations then reduce to

$$\nabla^2 \phi = -\rho/\epsilon_0. \quad (\text{F.31})$$



This has the solution

$$\phi(\mathbf{x}) = \frac{1}{4\pi\epsilon_0} \int d^3\mathbf{x}' \frac{\rho(\mathbf{x}')}{|\mathbf{x} - \mathbf{x}'|}, \quad (\text{F.32})$$

which is the *instantaneous Coulomb interaction*.

In free space the scalar potential  $\phi$  can be eliminated by a gauge transformation. Then the Lorenz condition (F.21) is automatically fulfilled in the Coulomb gauge. The field equation (F.4) then becomes

$$\nabla^2 \mathbf{A} - \frac{1}{c^2} \frac{\partial^2 \mathbf{A}}{\partial t^2} = 0. \quad (\text{F.33})$$

The relativistic interaction with an atomic electron (D.44) is then in the Coulomb gauge given by

$$H_{\text{int}} = ec \boldsymbol{\alpha} \cdot \mathbf{A}_{\perp} \quad (\text{F.34})$$

and in second quantization (see Appendix B)

$$\hat{H}_{\text{int}} = \sum_{ij} c_j^{\dagger} \langle i | ec \boldsymbol{\alpha} \cdot \mathbf{A}_{\perp} | j \rangle c_j, \quad (\text{F.35})$$

where  $c^{\dagger}$ ,  $c$  represent creation/annihilation operators for electrons. In the *interaction picture* this becomes

$$\hat{H}_{\text{int},1}(t) = \sum_{ij} c_i^{\dagger} \langle i | ec \boldsymbol{\alpha} \cdot \mathbf{A}_{\perp} | j \rangle c_j e^{i(\epsilon_i - \epsilon_j)t/\hbar}. \quad (\text{F.36})$$

## F.2 Quantized Radiation Field

### *Transverse Radiation Field*

Classically the transverse components of the radiation field can be represented by the vector potential [206, Eq. 2.14]

$$\mathbf{A}(\mathbf{x}, t) = \sum_{\mathbf{k}} \sum_{p=1}^2 \left[ c_{\mathbf{k}p} \boldsymbol{\varepsilon}_p e^{i(\mathbf{k}\cdot\mathbf{x} - \omega t)} + c_{\mathbf{k}p}^* \boldsymbol{\varepsilon}_p e^{-i(\mathbf{k}\cdot\mathbf{x} - \omega t)} \right], \quad (\text{F.37})$$

where  $\mathbf{k}$  is the wave vector,  $\omega = c|\mathbf{k}|$  the frequency, and  $c_{\mathbf{k}p}/c_{\mathbf{k}p}^*$  represent the amplitude of the wave with the a certain  $\mathbf{k}$  vector and a certain polarization  $\boldsymbol{\varepsilon}_p$ . The energy of this radiation can be shown to be equal to [206, p. 22]

$$E_{\text{rad}} = 2\epsilon_0 \sum_{\mathbf{k}p} \omega^2 c_{\mathbf{k}p}^* c_{\mathbf{k}p} = \epsilon_0 \sum_{\mathbf{k}p} \omega^2 (c_{\mathbf{k}p}^* c_{\mathbf{k}p} + c_{\mathbf{k}r} c_{\mathbf{k}p}^*). \quad (\text{F.38})$$

By making the substitution

$$c_{kp} \rightarrow \sqrt{\frac{\hbar}{2\epsilon_0 \omega V}} a_{kp} \quad \text{and} \quad c_{kp}^* \rightarrow \sqrt{\frac{\hbar}{2\epsilon_0 \omega V}} a_{kp}^\dagger,$$

where  $a_{kp}^\dagger, /a_{kp}$  are *photon creation/annihilation operators*, the radiation energy goes over into the hamiltonian of a collection of harmonic oscillators

$$H_{\text{harm.osc}} = \frac{1}{2} \sum_{kp} \hbar\omega (a_{kp} a_{kp}^\dagger + a_{kp}^\dagger a_{kp}).$$

Therefore, we can motivate that the quantized *transverse* radiation field can be represented by the operator [206, Eq. 2.60]

$$\boxed{A_\perp(\mathbf{x}, t) = \sum_{\mathbf{k}} \sqrt{\frac{\hbar}{2\epsilon_0 \omega V}} \sum_{p=1}^2 \left[ a_{\mathbf{k}p} \boldsymbol{\varepsilon}_p e^{i(\mathbf{k}\cdot\mathbf{x} - \omega t)} + a_{\mathbf{k}p}^\dagger \boldsymbol{\varepsilon}_p e^{-i(\mathbf{k}\cdot\mathbf{x} - \omega t)} \right].} \quad (\text{F.39})$$

### Breit Interaction

The exchange of a single transverse photon between two electrons is illustrated by the time-ordered diagram (left) in Fig. F.1, where one photon is *emitted* at the time  $t_1$  and *absorbed* at a later time  $t_2$ . The second-order *evolution operator* for this process, using the interaction picture, is given by (see Sect. 3.2)

$$U_\gamma^{(2)}(0, -\infty) = \left(\frac{-i}{\hbar}\right)^2 \int_{-\infty}^0 dt_2 \hat{H}_{\text{int},1}(t_2) \int_{-\infty}^0 dt_1 \hat{H}_{\text{int},1}(t_1) e^{\gamma(t_1+t_2)}, \quad (\text{F.40})$$

where  $\gamma$  is the parameter for the *adiabatic damping* of the perturbation. The interaction Hamiltonians are in the Coulomb gauge given by (F.36) with the vector potential (F.39)

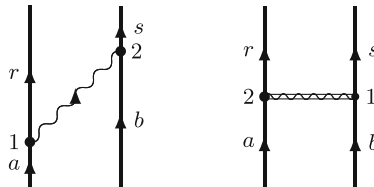


**Fig. F.1** Diagrammatic representation of the exchange of a single, transverse photon between two electrons (*left*). This is equivalent to a potential (Breit) interaction (*right*)

$$\begin{aligned}\hat{H}_{\text{int},1}(t_1) &= \sum_{k_1} \sqrt{\frac{\hbar}{2\epsilon_0\omega_1 V}} \sum_{p_1=1}^2 c_r^\dagger \langle r | (a_{k_p}^\dagger e c \boldsymbol{\alpha} \cdot \boldsymbol{\varepsilon}_{k_p} e^{-i\mathbf{k}\cdot\mathbf{x}})_1 | a \rangle c_a e^{-it_1(\varepsilon_a - \varepsilon_p - \hbar\omega_1)/\hbar}, \\ \hat{H}_{\text{int},1}(t_2) &= \sum_{k_2} \sqrt{\frac{\hbar}{2\epsilon_0\omega_2 V}} \sum_{p_2=1}^2 c_s^\dagger \langle r | (a_{k_p} e c \boldsymbol{\alpha} \cdot \boldsymbol{\varepsilon}_{k_p} e^{i\mathbf{k}\cdot\mathbf{x}})_2 | a \rangle c_b e^{-it_2(\varepsilon_b - \varepsilon_s + \hbar\omega_2)/\hbar},\end{aligned}\quad (\text{F.41})$$

which leads to the evolution operator

$$\begin{aligned}U_\gamma^{(2)}(0, -\infty) &= -c_r^\dagger c_a c_s^\dagger c_b \sum_k \frac{e^2 c^2}{2\hbar \epsilon_0 V \sqrt{\omega_1 \omega_2}} \\ &\quad \times \sum_{p_1 p_2} \langle rs | (a_{k_p} \boldsymbol{\alpha} \cdot \boldsymbol{\varepsilon}_p e^{i\mathbf{k}\cdot\mathbf{x}})_2 (a_{k_p}^\dagger \boldsymbol{\alpha} \cdot \boldsymbol{\varepsilon}_p e^{-i\mathbf{k}\cdot\mathbf{x}})_1 | ab \rangle \times I, \quad (\text{F.42})\end{aligned}$$

where  $I$  is the time integral. The *contraction* between the creation and annihilation operators (G.10) yields ( $\omega = \omega_1 = \omega_2$ )

$$\begin{aligned}&\sum_{p_1 p_2} \langle rs | (a_{k_p} \boldsymbol{\alpha} \cdot \boldsymbol{\varepsilon}_p e^{i\mathbf{k}\cdot\mathbf{x}})_2 (a_{k_p}^\dagger \boldsymbol{\alpha} \cdot \boldsymbol{\varepsilon}_p e^{-i\mathbf{k}\cdot\mathbf{x}})_1 | ab \rangle \\ &= \sum_{p=1}^2 \langle rs | (\boldsymbol{\alpha} \cdot \boldsymbol{\varepsilon}_p)_2 (\boldsymbol{\alpha} \cdot \boldsymbol{\varepsilon}_p)_1 e^{-i\mathbf{k}\cdot\mathbf{r}_{12}} \quad (\mathbf{r}_{12} = \mathbf{x}_1 - \mathbf{x}_2). \quad (\text{F.43})\end{aligned}$$

The time integral in (F.42) is

$$\begin{aligned}I &= \int_{-\infty}^0 dt_2 e^{-it_2(\varepsilon_b - \varepsilon_s + \hbar\omega + i\gamma)/\hbar} \int_{-\infty}^{t_2} dt_1 e^{-it_1(\varepsilon_a - \varepsilon_r - \hbar\omega + i\gamma)/\hbar} \\ &= -\frac{1}{(cq + cq' + 2i\gamma)(cq - \omega + i\gamma)}\end{aligned}\quad (\text{F.44})$$

with  $cq = (\varepsilon_a - \varepsilon_r)/\hbar$  and  $cq' = (\varepsilon_b - \varepsilon_s)/\hbar$ .

The result of the opposite time ordering  $t_1 > t_2$  is obtained by the exchange  $1 \leftrightarrow 2$  ( $\mathbf{r}_{12} \leftrightarrow -\mathbf{r}_{12}$ ),  $a \leftrightarrow b$ , and  $r \leftrightarrow s$ , and the total evolution operator, including both time-orderings, can be expressed

$$U_\gamma^{(2)}(0, -\infty) = c_r^\dagger c_a c_s^\dagger c_b \frac{e^2 c^2}{2\hbar \epsilon_0 \omega V} \sum_k \sum_{p=1}^2 \langle rs | (\boldsymbol{\alpha} \cdot \boldsymbol{\varepsilon}_p)_1 (\boldsymbol{\alpha} \cdot \boldsymbol{\varepsilon}_p)_2 \mathcal{M} | ab \rangle \quad (\text{F.45})$$

with

$$\mathcal{M} = \frac{e^{-i\mathbf{k}\cdot\mathbf{r}_{12}}}{(cq + cq' + 2i\gamma)(cq - \omega + i\gamma)} + \frac{e^{i\mathbf{k}\cdot\mathbf{r}_{12}}}{(cq + cq' + 2i\gamma)(cq' - \omega + i\gamma)}. \quad (\text{F.46})$$

This can be compared with the evolution operator corresponding to a *potential interaction*  $B_{12}$  between the electrons, as illustrated in the right diagram of Fig. F.1,

$$\begin{aligned} U_{\eta}^{(2)}(0, -\infty) &= c_r^{\dagger} c_a c_s^{\dagger} c_b \langle rs | B_{12} | ab \rangle \left( \frac{-i}{\hbar} \right) \int_{-\infty}^0 dt e^{-i(\varepsilon_a + \varepsilon_b - \varepsilon_r - \varepsilon_s + i\eta)t/\hbar} \\ &= \frac{c_r^{\dagger} c_a c_s^{\dagger} c_b}{\hbar} \frac{\langle rs | B_{12} | ab \rangle}{cq + cq' + i\eta}. \end{aligned} \quad (\text{F.47})$$

Identification then leads to

$$B_{12} = \frac{e^2 c^2}{2\epsilon_0 \omega V} \sum_{kp} (\boldsymbol{\alpha} \cdot \boldsymbol{\varepsilon}_p)_1 (\boldsymbol{\alpha} \cdot \boldsymbol{\varepsilon}_p)_2 \left[ \frac{e^{-i\mathbf{k} \cdot \mathbf{r}_{12}}}{cq - \omega + i\gamma} + \frac{e^{i\mathbf{k} \cdot \mathbf{r}_{12}}}{cq' - \omega + i\gamma} \right]. \quad (\text{F.48})$$

We assume now that *energy is conserved* by the interaction, i.e.,

$$\varepsilon_a - \varepsilon_r = \varepsilon_s - \varepsilon_b \quad \text{or} \quad q + q' = 0. \quad (\text{F.49})$$

It is found that the sign of the imaginary part of the exponent is immaterial (see Appendix J.2), and the equivalent interaction then becomes

$$B_{12} = \frac{e^2}{\epsilon_0 V} \sum_{kp} (\boldsymbol{\alpha} \cdot \boldsymbol{\varepsilon}_p)_1 (\boldsymbol{\alpha} \cdot \boldsymbol{\varepsilon}_p)_2 \frac{e^{i\mathbf{k} \cdot \mathbf{r}_{12}}}{q^2 - k^2 + i\gamma} \quad (\text{F.50})$$

with  $\omega = ck$ .

The  $\boldsymbol{\varepsilon}_p$  vectors are orthogonal unit vectors, which leads to [206, Eq. 4.312]

$$\sum_{p=1}^3 (\boldsymbol{\alpha} \cdot \boldsymbol{\varepsilon}_p)_1 (\boldsymbol{\alpha} \cdot \boldsymbol{\varepsilon}_p)_2 = \boldsymbol{\alpha}_1 \cdot \boldsymbol{\alpha}_2. \quad (\text{F.51})$$

This gives

$$\sum_{p=1}^2 (\boldsymbol{\alpha} \cdot \boldsymbol{\varepsilon}_p)_1 (\boldsymbol{\alpha} \cdot \boldsymbol{\varepsilon}_p)_2 = \boldsymbol{\alpha}_1 \cdot \boldsymbol{\alpha}_2 - (\boldsymbol{\alpha}_1 \cdot \hat{\mathbf{k}})(\boldsymbol{\alpha}_2 \cdot \hat{\mathbf{k}}), \quad (\text{F.52})$$

assuming  $\boldsymbol{\varepsilon}_3 = \hat{\mathbf{k}}$  to be the unit vector in the  $\mathbf{k}$  direction. The interaction (F.50) then becomes in the limit of continuous momenta (Appendix D)

$$B_{12} = \frac{e^2}{\epsilon_0} \int \frac{d^3 \mathbf{k}}{(2\pi)^3} \left[ \boldsymbol{\alpha}_1 \cdot \boldsymbol{\alpha}_2 - (\boldsymbol{\alpha}_1 \cdot \hat{\mathbf{k}})(\boldsymbol{\alpha}_2 \cdot \hat{\mathbf{k}}) \right] \frac{e^{i\mathbf{k} \cdot \mathbf{r}_{12}}}{q^2 - k^2 + i\gamma}. \quad (\text{F.53})$$

With the Fourier transforms in Appendix J this yields the **retarded Breit interaction**

$$B_{12}^{\text{Ret}} = -\frac{e^2}{4\pi\epsilon_0} \left[ \boldsymbol{\alpha}_1 \cdot \boldsymbol{\alpha}_2 \frac{e^{i|q|r_{12}}}{r_{12}} - (\boldsymbol{\alpha}_1 \cdot \nabla_1)(\boldsymbol{\alpha}_2 \cdot \nabla_2) \frac{e^{i|q|r_{12}} - 1}{q^2 r_{12}} \right]. \quad (\text{F.54})$$

Setting  $q = 0$ , we obtain the *instantaneous Breit interaction* (real part)

$$B_{12}^{\text{Inst}} = -\frac{e^2}{4\pi\epsilon_0} \left[ \frac{\boldsymbol{\alpha}_1 \cdot \boldsymbol{\alpha}_2}{r_{12}} + \frac{1}{2} (\boldsymbol{\alpha}_1 \cdot \nabla_1) (\boldsymbol{\alpha}_2 \cdot \nabla_2) r_{12} \right]$$

or using

$$(\boldsymbol{\alpha}_1 \cdot \nabla_1) (\boldsymbol{\alpha}_2 \cdot \nabla_2) r_{12} = -\frac{\boldsymbol{\alpha}_1 \cdot \boldsymbol{\alpha}_2}{r_{12}} + \frac{(\boldsymbol{\alpha}_1 \cdot \mathbf{r}_{12})(\boldsymbol{\alpha}_1 \cdot \mathbf{r}_{12})}{r_{12}^3}$$

we arrive at

$$B_{12}^{\text{Inst}} = -\frac{e^2}{4\pi\epsilon_0 r_{12}} \left[ \frac{1}{2} \boldsymbol{\alpha}_1 \cdot \boldsymbol{\alpha}_2 + \frac{(\boldsymbol{\alpha}_1 \cdot \mathbf{r}_{12})(\boldsymbol{\alpha}_1 \cdot \mathbf{r}_{12})}{2r_{12}^2} \right], \tag{F.55}$$

which is the standard form of the **instantaneous Breit interaction**.

### Transverse Photon Propagator

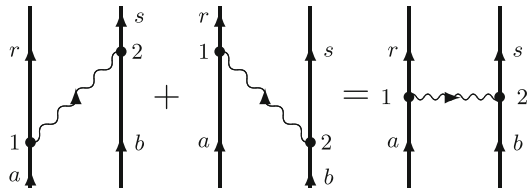
We shall now consider both time-orderings of the interaction represented in the Fig. F.2 simultaneously. The evolution operator can then be expressed

$$U_\gamma^{(2)}(0, -\infty) = \left(\frac{-i}{\hbar}\right)^2 \int_{-\infty}^0 dt_2 \int_{-\infty}^0 dt_1 T[\hat{H}_{\text{int,I}}(t_2) \hat{H}_{\text{int,I}}(t_1)] e^{-\gamma(|t_1|+|t_2|)}, \tag{F.56}$$

where

$$T[\hat{H}_{\text{int,I}}(t_2) \hat{H}_{\text{int,I}}(t_1)] = \begin{cases} \hat{H}_{\text{int,I}}(t_2) \hat{H}_{\text{int,I}}(t_1) & t_2 > t_1 \\ \hat{H}_{\text{int,I}}(t_1) \hat{H}_{\text{int,I}}(t_2) & t_1 > t_2. \end{cases} \tag{F.57}$$

**Fig. F.2** The two time-orderings of a single-photon exchange can be represented by a single *Feynman diagram*



In the Coulomb gauge the interaction is given by (F.36) and the vector potential is given by (F.39). The evolution operator for the combined interactions will then be

$$U_\gamma^{(2)}(0, -\infty) = -c_r^\dagger c_a c_s^\dagger c_b \frac{e^2 c^2}{\hbar^2} \times \int_{-\infty}^0 dt_2 \int_{-\infty}^0 dt_1 T[(\boldsymbol{\alpha} \cdot \mathbf{A}_\perp)_1 (\boldsymbol{\alpha} \cdot \mathbf{A}_\perp)_2] e^{-it_1(\varepsilon_a - \varepsilon_r + i\gamma)/\hbar} e^{-it_2(\varepsilon_b - \varepsilon_s + i\gamma)/\hbar}. \quad (\text{F.58})$$

Here

$$T[(\boldsymbol{\alpha} \cdot \mathbf{A}_\perp)_1 (\boldsymbol{\alpha} \cdot \mathbf{A}_\perp)_2] = \sum_{kp} \frac{\hbar}{2\omega\epsilon_0 V} (\boldsymbol{\alpha} \cdot \boldsymbol{\varepsilon}_p)_1 (\boldsymbol{\alpha} \cdot \boldsymbol{\varepsilon}_p)_2 \times \begin{cases} e^{-i(\mathbf{k}_1 \cdot \mathbf{x}_1 - \omega t_1)} e^{i(\mathbf{k}_2 \cdot \mathbf{x}_2 - \omega t_2)} & t_2 > t_1 \\ e^{-i(\mathbf{k}_2 \cdot \mathbf{x}_2 - \omega t_2)} e^{i(\mathbf{k}_1 \cdot \mathbf{x}_1 - \omega t_1)} & t_1 > t_2 \end{cases}$$

or with  $\mathbf{r}_{12} = \mathbf{x}_1 - \mathbf{x}_2$  and  $t_{12} = t_1 - t_2$ .

$$T[(\boldsymbol{\alpha} \cdot \mathbf{A}_\perp)_1 (\boldsymbol{\alpha} \cdot \mathbf{A}_\perp)_2] = \frac{\hbar}{\epsilon_0} \sum_{p=1}^2 (\boldsymbol{\alpha} \cdot \boldsymbol{\varepsilon}_p)_1 (\boldsymbol{\alpha} \cdot \boldsymbol{\varepsilon}_p)_2 \frac{1}{V} \sum_{\mathbf{k}} \frac{e^{\mp i(\mathbf{k} \cdot \mathbf{r}_{12} - \omega t_{12})}}{2\omega}, \quad (\text{F.59})$$

where the upper sign is valid for  $t_2 > t_1$ . This yields

$$U_\gamma^{(2)}(0, -\infty) = -c_r^\dagger c_a c_s^\dagger c_b \frac{e^2 c^2}{\epsilon_0 \hbar^2} \int_{-\infty}^0 dt_2 \int_{-\infty}^0 dt_1 \times \sum_{p=1}^2 (\boldsymbol{\alpha} \cdot \boldsymbol{\varepsilon}_p)_1 (\boldsymbol{\alpha} \cdot \boldsymbol{\varepsilon}_p)_2 \boxed{\frac{1}{V} \sum_{\mathbf{k}} \frac{e^{\mp i(\mathbf{k} \cdot \mathbf{r}_{12} - \omega t_{12})}}{2\omega}} e^{-icq t_{12}} e^{\gamma(t_1 + t_2)}, \quad (\text{F.60})$$

utilizing the energy conservation (F.49).

*The boxed part of the equation above is essentially the **photon propagator** (4.23)*

$$D_F(1, 2) = \frac{1}{V} \sum_{\mathbf{k}} \frac{e^{\mp i(\mathbf{k} \cdot \mathbf{r}_{12} - \omega t_{12})}}{2\omega} \Rightarrow \int \frac{d^3 \mathbf{k}}{(2\pi)^3} \frac{e^{\mp i(\mathbf{k} \cdot \mathbf{r}_{12} - \omega t_{12})}}{2\omega}. \quad (\text{F.61})$$

This can be represented by a complex integral

$$D_F(1, 2) = i \int \frac{d^3 \mathbf{k}}{(2\pi)^3} \int \frac{dz}{2\pi} \frac{e^{izt_{12}}}{z^2 - \omega^2 + i\eta} e^{i\mathbf{k} \cdot \mathbf{r}_{12}}, \quad (\text{F.62})$$

where  $\eta$  is a small, positive quantity. As before, the sign of the exponent  $i\mathbf{k} \cdot \mathbf{r}_{12}$  is immaterial. The integrand has poles at  $z = \pm(\omega - i\eta)$ , assuming  $\omega$  to be positive. For  $t_2 > t_1$  integration over the *negative* half plane yields  $\frac{1}{2\omega} e^{i\omega t_{12}} e^{i\mathbf{k} \cdot \mathbf{r}_{12}}$  and for  $t_1 > t_2$

integration over the *positive* half plane yields  $\frac{1}{2\omega} e^{-i\omega t_{12}} e^{i\mathbf{k}\cdot\mathbf{r}_{12}}$ , which is identical to (F.61). The evolution operator (F.60) can then be expressed

$$U_\gamma^{(2)}(0, -\infty) = -c_r^\dagger c_a c_s^\dagger c_b \frac{e^2 c^2}{\epsilon_0 \hbar} \int_{-\infty}^0 dt_2 \int_{-\infty}^0 dt_1 \\ \times \sum_{p=1}^2 (\boldsymbol{\alpha} \cdot \boldsymbol{\varepsilon}_p)_1 (\boldsymbol{\alpha} \cdot \boldsymbol{\varepsilon}_p)_2 D_F(1, 2) e^{-icq t_{12}/\hbar} e^{\gamma(t_1+t_2)\hbar}. \quad (\text{F.63})$$

### Comparison with the Covariant Treatment

It is illuminating to compare the quantization of the transverse photons with the fully covariant treatment, to be discussed in the next chapter. Then we simply have to replace the sum in (F.42) by the corresponding covariant expression

$$\sum_{p_1 p_2=1}^2 (a_{kp} \boldsymbol{\alpha} \cdot \boldsymbol{\varepsilon}_p)_1 (a_{kp}^\dagger \boldsymbol{\alpha} \cdot \boldsymbol{\varepsilon}_p)_2 \Rightarrow \sum_{p_1 p_2=0}^3 (a_{kp} \alpha^\mu \varepsilon_{\mu p})_1 (a_{kp}^\dagger \alpha^\nu \varepsilon_{\nu p})_2. \quad (\text{F.64})$$

The commutation relation (G.10) yields

$$\sum_{p_1 p_2=0}^3 (a_{kp} \alpha^\mu \varepsilon_{\mu p})_1 (a_{kp}^\dagger \alpha^\nu \varepsilon_{\nu p})_2 = \boldsymbol{\alpha}_1 \cdot \boldsymbol{\alpha}_2 - 1. \quad (\text{F.65})$$

We then find that the equivalent potential interaction (F.50) under energy conservation is replaced by

$$V_{12} = -\frac{e^2}{\epsilon_0} \int \frac{d^3\mathbf{k}}{(2\pi)^3} (1 - \boldsymbol{\alpha}_1 \cdot \boldsymbol{\alpha}_2) \frac{e^{i\mathbf{k}\cdot\mathbf{r}_{12}}}{q^2 - k^2 + i\gamma} \quad (\text{F.66})$$

and with the Fourier transform given in Appendix J.2

$$V_{12} = \frac{e^2}{4\pi\epsilon_0 r_{12}} (1 - \boldsymbol{\alpha}_1 \cdot \boldsymbol{\alpha}_2) e^{i|q|r_{12}}. \quad (\text{F.67})$$

We shall now compare this with the exchange of *transverse* photons, treated above. We then make the decomposition

$$1 - \boldsymbol{\alpha}_1 \cdot \boldsymbol{\alpha}_2 = \begin{cases} 1 - (\boldsymbol{\alpha}_1 \cdot \hat{\mathbf{k}})(\boldsymbol{\alpha}_2 \cdot \hat{\mathbf{k}}) \\ -\boldsymbol{\alpha}_1 \cdot \boldsymbol{\alpha}_2 + (\boldsymbol{\alpha}_1 \cdot \hat{\mathbf{k}})(\boldsymbol{\alpha}_2 \cdot \hat{\mathbf{k}}). \end{cases} \quad (\text{F.68})$$

The last part, which represents the exchange of *transverse* photons, is identical to (F.52), which led to the Breit interaction. The first part, which represents the exchange of *longitudinal and scalar* photons, corresponds to the interaction

$$V_C = -\frac{e^2}{\epsilon_0} \int \frac{d^3\mathbf{k}}{(2\pi)^3} [1 - (\boldsymbol{\alpha}_1 \cdot \hat{\mathbf{k}})(\boldsymbol{\alpha}_2 \cdot \hat{\mathbf{k}})] \frac{e^{i\mathbf{k}\cdot\mathbf{r}_{12}}}{q^2 - k^2 + i\gamma}. \quad (\text{F.69})$$

This Fourier transform is evaluated in Appendix J.3 and yields

$$V_C = -\frac{e^2}{\epsilon_0} \int \frac{d^3\mathbf{k}}{(2\pi)^3} \left(1 - \frac{q^2}{k^2}\right) \frac{e^{i\mathbf{k}\cdot\mathbf{r}_{12}}}{q^2 - k^2 + i\gamma} = \frac{e^2}{\epsilon_0} \int \frac{d^3\mathbf{k}}{(2\pi)^3} \frac{e^{i\mathbf{k}\cdot\mathbf{r}_{12}}}{k^2 - i\gamma}, \quad (\text{F.70})$$

provided that the orbitals are generated in a **local potential**. Using the transform in Appendix J.2, this becomes

$$V_{\text{Coul}} = \frac{e^2}{4\pi\epsilon_0 r_{12}}. \quad (\text{F.71})$$

Thus, we see that *the exchange of longitudinal and scalar photons corresponds to the instantaneous Coulomb interaction, while the exchange of the transverse photons corresponds to the Breit interaction*. Note that this is true only if the orbitals are generated in a **local potential**.

If instead of the separation (F.68) we would separate the photons into the scalar part ( $p = 0$ ) and the vector part ( $p = 1, 2, 3$ ),

$$1 - \boldsymbol{\alpha}_1 \cdot \boldsymbol{\alpha}_2 = \begin{cases} 1 \\ -\boldsymbol{\alpha}_1 \cdot \boldsymbol{\alpha}_2, \end{cases} \quad (\text{F.72})$$

then the result would be

$$\begin{aligned} V_{\text{Coul}}^{\text{Ret}} &= \frac{e^2}{4\pi\epsilon_0 r_{12}} e^{i|q|r_{12}} \\ V_{\text{Gaunt}}^{\text{Ret}} &= -\frac{e^2}{4\pi\epsilon_0 r_{12}} \boldsymbol{\alpha}_1 \cdot \boldsymbol{\alpha}_2 e^{i|q|r_{12}}, \end{aligned} \quad (\text{F.73})$$

which represents the *retarded Coulomb and the retarded magnetic (Gaunt) interaction*. This implies that **the longitudinal photon represents the retardation of the Coulomb interaction, which is included in the Breit interaction (F.54)**.

If we would set  $q = 0$ , then we would from (F.73) retrieve the *instantaneous Coulomb interaction (F.71)* and

$$-\frac{e^2}{4\pi\epsilon_0} \boldsymbol{\alpha}_1 \cdot \boldsymbol{\alpha}_2, \quad (\text{F.74})$$



which is known as the *Gaunt interaction*. The Breit interaction will then turn into the instantaneous interaction (F.55). This will still have some effect of the retardation of the Coulomb interaction, although it is instantaneous.

We shall see later that the interactions (F.73) correspond to the interactions in the Feynman gauge (4.56), while the instantaneous Coulomb and Breit interactions correspond to the Coulomb gauge.

# Appendix G

## Covariant Theory of Quantum Electro Dynamics

### G.1 Covariant Quantization. Gupta–Bleuler Formalism

With the Lorenz condition (F.21)  $\partial_\mu A^\mu = 0$  the Maxwell equations have a particularly simple form (F.22)

$$\square A = \mu_0 j. \quad (\text{G.1})$$

In this case the covariant electromagnetic radiation field can be expressed in analogy with the semiclassical expression (F.39) and represented by the four-component vector potential [143, Eq. 5.16]<sup>10</sup>

$$A_\mu(x) = A_\mu^+(x) + A_\mu^-(x) = \sqrt{\frac{\hbar}{2\omega\epsilon_0 V}} \sum_{kr} \varepsilon_{\mu r} [a_{kr} e^{-ikx} + a_{kr}^\dagger e^{ikx}]. \quad (\text{G.2})$$

However, different equivalent choices can be made, as further discussed in Sect. G.2. Here, we use the covariant notations

$$k = k^\mu = (k_0, \mathbf{k}); \quad k_0 = \omega/c = |\mathbf{k}|; \quad kx = \omega t - \mathbf{k} \cdot \mathbf{x},$$

defined in Appendix A.1, and  $r = (0, 1, 2, 3)$  represents the four polarization states. Normally, the polarization vector for  $r = 3$  is defined to be along the  $\mathbf{k}$  vector—*longitudinal component*—and for  $r = 1, 2$  to be perpendicular—*transverse components*. The component  $r = 0$  is referred to as the time-like or scalar component (see Sect. F.1).

<sup>10</sup>This is expressed in the interaction picture (IP). In the Schrödinger picture (SP) the time dependence is eliminated (c.f. (B.16)).

The electromagnetic-fields components are Heisenberg operators and should satisfy the canonical commutation (quantization) rules (E.24) at equal times

$$[A_\mu(t, \mathbf{x}), \pi^\nu(t, \mathbf{x}')] = i\hbar\delta_{\mu,\nu} \delta^3(\mathbf{x} - \mathbf{x}'), \quad (\text{G.3})$$

where  $\pi^\nu(x)$  is the conjugate field (E.21). With the Lagrangian (F.17) the field  $\pi^0$  vanishes according to the relation (F.19), which is inconsistent with the quantization rule (G.3). In order to remedy the situation, we add a term  $-\frac{\lambda}{2\mu_0} (\partial_\nu A^\nu)^2$  to the Lagrangian (F.17), where  $\lambda$  is an arbitrary constant [92, Eq. 1–49, Eq. 3–98]

$$\mathcal{L} = -\frac{1}{4\mu_0} F_{\mu\nu} F^{\mu\nu} - \frac{\lambda}{2\mu_0} (\partial_\nu A^\nu)^2 - j^\mu A_\mu. \quad (\text{G.4})$$

We can rewrite the extra term as

$$-\frac{\lambda}{2\mu_0} (\partial_\nu g^{\nu\sigma} A_\sigma) (\partial_\nu A^\nu).$$

Then the conjugate field (F.19) becomes [92, Eq. 3–100]

$$\pi^\mu(x) = \frac{\partial \mathcal{L}}{\partial(\partial^0 A_\mu)} = -\frac{1}{c\mu_0} F^{\mu 0} - \frac{\lambda}{\mu_0} g^{0\mu} \partial_\nu A^\nu \quad (\text{G.5})$$

and  $\pi^0 \neq 0$  for  $\lambda \neq 0$ .

The extra term in the Euler-Lagrange equations (F.14) leads to

$$\begin{aligned} \frac{\lambda}{2\mu_0} \partial_\nu \frac{\partial}{\partial(\partial_\nu A_\mu)} (\partial_\nu g^{\nu\sigma} A_\sigma) (\partial_\nu A^\nu) &= \frac{\lambda}{\mu_0} \partial_\nu g^{\nu\mu} (\partial_\sigma A^\sigma) \\ &= \frac{\lambda}{\mu_0} \partial_\mu g^{\mu\mu} (\partial_\sigma A^\sigma) = \lambda \partial^\mu (\partial_\sigma A^\sigma). \end{aligned}$$

The Maxwell equations (F.10) then take the modified form [92, Eq. 3–99]

$$\partial_\nu \partial^\nu A^\mu - (1 - \lambda) \partial^\mu (\partial_\nu A^\nu) = \mu_0 j^\mu. \quad (\text{G.6})$$

**Setting  $\lambda = 1$  we retrieve the same simple form of Maxwell's equations as with the Lorenz condition (G.1)—without introducing this condition explicitly.** This is usually referred to as the **Feynman gauge**.

The Lagrangian (G.4) is incompatible with the Lorenz condition, and to resolve the dilemma this condition is replaced by its expectation value

$$\langle \Psi | \partial_\mu A^\mu | \Psi \rangle = 0, \quad (\text{G.7})$$

which is known as the **Gupta–Bleuler proposal** [143, 5.35].

In the *Feynman gauge* the commutation relations (G.3) become [143, 5.23]

$$[A_\mu(t, \mathbf{x}), \dot{A}^\nu(t, \mathbf{x}')] = ic^2 \mu_0 \hbar g_{\mu\nu} \delta_{\mu,\nu} \delta^3(\mathbf{x} - \mathbf{x}'). \quad (\text{G.8})$$

To satisfy this relation, we can assume that the polarization vectors fulfill the orthogonality/completeness relations [143, Eq. 5.18, 19]

$$\begin{aligned} \varepsilon_{\mu r} \varepsilon_{\mu r'} &= g_{rr'} \\ \sum_r g_{rr} \varepsilon_{\mu r} \varepsilon_{\nu r} &= g_{\mu\nu}, \end{aligned} \quad (\text{G.9})$$

and the photon creation and absorption operators the commutation relation [143, Eq. 5.28]

$$[a_{kr}, a_{k'r'}^\dagger] = -\delta_{k,k'} g_{rr'}. \quad (\text{G.10})$$

Considering that the g-matric (A.5) used is diagonal, this leads to

$$\sum_{rr'} [\varepsilon_{\mu r} a_{kr}, \varepsilon_{\nu r'} a_{k'r'}^\dagger] = \sum_{rr'} \varepsilon_{\mu r} \varepsilon_{\nu r'} [a_{kr}, a_{k'r'}^\dagger] = -g_{\mu,\nu} \delta_{k,k'}, \quad (\text{G.11})$$

and then it follows that the field operators (G.2) satisfy the commutation relation (G.8).

With the Lagrangian (G.4) and the conjugate fields Eq. (G.5) the Hamiltonian of the free field (F.20) becomes in the Feynman gauge ( $\lambda = 1$ ) [143, Eq. 5.32]

$$H_{\text{Rad}} = - \sum_{k,r} \hbar \omega g_{rr} a_{kr}^\dagger a_{kr}. \quad (\text{G.12})$$

## G.2 Gauge Transformation

### G.2.1 General

The previous treatment is valid in the Feynman gauge, where the Maxwell equations have the form (G.1), and we shall here investigate how the results will appear in other gauges.

The interaction between an electron and the electromagnetic field is given by the Hamiltonian interaction density (D.44)

$$\mathcal{H}_{\text{int}} = j_\mu A^\mu, \quad (\text{G.13})$$

where  $j_\mu$  is the current density. The Maxwell equations are invariant for a *gauge transformation* (F.24)  $A \Rightarrow A + \nabla\Lambda$ , which transforms this interaction to

$$H_{\text{int}} = j_\mu A^\mu \Rightarrow \left( A^\mu + \frac{\partial\Lambda}{\partial x_\mu} \right) j_\mu.$$

Integration over space leads after partial integration to

$$\int d^3\mathbf{x} \frac{\partial\Lambda}{\partial x_\mu} j_\mu = - \int d^3\mathbf{x} \frac{\partial j_\mu}{\partial x_\mu} \Lambda = 0.$$

Since  $\Lambda$  is arbitrary, it follows that

$$\frac{\partial j_\mu}{\partial x_\mu} = \delta^\mu j_\mu = \nabla j = 0,$$

which is the *continuity equation* (F.23). In analogy with (F.30) the corresponding relation in the  $k$  space is

$$j_\mu(k) k^\mu = 0. \quad (\text{G.14})$$

The single-photon exchange is represented by the interaction (4.44)

$$I(x_2, x_1) = e^2 c^2 \alpha_1^\mu \alpha_2^\nu D_{F\nu\mu}(x_2, x_1), \quad (\text{G.15})$$

which corresponds to the interaction density  $j^\mu D_{F\nu\mu} j^\nu$ . In view of the relation (G.14) it follows that the transformation

$$D_{F\nu\mu}(k) \Rightarrow D_{F\nu\mu}(k) + k_\mu f_\nu(k) + k_\nu f_\mu(k),$$

where  $f_\mu(k)$  and  $f_\nu(k)$  are arbitrary functions of  $k$ , will leave the interaction unchanged.

## G.2.2 Covariant Gauges

In a *covariant gauge* the components of the electro-magnetic field are expressed in a covariant way. We shall consider three gauges of this kind.

### G.2.2.1 Feynman Gauge

The photon propagator in the Feynman gauge is given by the expression (4.28)

$$D_{F\nu\mu}(k) = -\frac{g_{\mu\nu}}{c\epsilon_0} \frac{1}{k^2 + i\eta}. \quad (\text{G.16})$$

### G.2.2.2 Landau Gauge

With

$$f_\mu(k) = \frac{1}{c\epsilon_0} \frac{k_\mu}{(k^2 + i\eta)^2}$$

the propagator (G.16) becomes

$$D_{F\mu\nu}(k) = -\frac{1}{c\epsilon_0} \frac{1}{k^2 + i\eta} \left( g_{\mu\nu} - \frac{k_\mu k_\nu}{k^2 + i\eta} \right). \quad (\text{G.17})$$

This leads to  $k^\mu D_{F\mu\nu} = 0$ , which is consistent with the Lorenz condition (F.21)

$$\nabla A = \partial^\mu A_\mu = 0$$

### G.2.2.3 Fried-Yennie Gauge

With

$$f_\mu(k) = \frac{1}{2c\epsilon_0} (1 - \lambda) \frac{k_\mu}{(k^2 + i\eta)^2}$$

the propagator (G.16) becomes

$$D_{F\mu\nu}(k) = -\frac{1}{c\epsilon_0} \frac{1}{k^2 + i\eta} \left( g_{\mu\nu} - (1 - \lambda) \frac{k_\mu k_\nu}{k^2 + i\eta} \right). \quad (\text{G.18})$$

With  $\lambda = 1$  this yields the Feynman gauge and with  $\lambda = 0$  we retrieve the Landau gauge. The value  $\lambda = 3$  yields the Fried-Yennie gauge [70], which has some improved properties, compared to the Feynman gauge, in the infrared region.

## G.2.3 Non-covariant Gauge

We consider only one example of a *non-covariant gauge*, the Coulomb gauge, which is of vital importance in treating the combined QED-correlation problem. Here, the Coulomb interaction is treated differently from the transverse part.

### G.2.3.1 Coulomb Gauge

With

$$f_0 = \frac{1}{2c\epsilon_0} \frac{1}{k^2 + i\eta} \frac{k_0}{\mathbf{k}^2}; \quad f_i = -\frac{1}{2c\epsilon_0} \frac{1}{k^2 + i\eta} \frac{k_i}{\mathbf{k}^2} \quad (i = 1, 2, 3)$$

the propagator (G.16) can be expressed

$$D_{F00}(k) = \frac{1}{c\epsilon_0} \begin{pmatrix} \frac{1}{k^2} & 0 \\ 0 & \frac{1}{k^2+i\eta} \left( \delta_{ij} - \frac{k_i k_j}{k^2} \right) \end{pmatrix}, \quad (\text{G.19})$$

where the first row/column corresponds to the component  $\mu = 0$  and the second row/column to  $\mu = 1, 2, 3$ .

This leads to  $k^i D_{Fij} = 0$ , which is consistent with the Coulomb condition (F.30)

$$\nabla \cdot \mathbf{A} = \partial^i A_i = 0 \quad (i = 1, 2, 3).$$

### G.3 Formulas for Dimensional Regularization

The formulas above can be generalized to be used in dimensional regularization (see Sect. 12.4), where the number of dimensions is non-integer (mainly from Adikins [1], see also 't Hooft and Veltman [241]).

Following the book by Peskin and Schroeder [194], we can by means of *Wick rotation* evaluate the integral

$$\begin{aligned} \int \frac{d^D l}{(2\pi)^D} \frac{1}{(l^2 - \Delta)^m} &= i(-1)^m \int \frac{d^D l}{(2\pi)^D} \frac{1}{(l_E^2 + \Delta)^m} \\ &= i(-1)^m \int \frac{d\Omega_D}{(2\pi)^4} \int_0^\infty dl_E^0 \frac{l_E^{D-1}}{(l_E^2 + \Delta)^m}. \end{aligned}$$

We have here made the replacements  $l^0 = il_E^0$  and  $\mathbf{l} = \mathbf{l}_E$  and rotated the integration contour of  $l_E$   $90^\circ$ , which with the positions of the poles should give the same result. The integration over  $d^D l_E$  is separated into an integration over the  $D$ -dimensional sphere  $\Omega_D$  and the linear integration over the component  $l_E^0$ . This corresponds in three dimensions to the integration over the two-dimensional angular coordinates and the radial coordinate (see below).

$$\int \frac{d^D k}{(2\pi)^D} \frac{1}{(k^2 + s + i\eta)^n} = \frac{i(-1)^n}{4\pi^{D/2}} \frac{\Gamma(n - D/2)}{\Gamma(n)} \frac{1}{s^{n-D/2}} \quad (\text{G.20})$$

$$\int d^4 k \frac{k^\mu}{(k^2 + s + i\eta)^n} = 0 \quad (\text{G.21})$$

$$\int \frac{d^D k}{(2\pi)^D} \frac{k^\mu k^\nu}{(k^2 + s + i\eta)^n} = \frac{i(-1)^n}{4\pi^{D/2}} \frac{\Gamma(n - D/2 - 1)}{\Gamma(n)} \frac{1}{s^{n-D/2-1}} \quad (\text{G.22})$$

### G.3.1 Covariant Gauge

Compared to Adkins [1] Eqs. (A1a), (A3), and (A5a):

$$p \rightarrow -q; M^2 \rightarrow -s; \omega \rightarrow D/2; \alpha \rightarrow n; \xi \rightarrow n; Q = p \rightarrow -q; \\ \times A_{\mu\nu} \rightarrow g_{\mu\nu}; \Delta \rightarrow w = q^2 - s$$

$$\int \frac{d^D k}{(2\pi)^D} \frac{1}{(k^2 + 2kq + s + i\eta)^n} = \frac{i(-1)^n}{(4\pi)^{D/2}} \frac{1}{\Gamma(n)} \frac{\Gamma(n - D/2)}{w^{n-D/2}} \quad (\text{G.23})$$

$$\int \frac{d^D k}{(2\pi)^D} \frac{k^\mu}{(k^2 + 2kq + s + i\eta)^n} = -\frac{i(-1)^n}{(4\pi)^{D/2}} \frac{1}{\Gamma(n)} q^\mu \frac{\Gamma(n - D/2)}{w^{n-D/2}} \quad (\text{G.24})$$

$$\int \frac{d^D k}{(2\pi)^D} \frac{k^\mu k^\nu}{(k^2 + 2kq + s + i\eta)^n} \\ = \frac{i(-1)^n}{(4\pi)^{D/2}} \frac{1}{\Gamma(n)} \left[ q^\mu q^\nu \frac{\Gamma(n - D/2)}{w^{n-D/2}} + \frac{g^{\mu\nu}}{2} \frac{\Gamma(n - 1 - D/2)}{w^{n-1-D/2}} \right] \quad (\text{G.25})$$

### G.3.2 Non-covariant Gauge

Compared to Adkins [1] Eqs. (A1b), (A4), (A5b):

$$p \rightarrow -q; M^2 \rightarrow -s; \omega \rightarrow D/2; \alpha \rightarrow n; \beta \rightarrow 1; \xi \rightarrow n + 1; \mathbf{k}^2 \rightarrow -\mathbf{k}^2; \\ \times Q = py \rightarrow -qy;$$

$$A_{\mu\nu} \rightarrow g_{\mu\nu} + \delta_{\mu,0}\delta_{\nu,0} \frac{1-y}{y}; (AQ)_\mu \rightarrow -q^\mu y - \delta_{\mu 0}(1-y)q_0$$

$$\Delta \rightarrow w = q^2 y^2 + (1-y)yq_0^2 - sy + \lambda^2(1-y) \\ = -\mathbf{q}^2 y^2 + yq_0^2 - sy + \lambda^2(1-y)$$

$$\int \frac{d^D k}{(2\pi)^D} \frac{1}{(k^2 + 2kq + s + i\eta)^n} \frac{1}{\mathbf{k}^2 - \lambda^2} \\ = \frac{i(-1)^n}{(4\pi)^{D/2}} \frac{1}{\Gamma(n+1)} \int_0^1 dy y^{n-1-1/2} \frac{\Gamma(n+1-D/2)}{w^{n+1-D/2}} \quad (\text{G.26})$$



$$\begin{aligned}
\int \frac{d^D k}{(2\pi)^D} \frac{k^\mu}{(k^2 + 2kq + s + i\eta)^n} \frac{1}{\mathbf{k}^2 - \lambda^2} &= -\frac{i(-1)^n}{(4\pi)^{D/2}} \frac{1}{\Gamma(n)} \\
&\times \int_0^1 dy y^{n-1-1/2} [q^\mu y + \delta_{\mu,0} q_0(1-y)] \\
&\times \frac{\Gamma(n+1-D/2)}{w^{n+1-D/2}} \quad (\text{G.27})
\end{aligned}$$

$$\not{k} \rightarrow -\not{q} y - \gamma^0 q_0(1-y) = \boldsymbol{\gamma} \cdot \mathbf{q} y - \gamma^0 q_0$$

$$\begin{aligned}
&\int \frac{d^D k}{(2\pi)^D} \frac{k^\mu k^\nu}{(k^2 + 2kq + s + i\eta)^n} \frac{1}{\mathbf{k}^2 - \lambda^2} \\
&= \frac{i(-1)^n}{(4\pi)^{D/2}} \frac{1}{\Gamma(n)} \\
&\times \int_0^1 dy y^{n-1-1/2} \left\{ [q^\mu y + \delta_{\mu,0} q_0(1-y)][q^\nu y + \delta_{\nu,0} q_0(1-y)] \right\} \\
&\times \frac{\Gamma(n+1-D/2)}{w^{n+1-D/2}} \\
&- \frac{1}{2} \left\{ [g^{\mu\nu} + \delta_{\mu,0} \delta_{\nu,0}(1-y)/y] \right\} \frac{\Gamma(n-D/2)}{w^{n-D/2}} \quad (\text{G.28})
\end{aligned}$$

$\not{k} \rightarrow \boldsymbol{\gamma} \cdot \mathbf{q} y - \gamma^0 q_0$  in first part and  $\not{k} \not{k} \rightarrow -\frac{1}{2} [\gamma^\mu \gamma_\mu + (1-y)/y]$  in second.

$$\begin{aligned}
&\int \frac{d^D k}{(2\pi)^D} \frac{k^i k^\mu k^j}{(k^2 + 2kq + s + i\eta)^n} \frac{1}{\mathbf{k}^2 - \lambda^2} \\
&= -\frac{i(-1)^n}{(4\pi)^{D/2}} \frac{1}{\Gamma(n)} \\
&\times \int_0^1 dy y^{n-1-1/2} \left\{ q^i q^\mu q^j y^3 + q^i q^\mu q^j \delta_{\mu 0} (1-y) y^2 \right\} \frac{\Gamma(n+1-D/2)}{w^{n+1-D/2}} \\
&+ \frac{1}{2} \left\{ y(g^{i\mu} q^j + g^{\mu j} q^i + g^{ji} q^\mu) + \delta_{\mu 0} g^{ij} q_0(1-y) \right\} \frac{\Gamma(n-D/2)}{w^{n-D/2}} \quad (\text{G.29})
\end{aligned}$$

## G.4 Gamma Function

The *Gamma function* can be defined by means of Euler's integral

$$\Gamma(z) = \int_{-\infty}^{\infty} dt t^{z-1} e^{-t}. \quad (\text{G.30})$$

For integral values we have the relation

$$\Gamma(n) = (n - 1)! \tag{G.31}$$

and generally

$$\Gamma(z) = (z - 1)\Gamma(z - 1). \tag{G.32}$$

The Gamma function can also be expressed by means of

$$\frac{1}{\Gamma(z)} = ze^{\gamma_E z} \prod_{n=1}^{\infty} \left(1 + \frac{z}{n}\right) e^{-z/n}, \tag{G.33}$$

where  $\gamma_E$  is Euler's constant,  $\gamma_E = 0.5772\dots$

The Gamma function is singular, when  $z$  is zero or equal to a negative integer. Close to zero the function is equal to

$$\Gamma(\epsilon) = \frac{1}{\epsilon} - \gamma_E + \mathcal{O}(\epsilon), \tag{G.34}$$

which follows directly from the expansion above. We shall now derive the corresponding expression close to negative integers.

### G.4.1 $z = -1 - \epsilon$

$$\frac{1}{\Gamma(-1 - \epsilon)} = -(1 + \epsilon) e^{-\gamma_E(1+\epsilon)} \prod_{n=1}^{\infty} \left(1 - \frac{1 + \epsilon}{n}\right) e^{(1+\epsilon)/n} \tag{G.35}$$

The first few factors of the product  $\prod$  are (to orders linear in  $\epsilon$ )

$$\begin{aligned} -\epsilon e^{1+\epsilon} &= -\epsilon e^1(1 + \epsilon) \\ \left(1 - \frac{1 + \epsilon}{2}\right) e^{(1+\epsilon)/2} &= \frac{1}{2} (1 - \epsilon) e^{1/2}(1 + \epsilon/2) \\ \left(1 - \frac{1 + \epsilon}{3}\right) e^{(1+\epsilon)/3} &= \frac{2}{3} (1 - \epsilon/2) e^{1/3}(1 + \epsilon/3) \\ \left(1 - \frac{1 + \epsilon}{4}\right) e^{(1+\epsilon)/4} &= \frac{3}{4} (1 - \epsilon/3) e^{1/4}(1 + \epsilon/4) \end{aligned}$$

which in the limit becomes

$$-e^{\gamma_E} \left( 1 + \epsilon \left[ 1 - 1/2 - 1/(2 \cdot 3) - 1/(3 \cdot 4) - \dots \right] \right) \approx -e^{\gamma_E}$$

using the expansion

$$1 + 1/2 + 1/3 + 1/4 + \dots + 1/M \Rightarrow \ln M + \gamma_E \quad (\text{G.36})$$

This gives

$$\Gamma(-1 - \epsilon) = \frac{1}{\epsilon} + \gamma_E - 1 + \mathcal{O}(\epsilon). \quad (\text{G.37})$$

This can also be obtained from (G.32).

#### G.4.2 $z = -2 - \epsilon$

$$\frac{1}{\Gamma(-2 - \epsilon)} = -(2 + \epsilon) e^{-\gamma_E(2+\epsilon)} \prod_{n=1}^{\infty} \left( 1 - \frac{2 + \epsilon}{n} \right) e^{(2+\epsilon)/n} \quad (\text{G.38})$$

The first few factors of the product  $\prod$  are (to orders linear in  $\epsilon$ )

$$-(1 + \epsilon) e^{2+\epsilon} = -(1 + \epsilon) e^2 (1 + \epsilon)$$

$$-\epsilon/2 e^{(2+\epsilon)/2} = -\epsilon/2 e^1 (1 + \epsilon/2)$$

$$\left( 1 - \frac{2 + \epsilon}{3} \right) e^{(2+\epsilon)/3} = \frac{1}{3} (1 - \epsilon) e^{2/3} (1 + \epsilon/3)$$

$$\left( 1 - \frac{2 + \epsilon}{4} \right) e^{(2+\epsilon)/4} = \frac{2}{4} (1 - \epsilon/2) e^{2/4} (1 + \epsilon/4)$$

$$\left( 1 - \frac{2 + \epsilon}{5} \right) e^{(2+\epsilon)/5} = \frac{3}{5} (1 - \epsilon/3) e^{2/5} (1 + \epsilon/5),$$

which in the limit becomes

$$e^{2\gamma_E} \left( 1 + \epsilon \left[ 5/2 - 2/(1 \cdot 3) - 2/(2 \cdot 4) - 2/(3 \cdot 5) - \dots \right] \right) \approx e^{2\gamma_E} (1 + \epsilon).$$

This gives

$$\Gamma(-2 - \epsilon) = -\frac{1}{2} \left[ \frac{1}{\epsilon} + \gamma_E - 1 - 1/2 + \mathcal{O}(\epsilon) \right]. \quad (\text{G.39})$$

This is consistent with the formula

$$\Gamma(2z) = (2\pi)^{-1/2} 2^{2z-1/2} \Gamma(z) \Gamma(z + 1/2). \quad (\text{G.40})$$

The step-down formula (G.32) yields

$$\Gamma(-3 - \epsilon) = \frac{1}{2 \cdot 3} \left[ \frac{1}{\epsilon} + \gamma_E - 1 - 1/2 - 1/3 \right], \quad (\text{G.41})$$

which can be generalized to

$$\Gamma(-N - \epsilon) = \frac{(-1)^{N-1}}{N!} \left[ \frac{1}{\epsilon} + \gamma_E - \sum_{n=1}^N \frac{1}{n} \right]. \quad (\text{G.42})$$

# Appendix H

## Feynman Diagrams and Feynman Amplitude

In this appendix we shall summarize the rules for evaluating Feynman diagrams of the different schemes, discussed in this book. These rules are based on the rules formulated by Feynman for the so-called *Feynman amplitude*, a concept we shall also use here.

### H.1 Feynman Diagrams for the S-Matrix

The S-matrix is given by (4.3)

$$S = \sum_{n=0}^{\infty} \frac{1}{n!} \left(\frac{-i}{c}\right)^n \int dx_1^4 \dots \int dx_n^4 T[\mathcal{H}(x_1) \dots \mathcal{H}(x_n)] e^{-\gamma(|t_1|+|t_2|+\dots|t_n|)}, \quad (\text{H.1})$$

where (4.4)

$$\mathcal{H}(x) = -\hat{\psi}^\dagger(x) e c \alpha^\mu A_\mu(x) \hat{\psi}(x). \quad (\text{H.2})$$

The Feynman diagram for the S-matrix is constructed by means of the following rules:

- There is an *outgoing* orbital line for each electron-field *creation* operator



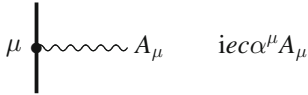
- and an *incoming* orbital line for each electron-field *absorption* operator



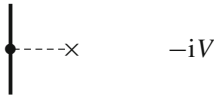
- There is a factor of  $-ie\alpha^\mu$  at each *vertex*



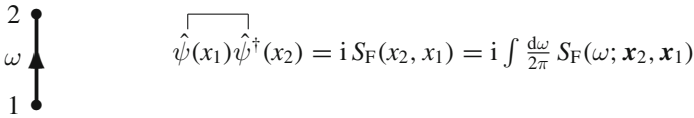
- For an interaction  $\mathcal{H}(x) = -\hat{\psi}^\dagger(x) e c \alpha^\mu A_\mu(x) \hat{\psi}(x)$  this leads to (including the factor  $-i$  from the vertex)



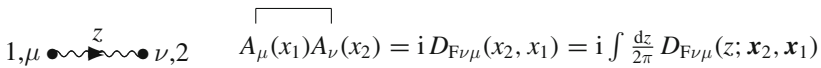
- For each energy potential  $V = -ecA_0$  this becomes



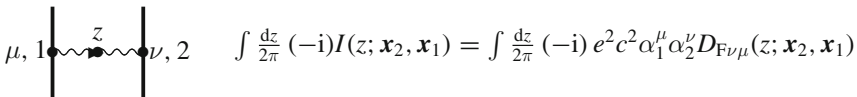
- There is an *electron propagator* for each contracted pair of electron-field operators:



- and a *photon propagator* for each contracted pair of photon-field operators:



- Thus, there is a *photon interaction*, **including the vertices**, for each photon exchange,




- For the Coulomb interaction this becomes




$$-iV_C = -i\frac{e^2}{4\pi\epsilon_0 r_{12}}$$

- Each electron self-energy leads, including the vertices, to



$$-i\Sigma$$

- and each vertex correction



$$-i\Lambda^\mu$$

- At each vertex space and time integrations are performed. The time integration leads to an integral  $2\pi\Delta_\gamma(arg)$ , where the argument is equal to incoming minus outgoing energy parameters. For an irreducible diagram with no internal model-space state, the gammas can go to zero independently at each vertex, which leads to energy conservation at each vertex as well as to an over-all energy conservation for the entire diagram.
- A factor of  $-1$  and a *trace symbol* for each closed orbital loop;

## H.2 Feynman Amplitude

### S-Matrix

For an irreducible S-matrix diagram the Feynman amplitude,  $\mathcal{M}$ , is defined by (see Sect. 4.7.2)

$$S = 2\pi\delta(E_{in} - E_{out})\mathcal{M}, \tag{H.3}$$

where  $E_{in}$ ,  $E_{out}$  are the incoming and outgoing energies, respectively. This implies that the rules for the Feynman amplitude are largely the same as for the Feynman diagram.

For corresponding diagrams the Feynman amplitude is the same also for the *Green's function* and the *covariant-evolution operator*, which are given by

$$G(x; x_0)P_{\mathcal{E}} = e^{-i(t-t_0)\mathcal{E}} \mathcal{M}P_{\mathcal{E}} \tag{H.4}$$

and

$$U(t, -\infty)P_{\mathcal{E}} = e^{-it(\mathcal{E}-H_0)} \mathcal{M}P_{\mathcal{E}}, \tag{H.5}$$

respectively, operating on a model-space state of energy  $\mathcal{E}$ .

**Illustrations**

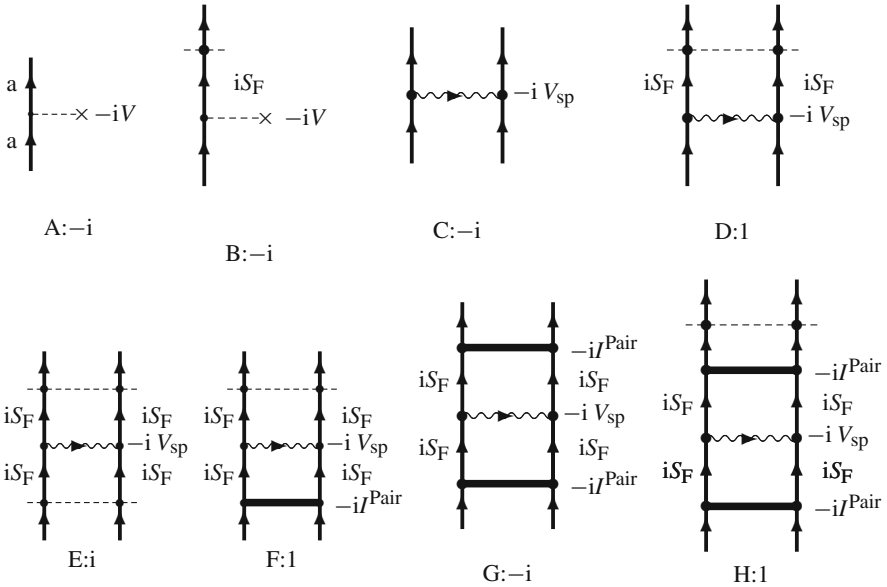


Diagram A is a first-order S-matrix with a potential interaction, and the Feynman amplitude is

$$\mathcal{M} = -iV$$

and the S-matrix

$$S = 2\pi \delta(E_{\text{in}} - E_{\text{out}}) \mathcal{M}$$

and the energy shift

$$\Delta E = \langle a | i\mathcal{M} | a \rangle = \langle a | V | a \rangle.$$

Diagram B is the corresponding CEO and Green's-operator diagram. The Feynman amplitude is

$$\mathcal{M}P_{\mathcal{E}} = iS_F(-i)V P_{\mathcal{E}} = S_F V P_{\mathcal{E}} = \frac{1}{\mathcal{E} - H_0} V P_{\mathcal{E}}$$



and the CEO

$$U(t, -\infty)P_{\mathcal{E}} = e^{-it(\mathcal{E}-H_0)}\mathcal{M}P_{\mathcal{E}},$$

which yields the same shift.

Diagram C is a first-order S-matrix for single-photon exchange (Sect. 4.4), and the Feynman amplitude is

$$\mathcal{M} = -iV_{\text{sp}}(E_0).$$

Diagram D is a corresponding CEO diagram with the unperturbed state as input and with outgoing electron propagators (Sect. 6.3). Here, there are three energy parameters and two subsidiary conditions. This leaves one non-trivial integration, giving a factor of  $-i$ . This gives a factor of  $i^2(-i)^2 = 1$  and

$$\mathcal{M} = \Gamma(E_0) V_{\text{sp}}(E_0).$$

Diagram E is a first-order CEO diagram with incoming and outgoing electron propagators (Sect. 8.1.1). Here, there are five parameters and three conditions, leaving two non-trivial integrations. This gives the factor  $i^4(-i)^3 = i$  and (8.9)

$$\mathcal{M} = \Gamma(E_0) iV_{\text{sp}}(E_0) \Gamma(E_0).$$

Diagram F is a first-order covariant evolution-operator diagram with incoming pair function (Sect. 6.4). This gives  $i^4(-i)^4 = 1$

$$\mathcal{M} = I^{\text{Pair}} \Gamma(E_0) V_{\text{sp}}(E_0) \Gamma(E_0) I^{\text{Pair}}.$$

Diagram G is an S-matrix diagram with incoming and outgoing pair functions (Sect. 6.4). This gives  $i^4(-i)^5 = -i$  and

$$\mathcal{M} = -iI^{\text{Pair}} \Gamma(E_0) V_{\text{sp}}(E_0) \Gamma(E_0) I^{\text{Pair}}.$$

Diagram H is a first-order covariant evolution-operator diagram with incoming and outgoing pair functions (Sect. 6.4). Here, there are 7 parameters and 4 subsidiary conditions, yielding  $i^6(-i)^6 = 1$  and

$$\mathcal{M} = \Gamma(E_0) I^{\text{Pair}} \Gamma(E_0) V_{\text{sp}}(E_0) \Gamma(E_0) I^{\text{Pair}}.$$

# Appendix I

## Evaluation Rules for Time-Ordered Diagrams

In non-relativistic (MBPT) formalism all interaction times are restricted to the interval  $(t, -\infty)$ , and the Goldstone diagrams are used for the graphical representation. In the relativistic (QED) formalism, on the other hand, times are allowed in the entire interval  $(\infty, -\infty)$ , and then Feynman diagrams, which contain all possible time orderings, are the relevant ones to use.

For computational as well as illustrative purpose it is sometimes useful also in the relativistic case to work with *time-ordered diagrams*. It should be observed, though, that *time-ordered Feynman diagrams are distinct from Goldstone diagrams*, as we shall demonstrate here.<sup>11</sup>

When only *particles states* (above the Fermi level) are involved, time runs in the *positive* direction, and the time-evolution operator can be expressed (3.21)

$$U(t, -\infty) = 1 - i \int_{-\infty}^t dt_1 V(t_1) + (-i)^2 \int_{-\infty}^t dt_1 V(t_1) \int_{-\infty}^{t_1} dt_2 V(t_2) + \dots, \tag{I.1}$$

where  $V(t)$  is the perturbation in the interaction picture (3.25)

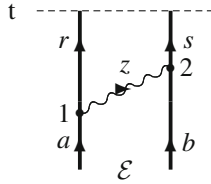
$$V(t) = - \int d^3\mathbf{x} \hat{\psi}^\dagger(x) e c \alpha^\mu A_\mu(x) \hat{\psi}(x). \tag{I.2}$$

Core states and negative energy states are regarded as *hole states* below the Fermi level with time running in the negative direction. Then the corresponding *time integration should be performed in the negative direction*.

---

<sup>11</sup>The treatment here is partly based upon that in [130, Appendices C and D].

### I.1 Single-Photon Exchange



We consider first the time-ordered diagram for single-photon exchange with only particle states involved. The time restrictions are here

$$t > t_2 > t_1 > -\infty,$$

which corresponds to the evolution operator (I.1)

$$(-i)^2 \int_{-\infty}^t dt_2 V(t_2) e^{-it_2 d_2} \int_{-\infty}^{t_2} dt_1 V(t_1) e^{-it_1 d_1}. \tag{I.3}$$

The contraction of the radiation-field operators gives rise to a photon propagator (4.18)

$$\overline{A_\nu(x_2) A_\mu(x_1)} = i D_{F\nu\mu}(x_2, x_1),$$

and this leads to the interaction (4.46)

$$I(x_2, x_1) = e^2 c^2 \alpha_1^\mu \alpha_2^\nu D_{F\nu\mu}(x_2, x_1) = \int \frac{dz}{2\pi} e^{-iz(t_2-t_1)} \int \frac{2c^2 k dk f(k; \mathbf{x}_1, \mathbf{x}_2)}{z^2 - c^2 k^2 + i\eta}.$$

The time dependence at vertex 1 then becomes  $e^{-it_1 d_1}$ , where

$$d_1 = \varepsilon_a - \varepsilon_r - z + i\gamma.$$

This parameter is referred to as the *vertex value* and given by *the incoming minus the outgoing orbital energies/energy parameters* at the vertex. Similarly, we define

$$\begin{aligned} d_2 &= \varepsilon_b - \varepsilon_s + z + i\gamma \\ d_{12} &= d_1 + d_2 = \mathcal{E} - \varepsilon_r - \varepsilon_s \end{aligned} \tag{I.4}$$

with  $\mathcal{E} = \varepsilon_a + \varepsilon_b$ . This leads to the time integrals

$$(-i)^2 \int_{-\infty}^t dt_2 e^{-it_2 d_2} \int_{-\infty}^{t_2} dt_1 e^{-it_1 d_1} = \frac{e^{-it d_{12}}}{d_{12}} \frac{1}{d_1}. \tag{I.5}$$

Together with the opposite time ordering,  $t > t_1 > t_2 > -\infty$ , the denominators become

$$\frac{1}{d_{12}} \left( \frac{1}{d_1} + \frac{1}{d_2} \right) = \frac{1}{\mathcal{E} - \varepsilon_r - \varepsilon_s} \left( \frac{1}{\varepsilon_a - \varepsilon_r - z + i\gamma} + \frac{1}{\varepsilon_b - \varepsilon_s + z + i\gamma} \right). \quad (I.6)$$

This leads to the Feynman amplitude (6.18)

$$\begin{aligned} \mathcal{M}_{\text{sp}} = & i \int \frac{dz}{2\pi} \frac{1}{\mathcal{E} - \varepsilon_r - \varepsilon_s} \left( \frac{1}{\varepsilon_a - \varepsilon_r - z + i\gamma} + \frac{1}{\varepsilon_b - \varepsilon_s + z + i\gamma} \right) \\ & \times \int \frac{2c^2 k \, dk f(k)}{z^2 - c^2 k^2 + i\eta} \end{aligned} \quad (I.7)$$

or

$$\langle rs | \mathcal{M}_{\text{sp}} | ab \rangle = \frac{1}{E - \varepsilon_r - \varepsilon_s} \langle rs | V_{\text{sp}}(\mathcal{E}) | ab \rangle \quad (I.8)$$

with

$$V_{\text{sp}}(\mathcal{E}) = \int c \, dk f(k) \left( \frac{1}{\varepsilon_a - \varepsilon_r - ck + i\gamma} + \frac{1}{\varepsilon_b - \varepsilon_s - ck + i\gamma} \right). \quad (I.9)$$

If the interaction is *instantaneous*, then the time integral becomes

$$-i \int_{-\infty}^t dt_{12} e^{-it_{12}d_{12}} = \frac{e^{-it} d_{12}}{d_{12}} = \frac{e^{-it} (\mathcal{E} - \varepsilon_r - \varepsilon_s)}{\mathcal{E} - \varepsilon_r - \varepsilon_s}, \quad (I.10)$$

which for  $t = 0$  is the standard MBPT result.

## I.2 Two-Photon Exchange

Next, we consider the diagrams in Fig. I.1.

We extend the definitions of the *vertex values*:

$$\begin{aligned} d_1 &= \varepsilon_a - \varepsilon_t - z; & d_2 &= \varepsilon_b - \varepsilon_u + z; & d_3 &= \varepsilon_t - \varepsilon_r - z'; & d_4 &= \varepsilon_u - \varepsilon_s + z' \\ d_{12} &= d_1 + d_2 = \mathcal{E} - \varepsilon_t - \varepsilon_u; & d_{13} &= \varepsilon_a - \varepsilon_r - z - z'; & d_{24} &= \varepsilon_b - \varepsilon_s + z + z' \\ d_{123} &= \mathcal{E} - \varepsilon_r - \varepsilon_u - z'; & d_{124} &= \mathcal{E} - \varepsilon_t - \varepsilon_s + z'; & d_{1234} &= \mathcal{E} - \varepsilon_r - \varepsilon_s, \end{aligned}$$

i.e., given by the *incoming minus the outgoing energies* of the vertex. There is a damping term  $\pm i\gamma$  for integration going to  $\mp\infty$ .

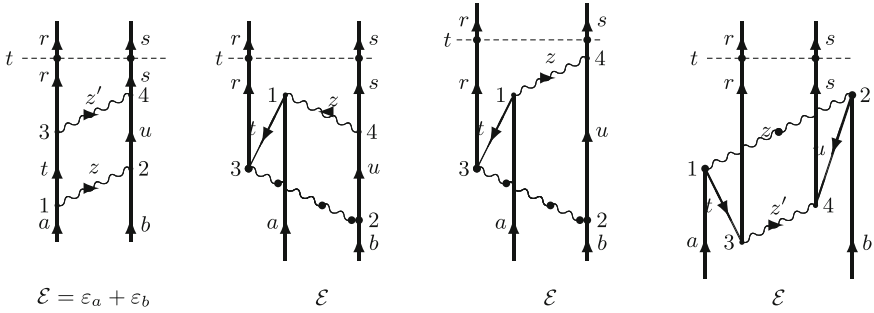


**Fig. I.1** Time-ordered Feynman diagrams for the two-photon ladder with only particle states (*left*) and with one and two intermediate hole states (*right*)

### No Virtual Pair

We consider now the first diagram above, where only particle states are involved. We assume that it is *reducible*, implying that the two photons do not overlap in time. Then the time ordering is

$$t > t_4 > t_3 > t_2 > t_1 > -\infty.$$

This leads to the time integrations

$$\begin{aligned} & (-i)^4 \int_{-\infty}^t dt_4 e^{-it_4 d_4} \int_{-\infty}^{t_4} dt_3 e^{-it_3 d_3} \int_{-\infty}^{t_3} dt_2 e^{-it_2 d_2} \int_{-\infty}^{t_2} dt_1 e^{-it_1 d_1} \\ &= \frac{e^{-it d_{1234}}}{d_{1234} d_{123} d_{12} d_1}. \end{aligned} \tag{I.11}$$

Changing the order between  $t_1$  and  $t_2$  and between  $t_3$  and  $t_4$  leads to the denominators

$$\frac{1}{d_{1234}} \left( \frac{1}{d_{123}} + \frac{1}{d_{124}} \right) \frac{1}{d_{12}} \left( \frac{1}{d_1} + \frac{1}{d_2} \right). \tag{I.12}$$

Here, all integrations are being performed upwards, which implies that all denominators are evaluated from below.

If the interaction 1-2 is *instantaneous*, then the integrations become

$$\begin{aligned} & (-i)^3 \int_{-\infty}^t dt_4 e^{-it_4 d_4} \int_{-\infty}^{t_4} dt_3 e^{-it_3 d_3} \int_{-\infty}^{t_3} dt_{12} e^{-it_{12} d_{12}} \\ &= \frac{e^{-it d_{1234}}}{d_{1234} d_{123} d_{12}} \end{aligned} \tag{I.13}$$

and together with the other time ordering

$$\frac{e^{-it d_{1234}}}{d_{1234}} \left( \frac{1}{d_{123}} + \frac{1}{d_{124}} \right) \frac{1}{d_{12}}. \tag{I.14}$$

If both interactions are instantaneous, we have

$$(-i)^2 \int_{-\infty}^t dt_{34} e^{-it_{34}d_{34}} \int_{-\infty}^{t_{34}} dt_{12} e^{-it_{12}d_{12}} = \frac{e^{-it d_{1234}}}{d_{1234} d_{12}}, \tag{I.15}$$

consistent with the MBPT result [124, Sect. 12.2].

### Single Hole

Next, we consider the two-photon exchange with a single hole, represented by the second diagram above. We still assume that the diagram is reducible, implying that the two photons do not overlap in time. The time ordering is now

$$t > t_4 > t_3 > t_2 > -\infty \quad \text{and} \quad \infty > t_1 > t_4,$$

but the order between  $t_1$  and  $t$  is not given.

If this is considered as a *Goldstone diagram*, all times (including  $t_1$ ) are restricted to  $t_n < t$ , which leads to

$$\begin{aligned} & \int_t^{-\infty} dt_1 e^{-it_1 d_1} \int_{-\infty}^{t_1} dt_4 e^{-it_4 d_4} \int_{-\infty}^{t_4} dt_3 e^{-it_3 d_3} \int_{-\infty}^{t_3} dt_2 e^{-it_2 d_2} \\ &= - \frac{e^{-it d_{1234}}}{d_{1234} d_{234} d_{23} d_2}. \end{aligned} \tag{I.16}$$

Note that the last integration is being performed in the negative direction, due to the core hole. This is illustrated in Fig. I.2 (left).

Considered as a *Feynman diagram*, the time  $t_1$  can run to  $+\infty$ , which leads to

$$\begin{aligned} & \int_{\infty}^{t_4} dt_1 e^{-it_1 d_1} \int_{-\infty}^t dt_4 e^{-it_4 d_4} \int_{-\infty}^{t_4} dt_3 e^{-it_3 d_3} \int_{-\infty}^{t_3} dt_2 e^{-it_2 d_2} \\ &= \frac{e^{-it d_{1234}}}{d_{1234} d_1 d_{23} d_2}. \end{aligned} \tag{I.17}$$

Here, the last integration is still performed in the negative direction, this time from  $+\infty$  to  $t_4$ , and this leads to a result different from the previous one. In the Goldstone case all denominators are evaluated from below, while in the Feynman case one of them is evaluated from above (see Fig. I.2, right). For *diagrams diagonal in energy* we have  $d_{1234} = 0$ , and hence  $d_1 = -d_{234}$ , which implies that in this case the two results are identical.

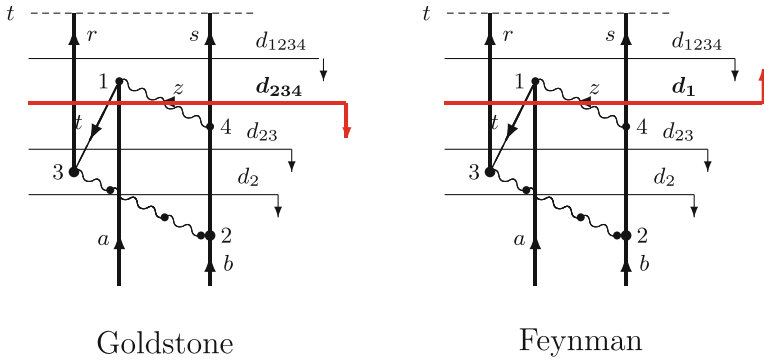


**Fig. I.2** Time-ordered Goldstone and Feynman diagrams, respectively, for two-photon exchange with one virtual pair. In the latter case one denominator (at vertex 1) is evaluated *from above*

Let us next consider the third diagram in Fig. I.1, where the time ordering is

$$t > t_4 > t_1 > t_3 > t_2 > -\infty.$$

Here, all times are limited from above in the Goldstone as well as the Feynman interpretation, and this leads in both cases to

$$\int_{-\infty}^t dt_4 e^{-it_4 d_4} \int_{t_4}^{-\infty} dt_1 e^{-it_1 d_1} \int_{-\infty}^{t_1} dt_3 e^{-it_3 d_3} \int_{-\infty}^{t_3} dt_2 e^{-it_2 d_2} = -\frac{e^{-it d_{1234}}}{d_{1234} d_{123} d_{23} d_2}. \tag{I.18}$$

### Double Holes

The last diagram in Fig. I.1, also reproduced in Fig. I.3, represents double virtual pair. Considered as a Goldstone diagram, the time ordering is

$$t > t_2 > t_1 > t_4 > t_3 > -\infty,$$

which yields

$$\int_{-\infty}^t dt_2 e^{-it_2 d_2} \int_{-\infty}^{t_2} dt_1 e^{-it_1 d_1} \int_{-\infty}^{t_1} dt_4 e^{-it_4 d_4} \int_{-\infty}^{t_4} dt_3 e^{-it_3 d_3} = \frac{e^{-it d_{1234}}}{d_{1234} d_{134} d_{34} d_3}. \tag{I.19}$$

This is illustrated in Fig. I.3 (left).

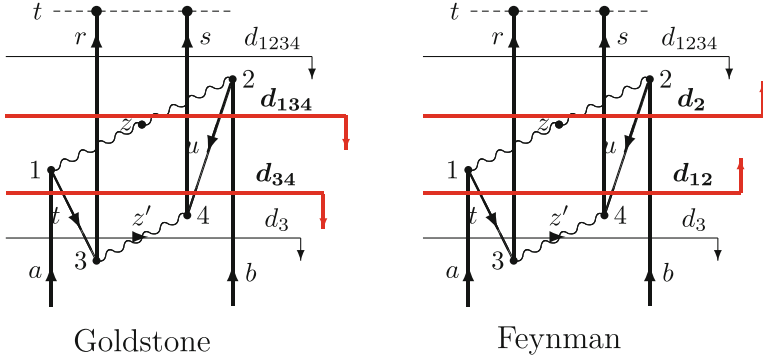


**Fig. I.3** Time-ordered Goldstone and Feynman diagrams, respectively, for two-photon exchange with two virtual pairs. In the latter case two denominators, (at vertices 1 and 2) is evaluated *from above*

Considered as a Feynman diagram, we have instead  $\infty > t_2 > t_1$ , which leads to

$$\begin{aligned}
 & \int_{-\infty}^t dt_4 e^{-it_4 d_4} \int_{-\infty}^{t_4} dt_3 e^{-it_3 d_3} \int_{\infty}^{t_4} dt_1 e^{-it_1 d_1} \int_{\infty}^{t_1} dt_2 e^{-it_2 d_2} \\
 &= \frac{e^{-it d_{1234}}}{d_{1234} d_3 d_{12} d_2}, \tag{I.20}
 \end{aligned}$$

where two integrations are performed in the negative direction.

### I.3 General Evaluation Rules

We can now formulate evaluation rules for the two types of diagrams considered here. For (non-relativistic) Goldstone diagrams the rules are equivalent to the standard **Goldstone rules** [124, Sect. 12.2]

- There is a matrix element for each interaction.
- For each vertex there is a denominator equal to the *vertex sum* (sum of vertex values: incoming minus outgoing orbital energies and  $z + i\gamma$  for crossing photon line (leading to  $-ck$  after integration) *below* a line immediately above the vertex).
- For particle/hole lines the integration is performed in the positive/negative direction.

For the relativistic **Feynman diagrams** the same rules hold, with the exception that

- for a vertex where time can run to  $+\infty$  the denominator should be *evaluated from above* with the denominator equal to the vertex sum *above* a line immediately below the vertex (with  $z - i\gamma$  for crossing photon line, leading to  $+ck$ ).



## Appendix J

### Some Integrals

#### J.1 Feynman Integrals

In this section we shall derive some integrals, which simplify many QED calculations considerably (see the books of Mandl and Shaw [143, Chap. 10] and Sakurai [206, Appendix E]), and we shall start by deriving some formulas due to Feynman.

We start with the identity

$$\frac{1}{ab} = \frac{1}{b-a} \int_a^b \frac{dt}{t^2}. \quad (\text{J.1})$$

With the substitution  $t = b + (a - b)x$  this becomes

$$\frac{1}{ab} = \int_0^1 \frac{dx}{[b + (a - b)x]^2} = \int_0^1 \frac{dx}{[a + (b - a)x]^2}. \quad (\text{J.2})$$

Differentiation with respect to  $a$ , yields

$$\frac{1}{a^2b} = 2 \int_0^1 \frac{x dx}{[b + (a - b)x]^3}. \quad (\text{J.3})$$

Similarly, we have

$$\begin{aligned} \frac{1}{abc} &= 2 \int_0^1 dx \int_0^x dy \frac{1}{[a + (b - a)x + (c - b)y]^3} \\ &= 2 \int_0^1 dx \int_0^{1-x} dy \frac{1}{[a + (b - a)x + (c - a)y]^3}. \end{aligned} \quad (\text{J.4})$$

Next we consider the integral

$$\int d^4k \frac{1}{(k^2 + s + i\eta)^3} = 4\pi \int |\mathbf{k}|^2 d|\mathbf{k}| \int_{-\infty}^{\infty} \frac{dk_0}{(k^2 + s + i\eta)^3}.$$

The second integral can be evaluated by starting with

$$\int_{-\infty}^{\infty} \frac{dk_0}{k_0^2 - |\mathbf{k}|^2 + s + i\eta} = \frac{i\pi}{\sqrt{|\mathbf{k}|^2 - s}},$$

evaluated by residue calculus, and differentiating twice with respect to  $s$ . The integral then becomes

$$\int d^4k \frac{1}{(k^2 + s + i\eta)^3} = \frac{3i\pi^2}{2} \int \frac{|\mathbf{k}|^2 d|\mathbf{k}|}{(|\mathbf{k}|^2 + s)^{5/2}} = \frac{i\pi^2}{2s}. \quad (\text{J.5})$$

The second integral can be evaluated from the identity

$$\frac{x^2}{(x^2 + s)^{5/2}} = \frac{1}{(x^2 + s)^{3/2}} - \frac{s}{(x^2 + s)^{5/2}}$$

and differentiating the integral

$$\int \frac{dx}{\sqrt{x^2 + s}} = \ln(x + \sqrt{x^2 + s}),$$

yielding

$$\int \frac{x^2}{(x^2 + s)^{5/2}} = \frac{1}{3s}.$$

For symmetry reason we find

$$\int d^4k \frac{k^\mu}{(k^2 + s + i\eta)^3} = 0. \quad (\text{J.6})$$

Differentiating this relation with respect to  $k_\nu$ , leads to

$$\int d^4k \frac{k^\mu k^\nu}{(k^2 + s + i\eta)^4} = \frac{g^{\mu\nu}}{3} \int d^4k \frac{1}{(k^2 + s + i\eta)^3} = \frac{i\pi^2 g^{\mu\nu}}{6s}, \quad (\text{J.7})$$

using the relations (A.4) and (J.5).

By making the replacements

$$k \Rightarrow k + q \quad \text{and} \quad s \Rightarrow s - q^2,$$

the integrals (J.5) and (J.6) lead to

$$\int d^4k \frac{1}{(k^2 + 2kq + s + i\eta)^3} = \frac{i\pi^2}{2(s - q^2)} \quad (\text{J.8})$$

and

$$\int d^4k \frac{k^\mu}{(k^2 + 2kq + s + i\eta)^3} = - \int d^4k \frac{q^\mu}{(k^2 + 2kq + s + i\eta)^3} = - \frac{i\pi^2 q^\mu}{2(s - q^2)}, \quad (\text{J.9})$$

respectively, Differentiating the last relation with respect to  $q_\nu$ , leads to

$$\int d^4k \frac{k^\mu k^\nu}{(k^2 + 2kq + s + i\eta)^4} = \frac{i\pi^2}{12} \left[ \frac{g^{\mu\nu}}{s - q^2} + \frac{q^\mu q^\nu}{(s - q^2)^2} \right] \quad (\text{J.10})$$

Differentiating the relation (J.8) with respect to  $s$ , yields

$$\int d^4k \frac{1}{(k^2 + 2kq + s + i\eta)^4} = \frac{i\pi^2}{6(s - q^2)^2}, \quad (\text{J.11})$$

which can be generalized to arbitrary integer powers  $\geq 3$

$$\int d^4k \frac{1}{(k^2 + 2kq + s + i\eta)^n} = i\pi^2 \frac{(n-3)!}{(n-1)!} \frac{1}{(s - q^2)^{n-2}}. \quad (\text{J.12})$$

This can also be extended to **non-integral powers**

$$\int d^4k \frac{1}{(k^2 + 2kq + s + i\eta)^n} = i\pi^2 \frac{\Gamma(n-2)}{\Gamma(n)} \frac{1}{(s - q^2)^{n-2}} \quad (\text{J.13})$$

and similarly

$$\int d^4k \frac{k^\mu}{(k^2 + 2kq + s + i\eta)^n} = -i\pi^2 \frac{\Gamma(n-2)}{\Gamma(n)} \frac{q^\mu}{(s - q^2)^{n-2}} \quad (\text{J.14})$$

$$\int d^4k \frac{k^\mu k^\nu}{(k^2 + 2kq + s + i\eta)^n} = i\pi^2 \frac{\Gamma(n-3)}{2\Gamma(n)} \left[ \frac{(2n-3)q^\mu q^\nu}{(s - q^2)^{n-2}} + \frac{g^{\mu\nu}}{(s - q^2)^{n-3}} \right]. \quad (\text{J.15})$$

## J.2 Evaluation of the Integral $\int \frac{d^3\mathbf{k}}{(2\pi)^3} \frac{e^{i\mathbf{k}\cdot\mathbf{r}_{12}}}{q^2 - \mathbf{k}^2 + i\eta}$

Using spherical coordinates  $\mathbf{k} = (\eta, \theta, \phi)$ , ( $\eta = |\mathbf{k}|$ ), we have with  $d^3\mathbf{k} = \eta^2 d\eta \sin\Theta d\Theta d\Phi$  and  $r_{12} = |\mathbf{x}_1 - \mathbf{x}_2|$

$$\begin{aligned} \int \frac{d^3\mathbf{k}}{(2\pi)^3} \frac{e^{i\mathbf{k}\cdot(\mathbf{x}_1 - \mathbf{x}_2)}}{q^2 - \mathbf{k}^2 + i\eta} &= (2\pi)^{-2} \int_0^\infty \frac{\eta^2 d\eta}{q^2 - \kappa^2 + i\eta} \int_0^\pi d\Theta \sin\Theta e^{i\kappa r_{12} \cos\Theta} \\ &= -\frac{i}{4\pi^2 r_{12}} \int_0^\infty \frac{\kappa d\kappa (e^{i\kappa r_{12}} - e^{-i\kappa r_{12}})}{q^2 - \kappa^2 + i\eta} \\ &= -\frac{i}{8\pi^2 r_{12}} \int_{-\infty}^\infty \frac{\kappa d\kappa (e^{i\kappa r_{12}} - e^{-i\kappa r_{12}})}{q^2 - \kappa^2 + i\eta}, \end{aligned} \quad (\text{J.16})$$

where we have in the last step utilized the fact that the integrand is an *even* function of  $\kappa$ . The poles appear at  $\kappa = \pm q(1 + i\eta/2q)$ .  $e^{i\kappa r_{12}}$  is integrated over the *positive* and  $e^{-i\kappa r_{12}}$  over the *negative* half-plane, which yields  $-e^{\pm iqr_{12}}/(4\pi r_{12})$  with the upper sign for  $q > 0$ . The same result is obtained if we change the sign of the exponent in the numerator of the original integrand. Thus, we have the result

$$\boxed{\int \frac{d^3\mathbf{k}}{(2\pi)^3} \frac{e^{\pm i\mathbf{k}\cdot(\mathbf{x}_1 - \mathbf{x}_2)}}{q^2 - \mathbf{k}^2 + i\eta} = \frac{1}{4\pi^2 r_{12}} \int_0^\infty \frac{2\kappa d\kappa \sin(\kappa r_{12})}{q^2 - \kappa^2 + i\eta} = -\frac{e^{i|q|r_{12}}}{4\pi r_{12}}.} \quad (\text{J.17})$$

The imaginary part of the integrand, which is an *odd* function, does not contribute to the integral.

## J.3 Evaluation of the Integral $\int \frac{d^3\mathbf{k}}{(2\pi)^3} (\alpha_1 \cdot \hat{\mathbf{k}})(\alpha_2 \cdot \hat{\mathbf{k}}) \frac{e^{i\mathbf{k}\cdot\mathbf{r}_{12}}}{q^2 - \mathbf{k}^2 + i\eta}$

The integral appearing in the derivation of the Breit interaction (F.53) is

$$\begin{aligned} I_2 &= \int \frac{d^3\mathbf{k}}{(2\pi)^3} (\alpha_1 \cdot \mathbf{k})(\alpha_2 \cdot \mathbf{k}) \frac{e^{i\mathbf{k}\cdot\mathbf{r}_{12}}}{q^2 - \mathbf{k}^2 + i\eta} \\ &= -(\alpha_1 \cdot \nabla_1)(\alpha_2 \cdot \nabla_2) \int \frac{d^3\mathbf{k}}{(2\pi)^3} \frac{e^{i\mathbf{k}\cdot\mathbf{r}_{12}}}{\mathbf{k}^2(q^2 - \mathbf{k}^2 + i\eta)}. \end{aligned} \quad (\text{J.18})$$

Using (J.16), we then have

$$\begin{aligned} I_2 &= -\frac{i}{8\pi^2 r_{12}} (\alpha_1 \cdot \nabla_1)(\alpha_2 \cdot \nabla_2) \int_{-\infty}^\infty \frac{d\kappa (e^{i\kappa r_{12}} - e^{-i\kappa r_{12}})}{(q^2 - \kappa^2 + i\eta)} \\ &= \frac{1}{4\pi^2 r_{12}} (\alpha_1 \cdot \nabla_1)(\alpha_2 \cdot \nabla_2) \int_0^\infty \frac{2\kappa d\kappa \sin(\kappa r_{12})}{\kappa^2(q^2 - \kappa^2 + i\eta)}. \end{aligned} \quad (\text{J.19})$$

The poles appear at  $\kappa = 0$  and  $\kappa = \pm(q + i\eta/2q)$ . The pole at  $\kappa = 0$  can be treated with half the pole value in each half plane. For  $q > 0$  the result becomes

$$-\frac{1}{4\pi r_{12}} \frac{e^{iqr_{12}-1}}{q^2}$$

and for  $q > 0$  the same result with  $-q$  in the exponent. The final result then becomes

$$\begin{aligned} & \int \frac{d^3\mathbf{k}}{(2\pi)^3} (\boldsymbol{\alpha}_1 \cdot \mathbf{k})(\boldsymbol{\alpha}_2 \cdot \mathbf{k}) \frac{e^{i\mathbf{k}\cdot\mathbf{r}_{12}}}{q^2 - \mathbf{k}^2 + i\eta} \\ &= -\frac{1}{4\pi r_{12}} (\boldsymbol{\alpha}_1 \cdot \nabla_1)(\boldsymbol{\alpha}_2 \cdot \nabla_2) \frac{e^{i|q|r_{12}-1}}{q^2} \\ &= \frac{1}{4\pi^2 r_{12}} (\boldsymbol{\alpha}_1 \cdot \nabla_1)(\boldsymbol{\alpha}_2 \cdot \nabla_2) \int_0^\infty \frac{2\kappa d\kappa \sin(\kappa r_{12})}{\kappa^2(q^2 - \kappa^2 + i\eta)}. \end{aligned} \quad (\text{J.20})$$

Assuming that our basis functions are eigenfunctions of the Dirac hamiltonian  $\hat{h}_D$ , we can process this integral further. Then the commutator with an arbitrary function of the space coordinates is

$$[\hat{h}_D, f(\mathbf{x})] = c \boldsymbol{\alpha} \cdot \hat{\mathbf{p}} f(\mathbf{x}) + [U, f(\mathbf{x})]. \quad (\text{J.21})$$

The last term vanishes, if the potential  $U$  is a **local function**, yielding

$$[\hat{h}_D, f(\mathbf{x})] = c \boldsymbol{\alpha} \cdot \hat{\mathbf{p}} f(\mathbf{x}) = -ic \boldsymbol{\alpha} \cdot \nabla f(\mathbf{x}). \quad (\text{J.22})$$

In particular

$$[\hat{h}_D, e^{i\mathbf{k}\cdot\mathbf{x}}] = -ic \boldsymbol{\alpha} \cdot \nabla e^{i\mathbf{k}\cdot\mathbf{x}} = c \boldsymbol{\alpha} \cdot \hat{\mathbf{k}} e^{i\mathbf{k}\cdot\mathbf{x}}. \quad (\text{J.23})$$

We then find that

$$(\boldsymbol{\alpha} \cdot \nabla)_1 (\boldsymbol{\alpha} \cdot \nabla)_2 e^{i\mathbf{k}\cdot\mathbf{x}} = \frac{1}{c^2} [h_D, e^{i\mathbf{k}\cdot\mathbf{x}}]_1 [h_D, e^{i\mathbf{k}\cdot\mathbf{x}}]_2 \quad (\text{J.24})$$

with the matrix element

$$\langle rs | (\boldsymbol{\alpha} \cdot \nabla)_1 (\boldsymbol{\alpha} \cdot \nabla)_2 e^{i\mathbf{k}\cdot\mathbf{x}} | ab \rangle = q^2 e^{i\mathbf{k}\cdot\mathbf{x}}, \quad (\text{J.25})$$

using the notation in (F.49). The integral (J.18) then becomes

$$I_2 = \int \frac{d^3\mathbf{k}}{(2\pi)^3} (\boldsymbol{\alpha}_1 \cdot \hat{\mathbf{k}})(\boldsymbol{\alpha}_2 \cdot \hat{\mathbf{k}}) \frac{e^{i\mathbf{k}\cdot\mathbf{r}_{12}}}{q^2 - \mathbf{k}^2 + i\eta} = \int \frac{d^3\mathbf{k}}{(2\pi)^3} \frac{q^2}{\mathbf{k}^2} \frac{e^{i\mathbf{k}\cdot\mathbf{r}_{12}}}{q^2 - \mathbf{k}^2 + i\eta}, \quad (\text{J.26})$$

provided that the orbitals are generated by a hamiltonian with a **local potential**.

# Appendix K

## Unit Systems and Dimensional Analysis

### K.1 Unit Systems

#### *SI System*

The standard unit system internationally agreed upon is the SI system or *System Internationale*.<sup>12</sup> The basis units in this system are given in the following table

Quantity	SI unit	Symbol
Length	Meter	m
Mass	Kilogram	kg
time	second	s
electric current	ampere	A
thermodynamic temperature	kelvin	K
amount of substance	mole	mol
luminous intensity	candela	cd

For the definition of these units the reader is referred to the NIST WEB page (see footnote). From the basis units—particularly the first four—the units for most other physical quantities can be derived.

---

<sup>12</sup>For further details, see *The NIST Reference on Constants, Units, and Uncertainty* (<http://physics.nist.gov/cuu/Units/index.html>).

### ***Relativistic or “Natural” Unit System***

In scientific literature some simplified unit system is frequently used for convenience. In relativistic field theory the *relativistic unit system* is mostly used, where the first four units of the SI system are replaced by

Quantity	Relativistic unit	Symbol	Dimension
mass	rest mass of the electron	$m$	kg
velocity	light velocity in vacuum	$c$	$\text{ms}^{-1}$
action	Planck's constant divided by $2\pi$	$\hbar$	$\text{kg m}^2\text{s}^{-1}$
dielectricity	dielectricity constant of vacuum	$\epsilon_0$	$\text{A}^2\text{s}^4 \text{kg}^{-1}\text{m}^{-3}$

In the table also the dimension of the relativistic units in SI units are shown. From these four units all units that depend only on the four SI units kg, s, m, A can be derived. For instance, *energy* that has the dimension  $\text{kg m}^{-2}\text{m}^{-2}$  has the relativistic unit  $m_e c^2$ , which is the rest energy of the electron ( $\approx 511 \text{ keV}$ ). The unit for *length* is

$$\frac{\hbar}{m_e c} = \lambda/2\pi \approx 0,386 \times 10^{-12} \text{ m},$$

where  $\lambda$  is *Compton wavelength* and the unit for *time* is  $2\pi c/\lambda \approx 7,77 \times 10^{-4} \text{ s}$ .

### ***Hartree Atomic Unit System***

In atomic physics the *Hartree atomic unit system* is frequently used, based on the following four units

Quantity	Atomic unit	Symbol	Dimension
mass	rest mass of the electron	$m$	kg
electric charge	absolute charge of the electron	$e$	As
action	Planck's constant divided by $2\pi$	$\hbar$	$\text{kg m}^2\text{s}^{-1}$
dielectricity	dielectricity constant of vacuum times $4\pi$	$4\pi\epsilon_0$	$\text{A}^2\text{s}^4 \text{kg}^{-1}\text{m}^{-3}$

Here, the unit for *energy* becomes

$$1H = \frac{me^4}{(4\pi\epsilon_0)^2\hbar^3},$$

which is known as the *Hartree unit* and equals twice the ionization energy of the hydrogen atom in its ground state ( $\approx 27.2$  eV). The atomic unit for *length* is

$$a_0 = \frac{4\pi\epsilon_0\hbar^2}{me^2},$$

known as the *Bohr radius* or the radius of the first electron orbit of the Bohr hydrogen model ( $\approx 0,529 \times 10^{-10}$  m). The atomic unit of *velocity* is  $\alpha c$ , where

$$\alpha = \frac{e^2}{4\pi\epsilon_0 c \hbar} \quad (\text{K.1})$$

is the dimensionless *fine-structure constant* ( $\approx 1/137,036$ ). Many units in these two systems are related by the fine-structure constant. For instance, the relativistic length unit is  $\alpha a_0$ .

### ***cgs Unit Systems***

In older scientific literature a unit system, known as the cgs system, was frequently used. This is based on the following *three* units

Quantity	cgs unit	Symbol
length	centimeter	cm
mass	gram	g
time	second	s

In addition to the three units, it is necessary to define a fourth unit in order to be able to derive most of the physical units. Here, two conventions are used. In the *electrostatic version* (ecgs) the proportionality constant of Coulombs law,  $4\pi\epsilon_0$ , is set equal to unity, and in the *magnetic version* (mcgs) the corresponding magnetic constant,  $\mu_0/4\pi$ , equals unity. Since these constants have dimension, the systems cannot be used for dimensional analysis (see below).

The most frequently used unit system of cgs type is the so-called *Gaussian unit system*, where electric units are measured in ecgs and magnetic ones in mcgs. This implies that certain formulas will look differently in this system, compared to a system with consistent units. For instance, the *Bohr magneton*, which in any consistent unit system will have the expression

$$\mu_B = \frac{e\hbar}{2m}$$



will in the mixed Gaussian system have the expression

$$\mu_B = \frac{e\hbar}{2mc},$$

which does not have the correct dimension. Obviously, such a unit system can easily lead to misunderstandings and should be avoided.

## K.2 Dimensional Analysis

It is often useful to check physical formulas by means of dimensional analysis, which, of course, requires that a consistent unit system, like the SI system, is being used. Below we list a number of physical quantities and their dimension, expressed in SI units, which could be helpful in performing such an analysis.

In most parts of the book we have set  $\hbar = 1$ , which simplifies the formulas. This also simplifies the dimensional analysis, and in the last column below we have (after the sign  $\Rightarrow$ ) listed the dimensions in that case.

$$[\text{force}] = \text{N} = \frac{\text{kg m}}{\text{s}^2} \Rightarrow \frac{1}{\text{ms}}$$

$$[\text{energy}] = \text{J} = \text{Nm} = \frac{\text{kg m}^2}{\text{s}^2} \Rightarrow \frac{1}{\text{s}}$$

$$[\text{action}, \hbar] = \text{Js} = \frac{\text{kg m}^2}{\text{s}} \Rightarrow 1$$

$$[\text{electric potential}] = \text{V} = \frac{\text{J}}{\text{As}} = \frac{\text{kg m}^2}{\text{As}^3} \Rightarrow \frac{1}{\text{As}^2}$$

$$[\text{electric field}, \mathbf{E}] = \text{V/m} = \frac{\text{kg m}}{\text{As}^3} \Rightarrow \frac{1}{\text{Ams}^2}$$

$$[\text{magnetic field}, \mathbf{B}] = \text{Vs/m}^2 = \frac{\text{kg}}{\text{As}^2} \Rightarrow \frac{1}{\text{Am}^2\text{s}}$$

$$[\text{vector potential}, \mathbf{A}] = \text{Vs/m} = \frac{\text{kg m}}{\text{As}^2} \Rightarrow \frac{1}{\text{Ams}}$$

$$[\text{momentum}, p] = \frac{\text{kg m}}{\text{s}} \Rightarrow \frac{1}{\text{m}}$$

$$[\text{charge density}, \rho] = \frac{\text{As}}{\text{m}^3}$$

$$[\text{current density}, \mathbf{j}] = \frac{\text{A}}{\text{m}^2}$$

$$[\mu_0] = \text{N}/\text{A}^2 = \frac{\text{kg m}}{\text{A}^2 \text{s}^2} \Rightarrow \frac{1}{\text{A}^2 \text{ms}}$$

$$[\epsilon_0] = [1/\mu_0 c^2] = \frac{\text{A}^2 \text{s}^4}{\text{kg m}^3} \Rightarrow \frac{\text{A}^2 \text{s}^3}{\text{m}}$$

### Fourier Transforms

$$D_{F\nu\mu}(x_1, x_2) = \int \frac{dz}{2\pi} D_{F\nu\mu}(z; \mathbf{x}_1, \mathbf{x}_2) e^{-iz(t_2 - t_1)}$$

$$[A(\omega, \mathbf{x})] = \text{s}[A(x)]$$

$$[A(\omega, \mathbf{k})] = \text{sm}^3[A(x)]$$

$$[A(k)] = \text{m}^4[A(x)]$$

### Photon Propagator

$$[D_{F\nu\mu}(x, x)] \Rightarrow \frac{1}{\text{A}^2 \text{m}^2 \text{s}^2}$$

$$[\epsilon_0 D_{F\nu\mu}(x, x)] \Rightarrow \frac{\text{s}}{\text{m}^3}$$

$$[\epsilon_0 D_{F\nu\mu}(k)] \Rightarrow \text{sm}$$

$$[\epsilon_0 D_{F\nu\mu}(k_0, \mathbf{x})] \Rightarrow \frac{\text{s}}{\text{m}^2}$$

$$[\epsilon_0 D_{F\nu\mu}(t, \mathbf{x})] \Rightarrow \frac{1}{\text{m}^2}$$

$$[\epsilon_0 D_{F\nu\mu}(z, \mathbf{x})] \Rightarrow \frac{\text{s}^2}{\text{m}^3} \quad z = ck_0$$

$$[\epsilon_0 D_{F\nu\mu}(z, \mathbf{k})] \Rightarrow \text{s}^2$$

$$[e^2 c^2 D_{F\nu\mu}(z, \mathbf{x}) = I(z, \mathbf{x})] \Rightarrow \frac{1}{\text{s}}$$

$$\left[ \frac{e^2}{\epsilon_0} \right] \Rightarrow \frac{\text{m}}{\text{s}}$$

***Electron Propagator***

$$S_F(x, x) \Rightarrow \frac{1}{\text{m}^3}$$

$$S_F(z, \mathbf{x}) \Rightarrow \frac{\text{s}}{\text{m}^3}$$

$$S_F(z, \mathbf{k}) \Rightarrow \text{s}$$

$$S_F(k) = cS_F(z, \mathbf{k}) \Rightarrow \text{m}$$

***S-Matrix***

$$S(x, x) \Rightarrow 1$$

$$S(z, \mathbf{x}) \Rightarrow \text{s}$$

$$S(z, \mathbf{k}) \Rightarrow \text{m}^4$$

***Self-Energy***

$$\Sigma(z) \Rightarrow \frac{1}{\text{s}}$$

$$\Sigma(z, \mathbf{x}) \Rightarrow \frac{1}{\text{sm}^3}$$

$$\Sigma(z, \mathbf{k}) \Rightarrow \frac{1}{\text{s}}$$

$$\Sigma(k) \Rightarrow \frac{\text{m}}{\text{s}^2}$$

***Vertex***

$$\Lambda(z, \mathbf{k}) \Rightarrow 1$$

$$\Lambda(p, p') \Rightarrow \frac{\text{m}}{\text{s}}$$

# References

1. Adkins, G.: One-loop renormalization of Coulomb-gauge QED. *Phys. Rev. D* **27**, 1814–1820 (1983)
2. Adkins, G.: One-loop vertex function in Coulomb-gauge QED. *Phys. Rev. D* **34**, 2489–2492 (1986)
3. Adkins, G.S., Fell, R.N.: Bound-state formalism for positronium. *Phys. Rev. A* **60**, 4461–4475 (1999)
4. Adkins, G.S., Fell, R.N., Mitrikov, P.M.: Calculation of the positronium hyperfine interval using the Bethe-Salpeter formalism. *Phys. Rev. A* **65**, 042103 (2002)
5. Araki, H.: Quantum-electrodynamical corrections to energy-levels of helium. *Prog. Theor. Phys. (Jpn.)* **17**, 619–642 (1957)
6. Artemyev, A.N., Beier, T., Plunien, G., Shabaev, V.M., Soff, G., Yerokhin, V.A.: Vacuum-polarization screening corrections to the energy levels of heliumlike ions. *Phys. Rev. A* **62**(1–8), 022116 (2000)
7. Artemyev, A.N., Holmberg, J., Surzhykov, A.: Radiative recombination of bare uranium; QED-corrections to the cross section and polarization. *Phys. Rev. A* **92**, 042510 (2015)
8. Artemyev, A.N., Shabaev, V.M., Yerokhin, V.A.: Vacuum polarization screening correction to the ground-state energy of two-electron ions. *Phys. Rev. A* **56**, 3529–3554 (1997)
9. Artemyev, A.N., Shabaev, V.M., Yerokhin, V.A., Plunien, G., Soff, G.: QED calculations of the  $n = 1$  and  $n = 2$  energy levels in He-like ions. *Phys. Rev. A* **71**, 062104 (2005)
10. Åsén, B.: QED effects in excited states of helium-like ions. Ph.D. thesis, Department of Physics, Chalmers University of Technology and University of Gothenburg, Gothenburg, Sweden (2002)
11. Åsén, B., Salomonson, S., Lindgren, I.: Two-photon exchange QED effects in the  $1s2s\ ^1S$  and  $^3S$  states of heliumlike ions. *Phys. Rev. A* **65**, 032516 (2002)
12. Avgoustoglou, E.N., Beck, D.R.: All-order relativistic many-body calculations for the electron affinities of  $\text{Ca}^-$ ,  $\text{Sr}^-$ ,  $\text{Ba}^-$ , and  $\text{Yb}^-$  negative ions. *Phys. Rev. A* **55**, 4143–4149 (1997)
13. Barbieri, R., Sucher, J.: General theory of radiative corrections to atomic decay rates. *Nucl. Phys. B* **134**, 155–168 (1978)
14. Bartlett, R.J.: Coupled-cluster approach to molecular structure and spectra: a step toward predictive quantum chemistry. *J. Phys. Chem.* **93**, 1697–1708 (1989)
15. Bartlett, R.J., Purvis, G.D.: Many-body perturbation theory, coupled-pair many-electron theory, and the importance of quadruple excitations for the correlation problem. *Int. J. Quantum Chem.* **14**, 561–581 (1978)
16. Beier, T., Djekic, S., Häffner, H., Indelicato, P., Kluge, H.J., Quint, W., Shabaev, V.S., Verdu, J., Valenzuela, T., Werth, G., Yerokhin, V.A.: Determination of electron's mass from g-factor experiments on  $^{12}\text{C}^{+5}$  and  $^{16}\text{O}^{+7}$ . *Nucl. Instrum. Methods* **205**, 35 (2003)

17. Beier, T., Häffner, H., Hermanspahn, N., Karshenboim, S.G., Kluge, H.J.: New determination of the electron's mass. *Phys. Rev. Lett.* **88**, 011603-1–011603-4 (2002)
18. Beier, T., Lindgren, I., Persson, H., Salomonson, S., Sunnergren, P., Häffner, H., Hermanspahn, N.:  $g_j$  factor of an electron bound in a hydrogenlike ion. *Phys. Rev. A* **62**, 032510 (2000)
19. Bethe, H.A.: The electromagnetic shift of energy levels. *Phys. Rev.* **72**, 339–341 (1947)
20. Bethe, H.A., Salpeter, E.E.: *An Introduction to Relativistic Quantum Field Theory. Quantum Mechanics of Two-Electron Atoms.* Springer, Berlin (1957)
21. Bjorken, J.D., Drell, S.D.: *Relativistic Quantum Fields.* Mc-Graw-Hill Publishing Co., New York (1964)
22. Bjorken, J.D., Drell, S.D.: *Relativistic Quantum Mechanics.* Mc-Graw-Hill Publishing Co., New York (1964)
23. Blanchard, P., Brüning, E.: *Variational Methods in Mathematical Physics. A Unified Approach.* Springer, Berlin (1992)
24. Bloch, C.: Sur la détermination de l'état fondamental d'un système de particules. *Nucl. Phys.* **7**, 451–58 (1958)
25. Bloch, C.: Sur la théorie des perturbations des états liés. *Nucl. Phys.* **6**, 329–47 (1958)
26. Blundell, S.: Calculations of the screened self-energy and vacuum polarization in Li-like, Na-like, and Cu-like ions. *Phys. Rev. A* **47**, 1790–1803 (1993)
27. Blundell, S., Mohr, P.J., Johnson, W.R., Sapirstein, J.: Evaluation of two-photon exchange graphs for highly charged heliumlike ions. *Phys. Rev. A* **48**, 2615–2626 (1993)
28. Blundell, S., Snyderman, N.J.: Basis-set approach to calculating the radiative self-energy in highly ionized atoms. *Phys. Rev. A* **44**, R1427–R1430 (1991)
29. Blundell, S.A.: Accurate screened QED calculations in high-Z many-electron ions. *Phys. Rev. A* **46**, 3762–3775 (1992)
30. Blundell, S.A., Cheng, K.T., Sapirstein, J.: Radiative corrections in atomic physics in the presence of perturbing potentials. *Phys. Rev. A* **55**, 1857–1865 (1997)
31. Blundell, S.A., Johnson, W.R., Liu, Z.W., Sapirstein, J.: Relativistic all-order calculations of energies and matrix elements for Li and  $\text{Be}^+$ . *Phys. Rev. A* **40**, 2233–2246 (1989)
32. Boldwin, G.T., Yennie, D.R., Gregorio, M.A.: Recoil effects in the hyperfine structure of QED bound states. *Rev. Mod. Phys.* **57**, 723–782 (1985)
33. Borbely, J.S., George, M.C., Lombardi, L.D., Weel, M., Fitzakerley, D.W., Hessel, E.A.: Separated oscillatory-field microwave measurement of the  $2^3P_1 - 2^3P_2$  fine structure interval of atomic helium. *Phys. Rev. A* **79**, 60503 (2009)
34. Brandow, B.H.: Linked-cluster expansions for the nuclear many-body problem. *Rev. Mod. Phys.* **39**, 771–828 (1967)
35. Breit, G.: Dirac's equation and the spin-spin interaction of two electrons. *Phys. Rev.* **39**, 616–624 (1932)
36. Brown, G.E., Kuo, T.T.S.: Structure of finite nuclei and the nucleon-nucleon interaction. *Nucl. Phys. A* **92**, 481–494 (1967)
37. Brown, G.E., Langer, J.S., Schaeffer, G.W.: Lamb shift of a tightly bound electron. I. *Method. Proc. R. Soc. Lond. Ser. A* **251**, 92–104 (1959)
38. Brown, G.E., Mayers, D.F.: Lamb shift of a tightly bound electron. II. Calculation for the K-electron in Hg. *Proc. R. Soc. Lond. Ser. A* **251**, 105–109 (1959)
39. Brown, G.E., Ravenhall, D.G.: On the interaction of two electrons. *Proc. R. Soc. Lond. Ser. A* **208**, 552–559 (1951)
40. Brueckner, K.A.: Many-body problems for strongly interacting particles. II. Linked cluster expansion. *Phys. Rev.* **100**, 36–45 (1955)
41. Bukowski, R., Jeziorski, B., Szalewicz, K.: Gaussian geminals in explicitly correlated coupled cluster theory including single and double excitations. *J. Chem. Phys.* **110**, 4165–4183 (1999)
42. Caswell, W.E., Lepage, G.P.: Reduction of the Bethe-Salpeter equation to an equivalent Schrödinger equation, with applications. *Phys. Rev. A* **18**, 810–819 (1978)
43. Chantler, C.T.: Testing three-body quantum-electrodynamics with trapped  $\text{T}^{20+}$  Ions: evidence for a Z-dependent divergence between experimental and calculation. *Phys. Rev. Lett.* **109**, 153001 (2012)

44. Chantler, C.T., et al.: New X-ray measurements in Helium-like Atoms increase discrepancy between experiment and theoretical QED. arXiv-ph, p. 0988193 (2012)
45. Cheng, K.T., Johnson, W.R.: Self-energy corrections to the K-electron binding energy in heavy and superheavy atoms. *Phys. Rev. A* **1**, 1943–1948 (1976)
46. Cheng, T.K., Johnson, W.R., Sapirstein, J.: Screened lamb-shift calculations for lithiumlike uranium, sodiumlike platinum, and copperlike gold. *Phys. Rev. Lett.* **23**, 2960–2963 (1991)
47. Čížek, J.: On the correlation problem in atomic and molecular systems. Calculations of wavefunction components in the Ursell-type expansion using quantum-field theoretical methods. *J. Chem. Phys.* **45**, 4256–4266 (1966)
48. Clarke, J.J., van Wijngaaren, W.A.: Hyperfine and fine-structure measurements of  ${}^6,7\text{Li}^+$   $1s2s^3S$  and  $1s2p^3P$  states. *Phys. Rev. A* **67**, 12506 (2003)
49. Connell, J.H.: QED test of a Bethe-Salpeter solution method. *Phys. Rev. D* **43**, 1393–1402 (1991)
50. Coster, F.: Bound states of a many-particle system. *Nucl. Phys.* **7**, 421–424 (1958)
51. Coster, F., Kümmel, H.: Short-range correlations in nuclear wave functions. *Nucl. Phys.* **17**, 477–85 (1960)
52. Curdt, W., Landi, E., Wilhelm, K., Feldman, U.: Wavelength measurements of heliumlike  $1s2s^3S_1 - 1s2p^2P_{0,2}$  transitions in  $\text{Ne}^{8+}$ ,  $\text{Na}^{9+}$ ,  $\text{Mg}^{10+}$ , and  $\text{Si}^{12+}$  emitted by solar flare plasmas. *Phys. Rev. A* **62**, 022502-1–022502-7 (2000)
53. Cutkosky, R.E.: Solutions of the Bethe-Salpeter equation. *Phys. Rev.* **96**, 1135–41 (1954)
54. Debnath, L., Mikusiński, P.: Introduction to Hilbert Spaces with Applications, 2nd edn. Academic Press, New York (1999)
55. Delves, L.M., Welsh, J.: Numerical Solution of Integral Equations. Clarendon Press, Oxford (1974)
56. Desiderio, A.M., Johnson, W.R.: Lamb shift and binding energies of K electrons in heavy atoms. *Phys. Rev. A* **3**, 1267–1275 (1971)
57. DeVore, T.R., Crosby, D.N., Myers, E.G.: Improved Measurement of the  $1s2s^1S_0 - 1s2p^3P_1$  Interval in Heliumlike Silicon. *Phys. Rev. Lett.* **100**, 243001 (2008)
58. Dirac, P.A.M.: *Roy. Soc. (Lond.)* **117**, 610 (1928)
59. Dirac, P.A.M.: *The Principles of Quantum Mechanics*. Oxford University Press, Oxford (1930, 1933, 1947, 1958)
60. Douglas, M.H., Kroll, N.M.: Quantum electrodynamic corrections to the fine structure of helium. *Ann. Phys. (N.Y.)* **82**, 89–155 (1974)
61. Drake, G.W.F.: Theoretical energies for the  $n = 1$  and  $2$  states of the helium isoelectronic sequence up to  $Z = 100$ . *Can. J. Phys.* **66**, 586–611 (1988)
62. Durand, P., Malrieu, J.P.: Multiconfiguration Dirac-Fock studies of two-electron ions: II. Radiative corrections and comparison with experiment. *Adv. Chem. Phys.* **67**, 321 (1987)
63. Dyson, F.J.: The radiation theories of Tomonaga, Schwinger, and Feynman. *Phys. Rev.* **75**, 486–502 (1949)
64. Dyson, F.J.: The wave function of a relativistic system. *Phys. Rev.* **91**, 1543–1550 (1953)
65. Eliav, E., Kaldor, U., Ishikawa, Y.: Ionization potentials and excitation energies of the alkali-metal atoms by the relativistic coupled-cluster method. *Phys. Rev. A* **50**, 1121–28 (1994)
66. Lindroth, E., Mårtensson-Pendrill, A.M.: Isotope shifts and energies of the  $1s2p$  states in helium. *Z. Phys. A* **316**, 265–273 (1984)
67. Fetter, A.L., Walecka, J.D.: *The Quantum Mechanics of Many-Body Systems*. McGraw-Hill, New York (1971)
68. Feynman, R.P.: Space-time approach to quantum electrodynamics. *Phys. Rev.* **76**, 769–788 (1949)
69. Feynman, R.P.: The theory of positrons. *Phys. Rev.* **76**, 749–759 (1949)
70. Fried, H.M., Yennie, D.M.: New techniques in the Lamb shift calculation. *Phys. Rev.* **112**, 1391–1404 (1958)
71. Froese-Fischer, C.: *The Hartree-Fock Method for Atoms*. Wiley, New York (1977)
72. Garpmann, S., Lindgren, I., Lindgren, J., Morrison, J.: Calculation of the hyperfine interaction using an effective-operator form of many-body theory. *Phys. Rev. A* **11**, 758–81 (1975)

73. Gaunt, J.A.: The triplets of helium. *Proc. R. Soc. Lond. Ser. A* **122**, 513–532 (1929)
74. Gell-Mann, M., Low, F.: Bound states in quantum field theory. *Phys. Rev.* **84**, 350–354 (1951)
75. George, M.C., Lombardi, L.D., Hessels, E.A.: Precision microwave measurement of the  $2^3P_1 - 2^3P_0$  interval in atomic helium: a determination of the fine-structure constant. *Phys. Rev. Lett.* **87**, 173002-1–173002-4 (2001)
76. Giusfredi, G., Pastor, P.C., DeNatale, P., Mazzotti, D., deMauro, C., Fallani, L., Hagel, G., Krachmalnicoff, V., Ingusio, M.: Present status of the fine structure of the  $2^3P$  helium level. *Can. J. Phys.* **83**, 301–310 (2005)
77. Goldstein, J.S.: Properties of the Salpeter-Bethe two-nucleon equation. *Phys. Rev.* **91**, 1516–1524 (1953)
78. Goldstone, J.: Derivation of the Brueckner many-body theory. *Proc. R. Soc. Lond. Ser. A* **239**, 267–279 (1957)
79. Grant, I.P.: *Relativistic Quantum Theory of Atoms and Molecules*. Springer, Heidelberg (2007)
80. Griffel, D.H.: *Applied Functional Analysis*. Wiley, New York (1981)
81. Gross, F.: Three-dimensional covariant integral equations for low-energy systems. *Phys. Rev.* **186**, 1448–1462 (1969)
82. Grotch, H., Owen, D.A.: Bound states in quantum electrodynamics: theory and applications. *Fundam. Phys.* **32**, 1419–1457 (2002)
83. Grotch, H., Yennie, D.R.: Effective potential model for calculating nuclear corrections to the energy levels of hydrogen. *Rev. Mod. Phys.* **41**, 350–374 (1969)
84. Grottsch, H.: *Phys. Rev. Lett.* **24**, 39 (1970)
85. Häffner, H., Beier, T., Hermanspahn, N., Kluge, H.J., Quint, W., Stahl, S., Verdú, J., Werth, G.: High-accuracy measurements of the magnetic anomaly of the electron bound in hydrogenlike carbon. *Phys. Rev. Lett.* **85**, 5308–5311 (2000)
86. Hedendahl, D.: *Towards a Relativistic Covariant Many-Body Perturbation Theory*. Ph.D. thesis, University of Gothenburg, Gothenburg, Sweden (2010)
87. Hedendahl, D., Holmberg, J.: Coulomb-gauge self-energy calculation for high-Z hydrogenic ions. *Phys. Rev. A* **85**, 012514 (2012)
88. Holmberg, J.: Scalar vertex operator for bound-state QED in Coulomb gauge. *Phys. Rev. A* **84**, 062504 (2011)
89. Holmberg, J., Salomonson, S., Lindgren, I.: Coulomb-gauge calculation of the combined effect of the correlation and QED for heliumlike highly charged ions. *Phys. Rev. A* **92**, 012509 (2015)
90. Hubbard, J.: The description of collective motions in terms of many-body perturbation theory. 3. The extension of the theory to non-uniform gas. *Proc. R. Soc. Lond. Ser. A* **243**, 336–352 (1958)
91. Udelichato, P., Gorceix, O., Desclaux, J.P.: Multiconfiguration Dirac-Fock studies of two-electron ions: II. Radiative corrections and comparison with experiment. *J. Phys. B* **20**, 651–63 (1987)
92. Itzykson, C., Zuber, J.B.: *Quantum Field Theory*. McGraw-Hill, New York (1980)
93. Jankowski, K., Malinowski, P.: A valence-universal coupled-cluster single- and double-excitations method for atoms: II. *Appl. Be. J. Phys. B* **27**, 829–842 (1994)
94. Jankowski, K., Malinowski, P.: A valence-universal coupled-cluster single- and double-excitations method for atoms: III. Solvability problems in the presence of intruder states. *J. Phys. B* **27**, 1287–98 (1994)
95. Jena, D., Datta, D., Mukherjee, D.: A novel VU-MRCC formalism for the simultaneous treatment of strong relaxation and correlation effects with applications to electron affinity of neutral radicals. *Chem. Phys.* **329**, 290–306 (2006)
96. Jentschura, U.D., Mohr, P.J., Soff, G.: Calculation of the electron self-energy for low nuclear charge. *Phys. Rev. Lett.* **61**, 53–56 (1999)
97. Jentschura, U.D., Mohr, P.J., Tan, J.N., Wundt, B.J.: Fundamental constants and tests of theory in rydberg states of hydrogenlike ions. *Phys. Rev. Lett.* **100**, 160404 (2008)

98. Jeziorski, B., Monkhorst, H.J.: Coupled-cluster method for multideterminantal reference states. *Phys. Rev. A* **24**, 1668–1681 (1981)
99. Jeziorski, B., Paldus, J.: Spin-adapted multireference coupled-cluster approach: linear approximation for two closed-shell-type reference configuration. *J. Chem. Phys.* **88**, 5673–5687 (1988)
100. Johnson, W.R., Blundell, S.A., Sapirstein, J.: Finite basis sets for the Dirac equation constructed from B splines. *Phys. Rev. A* **37**, 307–15 (1988)
101. Johnson, W.R., Blundell, S.A., Sapirstein, J.: Many-body perturbation-theory calculations of energy-levels along the sodium isoelectronic sequence. *Phys. Rev. A* **38**, 2699–2706 (1988)
102. Jones, R.W., Mohling, F.: Perturbation theory of a many-fermion system. *Nucl. Phys. A* **151**, 420–48 (1970)
103. Kaldor, U., Eliav, E.: High-accuracy calculations for heavy and super-heavy elements. *Adv. Quantum Chem.* **31**, 313–336 (1999)
104. Kelly, H.P.: Application of many-body diagram techniques in atomic physics. *Adv. Chem. Phys.* **14**, 129–190 (1969)
105. Kubiček, K., Mokler, P.H., Mäkel, V., Ullrich, J., López-Urrutia, J.C.: Transition energy measurements in hydrogenlike and heliumlike ions strongly supporting bound-state QED calculations. *PRA* **90**, 032508 (2014)
106. Kukla, K.W., Livingston, A.E., Suleiman, J., Berry, H.G., Dunford, R.W., Gemmel, D.S., Kantor, E.P., Cheng, S., Curtis, L.J.: Fine-structure energies for the  $1s2s\ ^3S-1s2p\ ^3P$  transition in heliumlike  $\text{Ar}^+$ . *Phys. Rev. A* **51**, 1905–1917 (1995)
107. Kümmel, H.: In: Caianiello, E.R. (ed.) *Lecture Notes on Many-Body Problems*. Academic Press, New York (1962)
108. Kümmel, H., Lührman, K.H., Zabolitsky, J.G.: Many-fermion theory in exp S (or coupled cluster) form. *Phys. Rep.* **36**, 1–135 (1978)
109. Kuo, T.T.S., Lee, S.Y., Ratcliff, K.F.: A folded-diagram expansion of the model-space effective Hamiltonian. *Nucl. Phys. A* **176**, 65–88 (1971)
110. Kusch, P., Foley, H.M.: Precision measurement of the ratio of the atomic ‘g values’ in the  $^2P_{3/2}$  and  $^2P_{1/2}$  states of gallium. *Phys. Rev.* **72**, 1256–1257 (1947)
111. Kusch, P., Foley, H.M.: On the intrinsic moment of the electron. *Phys. Rev.* **73**, 412 (1948)
112. Kutzelnigg, B.H.: *Adv. Quantum Chem.* **10**, 187–219 (1977)
113. Kvasnička, V., Laurinc, V., Hubac, I.: Many-body perturbation of intermolecular interactions. *Phys. Rev. A* **24**, 2016–2026 (1974)
114. Labzowski, L.N., Klimchitskaya, G., Dmitriev, Y.: *Relativistic Effects in Spectra of Atomic Systems*. IOP Publication, Bristol (1993)
115. Labzowsky, L.N., Mitrushenkov, A.O.: Renormalization of the second-order electron self-energy for a tightly bound atomic electron. *Phys. Lett. A* **198**, 333–40 (1995)
116. Lamb, W.W., Retherford, R.C.: Fine structure of the hydrogen atom by microwave method. *Phys. Rev.* **72**, 241–43 (1947)
117. Lindgren, I.: The Rayleigh-Schrödinger perturbation and the linked-diagram theorem for a multi-configurational model space. *J. Phys. B* **7**, 2441–70 (1974)
118. Lindgren, I.: A coupled-cluster approach to the many-body perturbation theory for open-shell systems. *Int. J. Quantum Chem.* **S12**, 33–58 (1978)
119. Lindgren, I.: Accurate many-body calculations on the lowest  $^2S$  and  $^2P$  states of the lithium atom. *Phys. Rev. A* **31**, 1273–1286 (1985)
120. Lindgren, I.: Can MBPT and QED be merged in a systematic way? *Mol. Phys.* **98**, 1159–1174 (2000)
121. Lindgren, I.: The helium fine-structure controversy. arXiv:quant-ph p. 0810.0823v (2008)
122. Lindgren, I.: Dimensional regularization of the free-electron self-energy and vertex correction in Coulomb gauge. arXiv:quant-ph p. 1017.4669v1 (2011)
123. Lindgren, I., Åsén, B., Salomonson, S., Mårtensson-Pendrill, A.M.: QED procedure applied to the quasidegenerate fine-structure levels of He-like ions. *Phys. Rev. A* **64**, 062505 (2001)
124. Lindgren, I., Morrison, J.: *Atomic Many-Body Theory*, 2nd edn. Springer, Berlin (1986, reprinted 2009)



125. Lindgren, I., Mukherjee, D.: On the connectivity criteria in the open-shell coupled-cluster theory for the general model spaces. *Phys. Rep.* **151**, 93–127 (1987)
126. Lindgren, I., Persson, H., Salomonson, S., Labzowsky, L.: Full QED calculations of two-photon exchange for heliumlike systems: analysis in the Coulomb and Feynman gauges. *Phys. Rev. A* **51**, 1167–1195 (1995)
127. Lindgren, I., Persson, H., Salomonson, S., Sunnergren, P.: Analysis of the electron self-energy for tightly bound electrons. *Phys. Rev. A* **58**, 1001–15 (1998)
128. Lindgren, I., Persson, H., Salomonson, S., Ynnerman, A.: Bound-state self-energy calculation using partial-wave renormalization. *Phys. Rev. A* **47**, R4555–58 (1993)
129. Lindgren, I., Salomonson, S.: A numerical coupled-cluster procedure applied to the closed-shell atoms Be and Ne. Presented at the Nobel Symposium on Many-Body Effects in Atoms and Solids, Lerum, 1979. *Physica Scripta* **21**, 335–42 (1980)
130. Lindgren, I., Salomonson, S., Åsén, B.: The covariant-evolution-operator method in bound-state QED. *Phys. Rep.* **389**, 161–261 (2004)
131. Lindgren, I., Salomonson, S., Hedendahl, D.: Many-body-QED perturbation theory: connection to the two-electron Bethe-Salpeter equation. Einstein centennial review paper. *Can. J. Phys.* **83**, 183–218 (2005)
132. Lindgren, I., Salomonson, S., Hedendahl, D.: Many-body procedure for energy-dependent perturbation: merging many-body perturbation theory with QED. *Phys. Rev. A* **73**, 062502 (2006)
133. Lindgren, I., Salomonson, S., Hedendahl, D.: Coupled clusters and quantum electrodynamics. In: Čárský, P., Paldus, J., Pittner, J. (eds.) *Recent Progress in Coupled Cluster Methods: Theory and Applications*, pp. 357–374. Springer, New York (2010)
134. Lindgren, I., Salomonson, S., Holmberg, J.: QED effects in scattering involving atomic bound states: radiative recombination. *Phys. Rev. A* **89**, 062504 (2014)
135. Lindroth, E.: Numerical solution of the relativistic pair equation. *Phys. Rev. A* **37**, 316–28 (1988)
136. Lindroth, E., Mårtensson-Pendrill, A.M.:  $2p^2\ ^1S$  state of Beryllium. *Phys. Rev. A* **53**, 3151–3156 (1996)
137. Lippmann, B.A., Schwinger, J.: Variational principles for scattering processes. I. *Phys. Rev.* **79**, 469–480 (1950)
138. Löwdin, P.O.: Studies in perturbation theory. X. Lower bounds to eigenvalues in perturbation-theory ground state. *Phys. Rev.* **139**, A357–A372 (1965)
139. Safronova, M.S., Sapirstein, J., Johnson, W.R., Derevianko, A.: Relativistic many-body calculations of energy levels, hyperfine constants, electric-dipole matrix elements, and static polarizabilities for alkali-metal atoms. *Phys. Rev. A* **56**, 4476–4487 (1999)
140. Mahan, G.D.: *Many-Particle Physics*, 2nd edn. Springer, Heidelberg (1990)
141. Mahapatra, U.S., Datta, B., Mukherjee, D.: Size-consistent state-specific multireference coupled cluster theory: formal developments and molecular applications. *J. Chem. Phys.* **110**, 6171–6188 (1999)
142. Malinowski, P., Jankowski, K.: A valence-universal coupled-cluster single- and double-excitation method for atoms. I. Theory and application to the  $C^{2+}$  ion. *J. Phys. B* **26**, 3035–56 (1993)
143. Mandl, F., Shaw, G.: *Quantum Field Theory*. Wiley, New York (1986)
144. Marrs, R.E., Elliott, S.R., Stöckler, T.: Measurement of two-electron contributions to the ground-state energy of heliumlike ions. *Phys. Rev. A* **52**, 3577–85 (1995)
145. Mårtensson, A.M.: An iterative, numerical procedure to obtain pair functions applied to two-electron systems. *J. Phys. B* **12**, 3995–4012 (1980)
146. Mårtensson-Pendrill, A.M., Lindgren, I., Lindroth, E., Salomonson, S., Staudte, D.S.: Convergence of relativistic perturbation theory for the  $1s2p$  states in low- $Z$  heliumlike systems. *Phys. Rev. A* **51**, 3630–3635 (1995)
147. Meissner, L., Malinowski, P.: Intermediate Hamiltonian formulation of the valence-universal coupled-cluster method for atoms. *Phys. Rev. A* **61**, 062510 (2000)

148. Meyer, W.: PNO-CI studies of electron correlation effects. 1. Configuration expansion by means of nonorthogonal orbitals, and application to ground-state and ionized states of methane. *J. Chem. Phys.* **58**, 1017–35 (1973)
149. Mohr, P.: Self-energy correction to one-electron energy levels in a strong Coulomb field. *Phys. Rev. A* **46**, 4421–24 (1992)
150. Mohr, P., Taylor, B.: CODATA recommended values of the fundamental constants 2002. *Rev. Mod. Phys.* **77**, 1–107 (2005)
151. Mohr, P., Taylor, B.: CODATA recommended values of the fundamental constants 2002. *Rev. Mod. Phys.* **661**, 287–289 (2008)
152. Mohr, P., Taylor, B.N.: CODATA recommended values of the fundamental physical constants: 1998. *Rev. Mod. Phys.* **72**, 351–495 (2000)
153. Mohr, P.J.: Numerical evaluation of the  $1s_{1/2}$ -state radiative level shift. *Ann. Phys. (N.Y.)* **88**, 52–87 (1974)
154. Mohr, P.J.: Self-energy radiative corrections. *Ann. Phys. (N.Y.)* **88**, 26–52 (1974)
155. Mohr, P.J.: Self-energy radiative corrections. *Ann. Phys. (N.Y.)* **88**, 26–51 (1974)
156. Mohr, P.J.: Lamb shift in a strong Coulomb field. *Phys. Rev. Lett.* **34**, 1050–1052 (1975)
157. Mohr, P.J.: Self-energy of the  $n = 2$  states in a strong Coulomb field. *Phys. Rev. A* **26**, 2338–2354 (1982)
158. Mohr, P.J.: Quantum electrodynamics of high-Z few-electron atoms. *Phys. Rev. A* **32**, 1949–57 (1985)
159. Mohr, P.J., Plunien, G., Soff, G.: QED corrections in heavy atoms. *Phys. Rep.* **293**, 227–372 (1998)
160. Mohr, P.J., Sapirstein, J.: Evaluation of two-photon exchange graphs for excited states of highly charged heliumlike ions. *Phys. Rev. A* **62**, 052501-1–052501-12 (2000)
161. Mohr, P.J., Soff, G.: Nuclear size correction to the electron self energy. *Phys. Rev. Lett.* **70**, 158–161 (1993)
162. Møller, C., Plesset, M.S.: Note on an approximation treatment for many-electron systems. *Phys. Rev.* **46**, 618–622 (1934)
163. Morita, T.: Perturbation theory for degenerate problems of many-fermion systems. *Progr. Phys. (Jpn.)* **29**, 351–369 (1963)
164. Morrison, J.: Many-Body calculations for the heavy atoms. III. Pair correlations. *J. Phys. B* **6**, 2205–2212 (1973)
165. Morrison, J., Salomonson, S.: Many-body perturbation theory of the effective electron-electron interaction for open-shell atoms. Presented at the Nobel Symposium., Lerum, 1979. *Physica Scripta* **21**, 343–50 (1980)
166. Mukherjee, D.: Linked-cluster theorem in the open-shell coupled-cluster theory for incomplete model spaces. *Chem. Phys. Lett.* **125**, 207–212 (1986)
167. Mukherjee, D., Moitra, R.K., Mukhopadhyay, A.: Application of non-perturbative many-body formalism to open-shell atomic and molecular problems—calculation of ground and lowest  $\pi - \pi^*$  singlet and triplet energies and first ionization potential of trans-butadine. *Mol. Phys.* **33**, 955–969 (1977)
168. Mukherjee, D., Pal, J.: Use of cluster expansion methods in the open-shell correlation problems. *Adv. Chem. Phys.* **20**, 292 (1989)
169. Myers, E.G., Margolis, H.S., Thompson, J.K., Farmer, M.A., Silver, J.D., Tarbutt, M.R.: Precision measurement of the  $1s2p^3P_2 - ^3P_1$  fine structure interval in heliumlike fluorine. *Phys. Rev. Lett.* **82**, 4200–4203 (1999)
170. Myers, E.G., Tarbutt, M.R.: Measurement of the  $1s2p^3P_0 - ^3P_1$  fine structure interval in heliumlike magnesium. *Phys. Rev. A* **61**, 010501R (1999)
171. Nadeau, M.J., Zhao, X.L., Garvin, M.A., Litherland, A.E.: Ca negative-ion binding energy. *Phys. Rev. A* **46**, R3588–90 (1992)
172. Nakanishi, N.: Normalization condition and normal and abnormal solutions of Bethe-Salpeter equation. *Phys. Rev.* **138**, B1182 (1965)
173. Namyslowski, J.M.: The relativistic bound state wave function. in light-front quantization and non-perturbative QCD. In: Vary, J.P., Wolz, F. (eds.) *International Institute of Theoretical and Applied Physics*, Ames (1997)

174. Nesbet, R.K.: Electronic correlation in atoms and molecules. *Adv. Chem. Phys.* **14**, 1 (1969)
175. Nooijen, M., Bartlett, R.J.: Similarity transformed equation-of-motion coupled-cluster theory: details, examples, and comparisons. *J. Chem. Phys.* **107**, 6812–6830 (1997)
176. Nooijen, M., Demel, O., Datta, D., Kong, L., Shamasundar, K.R., Lotrich, V., Huttington, L.M., Neese, F.: Multireference equation of motion coupled cluster: a transform and diagonalize approach to electronic structure. *Science* **339**, 417–20 (2014)
177. Oberlechner, G., Owono-N'Guema, F., Richert, J.: Perturbation theory for the degenerate case in the many-body problem. *Nouvo Cim. B* **68**, 23–43 (1970)
178. Onida, G., Reining, L., Rubio, A.: Electronic excitations: density-functional versus many-body Green's-function approaches. *Rev. Mod. Phys.* **74**, 601–59 (2002)
179. Pachucki, K.: Quantum electrodynamics effects on helium fine structure. *J. Phys. B* **32**, 137–52 (1999)
180. Pachucki, K.: Improved theory of helium fine structure. *Phys. Rev. Lett.* **97**, 013002 (2006)
181. Pachucki, K., Sapirstein, J.: Contributions to helium fine structure of order  $ma^7$ . *J. Phys. B* **33**, 5297–5305 (2000)
182. Pachucki, K., Yerokhin, V.A.: Reexamination of the helium fine structure. *Phys. Rev. Lett.* **79**, 62516 (2009)
183. Pachucki, K., Yerokhin, V.A.: Reexamination of the helium fine structure. *Phys. Rev. Lett.* **80**, 19902E (2009)
184. Pachucki, K., Yerokhin, V.A.: Fine structure of heliumlike ions and determination of the fine structure constant. *Phys. Rev. Lett.* **104**, 70403 (2010)
185. Pachucki, K., Yerokhin, V.A.: Reexamination of the helium fine structure (vol 79, 062516, 2009). *Phys. Rev. A* **81**, 39903 (2010)
186. Paldus, J., Čížek, J.: Time-independent diagrammatic approach to perturbation theory of fermion systems. *Adv. Quantum Chem.* **9**, 105–197 (1975)
187. Paldus, J., Čížek, J., Saute, M., Laforge, A.: Correlation problems in atomic and molecular systems. IV. Coupled-cluster approach to open shells. *Phys. Rev. A* **17**, 805–15 (1978)
188. Pauli, W., Willars, F.: On the invariant regularization in relativistic quantum theory. *Rev. Mod. Phys.* **21**, 434–444 (1949)
189. Persson, H., Lindgren, I., Labzowsky, L.N., Plunien, G., Beier, T., Soff, G.: Second-order self-energy-vacuum-polarization contributions to the Lamb shift in highly charged few-electron ions. *Phys. Rev. A* **54**, 2805–2813 (1996)
190. Persson, H., Lindgren, I., Salomonson, S., Sunnergren, P.: Accurate vacuum-polarization calculations. *Phys. Rev. A* **48**, 2772–2778 (1993)
191. Persson, H., Salomonson, S., Sunnergren, P.: Regularization corrections to the partial-wave renormalization procedure. Presented at the Conference Modern Trends in Atomic Physics, Hindås, Sweden, May 1996. *Adv. Quantum Chem.* **30**, 379–392 (1998)
192. Persson, H., Salomonson, S., Sunnergren, P., Lindgren, I.: Two-electron lamb-shift calculations on heliumlike ions. *Phys. Rev. Lett.* **76**, 204–207 (1996)
193. Persson, H., Salomonson, S., Sunnergren, P., Lindgren, I.: Radiative corrections to the electron g-factor in H-like ions. *Phys. Rev. A* **56**, R2499–2502 (1997)
194. Peskin, M.E., Schroeder, D.V.: *An Introduction to Quantum Field Theory*. Addison-Wesley Publication Co., Reading (1995)
195. Plante, D.R., Johnson, W.R., Sapirstein, J.: Relativistic all-order many-body calculations of the  $n = 1$  and  $n = 2$  states of heliumlike ions. *Phys. Rev. A* **49**, 3519–3530 (1994)
196. Pople, J.A., Krishnan, R., Schlegel, H.B., Binkley, J.S.: Electron correlation theories and their application to the study of simple reaction potential surfaces. *Int. J. Quantum Chem.* **14**, 545–560 (1978)
197. Pople, J.A., Santry, D.P., Segal, G.A.: Approximate self-consistent molecular orbital theory. I. Invariant procedures. *J. Chem. Phys.* **43**, S129 (1965)
198. Pople, J.A., Segal, G.A.: Approximate self-consistent molecular orbital theory. 3. CNDO results for AB<sub>2</sub> and AB<sub>3</sub> systems. *J. Chem. Phys.* **44**, 3289 (1966)
199. Purvis, G.D., Bartlett, R.J.: A full coupled-cluster singles and doubles model: the inclusion of disconnected triples. *J. Chem. Phys.* **76**, 1910–1918 (1982)

200. Pyykkö, P.: Relativistic effects in chemistry: more common than you thought. *Ann. Rev. Phys. Chem.* **63**, 45–64 (2012)
201. Quiney, H.M., Grant, I.P.: Atomic self-energy calculations using partial-wave mass renormalization. *J. Phys. B* **49**, L299–304 (1994)
202. Riis, E., Sinclair, A.G., Poulsen, O., Drake, G.W.F., Rowley, W.R.C., Levick, A.P.: Lamb shifts and hyperfine structure in  ${}^6\text{Li}^+$  and  ${}^7\text{Li}^+$ : theory and experiment. *Phys. Rev. A* **49**, 207–220 (1994)
203. Rosenberg, L.: Virtual-pair effects in atomic structure theory. *Phys. Rev. A* **39**, 4377–4386 (1989)
204. Safronova, M.S., Johnson, W.R.: All-Order Methods for Relativistic Atomic Structure Calculations, *Advances in Atomic Molecular and Optical Physics Series*, vol. 55 (2007)
205. Safronova, M.S., Sapirstein, J., Johnson, W.R.: Relativistic many-body calculations of energy levels, hyperfine constants, and transition rates for sodiumlike ions. *Phys. Rev. A* **58**, 1016–28 (1998)
206. Sakurai, J.J.: *Advanced Quantum Mechanics*. Addison-Wesley Publication Co., Reading (1967)
207. Salomonson, S., Lindgren, I., Mårtensson, A.M.: Numerical many-body perturbation calculations on be-like systems using a multi-configurational model space. Presented at the Nobel Symposium on Many-Body Effects in Atoms and Solids, Lerum, 1979. *Physica Scripta* **21**, 335–42 (1980)
208. Salomonson, S., Öster, P.: Numerical solution of the coupled-cluster single- and double-excitation equations with application to Be and  $\text{Li}^-$ . *Phys. Rev. A* **41**, 4670–81 (1989)
209. Salomonson, S., Öster, P.: Relativistic all-order pair functions from a discretized single-particle Dirac Hamiltonian. *Phys. Rev. A* **40**, 5548–5559 (1989)
210. Salomonson, S., Warston, H., Lindgren, I.: Many-body calculations of the electron affinity for Ca and Sr. *Phys. Rev. Lett.* **76**, 3092–3095 (1996)
211. Salomonson, S., Ynnerman, A.: Coupled-cluster calculations of matrix elements and ionization energies of low-lying states of sodium. *Phys. Rev. A* **43**, 88–94 (1991)
212. Salpeter, E.E.: Mass correction to the fine structure of hydrogen-like atoms. *Phys. Rev.* **87**, 328–343 (1952)
213. Salpeter, E.E., Bethe, H.A.: A relativistic equation for bound-state problems. *Phys. Rev.* **84**, 1232–1242 (1951)
214. Sandars, P.G.H.: Correlation effects in atoms and molecules. *Adv. Chem. Phys.* **14**, 365–419 (1969)
215. Sapirstein, J., Pachucki, K., Cheng, K.: Radiative corrections to one-photon decays of hydrogen ions. *Phys. Rev. A* **69**, 022113 (2004)
216. Sazdjian, H.: Relativistic wave equations for the dynamics of two interacting particles. *Phys. Rev. D* **33**, 3401–24 (1987)
217. Sazdjian, H.: The connection of two-particle relativistic quantum mechanics with the Bethe-Salpeter equation. *J. Math. Phys.* **28**, 2618–38 (1987)
218. Schäfer, L., Weidenmüller, H.A.: Self-consistency in application of Brueckner's method to doubly-closed-shell nuclei. *Nucl. Phys. A* **174**, 1 (1971)
219. Schiff, L.L.: *Quantum Mechanics*. McGraw-Hill Book Co., New York (1955)
220. Schweber, S.S.: *An Introduction to Relativistic Quantum Field Theory*. Harper and Row, New York (1961)
221. Schweber, S.S.: *QED and the Men Who Made It: Dyson, Feynman, Schwinger and Tomonaga*. Princeton University Press, Princeton (1994)
222. Schweppe, J., Belkacem, A., Blumenfeld, L., Clayton, N., Feinberg, B., Gould, H., Kostroun, V.E., Levy, L., Misawa, S., Mowat, J.R., Prior, M.H.: Measurement of the Lamb shift in lithiumlike uranium ( $\text{U}^{+89}$ ). *Phys. Rev. Lett.* **66**, 1434–1437 (1991)
223. Schwinger, J.: On quantum electrodynamics and the magnetic moment of the electron. *Phys. Rev.* **73**, 416 (1948)
224. Schwinger, J.: Quantum electrodynamics I. A covariant formulation. *Phys. Rev.* **74**, 1439 (1948)

225. Shabaev, V.M.: Quantum electrodynamic theory of recombination of an electron with a highly charged ion. *Phys. Rev. A* **50**, 4521–34 (1994)
226. Shabaev, V.M.: two-time Green's function method in quantum electrodynamics of high-Z few-electron atoms. *Phys. Rep.* **356**, 119–228 (2002)
227. Shabaev, V.M., Artemyev, A.N., Beier, T., Plunien, G., Yerokhin, V.A., Soff, G.: Recoil correction to the ground-state energy of hydrogenlike atoms. *Phys. Rev. A* **57**, 4235–39 (1998)
228. Shabaev, V.M., Yerokhin, V.A., Beier, T., Eichler, I.: QED corrections to the radiative recombination of an electron with a bare nucleus. *Phys. Rev. A* **61**, 052112 (2000)
229. Sinanoglu, O.: Electronic correlation in atoms and molecules. *Adv. Chem. Phys.* **14**, 237–81 (1969)
230. Slater, J.: *Quantum Theory of Atomic Spectra*. McGraw-Hill, New York (1960)
231. Snyderman, N.J.: Electron radiative self-energy of highly stripped heavy-atoms. *Ann. Phys. (N.Y.)* **211**, 43–86 (1991)
232. Sthöhlker, T., Beyer, H.F., Gumberidze, A., Kumar, A., Liesen, D., Reuschl, R., Spillmann, U., Trassinelli, M.: Ground state Lamb-shift of heavy hydrogen-like ions: status and perspectives. *Hyperfine Interact.* **172**, 135–140 (2006)
233. Stöhlker, T., Mokler, P.H., et al.: Ground-state lamb shift for hydrogenlike uranium measured at the ESR storage ring. *Phys. Rev. Lett.* **14**, 2184–2187 (1993)
234. Stueckelberg, E.C.G.: *Helv. Phys. Acta* **15**, 23 (1942)
235. Sucher, J.: Energy levels of the two-electron atom to order  $\alpha^3$  Ry; ionization energy of helium. *Phys. Rev.* **109**, 1010–1011 (1957)
236. Sucher, J.: S-matrix formalism for level-shift calculations. *Phys. Rev.* **107**, 1448–1454 (1957)
237. Sucher, J.: Ph.D. thesis, Columbia University Microfilm Internat., Ann Arbor, Michigan (1958)
238. Sucher, J.: Foundations of the Relativistic theory of many electron atoms. *Phys. Rev. A* **22**, 348–362 (1980)
239. Sunnergren, P.: Complete one-loop qed calculations for few-electron ions. Ph.D. thesis, Department of Physics, Chalmers University of Technology and University of Gothenburg, Gothenburg, Sweden (1998)
240. Taylor, A.E.: *Introduction to Functional Analysis*. Wiley, New York (1957)
241. 't Hooft, G., Veltman, M.: Regularization and renormalization of gauge fields. *Nucl. Phys. B* **44**, 189–213 (1972)
242. Todorov, I.T.: Quasipotential equation corresponding to the relativistic eikonal approximation. *Phys. Rev. D* **3**, 2351–2356 (1971)
243. Tolmachev, V.V.: The field-theoretic form of the perturbation theory for many-electron atoms. I. Abstract theory. *Adv. Chem. Phys.* **14**, 421–471 (1969)
244. Tomanaga, S.: *Phys. Rev.* **74**, 224 (1948)
245. Uehling, E.A.: Polarization effects in the positron theory. *Phys. Rev.* **48**, 55–63 (1935)
246. Čársky, P., Paldus, J., Pittner, J. (eds.): *Recent Progress in Coupled Cluster Methods: Theory and Applications*. Springer, New York (2009)
247. Walter, C., Peterson, J.: Shape resonance in  $\text{Ca}^-$  photodetachment and the electron affinity of  $\text{Ca}(^1\text{S})$ . *Phys. Rev. Lett.* **68**, 2281–84 (1992)
248. Wheeler, J.A.: On the mathematical description of light nuclei by the method of resonating group structure. *Phys. Rev.* **52**, 1107–1122 (1937)
249. Wichmann, E.H., Kroll, N.M.: Vacuum polarization in a strong Coulomb field. *Phys. Rev.* **101**, 843–859 (1956)
250. Wick, C.G.: The evaluation of the collision matrix. *Phys. Rev.* **80**, 268–272 (1950)
251. Wick, G.C.: Properties of Bethe-Salpeter wave functions. *Phys. Rev.* **96**, 1124–1134 (1954)
252. Yerokhin, V.A., Artemyev, A.N., Beier, T., Plunien, G., Shabaev, V.M., Soff, G.: Two-electron self-energy corrections to the  $2p_{1/2} - 2s$  transition energy in Li-like ions. *Phys. Rev. A* **60**, 3522–3540 (1999)
253. Yerokhin, V.A., Artemyev, A.N., Shabaev, V.M.: Two-electron self-energy contributions to the ground-state energy of helium-like ions. *Phys. Lett. A* **234**, 361–366 (1997)

254. Yerokhin, V.A., Artemyev, A.N., Shabaev, V.M., Sysak, M.M., Zharebtsov, O.M., Soff, G.: Evaluation of the two-photon exchange graphs for the  $2p_{1/2} - 2s$  transition in Li-like Ions. *Phys. Rev. A* **64**, 032109-1–032109-15 (2001)
255. Yerokhin, V.A., Indelicato, P., Shabaev, V.M.: Self-energy corrections to the bound-electron g factor in H-like ions. *Phys. Rev. Lett.* **89**, 134001 (2002)
256. Yerokhin, V.A., Indelicato, P., Shabaev, V.M.: Two-loop self-energy correction in high-Z hydrogenlike ions. *Phys. Rev. Lett.* **91**, 073001 (2003)
257. Yerokhin, V.A., Indelicato, P., Shabaev, V.M.: Evaluation of the self-energy correction to the g factor of S states in H-like ions. *Phys. Rev. A* **69**, 052203 (2004)
258. Zelevinsky, T., Farkas, D., Gabrielse, G.: Precision measurement of the three  $2^3P_J$  helium fine structure intervals. *Phys. Rev. Lett.* **95**, 203001 (2005)
259. Zhang, T.: Corrections to  $O(\alpha^7(\ln \alpha)mc^2)$  fine-structure splittings and  $O(\alpha^6(\ln \alpha)mc^2)$  energy levels in helium. *Phys. Rev. A* **54**, 1252–1312 (1996)
260. Zhang, T.: QED corrections to  $O(\alpha^7 mc^2)$  fine-structure splitting in helium. *Phys. Rev. A* **53**, 3896–3914 (1996)
261. Zhang, T.: Three-body corrections to  $O(\alpha^6)$  fine-structure in helium. *Phys. Rev. A* **56**, 270–277 (1997)
262. Zhang, T., Drake, G.W.F.: A rigorous treatment of  $O(\alpha^6 mc^2)$  QED corrections to the fine structure splitting of helium. *J. Phys. B* **27**, L311–L316 (1994)
263. Zhang, T., Drake, G.W.F.: Corrections to  $O(\alpha^7 mc^2)$  fine-structure splitting in helium. *Phys. Rev. A* **54**, 4882–4922 (1996)
264. Zhang, T., Yan, Z.C., Drake, G.W.F.: QED Corrections of  $O(mc^2\alpha^7 \ln \alpha)$  to the fine structure splitting of helium and He-like ions. *Phys. Rev. Lett.* **77**, 1715–1718 (1996)

# Index

## A

Action integral, 334  
Adiabatic damping, 48  
All-order method, 29  
Annihilation operator, 309  
Antisymmetry, 20

## B

Banach space, 301  
Bethe–Salpeter equation, 3, 108, 117, 158,  
177, 202, 219, 231  
    effective potential form, 226  
Bethe–Salpeter–Bloch equation, 6, 160, 177,  
219, 226  
Bloch equation  
    for Green’s operator, 152  
    generalized, 19, 21  
Bra vector, 316  
Breit interaction, 1, 36, 344, 346  
Brillouin–Wigner expansion, 157  
Brown-Ravenhall effect, 2, 36, 183

## C

Cauchy sequence, 301  
Charge renormalization, 252  
Closure property, 319  
Complex rotation, 35  
Configuration, 20  
Conjugate momentum, 13, 332  
Continuity equation, 340  
Contraction, 16  
Contravariant vector, 297  
Coordinate representation, 62, 318  
Counterterms, 141

Coupled-cluster approach, 29, 31  
    normal-ordered, 32  
Coupled-cluster expansion, 1  
Coupled-cluster-QED expansion, 205  
Covariance, 2  
Covariant evolution operator, 117  
Covariant evolution operator method, 3  
Covariant vector, 297  
Creation operator, 309  
Cut-Off procedure, 255  
Cutkosky rules, 279

## D

D’Alembertian operator, 298  
Damping factor, 302  
De Broglie’s relations, 11  
Delta function, 302  
Difference ratio, 142  
Dimensional analysis, 385  
Dimensional regularization, 167, 255  
Dirac–Coulomb Hamiltonian, 36  
Dirac delta function, 302  
Dirac equation, 2, 321  
Dirac matrices, 322  
Dirac sea, 36  
Discretization technique, 40  
Dot product, 136  
Dynamical process, 7, 140, 277  
Dyson equation, 107, 220, 249

## E

Effective Hamiltonian, 5, 18  
    intermediate, 35  
Effective interaction, 21, 29

Einstein summation rule, 315  
 Electron field operators, 311  
 Electron propagator, 60, 97  
 Energy diagram, 87  
 Equal-time approximation, 94, 118, 123,  
 177, 225, 229  
 Equations of the motion, 334  
 Euler-Lagrange equations, 334  
 Evolution operator, 44  
 Exponential Ansatz, 31  
 normal-ordered, 32  
 External-potential approach, 5, 229

**F**

Feynman amplitude, 79, 87, 94, 109, 112,  
 122, 179, 365, 367  
 Feynman diagram, 27, 38, 59, 87, 124, 365  
 First quantization, 11  
 Fock space, 134, 301  
 photonic, 6, 48, 133  
 Fock-space coupled-cluster, 33  
 Folded diagram, 21  
 Fourier transform, 62  
 Free-electron propagator, 244  
 Functional, 299  
 Furry picture, 19, 25  
 Furry's theorem, 85

**G**

Gamma function, 360  
 Gauge  
 Coulomb, 57, 66, 75, 80, 341, 351, 357  
 covariant, 57, 64, 122, 124, 356  
 Feynman, 57, 64, 80, 351, 354, 356  
 Fried-Yennie, 357  
 Landau, 357  
 non-covariant, 357  
 Gauge invariance, 341  
 Gauge transformation, 355  
 Gaunt interaction, 187, 351  
 Gell-Mann–Low theorem, 48, 49  
 relativistic, 131  
 G-factor, 168  
 Goldstone diagram, 23  
 Goldstone rules, 22, 26, 124  
 Green's function, 3, 89  
 projected, 111  
 two-time, 110  
 Green's operator, 117, 135  
 Fourier transform, 138  
 time dependence, 156  
 Green's operator method, 3, 117

Grotrsch term, 168  
 Gupta–Bleuler formalism, 353

**H**

Hamilton operator, 336  
 Hamiltonian density, 335, 336  
 Hartree-Fock model, 24  
 Heaviside step function, 307  
 Heisenberg commutation rules, 335  
 Heisenberg picture, 222, 312  
 Heisenberg representation, 90  
 Helium fine structure, 231  
 Hilbert space, 301  
 Hole state, 117  
 Hylleraas function, 5, 167

**I**

Incomplete model space, 28  
 Interaction density, 336  
 Interaction picture, 44  
 Intermediate normalization, 19  
 Intersection, 299  
 Intruder state, 21, 33  
 Irreducible diagram, 38, 128

**K**

Ket vector, 316  
 Klein-Gordon equation, 321  
 Knstantaneous Breit interaction, 72  
 Kronecker delta factor, 302, 303

**L**

Lagrange equations, 331  
 Lagrangian density, 334, 336  
 Lagrangian function, 335  
 Lamb shift, 2, 78, 83, 162, 259  
 Laplacian operator, 299  
 Lehmann representation, 95  
 Linked diagram, 26, 105  
 Linked-diagram theorem, 1  
 Lippmann-Schwinger equation, 226  
 Lorentz covariance, 2, 37, 58, 93, 117  
 Lorentz force, 334  
 Lorentz transformation, 2  
 Lorenz condition, 340

**M**

Many-body Dirac Hamiltonian, 134  
 Mass counterterm, 250  
 Mass renormalization, 251, 255



Matrix elements, 317  
Matrix representation, 317  
Maxwell's equations, 338  
Maxwell's equations form, 337  
Metric tensor, 297  
Minimal substitution, 333, 336  
Model state, 18  
Model space, 18  
    complete, 21  
    extended, 21  
Model-space contribution (MSC), 27, 53,  
    127, 140, 145  
Momentum representation, 327  
Multi-photon exchange, 127

## N

Non-radiative effects, 37  
Norm, 300  
Normal order, 16  
No-virtual-pair approximation, 2, 36

## O

Off the mass-shell, 245  
Optical theorem, 277–279

## P

Pair correlation, 29  
Parent state, 49, 50, 132  
Partitioning, 19  
Pauli spin matrices, 322  
Pauli-Willars regularizaition, 256  
Perturbation  
    Brillouin-Wigner, 109  
    Rayleigh-Schrödinger, 1, 22  
Photoionization, 281, 293  
Photon propagator, 63  
Photonic Fock space, 186  
Poisson bracket, 13, 332  
Polarization tensor, 86  
Principal-value integration, 63

## Q

QED effects, 37, 57, 78  
    non-radiative, 178  
    radiative, 196  
Quantization condition, 13  
Quasi-degeneracy, 21, 53, 60  
Quasi-potential approximation, 4  
Quasi-singularity, 53

## R

Radiative effects, 37  
Radiative recombination, 7, 281, 286  
Reaction operator, 138  
Reducible, 125  
Reducible diagram, 38, 128, 204  
Reference-state contribution, 76, 145  
Regularization, 78, 243  
    Brown-Langer-Schaefer, 259  
    dimensional, 264  
    partial-Wave, 262  
    Pauli-Willars, 255  
Renormalization, 78, 243  
    charge, 251  
    mass, 249  
Resolution of the identity, 317  
Resolvent, 22  
    reduced, 22

## S

Scalar potential, 338  
Scalar product, 298  
Scalar retardation, 187  
Scattering amplitude, 291  
Scattering cross section, 277  
Scattering matrix, 58  
Schrödinger equation, 13  
Schrödinger picture, 44  
Schwinger correction, 168  
Second quantization, 14, 309  
Self-energy, 107  
    electron, 37, 78, 161, 245, 251  
    photon, 86, 253  
    proper, 107  
Sequence, 300  
Set, 299  
Size consistency, 28  
Size extensive, 228  
Size extensivity, 28, 228  
Slater determinant, 20, 310  
S-matrix, 3, 58, 161  
Spin-orbital, 20  
Spline, 39  
State-specific approach, 35  
State-universality, 34  
Subset, 299  
Sucher energy formula, 59

## T

Target states, 18  
Time-ordering, 46  
    Wick, 16

Trace, 84, 86  
Transition rate, 7, 43, 44, 280  
Transverse-photon, 76  
Two-time Green's function, 3

**U**

Uehling potential, 85, 128  
Union, 299  
Unit system, 385  
  cgs, 387  
  Hartree, 386  
  mixed, 326  
  natural, 386  
  relativistic, 57, 386  
  SI, 385

Unlinked diagram, 26

**V**

Vacuum polarization, 2, 37, 83, 86  
Valence universality, 19, 34  
Vector potential, 337  
Vector space, 299  
Vertex correction, 37, 81, 247, 252

**W**

Ward identity, 82, 248, 286  
Wave operator, 18  
Wichmann–Kroll potential, 85  
Wick's theorem, 17